

**Proceedings of the
2019
Society of Wood Science and
Technology
International Convention**

**Convention Theme: Renewable
Materials and the Wood-based
Bioeconomy**

Edited by Susan LeVan-Green

*Overall General Chair: Eve Haviarova,
Purdue University, USA*

**October 20-25, 2019
Tenaya Lodge
Yosemite National Park, California, USA**

*Proceedings of the 62nd International Convention of
Society of Wood Science and Technology
October 20-25, 2019 – Tenaya Lodge, Yosemite, California USA*

Table of Content

Keynote Speaker

Monday, October 21, 2019

The Dilemma of Fire and Firefighting

Chris Schow1

Early Stage Researchers

Monday, October 21, 2019

Activity of Organic Acids and Their Synergy Against the Wood-Decaying Fungus *Coniophora Puteana*

Alitor Barbero-López, Md Mokbul Hossain, Antti Haapala2

Study on VOCs Emissions from Veneered Plywood at Closed Circumstances

Tianyu Cao, Jun Shen11

Investigation of A Waste Newspaper Reinforced Soybean Based Adhesives for Interior Plywood

Hao Yin, Qiaojia Lin, Qinzhi Zeng, Jiuping Rao, Nairong Chen17

Measuring Device Development for a Hardwood High-Speed Disintegration Process Analysis

Ondrej Dvoracek.....24

Structure-related Vapor Sorption Phenomena in Wood

Raphaela Hellmayr, Rupert Wimmer.....25

Industry 4.0 Readiness in the US Forestry Industry

Brooklyn Legg, Bettina Dorfner, Scott Leavengood, Eric Hansen.....33

Reducing the set-Recovery of Surface-Densified Scots Pine by Furfuryl Alcohol Modification

Han Lei34

Composition Analysis and Health Risk Assessment of Benzene Series for Nitrocellulose Paint Lacquered MDF

Huifang Li, Jun Shen.....35

Investigating the Thermal and Mechanical Properties of Fly Ash/Metakaolin-Based Geopolymer Reinforced with Alien Invasive Wood Species

Hamed Olafiku Olayiwola.....43

Evaluating Stem and Wood Quality of Planted Longleaf Pines Using Bio-Imaging Techniques

Sameen Raut, Joe Dahlen.....44

Improvement of Leaching Resistance of Fire-Retardant Wood by Formation of Insoluble Compounds

Alexander Scharf.....46

Understanding Silvicultural and Process Variation and Its Influence on Life-Cycle Carbon Emissions for Durable Wood Products

Adam Scouse.....48

Cellulose Nanocrystals vs Cellulose Nanofibrils: Which One Performs Better in Flexible, Biodegradable and Multilayer Films for Food Packaging?

Lu Wang.....49

Influence of Particleboard Thickness and Veneers on Odor Emissions

Qifan Wang, Jun Shen.....50

Effects of Pyrolysis Temperature on Properties of Cardboard Biochar and the Resulting Biochar/High Density Polyethylene Composites

Xiaoqian Wang.....64

*Proceedings of the 62nd International Convention of
Society of Wood Science and Technology
October 20-25, 2019 – Tenaya Lodge, Yosemite, California USA*

**Impact of Forest Disturbances on Wood Quality
Monday, October 21, 2019**

Evaluating the Role of Europe’s Wood Value Chain in the Circular Bioeconomy: the WoodCircus Project Mike Burnard.....	65
Comparison of Juvenile Wood Depictions to Wood Property Maps from Mature Longleaf Pine Thomas Eberhardt, Chi-Leung So, Daniel J. Leduc, Joe Dahlen.....	66
Life Cycle Assessment of Mass Timber Building Structural System Shaobo Liang, Hongmei Gu, Rick Bergman, Steve Kelley.....	74
Understanding the Uncertainty in Environmental Life Cycle Analysis for Biofuel Production from Forest Residue in the United States Kai Lan, Stephen S. Kelley, Sunkyu Park, Longwen Ou, Prakash Nepal, Yuan Yao.....	75
The Wood Density Variability of the French Forest Species, a New Data Base Jean-Michel Leban.....	77
Managed Forest Carbon Sustainability: Myths and Metrics Elaine Oneil.....	78
Life Cycle Assessment Can Improve Decisions to Optimize Wood Use Maureen Puettmann.....	79
Converting Industrial Waste Cork to Biochar as Cu (II) Absorbents via Effective Pyrolysis Qihang Wang, Zongyuan Lai, Demiao Chu, Jun Mu.....	80
The Contribution of the New Zealand Forest Harvest to Greenhouse Gas Emission Reduction Anne Wekesa, Bruce Manley, David Evison.....	81

**International Innovation, Trends and Education in Wood Science
Monday, October 21, 2019**

Perspectives of Female College Student Leaders on Gender Aspects in the Forest Sector Taylor Barnett.....	82
Suggestions for the Sustainable Development Goals of United Nations, Based on the 30-year Kenaf Research and Development in Japan Kazuhiko Sameshima.....	83
Development of Nano-cellulose Based Thermal Insulating and Encapsulated Phase Change Materials for Energy Efficient Buildings David DeVallance.....	84
Nature-inspired Sustainable Solutions for an Architectonic Environment – A Collection of Case Studies Eva Haviarova, Manja Kitek Kuzman, Zuzana Tončíkova, Denis Plavčák.....	85
Future Developments in the Forest Sector Ed Pepke, Kathryn Fernholz.....	87
Integrating Wood Science, Architecture, and Engineering in Research and Education: The TallWood Design Institute and the Renewable Materials Program at Oregon State University Evan Schmidt.....	98
The Forest for the Trees: Understanding the Experiences of Female PhDs in Forestry-Related Academia Amy Simmons.....	99

**Biodegradation and Preservation
Tuesday, October 22, 2019**

The Effect of Cattle Blood Based Coatings on Wood-rotting Fungi Growth Jan Baar.....	100
Search for the Decay Resistance Scots Pine, <i>Pinus sylvestris</i> L., Heartwood Anni Harju.....	102

*Proceedings of the 62nd International Convention of
Society of Wood Science and Technology
October 20-25, 2019 – Tenaya Lodge, Yosemite, California USA*

Influence of Thermo-Mechanical Timber Modification on the Decay and Mechanical Deterioration against <i>Coniophora puteana</i>	
Juhani Marttila, Victoria Nwachukwu, Aitor Barbero-López, Vitaly Bulavtsev, Antti Haapala.....	103
Revisiting the Role of Bacteria in Wood Decay	
Lakshmi Narayanan.....	112
Evaluation of the Durability of Mass Timber Products Against Termites (<i>Reticulitermes spp.</i>) Using Choice Testing	
Jazmine A. McGinnis, Tamara S.F.A. França, C. Elizabeth Stokes, Juliet D. Tang, Iris B. Montague.....	113
Portable MicroNIR Sensor for the Evaluation of Mould Contamination on Wooden Surfaces	
Olena Myronycheva, Olov Karlsson, Margot Sehlstedt-Persson, Micael Öhman, Dick Sandberg.....	114

Composites and Adhesives 1
Tuesday, October 22, 2019

Anisotropy of 3D Printed Parts Using Bio-Filaments	
Levente Dénes.....	120
Improve the Performance of Soy Protein-Based Adhesives by a Polyurethane Elastomer	
Qiang Gao.....	121
Thermo-Hydrolytic Recycling of Urea Formaldehyde Resin-Bonded Laminated Particleboards	
Qilan Fu.....	123
Wood-Based Material Applications in 3D Printing for Composites	
Douglas Gardner.....	124
Characterizing Accelerated Weathering Conditions	
Micah Sutfin, Fred Kamke.....	125
Effect of Element Morphology on Strength of Wood-PLA Composite	
Tibor Alpár.....	126
Improvement of Ash (<i>Fraxinus Excelsior</i> L.) Bonding Quality with One Component Polyurethane Adhesive and a Primer for Glued Laminated Timber	
Peter Niemz, Gaspard Clerc, Milan Gaff.....	136
Synchrotron-based Analysis of Densified Wood Impregnated with Curing Resin	
Matthew Schwarzkopf.....	143

Wood Chemistry
Tuesday, October 22, 2019

Lignocellulosic Materials as Biocompatible Drug Delivery System for Opioid Addiction Treatment	
Gloria Oporto, Kelsey O'Donnel, Noelle Comolli, Luis Arroyo, Marina Galvez-Peralta, Gustavo Cabrera	144
Dewatering Wood Using Supercritical CO₂	
Salonika Aggarwal, Shelly Johnson, Marko Hakovirta, Bhima Sastri, Sujit Banerjee.....	145
Selective Extraction of High-Value Molecules from Forest Products Processing Residues in the Speciality Chemicals Sector	
Andreja Kutnar.....	151
Cellulose I and II Nanocrystals Derived from Sulfuric Acid Hydrolysis of Cellulose I Substrates	
Jin Gu, Lichao Sun, Lida Xing, Yun Hong, Chuanshuang Hu.....	152
Mineralization in Situ of Tropical Hardwood Species: Calcium Carbonate Formation and Wood Properties	
Roger Moya.....	153
In-Situ Penetration of Ionic Liquids into Surface-Densified Scots Pine	
Benedikt Neyses, Kelly Peeters, Lauri Rautkari, Michael Altgen.....	154
Biomass Derived High Surface Area Carbon Materials for Shale Gas Flowback Water Purification	
Jingxin Wang.....	157

*Proceedings of the 62nd International Convention of
Society of Wood Science and Technology
October 20-25, 2019 – Tenaya Lodge, Yosemite, California USA*

**Student Posters
Tuesday, October 22, 2019**

Characterization and Utilization of Epoxy/Pyrolysis Bio-Oil in Oriented Strand Board Production	
Osei Asafu-Adjaye.....	157
Membrane-Based Thermal Energy Recovery System to Improve the Energy Efficiency of Kiln Drying Processes	
Nasim Alikhani, Darien Dewar, Ling Li, Jinwu Wang, Douglas Bousfield, Mehdi Tajvidi.....	158
Evaluation of NHLA Graded Yellow-Poplar Lumber Regraded for Structural Use in CLT Panel Production	
Rafael Azambuja.....	167
Design Validation of Cross Laminated Timber Rocking Shear Walls	
Esther Baas.....	169
Activity of Organic Acids and Their Synergy Against the Wood Decaying Fungus <i>Coniophora puteana</i>	
Aitor Barbero-López, Md Mokbul Hossain, Antti Haapala.....	170
Evaluation of Shear Performance of Cross-Laminated Timber Shear Wall Connections under the Effects of Moisture	
Shrenik Bora, Arijit Sinha, Andre Barbosa.....	179
Study on VOCs Emissions from Veneered Plywood at Closed Circumstances	
Tianyu Cao, Jun Shen.....	180
UV-light Protection Cellulose Nanocrystals Films Prepared through Trivalent Metal Ions	
Cong Chen, Lu Wang, Jinwu Wang, Douglas Gardner.....	186
Structure-Related Vapor Sorption Phenomena in Wood	
Raphaela Hellmayr, Rupert Wimmer.....	187
The Effect of Pore Size on Specific Capacitance for Activated Carbon Supercapacitors	
Jiyao Hu, Changlei Xia, Sheldon Shi.....	195
Sustainable Development – International Framework – Overview and Analysis in the Context of Forests and Forest Products with Quality	
Annika Hyytiä.....	196
Evaluation of Bond Integrity in Low-Value Blue-Stain Ponderosa Pine CLT	
Sina Jahedi, Lech Muszynski, Mariapaola Riggio, Rakesh Gupta.....	197
A Science Comic Poster: The Gender Diversity Tale in the US, Canada, Finland and Sweden Forest Sector	
Pipiet Larasatie, Eric Hansen.....	205
Rayleigh Mode Excitation at the Half-Space Boundary in Wood Using Embedded Elastic Waveguides	
Yishi Lee, Mohammad Mahoor, Wayne Hall.....	206
Industry 4.0 Readiness in the US Forestry Industry	
Brooklyn Legg, Bettina Dorgner, Scott Leavengood, Eric Hansen.....	214
Reducing the Set Recovery of Surface-Densified Scots Pine by Furfuryl Alcohol Modification	
Han Lei, Dick Sandberg.....	215
Composition Analysis and Health Risk Assessment of Benzene Series for Nitrocellulose Paint Lacquered MDF	
Huifang Li, Jun Shen.....	216
Using Crack-Growth Experiments to Study the Moisture and Thermal Durability of MDF, OSB and PB	
Sweta Mahapatra, Arijit Sinha, John Nairn.....	224
Moment-Rotation Behavior of Beam-Column Connections Fastened Using Compressed Wood Connectors	
Sameer Mehra, Iman Mohseni, Conan O’Ceallaigh, Zhongwei Guan, Adeayo Sotayo, Annette M. Harte.....	225
Evaluation of a Renewable Wood Composite Sandwich Panel for Building Construction	
Mostafa Mohammadabadi, Vikram Yadama.....	226
Dynamic Assessment of Dimensional Change of Wood-Based Composite Materials in Moist Environments	
Luis Molina, Fred Kamke.....	227
Investigating the Thermal and Mechanical Properties of Fly Ash/Metakaolin-Based Geopolymer Reinforced with Alien Invasive Wood Species	
Hamed Olafiku Olayiwola, Stephen Amiandamhen, Luvuyo Tyhoda.....	228
Evaluating Stem and Wood Quality of Planted Longleaf Pines Using Bio-Imaging Techniques	
Sameen Raut, Joe Dahlen.....	229

*Proceedings of the 62nd International Convention of
Society of Wood Science and Technology
October 20-25, 2019 – Tenaya Lodge, Yosemite, California USA*

Development of a Leach Resistant Fire-Retardant System for Wood	
Alexander Scharf.....	231
Mycelium-Assisted Bonding: Influence of the Aerial Hyphae on the Bonding Properties of White-Rot Modified Wood	
Wenjing Sun, Mehdi Tajvidi.....	233
Influence of Particleboard Thickness and Veneers on Odor Emissions	
Qifan Wang, Jun Shen.....	234
Converting Industrial Waste Cork to Biochar as Cu (II) Absorbents via Effective Pyrolysis	
Qihang Wang, Zongyuan Lai, Demiao Chu, Jun Mu.....	248
A Novel Method for Fabricating an Electrospun poly (vinyl alcohol)/Cellulose Nanocrystals Composite nanofibrous Filter with Low Air Resistance for High-Efficiency Filtration of Particulate Matter	
Qijun Zhang, Siqun Wang.....	249

Regular Posters
Tuesday, October 22, 2019

Environmental Impacts of Redwood Lumber: A Cradle-to-Gate Assessment	
Kamalakanta Sahoo, Richard D. Bergman.....	250
Data Science at the University of Primorska: Combining Fundamentals with Data and Challenges from Buildings, Wood and Processing Science	
Mike Burnard, Klavdija Kutnar.....	262
Quantifying Dimensional Changes in Wood Pellets as a Function of Relative Humidity	
Daniel Burnett, Fahimeh Yazdan Panah, Shahabaddine Sokhansanj, Hamid Rezaei.....	263
A Potential Thermal Energy Storage Material Used for Green Buildings	
Xi Guo, Jinzhen Cao.....	264
Improvement of Weathering Performance of Painted Wood Applying Laser Micro Incisions	
Satoshi Fukuta.....	265
Performance Test of Chairs – Joints Design by Use of Lower Tolerance Limits	
Eva Haviarova, Mesut Uysal.....	266
Mechanical Properties of 3D Printable Sustainable Bio-based Sandwich Structures	
Eva Haviarova, Nadir Ayrimis, Manja Kitek Kuzman.....	267
Applying Zero-Slot Learning to Wood Identification	
Eva Haviarova, Fanyou Wu, Rado Gazo Bedrich Benes.....	268
Fire Resistance of Unprotected Cross-Laminated Timber Assemblies of Walls and Floors Made in U.S	
Seung Hyun Hong, Lech Muszynski, Rakesh Gupta, Brent Pickett.....	269
Preparation of Biomorphic Porous SiC Ceramics from Bamboo by Combining Sol-Gel Impregnation and Carbothermal Reduction	
Ke-Chang Hung, Tung-Lin Wu, Jin-Wei Xu, Jyh-Horng Wu.....	270
Fire-Retardant and Sound Absorption Performance of WM Board	
Seok-un Jo, Hee-jun Park, Chun-won Kang.....	278
Thermal Stability of Glued Wood Joint Reinforced with Nanocrystalline Cellulose in Shear Loading	
Gourav Kamboj, Milan Gaff, Vladimír Záborský, Gianluca Ditommaso, Robert Corleto, Adam Sikora, Fatemeh Rezaei, Miroslav Sedlecký, Štěpán Hýsek.....	283
Wood Modification Using in situ Polyesterification Treatment with Cost-Effective and Eco-friendly Biomass Material	
Shanming Li, Enguang Xu, Xuefeng Xing, Lanying Lin, Yongdong Zhou, Feng Fu.....	284
Effects of Physical Extraction on the Acoustic Vibration Performance of <i>Picea jezoensis</i>	
Yuanyuan Miao, Rui Li, Xiaodong Qian, Yuxue Yin, Xianglong Jin, Bin Li, Zhenbo Liu.....	292
The Stress-Strain Behavior of Joint Components in the Surrounding of Oak Dowels	
Jaromir Milch, Pavlina Suchomelova, Hana Hasnikova, Martin Hataj, Martin Brabec, Jiri Kunecky.....	293

**Proceedings of the 62nd International Convention of
Society of Wood Science and Technology
October 20-25, 2019 – Tenaya Lodge, Yosemite, California USA**

Intensified Pulping Process to Produce High Value Materials from Underutilized Appalachian Hardwood Biomass	
Gloria Oporto, Rory Jara-Moreno, Joseph McNeel	295
Comparison of Small- and Intermediated-Scale Fire Performance Tests of Southern Pine Cross-Laminated Timber	
Bryan Dick, Perry Peralta, Phil Mitchell, Ilona Peszlen	296
Hierarchy of Efficient Carbon Displacement and Storage in Products	
Bruce Lippke, Maureen Puettmann, Elaine Oneil	297
Optimization of Milling Process of Iroko Wood (<i>Chlorophora excelsa</i>) Depending on Temperature of Thermal Modification	
Miroslav Sedlecký, Milan Gaff, Fatemeh Rezaei, Gourav Kamboj, Gianluca Ditommaso, Roberto Corleto, Monika Sarvasová, Kvietková, Adam Sikora, Štěpán Hýsek	298
Behavior of Layered Beech Wood Reinforced with Glass and Carbon Fibers under Bending Loading	
Adam Sikora, Milan Gaff, Tomás, Štěpán Hýsek	299
Impact of Gas Concentrations on the Self-Activation of Wood Biomass throughout its Processing	
Lee Smith, Sheldon Q. Shi	300
Survey of the Needed Changes in Forestry Related Curricula – For Improving the Competitiveness of Estonian Forest Sector	
Meelis Teder	301
Comparison of Acoustic Non-Destructive Methods and Semi-Destructive Methods for Logs and Timber Assessment	
Jan Tippner, Michal Kloiber, Jaroslav Hrivnák, Jan Zlámal, Václav Sebera	303
Preparation and UV-Aging Resistance Properties of Eu(III) Complex-Modified Poplar Wood Based Materials	
Di Wang	311
Impact of Torrefaction on the Chemical Component of Nigerian Grown <i>Pinus caribaea Morelet</i>	
F.A. Faruwa, M. Anyacho, E.A. Iyiola, A. Wekesa	312
Novel Enzyme-Modified Lignin Adhesive to Substitute PVAc Carpenter’s Glue?	
Raphaela Hellmayr, Sabrina Bischof, Georg M. Guebitz, Gibson Stephen Nyanhongo, Rupert Wimmer	321

**Composites and Adhesives 2
Thursday, October 24, 2019**

Characterization of Plastic Bonded Composites Reinforced with <i>Delonix regia</i> Pods	
B. Ajayi, A.T. Adeniran, O.E. Falade, B.O. Alade	325
Mycelium-Assisted Bonding, Influence of the Aerial Hyphae on the Bonding Properties of White-Rot Modified Wood	
Wenjing Sun, Mehdi Tajvidi	334
Characterization and Properties of PLA-Based Biomass Composites for FDM Technology	
Rui Guo, Min Xu	335
Evaluation of a Renewable Wood Composite Sandwich Panel for Building Construction	
Mostafa Mohammadabadi, Yikram Yadama	337
The Use of Soy Flour to Replace pMDI in Wood Composites	
Brian Via, Osei Asafu-Adjaye, Sujit Banerjee	338
UV-Light Protection Cellulose nanocrystals Films Prepared through Trivalent Metal Ions	
Cong Chen, Lu Wang, Jinwu Wang, Douglas Gardner	339
Study of Refiner Plates as a Possibility to Improve the Production of Wood Fiber Insulation Materials	
Simon Barth, Andreas Michanickl	340
Environmentally-Friendly Bio-adhesives from Renewable Resources – WooBAdh Project	
Milan Sernek, Jasa Sarazin, Siham Amirou, Antonio Pizzi, Marie-Pierre Laborie, Detlef Schmiedl, Thelmo A Lú Chau, María Teresa Moreira	341

*Proceedings of the 62nd International Convention of
Society of Wood Science and Technology
October 20-25, 2019 – Tenaya Lodge, Yosemite, California USA*

**Business, Marketing and Regulations
Thursday, October 24, 2019**

Keeping the Home Fires from Burning: The Latest on Fire-Retardant-Treated Wood and the Model Codes Mike Eckhoff	342
Marketing of Urban and Reclaimed Wood Products Omnar Espinoza, Anna Pitti, Robert Smith	351
Drivers Impacting Supplying Decisions of Construction Companies: A Case Study in the Southeastern Region of the US Henry Quesada, Robert Smith, Alison Bird, Joe Pomponi	352
Productivity of Firms in the Swedish Industry for Wooden Single-Family Houses Tobias Schauerte, Alexander Vestin	353
Building the Future with Social Media Candra Burns	362

**Wood Physics and Mechanics
Thursday, October 24, 2019**

Sorption Hysteresis in Wood and Its Coupling to Swelling Investigated by Atomic Modeling Jan Carmeliet, Mingyang Chen, Benoit Coasne, Dominique Derome	363
Sorption, Swelling and Mechanical Behavior of Wood: A Multiscale Study Chi Zhang, Mingyang Chen, Benoit Coasne, Jan Carmeliet	364
Effect of Pyrolysis-Oil Based Microemulsions on Mechanical Properties of Scots Pine Antti Haapala, Vitaly Bulavtsev, Aitor barber-López, Juhani Marttila	365
Thermal Modification Influences on Permeability and Sorption Properties of Wooden Shingles Dominik Hess	370
Rayleigh Mode Excitation at the Half-Space Boundary in Wood Using Embedded Elastic Waveguides Yishi Lee, Mohammad Mahoor, Wayne Hall	371
The Mechanics of Engineered Wood Flooring Joseph R. Loferski	379
“Water in Wood – the Gel-Theory Revised” Martin Nopens, Michael Fröba, Bodo Saake, Uwe Schmitt, Andreas Krause	381
Cell Morphology and Mechanical Properties of Transgenic Poplar with Reduced Cellulose Content Ilona Peszlen, Zhouyang Xiang, Perry Peralta	383
Triboelectrical Charging of Wood: A Neglected Wood Property with Potential Applications Roman Myna, Stephan Frybort, Raphaela Hellmayr, Falk Lieber, Rupert Wimmer	384

**Timber Engineering and Mass Timber
Friday, October 25, 2019**

Evaluation of NHLA Graded Yellow-Poplar Lumber Regraded for Structural Use in CLT Panel Production Rafael Azambuja, David DeVallance, Joseph McNeel, Curt Hassler	392
Evaluation of Shear Performance of Cross Laminated Timber Shear Wall Connections under the Effects of Moisture Intrusion Shrenik bora, Arijit Sinha, Andre Barbosa	394
Evaluation of Bond Integrity on Low-Value Blue Stain Ponderosa Pine CLT Sina Jahedi, Lech Muszynski, Mariaapaola Riggio, Rakesh Gupta	395
Flexural Properties of Dowel-Type Fastener-Laminated Timber Olayemi Ogunrinde, Meng Gong, Ying-Hei Chui, Ling Li	403

*Proceedings of the 62nd International Convention of
Society of Wood Science and Technology
October 20-25, 2019 – Tenaya Lodge, Yosemite, California USA*

Mass Timber Building Construction Cost and Life Cycle Cost Analysis with Comparison to Concrete and Steel Buildings	
Hongmei Gu, Shaobo Liang	404
Potential Use of Hardwood Lumber in Cross Laminated Timber: A Manufacturer Perspective	
Henry Quesada.....	405
Moment-Rotation Behavior of Beam-Column Connections Fastened using Compressed Wood Connectors	
Sameer Mehra, Iman Mohseni, Conan O’Ceallaigh, Zhongwei Guan, Adeayo Sotayo, Annette M. Harte	406
Experimental Investigation of a Mass Plywood Panel Self-Centering Rocking Wall System	
Ian Morrell, Rajendra Soti, Arijit Sinha, Byrne Miyamoto Dillon Fitzgerald	407
Hardwoods for CLTs: Opportunities, Issues and Barriers	
David DeVallance.....	408
SPONSORS	409

Monday, October 21st
Keynote Speaker
8:35-9:15

The Dilemma of Fire and Firefighting

Chris Schow, Retired Deputy Director Fire and Aviation
US Forest Service, Pacific Southwest Region

Abstract

Fire and firefighting are woven into the fabric of the western United States. In 1910 the United States Forest Service bet its existence on the theory it could alter western forests to be fireproof and made an enemy of a natural disturbing agent that created the forests early settlers found. Recent fire seasons, especially in California, have increasingly proven that a losing bet.

I have spent 36 years as a wildland firefighter for the USFS – the last 7 in California and recently retired as the Deputy Director for Fire and Aviation Management in Region 5. I have experienced the dilemma of aggressively suppressing fire in fire adapted ecosystems and the impact to communities at many scales.

The “war on fire” cannot be won. Learning to live with fire is critical to community resilience at the local, state and federal level. This paradigm shift is not only on the shoulders of the USFS, but part the weave of federal land management, state protection responsibilities, utility infrastructure, county building codes, and a host of interconnected subjects that made the same bet.

Monday, October 21st

EARLY STAGE RESEARCHERS

9:30-10:45

Chair: Hui Li, Washington State University, USA

ACTIVITY OF ORGANIC ACIDS AND THEIR SYNERGY AGAINST THE WOOD-DECAYING FUNGUS *CONIOPHORA PUTEANA*

Aitor Barbero-López^{1}, Md Mokbul Hossain², Antti Haapala³*

¹Early Stage Researcher, School of Forest Sciences, University of Eastern Finland, Joensuu, FI-80101, Finland. *Corresponding author, *aitorb@uef.fi*

²Junior Researcher, School of Forest Sciences, University of Eastern Finland, Joensuu, FI-80101, Finland. *mdho@student.uef.fi*

³Associate Professor, School of Forest Sciences, University of Eastern Finland, Joensuu, FI-80101, Finland. *antti.haapala@uef.fi*

Abstract

Wood industry is seeking for new wood preservatives that harm the environment less than the ones used nowadays. Bio-based chemicals, usually extracted from forestry side-streams, are being studied as a possible new wood preservative. Organic acids are one of the most common constituents found in bio-based chemicals and are often considered responsible of their antimicrobial activity against fungi and insects. The aim of this study is to understand the independent and synergetic activity of acetic, formic and propionic acid against the wood-decaying fungus *Coniophora puteana*, performing *in vitro* antifungal and wood decay tests. Within all the acids and acid mixtures tested, that showed a high antifungal activity against *C. puteana*, propionic acid was the best performing one, with an estimated minimum inhibitory concentration to completely inhibit the fungus around 0.03%. The wood decay test showed that

even the acids are successfully impregnated into the wood, they are easily leached out and don't protect the wood from fungal decay well enough. Thus, the high wood preserving activity of bio-based chemicals, such as pyrolysis distillates, is not coming only from the organic acids, but from their combination with other constituents.

Key words: Wood Preservatives; Pyrolysis; Organic Acids; Fungal Inhibition; Wood Degradation; Wood Decay.

1 INTRODUCTION

Wood decays naturally due to many factors, as fungi or bacteria, when used outdoors. To avoid decay, many kinds of wood preservatives have been tried and many already substituted during the years due to their toxic nature, as chromated-copper-arsenate (CCA) (Mohajerani et al. 2018). Further limitations are expected because of environmental awareness and increasingly strict chemical legislation driving the industry towards new green alternatives.

Bio-based chemicals are being broadly studied as the already cited green alternatives for wood preservation. Several extractives are known to play a role in wood decay prevention due to their antifungal and antioxidant activities, such as tannins (Anttila et al. 2013), stilbenes (Lu et al. 2016) or spent coffee's cinnamates (Barbero-López et al. 2018). These antifungals can be extracted from forestry side streams, such as bark, via different methods, such as pyrolysis, resulting in chemical mixtures rich in phenolics and organic compounds, able to inhibit wood-decaying fungi (Temiz et al. 2013; Barbero-López et al. 2019). Organic acids have been identified by previous researchers as fungal inhibitors against wood-decaying fungi, as propionic and acetic acid protect date and oil palm against decay (Bahmani et al. 2016). Acid anhydrides from formic and acetic acid are also used in commercial modified wood such as Accoya® and Kebony®, that are more durable than non-treated wood.

The aim of this study is to understand the independent and synergetic antifungal activity and wood decay retardancy of organic acids broadly found in wood pyrolysis distillates - propionic acid, acetic acid and formic acid - against the brown-rot fungus *Coniophora puteana*. The results of the study will help understanding if organic acids are the main responsible of the antifungal activity of the pyrolysis distillates, or if other constituents play also a role. The antifungal activity of the acids was tested measuring the inhibition caused by the chemicals to the fungal growth in petri dish, while the wood decay retardancy was studied exposing Scots pine sapwood impregnated with acids – and non-impregnated as control – to fungal cultures of *C. puteana* and assessing the mass loss caused by this fungus.

2 MATERIALS AND METHODS

2.1 Antifungal test

Growth media amended with acetic, propionic and formic acid (Merck KGaA, Darmstadt, Germany) and their mixtures were prepared in petri dish (Ø 90 mm). The pH of the acids and acid mixtures was neutralized adding few drops 0.1M NaOH, until pH was 4, to ensure later

agar setting. The media for the antifungal test were prepared in Milli-Q water, with 4% malt powder, 2% agar and one of the organic acids or their mixtures as presented in table 1. The growth media for the control samples was prepared by mixing 4% malt powder and 2% agar in Milli-Q water, without adding acids. In each petri dish 15 mL of 1 of the media was poured. Eight replicates were prepared for each organic acid, mixture and concentration.

Table 1: concentrations of the individual organic acids and their mixtures tested in the antifungal test.

Organic acid and its mixtures	Total tested concentrations (%)			
Acetic acid	0.01	0.025	0.05	0.1
Propionic acid	0.01	0.025	0.05	0.1
Formic acid	0.01	0.025	0.05	0.1
Acetic + propionic acid (1:1, w/w)	0.02	0.05	0.1	
Propionic + Formic acid (1:1, w/w)	0.02	0.05	0.1	
Acetic + Formic acid (1:1, w/w)	0.02	0.05	0.1	
Acetic + propionic + formic acid (1:1, w/w)	0.03	0.075	0.1	

In the center of each acid-amended petri dish and in each control petri dish a spherical piece (\emptyset 5.5 mm) of an active colony of *C. puteana* (strain BAM 112), purchased to the Federal Institute for Materials Research and Testing (BAM, Berlin, Germany), was put under sterile conditions. The petri dish were then sealed with parafilm and put in a growing chamber ($22 \pm 2^\circ\text{C}$ and $65 \pm 5\%$ relative humidity), and the growth of the fungal colonies was checked daily, until the mycelia of the controls reached the edge of the petri dish (between 11 and 14 days). Fungal growth inhibition was measured by modifying the formula proposed by Chang et al. (1999):

$$\text{Inhibition (\%)} = (1 - (AT - IA)/(AC - IA)) * 100$$

Here, AT is the area of the experimental plate, AC is the area of the control plate, and IA is the surface area (mm^2) of the inoculated plug. The minimum inhibitory concentration (MIC) to inhibit the growth of the fungus completely was estimated based on this result.

2.2 Wood decay test

Scots pine (*Pinus sylvestris*) sapwood pieces of $5 \times 40 \times 10 \text{ mm}^3$ (radial x longitudinal x tangential) bought from Kerimäki sawmill, Finland, were used as wood substrate. These sapwood pieces were tagged and oven dried at 50°C until constant mass was reached, and their mass was recorded. Propionic, acetic and formic acid were prepared at 3% and 6% concentration for wood impregnation. Formic and propionic acid mixture (1:1) and acetic, formic and propionic acid mixture (1:1:1) at a total acid concentration of 3% and 6% were also prepared for wood impregnation. Wood decay test was carried out by following a modified version of EN 113 test described by Lu et al. (2016). In each acid and acid mixture, 16 sapwood pieces were submerged, and, using the PUUMA impregnation platform of the University of Eastern Finland, they were exposed to a modified Bethel impregnation process. First, wood pieces were exposed to vacuum in 0.15 bar for 20 minutes. Afterwards, the pressure was slowly increased until 10 bar, held for 60 minutes and released, and no final vacuum was applied. The wet mass of the

impregnated wood specimens was then measured to ensure proper impregnation, and afterwards the wood pieces were oven dried at 50°C until constant mass was reached, and their mass was recorded to calculate the chemical retention.

Eight sapwood specimens of each treatment were then exposed to leaching following the norm EN84. After leaching, the wood specimens were oven dried at 50°C until constant mass was reached, and their mass was recorded. Then, the wood specimens – impregnated and non-treated – were sterilized in the Scandinavian Clinics Estonia OÜ (Alliku, Estonia) using gamma radiation (31.7 kGy to 32.3 kGy).

Petri dish (Ø 90 mm and 15 mm height) were prepared with 30 ml of 4% malt powder and 2% agar growth media, and a plug (Ø 5.5 mm) of the fresh *C. puteana* cultures was put in the center of the petri dish under sterile conditions. The petri dish were sealed with parafilm and kept in a growing chamber (22 ± 2°C and 65 ± 5 % relative humidity) until the mycelia covered the whole surface of the petri dish. Then, under sterile conditions, four plastic meshes (~50 x 15 mm²) were put in each petri dish, and four wood pieces were placed in each petri dish over the meshes. All the wood pieces in each petri dish were leached and non-leached specimens of different concentrations (3% and 6%) of the same acid or acid mixtures (see figure 1). In case of controls, two wood specimens were put in each petri dish, and two extra wood specimens – not part of the experiment – were added to the petri dish to have 4 specimens per dish. 8 replicates per treatment were used in this experiment. Then, the petri dish were sealed with parafilm and kept in a growing chamber at 22 ± 2°C and 65 ± 5 % relative humidity. After eight weeks, the wood specimens were taken out of the petri dish, the fungal mycelia was smoothly removed with the help of a brush and the wood specimens were oven dried at 50°C until constant mass was reached. The mass of the wood specimens was measured to calculate the decay rate caused by *C. puteana* to the wood pieces.

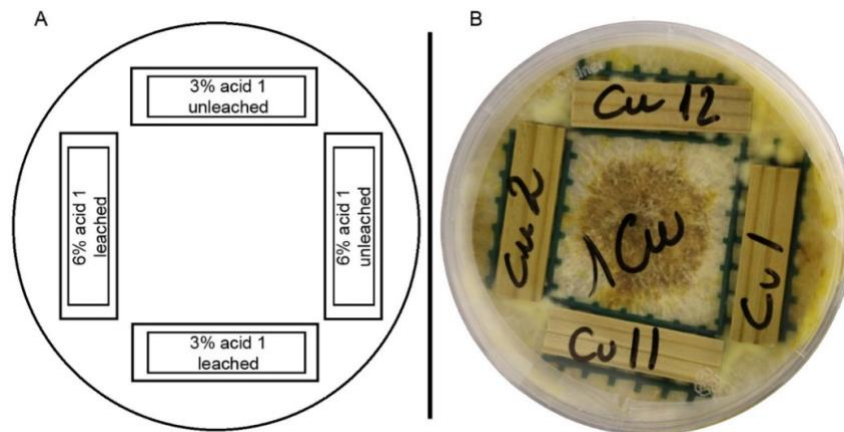


Fig 1: Schematic (A) and visual example (B) of the setup of the sapwood pieces, over the plastic meshes, in a petri dish inoculated with *C. puteana*.

3 RESULTS

3.1 Antifungal test

All the studied acids showed antifungal activity even at the lowest tested concentrations (Table 2). At 0.01%, formic acid was the most effective acid inhibiting *C. puteana* about 70%, while acetic acid and propionic acid inhibited this fungus about 40%. When the acid concentration was increased to 0.025% propionic acid was the most effective acid as it almost fully inhibited *C. puteana*. Acetic acid caused about 70% inhibition of the fungus while formic acid was able to inhibit it about 80%. At 0.05% concentration, propionic acid completely inhibited *C. puteana*, and acetic and formic acid inhibited this fungus about 90%. The decay fungus was completely inhibited by the acids at 0.1%.

The two acid mixtures were also successful inhibitors of *C. puteana* at concentration of 0.2%, the acetic acid and formic acid mixture caused *C. puteana* inhibition of 25%. Acetic acid and propionic acid mixture inhibition was 35%. The mixture of formic acid and propionic acid caused a growth increment of *C. puteana* of about 9%. The inhibition by acetic and formic acid at 0.05% did not differ from the inhibition caused at 0.02%. The formic and propionic acid mixture inhibited the fungus at 76%, while the acetic acid and propionic acid mixture caused over 90% fungal inhibition. The fungus was completely inhibited by mixtures at 0.1%. The three acid mixture inhibited *C. puteana* over 75% at 0.03% concentration, and completely at higher concentrations. Out of all the tested acids and acid mixtures, propionic acid has the lowest estimated MIC (about 0.03%). Acetic acid and the mixture of acetic acid and propionic acid have a MIC of 0.06%. Formic acid, its mixture with propionic acid and the mixture of acetic, formic and propionic acid have MIC between 0.07 and 0.08%. The highest MIC - about 0.1% - was estimated for the acetic and formic acid mixture.

Table 2. Growth inhibition (%) of *Coniophora puteana* caused by the different acids and their mixtures, and the estimated minimum inhibitory concentration (MIC) to fully inhibit *C. puteana*. Results are presented as mean \pm standard error.

Acids	0.01%	0.025%	0.05%	0.1%	MIC
Acetic acid	41.8 \pm 3.8	70.8 \pm 2.4	93.5 \pm 1.2	100 \pm 0	~ 0.06%
Formic acid	71.3 \pm 2.8	79.1 \pm 3.8	86.6 \pm 1.7	100 \pm 0	~ 0.07%
Propionic acid	38.8 \pm 4.3	98.1 \pm 0.2	100 \pm 0	100 \pm 0	~ 0.03%
	0.02%	0.05%	0.1%		
Acetic + formic acid	24.6 \pm 7.1	23.6 \pm 3.0	100 \pm 0		~ 0.1%
Acetic + propionic acid	35.4 \pm 4.8	92.4 \pm 1.2	100 \pm 0		~ 0.06%
Formic + propionic acid	-9.3 \pm 2.6	76.0 \pm 3.4	100 \pm 0		~ 0.08%
	0.03%	0.075%	0.1%		
Acetic + formic + propionic acid	77.4 \pm 3.2	100 \pm 0	100 \pm 0		~ 0.07 – 0.08%

3.2 Chemical retention in wood

All the acids and their mixtures were successfully impregnated into the wood, with retention values of 8-20 kg·m⁻³. When the dry impregnated specimens were exposed to leaching, all the treated wood presented a negative retention values between 1-6 kg·m⁻³.

3.3 Wood decay test

The acid treatment of the sapwood specimens produced in most of the cases a decrement in the mass loss caused by *C. puteana* in non-leached sapwood specimens (Table 3). Acetic acid at 3% concentration presented the best performance against wood decay caused by *C. puteana*, as it had the lowest sapwood mass loss out of all the acids and acid mixtures tested. Propionic acid at 6% presented the lowest mass loss out of all the acid and mixtures at that concentration. All the other tested acids and mixtures had a mass loss of between 15-20%, while the mass loss of the untreated controls was close to 24%.

Table 3. Dry mass loss (%) caused by *C. puteana* to acid treated leached and non-leached Scots pine sapwood specimens. Results are presented as mean ± standard error.

Acids	Concentration (%)	Non-leached (%)	Leached (%)
Acetic acid	3	10.32 ± 2.14	17.55 ± 2.83
	6	13.86 ± 3.37	20.56 ± 3.18
Formic acid	3	17.10 ± 3.19	25.40 ± 4.13
	6	17.66 ± 2.17	18.65 ± 2.31
Propionic acid	3	13.52 ± 3.01	21.62 ± 2.54
	6	10.47 ± 3.02	16.90 ± 2.39
Formic + propionic acid	3	18.93 ± 3.36	21.26 ± 2.95
	6	19.69 ± 3.54	16.42 ± 2.06
Acetic + Formic + propionic acid	3	15.31 ± 1.84	23.85 ± 3.29
	6	19.68 ± 3.43	22.53 ± 2.87
Control		23.75 ± 2.59	

The leached sapwood specimens has a higher mass loss than the non-leached specimens treated with the same acid and mixtures (Table 3). Only sapwood specimens treated with 3% acetic acid and 6% formic acid, propionic acid and the mixture of propionic and formic acid had less mass loss than the control specimen.

4 DISCUSSION

The results of the antifungal test proved the high inhibitory effect of the different acids against the wood-decaying fungus *C. puteana*, causing fungal inhibition even at 0.01% concentration. Propionic acid was found to be the most effective acid out of the tested independent acids, as it has a MIC value that is at least half the MIC value of the other tested acids and mixtures. These results agree with previous findings that suggested a high inhibitory effect of propionic acid against wood-decaying fungi (Barbero-López et al. 2019) and the relevance of total acid content

of different chemicals, as pyrolysis distillates, in their antifungal activity (Oramahi and Yoshimura 2013).

The results of our study found that the tested acid mixtures inhibit *C. puteana* in a similar manner to independent acids, but it does not have a stronger effect. Barbero-López et al. (2019) concluded that pyrolysis distillates present a high antifungal activity due to the mixture of different organic acids and other chemicals, such as phenolics, what supports the findings of this study.

All the acids and their mixtures were successfully impregnated into the wood, but after leaching the mass of the specimens was slightly lower than their mass before impregnation, presenting a maximum estimated mass loss of about 1%. This showed that these acids and mixtures have a high leachability from wood and a possible chemical degradation of the specimens by strong acidic solutions (Kass et al. 1970).

Although some of the acids decreased the decay rate of the sapwood specimens, based on the European norms (EN 113), none of the acids provided adequate protection as the mass loss of all the sapwood specimens was over 3%. However, non-leached propionic acid and acetic acid impregnated wood showed the best performance out of all the tested acids against wood decay caused by *C. puteana*.

Both tested mixtures of acids presented very low mass loss reductions compared to control specimens, despite their higher impregnation rate compared to independent acids and although organic acids are present in chemicals with known antifungal and decay retardant properties, as pyrolysis distillates (Oasmaa and Czernik 1999; Barbero-López et al. 2019). This results show that the antifungal properties and decay retardancy caused by pyrolysis distillates it's not coming merely from the organic acids tested in this study, but from other distillates' constituents. Baimark and Niamsa (2009) concluded that the antifungal activity of these distillates was dependent in their amount of phenolics and recently, Mattos et al. (2018) highlighted that based on literature, the antimicrobial activity of these distillates are coming from their phenolics, fatty acids and acetic acid. Based on the cited literature and our findings, it could be concluded that the pyrolysis distillates' antifungal activity is based in the combined effect of their constituents and not just by the organic acids or phenolics.

The present paper focused in understanding the activity of the several organic acids against *C. puteana*. The results help understanding the pyrolysis liquids' constituents' activity against *C. puteana*, and discard the acid impregnation as such as a wood preservative, due to their low performance against the decay. Nevertheless, the study needs to be expanded to more fungi and wood species. Due to the high antifungal activity of propionic and acetic acid at very low concentration, the addition of these acids in wood preservatives formulations need to be studied further. Further studies are also necessary to understand the mechanical properties of wood are affected by these acids at low concentration and how would they affect the wood properties and durability if their pH is neutralized prior to impregnation.

5 CONCLUSIONS

Acetic, formic and propionic acid, as well as their mixtures, showed a very high antifungal activity *in vitro* against *Coniophora puteana*, but did not retard Scots pine sapwood decay caused by *C. puteana* sufficiently to meet the requirements in EN 113 standard. Propionic acid exhibited the highest inhibitory effect against *C. puteana*. Additionally, it was found that the organic acids of pyrolysis distillates are not the alone responsible of the antifungal activity of pyrolysis distillates, but their efficiency arises in combination with other constituents.

6 REFERENCES

- Anttila AK, Pirttilä AM, Häggman H, Harju A, Venäläinen M, Haapala A, Holmbom B, Julkunen-Tiitto R (2013) Condensed conifer tannins as antifungal agents in liquid culture. *Holzforschung* 67: 825–832.
- Bahmani M, Schmidt O, Fathi L, Frühwald A (2016) Environment-friendly short-term protection of palm wood against mould and rot fungi. *Wood Mater. Sci. Eng.* 11: 239–247.
- Baimark Y, Niamsa N, (2009) Study on wood vinegars for use as coagulating and antifungal agents on the production of natural rubber sheets. *Biomass Bioenergy* 33: 994-998.
- Barbero-López A, Chibily S, Tomppo L, Salami A, Ancin-Murguzur FJ, Venäläinen M, Lappalainen R, Haapala A (2019) Pyrolysis distillates from tree bark and fibre hemp against wood-decaying fungi. *Ind. Crop. Prod.* 129: 604–610.
- Barbero-López A, Ochoa-Retamero A, López-Gómez Y, Vilppo T, Venäläinen M, Lavola A, Julkunen-Tiitto R, Haapala A (2018) Activity of spent coffee ground cinnamates against wood-decaying Fungi *in vitro*. *BioResources* 13: 6555–6564.
- EN 113. “Wood preservatives – Test method for determining the protective effectiveness against wood destroying basidiomycetes - Determination of the toxic values”. European Committee for Standardization, Brussels, BE, 1996.
- Kass A, Wangaard FF, Schroeder HA (1970) Chemical Degradation of Wood: The Relationship Between Strength Retention and Pentosan Content. *Wood Fiber Sci.* 1: 31-39.
- Lu J, Venalainen M, Julkunen-Tiitto R, Harju AM (2016) Stilbene impregnation retards brown-rot decay of Scots pine sapwood. *Holzforschung* 70: 261–266.
- Mattos C, Romeiro GA, Folly E (2018) Potential biocidal applications of pyrolysis bio-oils. *J. Anal. Appl. Pyrol.* DOI: 10.1016/j.jaap.2018.12.029
- Mohajerani A, Vajna J, Ellcock R (2018) Chromated copper arsenate timber: a review of products, leachate studies and recycling. *J. Clean. Prod.* 179: 292–307.
- Oasmaa A, Czernik S (1999) Fuel oil quality of biomass pyrolysis oils - state of the art for the end users. *Energ. Fuels* 13: 914-921.
- Oramahi HA, Yoshimura T (2013) Antifungal and antitermitic activities of wood vinegar from *Vitex pubescens* Vahl. *J. Korean Wood Sci. Technol.* 59: 344–350.

***Proceedings of the 62nd International Convention of
Society of Wood Science and Technology
October 20-25, 2019 – Tenaya Lodge, Yosemite, California USA***

Temiz A, Akbas S, Panov D, Terziev N, Alma MH, Parlak S, Kose G (2013) Chemical composition and efficiency of bio-oil obtained from giant cane (*Arundo donax* L.) as a wood preservative. *BioResources* 8: 2084-2098. doi:10.15376/biores.8.2.2084-2098

Study on VOCs Emissions from Veneered Plywood at Closed Circumstances

Tianyu Cao^a, Jun Shen^b, *

^a College of Material Science and Engineering, Northeast Forestry University, Harbin, China
18504616802@163.com

^b College of Material Science and Engineering, Northeast Forestry University, Harbin, China
shenjun@nefu.edu.cn

Abstract

In order to explore the emission characteristics of VOCs and different VOC-components from plywood in a sealed environment, three kinds of plywood with thickness of 8 mm were tested as experimental materials. Polyvinyl chloride overlaid veneered plywood (PVC-VP), melamine-impregnated paper overlaid veneered plywood (MI-VP) and unfinished plywood (UF-P) were released in a 15 L small environment cabin with the temperature of $23.5^{\circ}\text{C}\pm 0.5^{\circ}\text{C}$ and gas exchange of 0 time $\cdot\text{h}^{-1}$. The gas was collected after sealed 2h, 4h, 6h, 8h, 12h, 18h, 24h and 30h separately under the panel area to volume ratios were $1\text{m}^2\cdot\text{m}^{-3}$, $1.5\text{m}^2\cdot\text{m}^{-3}$, $2\text{m}^2\cdot\text{m}^{-3}$, $2.5\text{m}^2\cdot\text{m}^{-3}$. The gas chromatography-mass spectrometer was used to analysis the changes of VOCs concentration and VOC-components with the panel area to volume ratios. The results show that the VOCs concentration released from the panel increased gradually until equilibrium with the increase of the hermetical time, and the trend was non-linear. PVC-VP and MI-VP were reached equilibrium state after sealed 12h, but UF-P needed 18h. The higher the panel area to volume ratio is, the earlier VOC concentration reached equilibrium, and veneered plywood (PVC-VP and MI-VP) reached equilibrium earlier than unfinished plywood. Among them, concentration of MI-VP is the highest in equilibrium. Among the various components of VOC, categories that account for larger proportion such as aromatic hydrocarbons, esters and aldehydes changed obviously with time. The concentration of aromatic hydrocarbons increased most obviously with the increase of sealing time, also with the panel area to volume ratios. The UF-P reached equilibrium after 24h of sealing, but the veneered plywood reached fluctuation equilibrium after 12h. The concentration of esters released from PVC-VP and MI-VP changed more regularly, which increased with time and had no equilibrium period. However, only the esters released from UF-P showed a weak positive correlation with the increase of the panel area to volume ratios. The regularity of aldehydes changes with time and the panel area to volume ratios were weak, which showed an unstable upward trend. The other VOC-components had small proportion and the trends of them were not obvious.

Keywords: plywood; veneer material; closed circumstances; the panel area to volume ratio; VOC-components

INTRODUCTION

In recent years, more and more attention has been paid to the pollution caused by family decoration. And wood-based panel such as plywood and particleboard has been used more and more widely in furniture decoration. Plywood has many advantages such as not easy to deform, good transverse tensile properties, large breadth and so on. But volatile organic compounds could release from plywood when manufacturing and using, which causing indoor air pollution. VOC can do harm to human health, especially elderly and children, which can lead to cancer and even death [1-2]. Formaldehyde and benzene were mainly toxic substance which can irritate eyes and mucosa, leading headache, fatigue and nausea, and resulting in sick building syndrome (SBS) [3]. Therefore, the research of VOCs has been paid more and more attention.

There are many studies on the impact of VOCs on indoor air and health risk assessment. The level of indoor air pollution could be calculated the comprehensive index to determine according to Bernd's research [4-5]. The concentration and odor of TVOC could also be affected by changes of indoor environmental factors. The odor will be stronger when indoor temperature and relative humidity increase [6]. VOCs released from wood itself and wood surface coatings, decorative materials can also be a source of odor [7-9]. As a common decorative material, PVC is a thermoplastic polymer made from vinyl chloride monomer. The VOC released by PVC mainly includes dibutyl phthalate and dioctyl phthalate [10]. It is irritating and easy to release vinyl chloride, trichloromethane and trichloroethylene after heating, showing acid and plastic taste [11].

**Proceedings of the 62nd International Convention of
Society of Wood Science and Technology
October 20-25, 2019 – Tenaya Lodge, Yosemite, California USA**

The emission of VOCs can be affected by many factors such as environmental parameters, production process and finishing materials. The research shows that the increase of temperature can promote the release of formaldehyde and VOCs in wood-based panels more than the increase of relative humidity [12-13]. The release rate of VOCs will increase by increasing the hot-pressing temperature and time in the production process [14]. Most wood-based panels were decorated by veneers and edges, and different veneers have different sealing rates for formaldehyde and TVOC [15-17]. Not only veneer treatment, surface painting can effectively reduce TVOC release from particleboard, but surface painting and wood modification with chemical reagents often lead to increased TVOC release, which brings hidden dangers to human health [18-19].

In this experiment, the VOCs emission of three kinds of plywood were tested under the condition of air exchange rate was 0 times/h. Four panel area to volume ratios ($1\text{m}^2\cdot\text{m}^{-3}$, $1.5\text{m}^2\cdot\text{m}^{-3}$, $2\text{m}^2\cdot\text{m}^{-3}$, $2.5\text{m}^2\cdot\text{m}^{-3}$) and eight airtight storage periods (2h, 4h, 6h, 8h, 12h, 18h, 24h and 30h) were set. The total concentration and composition of VOCs were qualitatively and quantitatively analyzed by GC-MS. The characteristic curve of VOCs release from plywood under closed condition was explored, and the effects of finishing materials and panel area to volume ratios on the release of VOCs from plywood were analyzed. It is of great guiding significance to choose plywood for furniture decoration.

EXPERIMENTAL

Materials

In this experiment, three kinds of plywood were from a furniture manufacturer in Guangzhou. The length×width×thickness was 1200mm×1200mm×8mm, and the pH was 7.2-7.4. The hot-pressing temperature was 190-200°C and hot-pressing time was 210s. The initial moisture content of plywood ranges from 8.5% to 10.5%. Three kinds of plywood were cut to 150mm×50mm×8mm and 150mm×75mm×8mm. Aluminum foil was used to seal the edges of the specimens so that the VOCs do not escape from the edges, then stored at -30°C.

Equipment

The main equipment conditions are as follows:

- (1) A 15 L small environment cabin was used as the VOCs sampling chamber, which was made by Northeast Forestry University independently. 15 L small environment cabin has the advantage that simple assembly, low cost and has good correlation with 1m^3 environment cabin. Nitrogen (purity was 99.99%) was used as carrier gas, the temperature was $23.5^\circ\text{C}\pm 0.5^\circ\text{C}$ and gas exchange rate was 0 h⁻¹.
- (2) Tenax-TA tubes (200mg filler inside, L×R=89mm×3.2mm, BeifenTianpu Instrument Technology Co., Led. Beijing, China) were used to collect the gas released from plywood in the cabin.
- (3) A vacuum sealing machine (VS2110GB, Dongguan Yinger Electrical Appliances Co., Ltd.) was used to vacuum samples into polytetrafluoroethylene bags.
- (4) Analytical Tube Processor (TP-2040, Beijing Beifen Tianpu Instrument Technology Co., Ltd.) was used to thermal desorption of the Tenax-TA tubes and removal of residues in the tubes.
- (5) A miniature vacuum pump (ANJ6513-220V, Chengdu Xinweicheng Technology Co., Ltd.) was used as one of the sampling equipment. A Tenax-TA tubes was set between 15L small cabin and vacuum pump, and gas was collected into the tube by vacuum extraction.
- (6) Thermal Desorber (ultra&unity, Markes International Inc., Llantrisant, UK) were used as the thermal desorption equipment. The cold trap adsorption temperature is -15°C, analytical temperature is 300°C and pipeline temperature is 180°C.
- (7) GC-MS (DSQ II, Thermo Scientific, Germany) was used to characterize and quantified the VOCs. The basic parameters were as follows: the type of chromatographic column is DB-5MS, 30m×0.25mm×0.25 μm , the carrier gas was helium of 99.996%, the injection port temperature was 250°C and the distribution ratio was 40. The temperature program is three steps: first kept at 40°C for 2 min, then increased to 150°C by 4°C/min and kept for 4 min, finally increased to 250°C by 10°C/min and kept for 8 min. By ionizing with EI and the energy was 70eV, the ionization temperature was 230°C, transmission line temperature was 250°C and the mass scan range was 40-450 amu with full scan.

Methods

Sampling

The samples were divided into three groups: PVC-VP, MI-VP and UF-P, and have two pieces 150mm×75mm×8mm and four pieces 150mm×50mm×8mm according to the panel area to volume ratios and exposure area of panel ($1\text{m}^2/\text{m}^3-0.015\text{m}^2$, $1.5\text{m}^2/\text{m}^3-0.225\text{m}^2$, $2\text{m}^2/\text{m}^3-0.03\text{m}^2$, $2.5\text{m}^2/\text{m}^3-0.0375\text{m}^2$).

The interior walls of 15L small cabin was cleaned by anhydrous ethanol and distilled water. Then the fan was turned on and kept for more than 30 minutes and nitrogen with 99.99% purity was injected. The main experimental parameters were: temperature $23.5^\circ\text{C}\pm 0.5^\circ\text{C}$ controlled by air conditioner, and gas exchange rate was zero. Put samples into the cabin and then turn down the fan and nitrogen to keep the airtight condition.

Before collection, the Tenax-TA tubes should be desorbed by the analytic tube processor for 30 minutes at 325°C . A miniature vacuum pump was used to collection 3L gas in the cabin. In this way, eight experiments were conducted in each group and the airtight time was 2h, 4h, 6h, 8h, 12h, 18h, 24h and 30h, respectively.

Analytical method

Toluene-D₈ was used as the solute and dissolved in methanol to make a standard curve. $2\mu\text{L}$ of Toluene-D₈ was injected into a Tenax-TA tube and prepurge for 5 minutes. DSQII gas chromatography-mass spectrometer was used to characterize and quantified the VOCs. In the analysis of VOCs, firstly the volatile components with matching degree greater than 90% and the number of carbon atoms is 6-16 were selected, then determination the volatile components by retention time. Finally, the peak area of C₇D₈ was used to quantify VOCs concentration.

RESULTS AND DISCUSSION

Trend of VOCs of plywood with time under four panel area-volume ratios

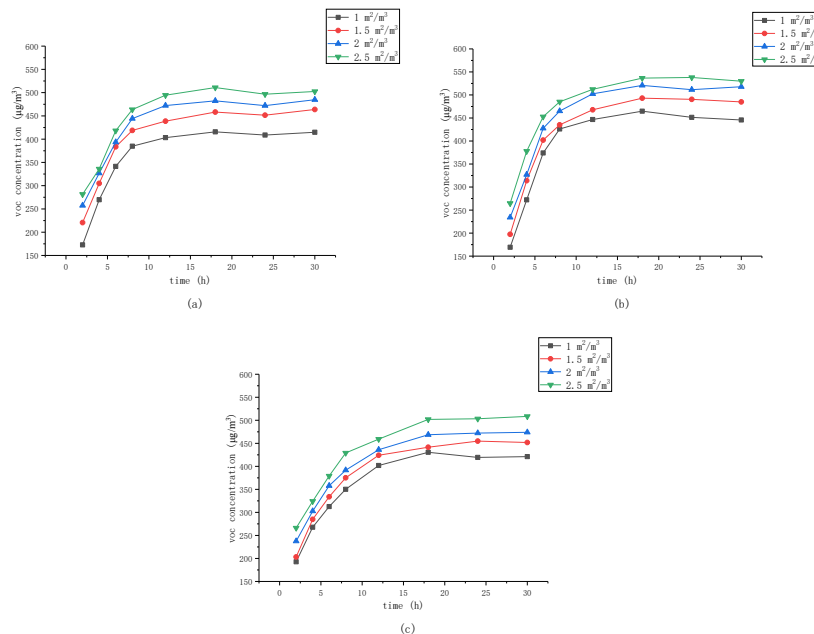


Fig. 1 Trend of VOCs with airtight time under different panel area-volume ratios: PVC-VP (a), MI-VP (b), UF-P(c)

Fig.1 shows the concentration of the VOCs released from PVC-VP, MI-VP, and UF-P after storage for 2h, 4h, 6h, 8h, 12h, 18h, 24h, and 30h respectively in airtight environment cabin. Regardless of the plywood type, VOCs concentration increased with the airtight time, and gradually reached saturation. But the speed of saturation of plywood with different veneer materials was different. The concentration of VOCs of PVC-VP after storage for 12h was 97.15% higher than after storage for 2h. MI-VP was 127.27% after storage for 12h compared with 2h. While the concentration after storage for 30h was only 3.22% (PVC-VP), 2.5% (MI-VP) higher than 12h. Therefore, the concentration of VOCs growth rapidly when storage for 2h-12h, and the growth rate slows down greatly after 12h. What's more, the concentration of VOCs released from veneered plywood (PVC-VP, MI-VP) reached saturation faster, and about only 12h needed. However, the VOCs concentration of UF-P needs 18h to reach the saturation, and increased only 0.66% from 18h to 30h.

UF-P only releases VOCs from the interior plywood, but veneer materials released VOCs along with the inner board because the veneer covered by the surface itself contains VOCs. In terms of VOCs concentration at saturation, the pollution degree of veneered plywood is PVC-VP better than MI-VP. Also, the concentration of VOCs from MI-VP is the highest among the three plywood. The higher the panel area to volume ratio is, the earlier VOC concentration reached equilibrium, and veneered plywood (PVC-VP and MI-VP) reached equilibrium earlier than unfinished plywood.

Analysis of Mainly VOC-components

VOCs are aggregates of many volatile organic compounds; they are classified into eight categories according to their composition (aromatics, alkanes, olefins, aldehydes, ketones, alcohols, esters and others). Among the various components of VOC, categories that account for larger proportion such as aromatic hydrocarbons, esters and aldehydes changed obviously with time. Figure 2 shows the trend of aromatic hydrocarbons, aldehydes and esters with the airtight time and different panel area to volume ratios at 30h.

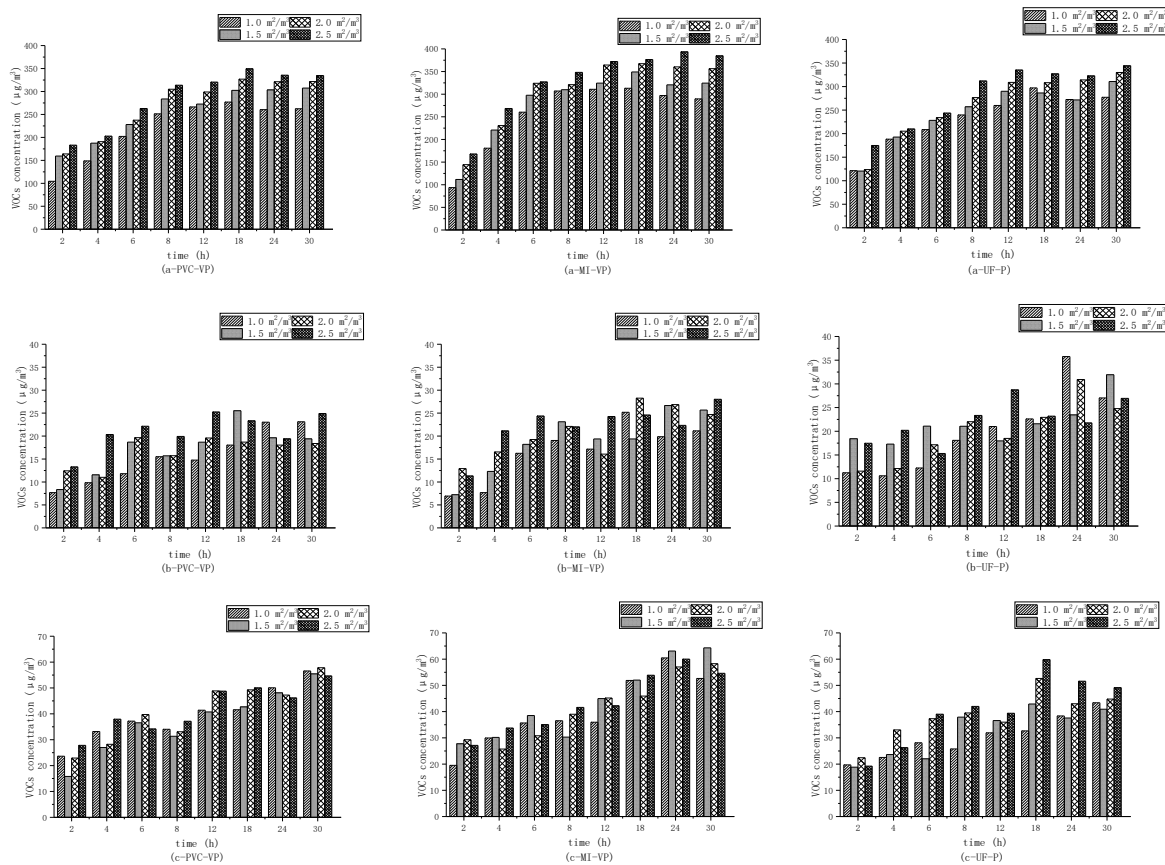


Fig. 2 trend of aromatic hydrocarbons (a), aldehydes (b) and esters (c) released from PVC-VP, MI-VP and UF-P at 30h

Aromatic hydrocarbons account for the largest proportion of VOCs, because the components with higher release rate can better represent the release characteristics of VOCs [20]. The proportion of aromatic hydrocarbons in VOC released by three kinds of plywood was 65.63% (PVC-VP), 68.34% (MI-VP) and 67.98% (UF-P), respectively. The concentration of aromatic hydrocarbons showed a good trend with the increase of airtight time, also with the panel area to volume ratios. The aromatic hydrocarbons released from MI-VP reached the saturation fastest, and its concentration was the highest. The aromatic hydrocarbons of UF-P reached equilibrium after 24h of sealing, but the aromatic hydrocarbons of veneered plywood reached fluctuation equilibrium after 12h. The concentration of aromatic hydrocarbons released from three kinds of plywood increased by more than 120% when the panel area to volume ratios from 1m²-m⁻³ to 2.5m²-m⁻³, such as PVC-VP was 127.58%, MI-VP was 132.89% and UF-P was

**Proceedings of the 62nd International Convention of
Society of Wood Science and Technology
October 20-25, 2019 – Tenaya Lodge, Yosemite, California USA**

124.19%. It shows that MI-VP is most strongly affected by the panel area to volume ratios. On the other hand, Polyvinyl chloride can prevent the release of aromatic hydrocarbons from the inside of the plywood effectively cause its concentration was lowest among the three plywood.

The regularity of aldehydes changes with time and the panel area to volume ratios were weak, which showed an unstable upward trend. The aldehydes released from PVC-VP and MI-VP increased more obviously with airtight time than those released by UF-P, and influenced by the panel area to volume ratios more obviously when the airtight time were 2h-12h. The influenced was weakened by the panel area to volume ratios after 12h. The concentration of esters released from PVC-VP and MI-VP changed more regularly, which increased with time and had no equilibrium period. However, only the esters released from UF-P showed a weak positive correlation with the increase of the panel area to volume ratios. The concentration of aldehydes from PVC-VP and MI-VP were lower than UF-P, which shows polyvinyl chloride and melamine-impregnated paper can reduce the release of aldehydes emissions. On the contrary, the concentration of esters from PVC-VP and MI-VP were higher than UF-P. This is due to the lack of decorative materials on the surface of veneer plain board, so a part of the source of esters is missing. Shen Jun, Jiang Liqun's research found that veneer treatment reduced the total amount of TVOC released from sheets, but also increased the amount of a compound released [21], which also explains the increase of esters concentration released from MI-VP and PVC-VP.

It can be seen that not all the release characteristics trend was logarithmic function growth as expected, but shows different characteristic curves because of the influence of decoration materials. Results show that the panel area to volume ratios does not have a linear relationship with VOCs concentration [22]. And the emission of VOCs from the inside of plywood could be limited when the concentration increased to maximum under the condition that the air exchange rate was zero [23], which explained the different characteristic curves above. However, the obtained characteristics curve is limited because the panel area to volume ratios chosen in this experiment was only $1\text{m}^2\cdot\text{m}^{-3}$ to $2.5\text{m}^2\cdot\text{m}^{-3}$. Therefore, it is necessary to carry out follow-up experiments which have the panel area to volume ratios greater than $2.5\text{m}^2\cdot\text{m}^{-3}$.

CONCLUSIONS

(1) VOCs concentration increased with the airtight time, and gradually reached saturation. But the speed of saturation of plywood with different veneer materials was different. PVC-VP and MI-VP reached saturation faster, and about only 12h needed, but UF-P needs 18h. The concentration of VOCs growth rapidly when storage for 2h-12h, and the growth rate slows down greatly after 12h. In terms of VOCs concentration at saturation, the pollution degree of veneered plywood is PVC-VP better than MI-VP. Also, the concentration of VOCs from MI-VP is the highest among the three plywood. The higher the panel area to volume ratio is, the earlier VOC concentration reached equilibrium, and veneered plywood (PVC-VP and MI-VP) reached equilibrium earlier than unfinished plywood.

(2) Aromatic hydrocarbons account for the largest proportion of VOCs and showed a good trend with the increase of airtight time, also with the panel area to volume ratios. The aromatic hydrocarbons released from MI-VP reached the saturation fastest, and its concentration was the highest. Polyvinyl chloride can prevent the release of aromatic hydrocarbons from the inside of the plywood effectively. The regularity of aldehydes changes with time and the panel area to volume ratios were weak, which showed an unstable upward trend. The concentration of esters released from PVC-VP and MI-VP changed more regularly, which increased with time and had no equilibrium period. However, only the esters released from UF-P showed a weak positive correlation with the increase of the panel area to volume ratios. the concentration of esters from PVC-VP and MI-VP were higher than UF-P. It can be seen that not all the release characteristics trend was logarithmic function growth as expected, but shows different characteristic curves because of the influence of decoration materials. The other VOC-components had small proportion and the trends of them were not obvious.

ACKNOWLEDGEMENTS

This study was supported by the National Key Research and Development Program of China (Grant 2016 TFD 0600706).

REFERENCES CITED

- [1] Shao, Y. L., Shen, J., Shen, X. W. & Qin, J. K. Effect of panel area–volume ratio on TVOC released from decorative particleboards. *Wood Fiber Sci.* 50, 132–142 (2018).

**Proceedings of the 62nd International Convention of
Society of Wood Science and Technology
October 20-25, 2019 – Tenaya Lodge, Yosemite, California USA**

- [2] Liu WJ, Shen J, Wang QF (2017) Design of DL-SW micro-cabin for rapid detection and analysis of VOCs from wood-based panels. *J. Forestry Eng* 4:40–45. (In Chinese)
- [3] Jiang C, Li D, Zhang P, et al. Formaldehyde and volatile organic compound (VOC) emissions from particleboard: Identification of odorous compounds and effects of heat treatment [J]. *Building and Environment*, 2017, 117:118-126.
- [4] Zhao Y, Shen J, Zhao GL. Measurement of VOC release rate of plywood and its impact on indoor environment [J]. *Journal of Safety and Environment*, 2015, 15 (01): 316-319. (In Chinese)
- [5] Liu Y, Zhu XD. Application of comprehensive index method in the evaluation of volatile organic compound pollution from wood-based panel[J]. *Journal of Environment and Health*, 2012, 28(4) : 369-370.
- [6] Wang QF, Shen J, Shen XW, Du JH (2018) Volatile Organic Compounds and Odor Emissions from Alkyd Resin Enamel-coated Particleboard. *BioResources* 13(3): 6837-6849
- [7] Liu R, Huang AM, Wang C, Lu B. Review of Odor Source and Controlling Technology for Furniture [J]. *Wood Industry*, 2018, 32 (03): 34-38. (In Chinese)
- [8] Filipy J, Rumburg B, Mount G, et al. Identification and quantification of volatile organic compounds from a dairy[J]. *Atmospheric Environment*, 2006, 40(8): 1480-1494.
- [9] Järnström H, Saarela K, Kalliokoski P, et al. Comparison of VOC and ammonia emissions from individual PVC materials, adhesives and from complete structures[J]. *Environment International*, 2008, 34(3):420-427.
- [10] Wang QF, Shen J, Jiang LQ, Dong HJ. Comprehensive evaluation on impact of melamine veneer particleboard on indoor environment [J]. *Journal of Central South Forestry University*, 2019, 39 (03): 99-106. (In Chinese)
- [11] Li ZJ, Shen J, Jiang LQ, Li XB, Dong HJ, Wang QF. Odor emission analysis of melamine faced MDF [J]. *Journal of Beijing Forestry University*, 2018, 40 (12): 117-123. (In Chinese)
- [12] Cao TY, Shen J, Liu WJ, Shao YL. Effect of Environment on the Release of VOCs from Wood-based Panel which Detected by DL-SW Micro-cabin [J]. *Journal of Northeast Forestry University*, 2018, 46 (02): 72-76. (In Chinese)
- [13] Liang W, Lv M, Yang X. The effect of humidity on formaldehyde emission parameters of a medium-density fiberboard: Experimental observations and correlations[J]. *Building and Environment*, 2016, 101:110-115.
- [14] Liu Y, Shen J, Zhu XD. Effect of hot-pressing parameters on the emission of volatile organic compounds from particleboard [J]. *Journal of Beijing Forestry University*, 2008 (05): 139-142. (In Chinese)
- [15] Shen J, Liu Y, Zhang XW, et al. Study on the volatile organic compounds emission from wood-based composites [J]. *China Forest Products Industry*, 2006, 33(1): 5—9. (In Chinese)
- [16] Shen J, Liu Y, Zhang WC, et al. Study on particleboard VOCs release [M]. Beijing: Science Press, 2013. (In Chinese)
- [17] Chen F. Study on the release characteristics and influence factors of volatile organic compounds emission from surface finishing particleboard [D]. Harbin: Northeast Forestry University, 2010. (In Chinese)
- [18] Zhang YF. Several environmentally-friendly finishing products for panel and their production technology [J]. *Forest Industry*, 2002 (04): 26-28. (In Chinese)
- [19] Deng FJ, Shen J, Li YB, Wang JX. Impacts of isocyanate concentration on TVOC emission from treated poplar wood [J]. *Forest Engineering*, 2016, 32 (04): 46-50. (In Chinese)
- [20] Li S, Shen J, Jiang SM. Characteristics of VOC Emission from Plywood in Different Environment Factors [J]. *Forestry Science*, 2013, 49 (01): 179-184.
- [21] Shen J, Jiang LQ. A review of research on VOCs release from wood-based panels [J]. *Journal of Forestry Engineering*, 2018, 3(06): 1-10.
- [22] Shao YL, Shen J, Deng FJ, Li YB, Shen XW. The influence of surface coating on TVOC emissions from the treated populus wood [J]. *Journal of Central South Forestry University*, 2018, 38 (02): 114-121.
- [23] Li CY, Shen XB, Shi Y. Study on VOC Emissions from Plywood Using a Climate Chamber [J]. *Wood Industry*, 2007 (04): 40-42.

Investigation of A Waste Newspaper Reinforced Soybean Based Adhesives for Interior Plywood

Hao Yin, Qiaojia Lin, Qinzhi Zeng, Jiuping Rao, Nairong Chen*
College of Material Engineering, Fujian Agriculture and Forestry University,
Fuzhou, 350002, China

*Corresponding author. Nairong Chen, Phone: + 86-591-83715175, Fax: + 86-591-83715175, E-mail: fafucnr@163.com

Abstract

A formaldehyde-free wood adhesive composed of waste newspaper, defatted soybean flour, and polyamide epichlorohydrin was developed for preparing three-ply plywood. The newspaper sizes and pH in the adhesive formulation and hot-pressing temperature and time for preparing plywood were investigated. The performance of adhesives were evaluated by shear strength of the bonded plywood. When the following optimum conditions: sizes with 80-120 mesh of waste newspaper, pH 6.0 of the adhesive, hot pressing temperature 130 ° C, and hot pressing time 3 min was used to prepare plywood. The plywood with shear strength of 1.24 MPa, which meet the requirements of the Chinese National Standard GB/T 9846-2015 for interior application. The cost of the adhesives decreased by 8% after using waste newspaper as reinforcement materials. Fourier transform infrared spectroscopy analysis indicated the reactions between carboxylate groups, amino, and hydroxyl groups of soybean flour and hydroxyl groups of wood fiber and polyamide epichlorohydrin lead to three-dimensional crosslinked structure, which improved the water resistance of the resulting plywood panels.

Key words: wood adhesive, biomass, environmentally friendly, waste newspaper, wood based panel

Introduction

Due to the increasing concerned on environmental pollution derived from petrochemical products, replaced such products to renewable environmentally friendly biomass resources have received widespread attentions. Adhesive, as a key component in wood industry, which consumed the most volume adhesives all over world [1]. Formaldehyde based wood adhesives, such as phenolic resin and urea-formaldehyde resin, derived from fossil resources account for more than 80% volume of consumption in wood adhesives. Besides, formaldehyde based wood adhesives can release a large amount of harmful substances (e.g., formaldehyde, phenol) during its production and application. Therefore, it is important to find a renewable and environmentally friendly adhesive derived from biomass to replace these adhesives for wood industry.

Soy protein, as a kind of biomass, is widely used as raw material for preparing wood adhesives due to its many advantages such as environmentally safe, readily available, and high chemical activity [2]. Defatted soy flour (DSF), containing 50% soy protein, is characterized by its low cost compared to other raw materials such as soy protein isolate, soy protein concentrate, etc. It is an ideal raw material for soybean-based adhesives, but poor gluability in the moisture condition is one of the challenges influencing the use of soy-based adhesives both in traditional wood composite products applications and as substitutions for formaldehyde-based adhesives. There are a large number of reports focused on chemical-supported modifiers, such as tannins [3], polyamidoamine-epichlorohydrin (PAE) resin [4], polyethylenimine and maleic anhydride [5], epoxy resin [6], undecylenic acid [7], and magnesium oxide [8] to improve the adhesives' gluability under the moisture conditions. None of these received much commercial acceptance except an adhesive system, consisting of PAE resin and soy-based raw materials [9, 10], which occupied 60% of the plywood market in the US and the inventor Dr. Li was awarded the Golden Goose Award [11]. The PAE resin has received special attention due to the fact that it is readily cross-links and grafts onto carboxyl and hydroxyl groups in DSF components during the heating process. However, the DSF-PAE adhesive system is expensive than traditional formaldehyde-based adhesive [2].

Worldwide paper industry produce more than 450 million tons of paper per annual [12]. The environment pollution caused by waste paper is a big problem. For example, the recycling of waste newspapers is mainly used for papermaking through a series of physical and chemical treatments, such as crushing, dissociation, deinking, etc. During this process, a large amount of chemicals, e.g., alkali, oxidant, surfactant, etc., will be released and cause environment pollution. Waste newspapers have a large number of reactive groups such as hydroxyl groups, carboxyl groups, etc., which provides the possibility of further reaction with PAE resin, e.g., PAE resin is widely used in paper industry to strengthen wet paper [13]. Hence, We hypothesized that waste newspaper may be used as a chemical reinforcement material for preparing environmentally friendly soy-based adhesives with improved wet cohesion and declined cost for interior plywood.

In this work, we tried to prepare soy-based adhesives by combining waste newspapers and DSF with PAE as a crosslinking agent. In addition, Fourier transform infrared spectroscopy (FTIR) was used to characterize the cross-linking reaction between waste newspaper and PAE. The gluability of the soy-based adhesive was evaluated by analyzing its application in plywood. Our work will provide new ideas for the development of environmentally friendly wood adhesives, and have important practical significance in the field of wood composites.

Experimental Materials

Defatted soybean flour (DSF, 53.4% of crude protein, 36.3% of carbohydrate, and 7.5% of moisture) purchased from Shandong Wonderful Industrial Group Co., Ltd. (Kenli, Shandong, China). Polyamide epichlorohydrin (PAE, solid content 12.5%), purchased from Qingzhou Jinhao Industry & Trade Co., Ltd. (Qingzhou, Shandong, China). Waste newspaper with 4.5% moisture content was obtained from the people's daily press (Beijing, China). Pinus massoniana veneers

(30 cm × 30 cm in size, 1.2 to 1.3 mm in thickness, and 10% to 12% of moisture contents) were obtained from Jianyang Luban Wood Industry Co., Ltd. (Jian Yang, Fujian, China). The other chemical reagents such as hydrochloric acid and sodium hydroxide, were analytical grade and purchased from Sinopharm Chemical Reagent Beijing Co., Ltd. (Beijing, China).

Preparation of soy based adhesive

Waste newspaper was placed in an air drying oven for 1 h, and then pulverized into powder with a pulverizer, and was further sieved with a standard sieve. DSF (50 g) and waste newspaper powder (20 g) were added to deionized water (63 g), and stirred at room temperature for 20 min until the components were uniformly mixed. PAE (75 g) was then added to the mixture and stirred at room temperature for 10 min. After stirring, the mixture was adjusted to different pH with sodium hydroxide or hydrochloric acid solution, and further stirred at room temperature for 1 h to obtain the waste newspaper reinforced soy-based adhesive.

Fourier transform infrared (FTIR) spectroscopy

The uncured and cured adhesive samples were ground into powder and scanned via a Nicolet 380 FTIR spectrometer (Thermo Fisher Scientific, Waltham, MA, USA) at a resolution of 4 cm⁻¹ for 32 scans in the spectral range of 500–4000 cm⁻¹.

Gluability test

The soy-based adhesive (170g/m² for a single side) was evenly applied to the surface of the veneer. The glued *Pinus masson* veneer was sandwiched between two pieces of un-glued veneers. Hot pressing parameters of plywood as follow: hot pressing temperature, pressure, and time were 130 °C, 1.0 MPa, and 3 min/mm, respectively. The plywood was conditioned at room temperature for 24 h before test. The gluability of adhesive was evaluated by shear strength of the plywood using the conditions and methods described by the Chinese National Standards GB/T 9846-2015 for plywood type II. A piece of plywood was cut into ten 10.0 cm × 2.5 cm specimens which were soaked in 63°C water for 3 h and then dried at room temperature for 10 min. After that, the specimens were tested in a tensile testing machine (MTS, Shenzhen, China) with a crosshead speed of 5 mm/min. Two replicates were used for each soy-based adhesive. Microsoft Office Excel 2007 (Redmond, WA, USA) was the software used for data analysis.

Results and discussion

FTIR analysis

The effect of PAE cross-linking with waste newspaper and DSF on the functional groups variation of adhesive was further analyzed by FTIR. We analyzed three kinds of adhesives. (i) DSF blended with PAE, the sample DP. (ii) waste newspaper blended with PAE, the sample WP. (iii) DSF and waste newspaper blended with PAE, the sample DWP. As shown in Figure 1, a large number of peaks appear at 3300-3500 cm⁻¹, which is usually due to the overlap of O-H and N-H groups. Generally, the reaction between PAE and soybean protein is mainly the ring-opening reaction between hydroxy-azetidium (the cationic four-membered ring structure) groups on PAE and carboxyl groups and amino groups on soybean protein [4]. However, compared with soybean protein isolate, DSF is more complex and its functional groups overlap with each other in FTIR, which is difficult to distinguish.

The amide I region is located at approximately 1640 cm⁻¹, representing the effect of C=O stretching vibration and a small amount of C-N stretching vibration. 1535 cm⁻¹ is the amide II

region representing the N-H bond vibration and a small amount of C-N stretching vibration. The amide III region represents the stretching vibration of C-N at 1242 cm^{-1} . A smaller peak was located at 1405 cm^{-1} , which represents the symmetric stretching vibration of COO^- at 1236 cm^{-1} . As shown in Figure 1, after a comparison of un-cured and cured DP, WP, and DWP adhesive, we could find that the DP amide I region changed from 1640 to 1652 cm^{-1} as the adhesive curing, and the amide II region changed from 1535 to 1543 cm^{-1} (blue shift). Amide I region of WP adhesive changed from 1630 to 1640 cm^{-1} (blue shift), and the region in DWP adhesive changed from 1640 to 1655 cm^{-1} (blue shift), indicating that the in deeded chemical reaction occurred during the curing process of adhesive. Moreover, compared with the un-cured samples, the cured WP adhesive showed a significant increase in the peak area of 1740 cm^{-1} , which indicates that the carboxyl group in the waste newspaper may undergo ring-opening reaction with the hydroxy-azetidium groups in the PAE to form an ester group. After curing, the amide II peak in DWP adhesive decreased, and the amide III peak increased, further indicating that PAE had crosslinked with DSF and waste newspaper during the curing process of adhesive.

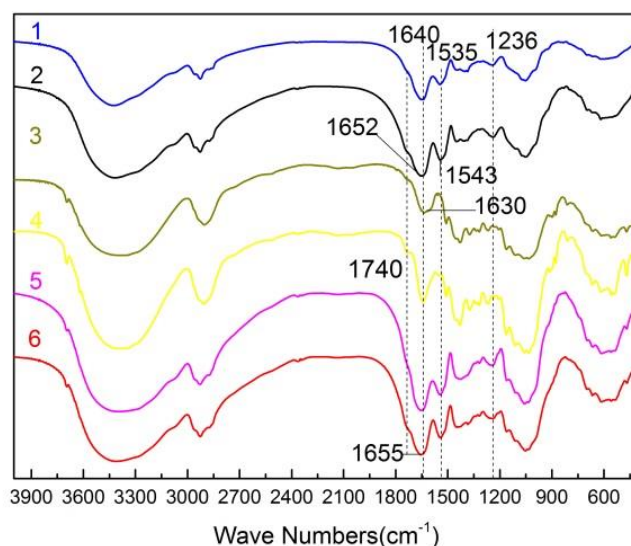


Figure 1. FTIR spectra of soy based adhesive. (samples 1, 2, and 3 represent un-cured DP, WP, and WDP adhesives, respectively. Samples 4, 5, and 6 represent cured DP, WP, and WDP adhesives, respectively.)

Effect of particle sizes of waste newspaper

Figure 2(I) shows the shear strength of soy-based adhesive reinforced by different particle sizes of waste newspaper and with different pH. As shown in Fig. 2(I), the shear strength of all samples increased first and then decreased as particle sizes was decreased. It is possible that this is because the small particle sizes of waste newspaper is readily aggregation with a huge number of hydrogen bonds, which may lead to its poor dispersion during the soy-based adhesive preparation process. As we known, poor dispersion of reinforcement materials can give rise to detrimental properties of final composites[14, 15]. When particle sizes of waste

newspaper was 80, 100, or 120 mesh, all the shear strength of adhesive was higher than 1.00 MPa and was no significant different ($p>0.05$), indicating that we can control the pulverized waste newspaper powder particle sizes range from 80 to 120 mesh.

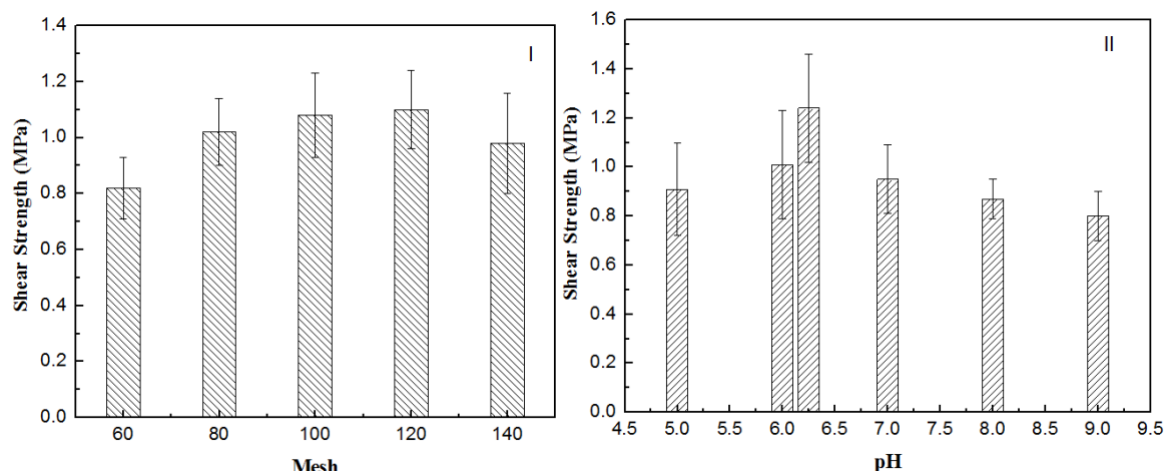


Figure 2 Effect of particle sizes of waste newspaper (I) and pH (II) on shear strength of adhesive

Effect of pH

Figure 2(II) shows the shear strength of soy-based adhesive with different pH reinforced by 80-120 mesh waste newspaper powder. As shown in Fig. 2(II), the shear strength of all samples increased first and then decreased as the adhesives' pH was decreased. This is might due to the synergistic effect of pH on soy protein and PAE molecular. The PAE is a cationic resin with the highest reactivity at neutral and weak base [16]. However, increased the pH of soy-based adhesives would unfold the soy protein molecular, resulting in the adhesive with sharply increased viscosity and poor flowing property. The adhesive would be hard to penetrate into crack of veneer, which decreased the mechanical property of cured adhesive. When the pH of adhesives were adjusted to 5.0, 6.0, 7.0, 8.0, and 9.0, respectively, the highest shear strength (1.01 MPa) was observed at the pH 6.0, which was closed to the original pH of DSF (about pH 6.25). Thus, we prepared a soy-based adhesive with pH 6.25, and the highest shear strength 1.24 MPa was obtained.

Cost analysis

According to the raw materials cost (DSF, 6000 ¥/t, PAE 10500 ¥/t, and waste newspaper 1000 ¥/t) in the China market, we calculated the cost of adhesive (Table 1). The cost of soy-based adhesive was higher than urea formaldehyde resin, but no formaldehyde released from soy-based adhesive. The adhesive with 8.0% decreased cost and improved properties. This result will promote the industry application of soy-based adhesive.

Table 1 cost of the adhesives

*Proceedings of the 62nd International Convention of
Society of Wood Science and Technology
October 20-25, 2019 – Tenaya Lodge, Yosemite, California USA*

Adhesive	Solid content (%)	Shear strength (MPa)	Formaldehyde	Dried adhesive cost(¥/t)	Wet adhesive cost(¥/t)
Urea formaldehyde resin	48.7	≧0.80	Yes	6160	3000
Soy-based adhesive	36	0.83	No	15850	5706
Waste newspaper reinforced soy-based adhesive	36	1.24	No	14600	5256

Conclusion

In the present study, a waste newspaper reinforced soy-based adhesive with water resistance comparable to urea formaldehyde resin was successfully developed. FTIR confirmed the reaction of the functional groups in DSF and waste newspaper crosslinked with hydroxy-azetidium groups in the PAE during curing process of adhesives. The gluability of all samples increased first and then decreased as particle sizes of waste newspaper powder was decreased. The particle sizes range from 80 to 120 mesh were suitable as a reinforcement material for soy-based adhesives. The weak acid condition of soy-based adhesive was good for its gluability. When soy-based adhesive was adjusted to pH 6.25, the plywood bonded with soy-based adhesive had the highest shear strength 1.24 MPa, which met the Chinese National Standard GB/T 9846-2015 requirement for interior plywood. The waste newspaper reinforced soy-based adhesive with reduced cost 8.0% show potentials application in the wood based panels industry.

Acknowledgments

The authors thank the National Natural Science Foundation of China (grant number 31500477) and the Natural Science Foundation of Fujian province (grant number 2019J01389) for providing financial support for this research.

References

- [1] Chen N., Lin Q., Zheng P., Rao J., Zeng Q., Sun J., A sustainable bio-based adhesive derived from defatted soy flour and epichlorohydrin, *Wood Sci Tech* 2019; 73: 801-17.
- [2] Chen N., Huang J., Li K., Investigation of a new formaldehyde-free adhesive consisting of soybean flour and Kymene® 736 for interior plywood, *Holzforschung* 2019; 73: 409-14.
- [3] Ghahri S., Pizzi A., Improving soy-based adhesives for wood particleboard by tannins addition, *Wood Science and Technology* 2017: 1-19.
- [4] Li K., Peshkova S., Geng X., Investigation of soy protein-Kymene® adhesive systems for wood composites, *J. Am. Oil Chem. Soc.* 2004; 81: 487-91.
- [5] Huang J., Li K., A new soy flour-based adhesive for making interior type II plywood, *J. Am. Oil Chem. Soc.* 2008; 85: 63-70.

***Proceedings of the 62nd International Convention of
Society of Wood Science and Technology
October 20-25, 2019 – Tenaya Lodge, Yosemite, California USA***

- [6] Chen N., Zheng P., Zeng Q., Lin Q., Rao J., Characterization and performance of soy-based adhesives cured with epoxy resin, *Polymers* 2017; 9: 514.
- [7] Liu H., Li C., Sun X.S., Improved water resistance in undecylenic acid (UA)-modified soy protein isolate (SPI)-based adhesives, *Ind. Crop. Prod.* 2015; 74: 577-84.
- [8] Jang Y., Li K., An all-natural adhesive for bonding wood, *J. Am. Oil Chem. Soc.* 2015; 92: 431-8.
- [9] Frihart C.R., Satori H., Soy flour dispersibility and performance as wood adhesive, *J. Adhes. Sci. Technol.* 2013; 27: 2043-52.
- [10] Frihart C.R., Birkeland M.J., Soy properties and soy wood adhesives, *Soy-based chemicals and materials*, ACS Publications, 2014, pp. 167-92.
- [11] Northeast S., Grants N.S.F., Science Policy Report, Policy 2017; 2017: 09-6.
- [12] Akinwumi I.I., Olatunbosun O.M., Olofinnade O.M., Awoyera P.O., Structural evaluation of lightweight concrete produced using waste newspaper and office paper, *Civil and Environmental Research* 2014; 6: 160-7.
- [13] Gustafsson E., Pelton R., Wågberg L., Rapid development of wet adhesion between carboxymethylcellulose modified cellulose surfaces laminated with polyvinylamine adhesive, *ACS Appl. Mater. Interfac.* 2016; 8: 24161-7.
- [14] Ramasubramaniam R., Chen J., Liu H., Homogeneous carbon nanotube/polymer composites for electrical applications, *Applied Physics Letters* 2003; 83: 2928-30.
- [15] Ajayan P.M., Tour J.M., Materials science: nanotube composites, *Nature* 2007; 447: 1066.
- [16] Khosravi S., Khabbaz F., Nordqvist P., Johansson M., Wheat - Gluten - Based Adhesives for Particle Boards: Effect of Crosslinking Agents, *Macromolecular Materials & Engineering* 2014; 299: 116-24.

Measuring Device Development for a Hardwood High-Speed Disintegration Process Analysis

Ondrej Dvoracek
Wood K Plus, Austria

Abstract

Climatic changes forced the European forestry to a transformation process concerning the forest composition, i.e. by increasing the share of deciduous species. In contrast, industrial processes are not prepared for changes in the raw material yet. Within the past, cutting process parameters were usually optimized by the trial and error method, therefore a knowledge-based adaption to changes of the raw material is not possible. Hence, the aim of this study is to gain an understanding of the disintegration mechanisms of hardwood by means of a novel test set-up, enabling a thorough analysis of the high-speed disintegration process. The self-designed machine enables the simultaneous examination of cutting forces and deformations of linear cutting processes at cutting speeds of up to 100 m/s. Therefore, the tool (a single knife) is installed on a three-dimensional force sensor, which is fixed on a machine. Thereby cutting forces of a minimum chip thickness of 0.02 mm can be analyzed. The specimen, that is mounted on a rotating arm of 4 m in diameter, passes the knife where the cutting process takes place. The process is simultaneously recorded by means of a sensitive piezo force sensor and high-speed cameras with a frame rate of up to 1,000,000 fps. Captured data are used for an analysis of deformations using the digital image correlation. The measurement process (triggering, data recording etc.) is controlled by a computer and fully automated. High rotation speed (up to 477 rpm) cause vibrations which are also measured by means of several accelerometers. This data are used for a raw data filtering minimizing the data bias. Results are the basis for the development of a cutting process model including the utilization of the finite element method, which subsequently serves as a tool for knowledge-based process parameters optimization.

Structure-related Vapor Sorption Phenomena in Wood

Raphaela Hellmayr^{1} – Rupert Wimmer²*

¹ Graduate Student, University of Natural Resources and Life Sciences, Vienna, Austria * *Corresponding author*
raphaela.hellmayr@boku.ac.at

² Professor, University of Natural Resources and Life Sciences, Vienna, Austria
rupert.wimmer@boku.ac.at

Abstract

Wood-water relations have been studied for more than a century. Doubts exist if equilibrium moisture content can be ever reached in full for wood in service, since ambient climate conditions are changing within a day. The objective of this research was to analyse vapor sorption, i.e. swelling phenomena of several wood species, by using Dynamic Vapour Sorption (DVS) in combination with a built-in video camera. DVS is a gravimetric method able to record sorption behaviour of materials by continuously monitoring the sample mass. Different softwoods and hardwoods were tested at 20 % steps of relative humidity. With the built-in video camera sample images were taken when the equilibrium moisture content was reached at each step, with the hygroexpansion coefficients determined at the acquired images. Results show that the adsorption phases were longer than the desorption phases across the species measured, with exception of beech. During adsorption the required time per step increased at higher relative humidity levels, whereas the duration in desorption was comparably stable. Different to spruce, larch responded slower to relative humidity changes. Radial swelling in earlywood of softwoods was roughly one-third of the one measured in latewood. It can be stated that a DVS apparatus with a built-in camera is suitable for determining swelling and shrinking of wood. As a next step, consecutive images will be evaluated by applying digital image correlation, delivering high spatial-resolution data for even better understanding.

Key words: Sorption, swelling, wood physics, wood anatomy, DVS, beech, oak, spruce, pine, larch

Introduction

Wood is a heterogeneous and anisotropic material with a specific multiscale anatomic structure. The orientation of the cells has a big influence on the mechanical and hygroexpansive properties. Dimensional changes occur when the moisture content drops below the fibre saturation point (FSP), with the content of bonded water in the wooden cell wall declining (Chirkova et al., 2007). According to Walker (2006) reasons for swelling differences in the radial vs. tangential direction are (1) the arrangement and density of earlywood and latewood within the annual ring, (2) microfibril angle differences of the radial vs. tangential cell walls and (3) directional influences of the radially arranged wood rays. Siau (1984) stated that swelling and shrinkage is directly proportional to density. Since the relative humidity in housings (Fischer et al., 2008) and outdoor is changing throughout the year, wood as a hygroscopic material is constantly adjusting to the ambient climate. Thybring et al. (2017) reported that the hydroxyl groups accessibility in wood is affected by drying and re-wetting procedures. A method to study swelling of wood at a cellular scale is phase-contrast X-ray tomography (Derome et al., 2011). A digital X-ray imaging system with a humid air conditioner was developed by Badel et al. (2006). With this configuration it was possible to investigate swelling phenomena at high spatial resolution, including anatomical patterns and density variations. El Hachem et al. (2017) studied the swelling of spruce during sorption cycles at the microscale. Here, the lumen as well as cell wall dimensional changes during swelling at different relative humidities were observed. Stuckenberg et al. (2018) determined the swelling velocity of different wood species relative to the anatomical cutting directions, using 50µm thick microtomed sections. The proportions of earlywood and latewood had a significant influence on the swelling velocity, with the latter being highest in tangential direction. Chau et al. (2015) have measured adsorption and hygroexpansion in southern pine. In this research radial and tangential swelling showed a linear relationship along with the moisture content. As reviewed by Engelund et al. (2013) wood-water relations have been studied for more than a century. It is seen doubtful that moisture equilibrium is ever fully reached in applications, since it takes a long time until wood is fully adjusted to an ambient climate. The technical development of Dynamic Vapor Sorption (DVS) apparatus enable the monitoring of adsorption and desorption processes (Wilkinson and Williams, 2016). Pfriem et al. (2007) recorded differences in sorption dynamics at high vs. low wood moisture contents. So far, no data on the sorption behaviour of wood prior to a reached moisture equilibrium.

In this research the following hypotheses are stated and tested: (a) Adsorption and desorption dynamics in wood alter with relative humidity levels, along with the prevalent moisture content. Chemisorption, physisorption and capillary condensation are mechanisms that result from different moisture uptake behavior. (b) A dynamic vapor sorption apparatus with a built-in video camera is in the position to determine high-spatial resolution swelling and shrinking movements in wood, allowing a combination of sorption dynamics with hygroexpansion. (c) Radial swelling in softwood species differs between earlywood and latewood, due to the existing density differences.

Materials & Methods

Nine wood species (Table 1) were analysed with samples having a size of 10 mm in radial

direction, 10 mm in tangential direction, and a thickness of 1 mm cut in longitudinal direction. Surfaces were sanded with a fine grit sandpaper (up to 600-grit).

Table 1: Tested wood species and samples

Scientific name	Common name	Number of samples
<i>Picea abies (L.) Karst</i>	Norway spruce	5
<i>Pinus sylvestris L.</i>	Scots pine	5
<i>Larix decidua Mill.</i>	European larch	4
<i>Fagus sylvatica L.</i>	European beech	11
<i>Quercus robur L. / petraea (Matt.) Liebl.</i>	European oak	4
<i>Fraxinus excelsior L.</i>	European ash	2
<i>Acer pseudoplatanus L.</i>	Sycamore maple	2
<i>Prunus avium L.</i>	Wild cherry	2
<i>Eucalyptus spp.</i>	Eucalyptus	3
Total		38

Dynamic Vapor Sorption (DVS, Advantage 1 by Surface measurement systems®) is a gravimetric measurement method, which is recording the sorption of the solvent in the sample by a continuous monitoring of the mass changes. The heart of the DVS is a micro-balance ($\pm 0.1 \mu\text{g}$) in a small chamber with controlled climate. The relative humidity range is between 0 % and 98 % and can be set by a mixture of two flows, one with water vapor and one with nitrogen at an accuracy of ± 1.5 %. All tests were performed at a nitrogen flow of 200 sccm. Equilibrium was defined as a relative change-rate in mass over time (dm/dt), which must be below 0.002 for 10 minutes. The built-in video camera (Dino-Lite ProX®) was mounted beneath the sample, to take sample images at each equilibrium moisture content state. The sample-surrounding climate gets changed by approaching a next climate step.

$$\alpha [\%] = \frac{d_{95} - d_0}{d_0} * 100 \quad (1)$$

The sequence was programmed with 20 % relative humidity steps starting from zero to 95 %, and back to 0 %, at a constant temperature of 25 °C. Sample mass was recorded every second and the minute averages saved. Data analysis and statistics were processed with the software SPSS (IBM, Version 24.0). ImageJ was used for image analysis and distances in radial and tangential direction were measured at 0 % and 95 % relative humidity. The resolution of the images was 1780 dpi. As shown in Equation (1), swelling was calculated by dividing the distance change by the initial distance.

Results and Discussion

Sorption dynamics

The overall sorption cycle duration is representing the speed of sorption reaching equilibrium at the ambient climate. This duration is ranging between 32 and 50 hours. The equilibrium moisture contents reached at each step, the produced isotherms as well as the hysteresis curves all showed similar levels across the species spruce, larch and pine, though spruce was adjusting

significantly faster to equilibrium moisture contents than larch (Figure 1). The saturated state at 95 % relative humidity corresponded with 16 to 18 % moisture content. For all species, adsorption required on average more time than desorption, with the exception of beech. Pfriem et al. (2007) showed that the speed of adsorption for Norway spruce was increasing with higher starting relative humidity, which is the opposite trend compared to the results obtained in this work. Compared to the other species, larch was slower in adsorption between 0 % and 60 % relative humidity, reaching a similar equilibrium moisture content. In desorption larch was slower and spruce faster than the average, a fact that was also found by Žlahtič and Humar (2017). Meyer-Veltrup et al. (2017) confirmed our finding, by reporting that the moisture uptake of European larch was significantly lower than for the other domestic wood species.

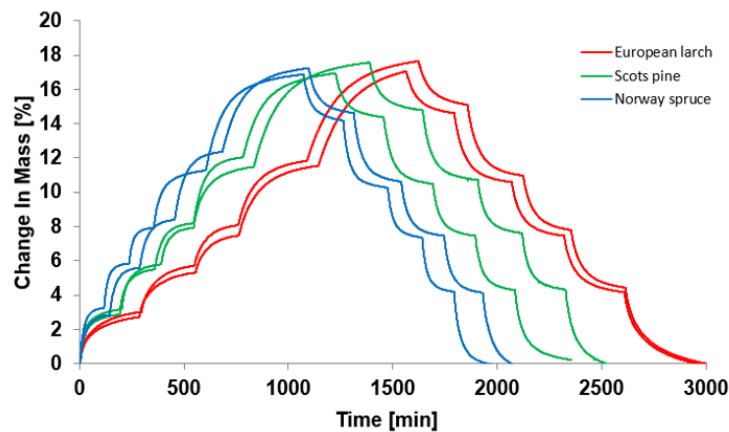


Figure 1: Change in mass over time, for spruce, larch and pine

As shown in Figure 2 (left) there is a significant difference between the time required for a complete adsorption and for a desorption cycle. The duration for desorption was longer for the lowest relative humidity step, and shorter at the highest humidity step. Moisture content changes per step followed the trend of relative humidity, (Figure 2, right) with changes per step varying between 1.5 % and 7 %. The visible outlier data in Figure 2 refer to eucalyptus, which showed high moisture uptake at low relative humidity. With eucalyptus, the first adsorption step created a 4 % change in moisture content, while in desorption it was slightly below 6 %. The continued sorption course did follow the general trend of all other species. The duration in desorption lasted longer than in adsorption, between 0 % and 60 % relative humidity, and shorter for the steps above that given range. Adsorption took longest for the step from 80 % to 95 % relative humidity, with an average of 7.5 hours. Steps between 0 % and 60 % relative humidity had no significant difference in their duration of adsorption, which equalled to an average of 2.5 hours. The same trend was observed for the change in moisture content per step, which laid between 2 % and 6 %. The achieved moisture content at half time of the step was slightly increasing and values between 80 % and 90 % were obtained. Here, Hill et al. (2010) reported similar sorption kinetics curves with Sitka spruce. The variation of the required desorption time between the steps was beyond the one for adsorption. Desorption between 20 % and 0 % relative humidity took longest with 5.5 hours on average, and the largest change in moisture with 4.5 %. The humidity step from 40 % to 20 % took the least time with only three hours. The lowest change

in moisture content was obtained for the 95 % and 80 % relative humidity step.

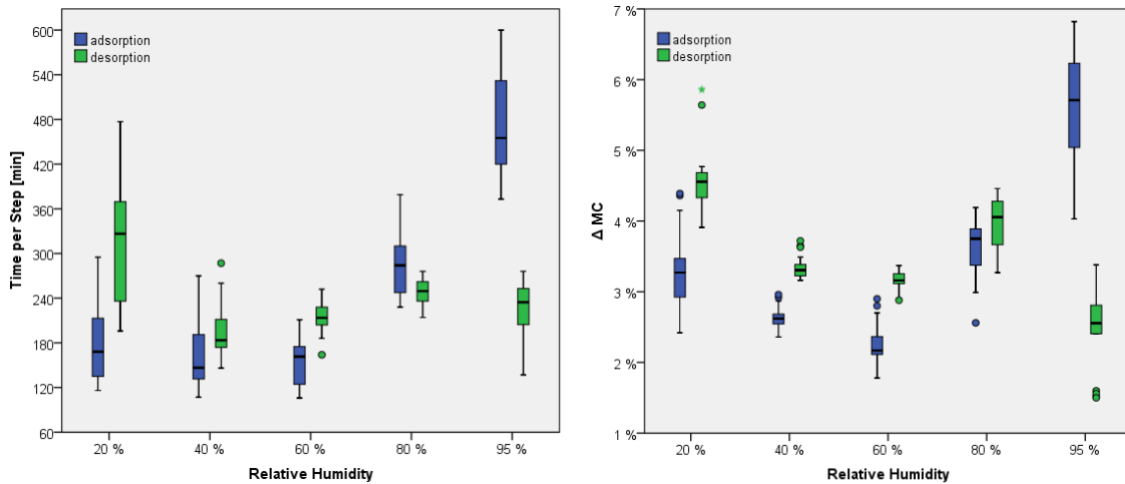


Figure 2: Sorption time per step (left) and change in moisture content (right) for adsorption and desorption

The reached moisture content at half time of the step was around 90% of the equilibrium, which showed the lowest values for the highest relative humidity step. Glass et al. (2018) described that the errors with a setting of dm/dt at 0.002, which must be held over ten minutes, are up to 1.2 % of the equilibrium moisture content and can be minimized by a stricter criterion. Since the objective of this study was to analyse the difference between relative humidity and species, including the path to get there, the accuracy of equilibrium was less critical. All samples reached more than 80 % of the equilibrium moisture content at half time of the step.

Swelling properties

The analysis of earlywood and latewood of softwoods individually in radial direction showed that there are significant difference in swelling (Figure 3). Swelling in earlywood was approximately one third of the one for latewood, which was also more or less equivalent to the total tangential swelling. Patera et al. (2018) showed that latewood is isotropic, while earlywood is orthotropic, a result that was also confirmed here. Combined swelling of earlywood and latewood showed no significant difference to total swelling in radial direction. The variance of swelling in latewood could be caused by the small distances and the limited measuring accuracy. For example, if the distance is 8 mm, one pixel is equivalent to 0.2 %, whereas if the distance is only 0.5 mm, one pixel equals to 1.5 %. It was not possible to identify the hygroexpansion of pores or single wood rays and the swelling in latewood showed a notable deviation. Latewood has a density gradient and the highest value is probably linked to the highest density. Panshin and Zeeuw (1980) stated that decreased shrinkage in radial direction is caused by wood rays and the change in density between earlywood and latewood. In tangential direction the latewood controls shrinkage and forces earlywood to shrink in the same amount. Earlywood and latewood were visually identified by the lighter and darker colour.

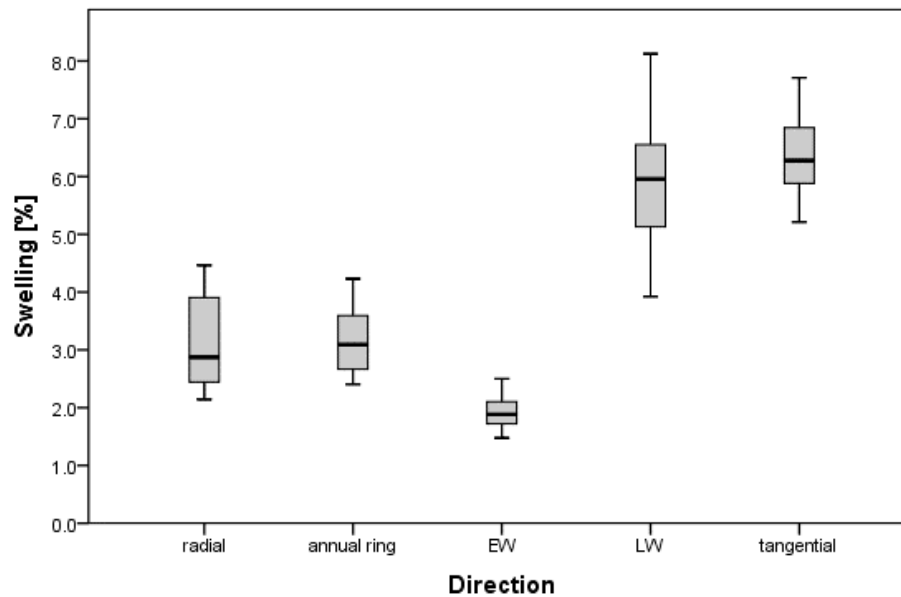


Figure 3: Radial (annual ring, earlywood (EW), latewood (LW)) and tangential swelling of softwoods

Total tangential swelling was approximately twice the swelling in radial direction for all domestic wood species. This well-known fact has been observed in various studies (e.g. Niemz and Sonderegger, 2017), and simply approved the validity of the DVS measurement method, in combination with an in-situ video camera to determine wood sorption. Chau et al. (2015) showed the moisture adsorption and hygroexpansion of southern pine and found that the swelling ratio between tangential and radial direction is increasing with moisture content. The same authors also stated that a linear correlation exists between swelling and the moisture content in wood. Tangential swelling of eucalyptus was approximately half of the one found for the domestic hardwood species. In radial direction the eucalyptus swelling was slightly lower than the one for the other species, which results in a radial to tangential ratio of 10:15. Spruce, pine and larch had a similar swelling behaviour in tangential direction, with the radial swelling being slightly higher for Scots pine than the other species. A reason for this deviation might be founded in earlywood and latewood differences, as determined by the density of the samples. Siau (1984) showed that density is directly proportional to swelling. European larch showed a high latewood proportion of approximately 40 %. The latewood proportion in Norway spruce and Scots pine was significantly less. It would be interesting to see if species differences are neglectable if the density difference is considered.

Summary and Conclusions

Sorption analyses confirmed that adsorption and desorption dynamics in wood are dependent on the prevalent relative humidities, and the moisture content levels. For the tested wood species with exception of beech the adsorption phase took longer than desorption. In adsorption the required time per relative humidity step increased as the moisture content was higher, whereas the duration in desorption was more constant. Larch reacted slower to a changed relative humidity than spruce. Dynamic vapor sorption (DVS) with a built-in video camera was

suitable for the determination of swelling and shrinkage in wood. For the combination of sorption with hygroexpansion, the spatial resolution of 1.3 megapixel of the used camera was insufficient. The difference of radial swelling in earlywood and latewood of domestic softwood species was quantified as well. DVS with a built-in camera having high-resolution has utility to analyse swelling properties of wood below the equilibrium moisture content. This would help to understand sorption in wood during real-life humidity cycles, checking also if there is a difference in swelling during adsorption and shrinkage during desorption. Further, digital image correlation could be applied to analyse the sorption images as well. Future studies are planned to better understand the swelling properties of heartwood, of coloured heartwood and of sapwood, especially of beechwood.

References

- Badel, E., Bakour, R. and Perré, P. (2006): Investigation of the relationships between anatomical pattern, density and local swelling of oak wood, *IAWA Journal*, 27(1), pp. 55–71.
- Chau, T., Ma, E. and Cao, J. (2015): Moisture Adsorption and Hygroexpansion of Paraffin Wax Emulsion-treated Southern Pine (*Pinus spp.*), *BioResources*, 10(2), pp. 2719–2731.
- Chirkova, J., Andersons, B. and Andersone, I. (2007): Study of the structure of wood-related biopolymers by sorption methods, *BioResources*, 4(3), pp. 1044–1057. doi: 10.15376/biores.4.3.1044-1057.
- Derome, D. et al. (2011): Hysteretic swelling of wood at cellular scale probed by phase-contrast X-ray tomography, *Journal of Structural Biology*. Elsevier Inc., 173, pp. 180–190. doi: 10.1016/j.jsb.2010.08.011.
- El Hachem, C., Abahri, K. and Bennacer, R. (2017): Microscopic swelling analysis of spruce wood in sorption cycle, *Energy Procedia*. Elsevier B.V., 139, pp. 322–327. doi: 10.1016/j.egypro.2017.11.215.
- Engelund, E. T. et al. (2013): A critical discussion of the physics of wood-water interactions, *Wood Science and Technology*, 47, pp. 141–161. doi: 10.1007/s00226-012-0514-7.
- Fischer, H.-M. et al. (2008): *Lehrbuch der Bauphysik*, Wiesbaden:Vieweg+Teubner Verlag.
- Glass, S. V. et al. (2018): Quantifying and reducing errors in equilibrium moisture content measurements with dynamic vapor sorption (DVS) experiments, *Wood Science and Technology*. Springer Berlin Heidelberg, 52, pp. 909–927. doi: 10.1007/s00226-018-1007-0.
- Hill, C. A. S., Norton, A. J. and Newman, G. (2010): The water vapour sorption properties of Sitka spruce determined using a dynamic vapour sorption apparatus, *Wood Science and Technology*, 44(3), pp. 497–514. doi: 10.1007/s00226-010-0305-y.
- Meyer-Veltrup, L. et al. (2017): The combined effect of wetting ability and durability on outdoor performance of wood: development and verification of a new prediction approach, *Wood Science and Technology*, 51, pp. 615–637. doi: 10.1007/s00226-017-0893-x.
- Niemz, P. and Sonderegger, W. (2017): *Holzphysik: Physik des Holzes und der Holzwerkstoffe*. München: Fachbuchverlag Leipzig im Carl Hanser Verlag.
- Panshin, A. J. and Zeeuw, C. (1980): *Textbook of wood technology: structure, identification, properties, and uses of the commercial woods of the United States and Canada*. 4th edition, New York: McGraw-Hill.

***Proceedings of the 62nd International Convention of
Society of Wood Science and Technology
October 20-25, 2019 – Tenaya Lodge, Yosemite, California USA***

- Patera, A. et al. (2018): Swelling interactions of earlywood and latewood across a growth ring: global and local deformations, *Wood Science and Technology*. Springer Berlin Heidelberg, 52(1), pp. 91–114. doi: 10.1007/s00226-017-0960-3.
- Pfriem, A., Grothe, T. and Wagenführ, A. (2007): Einfluss der thermischen Modifikation auf das instationäre Sorptionsverhalten von Fichte (*Picea abies* (L.) Karst.), *Holz als Roh- und Werkstoff*, 65, pp. 321–323. doi: 10.1007/s00107-006-0167-z.
- Siau, J. F. (1984) *Transport processes in wood*. Berlin: Springer.
- Stuckenberg, P., Wenderdel, C. and Zauer, M. (2018): Determination of the swelling velocity of different wood species and tissues depending on the cutting direction on microtome section level, *Results in Physics*. Elsevier, 9, pp. 1388–1390. doi: 10.1016/j.rinp.2018.04.059.
- Thybring, E. E., Thygesen, L. G. and Burgert, I. (2017): Hydroxyl accessibility in wood cell walls as affected by drying and re-wetting procedures, *Cellulose*. Springer Netherlands, 24, pp. 2375–2384. doi: 10.1007/s10570-017-1278-x.
- Walker, J. C. (2006): *Primary wood processing: principles and practice*, 2nd edition, Dordrecht: Springer.
- Wilkinson, J. and Williams, D. (2016): The Latest Developments in Dynamic Vapor Sorption (DVS), <https://www.azom.com/article.aspx?ArticleID=13001>, 15.03.2019.
- Žlahtič, M. and Humar, M. (2017) 'Influence of Artificial and Natural Weathering on the Hydrophobicity and Surface Properties of Wood', *BioResources*, 12(1), pp. 117–142. doi: 10.15376/biores.11.2.4964-4989.

***Proceedings of the 62nd International Convention of
Society of Wood Science and Technology
October 20-25, 2019 – Tenaya Lodge, Yosemite, California USA***

Industry 4.0 Readiness in the US Forestry Industry

Ms. Brooklyn Legg, leggb@oregonstate.edu

Ms. Bettina Dorfner

Dr. Scott Leavengood

Dr. Eric Hansen

Oregon State University, USA

Abstract

Advances in technology have promoted evolution across all sectors of manufacturing. The forestry industry has also implemented many new manufacturing technologies and techniques. Given these changes, this work sought to identify the overall readiness of the industry with respect to implementing the principles and technologies associated with Industry 4.0 (the fourth industrial revolution). Preliminary results from a pilot study show that industry professionals feel well prepared for Digital Connectivity, Digital Customer Interaction and New Business Models, but the majority are not familiar with Virtualization, Robotics, Big Data, Predictive Analytics, Cloud Computing and Autonomous Systems. A survey of US-based primary wood products manufacturers will be conducted in summer 2019. Survey questions cover a variety of industry advancements including new technologies. We hope to develop insights that can help improve the sector by understanding the current technological growth and eliminating roadblocks that hinder the growth of future technologies.

Reducing the Set-Recovery of Surface-Densified Scots Pine by Furfuryl Alcohol Modification

Lei Han

Lulea Technology University, Sweden

Abstract

It is well known that there is a positive relationship between wood density and its mechanical properties. That means the densification process is a reasonable method to increase the value of low-density species like Scots Pine and Norway Spruce. In the past, most of the densification processes are aim to densify the whole thickness of the wood. However, the bulk densification not only consumes a quite long time and the huge amount of energy during the process but also lose most of the volume after the process which results in the lower total bending capacity and much higher price per unit. In some case, only one surface of the product is exposed during use periods such as the wooden flooring and worktop. Therefore, the surface densified wood is relative fast, low energy consuming, retained overall thickness and enough to provide favorable hardness and strength during the application period. How to avoid the moisture-induced set-recovery of the densified wood is still the main obstacle in wood densification. Although there are several methods like post heat treatment can almost eliminate the set-recovery, they are either time consuming or difficult to translate into a continuous process which makes the advantage of densification for cheap low-density species lost. On the point of fixing the deformation by increasing the dimensional stability of wood, furfurylation performs the best in improving the anti-swelling efficiency compared with other methods. Besides, furfuryl alcohol is a renewable and natural material which can be obtained from biomass waste. Furfurylation can also protect the wood from biodegradation at a high level without unharmed emission or leaching during the application period. Considering about wettability, curing conditions and viscosity, furfuryl alcohol owns similar properties like phenolic resin. Based on the above properties, it has been proved by the present study that the polymerization of furfuryl alcohol is able to be used to impregnate wood for fixing bulk densified deformation.

The objective of this thesis is to verify whether the furfuryl alcohol can also be used in reducing the set-recovery of surface densified Scots Pine. The study will focus on the interactive effect of the process parameters on the end properties such as immediately spring back, surface hardness, set-recovery under several dry-wet cyclic climate changes, etc. In order to achieve this objective and find the optimal processing parameter, the two-level full factorial design was used combined with following ANOVA and multivariate analysis. Microstructure and density profile measurement after the surface densification and dry-wet cyclic climate test were carried out at the same time as a supplementary tool to learn the mechanism of this two-step modification process further.

Keywords: surface densification; set-recovery; hardness; furfuryl alcohol; microstructure

Composition Analysis and Health Risk Assessment of Benzene Series for Nitrocellulose Paint Lacquered MDF

Huifang Lia, Jun Shen ^{b,*}

^a College of Material Science and Engineering, Northeast Forestry University, Harbin, China, 150040 lihuifang@nefu.edu.cn

^b College of Material Science and Engineering, Northeast Forestry University, Harbin, China, 150040 shenjun@nefu.edu.cn

Abstract: [objective] To evaluate the effect of board thickness and diluents of lacquered panel on human health. [method] The 18mm and 8mm MDF were used as the research object. The nitrocellulose paint was diluted by mixed solvent (alcohols, esters, benzene mixture), Anhydrous Ethanol and Ethyl Acetate, respectively. The 15L small climate chamber was used to simulate indoor environment, and GC – MS was used to analyze the concentration of benzene series released from nitro-lacquered panels. Health risk assessment was evaluated by EPA/US health risk assessment model, it showed the influence of different diluents on the release of benzene series to human body. [results] Under the simulated indoor condition of using MDF alone, 18 kinds of benzene series were detected from mixed diluent painted MDF (NC-M) with thickness of 18mm and 8mm. Thickness of board had no significant effect on the release of benzene. There were significant carcinogenic and non-carcinogenic risks to humans; MDF painted with Anhydrous Ethanol diluent (NC-A) released 14 kinds of benzene series with a total mass concentration of $174.82\mu\text{g}\cdot\text{m}^{-3}$, it had no significant non-carcinogenic risk to human body; MDF painted with Ethyl Acetate diluent (NC-E) released 16 kinds of benzene series with a total mass concentration of $218.76\mu\text{g}\cdot\text{m}^{-3}$, it had no significant non-carcinogenic risk to human body; [conclusion] Under the indoor conditions of using lacquered MDF alone, thickness has no significant effect on the release of benzene series. Of the three kinds of diluents, benzene series varieties and mass concentration releasing from NC-A and NC-E were both far lower than from NC-M, health risk of NC-A was the lowest. Choosing suitable organic solvent as the diluent of nitro-lacquer can greatly reduce the release of benzene series from the source.

Keywords: nitrocellulose paint; MDF; diluent; benzene series; health risk

Introduction

With the improvement of people's living standards and environmental protection consciousness, varieties of lacquered panel furniture are widely used for interior decoration [1]. Nitro-lacquered furniture is especially common in home storage, while is also getting more and more air irritating attention [2]. Studies have shown that indoor air pollution can cause diseases of the respiratory, nervous and circulatory systems [3]. Volatile organic compounds (VOCs) released from nitro-lacquered furniture, especially benzene series, can irritate people's skin, eyes and respiratory tract, and pose a serious threat to people's health [4]. Therefore, the nitro-lacquered MDF was tested to study the effect of different diluents on the release of benzene series and scientifically evaluated for air quality and human health risks. It is of great significance for ensuring indoor air quality and human health.

Health risk assessment is used to evaluate the degree of harm of toxic substances to human health [5]. It includes carcinogenic risk and non-carcinogenic risk [6]. Non-carcinogenic risk assessment is expressed by Hazard Index (HI), it's the ratio of long-term intake to reference dose. Carcinogenic risk is expressed in terms of risk value (Risk), it's expressed by the product of the reference intake and average exposure concentration of lifetime. The formula is as follows.

$$\text{HQ} = \text{EC} / (\text{Rfc} \times 1000) \quad (1)$$

$$\text{HI} = \sum \text{HQ}_i \quad (2)$$

$$\text{Risk} = \text{EC} \times \text{IUR} \quad (3)$$

Note: HQ is Hazard Quotient, EC is Exposure Concentration, Rfc is the concentration of inhaled carcinogenic risk ($\text{mg}\cdot\text{m}^{-3}$), HI is the sum of hazard quotients of pollutants, IUR is the reference concentration that causes a cancer risk ($\text{m}^3\cdot\mu\text{g}^{-1}$) [7].

To evaluate the effect of different thickness and diluents of lacquered panels on human health, in this study, 8mm and 18mm nitro-lacquered MDF panels were examined as the research object, the nitrocellulose paint was diluted by mixed solvent (alcohols, esters, benzene mixture), Anhydrous Ethanol and Ethyl Acetate, respectively. The panels were placed in a 15L small climate chamber, which was used to simulate indoor environment. Benzene series released from three kinds of nitro-lacquered panels was examined by GC – MS. The health risk assessment model was used to evaluate the risk of benzene series to human health. Based on assessment result, to protect human health, the study proposed to control benzene series pollution from the choice of paint diluent.

Materials and Methods

Experimental materials

Undecorated MDF panels, produced in Guangdong, were chosen as our experimental material. The panels had the dimensions (length × width × thickness) of 150mm×75mm×18mm and had a formaldehyde emission of level of E1. The adhesive used in MDF production was urea-formaldehyde resin adhesive.

Ash was used as veneer material for MDF with a thickness of 0.6mm, the hot-pressing temperature was 200°C, the hot-pressing time was 10min, and the thermal pressure was 4MPa^[8].

The nitrocellulose paint was diluted by three types of diluents, the first type was Anhydrous Ethanol (NC-A), the second was Ethyl Acetate (NC-E), and the last was mixed solvents that mixed with alcohol, ester and benzene (NC-M). Painting proportion was the main agent: diluent=2:1. Painted panels were placed in a naturally ventilated room with 23°C for 28 days^[9]. Tin foil is used to seal the side of the plate when collecting gas to prevent the benzene series from being released ^[10].

Experimental equipment

The following equipment was used in the experiments. (1) A small climate chamber with the volume of 15 liter. It had been verified had a good correlation ^[11] with 1m³ chamber ^[12]. The chamber simulated the indoor environment, with the temperature of 23°C, air humidity of 50%, air exchange rate of 1^[13]. (2) Tenax-TA sampling tubes were obtained from Beifen Tianpu Instrument Technology Limited Company^[14]. (3) A DSQ II series GC-MS (Thermo Fisher, America) was used^[15]. Thermal desorption apparatus made by MARKES UK performed with a DB-5 quartz capillary column, the carrier gas was Helium^[16].

Experimental design

Collection of benzene series- In this study, painted MDF were placed in a naturally ventilated room with 23°C for 28 days. The panels were placed horizontally in the center of the climate chamber, the benzene series released from the specimen surface was absorbed using Tenax-TA tubes. The collected gas was analyzed by thermal desorption apparatus for 5 minutes. The GC-MS and built-in software were used to analyze the concentration of benzene series according to GB/T29899-2013^[17]. The EPA/US health risk assessment model were used to evaluate the risk of harm of benzene series to human health.


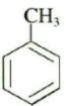
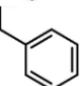

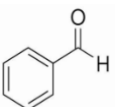
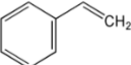
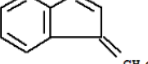
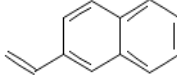
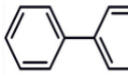
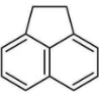
Results and Discussion

Benzenes eries components released from MDF with different thicknesses

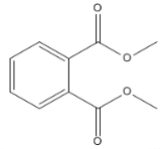
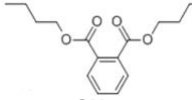
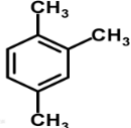
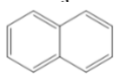
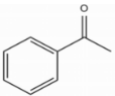
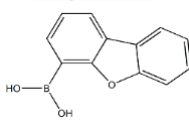
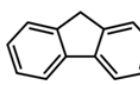
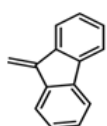
Table 1 summarizes the release of benzene series from MDF lacquered with different thickness. 18 kinds of benzene series were detected in 8mm and 18mm MDF, 13 kinds of benzene series were detected in undecorated MDF.

**Proceedings of the 62nd International Convention of
Society of Wood Science and Technology
October 20-25, 2019 – Tenaya Lodge, Yosemite, California USA**

Table 1 Release of benzene series components from three kinds of MDF

substance	chemical formula	structural formula	functional group	Toxicity	Concentration / ($\mu\text{g}\cdot\text{m}^{-3}$)		
					18mm MDF	8mm MDF	18mm undecorated MDF
benzene	C ₆ H ₆		/	high	45.61	45.42	44.4
toluene	C ₇ H ₈		methyl	high	27.65	14.75	60.24
ethylbenzene	C ₈ H ₁₀		ethyl	high	62.62	63.35	59.37
p-xylene	C ₈ H ₁₀		methyl	high	61.1	72.11	43.17
Benzaldehyde	C ₇ H ₆ O		Aldehyde group	high	3.09	3.82	/
styrene	C ₈ H ₈		carbon-carbon double bond	high	9.54	7.54	/
1-methylene-1H-indene	C ₁₀ H ₈		carbon-carbon double bond	low	2.57	2.45	/
2-vinylnaphthalene	C ₁₂ H ₁₀		carbon-carbon double bond	low	5.22	3.61	4.98
biphenyl	C ₁₂ H ₁₀		/	low	1.96	1.51	10.47
acenaphthene	C ₁₂ H ₁₀		/	low	3.14	3.79	12.38

**Proceedings of the 62nd International Convention of
Society of Wood Science and Technology
October 20-25, 2019 – Tenaya Lodge, Yosemite, California USA**

dimethyl phthalate	C ₁₀ H ₁₀ O ₄		/	low	3.45	3.58	3.15
dibutyl phthalate	C ₁₈ H ₂₂ O ₄		Ester group	low	28.57	27.65	21.49
1,2,4-trimethylbenzene	C ₉ H ₁₂		methyl	high	1.59	1.21	5.31
naphthalene	C ₁₀ H ₈		/	low	4.09	4.2	21.2
Acetophenone	C ₈ H ₈ O		/	low	1.49	2.42	/
Dibenzofuran	C ₁₂ H ₈ O		carboxyl	low	6.91	6.14	1.95
Fluorene	C ₁₃ H ₁₀		/	low	10.12	11.59	16.64
9H-Fluorene-9-methylene-	C ₁₄ H ₁₀		carbon-carbon double bond	low	5.72	5.92	/

The benzene series released from the nitro-lacquered MDF is mainly from the paint. Table 1 shows the total mass concentration of benzene series released from undecorated MDF was 316.24 $\mu\text{g}\cdot\text{m}^{-3}$, concentrations of Benzene, Toluene, Ethyl Benzene and P-xylene were 44.4 $\mu\text{g}\cdot\text{m}^{-3}$, 60.24 $\mu\text{g}\cdot\text{m}^{-3}$, 59.37 $\mu\text{g}\cdot\text{m}^{-3}$ and 43.17 $\mu\text{g}\cdot\text{m}^{-3}$ respectively. The mass concentration of Toluene was the highest, followed by Benzene and Ethyl Benzene. It can be seen that BTEX contributed the most to the benzene series of the undecorated MDF, it mainly derived from the tree itself and the adhesive applied when the wood fiber was produced.

The total concentration of 18 benzene series released from 18mm MDF was 284.44 $\mu\text{g}\cdot\text{m}^{-3}$, concentration of BTEX was 196.98 $\mu\text{g}\cdot\text{m}^{-3}$, Benzene, Toluene, Ethyl Benzene and P-xylene were 45.61 $\mu\text{g}\cdot\text{m}^{-3}$, 27.65 $\mu\text{g}\cdot\text{m}^{-3}$, 62.62 $\mu\text{g}\cdot\text{m}^{-3}$, 61.1 $\mu\text{g}\cdot\text{m}^{-3}$, respectively. The five highest components of total benzene series from high to low was Ethyl Benzene, P-xylene, Benzene, Dibutyl Phthalate and Toluene. The mass concentration of the other 13 benzene series was lower than 10.12 $\mu\text{g}\cdot\text{m}^{-3}$, and the concentration of Biphenyl was the lowest.

The total concentration of 18 benzene series released from 8mm MDF was 281.06 $\mu\text{g}\cdot\text{m}^{-3}$, concentration of BTEX was 195.65 $\mu\text{g}\cdot\text{m}^{-3}$, the mass concentrations of Benzene, Toluene, Ethyl Benzene and P-xylene were 45.42 $\mu\text{g}\cdot\text{m}^{-3}$, 14.75 $\mu\text{g}\cdot\text{m}^{-3}$, 63.35 $\mu\text{g}\cdot\text{m}^{-3}$, 72.11 $\mu\text{g}\cdot\text{m}^{-3}$, respectively. The concentration of P-xylene was the highest, then Ethyl Benzene and Benzene, and then Dibutyl Phthalate. The mass concentration of the other 14 kinds of benzene series were lower than 14.75 $\mu\text{g}\cdot\text{m}^{-3}$.

It was found that benzene series types released from 18mm and 8mm nitrocellulose lacquered MDF were same, the total mass concentration was not much different, and the concentration of BTEX was almost equal. It shows that under this experimental condition, thickness had no significant effect on the release of benzene series. The benzene series types of undecorated MDF were the least, but the total mass concentration was the highest. First, because the plate was veneered with ash before painting, it had a significant sealing effect on benzene series release from the plate itself. Secondly, the existence of paint film closed the contact between wood and air, and hindered the benzene series released from wood itself and adhesive, lacquer material becomes the main source of the benzene series released from lacquered MDF. This experiment also corrected

the general view that "unpainted board is more environmentally friendly". Reasonable painting can not only protect wood, but also hinder the release of volatile organic compounds, and protect the home environment.

Composition ratio of benzene series released from nitro-lacquered MDF with different diluents

Benzene series release mainly from main agent and diluents of the paint. Figures 1 to 3 visually show the composition and proportion of benzene series released from nitro- lacquered MDF using three diluents. The main ingredients include three major parts of BTEX (Benzene, Toluene, Ethyl benzene, P-xylene) which is the most harmful to humans, Styrene and other benzene-containing compounds.

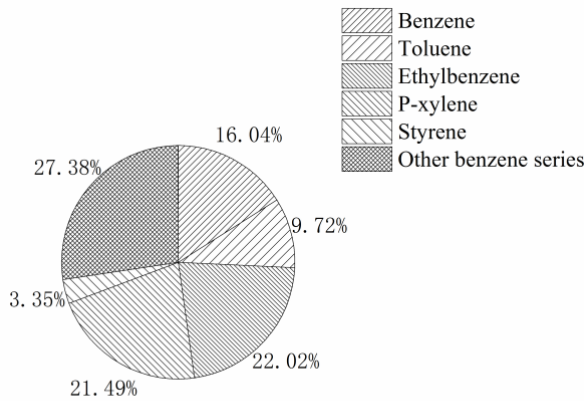


Figure 1 benzene series released from NC-M

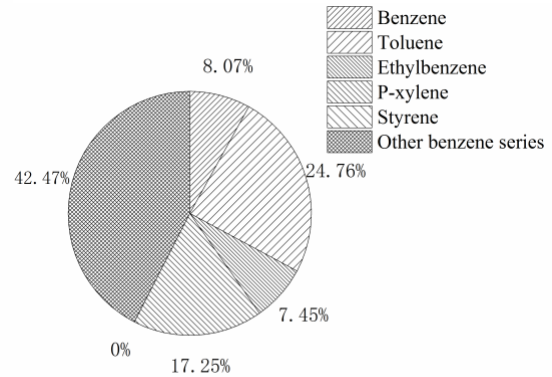


Figure 2 benzene series released from NC-A

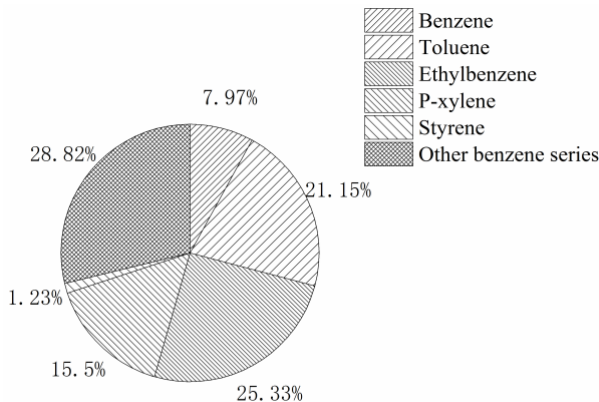


Figure 3 benzene series released from NC-E

Among the benzene series released from the nitro-lacquered MDF with three diluents, there were 12 common components, and BTEX accounted for the largest proportion.

BTEX accounted for 69.26% of the total mass concentration of benzene series released from NC-M lacquered MDF, Ethyl Benzene and P-xylene accounted for more than 1/5, which was 22.02% and 21.49%, respectively, and Styrene accounted for 3.35%, which may cause a potential health risks;

From NC-A lacquered MDF, BTEX accounted for 57.6% of the total mass concentration, Toluene and P-xylene accounted for 24.76% and 17.25% respectively, without releasing Styrene;

From NC-E lacquered MDF, BTEX accounted for 69.94% of the total mass concentration, Toluene and Ethyl Benzene accounted for 21.15%, 25.33% and Styrene for 1.23% respectively. Other compounds such as Naphthalene, Fluorene, Biphenyls, etc., had a lower release amount and a faster volatilization rate, causing less harm to health.

At present, the national standard limits the amount of benzenes added to the paint to not more than 0.5%, so that Benzene released from the lacquered panels get controlled. However, there is no specific limit of other single components of BTEX, and the potential hazards of various benzene series to human body still exist.

**Proceedings of the 62nd International Convention of
Society of Wood Science and Technology
October 20-25, 2019 – Tenaya Lodge, Yosemite, California USA**

Therefore, it is necessary to improve the monitoring of BTEX releasing level of lacquered panels, especially Toluene, Ethyl Benzene and P-xylene, in home life.

Health risk assessment

A health risk assessment is to further clarify the toxicity of the benzene series released from three lacquered MDF.

At present, only the Rfc and IUR values of Benzene, Toluene, Ethyl Benzene, P-xylene and Styrene can be found in the database of EPA/US Integrated Risk Information System (IRIS) [18]. Therefore, this study only evaluated the health risks of these five benzene series. Referring to the health risk assessment model, the daily average exposure concentration (EC), non-carcinogenic risk hazard quotient (HQ), hazard index (HI) and lifetime carcinogenic risk (Risk) of the five benzene series mentioned above in three kinds of lacquered MDF were calculated according to formulas (1) ~ (3), respectively. The results are shown in Table 2~4.

Table 2 Health Risk Assessment of Benzenes Released from NC-M

Benzenes	EC/($\mu\text{g}\cdot\text{m}^{-3}$)	Rfc/ ($\text{mg}\cdot\text{m}^{-3}$)	IUR/ ($\text{m}^3\cdot\mu\text{g}^{-1}$)	HQ	Risk
Benzene	45.61	0.03	7.80E-06	1.52	3.56E-04
Toluene	27.65	5	—	5.53E-03	—
Ethyl Benzene	62.62	1	—	6.26E-02	—
P-xylene	61.1	0.10	—	0.06	—
Styrene	9.54	1	—	9.54E-03	—
$\text{HI}_{\text{NC-M}}=\sum\text{iHQ}_{\text{NC-M}}=1.66$					

Table 3 Health Risk Assessment of Benzenes Released from NC-A

Benzenes	EC/($\mu\text{g}\cdot\text{m}^{-3}$)	Rfc/ ($\text{mg}\cdot\text{m}^{-3}$)	IUR/ ($\text{m}^3\cdot\mu\text{g}^{-1}$)	HQ	Risk
Benzenes	14.1	0.03	7.80E-06	0.47	1.1E-04
Toluene	43.28	5	—	8.66E-03	—
Ethyl Benzene	13.02	1	—	1.3E-02	—
P-xylene	30.16	0.10	—	0.3	—
Styrene	—	1	—	—	—
$\text{HI}_{\text{NC-A}}=\sum\text{iHQ}_{\text{NC-A}}=0.79$					

Table 4 Health Risk Assessment of Benzenes Released from NC-E

Benzenes	EC/($\mu\text{g}\cdot\text{m}^{-3}$)	Rfc/ ($\text{mg}\cdot\text{m}^{-3}$)	IUR/ ($\text{m}^3\cdot\mu\text{g}^{-1}$)	HQ	Risk
Benzene	17.44	0.03	7.80E-06	0.58	1.36E-04
Toluene	46.26	5	—	9.25E-03	—
Ethyl Benzene	55.41	1	—	5.54E-02	—
P-xylene	33.9	0.10	—	0.34	—
Styrene	2.69	1	—	2.69E-03	—
$\text{HI}_{\text{NC-E}}=\sum\text{iHQ}_{\text{NC-E}}=0.99$					

Note: “—” means no relevant data.

Assessment of non-carcinogenic risk

Table 2 shows in the benzene series released from NC-M, the HQ of Benzene was two to three orders of magnitude higher than the other four benzene series, Benzene was the most harmful benzene series. The EC

**Proceedings of the 62nd International Convention of
Society of Wood Science and Technology
October 20-25, 2019 – Tenaya Lodge, Yosemite, California USA**

ranged from 9.54 to 62.62 $\mu\text{g}\cdot\text{m}^{-3}$, HQ ranged from 5.53E-03 to 1.52, and HI was 1.66. According to the EPA/US standard, adverse reactions will occur when people are exposed to environmental conditions with HI of Benzene greater than 1 for a long time. In this study, the HI of benzene series was greater than 1, which indicated that the benzene series released from NC-M lacquered MDF had obvious non-carcinogenic risk to human body.

Table 3 shows the HI of benzene series released from NC-A lacquered MDF was the lowest, much lower than NC-M. The HQ of Benzene and P-xylene was one to two orders of magnitude higher than that of the other three benzene series. EC ranged from 3.64 to 17.67 $\mu\text{g}\cdot\text{m}^{-3}$, HQ ranged from 8.66E-03 to 0.47, HI was 0.79, and there was no obvious non-carcinogenic risk to human body.

Table 4 shows the HI of benzene series released from NC-E lacquered MDF was lower than NC-M, the HQ of Benzene and P-xylene was one to two orders of magnitude higher than that of the other three benzene series. The EC range of the five benzene series was 2.69~46.26 $\mu\text{g}\cdot\text{m}^{-3}$, the HQ range was 8.66E-03~0.47, and the HI was 0.99. The HI was lower than the NC-M, higher than the NC-A, close to 1, may have potential non-carcinogenic risks to the human body.

It should be pointed out that no obvious non-carcinogenic risk is not equal to no harm. The HI of benzene series released from NC-M lacquered MDF had exceeded 1. It is advisable to monitor the concentration of benzene series released from the nitrocellulose lacquered MDF for a long time, and be alert to the potential effects of benzenes in the environment on the human body.

Assessment of carcinogenic risk

According to the relevant definition of EPA/US, for the cancer risk, the acceptable carcinogenic risk value is in the range of 10^{-6} ~ 10^{-4} , when the risk value is less than 10^{-6} , it is considered to be acceptable, whereas the risk value is greater than 10^{-4} , it indicates that the benzene released from the lacquered board has a higher risk of cancer, and certain measures must be taken. Table 2~4 shows the risk value of benzene series released from NC-M lacquered MDF was 3.56E-04, which is 3.56 times the upper limit of carcinogenic risk. The carcinogenic risk values of benzenes released from NC-A and NC-E were significantly lower than those of NC-M, which were 1.1E-04 and 1.36E-04, respectively. The carcinogenic risk of these two kinds of paints has reached the upper limit, it indicates that benzene released from the two kinds of painted panels still has a certain carcinogenic risk to human body under this painting condition.

It can be seen that the type of diluents will directly affect the carcinogenic risk of gases. Using appropriate organic solvents as diluents can greatly reduce the toxicity of the released gases. Close attention should be paid to the release of benzene, and take measures such as window ventilation to promote the discharge of benzene.

The study shows that it feasible to use appropriate organic solvents as nitro-lacquer diluent, which not only guarantees the stable performance of the film, but also reduces the pollution of benzene series from the source. It has certain reference value for industrial improvement of nitro-lacquer.

Conclusion

- (1) Under the indoor conditions of using lacquered MDF alone, thickness has no significant effect on the release of benzene series.
- (2) The health risk of benzene series released from NC-A and NC-E lacquered MDF were both lower than NC-M, NC-A had the lowest health risk.
- (3) Choosing suitable organic solvent as the diluent of nitro-lacquer can greatly reduce the release of benzene series from the source.

Reference

- [1] Wang Zhenjie, Gao Li. Application and Demand of Wood-based Panel Products in Modern Interior Decoration [J]. *China Wood-based Panel*, 2018, 25 (04): 22-25.
- [2] Lu boqi. Effect of decoration materials on indoor air quality [J]. *Farmer's Staff*, 2018 (15): 210.
- [3] Peng Qi, Rao Jun, Yang Zhiwen, Zhou Chunliang. A review of the correlation between indoor inhalable particulate matter pollution and asthma and lung cancer [J]. *Practical preventive medicine*, 2018, 25 (08): 1022-1025.
- [4] Shen Jun, Jiang Liqun. Progress in VOCs release from wood-based panels [J]. *Journal of Forestry Engineering*, 2018,3(06): 1-10.

**Proceedings of the 62nd International Convention of
Society of Wood Science and Technology
October 20-25, 2019 – Tenaya Lodge, Yosemite, California USA**

- [5] Committee on the Institutional Means for Assessment of Risks to Public Health, National Research Council (US). Risk Assessment in the Federal Government: Managing the Process [R] . *Washington, DC: National Academy Press*, 1983.
- [6] Feng Huanyin, Fu Xiaoqin, Zhang Qian, et al. Residual status and health risk assessment of persistent toxic pollutants in agricultural soils in suburbs of Ningbo [J]. *Modern Scientific Instruments*, 2012 (4): 128-133.
- [7] Li Lei, Li Hong, Wang Xuezhong. Pollution characteristics and health risk assessment of volatile organic compounds (VOCs) in the ambient air of downtown Guangzhou [J]. *Environmental Science*, 2013, 34 (12): 4558-4564.
- [8] Tang Qiheng, Tan Hongwei, Wei Qifeng, Cui He Shuai, Guo Wenjing, Zhou Guanwu. Preparation and properties of low formaldehyde emission high density fiberboard [J]. *Journal of Forestry Engineering*, 2019, 4 (02): 26-30.
- [9] Xu Wei, Han Jiatong, Feng Yuefei, Wu Zhizhi, Luo Jianfeng. Effects of film thickness on sound absorption properties of spruce wood [J]. *Journal of Forestry Engineering*, 2016,1(04): 156-160.
- [10] Shao Yali, Shen Jun, Deng Fujie et al. Study on the effect of surface finishing on the release of TVOC from strengthened poplar wood [J]. *Journal of Central South University of Forestry Science and Technology*, 2018, 38 (2): 114-121.
- [11] Du Chao, Shen Jun. Comparison of VOCs rapid detection method and climatic box method for wood-based panels [J]. *Forestry Science*, 2015, 51 (3): 109-115.
- [12] Afshari A, Lundgren B, Ekberg L E. 2003. Comparison of three small chamber test methods for the measurement of VOC emission rates from paint. *Indoor Air*, 13: 156– 165
- [13] Du Chao, Shen Jun. Comparison of VOCs rapid detection method and climatic box method for wood-based panels [J]. *Forestry Science*, 2015, 51 (3): 109-115.
- [14] Du Chao, Shen Jun. Rapid Detection of Volatile Organic Compounds Release from MDF [J]. *Journal of Northeast Forestry University*, 2014, 42 (10): 115-117, 131.
- [15] Cao Tianyu, Shen Jun, Liu Wanjun, et al. Effects of environmental conditions on VOCs release from wood-based panels detected by DL-SW microchip [J]. *Journal of Northeast Forestry University*, 2018, 46 (2): 72-76
- [16] Zhao Yang, Shen Jun, Cui Xiaolei. VOC Release and Rapid Detection of 3-storey Solid Wood Composite Flooring [J]. *Forestry Science*, 2015, 51(2): 99-104.
- [17] Wu Qingsi, Wang Xuan, Xia Jinwei, Shen Lijin, Zhang Yaoli. Wood structural characteristics and GC-MS analysis of *Dalbergia alba* and *Dalbergia alba* [J]. *Journal of Forestry Engineering*, 2017, 2 (06): 26-30.
- [18] US EPA. Risk Assessment Guidance for Superfund Volume I: Human Health Evaluation Manual (Part F, Supplemental Guidance for Inhalation risk Assessment) [R] . Washington D C: Office of Superfund Remediation and Technology Innovation Environmental Protection Agency, 2009.

INVESTIGATING THE THERMAL AND MECHANICAL PROPERTIES OF FLY ASH/METAKAOLIN-BASED GEOPOLYMER REINFORCED WITH ALIEN INVASIVE WOOD SPECIES

HAMED OLAFIKU OLAYIWOLA
Stellenbosch University, South Africa

Abstract

Alien invasive wood species pose serious threat to the sustainable biodiversity of natural ecosystems. They add to the fuel load of above-ground biomass and lead to excessive loss of groundwater storage through evapotranspiration. The impacts have manifested in the incessant fire outbreaks and acute water shortage being experienced in South Africa in recent times. The prevailing approach of total clearing to contain the spread of these invasive plants is generating enormous biomass wastes. This study seeks to find alternative uses for these residues in geopolymer composite manufacturing, which can be applied in low cost building construction as an alternative beneficial control measure and a novel pathway of converting biomass and industrial wastes to value added products. *Acacia mearnsii* and *A. longifolia* were incorporated into geopolymer binder developed from a binary precursor system of fly ash and metakaolin. The production process was established using Central Composite Design (CCD) coded to utilize as much biomass as technically possible. Influence of factors related to the precursor materials and chemical activators such as binder to activator ratio, activator moduli ($\text{SiO}_2/\text{Na}_2\text{O}$), dosage ($\%\text{Na}_2\text{O}/\text{binder}$) and curing pattern on the thermal and mechanical properties of the final products were investigated. Preliminary results have indicated that the final products have comparable properties to conventional inorganic-bonded composite products.

Evaluating Stem and Wood Quality of Planted Longleaf Pines Using Bio-Imaging Techniques

Sameen Raut^{1} – Joe Dahlen²*

¹ MS Student, University of Georgia, Warnell School of Forestry and Natural Resources, Athens, GA, USA
sameen.raut@uga.edu

² Associate Professor, University of Georgia, Warnell School of Forestry and Natural Resources, Athens, GA, USA
jdahlen@uga.edu

Abstract

The conversion of forest land to agriculture resulted in the loss of 97 percent of longleaf pine forests in the southern U.S. Reforestation efforts in the 1950's established other southern pines across the southeast, namely loblolly and slash pine. However, recent efforts have led to the reestablishment of approximately 4 million acres of longleaf pine throughout the south on both converted agricultural fields and cutover forestlands. The application of modern silvicultural practices, combined with the lack of genetic improvement, has proven detrimental to longleaf pine stem wood and quality, with some sites having over 50% stem defect rate. Defects including sweep, forking, and ramicorn branching will result in the formation of compression wood which is undesirable for manufacturing. This study will investigate the applicability of bio-imaging techniques to quantify the amount of compression wood from longleaf pine. We are in the process of collecting cross sectional disks, extracted at multiple height levels, from approximately 400 trees. Green disk surfaces will be machined using a CNC router and subsequently photographed. An RGB image will be collected for making inferences about wood and bark volume and disk shape. A second image taken using circular polarized light will fluorescence the compression wood and allow for accurate quantification of the compression wood quantity.

*Proceedings of the 62nd International Convention of
Society of Wood Science and Technology
October 20-25, 2019 – Tenaya Lodge, Yosemite, California USA*

Following imaging, wood and bark volume, specific gravity and moisture content will be determined manually with comparisons made between the two volume measurements. Analysis of Variance using linear mixed models with stand and tree sampled as random factors will be conducted to determine differences in wood and bark properties between the converted agricultural fields and cutover forestland sites.

Results from this study will help inform forest landowners and state foresters about the quality of longleaf pine stem and wood so that they can better assess product quality and ultimately the economic returns on their investment. With growing interests of landowners towards planting longleaf pine in their cutover forestlands and old agricultural fields due to lucrative incentives, and the broader community of longleaf supporters making somewhat a leap of faith in attaching the same values of physical wood properties (specific gravity, moisture content, etc.) that natural, slow growing longleaf is known for to the more quickly grown plantation longleaf, our research, in my point of view, is of great importance.

Key words: Longleaf pine, compression wood, specific gravity, moisture content, bio-imaging

Improvement of Leaching Resistance of Fire-retardant Wood by Formation of Insoluble Compounds

Alexander Scharf

Luleå University of Technology, Sweden

Abstract

Wood is a traditional and promising raw material which can meet the increasing demands on building products regarding sustainability and environmental impact. Recent developments in wood modification and engineered wood products have proven that wood is a serious competitor for steel and concrete constructions, not only in regard to sustainability.

The fire performance of materials used for construction is one of the main selection criteria. By introducing chemicals into wood, the usually high instability of untreated wood to fire, can be strongly limited. The reduction in fire resistance of fire-retardant-treated wood by exposure to outdoor conditions is often an issue when developing new retardants. Commonly used fire-retardants are inorganic salts of the elements phosphorus, nitrogen and boron. These compounds alter the thermal degradation of wood as single compounds, but also by synergistic effects. However, the solubility of inorganic salts makes them susceptible to leaching. This may lead to a loss in fire-performance but also to a higher introduction of leached out chemicals into the environment.

The durability of fire-retardant-treated wood in outdoor use is dependent on the leaching resistance. Östman and Tsantaridis (2017) showed that commercially fire-retardant-treated wood may lose its improved fire performance over time under service conditions. High amount of chemicals or protective paint systems allow the wood to keep its fire performance. Furuno et al. (1993) introduced water glass solution (sodium silicate) and boron compounds into wood with subsequent precipitation of silicate by soaking specimens in aluminum sulphate. The treated samples showed improved fire resistance and increased hygroscopicity. The precipitation of insoluble inorganic substance like aluminum silicate may provide the wood with leaching resistance. It could lower the amount of needed chemicals and reduce the environmental impact of fire-retardant-treated wood.

In this project Scots pine (*Pinus Sylvestris*) samples with dimensions of 150x10x10mm³ (L x W x T) were treated in a two-step process. Initial pressure impregnation with an aqueous solution containing guanidylurea phosphate, borax and sodium silicate was followed by drying and then by soaking in aluminum sulphate for precipitation of insoluble compounds. The dried samples were exposed to leaching in water (EN 84) and limited oxygen index (LOI) was determined. The formed insoluble compounds may provide the material with leaching resistance to secure fire resistance under service conditions. The analyses were supported by thermogravimetric analysis, SEM and FTIR spectroscopy.

*Proceedings of the 62nd International Convention of
Society of Wood Science and Technology
October 20-25, 2019 – Tenaya Lodge, Yosemite, California USA*

The applied 2-step treatment of the samples led to a reduction in leaching compared to the single treatment reference. Samples lost 80-90% of the initially introduced material but still showed improved fire resistance despite the leaching losses. Without the second treatment all compounds were leached out and had a fire resistance similar to untreated wood. Different ratios of the chemicals were tested, and the results were evaluated by multivariate data analysis. Higher concentrations of chemicals did not lead to a significant improvement in leaching resistance or fire retardancy.

Key words: wood modification, wood-mineral composite, water glass, leaching resistance, fire resistance

Understanding Silvicultural and Process Variation and its Influence on Life-Cycle Carbon Emissions for Durable Wood Products

Adam Scouse

North Carolina State University, USA

Abstract

Woody biomass is currently used to produce of any array of valuable, durable wood products (DWP) like lumber, plywood, oriented strand board, laminated veneer lumber, and gluelam. These DWPs sequester carbon and serve as an alternative to metal or concrete products with high embodied energy content and other associated environmental burdens. The productivity and management of forests have a significant impact on the environmental life-cycle impacts of DWPs. In addition, the productivity and management of forests are also highly variable between species, e.g., Loblolly Pine or Douglas Fir.

This presentation will highlight the impacts of alternative forest management and processing variables on the overall greenhouse gas emissions generated by DWP production. Stochastic modeling tools will be coupled with forest growth and yield simulations and alternative manufacturing processes to evaluate the most likely outcomes for different combinations of forest management and DWP production activities. This research will specifically determine how plantation management, the distance from the harvest site to the processing mill, lumber yield, use of mill residues, duration of use for the DWP, and the final disposal of the DWP will contribute to the overall GHG cycle. Each step of the production process can have significant variation. Therefore, point estimates of the resulting energy consumption and greenhouse gas (GHG) emissions are also expected to be highly variable.

This work is part of a larger project that is focused on integrating biofuels, produced from forest thinnings and residues, with DWP production.

Cellulose Nanocrystals vs Cellulose Nanofibrils: Which One Performs Better in Flexible, Biodegradable and Multilayer Films for Food Packaging?

Lu Wang

University of Maine, USA

Abstract

Appropriate packaging techniques are essential in preserving food from deterioration and being disposed as waste, which accounts for 40% of all food produced in USA. To extend the shelf life of food, packaging should decelerate/prevent the transmission of gases from the ambient environment to food, especially oxygen and water vapor which are essential inputs for spoilage microbes. Polylactic acid (PLA), a favorable biodegradable polymer for the packaging industry, possesses medium water vapor barrier permeability $\sim 1,000 \text{ g um}/(\text{m}^2\text{day kPa})$ and high oxygen permeability $\sim 300,000 \text{ cm}^3 \text{ um}/(\text{m}^2 \text{ day atm})$ and is rated as low grade relative to oxygen barrier character. Cellulose nanomaterials (CNMs) are widely reported to be superior oxygen barriers at low to medium relative humidities ($<50\% \text{ RH}$). Among all the approaches scientists have searched to ameliorate PLA's barrier properties, utilizing CNMs is an interesting method because CNMs improved the barrier performance of PLA without deteriorating the biodegradability of the resulting package system. While both cellulose nanocrystals (CNCs) and cellulose nanofibrils (CNFs) are excellent oxygen barriers, paths available for gases to diffuse are different depending on their morphological properties. However, there is no conclusive knowledge regarding which nanomaterial performs better in reducing oxygen transmission. In rare cases, CNMs films can maintain oxygen barrier characteristics at high RH that meet industrial requirements without being laminated to more hydrophobic plastics. Multilayer packages where CNMs films as the core and plastic films as skin were reported to possess great commercial potential in several recent review articles. The purpose of this research was to provide meaningful data for PLA/CNMs/PLA multilayer packaging films and fairly compare the performance of CNCs and CNFs films in multilayer packages.

INFLUENCE OF PARTICLEBOARD THICKNESS AND VENEERS ON ODOR EMISSIONS

Qifan Wang¹, Jun Shen^{2*}

ABSTRACT

It is well known that the release of volatile organic compounds (VOCs) and odors from wood-based panels is harmful to human health. To reduce the problem of volatile organic compounds (VOCs) and odor emissions from veneered particleboard, this study focused on identifying odorant compounds and exploring the thickness and veneers on VOCs and odor emissions. Veneered particleboard coated with polyvinyl chloride (PVC) and melamine was studied via gas chromatography-mass spectroscopy/olfactometry. In total, 17 (55%) different odor types were identified from PVC-veneered particleboard among the 31 detected compounds. The predominant odor impressions of PVC veneered particleboard were *pungent*, *spicy* and *sweet*, and the main odorant compounds identified were aromatics, ketones, and esters. Over time, the odorant esters and ketones released from the PVC-covered particleboard decreased, whereas the release of alcohols and aldehydes odors increased, the release of aromatic compounds changed little. Among the 29 compounds detected from the melamine-veneered particleboard, 13 (45%) had odorant characteristics, the predominant odor impressions were *fresh*, *bitterness of plants* and *sour*, and the main odorant compounds identified were aromatics and esters. The release of odorant aromatic was relatively weak, but the release of ketones, esters, and aldehydes increased over time. In the early stage, the TVOC and total odor intensity was greatest, and over time, those values gradually decreased until a state of equilibrium was reached. There was no direct correlation between odor intensity and the mass concentration of different odorant compounds, but, for a odorant compound, its concentration affected the odor intensity somewhat. It is proved that veneer can help prevent the release of odors from particleboard, but it cannot completely prevent the emission for the voids in the structure of the veneer. Increasing thickness will increase the emission of VOCs and odor. Compared to veneered particleboard, the thickness influence odor emission from unvarnished particleboard more greatly.

Keywords: emission characteristics, melamine veneer, particleboard, PVC veneer, thickness, volatile organic compounds

INTRODUCTION

Volatile organic compounds (VOCs) from interior decorating have been identified as a silent killer by the medical community (Klepeis et al. 2001; Shen et al. 2001), and the problem of odor from furniture is receiving increasing attention (Nibbe 2017). People make subjective judgments about an environment based on its odors, and odors can affect a person's mood. Therefore, combining instrumental analysis with the subjective, human sense of smell provides more complete odor analysis and increases our ability to control VOCs.

In this study, a gas chromatography-mass spectroscopy-olfactometry (GC-MS-O) analysis combined the excellent separation techniques of gas chromatography, the abundant structural information produced by a mass spectrometer (Hsu and Shi 2013), and the human sense of smell, which can exceed that of many chemical detectors (Xia and Song 2006). This method has been widely used to select and evaluate active odor substances from complex mixtures (Zhang et al. 2009). At present, GC-MS-O has been used to analyze tobacco (Cotte et al. 2010), food (Frank et al. 2004; Gómez-Miguez et al. 2007; Machiels et al. 2003), and flavorings and spice (Choi 2005; Dharmawan et al. 2009) and has been used in environmental monitoring (Bulliner et al. 2006; Rabaud et al. 2002). However, GC-MS-O has not been widely used in the wood industry. GC-MS-O, based on GC-MS first proposed by Fuller et al. (1964) and Acree et al. (1976), analyzes the outflow components of GC-MS directly. In 1976, Acree et al. improved the original GC-MS technology by adding humidified air and by having evaluators smell the GC outflow after film chromatography processing. In

¹ Northeast Forestry University, 26 Hexing Road, Harbin 150040, China. Email: wangqifan66@163.com

² Northeast Forestry University, 26 Hexing Road, Harbin 150040, China. Email: shenjunnr@126.com. Corresponding author.

the mid-1980s, Acree et al. (1984) and Ullrich and Grosch (1987) used dilution-analysis to analyze the intensity of various odors at the same time, which made GC-MS technology widely applicable in many situations. Currently, there are four major GC-MS-O detection methods (Maarse and van der Heij 1994), including dilution analysis, time-intensity analysis, detection-frequency methods, and posterior-intensity evaluation. Time-intensity analysis was used in this study.

Polyvinyl chloride (PVC) and melamine veneers are widely used in furniture and interior decor composed of particleboard. In this study, those two types of veneered particleboards were analyzed. A Micro-Chamber/Thermal Extractor M-CTE250 (Markes International, Cardiff, UK) and GC-MS-O were used to analyze VOCs and odor emissions within a standard environment (temperature 23°C, relative humidity 40%). The characteristic odor of the compounds and their possible sources were identified, and variations caused by the thickness of the particleboard were investigated.

MATERIALS AND METHODS

Experimental Materials

In this experiment, PVC and melamine veneers were applied to particleboard ((Suofeiya, Guangdong, China). The density and moisture content of the particleboard were 0.60 g cm⁻³ and 8%, respectively. The samples were cut into round pieces (60 mm diameter) for the microchamber/thermal extractor apparatus, and the exposed surface area was 5.65 × 10⁻³ m². The samples were all taken from the center of the same plate to ensure the stability of the experimental material. For each experimental condition, four particleboard samples were used. After the edges of the specimens were sealed with aluminum foil to prevent the release of compounds, the samples were stored in polytetrafluoroethylene bags and refrigerated until needed.

Experimental Equipment

Sampling devices

The Micro-Chamber/Thermal Extractor μ -CTE 250 consists of four cylindrical micropools (each with a microcell diameter of 64 mm wide × 36 mm deep). The sampling temperature can be adjusted up to 250°C and can test four samples at the same time. The Tenax TA tube (Markes International Inc.) used had a stainless steel pipe body and contained 200 mg of 2,6-dibenzofurans porous polymer, which efficiently adsorbs or desorbs the VOC gases.

Detection and analysis device

Three detection and analysis devices were used. The Unity thermal analysis desorption unit (Markes International Inc.) used nitrogen as the carrier gas and was set with the following related parameters: thermal desorption temperature, 280°C; cold-trap adsorption temperature, -15°C; thermal analysis time, 10 min; and injection time, 1 min.

The second device used was a DSQ II series GC-MS (Thermo Fisher Scientific, Schwerte, Germany). Chromatography was performed with a DB-5 quartz capillary column (3,000 mm [length] × 0.26 mm [inner diameter] × 0.25 μ m [particle sizes]). Helium was used as the carrier gas with a constant velocity of 1.0 mL min⁻¹ by splitless injection. The chromatographic column was initially kept at 40°C for 2 min; then, the temperature was increased to 50°C (in 2°C min⁻¹ increments) and was held at that temperature for 4 min. Finally, the temperature was increased to 250°C (in 10°C min⁻¹ increments) and held at that temperature for 8 min. The injection port temperature was 250°C. The following GC-MS parameters were used: ionization mode, electron ionization; ion energy, 70 eV; transmission line temperature, 270°C; ion source temperature, 230°C; and mass scan range, 50 to 650 atomic mass units.

The third detection device used was a Sniffer 9000 Olfactory Detector (Brechtbühler, Echallens, Switzerland). Combined with GC-MS, quantitative and qualitative analyses can be made, and the compound's odor intensity can be reflected directly and recorded. The effluent of the GC capillary is divided into two parts, one part enters the mass spectrometer, and the other part is used for human sensory evaluation (ratio 1:1). The transmission line temperature was 150°C, and nitrogen was used as the carrier gas through a purge valve. Humidified air was added to prevent dehydration of the nasal mucosa.

Experimental Method

Sampling method

The experiment used the Tenax TA sampling tubes to adsorb a 2 liter amount of VOCs from the alkyd resin enamel coating on the particleboards under constant experimental conditions. Four samples were collected under each condition, with a sampling cycle of 8 hours; 2 L of the content was sampled and analyzed. After sampling, the Tenax TA sampling tubes were wrapped in polytetrafluoroethylene plastic bags until needed. The experimental scheme is shown in Table 1.

Analytic method

GC-MS and its built-in software were used to analyze the VOCs. The MS detection peaks were identified in the 2008 spectral library of the National Institute of Standards and Technology (NIST, Gaithersburg, MD) (matching degrees up to 800 or above). An internal-standard method was used in this experiment, with deuterium substituted for toluene at a concentration of 200 ng μL^{-1} , which added 2 μL . The internal-standard quantitative-analysis method used the following equation:

$$M_i = A_i \times \left(\frac{M_s}{A_s} \right) \quad (1)$$

where M_i is the mass of the internal standard added to the calibration standard; A_i and A_s are the peak areas of the products tested and the internal standard, respectively; and M_s is the amount of internal standard.

The time-intensity method was chosen for analysis of the compounds. As the sample was injected and the chromatogram yielded peaks, the human sensory-evaluation assessors perceived and described the column outflow from the odor port simultaneously. The timing of the odor, the odor type, and the intensity of the odor were recorded. After specific training, four assessors (with ages between 20 and 30 y, no history of smoking, and no olfactory organ disease) formed an odor-analysis evaluation group. The experimental environment was set to reference standard EN 13725-2003 (NSAI 2003). The room was well ventilated, and there were no peculiar smells within the room. The temperature was kept $23^\circ\text{C} \pm 2^\circ\text{C}$ throughout the entire experiment. Activities, such as eating, which might have an effect on indoor odors, were forbidden for 5 h before the experiment. Experimental results were recorded when the same odor characteristics were described by at least two assessors at the same time. The intensity value was based on the average value of the four assessors. The experiment's discrimination of odor intensity was based on the human sense of smell according to Japanese standards (Table 2; Ministry of Japan 1971).

After detection by GC-MS, the compounds were identified through the NIST (2008 standard spectrum) and Wiley (Hoboken, NJ) MS libraries. The primary odor compounds were identified by GC-MS-O. The refractive index value was calculated by the retention time of *n*-alkane under the same conditions (van Den Dool and Kratz 1963).

RESULTS AND DISCUSSION

Odor Constituents From Two Types of Veneered Particleboard

The odor constituents arising from 8-mm-thick, PVC-veneered particleboard, melamine-veneered particleboard, and unfinished particleboard were identified within a standard environment (temperature, 23°C ; relative humidity, 40%). Figure 1 shows the intensities of the odor-time spectrum for the two types of veneered particleboard. The greatest odor intensities from the PVC- and melamine-veneered particleboard were less than that arising from the unvarnished particleboard, that is, both veneer coatings lessened the odor intensity of the particleboard alone. The odor intensities from the two veneered particleboard were not high, with an average intensity of about 1. Odors from the PVC veneer reached their maximum intensity at about 4 min and 30 min, whereas those from the melamine veneer reached their maximum in about 27 min and had a maximum intensity of 2.

Table 3 shows the primary odor constituents emitted from the two types of veneered particleboard and the particleboard alone. Aromatics comprised most of the VOCs in both the veneered boards and the particleboard itself. For comparison and analysis, Table 4 shows the composition of the odorant compounds from the particleboard. Table 5 shows the acute-toxicity classification by the World Health Organization of the various

**Proceedings of the 62nd International Convention of
Society of Wood Science and Technology
October 20-25, 2019 – Tenaya Lodge, Yosemite, California USA**

odorants released from each veneer and from the particleboard, whereas the actual constituents of the odor are shown in Tables 6 and 7.

Among the 31 compounds detected from PVC-veneered particleboard, 17 (55%) produced the odorant characteristics. According to the UL 2821-2013 standard (Greenguard Environmental Institute 2006), those of the greatest concern were benzene, *p*-xylene, butyl acetate, and 2-butanol, which are listed as VOCs from office furniture if measured in greater than 10% of all products. Aromatics, ketones, and esters primarily produced the odors, which also contained alcohol and aldehyde odorants. The odor from aromatics produces a plant aroma and was in the low-toxicity range (only *p*-xylene was categorized as slightly toxic). Aromatics were emitted from the particleboard itself, from the raw materials used in PVC film coating, from the polyester resin stabilizer, from adhesives used in hot pressing, and from high-temperature lubricants used in making PVC. Ketones produced an aroma of soil and spice and were in the low to slight toxicity range. Ketones were mainly produced from the adhesive mundificant, the preparation of the adhesives, and the use of solvents. Most esters produce a fruity odor and had only slight toxicity. Esters were primarily produced by the making of PVC, from adhesive solvents, and from the particleboard itself. Only one constituent was categorized as alcohol, and it had a sour and bitter aroma and was classified as low toxicity. The alcohol was produced by the adhesive detergent, the PVC plasticizer, and the cosolvent. Aldehydes, which produce an aroma described as green grass, belong to low-toxicity classification and were derived from releases from the particleboard itself.

Among the 29 compounds detected from the melamine-veneered particleboard, 13 (45%) had odorant characteristics. The compounds of greatest concern from this veneer board were benzene, *p*-xylene, butyl acetate, and 2-butano, according to the UL 2821-2013 standard. Those compounds were listed as VOCs from office furniture if measured in greater than 10% of all products. Most of the odors from this type of veneered particleboard were aromatics and esters and, in small amounts, ketones and aldehydes. These aromatics produced the same plant aromas and were listed as being of low toxicity (only *p*-xylene was listed as slightly toxic, whereas naphthalene is moderately toxic). Aromatics were mainly produced by the particleboard itself, from the raw materials of synthetic ester, and from the adhesives and lubricants used in hot pressing. There was only a single compound in the ketone category—acetone—which has a slight toxicity classification, produces spicy odors, and is produced primarily from the adhesives, mundificants, and ester solvents. Esters produce fruity odors with only slight toxicity and are primarily produced by the adhesive solvents, resin solvents, organic solvents, and the particleboard itself. Aldehydes smell like green grass and have a low-toxicity classification. They were derived from the particleboard itself; however, the mass concentration from the aldehydes was greater than that released from the particleboard itself, so it may also be derived from the synthesis of resin in melamine-impregnated paper.

We found no direct correlation between odor intensity and the number of different odorant compounds in either veneered particleboard. A greater concentration of a single odorant compound, however, affected the odor intensity to a certain extent. The extent to which a constitution added to the overall atmosphere is related to the threshold of that species (Sun 2003). When a compound's mass concentration was relatively low, the sensory evaluators might not even perceive it as they would at a higher threshold. For example, the ethyl acetate (which smells fresh and sweet) and the acetic acid 1-methylpropyl ester (which smells like fresh and sweet fruit) from the melamine-veneered particleboards, which obviously have odor characteristics, were not detected at low mass concentrations.

Effect of Particleboard Thickness on VOCs and Odor Release

Figure 2 shows the TVOC and total odor intensity released by the different thicknesses of particleboard with PVC and melamine veneer coatings were basically the same. In the early stage, the TVOC and total odor intensity reached their maximum values; then, they decreased over time until a stable phase was achieved. The VOC concentrations decreased sharply on d 1 to d 7; after which, the rate of the decline slowed. That trend was due to the larger concentration difference between the VOCs and the external environment during the early release. According to the theory of mass transfer, the VOCs inside the particleboard plate continue to off-gas until the concentration difference disappears (Liu et al. 2017). The TVOC and total odor intensity for the two types of veneer studied were all less than particleboard itself with the same thickness. In the initial stages, PVC and melamine veneers effectively prevent the release of VOCs and odor from the particleboard, but over time, those distinctions gradually diminish, until no difference is seen between the veneers and the particleboard alone.

The TVOC and total odor intensity increases as the thickness of the particleboard increased. Compared with the TVOC, the increasing trend from the total odor intensity was not large. In the early stages, the TVOC and total odor intensity from 18-mm-thick PVC-veneered particleboard was greater than it was from the 8-mm-thick PVC-veneered particleboard at about $106.53 \mu\text{g m}^{-3}$ and $0.75 \mu\text{g m}^{-3}$, respectively. The TVOC and total odor intensity of 18-mm-thick melamine-veneered particleboard was stronger than it was for 8-mm-thick melamine-veneered particleboard at about $113.73 \mu\text{g m}^{-3}$ and $0.5 \mu\text{g m}^{-3}$, respectively. When the emissions reached a plateau, the TVOC and total odor intensity of 18-mm-thick PVC-veneered particleboard were still more than they were in the 8-mm-thick boards at about $31 \mu\text{g m}^{-3}$ and $0.5 \mu\text{g m}^{-3}$, respectively. The TVOC of 18-mm-thick melamine-veneered particleboard was greater than it was for the 8-mm-thick board at about $12.72 \mu\text{g m}^{-3}$, whereas the total odor intensity remained the same. Substrate thickness produced those results, with the 18-mm-thick particleboard emitting more VOCs than 8-mm-thick board did (Sun 2011). The veneer prevented the release of only some of the particleboard gases, but because of the void structure within the veneer, it could not completely deter their release. The amount off-gassing from particleboard at various thicknesses was greater than it was for veneered particleboard. In their initial state, the concentration difference between two different thicknesses of particleboard was $549.69 \mu\text{g m}^{-3}$, whereas the concentration difference from two different thicknesses for the PVC-veneered particleboard was $106.53 \mu\text{g m}^{-3}$ and was $113.73 \mu\text{g m}^{-3}$ from the melamine surface. Similarly, at equilibrium, the concentration differences between the two different thicknesses of particleboard was $92.91 \mu\text{g m}^{-3}$, whereas the difference in the thickness of PVC veneer was $31.00 \mu\text{g m}^{-3}$ and was $12.72 \mu\text{g m}^{-3}$ for the melamine surface.

VOCs and Odors Released From Two Types Of Veneered Particleboards

Figure 3 shows the percentage of TVOC and total odor intensity in the initial and stable phases of PVC- and melamine-veneered particleboard. The gases released from the particleboard with a PVC veneer included aromatics, alkanes, ketones, esters, alcohols, aldehydes, and alkenes; among which, aromatics, ketones, esters, alcohols, and aldehydes had odorant characteristics. The gases released from melamine-veneered particleboard included aromatics, alkanes, ketones, esters, aldehydes, and alkenes; among which, aromatics, ketones, esters, and aldehydes had odorant characteristics.

For the PVC-veneered particleboards, over time, the odorant compounds emitted were esters and ketones, which decreased, whereas the release of alcohols and aldehydes strengthened over time. Aromatics showed little change in odor intensity over time. In a state of equilibrium, the proportion of VOC components, from most to least, were esters (34.26%), aromatics (16.98%), alkanes (14.16%), ketones (13.26%), alcohols (11.48%), and aldehydes (9.86%) from the PVC veneer. The proportion of gases with odor components, from most to least were esters (50.26%), aromatics (15.29%), ketones (13.11%), alcohols (11.48%), and aldehydes (9.86%).

For melamine-veneered particleboards, emissions of aromatics decreased over time, whereas the release of ketones, esters, and aldehydes increased somewhat. In a state of equilibrium, the proportion of VOC components, from most to least, were aromatics (59.58%), esters (26.58%), aldehydes (7.26%), and ketones (6.58%). The proportions of gases with odor components, most to least, were aromatics (44.25%), esters (20.01%), aldehydes (14.89%), alkanes (12.58%), and ketones (8.27%).

CONCLUSIONS

PVC- and melamine-veneered particleboards were analyzed by GC-MS-O in this experiment. The results showed that the primary odor emissions released from PVC particleboards were aromatics, ketones, and esters, whereas the melamine particleboard off-gassed aromatics and esters. Both the TVOC and the odor intensity increased with thicker particleboards, even when coated with either veneer. The release characteristics of TVOC and total odor intensity from PVC and melamine particleboards remained consistent with the different thicknesses. In the early stage, the TVOC and total odor intensity was greatest, and over time, those values gradually decreased until a state of equilibrium was reached. Both veneers slowed the release of gas from the particleboard, but because of the void structure of veneers, they could not completely prevent the release. Thickness had a greater effect on the particleboard itself than it did on the veneered particleboard. There was no direct correlation between odor intensity and the number of different odorant compounds, but, for any particular odorant compound, its concentration affected the odor intensity somewhat. Over time (28 d), the off-gassing of esters and ketones from the PVC particleboard weakened, whereas the release of alcohols and

**Proceedings of the 62nd International Convention of
Society of Wood Science and Technology
October 20-25, 2019 – Tenaya Lodge, Yosemite, California USA**

aldehydes increased. The release of aromatic compounds changed little with time. For the melamine particleboard, the aromatic compounds weakened over time, whereas the release of ketones, esters, and aldehydes increased.

LIST OF FIGURES

Figure 1. Odor–time intensity spectrum from particleboard and two types veneered particleboard. (a) Particleboard. (b) Particleboard with polyvinyl chloride (PVC) veneer. (c) Particleboard with melamine veneer.

Figure 2. The trends in total volatile organic compound (TVOC) and odors released from different thicknesses of particleboard coated with polyvinyl chloride (PVC) and with melamine. (a) TVOC of PVC-veneered particleboard. (b) Total odor intensity from PVC-veneered particleboard. (c) TVOC from melamine-veneered particleboard. (d) Total odor intensity from the melamine-veneered particleboard

Figure 3. The percentage of various constituents of the gases released from polyvinyl chloride (PVC) and melamine particleboard and the mass concentration of the odorant substances during the initial and stable phases (a) Volatile organic compounds (VOC) from PVC-coated particleboard. (b) Odorant components from PVC-veneered particleboard. (c) VOC compounds from melamine particleboard. (d) Odorant components from the melamine particleboard.

REFERENCES

- Acree TE, Barnard J, Cunningham DG (1984) A procedure for the sensory analysis of gas chromatographic effluents. *Food Chem* 14(4):273-286.
- Acree TE, Butts RM, Nelson PR, Lee, CY (1976) Sniffer to determine the odor of gas chromatographic effluents. *Anal Chem* 48(12):1821-1822.
- Bulliner EA, Koziel JA, Cai LS, Wright, D (2006) Characterization of livestock odors using steel plates, solid-phase microextraction, and multidimensional gas chromatography-mass spectrometry-olfactometry. *J Air Waste Manag Assoc.* 56(10):1391-1403.
- Choi HS (2005) Characteristic odor components of kumquat (*Fortunella japonica* Swingle) peel oil. *J Agric Food Chem* 53(5):1642-1647.
- Cotte VME, Prasad SK, Wan PHW, Linforth, RST, Taylor, AJ (2010) Cigarette smoke: GC-Olfactometry analyses using two computer programs. Pages 498-502 in I Blank, M Wüst, C. Yeretziyan, eds. *Expression of Multidisciplinary Flavour Science–Proc 12th Weurman Symposium, July 2008, Interlaken, Switzerland.* Zürcher Hochschule für Angewandte, Wissenschaften, Winterthur.
- Dharmawan J, Kasapis S, Sriramula P, Lear MJ, Curran P. (2009) Evaluation of aroma-active compounds in Pontianak orange peel oil (*Citrus nobilis* Lour. Var. *micropa* Hassk) by gas chromatography-olfactometry, aroma reconstitution, and omission test. *J Agric Food Chem* 57(1):239-244.
- Frank CO, Owen CM, Patterson J. (2004) Solid phase microextraction (SPME) combined with gas-chromatography and olfactometry-mass spectrometry for characterization of cheese aroma compounds. *LWT Food Sci Technol* 37(2):139-154.
- Fuller GH, Stellencamp R, Tisserand GA. (1964) The gas chromatograph with human sensor: perfumer model. *Ann N Y Acad Sci.* 116:711-724.
- Gómez-Miguez MJ, Cacho JF, Ferreira V, Vicario IM, Heredia FJ (2007) Volatile components of Zalema white wines. *Food Chem* 100(4):1464-1473.
- Greenguard Environmental Institute (2006) Standard Method for Measuring and Evaluating Chemical Emissions From Building Materials, Finishes and Furnishings Using Dynamic Environmental Chambers. GG Publications UL 2821-2013, Marietta, GA.
- Hsu CS, Shi Q. (2013) Prospects for petroleum mass spectrometry and chromatography. *Sci. China Chem.* 56(7):833-839.

**Proceedings of the 62nd International Convention of
Society of Wood Science and Technology
October 20-25, 2019 – Tenaya Lodge, Yosemite, California USA**

- Klepeis NE, Nelson WC, Ott WR, Robinson JP, Tsang AM, Switzer P, Behar JV, Hern SC, Engelmann WH (2001) The National Human Activity Pattern Survey (NHAPS): A resource for assessing exposure to environmental pollutants. *J Expo Anal Environ Epidemiol* 11(3): 231-252.
- Liu WJ, Shen J, Wang QF (2017) Design of DL-SW micro-cabin for rapid detection and analysis of VOCs from wood-based panels. *J For Eng* 2(4):40-45. In Chinese.
- Maarse H, van der Heij DG, eds. (1994) Pages 211–220 in *Trends in flavour research*, Proc 7th Weurman Flavour Res Symp, 15-18 June 1993, Noordwijkerhout, Netherlands. Elsevier, Amsterdam.
- Machiels D, van Ruth SM, Posthumus MA, Istasse L (2003) Gas chromatography-olfactometry analysis of the volatile compounds of two commercial Irish beef meats. *Talanta* 60(4):755-764.
- Ministry of the Environment. (1971) Law No. 91: Offensive Odor Control Law. Government of Japan, Tokyo, Japan.
- NSAI. National Standards Authority of Ireland. (2003) Air Quality—Determination of Odour Mass Concentration by Dynamic Olfactometry. SN EN 13725-2003. NSAI, Dublin, Ireland.
- Nibbe N (2017) How to select train and maintain a human sensory panel. *In Olfasense: Proc Odour Workshop on Product and Material Testing*. 26-27 January 2017, Kiel, Germany.
- Rabaud N, Ebeler SE, Ashbaugh LL, Flocchini RG (2002) The application of thermal desorption GC/MS with simultaneous olfactory evaluation for the characterization and quantification of odor compounds from a dairy. *J Agric Food Chem*. 50(18):5139-5145.
- Shen XY, Luo XL, Zhu LZ (2001) Progress in research on volatile organic compounds in ambient air. *J Zhejiang Univ (Sci Ed)* 28(5):547-556. In Chinese with abstract in English.
- Sun BG (2003) Edible flavoring surgery. Chemical Industry Publishing House, Beijing, China. In Chinese.
- Sun SJ. (2011) Study on evaluation of the influencing factors for VOC emissions from wood-based panels. MS thesis. Northeast Forestry University, Harbin, China.
- Ullrich F, Grosch W (1987) Identification of the most intense volatile flavor compounds formed during autoxidation of linoleic acid. *Z Lebensm Unters Forsch*. 1987; 184(4):277-282.
- van Den Dool, H., Kratz, PD (1963) A generalization of the retention index system including linear temperature programmed gas-liquid partition chromatography. *J. Chromatogr.* 11:463–470.
- Xia LJ, Song HL (2006) Aroma detecting technique—application of the GC-olfactometry. *Food Ferment Ind.* 32(1):83-87. In Chinese.
- Zhang Q, Wang XC, Liu Y (2009) Applications of gas chromatography-olfactometry (GC-O) in food flavor analysis. *Food Sci* 30(3):284-287.

TABLE 1 Testparameters

Testparameters	Condition
Exposure area /m ²	5.65×10 ⁻³
Cabin volume /m ³	1.35×10 ⁻⁴
Loading rate /(m ² /m ³)	41.85
The ratio of air exchange rate and loading factor /(m ³ ·m ⁻² ·h ⁻¹)	0.5±0.05
Temperature /°C	23±1
Relative humidity /%	40±5

TABLE 2 Odor intensity Criteria (Japan)

Odor intensity	0	1	2	3	4	5
Representation	Odorless	Barely perceptible (Detection threshold)	Slightly perceptible (Identification threshold)	Obvious perceptible	Strong smell	Extremely strong smell

**Proceedings of the 62nd International Convention of
Society of Wood Science and Technology
October 20-25, 2019 – Tenaya Lodge, Yosemite, California USA**

TABLE 3 Main components emitted from two types veneer particleboards and particleboards

Classification	VOCs components of particleboard	VOCs components of PVC veneer particleboard	VOCs components of melamine veneer particleboard
Aromatic compounds	Benzene, Toluene, Ethylbenzene, 1,3-dimethyl-Benzene, Styrene, 1-ethyl-2-methyl-Benzene, propyl-Benzene, 1-ethyl-3-methyl-Benzene, 1-ethyl-4-methyl-Benzene, 1,2,4-trimethyl-Benzene, 1-methyl-2-(1-methylethyl)-Benzene, 1-methylene-1H-Indene, 1,2-Benzisothiazole, hexyl-Benzene, 1-methyl-Naphthalene, Acenaphthene, Fluorene, Phenanthrene, Dibutyl phthalate	Benzene, Toluene, Ethylbenzene, 1,3-dimethyl-Benzene, p-Xylene, 1-ethyl-3-methyl-Benzene, 1-ethyl-4-methyl-Benzene, 1,3,5-trimethyl-Benzene, 1,2,3-trimethyl-Benzene, 1-methylene-1H-Indene, 1-methyl-Naphthalene, Dibenzofuran	Benzene, Toluene, Ethylbenzene, p-Xylene, 1,3-dimethyl-Benzene, 1-ethyl-3-methyl-Benzene, 1-ethyl-4-methyl-Benzene, 1,2,3-trimethyl-Benzene, 1,2,4-trimethyl-Benzene, 1-methyl-3-(1-methylethyl)-Benzene, Naphthalene, 2-methyl-Naphthalene, 1-methyl-Naphthalene, Acenaphthene, Dibenzofuran, Fluorene
Alkanes	hexamethyl-Cyclotrisiloxan, octamethyl-Cyclotetrasiloxane, Undecane, dodecamethyl-Cyclohexasiloxane	dimethoxy-Methane, 3-methylene-Heptane, 2,2,4,6,6-pentamethyl-Heptane, Decane	dimethoxy-Methane, Hexane, Decane, 5-ethyl-2,2,3-trimethyl-Heptane
Ketones	(1S)-1,7,7-trimethyl-Bicyclo[2.2.1]heptan-2-one	Acetone, 2-Butanone, Methyl Isobutyl Ketone, 2-methyl-Cyclopentanone, (1S)-1,7,7-trimethyl-Bicyclo[2.2.1]heptan-2-one	Acetone, Cyclohexanone, (1S)-1,7,7-trimethyl-Bicyclo[2.2.1]heptan-2-one
Esters	Acetic acid, butyl ester	2-methyl-2-Propenoic acid, methyl ester, Acetic acid, 1-methylpropyl ester, Acetic acid, 2-methylpropyl ester Acetic acid, butyl ester, 2-Pentanol, acetate, 2-methyl-2-Propenoic acid, butyl ester, Ethyl Acetate	Ethyl Acetate, Acetic acid, 1-methylpropyl ester, Acetic acid, 2-methylpropyl ester, Acetic acid, butyl ester, 2-Pentanol, acetate
Alcohols	2-ethyl-1-Hexanol	2-Butanol, 2-methyl-1-Propanol	-
Aldehydes	Hexanal, Nonanal	Hexanal	Hexanal
Alkenes	(ñ)-2,6,6-trimethyl-Bicyclo[3.1.1]hept-2-ene, D-Limonene	2-Butene, 3,6,6-trimethyl-Bicyclo[3.1.1]hept-2-ene	Copaene

**Proceedings of the 62nd International Convention of
Society of Wood Science and Technology
October 20-25, 2019 – Tenaya Lodge, Yosemite, California USA**

TABLE 4 Composition of odorant compounds of particleboard

Compounds	Retention time(RT)	Retention index(RI)	Mass concentration/ $\mu\text{g}\cdot\text{m}^{-3}$	Odor character	Odor intensity
Aromatic compounds					
Benzene	6.42	642	4.56	Burnt	1
Ethylbenzene	15.00	849	187.25	Aromatic	1
1,3-dimethyl-Benzene	15.46	858	152.56	Aromatic, sweet	2
Styrene	16.37	875	101.16	Charcoal, cream	3
1-ethyl-2-methyl-Benzene	18.25	912	2.42	Mixed smell	0
1,2,4-trimethyl-Benzene	21.38	981	4.15	Aromatic	0
1-methylene-1H-Indene	28.13	1165	75.60	Bitter, oil	2
1-methyl-Naphthalene	31.67	1340	9.44	Wheat	1
Aldehyde					
Hexanal	11.20	775	6.25	Sweet	2
Nonanal	25.43	1085	3.31	Oil, flower, fresh	1
Esters					
Acetic acid, butyl ester	12.39	800	20.47	Fresh and sweet fruit	1
Alkenes					
D-Limonene	23.09	1023	3.36	Lemon	0

TABLE 5 Acute toxicity classification of compounds by World Health Organization

Toxicity classification	Rats orally LD50 (mg/kg)	Rats inhalation and dead 1/3-2/3 in 4 hours	Rabbit transdermal LD50 (mg/kg)
Severe toxicity	≤ 1	≤ 10	≤ 5
Highly toxicity	1-50	10-100	5-43
Moderate toxicity	51-500	101-1000	44-350
Low toxicity	501-5000	1001-10000	351-2180
Slight toxicity	5001-15000	10001-100000	2181-22590
Non-toxic	>15000	>100000	>22600

**Proceedings of the 62nd International Convention of
Society of Wood Science and Technology
October 20-25, 2019 – Tenaya Lodge, Yosemite, California USA**

TABLE 6 Composition of odorant compounds from PVC veneer particleboards

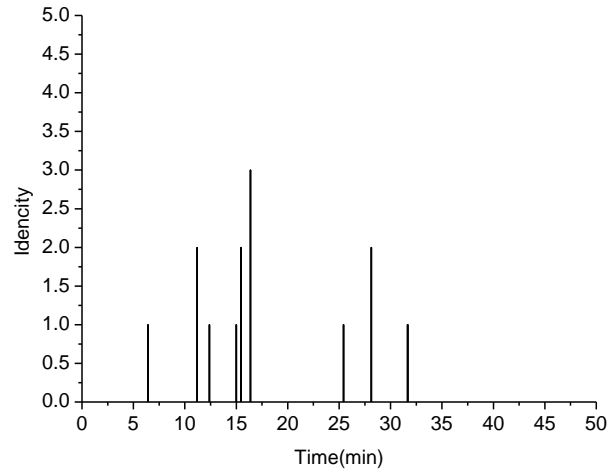
Compounds Retention Time	Retenti on index(RI)	Mass concentr ation/ $\mu\text{g}\cdot$ m^{-3}	Toxicity classificati on	Odor character	Odor intensit y	Possible sources
Aromatic compounds						
Benzene	5.05	3.73	Low toxicity	Burnt	0.5	Particleboard emission
1,3-dimethyl-Benzene	13.55	43.00	Low toxicity	Fresh	1	Particleboard emission
p-Xylene	13.63	13.62	Slight toxicity	Pungent, aromatic	0	PVC film coating agent and adhesive
1,3,5-trimethyl-Benzene	19.88	4.63	Low toxicity	Mixed smell	1.75	Stabilizer of polyester resin
1-methylene-1H-Indene	27.32	9.53	Low toxicity	Bitter, oil	0	Particleboard emission
1-methyl-Naphthalene	30.90	4.55	Low toxicity	Wheat	1	Particleboard emission
Dibenzofuran	38.36	2.41	Low toxicity	Almond, licorice	0	High temperature lubricant in the preparation of PVC
Ketones						
Acetone	3.34	6.39	Slight toxicity	Special spicy	0	Adhesive mundificant
2-Butanone	4.11	7.27	Low toxicity	Pungent, spicy, sweet	2	Adhesive mundificant
Methyl Isobutyl Ketone	6.97	64.00	Low toxicity	Pleasant fragrance	1.25	Adhesive
2-methyl-Cyclopentanone	14.96	92.44	Low toxicity	Soil	1	Solvent
Esters						
Acetic acid, 1-methylpropyl ester	7.60	330.67	Slight toxicity	Fresh and sweet fruit	0.75	Preparation of PVC
Acetic acid, 2-methylpropyl ester	8.30	1.20	Slight toxicity	Fresh and sweet fruit	0	Preparation of PVC
Acetic acid, butyl ester	10.27	18.38	Slight toxicity	Fresh and sweet fruit	0	Particleboard emission, organic solvent
Ethyl Acetate	4.31	5.84	Slight toxicity	Fresh and sweet	0	Adhesive solvent
Alcohols						
2-Butanol	4.19	1.38	Low toxicity	Sour, bitter	0	Adhesive mundificant, PVC plasticizer and cosolvent
Aldehydes						
Hexanal	9.50	5.10	Low toxicity	Grass	0	Particleboard emission

**Proceedings of the 62nd International Convention of
Society of Wood Science and Technology
October 20-25, 2019 – Tenaya Lodge, Yosemite, California USA**

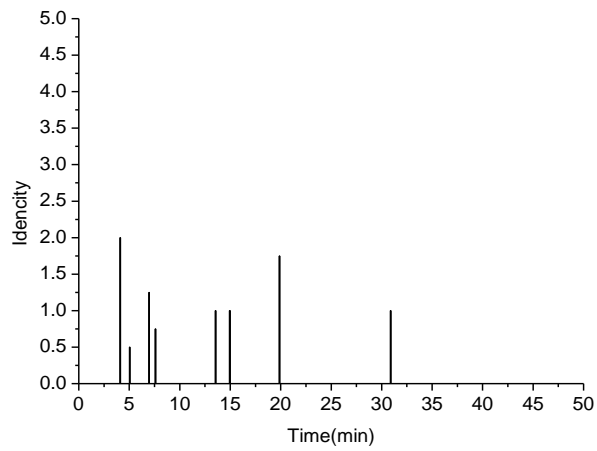
TABLE 7 Composition of odorant compounds from melamine veneer particleboards

Compounds Retention Time	Retention index(RI)	Mass concentration/ $\mu\text{g}\cdot\text{m}^{-3}$	Toxicity classification	Odor character	Odor intensity	Possible sources
Aromatic compounds						
Benzene	5.06	8.91	Low toxicity	Burnt	0.75	Particleboard emission, additive
Ethylbenzene	13.05	104.30	Low toxicity	Aromatic	0	Particleboard emission
p-Xylene	13.57	133.95	Slight toxicity	Pungent, aromatic	1	Adhesive
1,3-dimethyl- Benzene	14.84	80.79	Low toxicity	Fresh	0.75	Particleboard emission
Naphthalene	27.33	69.56	Moderate toxicity	Fresh, bitterness of plants, sour	1.75	Raw material of resin
1-methyl- Naphthalene	31.39	15.16	Low toxicity	Wheat	1	Particleboard emission
Dibenzofuran	38.35	11.42	Low toxicity	Almond, licorice	1	Lubricant
Ketones						
Acetone	3.36	16.28	Slight toxicity	Special spicy	0	Adhesive mundificant, Resin solvent
Esters						
Ethyl Acetate	4.33	10.65	Slight toxicity	Fresh and sweet	0	Adhesive solvent
Acetic acid, 1- methylpropyl ester	7.65	27.72	Slight toxicity	Fresh and sweet fruit	0	Resin solvent
Acetic acid, 2- methylpropyl ester	8.33	5.03	Slight toxicity	Fresh and sweet fruit	0	Resin solvent
Acetic acid, butyl ester	10.32	77.10	Slight toxicity	Fresh and sweet fruit	0.5	Particleboard emission, organic solvent
Aldehydes						
Hexanal	9.53	16.58	Low toxicity	Grass	1	Particleboard emission, Synthesis of resin

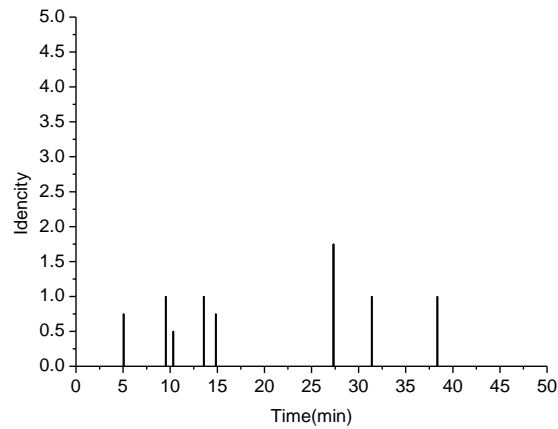
FIGURE 1



(a)

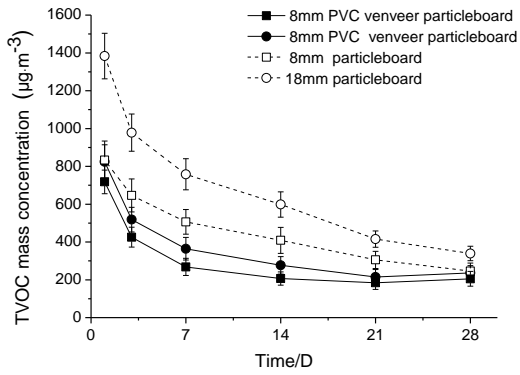


(b)

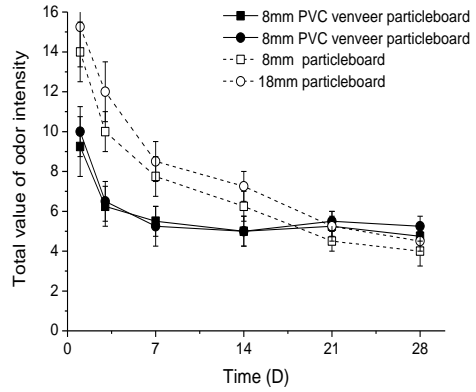


(c)

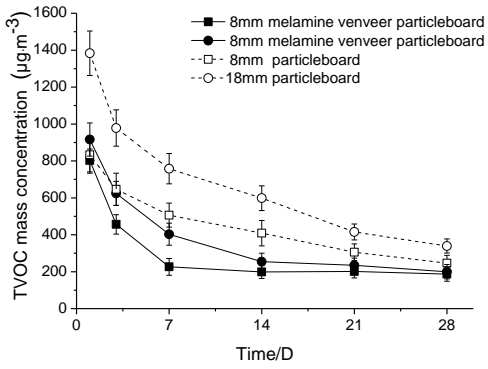
FIGURE 2



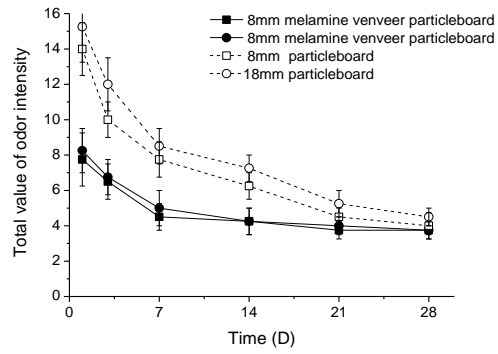
(a)



(b)

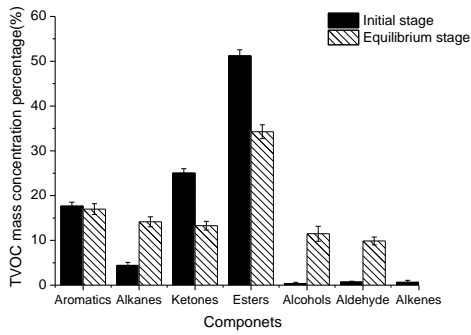


(c)

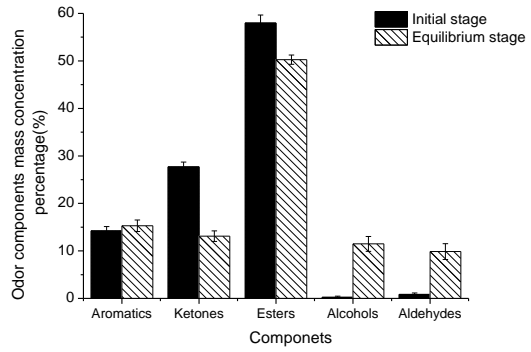


(d)

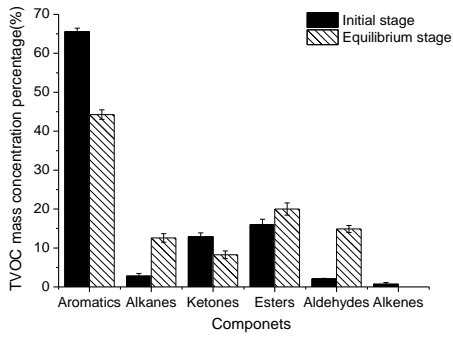
FIGURE 3



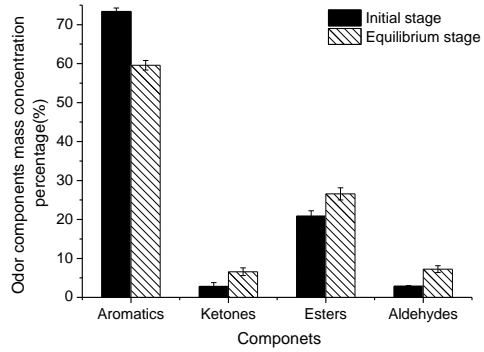
(a) VOCs component of PVC particleboards



(b) Odorant Components of PVC particleboards



(c) VOCs component of melamine particleboards



(d) Odorant Components of melamine particleboards

Effects of Pyrolysis Temperature on Properties of Cardboard Biochar and the Resulting Biochar/high density Polyethylene Composites

Xiaoqian Wang

Beijing Forestry University

Beijing, China

Abstract

Municipal solid waste (MSW) has become a serious environmental issue because of the increase of waste quantities and sustainable waste management. Thermal conversion is a feasible solution to treat MSW (especially packing and paper materials) into value added products or energy. Corrugated cardboard (CCB) is a common packing material, which consists mainly of hemicellulose and cellulose. Pyrolysis is a thermochemical decomposition process applied to organic materials (biomass) which can be converted into a carbon-rich solid (biochar) and volatile matter (bio-oil and gases) by heating in the absence of oxygen. Biochar is widely used due to its distinctive characteristics (high adsorption capacity, high ion exchange, high carbon sequestration, etc.). Moreover, biochar is thermally stable and hydrophobic; therefore, a good candidate as a reinforcing filler in polymer matrix.

In this study, CCB was pyrolyzed at 350, 400, and 450 °C to produce biochars. The chemical features, fiber length, thermal stability, proximate analysis for biochars were determined. The original CCB and biochars were compounded with high density polyethylene (HDPE) and the composites properties (thermal, tensile, water soak, rheological, weatherability and biodurability) were determined. The CCB composite melts showed higher modulus and viscosity than biochar composites. Compared with CCB composites, an increase of tensile strength (4%) and tensile modulus (30%) could be observed in CCB350 composite. In addition, the CCB350 composite showed lower $\tan \delta$ and adhesion factor, indicating strong interfacial interaction between CCB350 particles and HDPE. The degree of HDPE crystallinity in the biochar composites decreased relative to the CCB composites, while the thermal properties of the composites improved. The CCB composite displayed the highest water absorption (3.9%) and thickness swell (3.8%). CCB450 composite experienced the least color change, lightness and carbonyl concentrations due to weathering. Pyrolysis of CCB reduced the weight loss in the resulting composites exposed to fungi compared with the CCB composite.

Monday, October 21st

Impact of Forest Disturbances on Wood Quality

11:00-12:30

Chair: Scott Leavengood, Oregon State University, USA

**Evaluating the role of Europe’s wood value chain in the circular bio-economy:
the WoodCircus project**

Mike Burnard

InnoRenew CoE and University of Primorska, Slovenia

Abstract

As demand for structures grows worldwide and the need to limit their environmental impact has become critical, increasing pressure is placed on renewable resources to supply the material necessary to support a growing and urbanizing population. To address these demands there is a need to understand current best practices and identify areas of improvement for forest sector companies to improve their resource efficiency. A new project was developed to examine the role of the wood value chain in the circular economy: the “Underpinning the vital role of the forest-based sector in the Circular Bio-Economy” (WoodCircus). The WoodCircus project is a Horizon 2020 project coordinated by VTT (Finland) with a consortium of 7 research organisations, 7 companies, and 3 European associations from 7 countries. The project was created to identify and study best practices and develop policy recommendations, business strategies, and identify research, development, technology, and innovation (RTDI) priorities for the forest sector to solidify its strong role in the circular bio-economy. The WoodCircus project emphasizes the role of the construction sector and examines practices, conducts environmental impact assessments, and builds a lasting network of international stakeholders to carry the project work forward after the end of the project. The main outputs of the project are a best practices database, a policy white paper, a RTDI plan for companies and researchers, and a well-established network of stakeholders. The policy and RTDI implications of the current state of the art will be presented, along with up-to-date information about the project outputs.

Comparison of juvenile wood depictions to wood property maps from mature longleaf pine

Thomas L. Eberhardt^{1} – Chi-Leung So² – Daniel J. Leduc³ – Joe Dahlen⁴*

¹ Research Scientist and Project Leader, USDA Forest Service, Forest Products Laboratory, Madison, WI, USA * *Corresponding author*
thomas.l.eberhardt@usda.gov

² Consultant, Cenla Wood Science, Pineville, LA, USA
chi.so@usda.gov

³ Statistician, USDA Forest Service, Southern Research Station, Pineville, LA, USA
daniel.leduc@usda.gov

⁴ Associate Professor, University of Georgia, Warnell School of Forestry and Natural Resources, Athens, GA, USA
jdahlen@uga.edu

Abstract

Early illustrations of juvenile wood in hard pines have depicted a central core of wood, varying little by diameter or cambial age, to be nested within mature wood tapering to the upper portion of the stem; other depictions show greater complexity in attributing the variability of this central core of wood with its proximity to the crown and/or actual maturity of the tree when the wood was formed. The present discussion addresses the degree to which different representations of juvenile wood (corewood) are applicable to mature longleaf pine (*Pinus palustris* Mill.) trees. Wood property maps were derived from X-ray densitometry data gathered from different tree heights. Results suggest that the more complex illustrations of juvenile wood appear to align with the study trees, attributable in part to their maturity, and near maximum attainable height.

Key words: Corewood, juvenile wood, mature wood, southern pine, wood properties

Introduction

Juvenile wood (corewood) has been widely studied given its high contribution to the wood resource, especially for usable timber obtained at short rotation ages. Reviews of juvenile wood in the literature provide insight into its physiological origin, anatomical features, properties (e.g., chemical, physical) and utilization (Zobel and van Buijtenen 1989; Zobel and Sprague 1998; Larson et al 2001; Lachenbruch et al 2011; Moore and Cown 2017). Juvenile wood is

commonly shown as a central core of wood within mature wood tapering to the upper portion of the stem (Fig. 1a). Taking into account that wood juvenility may be attributed to the proximity to the tree crown when formed, Lachenbruch et al (2011) provides a novel illustration (Fig. 2b) showing nested growth rings shown as being juvenile near the crown, but maturing as they progress down the bole of the tree to its base. An illustration put forth by Kibblewhite (1999) shows even greater complexity in attributing the variability of this zone of wood with its proximity to the crown and/or actual maturity of the tree when the wood was formed; thus, juvenile wood terminology being reserved for that wood formed when the tree itself was of a juvenile age (Fig. 1c).

Wood property data gathered at different heights and radial positions have been used to generate tree maps that generally show a central core of wood that is lower in specific gravity (SG) from the base of the tree to the top. The reader is referred to maps reported in the literature (Auty et al 2014; Dahlen et al 2018; Longuetaud et al 2016; Schimleck et al 2018). A few tree maps depict variability in the central core with respect to tree height for individual trees (Trendelenburg 1935; Downes et al 2009); trees used for these two studies were well over 100 years in age. The objective of this report is expand upon the discussion of wood properties from a sampling of mature longleaf pine (*Pinus palustris* Mill.) trees in the context of the aforementioned illustrations of juvenile and mature wood zones.

Materials and Methods

Ten 70-year-old longleaf pine trees covering a range of diameters at breast height (14.5 to 49.8 cm) and total heights (17.6 to 27.5 m) were sampled in the Palustris Experimental Forest, Alexandria, LA, USA. Tree-specific data and the experimental procedures can be found in Eberhardt et al. (2018, 2019). Briefly, all study trees were marked to retain the northern and southern cardinal directions on 5-cm-thick disks cut at stump height (15 cm), followed by 77 cm above ground level, then every 61 cm along the tree bole. Densitometry afforded bark to pith data that were processed to provide wood property data (e.g., ring SG) and width for each growth ring. To create the wood property maps, the actual position for each data point was converted to a relative position in each tree. These positions were rounded to the nearest 0.05 increment and a mean parameter value was then calculated for each point across all of the sample trees. Further details and references for the generation of the maps can be found in Eberhardt et al. (2019).

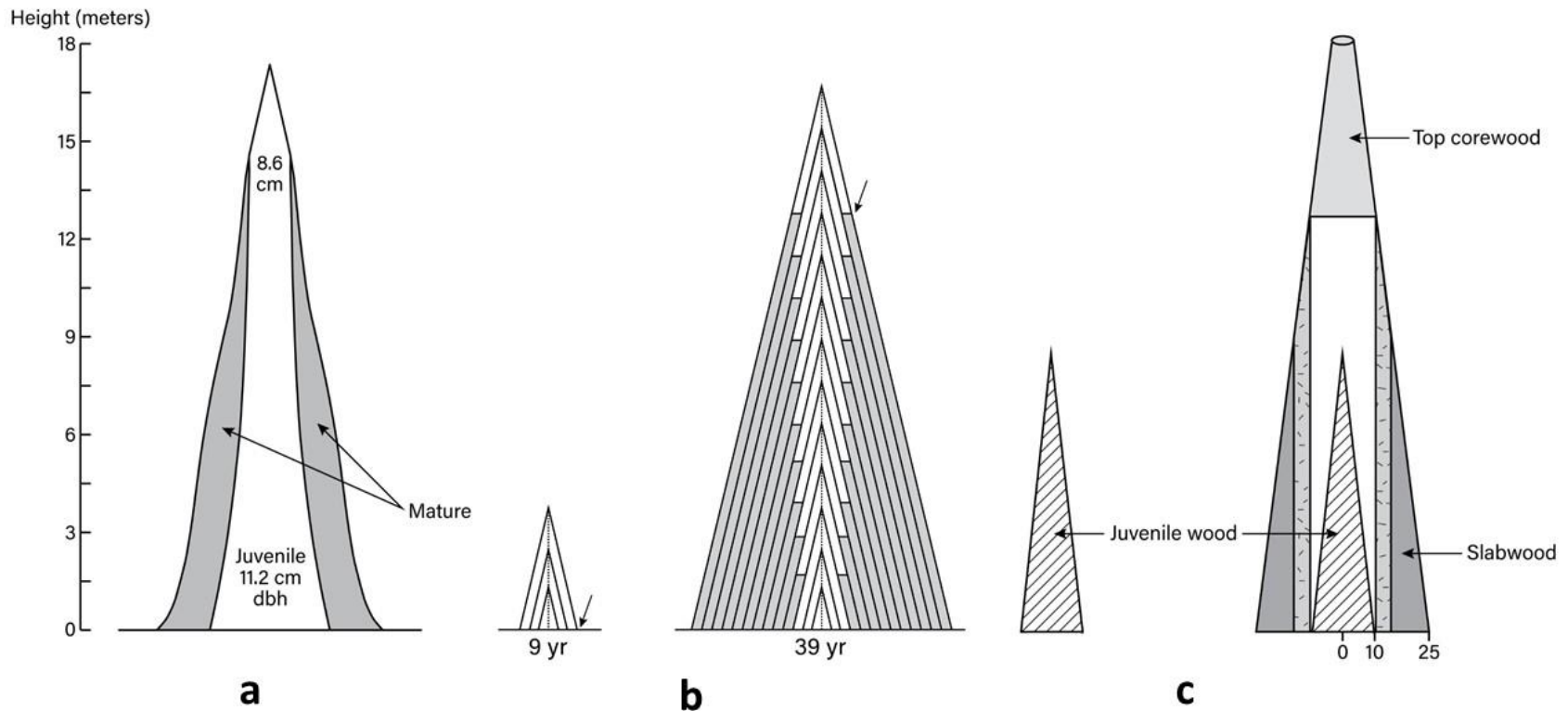


Figure 1: Illustrations of juvenile wood adapted/redrawn from the literature: a, Zobel and Blair (1976); b, Lachenbruch et al. (2011); c, Kibblewhite (1999).

Results and Discussion

Similar to other maps of the southern pines, either based on single trees, averaged data among many trees, or models representative of even larger groups of trees, the map in Figure 2a shows a central core of lower density wood ($SG < 0.475$) running the length of the tree bole. This essentially continuous zone of lower SG wood, that may be attributed to juvenile wood (corewood), supports the illustrations by Zobel and Blair (1976) and Lachenbruch et al. (2011) shown in Figures 1a and 1b, respectively. Also similar to these illustrations, the mature wood tapers to the upper regions of the stem; however, in the tree map the zone of lower SG wood does not extend from the pith to the bark at the top of the tree. In other words, similar to the lower relative heights, ring SG increases moving from pith to bark over the tree map profile.

Also, it is readily apparent in the tree map that there is zone of lower SG wood that is wider at mid-height than at the lower and higher relative heights. This observation is not restricted to mature longleaf pine, with a zones of low SG wood near the mid-height being wider for loblolly pine at relatively young ages of 13 and 22 years (Schimleck et al 2018). Such observations do not invalidate the juvenile wood illustrations but instead demonstrate that more complex density profiles for specific groupings of trees may be present and measurable.

Typical of other tree maps reported in the literature, there is higher ring SG wood towards the base of the tree; however, in said tree SG maps, this does not extend all the way to the wood closest to the bark. In the tree map shown here (Fig. 2a) this pattern is more consistent with density traces taken at breast height where ring SG increases through juvenile wood formation, plateaus in the mature wood zone, and declines in the wood close to the bark (Eberhardt and Samuelson 2015; Jordan et al 2008; Spurr and Hsiung 1954). Also of interest is the fairly symmetrical regions of high ring SG above the relative height of 0.7. This observation is consistent with Kibblewhite's (1999) illustration (Fig. 1c) showing the wood in the crown (so called "top corewood") to be different than the juvenile wood zone at the base of the tree, and have properties similar to mature wood.

For the study trees, the average top disk diameter was 2.8 cm and the average number of rings included was 7. Indeed, ring widths within the juvenile core (ca. ≤ 7 annual rings) are quite narrow well into the top of the tree crown. Thus, the tree map for ring width shows narrow rings at the top of the tree and extending down the bole to the base, in the outermost zone of wood near the bark. Superficially this may seem to be contradictory to what we know about southern pine wood quality, with narrow rings and higher ring SG as a feature normally associated of higher wood quality in the mature wood zone; however, since the study trees are mature and near their maximum attainable height, it can be easily rationalized that ring widths would be narrow at the top, and extending down the mature wood to the base. A parallel can be drawn to the illustration by Lachenbruch et al. (2011), with the outermost growth ring extending from the top of the tree to the base, irrespective any maturation that may occur with increasing distance from the crown. Altogether, the tree maps generated here for a group of

***Proceedings of the 62nd International Convention of
Society of Wood Science and Technology
October 20-25, 2019 – Tenaya Lodge, Yosemite, California USA***

mature longleaf pines appear to support tree profile put forth by Kibblewhite (1999). Finally, the more recent conceptualization of juvenile wood has been described by Burdon et al (2004) is not provided

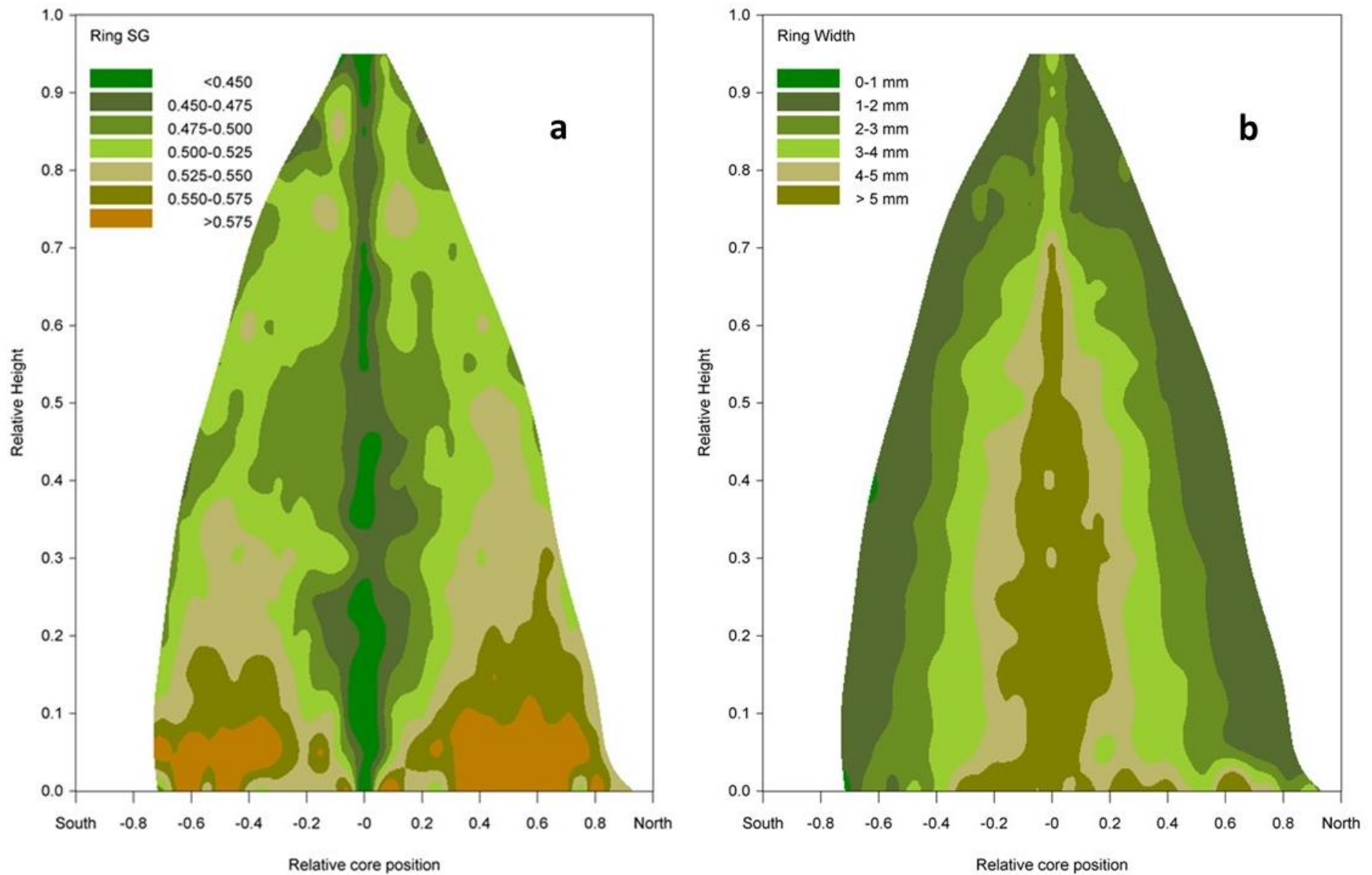


Figure 2: Wood property maps for mature longleaf pine: a, ring specific gravity (SG); b, ring width.

***Proceedings of the 62nd International Convention of
Society of Wood Science and Technology
October 20-25, 2019 – Tenaya Lodge, Yosemite, California USA***

here, but parallels that by Kibblewhite (1999) having the central core of wood (≤ 10 growth rings) maturing from the base of the tree to the top.

Summary and Conclusions

Results suggest that the more complex illustrations of juvenile wood appear to align with the study trees, attributable in part to their maturity, and near maximum attainable height.

Acknowledgements

Karen K. Nelson at the UDSA Forest Service, Forest Products Laboratory, skillfully prepared the illustrations of juvenile wood redrawn/adapted from those in the literature.

References

- Auty D, Achim A, Macdonald E, Cameron AD, Gardiner BA (2014) Models for predicting wood density variation in Scots pine. *Forestry* 87:449-458.
- Burdon RD, Kibblewhite RP, Walker JCF, Megraw RA, Evans R, Cown DR (2004) Juvenile versus mature wood: A new concept, orthogonal to corewood versus outerwood, with special reference to *Pinus radiata* and *Pinus taeda*. *Forest Sci* 50(4):399-415.
- Dahlen J, Montes C, Eberhardt TL, Auty D. 2018. Probability models that relate nondestructive test methods to lumber design values of plantation loblolly pine. *Forestry* 91:295-306.
- Downes GM, Drew D, Battaglia M, Schulze D (2009) Measuring and modelling stem growth and wood formation: An overview. *Dendrochronologia* 27:147-157.
- Eberhardt TL, Samuelson LJ (2015) Collection of wood quality data by X-ray densitometry: A case study with three southern pines. *Wood Sci Technol* 49:739-753.
- Eberhardt TL, So C-L, Leduc DJ (2018) Wood variability in mature longleaf pine: Differences related to cardinal direction for a softwood in a humid subtropical climate. *Wood Fib Sci* 50(3):323-336.
- Eberhardt TL, So C-L, Leduc DJ (2019) Wood property maps showing wood variability in mature longleaf pine: does getting old change juvenile tendencies. *Wood Fib Sci* 51(2):193-208.
- Jordan L, Clark A III, Schimleck LR, Hall DB, Daniels RF (2008) Regional variation in wood specific gravity of planted loblolly pine in the United States. *Can J For Res* 38:698-710.

*Proceedings of the 62nd International Convention of
Society of Wood Science and Technology
October 20-25, 2019 – Tenaya Lodge, Yosemite, California USA*

Kibblewhite RP (1999) Designer fibres for improved papers through exploiting genetic variation in wood microstructure. *Appita J* 52(6):429-435.

Lachenbruch B, Moore JR, Evans R (2011) Radial variation in wood structure and function in woody plants, and hypotheses for its occurrence. In: *Size- and Age-Related Changes in Tree Structure and Function*. FC Meinzer, B Lachenbruch, TE Dawson, Eds. Springer: Berlin, Germany. pp. 121-164.

Larson PR, Kretschmann DE, Clark A III, Isebrands JG (2001) Formation and properties of juvenile wood in the southern pines: A synopsis. USDA Forest Service, For. Prod. Lab. Gen. Tech. Rep. FPL-GTR-129, 42 pp.

Longuetaud F, Mothe F, Fournier M, Dlouha J, Santenoise P, Deleuze C (2016) Within-stem maps of wood density and water content for characterization of species: a case study on three hardwood and two softwood species. *Ann For Sci* 73:601-614.

Moore JR, Cown DJ (2017) Corewood (juvenile wood) and its impacts on wood utilization. *Curr Forestry Rep* 3:107-118.

Schimleck L, Antony F, Mora C, Dahlen J (2018) Comparison of whole-tree wood property maps for 13- and 22-year-old loblolly pine. *Forests* 9:287

Spurr SH, Hsiung W-Y (1954) Growth rate and specific gravity in conifers. *J For* 52(3):191-200.

Trendelenburg R (1935) Schwankungen des Raumgewichts wichtiger Nadelhölzer nach Wuchsgebiet, Standort und Einzelstamm. *Zeitschrift des Vereines deutscher Ingenieure* 79(4):85-89 [in German].

Zobel B, Blair R (1976) Wood and pulp properties of wood and topwood of the southern pines. *Appl Polym Symp* 28:421-433.

Zobel BJ, Sprague JR (1998) *Juvenile Wood in Forest Trees*. Springer-Verlag, Berlin. 300 pp.

Zobel BJ, van Buijtenen JP (1989) *Wood Variation: Its Causes and Control*. Springer-Verlag, Berlin. 363 pp.

Life cycle assessment of mass timber building structural system

Shaobo Liang¹, Hongmei Gu², Rick Bergman², Steve Kelley¹

¹Department of Forest Biomaterials North Carolina State University Raleigh, NC 27695, USA

²USDA Forest Service, Forest Products Laboratory, Madison, WI 53726 USA

Abstract

The use of mass timber as a building material has become increasingly prevalent in the world building sector. Mass timber products including cross laminated timber (CLT), glulam, and nail laminated timber have been demonstrated as green building materials with a lower carbon footprint than their concrete and steel alternatives. The use of mass timber brings improved sustainability metrics and efficient construction processes to the building industry. Using mass timber products in building systems has been a boost to the wood industry sector but requires rigorous scientific analysis on many attributes including its environmental impact to support green building policies. To show the environmental impacts of buildings, whole building life-cycle assessments are conducted according to ASTM E2921:2016 and EN 15978:2011 standards. This study conducted a whole building LCA for a mass timber building comprised of CLT and glulam with a comparison to a concrete building structural system. The environmental impacts of materials types and structural building components of the two functionally equivalent buildings will be analyzed and reported. The results will provide the scientific evidence of the environmental performance metrics of mass timber buildings necessary to inform the public, building industry, and policy makers.

Understanding the Uncertainty in Environmental Life Cycle Analysis for Biofuel Production from Forest Residue in the United States

Kai Lan¹, Stephen S. Kelley¹, Sunky Park¹, Longwen Ou², Prakash Nepal³, Yuan Yao^{1,}*

¹ Department of Forest Biomaterials, North Carolina State University, 2820 Faucette Drive,
Raleigh, NC, 27606

² Argonne National Laboratory

³ Department of Forestry and Environmental Resources, North Carolina State University, 2820
Faucette Drive, Raleigh, NC, 27606

As an alternative to fossil fuel, biofuel has many potential energy, economic, and environmental benefits. Woody biomass is one of the most abundant renewable resources in the U.S. A significant amount of forest residues are generated annually from forest management and wood product manufacturing (e.g., potentially 30-108 million dry metric ton/year in the U.S.¹). Most of forest residues are either left onsite as waste or combusted for energy recovery that is a low-value use. Converting forest residues to biofuel could provide a value-added and environmentally sustainable approach. Understanding the environmental and economic implications of the biofuel derived from forest residues is critical for decision-making related to investment and management in the forest sector. Many Life Cycle Analysis (LCA) have been conducted to understand the implications of making biofuels from woody biomass, but few of them evaluated the impacts of variations. For example, large variations and uncertainties exist in biomass production such as tree growth rates, management intensities, forest operations, and end-of-life of residues (e.g., left for decay, burning, or sent for biofuel). Those variations may have large impacts on LCA results, thus it is crucial to quantify the impacts and identify the key parameters driving the environmental impacts such as the life-cycle carbon footprints (e.g. biogenic and fossil).

In this work, a cradle-to-gate LCA was developed for a biofuel produced from pine residues in the Southern U.S.. The LCA includes biomass production, transportation, and biomass conversion in a biorefinery using fast pyrolysis. Life Cycle Inventory data were collected from literature and process simulation models for pine and biorefinery. Key parameters in each life-cycle stage that may drive the LCA results are first identified through sensitivity analysis and literature. Most of those parameters are related to either forest management (e.g., planting density, use of fertilizers and herbicides) and biomass quality (e.g., moisture, ash, and carbon contents). The variations (i.e., ranges and distributions) of each parameter were used as inputs for a Monte Carlo Simulation (MCS). MCS is a commonly used approach to understand the impacts of uncertainty and has been widely used in LCA.² Through the MCS, we quantified the variations of life-cycle primary energy consumption and Greenhouse Gas (GHG) emissions. Comparative scenarios were developed to quantify the environmental benefits of turning forest residues into biofuel and identify the key parameters that could potentially maximize the benefits and reduce the adverse environmental impacts. Preliminary results showed that forest management strategies such as those related to

**Proceedings of the 62nd International Convention of
Society of Wood Science and Technology
October 20-25, 2019 – Tenaya Lodge, Yosemite, California USA**

planting, thinning, and rotation had large impacts on the life cycle GHG footprints of biofuels, while life cycle primary consumption was mainly contributed by biorefinery.

Reference

1. Perlack, R. D., Eaton, L. M., Turhollow Jr, A. F., Langholtz, M. H., Brandt, C. C., Downing, M. E., ... & Nelson, R. G. (2011). US billion-ton update: biomass supply for a bioenergy and bioproducts industry.
2. Lo, S. C., Ma, H. W., & Lo, S. L. (2005). Quantifying and reducing uncertainty in life cycle assessment using the Bayesian Monte Carlo method. *Science of the total environment*, 340(1-3), 23-33.

Key words: pine residue, biofuel, life cycle assessment, variabilities, energy consumption, greenhouse gas emission, Monte Carlo simulation.

The Wood Density Variability of the French Forest Species, a New Data Base

Jean-Michel Leban

INRA

Abstract

Introduction

There is an increasing demand on the monitoring of the forest resources, on forests statistics, and on projections of future forest resource availability especially in terms of biomass (Leban & Bontemps, 2016). We developed a new method to enrich the forest information produced by the French National French Inventory by the measurement of the wood density.

Materials and methods

This technological innovation permits the fast and reliable measurement of the wood density on unprepared increments cores collected in the forests by the NFI staff. The cores are passed through a medical Xray scanner. Since 2015, about thirty thousand cores were sampled each year. In November 2019 we will have a novel data base with wood density measurements on more than one hundred thousand increment cores.

Results

We will present results that illustrate the different ways to enrich forest information with these new data, e.g. (i) the reassessment of the total standing biomass for all the forest species and (ii) the wood density variability maps for each species that can be used for the assessment of the forest biomass changes as well as for new strategies for wood procurement at national or regional scales.

Conclusion

We will discuss the perspective for the sharing of this new data base that combines at the national scale level wood density and the usual forest inventory measurements such as DBH, height, age etc. Such data base pave the avenue for a better knowledge of our forest resources and for understanding of the biomass production along different silvicultural, climatic and trophic gradients.

References

- Hervé J.-C., 2016. France, pp 385-404, in “*National forest inventories: Assessment of wood availability and use*” Vidal, C., Alberdi, I., Hernández, L., Redmond, J.J. (Eds.) Springer
- Jacquin, P., Mothe, F., Longuetaud, F., Billard, A., Kerfriden, B., & Leban, J.-M. (2019). CarDen: A software for fast measurement of wood density on increment cores by CT scanning. *Computers and Electronics in Agriculture*, 156(1), 606–617.
- Leban, JM., & Bontemps, J.-D., 2016. Editorial: “Forest Inventories at the European level”. *Annals of Forest Science*, 73(4), pp 1–4.

Monday, October 21st

13:45-15:00

Managed Forest Carbon Sustainability: Myths and Metrics

Elaine Oneil

Consortium for Research on Renewable Industrial Materials

(CORRIM)

Abstract

Ample empirical evidence from life cycle inventory and assessments demonstrates the low carbon footprint of growing, harvesting, and manufacturing wood products in North America. Placing that footprint within the context of land-use, and alternative use, strategies for forest land, demands a rigorous assessment of forest conditions including growth, harvest, disturbance, and conversion risk. Placing these forestry variables within the context of the prevailing market and regional socioeconomic conditions generates a more complete picture of the overall carbon footprint of using harvested wood products as a carbon mitigation strategy, while dispelling the myth of forest carbon debt at the system wide scale.

Life Cycle Assessment Can Improve Decisions to Optimize Wood Use

Maureen Puettmann

The Consortium for Research on Renewable Industrial Materials
(CORRIM)

Abstract

Higher expectations for greenhouse gas reductions and public pressure to reduce the use of fossil fuels has led to increasing interests in using wood residues for energy and fuels and brings up the question about the optimal use of wood. For example, the shift of using mill residues for energy, rather than for alternative uses in e.g., long term products, may have unintended consequences such as greater carbon emission in the short-term. The US softwood lumber industry produces an estimated 19 million metric tons per year of chips and residues (bark, sawdust, and shavings) and I present the implications of the choice how to use this material. Historically, about half of these “coproducts” have gone to the pulp and paper industry. Recent surveys from long term wood panel products such as medium density fiberboard, particle board, hardboard, and fiberboard have estimated a softwood residue demand of 7.4 million metric tons per year. In addition, softwood lumber producers use another 3.8 million metric tons per year of wood residues for energy generation for processing facilities; a direct substitution of fossil fuels and a direct carbon emission reduction. Alternatively, structural wood building assemblies can displace 2 – 6 times the carbon emissions compared to non-wood assemblies (steel, concrete). This presentation will focus on comparing carbon storage in short-and long term products and its implication for net carbon emissions and substitution of fossil fuels to determine the best use of wood for maximal carbon mitigation.

Converting Industrial Waste Cork to Biochar as Cu (II) Absorbents via Effective Pyrolysis

Qihang Wang, Zongyuan Lai, Demiao Chu, Jun Mu*

Key Laboratory of Wood Material Science and Utilization (Beijing Forestry University), Ministry of Education, Beijing, 100083, P.R. China;

*Corresponding author: mujun@bjfu.edu.cn

Abstract:

Cork is a renewable biomass material with many excellent properties, which makes it widely applicable to a diverse array of applications all over the world. Cork powders being generated throughout the fabrication stages of various cork products is the main waste of the cork industry. It is with an annual production estimated to reach around 50,000 t only by the granulation process. This aspect of cork manufacturing is considered highly problematic, as the cork powders has almost no commercial value, and thus, has been mainly combusted for energy generation, due to its high calorific value. The purpose of this study was to use cork waste to prepare cork-based biochar (CBC) that can be used to removal heavy metal ions from wastewater, which could be a more eco-friendly, cost-effective, and sustainable cork waste recycling method.

The cork powders were heated under different pyrolysis temperatures (450, 550, 650, and 750°C) and pyrolysis time (0.5, 1.0, 1.5, and 2.0 hr) at 10 °C/min in a tubular electric furnace under nitrogen gas to obtain CBC. The physicochemical properties of CBC were characterized by elemental analysis, FT-IR, XRD, N₂ adsorption and SEM. The adsorption capacity of CBC on heavy metal ions was further evaluated by Cu ion adsorption testing.

The results showed that the CBC produced under conditions of higher pyrolysis temperature and time, has a more stable carbon structure, larger specific surface area, and enhanced Cu ion adsorption capacity. The maximum specific surface area of CBC prepared at 750°C for 0.5 h was 392.5m²/g, which surpasses most other biochars reported in previous studies, which are beneficial to the application of wastewater management. The SEM image demonstrated that the biochar retains the special hollow polyhedral cell structure of raw material cork. Furthermore, a large number of pores formed on the cell wall after high temperature pyrolysis, causing independent cells to communicate with each other. Finally, CBC exhibits superior Cu ion adsorption capacity (18.5mg/g) with a shorter equilibrium time, which gives it a competitive advantage to similar adsorbents.

In summary, pyrolysis of cork waste to obtain biochar is a solution to recycling these large residues, and facilitates adsorbent development with no exploitation of natural resources. In addition, it also reduces the carbon footprint by taking advantage of industrial by-products that have no significant value. Therefore, regardless of ecological or economic perspective, this method can be regarded as a feasible alternative to recycling waste in the cork industry.

Key words:

Industrial Waste Cork, Biochar, Cu (II) Absorbents, Pyrolysis

The Contribution of the New Zealand Forest Harvest to Greenhouse Gas Emission Reduction

Anne Wekesa, Bruce Manley, David Evison
University of Canterbury, New Zealand
Corresponding author: anne.wekesa@pg.canterbury.ac.nz

This study aims to provide separate carbon stock estimates from harvested wood products (HWP) in the domestic and export markets. In New Zealand, carbon stocks estimates from HWP are assessed using the production approach suggested by the Intergovernmental Panel on Climate Change (IPCC) guidelines. However, lack of information of identical HWP categories in the domestic and export markets and their respective half-life values has hindered distinctly reporting HWP carbon stock estimates in these markets as advised by IPCC guidelines. This separation is important as it boosts the accuracy of the estimates. In addition, utilising country specific half-life values and activity data allows for the adoption of higher tiered accounting methods which result into better estimates. The results of this research will provide this information for the domestic market so that the separation of carbon stock estimates from HWP in both markets can be carried out. In addition, this data will allow New Zealand to accurately provide estimates of carbon stocks for all HWP resulting from its domestic harvest as well as identify if carbon storage is highest in the domestic or in the export market.

Currently, there is information on the life cycle and half-life values of HWP for roundwood logs processed by sawmills, plywood, veneer, medium density fibreboard (MDF) and particleboard companies in New Zealand's major export markets. This information is however not available for roundwood logs processed by similar companies in the domestic wood industry. This study utilises questionnaires to collect information on the life cycle of HWP resulting from roundwood logs processed by domestic wood processing companies across the country manufacturing HWP, namely, sawn timber, plywood, veneer, medium density fibreboard (MDF) and particleboard. The life cycle of HWP will be traced by collecting information on the current typical grade out-turns, namely, appearance, structural and industrial from the different log grades processed, their waste flows and final markets of wood products. This approach is important because different product grades have unique end uses due to differences in their qualities and characteristics. In addition, disaggregation of HWP categories reduces uncertainty in estimates. Furthermore, information on the service life of these products will be collected in order to calculate their half-life values. The findings of this study will be presented.

***Proceedings of the 62nd International Convention of
Society of Wood Science and Technology
October 20-25, 2019 – Tenaya Lodge, Yosemite, California USA***

Blank Page

Monday, October 21st

International Innovation, Trends and Education in Wood Science

15:30-17:30

**Chair: Rupert Wimmer, University of Natural Resources and Life Sciences,
Vienna, Austria and Michael Burnard, InnoRenew, Slovenia**

**The more the merrier? Perspectives of female college student leaders on gender aspects in
the forest sector**

Taylor Barnett
Oregon State University, USA

Abstract:

In developed societies, there have been overall continuous efforts in recent years to increase gender diversity that resulted in some positive benefits such as an increased number of women in education, paid employment, and top management positions. It can be argued that increasing gender diversity in the workplace is not only the right thing to do, but the smart thing to do. However, prevalent economic exclusion still plays a role in the workplace, as evidenced by women averaging 15-20 percent less earnings than men.

This qualitative study employs semi-structured interviews to examine perspectives of female college students in leadership roles on gender aspects in the forest sector. Our participants are 28 female student organization leaders from the top four forestry universities in the world as reported by The Center for World University Rankings: Swedish University of Agricultural Sciences, Oregon State University, University of British Columbia, and University of Helsinki.

The questions being researched are as follows: (1) What are perceptions of female college student leaders on the current situation with respect to gender diversity in forest sector education? (2) What motivates female students to enter forest sector education and industry? (3) In what ways do gender stereotypes and expectations influence the experiences of a collegiate forest student organization leader? and (4) In what ways do female college student leaders think the forest sector education and industry could be made more attractive to young females?

Preliminary results suggest that female representation in the forest sector is one of the top influencers in retention rates of females in forestry, whether it be academic or professional, as well as creating an inviting atmosphere for more young women to join. Many women find that having a more gender balanced environment in forestry creates opportunities for female mentorship and a welcoming sense of community where they feel comfortable to speak up about their opinions to collaborate with one another. As the image of forestry changes, their perspective changes as well, motivating women to stay in the field and pursue careers in the field.

Suggestions for the Sustainable Development Goals of United Nations, Based on the 30year Kenaf Research and Development in Japan

Kazuhiko Sameshima
Kochi University, Japan

Abstract

The full-fledged Japanese research and development of kenaf (*Hibiscus cannabinus*) has started with the opening of the Heisei Era (1989). The 30year history of Heisei Era ends this year (May,2019). The new steps of kenaf R&D should also start again in new Japanese Era. Through the Heisei kenaf R&D, the attractiveness and potential of kenaf plant has been confirmed by many people from an individual to an enterprise in Japan. The wave of passion of this kenaf research and development should continue even in the new era to come.

Japan has the various climates and geological features and the kenaf research findings in Heisei Era will be useful not only at every corner of Japan archipelago but also at many parts of the world. The kenaf application can be from a large-scale industrial use to a personal use. There are a lot of points where kenaf can play important role in the possible target works of Sustainable Development Goals that UN propose. The suggestions will be made for the next generation to make kenaf useful to establish a sustainable system in many parts in the world. The suggestions are based on the 30year experience of a "wood chemist" of a Japanese local university and a NGO "Japan Kenaf Association" which has been the main NGO to promote the kenaf research and development in Japan.

Keywords: climate change, kenaf (*Hibiscus cannabinus*), plant fibers, sustainable system, biomass, education, agroforestry, biorefinery, nanotechnology.

Development of Nano-cellulose Based Thermal Insulating and Encapsulated Phase Change Materials for Energy Efficient Buildings

David DeVallance
InnoRenew CoE and University of Primorska, Slovenia

Abstract

Nanocellulose has been gaining more attention for use as a light-weight, bio-based, highly insulative material. Specifically, researchers and industry are looking to use waste materials, such as wood fibers, waste textiles, and under-utilized cellulosic sources for producing innovative building materials with enhanced insulative properties. In addition to insulating materials, building efficiency can be achieved through the use of phase change materials (PCMs). Organic phase change materials such as paraffin wax, polyethylene glycol, fatty acids, polyalcohol, and polyethylene have shown potential as sufficient PCMs. PCMs, especially organic based types, are generally hindered with low heat transfer rate that results in incomplete melting/freezing and losses in extraction of stored energy. Some approaches to overcome these hindrances include macro and micro encapsulating the PCMs, incorporating porous materials into PCMs, filling PCMs with highly conductive particles and fibrous materials. The overall goal of this research is to develop high performance nano-cellulose based thermal insulation material and a new generation of encapsulated PCMs with thermal conductivity-enhancing cellulose-based shells. Specifically, this presentation covers the laboratory design and development of new enhanced cellulose-based shells and the development of the encapsulation process for PCM. To evaluate the emulsification process of PCMs, heated homogenous mixtures of palmitic acid (PA) and cellulose triacetate (CTA) were prepared at 80 degrees Celsius in dimethyl sulfoxide (DMSO). To evaluate improvement in thermal conductivity, highly conductive particles of carbon black and from carbonized wood were incorporated into shells of PCM capsules. The presentation will cover the results from the emulsification studies and improvements in thermal performance of the PCMs containing conductive carbon materials.

Nature-inspired Sustainable Solutions for an Architectonic Environment – A Collection of Case Studies

Eva Haviarova¹, Manja Kitek Kuzman², Zuzana Tončíkova³, Denis Plavčák²,

¹Purdue University, Department of Forestry and Natural Resources,
West Lafayette, IN, USA;

ehaviar@purdue.edu

²University of Ljubljana, Department of Wood Science and Technology,
Ljubljana, Slovenia;

Manja.KitekKuzman@bf.uni-lj.si

denis.plavcak@bf.uni-lj.si

³Technical University of Zvolen, Department of Furniture Design and
Wood Products, Zvolen Slovakia

xholecyova@tuzvo.sk

Abstract

The deeper understanding and use of light-weight principles, such as a high degree of differentiation of material and structure, in combination with the development of computational strength design, simulation, and fabrication methods, enables novel constructions in design and architecture. The use of different lightweight materials, such as engineered wood products (EWPs), now makes it possible to implement nature-inspired and bio-based solutions in interior design and building sectors. An adaptive robotic fabrication process makes possible a necessary scaling-up and handling of complex interrelations between the pattern shapes and the behavior of novel materials. In contrast to repetitive manufacturing processes where automation relies on the execution of predetermined and fully defined steps, sensing technology is employed to enable a workflow that synthesizes material computation and robotic fabrication in real time. In this process, the shape of the tailored work piece is repetitively scanned. Some contemporary case studies will be presented, such as: Material efficient shell structures inspired by bio-silica of the marine life planktons; Kinetic – movable & adaptive energy minimizing façades, inspired by the wings of insects; Origami-based building structures inspired by folding leaves; Fibrous anisotropic structures inspired by wood and cactus; Environmentally neutral, thermo-regulating ventilation systems using solar effects; Multi-combinations of lightweight principles, structurally optimized by combing nature inspired fiber reinforced composites; Interior spaces and accessories created based on biophilic principles and designed according to the biomimicry methods. A variety of natural processes using biomimicry and nature-inspired solutions were studied and taken into consideration.

Keywords: architecture; timber construction; digital design; interior design objects; nature-inspired; biophilia; wood processing

Future developments in the forest sector

Dr. Ed Pepke^{1} – Ms. Kathryn Fernholz²*

¹ Associate, Dovetail Partners, Minneapolis, Minnesota, United States

** Corresponding author. ed@dovetailinc.org*

² President, Dovetail Partners, Minneapolis, Minnesota, United States

katie@dovetailinc.org

Abstract

Future developments in the forest sector are highlighted at the Society of Wood Science and Technology conventions which bring together the brightest minds in the forest sector. The technical session chairs of the 2019 convention were surveyed to learn their forecasts of developments in the 2020s, and the impacts and risks of those developments. The chairs responded positively about the future of the sector emphasizing that sustainable production of wood and wood fiber is essential and must be ensured by sustainable forest management that protects biodiversity. Continued market development is critical, especially for new products and applications. Efficient manufacturing is necessary for traditional products and for new products. A revitalization of the forest industry was called for and respondents recommended viable products and processes. Strong, ongoing support is important for university-level education and research in all aspects of the forest sector. International cooperation, one of the tenants of the SWST, is and always will be a key for continued forest sector development.

Keywords

Future developments, forest sector, cross-laminated timber, nanotechnology, sustainable forest management, sustainable development, new products, new applications, market development

***Proceedings of the 62nd International Convention of
Society of Wood Science and Technology
October 20-25, 2019 – Tenaya Lodge, Yosemite, California USA***

Introduction

The Society of Wood Science and Technology (SWST) is an international organization with approximately 500 members in academia, industry and government. Its mission is “to provide service to SWST members; to develop, maintain, and promulgate the educational, scientific and ethical standards that define the profession; and to advocate the socially responsive production and use of wood and lignocellulosic materials.”

SWST conventions bring together some of the brightest minds in the forest sector. They represent expertise in a variety of fields and present their discoveries. For this report Dovetail Partners tapped their knowledge with a focus on their expectations and forecasts for future developments (positive and negative) in their fields. Based on their forecasts, Dovetail produced this forward-looking report about the forest sector in 2020 and beyond.

Methodology

The structure of the SWST convention lends itself to gathering information for this report. The convention is organized in these topical sessions:

1. Wood Physics and Mechanics
2. Wood Chemistry
3. Advances in Cell Biology
4. Biodegradation and Preservation
5. Timber Engineering and Mass Timber
6. Composites and Adhesives 1
7. Composites and Adhesives 2
8. Business, Marketing and Regulations
9. International Innovation, Trends and Education in Wood Science
10. Impact of Forest Disturbances on Wood Quality

In addition there is a poster session where additional ideas can be gathered from presenters.

Each of the 11 sessions (including the poster session) has a chair that responded to a short, 7-question survey in preparation of this report before the convention. The chairs responded via an online survey

After identifying their topical session, the chairs were asked these questions:

1. What will be the most important topic in the 2020s?
2. How does your topic address a broader, umbrella issue such as sustainable development or sustainable forest management or climate change?
3. What are the potential risks associated with this development? How could those risks limit or preclude the development?
4. What new products or product applications will become available?

5. And will they substitute for other current products or raw materials (wood- or non-wood-based products/materials)?
6. Are developments likely to increase or decrease demand for wood or wood fiber?
7. Could developments lead to reductions in the environmental impacts of wood-based products production and use, and if so, what indicators are most likely to show improvement?

Results and Discussion

Overarching developments. Despite differences in their fields of expertise, the technical session chairs all were positive about future developments in the forest sector. Repeatedly the word “sustainable” was used in conjunction with the production of forest products and their markets. Sustainable production of wood and wood fiber is essential and is ensured by sustainable forest management (SFM) that protects biodiversity. Widespread development of forest plantations of fast-growing, often exotic species to achieve higher growth rates was mentioned, with the caveat that these species’ physical properties are known and are suitable to end uses. SFM will improve when less-utilized species are processed into value-added products.

Market development continues to be needed, especially for new products and their applications. Then efficient manufacturing is necessary for traditional products, e.g. lumber and panel products, and for new products.

A revitalization of the global forest industry was called for, especially in the United States. Some of the products and processes mentioned below directly address this need. Respondents supported university-level education and research in all aspects of the forest sector. International cooperation, one of the tenants of the SWST, is and always will be important for continued forest sector development.

Question 1. What will be the most important topic in the 2020s?

New products and processes. Cross-laminated timber (CLT) was the most commonly mentioned new product. Its current production is most-often from softwood species, but its manufacture from suitable hardwood species and small-diameter timber was called for. Mass timber construction will be enabled through improvements in connections. These buildings will show more advantages as improvements come in seismic design and long-term durability. Research

will discover how to manufacture panels and construct CLT buildings for different climates, e.g. humid regions.¹

The pulp and paper sector is evolving from traditional products which are declining in demand, e.g. newspaper, into bio-refineries.² These new factories can produce a variety of traditional products and in addition new fiber-based products and wood-based energy. Some of these products are either primary outputs or are byproducts. Heretofore byproducts, e.g. lignin, are elevated to primary- or secondary-products. Refineries will need to produce cellulose and lignin for nano-fibers for their increasing applications.³

Ingenuity in breaking down wood into its fibers and chemical components and then reforming them into composite products is forecast to continue. Biomolecular engineering of wood structure and its chemical composition will lead to enhanced materials. New applications of lignin and cellulose will produce the components for nanotechnology. Improvements in bonding of wood-to-wood composites and wood-to-other materials composites will facilitate new structural products. Adhesives derived from natural products, presumably as opposed to synthetic chemical sources, will be more environmentally friendly. Science will continue to achieve greater wood stability in composite products.

Another avenue for more environmentally friendly processes is in preservation of wood. Biodegradation and biodeterioration are natural processes which have been traditionally reduced by chemical and heat treatments. New treatments will be developed that have lower environmental impacts. Thermally modified wood products will provide a variety of advantages in addition to resistance to decay.

Question 2. How does your topic address a broader, umbrella issue such as sustainable development or sustainable forest management or climate change?

Effects on sustainable forest management, sustainable development and climate change. All the developments for the future occur within the context of these three broad, interconnected issues. Wood is recognized as a sustainable and renewable

¹ For more information, see the Dovetail Report, *Modern Tall Wood Buildings: Opportunities for Innovation* available at:

http://www.dovetailinc.org/report_pdfs/2016/dovetailtallwoodbuildings0116.pdf

² For further discussion of the potential for biorefineries, see the Dovetail Report examining the U.S. Pulp and Paper Industry, available at:

http://www.dovetailinc.org/report_pdfs/2005/dovetailpulppaper0705new.pdf

³ For background information about nanotechnology, see *Nanotechnology and the Forest Products Industry: Commercial Opportunities*, available at:

http://www.dovetailinc.org/report_pdfs/2016/dovetailnanotech1016.pdf

material that sequesters carbon and thereby helps to mitigate climate change⁴. Carbon sequestration occurs from standing trees through end-products of wood and paper. Sustainable forest management will be enhanced through the use of small-diameter timber in products such as CLT. Heretofore pre-commercial thinnings will become profitable when end-products use this low value fiber source. Thinning forests will reduce fire hazard and provide raw material for wood-based energy. When using wood in construction, it has a much smaller carbon footprint than concrete or steel buildings.⁵ As the long-cycle CO₂ footprint decreases, the short cycle will increase, providing a more sustainable balance.

Realizing that wood has attributes as a building material, it needs to be used in the right applications. It is a biological material subject to degradation by insects and diseases. In addition it can be damaged by non-biological agents such as fire, heat and weather. Protection of wood in its various uses is essential not only to extend its lifespan, but also to maintain its reputation. Research must continue to develop environmentally friendly protection strategies to extend the service life of wood products.

Question 3. What are the potential risks associated with this development? How could those risks limit or preclude the development?

Risks associated with the developments. A positive perception of wood and paper products is critical to its current and future use. Promotion of all the advantages of living with wood and using wood and paper products is essential. Communication is necessary to counter arguments against wood which hinder its fuller use. For some exterior applications wood needs to be treated which makes some consumers doubt its sustainability – again, communication at the market level is necessary. Communication must target key audiences, e.g. architects. The durability of wood in service is essential to its reputation and risks can be limited through sound, applied scientific research.⁶ Ongoing education in schools is required to sensitize students on the concepts of sustainability and the life cycle of wood and paper products. Public relations aimed at producers and consumers must be continued too.

Lack of investment and support for research and development is a major risk for the forest sector. Likewise support is critical to preserve the remaining forest products

⁴ For further discussion, *Managing Forests for Carbon Mitigation*
http://www.dovetailinc.org/report_pdfs/2011/dovetailmanagingforestcarbon1011.pdf

⁵ http://www.dovetailinc.org/report_pdfs/2015/building_with_wood.pdf

⁶ Wood Science Research - Not Trendy, But Necessary, available at:

http://www.dovetailinc.org/report_pdfs/2006/dovetailresearch0506.pdf

*Proceedings of the 62nd International Convention of
Society of Wood Science and Technology
October 20-25, 2019 – Tenaya Lodge, Yosemite, California USA*

education programs and the precious knowledge they generated over time. Politicians and the populations they serve must be convinced that the forest sector delivers sustainable products.

Products that are not sustainable are a risk to wood products. For example some of the best and least-expensive adhesives are petroleum-based, and thus not sustainable. Some byproducts can have a negative effect on main products entire life cycle.

Any changes to current economies and markets carry risks of some loss of employment and increased prices. Whether society supports such negative effects is dependent on how it responds to signs of climate change and depleting resources.

Achieving some developments necessitates solving the skilled labor shortage. Continued implementation of robotics in wood process will help, but attracting and training workers will be a challenge.

The sustainable supply of wood raw materials is essential to avoid any interruptions in supply chain. The supply chain itself needs to conform to the entire lifecycle of wood, i.e. from trees, to products and byproducts, to recycling and final uses such as fuel. New products based on nanotechnology need a stable supply of nanofibers.

Another risk is declining demand for solid wood and veneer products for interior applications such as furniture. Increasing demand will require mitigating some of the problems for reduced demand including high costs, complexity of processing and moisture movement. Lacking solutions solid wood will only be used for custom-made wood products. Some solutions include: use of composite materials for their uniformity and workability; simplifying and economizing in manufacturing via computer numerically controlled technology.

Excessive demand for highly fashionable species has always been a challenge for the forest sector. Since trees grow slowly to the size needed for solid wood products, overharvesting of desirable species occurs. Substitution of species and promotion of alternative species is needed.

Plantations are important in maintaining a stable, affordable source of wood fiber. Knowledge of plantation-wood's characteristics, qualities and variabilities are important to mitigate the risk of these fast growing species. Some plantation species

and some manufacturing processes consume important quantities of water and energy which can hinder the advancement and economic viability of new materials.⁷

Question 4. What new products or product applications will become available?

New products Respondents proposed a multitude of exciting new products and their applications. New products will come about by modifying wood, for example through thermal treatments or chemical treatments or combinations of both. Acetylated⁸- and furfurylated⁹ and polymeric¹⁰-based wood products will be developed. Nano technology will continue to evolve with a variety of end products commercialized based on wood's chemical components. Chemicals extracted from wood will be turned into organic textiles, pharmaceutical and other consumer products.

Mixes of wood and plastics is commonly known for some products such as decking.¹¹ Wood fibers can provide valuable characteristics when combined with other materials, for example recycled glass fiber (rock wool, fiberglass insulation). Mixes of wood with agricultural residues will yield new composite products.

New applications. Mass timber is in fashion. While CLT is not new, the applications of CLT are growing. It had been in use for many years in Europe prior to the more recent developments in North America. New species will be incorporated into CLT, including hardwoods as mentioned above. "Hybrid panel" construction in CLT will incorporate well-known, commonly used species for the main structural elements with other parts of the panel constructed from fast growing and/or naturally durable species. Hybrid panels will incorporate structural composite lumber and panels. Advances in adhesives, with higher concentrations of natural products, will enable better bonding in structural applications.

⁷ Fast-Growth Tree Plantations for Wood Production, available at:

http://www.dovetailinc.org/report_pdfs/2005/dovetailplant1005b.pdf

⁸ Acetylation alters the cellular structure of wood in a process involving heat, pressure and acetic anhydride. The wood becomes more durable and dimensionally stable.

https://www.deckmagazine.com/products/acetylated-decking_o

⁹ Furfurylated wood is treated with furfuryl alcohol to improve hardness, resist microbial and insect attack, increase the modulus of rupture, increase the modulus of elasticity and to improve dimensional stability.

<https://www.tandfonline.com/doi/full/10.1080/0282758041001915?src=recsys>

¹⁰ Polymeric woods have advantages of corrosion-resistance and thermal insulation. They can be coatings or mixed with wood fibers and/or other materials such as plastic.

<https://advances.sciencemag.org/content/4/8/eaat7223.full>

¹¹ Wood-Plastic Composite Lumber vs. Wood Decking, available at:

http://www.dovetailinc.org/report_pdfs/2010/dovetailplasticdeck0710.pdf

Advances in structural panels such as CLT, along with other structural wood components, such as glulam, will result in taller and taller wooden buildings.

For some applications wood's attribute of biodegradability property is an attribute; it will be developed with certain polymers. Decomposition has always been important in forests and for products at the end of their useful life. Biodegradability and decomposition properties will be further promoted.

Labor shortages can be alleviated in wood processing with advances in scanning technologies. Robotic utilization for repetitive and dirty jobs can allow labor to be allocated to more meaningful and healthful tasks.

Internet shopping has spurred the need for cardboard boxes. Wood-based packaging will replace some fossil-fuel based packaging. Bio-based, biodegradable plastics will increase in use and replace petroleum-based plastics.

Question 5 And will they substitute for other current products or raw materials (wood- or non-wood-based products/materials)?

Many, if not most, of the future products under development will substitute for currently used wood, or non-wood, materials. In a circular economy the use of bio-based resources will replace petroleum-based materials. Naturally durable temperate species, and heat- and chemical-treated temperate species, will continue to substitute for naturally durable tropical timber.¹² Composites, be they from fine particles or large pieces of wood, will continue substituting for solid wood products.

Respondents were almost universal in saying that wood-based materials will substitute for petroleum-based products, e.g. plastics. Substitution will continue for other competitors of wood, e.g. concrete and metals. Biodegradable, wood-based plastics, or fibrous materials will directly replace low- and medium-quality petroleum-based thermoplastics with long lives, such as LDPE, HDPE and PVC. To accomplish this replacement, biomolecular engineering of wood structure and chemical composition are necessary. However, these other materials will continue to be needed when more advantageous in their applications than wood.

Improved treatment methods for biological damage, i.e., disease and decay, will replace older treatment methods. Treatment techniques which are more environmentally safe will continue to be developed and employed.

¹² Impact of market forces and government policies on the tropical timber trade, available at: http://www.dovetailinc.org/report_pdfs/2018/dovetailtroptimber0118.pdf

Question 6 Are developments likely to increase or decrease demand for wood or wood fiber?

Survey respondents were unanimous in saying the developments will increase the demand for wood and wood fiber. First, because with increasing populations and standards of living the demand for wood and paper products will increase. Secondly, as wood-based products substitute for less environmentally friendly materials, the demand for wood will rise. And third, as we continue to address climate change the need increases for materials that store and emit less carbon in their manufacturing, lifespan and disposal.

CLT and other engineered wood products will certainly increase the demand for wood. The advantage of developments such as mass-timber buildings is that they will offset decreases in demand for wood and fiber for products such as newspaper and other paper grades where demand is declining.

As knowledge rises about the attributes of wood by students, architects and designers the applications will increase accordingly. The growing need for efficient and comfortable living and working spaces, for example by Millennials, will increase the demand for wood-based construction and products. Modern wooden buildings offer the desired combination of comfortable and healthy living environments as well as high-tech, stylish designs and even artistic qualities.

A question raised was about the future increase in wood-based energy. Obviously wood is first directed into its higher value uses. But will wood energy expand broadly, or will it continue to remain as regional uses? Will wood-based ethanol, pellets and pyrolysis be cost competitive without government subsidies? Respondents raised these questions for continued research.

Question 7. Could developments lead to reductions in the environmental impacts of wood-based products production and use, and if so, what indicators are most likely to show improvement?

Almost all respondents said that wood products production and use will reduce impacts on the environment. One example is in wooden construction which has a lower environmental impact than construction with competitive materials such as

***Proceedings of the 62nd International Convention of
Society of Wood Science and Technology
October 20-25, 2019 – Tenaya Lodge, Yosemite, California USA***

concrete, metal and plastic.¹³ Wood is a much better energy and sound insulator than the competitors.

The benefits of carbon sequestration were often cited. These span from forest environments to end-use wood and paper products. Forest productivity and sustainability will continue to improve through applied genetic research.

Increasing the service life of wood through various non-toxic treatments will reduce the environmental impact of earlier replacement.

With a market approach by researchers, new products will meet evolving consumer needs. These products will need to reduce any prior impacts on the environment either by wood-based products or by their competitors.

The best indicator to show improvement is by life cycle assessment (LCA).¹⁴ The measurements could be in kilograms of CO₂ equivalent or other measures of health and energy.

Summary and Conclusions

The session chairs responding to the survey about future developments in the forest sector were positive and made forecasts of product and process developments in their sectors. At a macro-level CLT was most often mentioned for its multiple attributes such as carbon sequestration, sustainable development, healthy living, etc. On a micro-level nanotechnology was often cited for its increasing applications.

To achieve these developments synergies are necessary throughout the industry. Timing is perfect for wood-based construction which fits into the “new green economy”. Government policies are necessary to enable research to be applied.

At the heart of SWST the need for continued higher education reform was called for. Forestry and wood science education must be modernized to meet current and future industry and consumer demands. And forestry and wood science education must meet current and future environmental considerations.

¹³ Life Cycle Cost Analysis of Non-Residential Buildings,
http://www.dovetailinc.org/report_pdfs/2013/dovetailccareport1013.pdf

¹⁴ A Review of Life Cycle Assessment Tools,
<http://www.dovetailinc.org/dovetailcatools0217.pdf>

***Proceedings of the 62nd International Convention of
Society of Wood Science and Technology
October 20-25, 2019 – Tenaya Lodge, Yosemite, California USA***

Communication by everyone in the wood chain, from foresters to scientists to architects and builders must support the attributes of wood. The forest sector must continue to modernize along with new needs and demands.

Acknowledgements

All information came from the survey of the chairs of the SWST Technical Sessions to whom we express our gratitude:

- Wood Physics and Mechanics, Dr. Tetsuya Inagaki, Nagoya University
- Wood Chemistry, Dr. Steven Keller, Miami University in Ohio
- Composites and Adhesives 1, Dr. Roger Moya, Costa Rica Tech
- Composites and Adhesives 2, Dr. Ilona Peszlen, North Carolina State
- Biodegradation and Preservation, Dr. Tamra Franca, Mississippi State University
- Timber Engineering and Mass Timber, Dr. Dave Devallance, InnoRenew
- Business, Marketing and Regulations , Dr. Henry Quesada, Virginia Tech
- Innovation, Trends and Education in Wood Science, Dr. Rupert Wimmer, Boku University and Dr. Mike Burnard, InnoRenew
- Impact of Forest Disturbances on Wood Quality, Dr. Scott Leavengood, Oregon State University
- Early Stage Researcher, Dr. Hui Li, Washington State University
- Poster Session, Dr. Gloria Oporto, West Virginia University
- and Dr. Eva Haviarova. Chair, SWST

Integrating Wood Science, Architecture, and Engineering in Research and Education: The TallWood Design Institute and the Renewable Materials Program at Oregon State University

Evan Schmidt
TallWood Design Institute, USA

Abstract

The landscape of education and work in wood-related fields is facing new opportunities and challenges, particularly with a changing student body and work-place dynamic, evolving environmental awareness, and the advent of new technologies, such as those related to mass timber building. TallWood Design Institute (TDI), based out of Corvallis, Oregon, is a unique academic partnership that recognizes the need for both a more interdisciplinary approach to research and education, as well as a more integrated relationship with various external stakeholders, including industry, environmental, and governmental groups. TDI specifically represents a partnership between researchers and educators at the Colleges of Forestry and Engineering (e.g. Wood Science and Civil Engineering) at Oregon State University and the College of Design (e.g. Architecture) at University of Oregon. Through diverse faculty expertise, cutting-edge facilities and dynamic partnerships with manufacturers, designers and other stakeholders, TDI conducts a wide range of testing and state-of-the-art mass timber research, and provides unique educational opportunities for students and a 21st century workforce.

This presentation will cover the general structure of TDI, with a dual focus on our research/testing activities and our educational programs. Educational programs will cover general curriculum, research/work opportunities for undergraduate and graduate students, and professional education geared towards manufacturers, builders, designers, and code officials. The presentation will also focus on our new facility, the "A.A. 'Red' Emerson Advanced Wood Processing Laboratory," which when completed in summer of 2019, will house educational and research functions relating to advanced manufacturing and fabrication processes with wood products, as well as full-scale structural testing. Finally, this presentation will touch on the evolution of the curriculum at the Wood Science department at Oregon State University, with a focus on the undergraduate curriculum, "Renewable Materials".

The Forest for the Trees: Understanding the Experiences of Female PhDs in Forestry-Related Academia

Amy Simmons
InnoRenew CoE and University of Primorska, Slovenia

Abstract

In science, technology, education, and mathematics (STEM) fields men and women are pursuing undergraduate degrees in similar numbers. However there is a leaky pipeline - women comprise less than 30% of researchers. This is especially true in the forest research sector, which remains traditionally male dominated. This study focuses on the experiences of female researchers with PhDs working within forestry-related research. The traditional and perhaps even chauvinistic culture of the field contributes to its ongoing gender disparity; indeed, it was difficult to find women and non-binary doctoral candidates to interview for this study, as the field remains male dominated and somewhat unwelcoming to anyone but cisgender men.

Fifteen female, PhD-level researchers were interviewed to assess their experiences and perceptions in the framework of gender diversity at forestry-related research universities and institutes in Europe and North America. Interviewees answered questions on topics like the atmosphere and culture of their workplace; the advantages and disadvantages of being a female in research; and challenges experienced during the promotion processes. Researchers discussed many common themes, such as, diverse teams do better research and positive change is slowly occurring. However many interviewees also stated that females are often isolated or excluded from 'old boy' networks and that having a family while meeting requirements for promotion within the existing structure is challenging. The study gave us insights regarding the lack of females in forestry research, and enabled us to identify ways to increase gender equality in research and innovation.

KEYWORDS: gender gap; forestry; academia; science, technology, engineering, and mathematics (STEM); gender diversity; gender disparity;

Tuesday, October 22nd

Biodegradation and Preservation

8:30 – 10:00

Chair: Tamara Franca, Mississippi State University, USA

The Effect of Cattle Blood Based Coatings on Wood-rotting Fungi Growth

Jan Baar^{1}*

¹ Assistant professor, Mendel University in Brno, Brno, Czech Republic *

Corresponding author

jan.baar@mendelu.cz

Abstract

To preserve historical authenticity of wooden structures it is necessary to follow choices that previous generation of craftsmen made. This means that techniques identical to those used originally, not only for wood-working, but for wood surface finishing as well, should be used. It is fundamental to preserve such traditional techniques because their resurrection becomes extremely difficult once they are forgotten. One of these techniques is use of cattle (ox) blood as wood coating of mainly interior wooden elements (ceilings, chests) in the middle Europe. The composition of the solution was generally based on combination of blood or blood proteins, lime, curd, egg white, milk and bile. Ingredients and their ratios vary from author to author. It is not at all certain, what was its purpose, but it is believed that the wood coating based on blood was efficient against bio deterioration from wood-rotting fungi or wood-boring insect, or as fire retardant.

To examine some of the expected effects of the solutions based on cattle blood, the aim of this study was to test solutions as protective agent against wood-decaying fungi, both brown-rot (*Poria placenta*, BAM 113) and white-rot (*Trametes versicolor*, BAM 116). Three different recipes were selected and prepared based on former experiences and literature review. First was fresh cooled cattle blood itself, second was fresh cooled cattle blood mixed with defatted milk, lime oil and bile (400:50:20:20 ml respectively), last solution was made from blood, casein paste (1500:60 ml respectively) and egg white, where casein paste consisted of lime, curd and ammonia water. Because of higher viscosity of solution and in respect with traditional application by brushing the surface protection according to modified EN 839 was chosen. The mass loss of treated pine samples ranged from 38 % to 41 %, while for control samples the mass loss was only 29 %. Obviously the brown-rot fungus decay ability was supported, especially if we take the end grain sealing of treated samples into consideration. On the other hand, slightly lower mass loss (29 %) compared to control samples (39 %) was found in case of

*Proceedings of the 62nd International Convention of
Society of Wood Science and Technology
October 20-25, 2019 – Tenaya Lodge, Yosemite, California USA*

white-rot fungus. The effect of solution composition on decay rate was not proved. Based on our results, traditional blood based wood coating certainly did not serve as an effective fungicide agent, but its surface layer could act partly as mechanical barrier against fungi infection.

Key words: blood, coating, decay, wood preservation

Acknowledgements

This contribution was created with financial supports from project “Historical Timber Structures: Typology, Diagnostics and Traditional Wood Working” NAKI II, reg. No, G16P02M026, provided by the Ministry of Culture of the Czech Republic.

Search for the Decay Resistant Scots pine, *Pinus sylvestris* L., Heartwood

Anni Harju
Natural Resources Institute Finland (Luke), Finland

Abstract

Scots pine, *Pinus sylvestris* L., heartwood is abundant, but underutilized renewable natural resource in northern Europe. It has favorable characteristics such as the stability of form under varying moisture conditions and decay resistance, which make it valuable material for safe and ecological wood products. However, individual pieces of sawn timber or the heartwood of individual trees vary widely in their decay resistance. This is mainly due to their varying content of extractives, especially of phenolic stilbenes. Grading of Scots pine heartwood would optimize its' use and would offer high quality raw material for the above-ground constructions outdoors.

We have studied, whether a method based on UV-fluorescence of stilbenes could be used to predict decay resistance of Scots pine heartwood. Because of large number of samples the measurement should be cost-effective and fast thus preferably running automatically. Our first aim has been to develop a technological solution to be used in the forest tree breeding in selecting the plus trees based on the stilbene content in their heartwood. The fluorescence of stilbenes has been measured from the solid surface of increment core specimen collected from standing trees. If the methodology works well in this application, it could be scaled up to be used in industrial grading. In the symposium, we shall present preliminary results from our studies.

To direct the assorted timber for optimal uses would add the value of heartwood in the whole production chain. Optimal and sparing use of non-hazardous naturally decay resistant heartwood will enhance the green bioeconomy.

Key words: Scots pine, heartwood, biodegradation, resistance, phenolic stilbenes, variation, sorting, fluorescence

Influence of Thermo-Mechanical Timber Modification on the Decay and Mechanical Deterioration against *Coniophora puteana*

Juhani Marttila^{1*} – *Victoria Nwachukwu*¹ – *Aitor Barbero-López*¹ –
*Vitaly Bulavtsev*² – *Antti Haapala*³

¹Early Stage Researcher, School of Forest Sciences, University of Eastern Finland,
FI-80101 Joensuu, Finland * *Corresponding author, juhani.marttila@uef.fi*

²Senior Researcher, School of Forest Sciences, University of Eastern Finland, FI-
80101 Joensuu, Finland,
bulavtsevv@yandex.ru

³Associate Professor, School of Forest Sciences, University of Eastern Finland,
Joensuu, FI-80101 Joensuu, Finland.
antti.haapala@uef.fi

Abstract

Scots pine (*Pinus sylvestris*) and Norway spruce (*Picea abies*) are among the major commercial European softwood species. Natural biological decay leads to mass loss and deterioration of mechanical properties, which are among the main factors limiting the use of wood. Susceptibility to decay depends substantially on structural and chemical composition of wood. Thermo-mechanical timber modification process (TMTMTM), developed and commercialized by Nextimber Ltd, Finland, enables drying, compression and thermal modification of sawn timber in a single treatment unit. Besides improvements in dimensional stability and mechanical properties, this treatment is also a potential method for improving decay resistance. The aim of this study was to analyze the effects of densification and thermal modification on decay resistance against brown-rot fungus *Coniophora puteana*.

A total of 360 clear wood specimens were manufactured from TMTMTM modified boards. Boards were either densified, thermally treated, or they had a combination of these treatments. Untreated wood and copper treated wood were used as negative and positive control group, respectively. Procedures in decay test were implemented according to the standard EN 113 with modifications presented by Lu et al. (2016). Wood pieces of each modified wood grade (12 pcs) were recovered from decay at intervals of 8, 12 and 16 weeks of exposure. Mass loss over the experiment was monitored. Subsequent mechanical tests according to were applied to determine modulus of elasticity and modulus of rupture of the specimens. Impacts of densified wood structure on its wetting kinetics and strength after decay have not been previously presented. The results show clear differences in the decay resistance between the groups that can be explained by physical and chemical changes in wood specimens.

Keywords: Scots pine, Norway spruce, brown rot fungus, thermo-mechanical modification, modulus of elasticity, modulus of rupture

1 INTRODUCTION

1.1 DETERIORATION OF WOOD BY BROWN-ROT FUNGI

Many biological agents including fungi, bacteria, and insects decompose wood in adequate environmental conditions. Structural polymers gradually reduce to simpler molecules and finally to CO₂ and water. Fungi colonize wood and degrade its cell wall components forming brown, soft or white rot (Blanchette et al. 1990). Brown rot fungi degrade mainly the polysaccharide components of wood (hemicellulose and cellulose) and leave a lignin framework (Blanchette et al. 1990, Schwarze 2007). In brown-rot fungi cellulose chains are depolymerized (Kaneko et al. 2005) and then lignin is modified chemically (Eriksson et al. 1990) by non-enzymatic methods. *Coniophora puteana* (cellar fungus) is a common brown rot fungus. It preferentially attacks softwoods and has also an impact on hardwoods (Eaton & Hale 1993). The fungus tolerates cold and it prefers moisture content of 50–60% (Eaton & Hale 1993, Lundell et al. 2014). According to Highley (1988), *Coniophora* brown rots produce an enzyme with cellobiohydrolase activity, which is capable of processing crystalline cellulose, and even production of ligninolytic enzymes has been reported (Lee et al. 2004). In general, wood degradation by brown-rot fungi progresses through ray parenchyma cells, and then spreads out through pits in transverse direction (Daniel et al. 2014). The hyphae of fungus grow inside the lumens and close to the wood cell wall (Schwarze 2007).

Natural recycling of organic becomes a problem when wood products in applications such as in construction are disintegrated (Blanchette et al. 1990). Decay by brown-rot fungi causes substantial strength losses in wood already before measurable weight loss occurs. Curling et al. (2002) reported that *Pinus* spp. sapwood lost 40% of its MOR before measurable weight loss was detected, and after 20% weight loss, decrease both in MOR and MOE was approximately 80%.

1.2 DECAY RESISTANCE OF THERMO-MECHANICAL MODIFICATION

Numerous preservatives and processes enhance resistance of wood from being destroyed by fungi and other corresponding factors. Those can be divided into three groups (Irbe et al. 2014): hydro-thermal treatments, chemical modification and impregnation with monomeric compounds. Increasing awareness and concern over health and environmental impacts of preservation substances has led to efforts to find treat wood in safer and more environmentally friendly ways. Wood densification is a process where density is increased by reducing void volume of lumens. Densification process is effective when wood is heated above the glass transition temperature of amorphous polymers of wood – hemicellulose and lignin (Kunesh 1968, Wolcott et al. 1994, Tabarsa & Chui 2001). The primary purpose of densification is to improve mechanical strength, moisture sorption behavior, and physical properties of wood (Fukuta et al. 2008). Densified wood tends to lose its state as a result of separation of hydrogen bonds by moisture and heat. Therefore, a method for fixation of the new state is needed. There are several mechanisms for this, including changing the hygroscopicity of the cell wall and forming covalent crosslinks between the components of wood in the deformed state (Morsing & Hoffmeyer 1998). Thermal modification degrades or modifies hemicelluloses and amorphous cellulose in wood (Morsing & Hoffmeyer 1998). In addition to elimination of the spring back effect, thermal

modification increases the biological durability of wood. Significant improvement in decay resistance against *Coniophora puteana* after heat treatment was noticed in *Picea abies* (Norway spruce) (Viitanen et al. 1994, Metsä-Kortelainen & Viitanen 2009) and in *Pinus sylvestris* (Scots pine) (Metsä-Kortelainen & Viitanen 2009, Ayata et al. 2017). Increased hydrophobicity limits water absorption into the wood which might hinder fungal growth (Metsä-Kortelainen & Viitanen 2009). According to Kotilainen (2000) and Weiland & Guynnoet (2003), changes in chemical composition might generate new extractives which acts as fungicides, and degraded polymers do not act as nutrition for fungi.

Besides, Schwarze & Spycher (2005) report that densification likely causes occlusion of cell lumina and reduces the size of voids within the cell walls. This might be particularly important in resistance against brown rot due to its mechanism to diffuse of degradative substances rather than direct erosion of cell walls caused by fungal hyphae. However, opposite results exist: Lesar et al. (2013) discovered that in case of hybrid poplar (*Populus deltoides* × *Populus trichocarpa*) and Douglas fir (*Pseudotsuga menziesii*) decay resistance of thermo-hydro-mechanically treated wood against brown-rot *Gloeophyllum trabeum* and white-rot *Trametes versicolor* was at the same level or worse than decay resistance of non-densified controls. Therefore, this phenomenon requires further examination.

1.3 AIM OF THE STUDY

The aim of this study is to investigate the effects of several combinations of densification and thermal modification of Scots pine and Norway spruce into decay resistance and mechanical deterioration resistance against *Coniophora puteana* with thermo-mechanical timber modification (TMTM_{TM}).

2 MATERIALS AND METHODS

Scots pine and Norway spruce boards were sawn in 2016 from freshly harvested logs to boards with cross-cut dimensions of 40 × 100 mm. The modifications were executed in a pilot modification kiln (Nextimber Ltd, Juankoski, Finland). The length of the boards was adjusted to 2,700 mm. In addition, commercial thermally modified pine and spruce samples without densification were used in the study. Untreated pine and spruce sapwood and copper treated pine wood were used as references.

The modification equipment allows drying, compressing and thermal modification in a single process. Different combinations of process and modification parameters as temperature and humidity can be used. The boards are stacked between hollow and perforated aluminum plates and compression is executed using hydraulic press. During the modification process, moisture evaporates from the wood surface and flows out through the aluminum plate (Marttila et al. 2017). Air and wood temperature, moisture content (MC) of wood, compression force and degree of compression (relative thickness decrease) were monitored during the compression. During the process, temperature in wood was first elevated gradually up and then stabilized until the moisture content of wood decreased. Then wood temperature was elevated up to 130 °C for the rest of the drying phase. The target degree of compression was set to 30%. Later, half of the material of was thermally modified at 190 °C after the drying and compression phases. Samples for the decay test were prepared from the core layer of the radially sawn boards. A total of 360 clear wood specimens with dimensions of 40 mm × 10 mm × 5 mm were manufactured

from TMTM™ modified boards. The specimens were dried in 75 °C to avoid structural changes in untreated wood and oven dry weight of samples were recorded. All the wood blocks

Group	Type	Densification	Thermal mod.	Specimens, total
Pine, D+TM	Heartwood	×	×	36
Pine, D	Heartwood	×	–	36
Pine, TM	Heartwood	–	×	36
Pine, control, HW	Heartwood	–	–	36
Pine, control, SW	Sapwood	–	–	36
Pine, Cu	Sapwood	–	–	36
Spruce, D+TM	Mixed	×	×	36
Spruce, D	Mixed	×	–	36
Spruce, TM	Mixed	–	×	36
Spruce, control	Mixed	–	–	36
Total				360

underwent gamma radiation with 32 kGy dose for sterilization before cultivation. Norm EN 113 was followed in the treatment. Malt extract agar media containing 4% malt and 2% agar was prepared into sterile 100 mm plates. Then MEA plates were inoculated using fungus from mother plate. Inoculated plates were sealed and incubated in normal conditions for proper growth. All fungi handling was done in a sterile condition. After reaching maximum growth (1–3 weeks), sterilized metal mesh was used between the fungus and the specimen prior to incubation. Then decay test was performed for the previously treated woods. Twelve replicates of each wood treatment types were used with each petri-dish containing 3 blocks for three different harvests (Table 1, Figs. 1 and 2.)

Table 1. Treatment groups in the experiment, D denotes densification, TM thermal modification, HW heartwood, SW sapwood and Cu the commercial copper preservative.



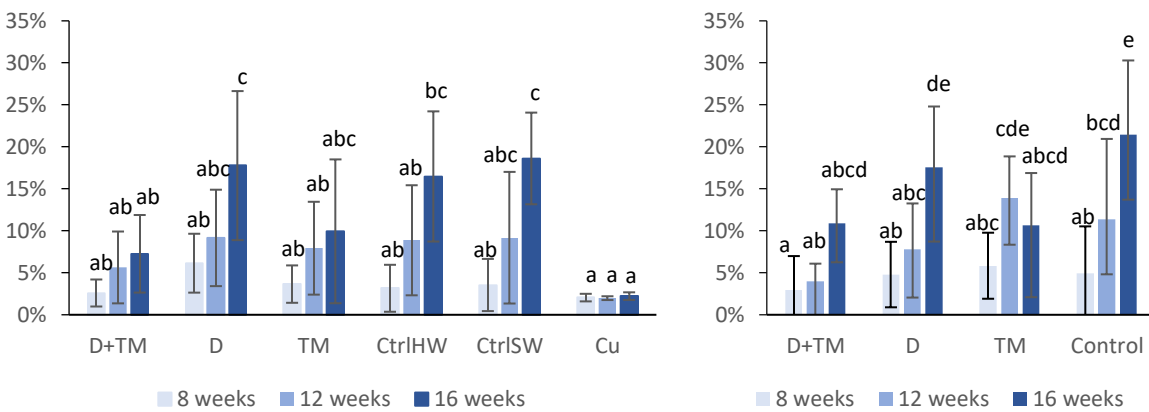
Figure 1 (left). After densification and thermal treatment fungus avoided to grow in some samples (left, before 1. harvesting). **Figure 2** (right). On the right side a sample is fully covered with mycelium (before 3rd harvesting).

Wood pieces were harvested at 8, 12 and 16 weeks from cultivation day. Harvested pieces were brushed and weighted. They were dried at 75°C until equilibrium moisture content was reached.

The relative mass loss due to fungal degradation was determined. After fungal exposure, subsequent mechanical tests according to ISO 13061-3 and 13061-4 were applied to determine modulus of elasticity and modulus of rupture of the specimens. Span (35 mm) and size of supports and load bearing block differed from standard due to small size of the samples. Differences between the groups were studied using analysis of variance (ANOVA) with Tukey HSD post-hoc test.

4 RESULTS

From our visual observations, heat treated wood was not completely covered by fungal mycelia mass. The thickness was, however, clearly increased in samples with only densification due to moisture absorption. Mass loss of species are presented in Figs. 3 and 4. Different letters denote significant differences ($p < 0.05$) between means in Tukey HSD test.

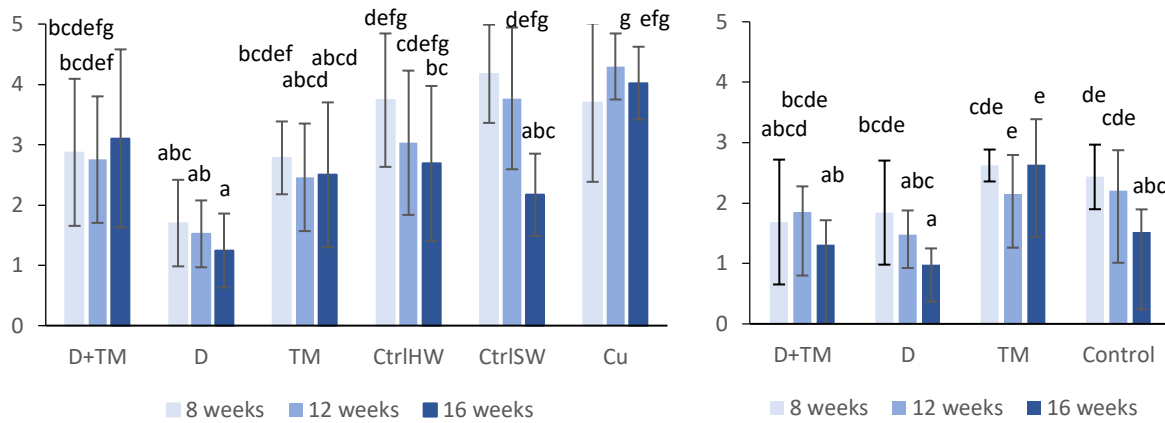


Figures 3 and 4. Mass loss of pine (left) and spruce (right) with different treatments after 8, 12 and 16 weeks of exposure to *Coniophora puteana*.

Average mass loss of pine after D+TM treatment was 7% after 16 weeks of fungal exposure. This was significantly less than untreated control with 18% mass loss in heartwood and 16% in sapwood for the same period. Thermo-mechanically treated pine can be described to some extent as durable against fungal attack since observed mass loss was only 5%-points higher than the copper-treated control group. Statistically significant differences in mass loss of between untreated pine sapwood and heartwood were not detected.

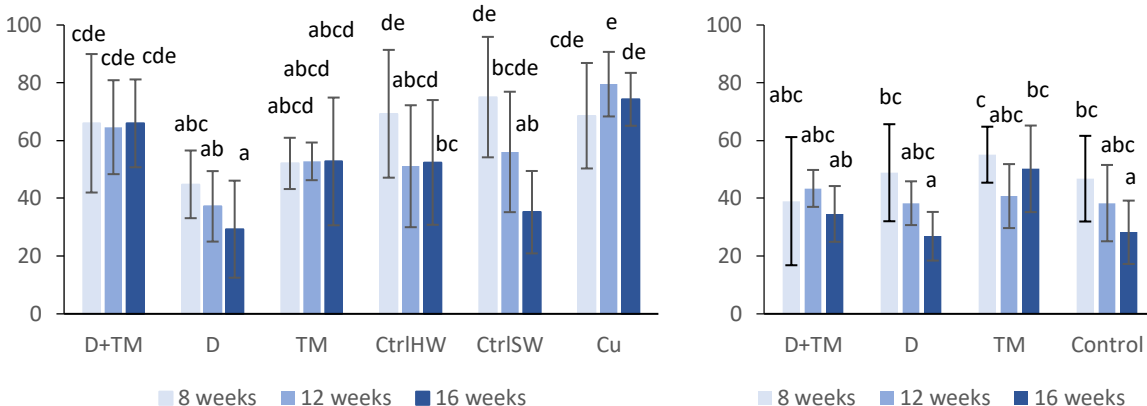
Modulus of elasticity (MOE) is presented in Figs. 5 and 6. Long exposure times decreased modulus of elasticity both in pine and in spruce. Mass loss and MOE have negative correlation in both species. Especially untreated sapwood had a substantial decrease in MOE after 16 weeks of exposure.

**Proceedings of the 62nd International Convention of
Society of Wood Science and Technology
October 20-25, 2019 – Tenaya Lodge, Yosemite, California USA**



Figures 5 and 6. Modulus of elasticity (in GPa) of pine (left) and spruce (right) with different treatments after 8, 12 and 16 weeks of exposure to *Coniophora puteana*.

Modulus of rupture is presented on Figs. 7 and 8. The trend follows same trend as in modulus of elasticity. A notable detail is that pine samples with combined densification and thermal treatment are statistically clearly better than with thermal treatment without densification. This phenomenon was not detected on spruce.



Figures 7 and 8. Modulus of rupture (in MPa) of pine (left) and spruce (right) with different treatments after 8, 12 and 16 weeks of exposure to *Coniophora puteana*.

5 DISCUSSION

There are clear evidences that combined densification and thermal treatment enhances decay resistance compared with sole densification or thermal treatment. This is probably partially due to decreased hygroscopicity and chemical changes in wood. Esteves et al. (2014) reported that the extent of resistance depends on the temperature and duration of modification process. Thermal modification also effectively disallows the springback effect of wood. This keeps voids small and cell lumina occluded (Schwartz & Spycher, 2005). This phenomenon needs still more examination on a microscope level. In terms of fungal resistance, pine showed better durability in the test. Spruce had worse performance but densification with subsequent thermal modification seem to improve also properties of spruce.

In our study pace of deterioration of mechanical properties was moderate. Small size of the specimens required very short span in mechanical test, and ratio of sample height to span differed from the standard. Therefore, MOE and MOR values in this study are not directly comparable with corresponding values of larger samples. Due to relatively small number of replicates per each treatment and high variation in results, statistically significant differences in many cases were not detected.

6 REFERENCES

- Ayata Ü, Akçay C, Esteves B (2017) Determination of decay resistance against *Pleurotus ostreatus* and *Coniophora puteana* fungus of heat-treated scotch pine, oak and beech wood species. *Maderas. Ciencia y tecnología* 19(3): 309–316.
- Blanchette R A, Nilsson T, Daniel G. & Abad A (1990) *Biological Degradation of Wood*.

**Proceedings of the 62nd International Convention of
Society of Wood Science and Technology
October 20-25, 2019 – Tenaya Lodge, Yosemite, California USA**

- EN 113 “Wood preservatives – Test method for determining the protective effectiveness against wood destroying basidiomycetes - Determination of the toxic values”. European Committee for Standardization, Brussels, BE, 1996.
- Eriksson K L, Blanchette R., Ander P (1990) Microbial and Enzymatic Degradation of Wood and Wood Components. Springer-Verlag, 407 p.
- Curling S F, Clause C A, Winandy J E (2002) Relationships between mechanical properties, weight loss and chemical composition of wood during incipient brown-rot decay. *Forest Products Journal* 52 (7/8): 34–39.
- Daniel G, Products F, Science, W (2014) Fungal and Bacterial Biodegradation: White Rots, Brown Rots, Soft Rots-, White Rot Decay of Wood and Lignocellulose. In *Deterioration and Protection of Sustainable Biomaterials*, 23–58. Symposium of the American Chemical Society.
- Eaton R A, Hale M D C (1993) *Wood: Decay, Pests and Protection*. London, New York: Chapman & Hall.
- Fukuta S, Asada F, Sasaki Y (2008) The simultaneous treatment of compression drying and deformation fixation in the compression processing of wood. *Forest Products Journal* 58 (7–8): 82–88.
- Highley T (1988) Cellulolytic activity of brown-rot and white-rot fungi on solid media. *Holzforschung* 42: 211–216.
- Irbe I, Elisashvili V, Asatiani M D, Janberga A, Andersone I, Andersons B, Biziks V, Grinins, J (2013) Lignocellulolytic activity of *Coniophora puteana* and *Trametes versicolor* in fermentation of wheat bran and decay of hydrothermally modified hardwoods. *International Biodeterioration & Biodegradation* 86: 71–78.
- ISO-13061-3:2014(E) Determination of ultimate strength in static bending.
- ISO-13061-4:2014(E) Determination of modulus of elasticity in static bending.
- Kaneko S, Yoshitake K, Itakura S, Tanaka H, Enoki A (2005) Relationship between production of hydroxy radicals and degradation of wood, crystalline cellulose, and a lignin related compound or accumulation of oxalic acid in cultures of brown rot fungi. *Journal of Wood Science* 51:262–269.
- Kotilainen R (2000) Chemical changes in wood during heating at 150–260°C. Doctoral thesis, University of Jyväskylä, Finland.
- Kunesh R H (1968) Strength and elastic properties of wood in transverse compression. *Forest Products Journal* 18: 65–72.
- Lee K H, Wi S G, Singh A P., Kim Y S (2004) Micromorphological characteristics of decayed wood and laccase produced by the brown-rot fungus *Coniophora puteana*. *Journal of Wood Science* 50: 281–284.
- Lesar B, Humar M, Kamke F, Kutnar A (2013) Influence of the thermo-hydro-mechanical treatments of wood on the performance against wood-degrading fungi. *Wood Science and Technology* 47: 977–992.
- Lu J, Venäläinen M, Julkunen-Tiitto R, and Harju A M (2016) Stilbene impregnation retards brown-rot decay of Scots pine sapwood. *Holzforschung* 70(3): 261–266.
- Lundell T K, Mäkelä M R & De Vries R P 2014. Genomics, Lifestyles and Future Prospects of Wood-Decay and Litter-Decomposing Basidiomycota. Vol. 70, in *Fungi*, by F. M. Martin, 329–370. *Advances in Botanical Research*.

***Proceedings of the 62nd International Convention of
Society of Wood Science and Technology
October 20-25, 2019 – Tenaya Lodge, Yosemite, California USA***

- Marttila J, Owusu Sarpong B, Möttönen V & Heräjärvi H (2017) Case hardening and equilibrium moisture content of European aspen and silver birch after industrial scale thermo-mechanical timber modification. In: Möttönen, V. & Heinonen, E. (eds.): 6th International Scientific Conference on Hardwood Processing: 156–165.
- Metsä-Kortelainen S & Viitanen H (2009) Decay resistance of sapwood and heartwood of untreated and thermally modified Scots pine and Norway spruce compared with some other wood species. *Wood Material Science & Engineering* 3–4: 105–114.
- Morsing N, Hoffmeyer P (1998). *Densification of Wood.: The influence of hygrothermal treatment on compression of beech perpendicular to grain*. Kgs. Lyngby, Denmark: Technical University of Denmark (DTU). (BYG-Rapport; No. R-79).
- Schwarze F W M R (2007) Wood decay under the microscope. *Fungal Biology Reviews* 21: 133–170.
- Schwarze F W M R, Spycher M (2005) Resistance of thermo-hygro-mechanically densified wood to colonisation and degradation by brown-rot fungi. *Holzforschung*, 59: 358–363.
- Tabarsa T., Chu Y H (2001) Characterizing microscopic behavior of wood under transverse compression. Part II. Effect of species and loading direction. *Wood and Fiber Science* 33: 223–232.
- Viitanen H, Jämsä S, Paajanen L, Nurmi A & Viitaniemi P (1994). The effect of heat treatment on the properties of spruce (Doc. No. IRG/WP 94-40032). International Research Group on Wood Preservation.
- Weiland J J, Guyonnet R (2003) Study of chemical modifications and fungi degradation of thermally modified wood using DRIFT spectroscopy. *Holz als Roh- und Werkstoff*, 61, 216–220.
- Wolcott M P, Kamke F A & Dillard D A (1994) Fundamental aspects of wood deformation pertaining to manufacture of wood-base composites. *Wood and Fiber Science*, 26(4): 496–511.

Revisiting the Role of Bacteria in Wood Decay

Lakshmi Narayanan
Mississippi State University, USA

Abstract

Wood is one of the primary construction materials used in the United States. However, it is susceptible to decay over time, leading to its reduced service life. Development of targeted wood protection methods requires detailed understanding of microbial wood-decay mechanisms. Fungi are the most destructive microorganisms to attack wood and much research effort has been directed towards understanding their mechanisms of decay. The role of bacteria in wood-decay is less studied. The objective of our research was to compare bacterial communities colonizing treated and untreated-wooden field stakes using next generation sequencing technology. MCA, ACA and CCA-treated and untreated wooden field stakes of size 3/4"H x 3/4"W x 18"L were installed in field test sites in Saucier, MS, and Madison, WI. Stakes were collected at three different time points within a year of installation. DNA was extracted from sawdust derived from the A-horizon (within 7.62 cm of the soil line) of the treated and untreated stakes and then used for 16S metagenomic library preparation. Metagenomic libraries were sequenced using the Illumina MiSeq platform. Data analysis from the three-month collection revealed sufficient sampling depth and species diversity that is a validation of the methodologies employed leading up to sequencing. Results of bacterial colonization in treated and untreated field stakes from at least the first two time-points will be discussed.

**Evaluation of the durability of mass timber products against termites
(*Reticulitermes* spp.) using choice testing.**

Jazmine A. McGinnis
Tamara S.F.A. França
C. Elizabeth Stokes
Mississippi State University
Mississippi State, Mississippi

Juliet D. Tang
Iris B. Montague
USDA Forest Service, Forest Products Laboratory
Starkville, Mississippi

ABSTRACT

Cross Laminated Timber (CLT) is rapidly growing in fascination and popularity across the North American construction timber market. Presently, the American Wood Protection Association E1 Standard calls for a test sample size of 2.54cm x 2.54cm x 0.64cm, which is too small to encompass the large spacing between the bond lines of CLT, a multilayered mass timber product composed of layers of kiln-dried lumber alternating in grain direction. The objective of this study is to evaluate the resistance of untreated CLT against subterranean termites (*Reticulitermes* spp.) found in the southeastern United States using two-sample choice testing and extend the AWP A E1-15 Standard to accommodate the larger material. From spring to mid-fall of 2019, trials will be set up using 10.16cm x 5.08cm x 2.54cm CLT samples of Douglas- fir, Spruce-Pine-Fir, and southern yellow pine against solid southern yellow pine without adhesive. Choice-testing methods will be evaluated over a 4 – 8 week period for mass loss, visual rating, mold formation, and termite mortality. In addition, an alternative visual rating system, based on the AWP A standard but including photos of termite-exposed CLT as reference points, will be tested with the intent of expediting the visual rating process for similarly constructed mass timber products with the use of a transparent film grid. The transparency grid will be a 10.16cm x 5.08cm x 2.54cm piece of film that will have 100 small points that represents 1% of surface area, which would aid in a more consistent visual rating among constituents.

Portable microNIR sensor for the evaluation of mould contamination on wooden surfaces

Olena Myronycheva, Olov Karlsson, Margot Sehlstedt-Persson, Micael Öhman,
Dick Sandberg

Luleå University of Technology, Wood Science and Engineering, Skellefteå, Sweden

Keywords: mould fungi, microNIR, wood, naturally seasoned, kiln-dried, multivariate model

Abstract: The traditional assessment of mould growth is sometimes subjective and can differ from person to person. By applying spectroscopic tools, it is possible to create an individual fingerprint of a wooden material and create databases for obtaining more objective information related to the chemical and biological composition.

Side-boards (the flat-sawn sapwood part of the log) of Scots pine were single stacked on stickers and naturally dried indoors at 20°C to an average moisture content (MC) of 4.6%. Another ten side-boards were dried in a small-scale laboratory air-circulation kiln to an average MC of 14%. Another group of side-boards were double-stacked with the bark-side surfaces of each pair turned outwards in order to get a high extractive concentration on these surfaces, and less concentration on opposite surfaces. The different flat-side surfaces were planed according to a planing-depth scheme : 0 mm (unplanned), 0.25, 0.75, and 1.75 mm depth from the surface, and the residual wood particles were collected for further analysis.

The planned surfaces were exposed to a mould test, performed by spraying a spore suspension of five mould fungi on the wood surfaces followed by incubation at the temperature of 24°C and 95±3%RH for 35 days. Thereafter, the surfaces were graded according to mould growth. A portable microNIR sensor (wave-length range 900-1670 nm, step 6 nm) was used for NIR-spectra detection on the surfaces after mould test, and a data matrix was created. Multivariate analysis of obtained spectra was performed.

The results show that the principal component analysis (PCA) can describe and predict 99.7% of the spectroscopic data obtained. No influence of the drying method or planned depth was discovered during classification. Two mould-classes could, however, be clearly separated; no mould, and with mould growth respectively, and the separation could be detected on a 93.4% level.

The study demonstrates that mould growth on the wooden surface could be evaluated by portable MicroNIR spectrometer, which is sensitive enough to detect chemical differences caused by fungal contamination.

INTRODUCTION

The transition towards a digital society pushes the wood industry to apply smart and robust methods for material properties evaluation.

A hypothesis about a strong influence of drying on contamination and growth of mould fungi on the wooden surface was developed by Terziev and Boutelje [1]. They found that the movement of low-molecular sugars and nitrogenous compounds during drying were significant

and related to type of drying [2]. Later studies found that not only sugars but also acetone soluble extractives migrates during drying and influence the degree of mould attack on the wooden surfaces [3, 4]. The wet chemistry these studies [3, 4] are tedious and it is hard to make fast and reliable conclusion about wooden properties and its relation on mould fungi growth, especially when also the degree mould contamination must be judged by visual assessment by the human eye, which is a subjective method. Therefore, researchers are looking for different non-destructive methods that allow detecting changes in wooden surfaces with high accuracy and precision, e.g. for the detection of mould.

By applying spectroscopic tools, it is possible to create an individual fingerprint of a material and create databases for obtaining more objective information related to the chemical and biological composition [5–7].

This study *aimed at* exploring near-infrared (NIR) portable spectrometer for the detection of differences in mould growth on the surface of the Scots pine side-boards. To study the influence of mould contamination, drying type and planning-depth variables on the multivariate-model efficiency was the *objective* of the study.

MATERIALS AND METHODS

Ten Side-boards (the flat-sawn sapwood part of the log) of Scots pine were single stacked on stickers and naturally dried indoors at 20°C to an average moisture content (MC) of 4.6%. after drying for 30 days. Another ten side-boards were dried in a small-scale laboratory air-circulation kiln. The boards were double-stacked with the bark-side surfaces (the surface of the boards oriented to the bark-side of the tree) in each pair oriented outwards in order to get a high flow of moisture from the inner part of the boards towards the bark-side surfaces. In this way, extractives could migrate with the water transport during drying and accumulate on the wood surfaces. The total drying time was 44 hours of which 1.7 hours was a heating regime, and the cycle ended with a 5-hour cooling regime giving a final moisture content of 14%. No conditioning regime was applied in order to prevent the influence of re-distribution of extractives after drying. The side-boards were prepared to specimens for further studies (Table 1).

**Proceedings of the 62nd International Convention of
Society of Wood Science and Technology
October 20-25, 2019 – Tenaya Lodge, Yosemite, California USA**

Table 1. Test groups

No.	Drying	Planing depth (mm)	Mould	No. of specimens
1	Seasoned	0	No	10
		0.25		10
		0.75		10
		1.75		10
2	Kiln	0	No	10
		0.25		10
		0.75		10
		1.75		10
3	Seasoned	0	Yes	10
		0.25		10
		0.75		10
		1.75		10
4	Kiln	0	Yes	10
		0.25		10
		0.75		10
		1.75		10

The different flat-side surfaces were planed according to a planing depth scheme: 0 mm (unplanned), 0.25, 0.75, and 1.75 mm depth from the surface, and the residual wood particles were collected for further analysis.

The planned surfaces were exposed to a mould test, performed by spraying of a spore suspension of five mould fungi on the wood surfaces and incubation at the temperature 24°C and 95±3%RH for 35 days, and thereafter surfaces were graded according to mould growth by human.

A microNIR OnSite Spectrometer (VIAVI Solutions Inc., San Jose, CA, USA) with NIR wavelengths from 908 to 1676 nm with step 6 nm was used (Figure 1) was used for samples evaluation. The assessment classes were: *No mold\Mold, Drying type, Planing depth, and NIR wavelengths.*



Figure 1. MicroNIR portable spectrometer.

Each measurement of mould exposure and reference (no mould) surface was taken in 5 replicates and the data matrix combined from the average value of those replicates. The multivariate analysis of obtained spectra [8] was performed by using Evince software version 2.7.9 software, Prediktera, Umea, Sweden. Data pre-processing was centring and UV scaling.

Results and Discussion

The exploratory PCA model was initially built from data from air and kiln-dried samples containing no mould, and the same samples after mould test for discovering the grouping pattern. The drying type and planing depth were not efficient for classification of the spectroscopic data. Figure 2 clearly demonstrates the differentiation between samples with classes **No mould** (green group of dots) and with **Mould** (blue group of dots). Obtained PCA model (Table 2) had a good fit. Therefore, the decision was made towards using Soft Independent Modelling of Class Analogy (SIMCA) that allows identifying local models around those classes (Table 2).

Table 2. Multivariate models of NIR spectra of air- and kiln-dried side-boards; **No mould** and **Mould** Classes. Data pre-processing - Centred + UV scaled.

Type	Comp	R2X_cum	Q2X_cum	Eigen value
PCA	3	0.997	0.997	1.1
SIMCA				
Class "No mould"	3	0.999	0.999	0.1
Class "Mould"	4	0.998	0.998	0.2

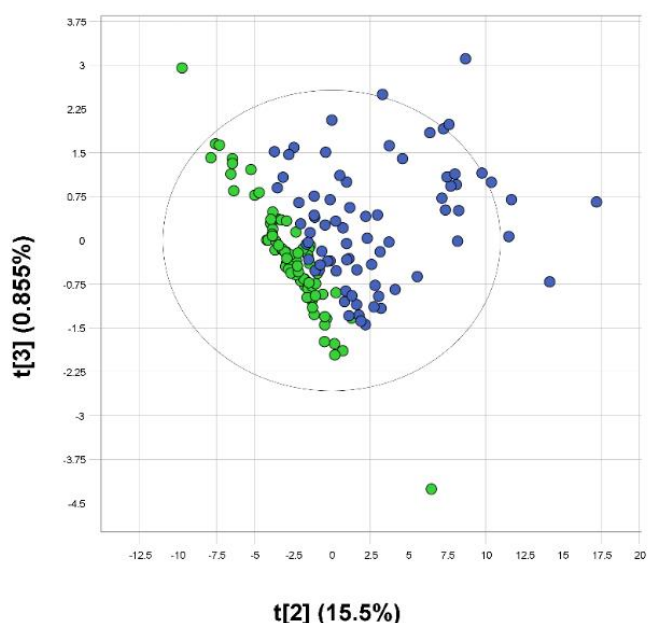


Figure 2. The score plot PC2 against PC3 where green - no mould class and blue - mould class.

Two models were adopted: a local 3-component for **No mould** class, and a 4-component for **Mould class** models. As can be seen in Table 1, the performance of the SIMCA models was

improved compare to PCA model and eigenvalues that represent self-projection of eigenvector was quite small due to a good data fit.

Figure 3 shows a Coomans' plot, which graphically presents the classification analysis. It is notable that data for air-dried and kiln-dried samples overlap (a green coloured group of the samples) and cannot be totally separated. Samples from **Mould** class (a blue group of the dots) are quite different from those in **No mould** class (red dots) as could be seen in Figure 3, as well as shown in the prediction table (Table 2).

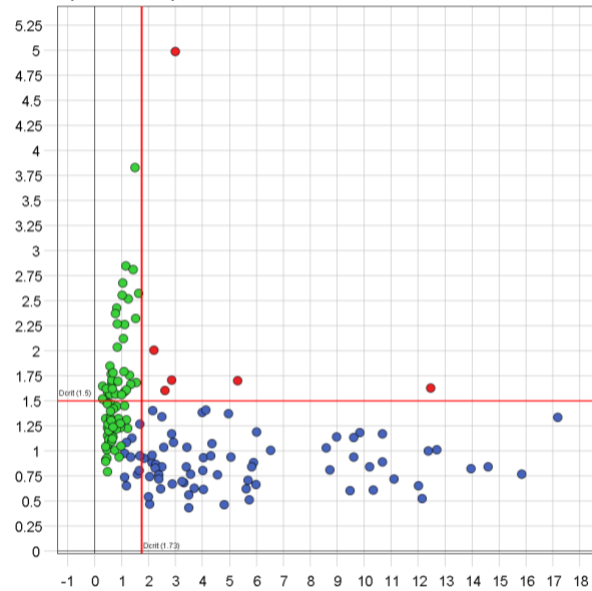


Figure 3. Coomans' Plot where green - class **No mould**, blue – class **Mould** and red – class **No class**.

The 6 observations out of totally 151 observations (total data matrix used for analysis) representing about 4% of the data the program algorithm could not be classified (Table 3). Still 141 observations were predicted correctly, that is 93.4% of accuracy whereas 10 were assigned not correctly in general.

Table 3. Prediction table from SIMCA model.

Classes	Total observations	No classes	Class No mould	Class Mould
No classes	6 (3.97%)		2 (33.3%)	4 (66.7%)
Class No mould	70 (46.4%)		70 (100%)	
Class Mould	75 (49.7%)		4 (5.33%)	71 (94.7%)
Predicted	151 (100%)	0 (0%)	76 (50.3%)	75 (49.7%)
- correctly	141 (93.4%)			
-not correctly	10 (6.62%)			

Conclusion

This study demonstrates that mould growth on a wooden surface can be evaluated by a portable MicroNIR spectrometer. The Micro NIR was sensitive enough to detect chemical differences from biological contamination such as mould growth on the wooden surfaces. Unfortunately, the sensitivity was not enough to differentiate the drying type and planning depth at current experimental conditions. We suggests that an increased number of specimens will give a better differentiation, but that is a question for future studies.

References

1. Terziev, N.; Boutelje, J. Effect of Felling Time and Kiln-Drying on Color and Susceptibility of Wood to Mold and Fungal Stain During an Above-Ground Field Test. *Wood Fiber Sci.* **2007**, *30*, 360–367.
2. Terziev, N. Migration of Low-Molecular Sugars and Nitrogenous Compounds in *Pinus sylvestris* L. During Kiln and Air Drying. *Holzforsch. - Int. J. Biol. Chem. Phys. Technol. Wood* **2009**, *49*, 565–574.
3. Myronycheva, O.; Karlsson, O.; Sehlstedt-Persson, M.; Öhman, M.; Sandberg, D. Distribution of low-molecular lipophilic extractives beneath the surface of air- and kiln-dried Scots pine sapwood boards. *PLOS ONE* **2018**, *13*, e0204212.
4. Karlsson, O.; Myronycheva, O.; Sehlstedt-Persson, M.; Öhman, M.; Sandberg, D. Multivariate modeling of mould growth in relation to extractives in dried Scots pine sapwood. In Proceedings of the 48th Conference of the International Research Group on Wood Protection, IRG48; Ghent, Belgium, 2017.
5. Thumm, A.; Riddell, M.; Nanayakkara, B.; Harrington, J.; Meder, R. Mapping Within-Stem Variation of Chemical Composition by near Infrared Hyperspectral Imaging. *J. Infrared Spectrosc.* **2016**, *24*, 605–616.
6. Williams, P.J.; Geladi, P.; Britz, T.J.; Manley, M. Near-infrared (NIR) hyperspectral imaging and multivariate image analysis to study growth characteristics and differences between species and strains of members of the genus *Fusarium*. *Anal. Bioanal. Chem.* **2012**, *404*, 1759–1769.
7. Via, B.K.; Eckhardt, L.G.; So, C.-L.; Shupe, T.F.; Groom, L.H.; Stine, M. The Response of Visible/Near Infrared Absorbance to Wood-Staining Fungi. *Wood Fiber Sci.* **2007**, *38*, 717–726.
8. Eriksson, L.; Byrne, T.; Johansson, E.; Trygg, J.; Vikström, C. *Multi- and megavariate data analysis: basic principles and applications*; 2013; ISBN 978-91-973730-5-0.

Tuesday, October 22nd

Composites and Adhesives, Session 1

10:30 – 12:30

Chair: Roger Moya, Instituto Tecnológico de Costa Rica, Costa Rica

Anisotropy of 3D printed parts using bio-filaments

Levente Dénes
University of Sopron, Hungary

Abstract

The fast developing additive manufacturing enables the tool-free manufacture of complex structures with minimal waste. However, the insufficient knowledge about physical and mechanical properties of bio-based printing materials limits the widespread adoption of large-scale 3D printing for bioproducts fabrication. This article studies the effect of filament orientation angle on mechanical properties of 3D printed parts using the fused deposition modeling (FDM) technique. This method build-up the models by the deposition of thermoplastic material through a nozzle on a layer-by-layer basis. Four filaments with different wood content, a biodegradable laboratory extruded printing material with lignin content, a carbon fiber reinforced filament were used beside the conventional PLA filament used as control. The samples were printed with five orientations (0°, 30°, 45°, 60°, 90°) and two building directions (flatwise, edgewise). The modulus of elasticity, tension strength and bending strength of the specimens were measured in a universal testing machine based on standard methodologies. For anisotropy modeling the Hankinson's equation and the tensor theory for orthotropic materials were employed. Results indicated that orientation has a significant influence on the mechanical properties of bio-filaments and both models used fit well on the measured data. The analysis of the effect of printing orientation on mechanical properties of 3d printed parts made of biofilaments can contribute to the propagation of additive manufacturing technologies in bio-materials processing industries.

Key-words: 3d printing, bio-filaments, printing orientation, fused deposition modeling, Hankinson's equation

Improve the performance of soy protein-based adhesives by a polyurethane elastomer

Qiang Gao

Key Laboratory of Wood Material Science and Utilization, Beijing Forestry University, Beijing 100083, China.

In recent years, soy protein-based adhesives (SPAs) have garnered great research attention as a substitute for the formaldehyde-based adhesives to eliminate formaldehyde emission from the wood-based panel [1]. As the most important raw material of SPAs, soybean meal is abundant, inexpensive, renewable, biodegradable, and nontoxic [2-3]. But the practical application of SPAs has been limited due to the low water resistance [4]. Chemical and physical methods were applied to enhance water resistance of the SPAs, including denaturation [5], cross-linking agents [6], synthetic resin [7], nano-material [8] and biomimetic modification [9]. Among those modifications, the most effective way is using cross-linking agents and synthetic resins, such as phenol formaldehyde resin [10], polyisocyanates [11], polyamidoamine-epichlorohydrin resin [12] and epoxide [13]. The active functions of the cross-linker or synthetic resin react with the $-NH_2$, $-NH-$, $-COOH$ of protein to generate a cross-linked structure, which improves the water resistance of the adhesive. However, our previous research showed the SPAs is brittle, and this brittleness of the adhesive further increases after modifying by cross-linker, resulting in a low dry bond strength and impact resistance property of the bonded panel. This is because the interior force of the wood panel is inevitable from the manufacture process and this interior force will increase with the moisture content change of the panel during the using process. These interior forces usually balanced by the bond force of cured adhesive, however, if the cured adhesive is brittle, this balance will be easily broken when the interior force increasing. Also, the previous research showed an increase of the crosslinker dosage created a more compact structure of the adhesive, but this decreased the bond strength of the resultant panel. Therefore, increasing the toughness of the SPAs will benefit for balancing the interior forces, which improves the bond strength and water resistance of the adhesive.

In this study, the soy protein isolate (SPI) and a laboratory-synthesized crosslinker- triglycidylamine (TGA) was used to develop a SPI-based adhesive. In order to improve the toughness of the adhesive, thermoplastic polyurethane elastomer (TPU) and γ -(2,3-epoxypropoxy) propyltrimethoxysilane (KH-560) were used to develop a novel high performance SPI-based adhesive. The effects of TPU and KH-560 addition on the performance of the adhesive and the resultant plywood were investigated. Three-ply plywood was fabricated and their dry/wet shear strength was tested according to China National Standards (GB/T 9846.3-2004). The functional groups, fracture morphology, thermal behavior, residual rate after hydrolyzing, and fracture section and cracks observation of the resultant adhesives were examined.

Results showed introducing TGA and KH-560 as a cross-linker reacted with the functions of the soy protein and effectively increased the water resistance of the soy protein isolate adhesive. The wet shear strength of plywood bonded by TSPI and TSPI/KH-560 adhesive was 0.96 and 1.39 MPa, improving by 26.3% and 82.9% compared to plywood bonded by SPI adhesive, which meet the interior-use plywood requirement (≥ 0.7 MPa). When 1% KH-560 was added into the SPT/TGA (TSPI) adhesive, the dry and wet shear strength of the plywood bonded by the resultant adhesive increased by 60.4% to 1.99MPa and 82.9% to 1.39 MPa, respectively. TPU physically combined with TSPI adhesive to form a interpenetration network, which improved the performance of the adhesive. When TPU was introduced to the TSPI adhesive, the residual rate of the adhesive increased by 5.2% comparing with TSPI adhesive, and the dry and wet shear strength of plywood bonded by TSPI/TPU adhesive increased by 10.7 and 67.7%, respectively, compared with that of TSPI adhesive. KH560 act as a bridge to connect TPU and TSPI, forming a joined crosslinking

network, which improved the thermostability/toughness of the adhesive and created a uniform ductile fracture section of the adhesive. This resulted in an improvement of the residual rate of the adhesive by 0.9% compared with that of TSPI/TPU adhesive. The dry and wet shear strength of the plywood bonded by the TSPI/TPU/KG560 adhesive increased by 23.2 and 23.6% when compared with that of TSPI/TPU adhesive.

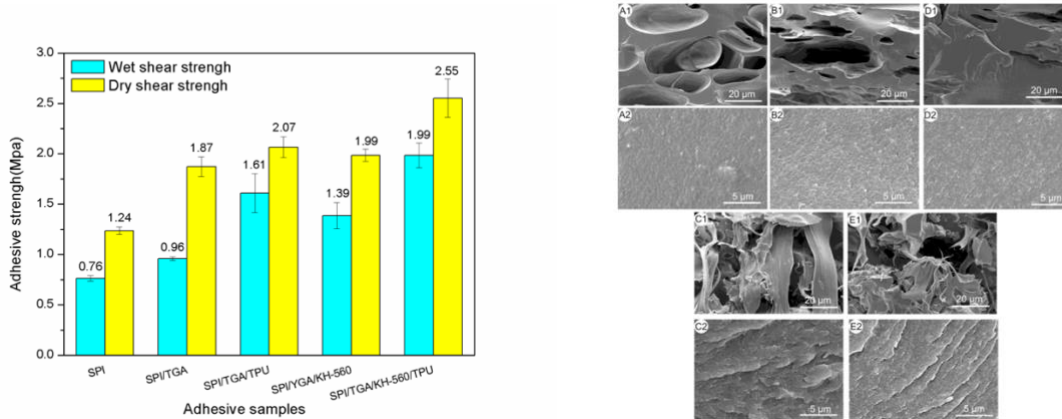


Figure 1. The bond strength and fracture surface micrographs of the cured adhesive: A1 and A2 (SPI), B1 and B2 (TSPI), C1 and C2 (TSPI/TPU), D1 and D2 (TSPI/KH-560), E1 and E2 (TSPI/KH-560/TPU)

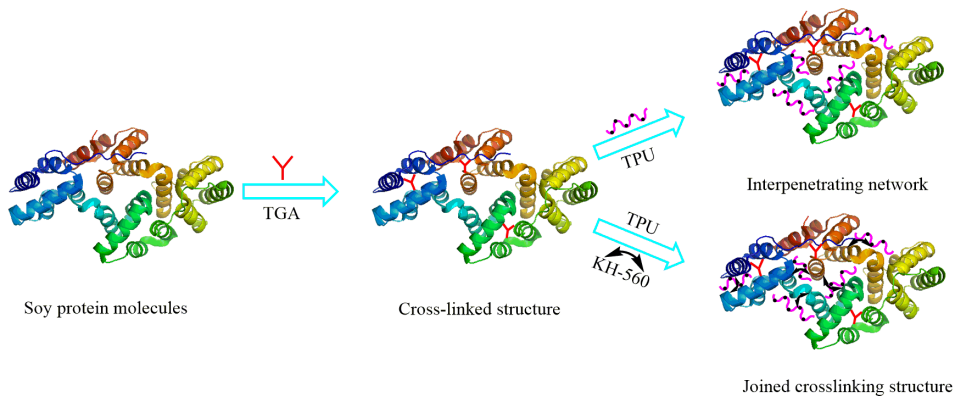


Figure 2. The reaction scheme of the adhesive

Thermo-hydrolytic Recycling of Urea Formaldehyde Resin-bonded Laminated Particleboards

Qilan Fu

Laval University and FPInnovations, Canada

Abstract

The large global production of particleboard creates equal quantity of particleboard waste after completing their service life. Given increasing demand for green products and new government's environmental policies, it is urgent to develop technologies to recycle these used composite panels into valuable raw materials for the manufacturing of other composites. This study was carried out to recover particles from waste laminated particleboards using various thermo-hydrolytic treatments. The recovered particles were used as raw materials with different substitutions of fresh particles to manufactured particleboard panels. The performance of the resulting particleboards was evaluated by their main mechanical properties and formaldehyde emissions. The results suggested that the particle size had more important effect on the internal bond strength (IB) of particleboard than the content of resin residue from the recycled particleboard. Particles recycled at 140 °C/20 min have the lowest nitrogen content value. About 65 % of UF resin can be removed from the particleboards treated at 140 °C/20 min. Particles recycled at 140 °C/20 min were comparable to fresh particles in terms of mechanical properties and formaldehyde emissions and 100% of the recycled particles can be used in the manufacture of particleboard without an adverse impact on the board performance.

Wood-based Material Applications in 3D Printing for Composites

Douglas Gardner
University of Maine, USA

Abstract

Wood-based material components including sawdust, wood flour, bamboo, lignin, and cellulose nanofibers are being explored as functional additive reinforcements in thermoplastic and thermosetting matrices used in additive manufacturing (AM) or 3D printing. The 3D printing processes most typically reported using wood-based materials include the extrusion-based fused filament fabrication, fused deposition modeling, and pellet-fed large scale AM, selective laser sintering, and liquid deposition modeling. The rationale for using wood-based components in 3D printing include enhancing the material properties of resulting printed parts such as increased mechanical properties, reduced dimensional instability, i.e. part warpage, improved aesthetics, providing a green alternative to carbon or glass filled polymer matrices as well as reducing material costs. This presentation will provide an overview of wood-based material applications in 3D printing for composites with a state of the art review of current research activities around the world.

Characterizing Accelerated Weathering Conditions

Mr. Micah Sutfin, micah.sutfin@oregonstate.edu

Dr. Fred Kamke

Oregon State University, USA

Abstract

Accelerated weathering (AW) is a type of weathering test to measure future possibilities of materials' durability under certain environmental conditions. Often methods of AW are intended to differentiate between the exterior durability of two or more adhesives, coatings and other treatments employed in engineered wood products. The goal of this project is to characterize the bondline conditions of test specimens undergoing standard accelerated weathering procedures. AW procedures depend on the standard test method chosen. Conditions may involve room temperature water soaking, hot water soaking, vacuum pressure soaking, submersion in boiling water, water spray, convection air drying, freezing, or some form of outside exposure to the weather. While there are few claims that AW testing provides data that can be used to predict service life, AW testing is useful as a comparative test among product alternatives. AW tests have become a requirement for many wood composite products.

This project will monitor temperature and moisture content of specimens undergoing AW exposure for the following standards: ASTM D3434 (automatic boil test), CSA O112.9 (boil-dry-freeze), PS2 (Section 7.17, 6-cycle VPS). Each AW procedure will be conducted with at least two types of specimens that differ by either geometry, adhesive employed, or density. Using fine-wire thermocouples, temperature will be measured in the center of the specimen during AW regimes. Average MC amongst specimens will be determined by weight measurements, and then a final oven-dry weight. MC gradient will be determined by periodic destructive testing, by removing a specimen from the AW environment and promptly cutting into sections for a gravimetric MC determination. Results will include plots of temperature and MC as a function of time and/or cycle. Appropriate mechanical tests will be performed on the weathered specimens, as well as unweathered control specimens.

Effect of Element Morphology on Strength of Wood-PLA Composite

*Tibor Alpár¹**

¹Simonyi Károly Faculty of Engineering, Wood Sciences and Applied Arts,
University of West Hungary, Sopron, Hungary *Corresponding author
tibor.alpar@skk.nyme.hu

Abstract

Typical reinforcers in polymer-based composites are different fibers, such as glass, carbon, aramid or even natural fibers. Most commonly wood flour or microparticles are used as filler in WPC, but recently wood fibers are also widely liked to reinforce polymers. Publications often do not distinguish among types of elements as wood flour, microparticles and real fibers. These element types are differing in their slenderness, specific surface and strength values based on their morphology depending on their production processes. These differences in shape and dimensions affect the processing and strength properties of the desired WPC product.

In this paper, the effect of shape or morphology of wood elements on the properties of wood-PLA composites were researched. Wood-PLA composites were produced in laboratory scale with wood flour, wood micro particles and real wood fibers as reinforcers. After compounding in twin screw extruder, standard bending and tensile test pieces were injection moulded and tested by standard test methods. As control, also neat PLA samples were produced and tested. The results were also compared to other results published in various research papers. As result it could be concluded that real fibers has the best reinforcing effect on wood-PLA composite and wood flour performs the lowest strength. So the morphology of wood elements has a significant effect on strength of WPC.

Keywords: wood flour, microparticles, wood fiber, fiber morphology, short fiber, continuous fiber

Introduction

There are three main applications to produce fiber reinforced composites: short, long and continuous fiber reinforcement. In continuous fiber technologies, the reinforcing fibers may be non-woven or woven, which can be uni-directional, bi- or triaxial. While continuous fibers are usually embodied in thermosetting polymer matrix, short and long fibers are compounded with thermoplastics (Czvikovszky et al. 2007). Short fiber technology usually uses extruders for compounding thermoplastic matrix material with fibers with limited length, up to 2 mm, which are usually below the length of the pelletized compound. The fibers are randomly embodied in a polymer. Long fiber WPC is produced by pultrusion and it has the feature of continuous fiber threads running the full length of the pellet, up to 25 mm (Calumby 2014). Here fibers run parallel to each other and to the length of pellet.

Publications often do not distinguish among types of elements as wood flour, microparticles and real fibers. These element types are differing in their slenderness, specific surface and strength values based on their morphology depending on their production processes. These differences in shape and dimensions affect the processing and strength properties of the desired WPC product.

Hardwood is built up from at least four cell types. Vessels (tracheas), parenchymas (shape is nearly spherical), rays and fibers. The fibers are 2-5 mm long, 20-30 μm thick, and the ratio of length/diameter is 100:1 (Peltola 2004, Molnár 2000, Carlquist 2010). Fibers in hardwood comprise around 60-65% of its volume (Winkler 1999, Deppe 1996). Softwood species contain only tracheids for transport and support, and occasionally thin rays for storage. Tracheids of early wood are thin walled and result in low wood strength compared with late-wood, where thick cell walls provide support. (Molnár 2000, Wilson & White 2006). Fibers in softwood comprise around 90-95% of its volume (Winkler 1999, Deppe 1996). Length of fibers vary by species and by age of trees. Komán (2012) tested different poplar clones and he determined that in general the fiber length increases from 0.5 mm at age of 2 years to 1.25 mm at age of 20 years. Typical wood-based fillers or reinforcers in wood-polymer composites are wood flour, wood microparticles and wood fibers. All three element types are produced with completely different technologies and they differ in sizes and morphology (Figure 1.).



Figure 1. Image of wood flour (a.), microparticles (b.) and fibers (actually fiber bundles) (c.)

Various techniques are used to produce wood elements for WPC, but the three main technologies are: mechanical processing, hydro-thermal and mechanical processing, and chemo-mechanical processing (Winkler 1998, Winkler 1999, Deppe 1996, Heller 1995, Rowell 2005).

In mechanical process element sizes are reduced in size by cutting processes with geometrically defined or undefined cutting, which results particles (Thole 2006). These various processes affect the geometry of wood elements. Thole (2006) categorizes mechanical processing, where the most common equipment to produce suitable particles for WPC are the hammer mill, disk mill, cross beater mill or simple sawing (sawdust). These are the methods of wood processing, but all are mostly based on a single cutting by a kind of knife. The geometry, size and surface microstructure of elements are influenced by the type and parameters of milling.

Wood may be divided into fibers or fiber bunches by hydro-thermal processes or chemical processes (Deppe 1996, Winkler 1999, Thole 2006). The defibrator is fed with wood chips, which are treated with saturated steam at 6 to 10 bar and an inner temperature of 175 – 195 °C for 3 to 7 minutes (Deppe 1996, Winkler 1999, Thoemen et al. 2010). During this hydro-thermal treatment, wood fibers absorb water and swell. Lignin is plasticized similarly to a thermoplastic polymer, and the hydrogen bonds between polyoses and cellulose partially break up. After plasticizing the wood, chips are fed into the refiner, which transforms them mechanically into fiber bundles by two large diameter discs (Deppe 1996, Winkler 1999, Thoemen et al. 2010).

Mechanical reduction is used to produce wood flour (wood dust), like impact reduction by beater mills, grinding reduction by milling with conidur sieves or disc mills or sanding of wood or wood-based panels. Sanding dust is typically a flour like raw material for WPC, and it is a by-product, which was formerly considered waste. It is cheaper to produce wood flour than real wood fibers, so in spite of its low aspect ratio it is more commonly used in WPC (Niska and Sain 2008). Reineke (1945) describes wood flour as follows: ‘...somewhat loosely to wood reduced to finely divided particles approximating those of cereal flours in size, appearance, and texture.

The shape of wood elements in WPC is significant. In many publications the real type of wooden elements used in composites is not clearly defined or have a misleading name. In this research we were intended to compare the effect of element morphology on strength of wood-PLA composites.

Materials and Methods

We compared various wood wastes (by-products) affecting wood-PLA composites (Figure 1). The results were partially summarized in diploma thesis of Horváth (2014). Three by-products were used during the experiments sanding dust and sawdust were obtained from a wood processing SME (Markó Co.) working with hardwood species and technical fibers were obtained from an MDF producing company (Kronospan-MOFA Hungary Ltd.). All three raw materials contained mixed species, and they were characterized by sieve analysis and the aspect ratio was measured by an image analyzer. The tests were done by a Fritsch Analysette vibrating separator fitted with sieve diameters of 1600, 1250, 800, 500, 250, 125, 80 microns and a bottom pan (#12,

#15, #20, #35, #60, #120, #180 respectively). Regarding image analysis results were based on ~500 measurements for each element type.

Image analysis is commonly used to characterize dimensions and shape of wood fibers and other elements. An image analysis system can measure and characterize the non-spherical particles as shown in Figure 2. using the shortest and longest diameters, perimeter and projected area.

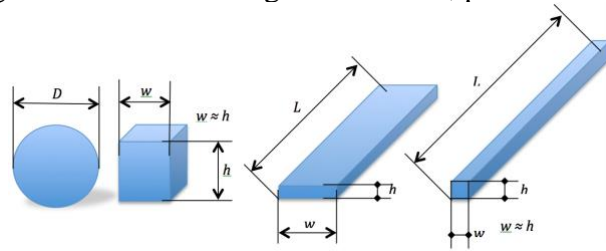


Figure 2. Basic shapes of wood particles

Various methods are available to characterize particles, like Feret diameter and Feret-ratio (Pabst & Gregorová 2007, Gescutti et al. 2006) or Martin diameter (D_M) (Stiess 1995, Thole 2006). Figure 3. shows the different diameters, where index t is for thickness, w is for width and l for length of the particle.

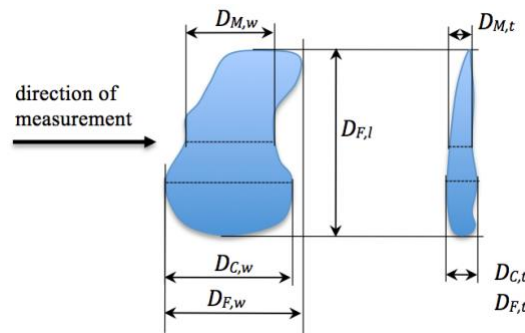


Figure 3. Particle size diameter definitions

Actually any ratios of two measures or two equivalent diameters of an element can be used as form factor. For elements that are not globular or cubical, it is more informative to use slenderness, which gives the ratio of a longer dimension to a shorter one. The best way to characterize a wood element is to use the methods of equivalent diameter and form factors. The following form factors are recommended:

- for wood flour: sphericity factor of Wadell,
- for microparticles and wood fibers: longitudinal slenderness (Ψ_{LS}), in general based on Figure 3.:

$$\Psi_{LS} = \frac{D_F^{\max}}{D_P}, \quad (\text{Eq.1})$$

where

D_P can be calculated based on Martin diameter:

$$D_P = \sqrt{\frac{4 \cdot (D_{M,w} \cdot D_{M,t})}{\pi}} \quad (\text{Eq.2})$$

To achieve a more precise approximation of shape characterization longitudinal slenderness (Eq.1) can be expanded by width slenderness:

$$\Psi_{LS} = \frac{D_F^{\max}}{D_P \cdot (\Psi_{WS})^2}, \quad (\text{Eq.3})$$

where

$$\Psi_{WS} = \frac{D_{F,w}^{\max}}{D_{F,t}^{\min}}. \quad (\text{Eq.4})$$

These methods are suitable to characterize technical fibers. When measuring different wood particles and applying form factor (Eq.5) to characterize slenderness, there is a limit value of $\Psi_{LS} > 1$, where the elements should be considered as fibers instead of particles or flour.

The matrix polymer was an ESun® PLA Polymer 2002D type polylactid acid product. No coupling agent was used. The composite was compounded in a Labtech Engineering LTE 26-48 twin-screw extruder with 12 heating zones (170-180 °C), at 15 RPM of extruder screw and a feeding speed of 5 k/h. Compounds were made with all three wood raw materials at 30 and 40 wt% load in PLA. The extruder was fed by two gravimetric feeders. The pellets were dried at 103 °C for 24 hours in a Heraeus UT-6 type drying cabin prior to injection moulding in an Arburg Allrounder Advance 370S 700-290 injection moulding machine. Standard test pieces for tensile tests and for flexure were made from all six compounds and from neat PLA as control. The samples were tested based on standards EN ISO 527-2 and EN ISO 128 by an INSTRON IN5566 testing machine.

Results and Discussion

The wood flour, so sanding dust contains ~35% of very fine elements below 80 microns, and another 30% measure 125 microns. The largest elements are 800 microns. 90% of microparticles are between 80 and 800 microns, and 30% are 250 microns. Comparing these by-products to standardized fillers of the American Wood Fibers company, the recommended use for sanding dust is ‘standard wood plastic composites’ and for microparticles is ‘foamed wood plastic composites’. It is more difficult to analyze wood fibers by sieving is since their length is much larger than their diameter. In Figure 4. the frequency of element sizes shows a wide range. The fibers contain a relatively high amount (17%) of fine elements below 80 microns.

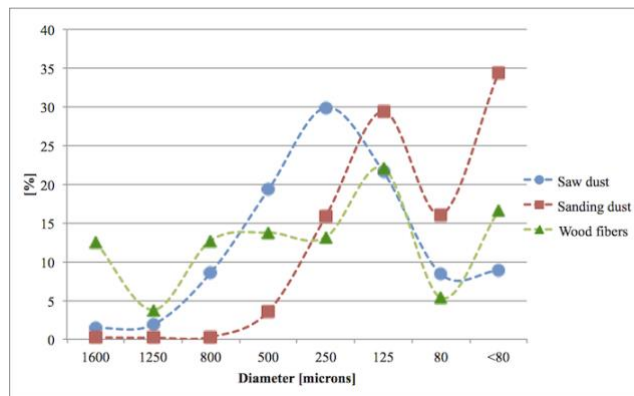


Figure 4. Element size distribution of sanding dust, sawdust and wood fibers (Horváth 2014)

In Figures 5. and 6., tensile strength and bending strength diagrams of wood-PLA composites are shown compounded with sanding dust, sawdust and technical fibers; (see the last section of Table 2. for values). In general, strength values of composites were lower than those of the neat PLA. It has to be emphasized that no coupling agent and no plasticizer were added. Composites with sanding dust (wood flour) filler were the most rigid compounds. They showed a 53% and 78% drop in tensile strength with 30 and 40 wt% wood load respectively. A similar decrease was observed in bending tests. By increasing the wood load in PLA from 30 to 40 wt%, a significant drop in strength was observed: a 45% drop for the bending test and 54% for the tensile test. Wood flour without any additives works only as filler in the composite.

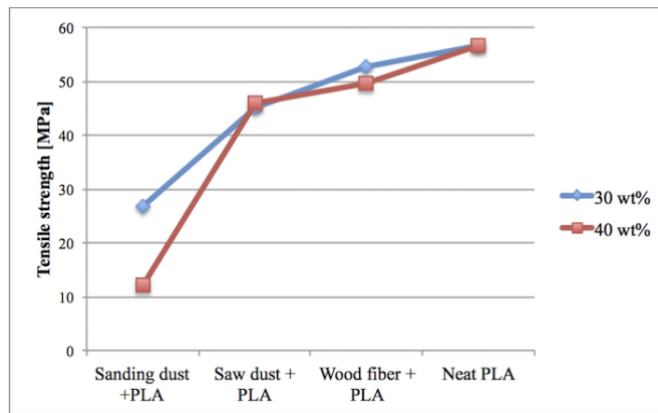


Figure 5. Tensile strength of wood-PLA composites from various wood elements and loads

Sawdust, considered as micro particles, has some slenderness and it showed better results compared to sanding dust. Tensile strength of a sawdust-PLA composite with 30 and 40 wt% wood loads was 20% lower for a 30 wt% wood load and 19% lower for a 40 wt% wood load than that of the neat PLA. Bending strength tests showed very similar results: 27% and 19% decrease. Still the higher sawdust content resulted in a higher bending strength: 79 vs. 88 MPa for 30 and 40 wt% wood loads respectively.

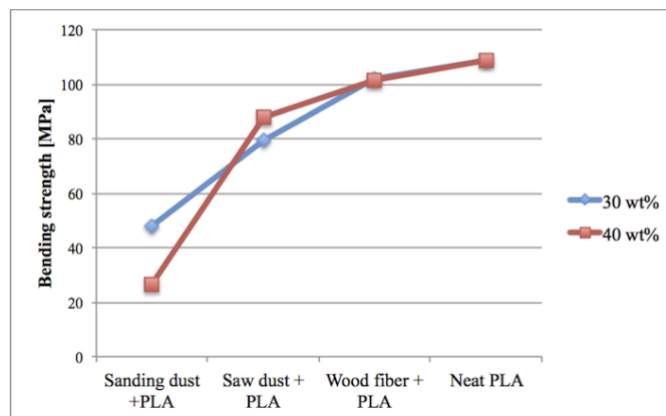


Figure 6. Bending strength of wood-PLA composites from various wood elements and loads

The best results were observed in wood fiber loaded PLA. The main reasons for higher strength are the large specific surface per element, the high aspect ratio, and good felting. Compared to neat PLA, the reduction in strength is very low - only 6-12%.

In Table 1. some important mechanical properties are compared based on various publications. Sawdust, considered as micro particles, has some slenderness and it showed better results compared to sanding dust. Tensile strength of a sawdust-PLA composite with 30 and 40 wt% wood loads was 20% lower for a 30 wt% wood load and 19% lower for a 40 wt% wood load than that of the neat PLA. Bending strength tests showed very similar results: 27% and 19% decrease. Still the higher sawdust content resulted in a higher bending strength: 79 vs. 88 MPa for 30 and 40 wt% wood loads respectively.

The best results were observed in wood fiber loaded PLA. The main reasons for higher strength are the large specific surface per element, the high aspect ratio, and good felting. Compared to neat PLA, the reduction in strength is very low - only 6-12%.

Table 1. Comparative strength properties of wood flour and wood fiber composites

Material	Wood load [wt%]	L [microns]	L/D	Tensile strength [MPa]	MOR [MPa]	Source
fiber BSKP + PLA	40	2280	73	61.5	-	
fiber TMP + PLA	40	1400	42	67.8	-	Peltola et al. (2014)
WFlour + PLA*	40	728	-	54.3	-	
fiber BSKP + PP	40	2280	73	22.5	-	
WPowder + comp. + PP*	50	200-2000	-	41.9	-	Nygård et al. (2008)
WFiber + comp. + PP	50	1.29	36.2	56.1	-	
fiber CTMP + comp. + PP	50	1.5	42	60.1	-	
sanding dust + PLA*	40	<500	1-2	12,1	26,2	Horváth (2014) and own data
saw dust + PLA*	40	80-1250	3-8	45,9	88,0	
wood fiber + PLA*	40	80-1600	40-140	49,7	101,5	
neat PLA	-	-	-	56,7	108,6	

*diameter in microns based on sieve analysis

Summary and Conclusions

Wood flour, micro particles, particles, flakes, chips and strands can be produced by clean mechanical size reduction processes. These elements are cut pieces of complete wood structure containing all chemical and anatomical components at various dimensions. These elements are NOT fibers regarding the anatomical structure of wood, because the fiber structure is damaged by mechanical processes. Of course, all of these elements contain fibers and fiber bunches, but in various fragmentations depending on the element size caused by the size reduction process. Figure 7. shows clearly the differences between mechanically processed wood flour, microparticles and thermo-mechanically processed wood fibers.

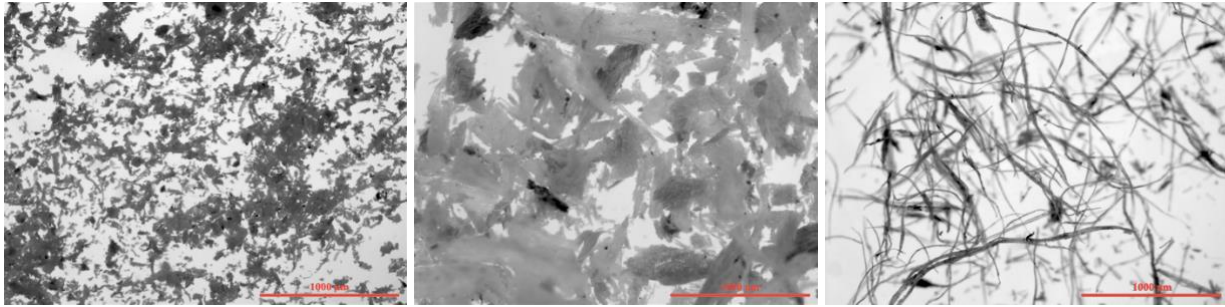


Figure 7. Microscopy images of wood flour (a), micro particle (b) and wood fibers (c) – photo: Sándor Fehér

Wood flour and micro-particles produced by mechanical size reduction processes are suitable for “short fiber” technologies or as fillers in thermoplastic WPCs. Wood fibers can be used in long fiber technologies, replacing other, non-wood fibers.

$$\Psi_{LS} = \frac{D_F^{\max}}{D_P \cdot (\Psi_{WS})^2} \quad (\text{Eq.1})$$

where:

Ψ_{LS} : longitudinal extended by width slenderness,

D_{Fmax} : Feret diameter,

Ψ_{WS} : width slenderness,

D_P : chord length diameter.

Thole (2006) determined a strong limit for form, determining when a particle should be considered as fiber. Based on research result and equation (1) the elements with form factor $\Psi_{LS} = 1$ are wood flour elements, in case of $1 < \Psi_{LS} \leq 10$ the elements are micro-particles and in case of $10 < \Psi_{LS}$ those are definitely fibers. These are technical fibers with significant slenderness, which means their length exceeds their width and thickness.

Various publications say that wood flour can be used only as a filler in WPC systems, but wood fibers have a significant reinforcing effect. The length of fibers and fiber load have a direct effect on strength values. It is also important to use coupling agents or surface modification on wood elements to increase the interaction between wood elements and matrix polymers as many researchers reported. (Alpár et al. 2017)

Acknowledgements

This article was made in frame of the „EFOP-3.6.1-16-2016-00018 – Improving the role of research+development+innovation in the higher education through institutional developments assisting intelligent specialization in Sopron and Szombathely”.

References

Alpár, T., Markó, G., Koroknai, L. 2017. Natural Fiber Reinforced PLA Composites: Effect of Shape of Fiber Elements on Properties of Composites. In: Vijay, Kumar Thakur; Manju, Kumari Thakur; Michael, R Kessler (szerk.) Handbook of Composites from Renewable Materials :

**Proceedings of the 62nd International Convention of
Society of Wood Science and Technology
October 20-25, 2019 – Tenaya Lodge, Yosemite, California USA**

- Volume 2 - Design and Manufacturing. New York, USA: John Wiley & Sons, Scrivener, (2017) pp. 287-312.
- Calumbi, R. 2014. *LONG FIBER REINFORCED THERMOPLASTICS A LIGHTWEIGHT SOLUTION FOR ENGINEERING APPLICATIONS*, SAMPE BRAZIL Conference 2014 (11th November 2014).
<http://www.feiplar.com.br/materiais/palestras/SAMPE/apresentacao/Celanese.pdf>
- Carlquist, S. 2010. *Comparative Wood Anatomy: Systematic, Ecological, and Evolutionary Aspects of Dicotyledon Wood*, Springer verlag
- Czvikovszky, T., Nagy, P., Gaál, J., 2006. *A polimertechnika alapjai (Fundamentals of polymertechnics)*, pp. 367-385, Műegyetemi Kiadó
- Deppe, H-J., Ernst, K., 1996. *MDF. Mitteldichte Faserplatten*, Drw Verlag Weinbrenner
- Gescutti, G., Müssig, J., Specht, K., Bledzki, A.K. 2006. Injection moulded natural fibre reinforced PP - Determination of fibre degradation by using image analysis and prediction of mechanical composites properties. in: Bledzki, A.K. & Sperber V.E. 2006. *6th Global Wood and Natural Fibre Composites Symposium*. (4-5. April 2006)
- Heller, W. 1995. *Die Spanplatten-Fibel (The Particleboard-Fable)*, Heller, Hameln
- Horváth, R. 2014. *Fa részecskék alakosságának hatása fa-PLA kompozitok tulajdonságaira (Effect of wood elements on properties of wood-PLA composites)*, Degree dissertation, University of West Hungary, Sopron
- Komán, S. 2012. *Nemesnyár-fajták korszerű ipari és energetikai hasznosítását befolyásoló faanatómiai és fizikai jellemzők (Anatomical and physical properties of poplar species regarding modern industrial and energetic utilization)*, pp. 41-44. PhD thesis, University of West Hungars, Sopron
- Ku, H., Wang, H., Pattarachaiyakoop, N., Trada, M. 2011. *A review on the tensile properties of natural fiber reinforced polymer composites*, Composites Part B: Engineering, Volume 42, Issue 4, pp. 856–873.
- Molnár, S., 2000. *Faipari Kézikönyv (Wood handbook)*, Faipari Tudományos Alapítvány
- Niska, K.O., Sain, M., 2008. *Wood-polymer composites*, Woodhead Publishing Ltd., Cambridge, pp. 13-14.
- Nygård, P., Tanem, B.S., Karlsen, T., Brachet, P., Leinsvang, B. 2008. *Extrusion-based wood fibre-PP composites: Wood powder and pelletized wood fibres – a comparative study*. Composites Science and Technology, Vol. 68. pp. 3418–3424.
- Pabst, W., and Gregorová, E. 2007. Characterization of particles and particle systems. ICT Prague, pp. 27-28
- Peltola, P., 2004 *Alternative fibre sources: paper and wood fibres as reinforcement*, in: „Green Composites – Polymer Composites and the Environment”, Ed.: Baillie C., Woodhead Publishing Limited, Cambridge, pp. 81-99
- Reineke, L.H. 1945. *Wood flour*, Report No. R565 USDA Forest Products Laboratory
- Rowell, R.M., 2005. *Handbook of wood chemistry and wood composites*, pp. 36., 365, Taylor & Francis.
- Stiess, M. 1995. *Mechanische Verfahrenstechnik - Vol.2*. Springer Verlag, pp. 231.

**Proceedings of the 62nd International Convention of
Society of Wood Science and Technology
October 20-25, 2019 – Tenaya Lodge, Yosemite, California USA**

- Thoemen, H., Irle, M., Sernek M. 2010. *Wood-Based Panels An Introduction for Specialists*, Brunel University Press, pp. 66-67.
- Thole, V. 2006. Mechanische und thermomechanische Verfahren zur Herstellung von Holzpartikeln für WPC (Mechanical and thermo-mechanical process to produce wood particles for WPC), in: Bledzki, A.K. & Sperber V.E. 2006. *6th Global Wood and Natural Fibre Composites Symposium*. (4-5. April 2006) University of Kassel
- Winkler, A. 1998. *Faforgácslapok (Particleboards)*, Dinasztia Kiadó
- Winkler, A., 1999. *Farostlemezőgyártás (Fiberboard production)*, pp. 11, Dinasztia Kiadó
- Yang, S. and Chin, W. 2004. *Mechanical properties of aligned long glass fiber reinforced polypropylene. II: Tensile creep behavior*, Volume 20, Issue 2, p. 207–215.
- http://www.awf.com/pdf/awf_industrial_fibers.pdf (12. 10. 2015)

IMPROVEMENT OF ASH (*FRAXINUS EXCELSIOR* L.) BONDING QUALITY WITH ONE COMPONENT POLYURETHANE ADHESIVE AND A PRIMER FOR GLUED LAMINATED TIMBER

Peter Niemz^{1,2}, Gaspard Clerc¹ and Milan Gaff²*

¹ em. Prof. Dr.Ing.habil.Dr.hc; Bern University of Applied Sciences, Institute for Materials and Wood Technology, Solothurnstrasse 102, POB 6096, CH -2500 Biel 6

e-mail: peter.niemz@bfh.ch and
niemzp@retired.ethz.ch

and

²⁾ Department of Wood Processing and Biomaterials, Faculty of Forestry and Wood Sciences, Czech University of Life Sciences Prague, Kamýcká 1176, Praha 6 - Suchdol, 16521 Czech Republic

¹⁾ M.Sc. Gaspard Clerc; PhD student; Bern University of Applied Sciences, Institute for Materials and Wood Technology; Solothurnstrasse 102, POB 6096, CH -2500 Biel 6

e-mail: gaspard.clerc@bfh.ch

²⁾ Doc. Dr. Milan Gaff, Department leader, Department of Wood Processing and Biomaterials, Faculty of Forestry and Wood Sciences; Czech University of Life Sciences Prague, Kamýcká 1176, Praha 6 - Suchdol, 16521 Czech Republic

e-mail: gaffmilan@gmail.com

Abstract

Glued laminated timber made from hardwood offer higher strength and stiffness properties than their equivalent in softwood. Also their visual aspect can be an attractive selling argument. However, their manufacturing still remains problematic. Nowadays, only phenol resorcinol formaldehyde adhesive (PRF) and special MF/MUF are able to provide a proper bonding quality concerning ash wood gluing. Despite their high bonding performance, these adhesives have several disadvantages (e.g. a dark brown bond line (PRF), emission of formaldehyde during the gluing for PRF/MUF). This paper focuses on the optimization of the gluing process of two different one-component polyurethane (1C-PUR) adhesives with ash wood in order to develop an industrial application process. The influence of the primer concentration and of the wood moisture content prior to bonding was investigated using tensile shear test according to DIN EN 302-1 and delamination test according to DIN EN 302-2. It was shown that low degree of

delamination (less than 10%) could be reached using special 1C-PUR adhesive under industrial conditions.

Key words: glued laminated timber, ash wood, gluing, delamination, 1C-PUR, priming, PRF (Aerodux), MUF

Introduction

The increase in hardwood harvest in Europe, particularly in Switzerland, encourages also the application of these species in construction engineering. The hardwood reserves in the forests are accumulating [1], [2] and thus another economic use besides the energetic use is desirable. The common hardwoods have better strength properties than the mostly used spruce wood and thus have a good potential in the construction sector. However, wooden construction designs usually need the wood to be adhesively bonded, e.g. as glued laminated timber (glulam) or laminated veneer lumber (LVL), to achieve the demanded load bearing capacity. Technical standards certain minimum requirements for such glue joints to guarantee safety and quality [3], [4].

The processing of glued laminated timber in hardwood is a more challenging task than for softwood. Nowadays the gluing of beech and especially ash glued laminated timber is only approved with special melamine urea formaldehyde (MF), phenol resorcinol formaldehyde and one component polyurethane with the adjunction of primer. Knorz et al. [5] showed that the gluing of ash wood is presenting higher difficulties than with beech wood. This paper presents the results of several projects which have been conducted with industrial partners concerning the gluing of ash wood for application in load bearing construction in order to develop a suitable process for an industrial application for ash wood. Fig. 1 shows the results from a first industrial test for gluing from ash wood under industrial conditions [8] for different adhesives (included 1 C PUR (producer 1) and priming with DMF) (see [6], [8]).

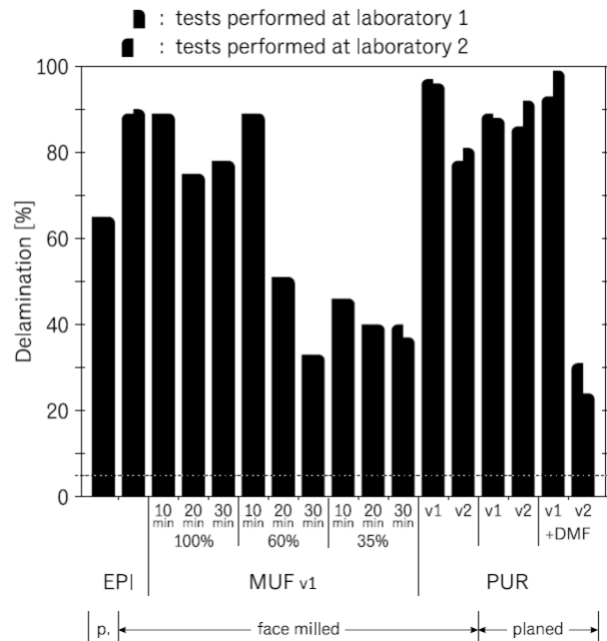


Figure 1. Delamination test from ash wood, measured at 2 different laboratories for ash wood and EPI, MUF (different closed assembly time) and 1 C PUR (producer (1) and DMF as a Primer for PUR (first test) [8], test serie 1

Preliminary experiments with EPI, MUF with different reactivity and CAT, PRF and 1 C PUR (producer 1) and DMF as primer showed that

- the delamination for all adhesives is higher than the allowed values in the standards (5%)
- for MUF delamination decreased with decreasing mixing ratio and decreases with the CAT
- 1 C PUR (manufacturer 1) without primer also did not meet the standard specification (5%), we have a difference between the 2 tested 1 C PUR, after priming with DMF get decreased the delamination (see also PhD thesis from Kläusler [9])

Materials & Methods

For the tensile shear strength and the delamination experiment, ash (*Fraxinus excelsior* L.) with a density of $674 \pm 68 \text{ kg/m}^3$ at a moisture content of 8 % was used. Different 1C-PUR with long CAT from Henkel AG (HBS 309, HBS 709 and the HB 181) were chosen. The primer Loctite PR 3105 developed by Henkel AG was used. The different 1C-PURs with long OAT from Henkel AG (LOCTITE HB S709 PURBOND and the LOCTITE HB 181 PURBOND) were chosen. HB S709 has an OAT of 70 minutes, and HB 181 has an OAT time of 120 minutes. The primer LOCTITE PR 3105 PURBOND, developed by Henkel AG, was used in combination with the 1C-PUR adhesives only. The PRF system Aerodux 185, with the hardener HRP 155 (mixing ratio of 100:20) from DYNEA, was used as a reference.

Lower delamination could also be obtained through a reduction of the lamellar thickness. Hering [10] calculated that a reduction of the thickness of the lamella reduces the moisture induced stresses in the section and hence reduces the delamination. For this reason, the lamellar thickness was reduced in the second part (series 2) from 30 to 25 mm.

DETERMIANTION OF TENSILE SHEAR STRENGTH (DIN EN 302-1)

Prior to gluing, the wood pieces were cut to 630 mm length, 130 mm width and 15 mm height and then acclimatized in three different climates according. The wood pieces were then planed to a thickness of 5 mm and cut in half prior to gluing.

The TSS (tensile shear strength) in dry state was tested according to the treatment A1 which consists in storing the sample at 20°C and 65% R.H. prior to testing the tensile shear strength. The TSS in wet state was tested according to the treatment A4 which consists in placing the sample into boiling water during 6 h before soaking them in water at 20°C during 2 hours, the samples were then directly tested. The treatment A5 consist in placing the sample into boiling water during 6 h before soaking them in water at 20°C during 2 hours before drying them in 20°C, 65% R.H climate until reaching constant mass. Each procedure was performed according to DIN EN 302-1.

DELAMINATION

The wood pieces were sorted out accordingly to DIN EN 302-2. The time between the primer application and the application is defined as the open primer time (OPT). The open assembly time (OAT) is defined as the time between the adhesive application and the assembly of the two wood pieces. The closed assembly time (CAT) is the time between the assembly of the different lamellas and the pressing. The total waiting time is defined as the sum of OPT, OAT and CAT. The delamination experiment was conducted according to the high temperature cycle described in DIN EN 302-2.

Results and Discussion

The results for series 1 of the delamination are shown in figure 2. In this experiment, the influence of two different primer concentrations and two different 1C-PUR adhesive was tested. As seen in the tensile shear strength experiment, the lower the wood moisture content, the better the bonding strength. The lamellas were conditioned at a humidity of 8 % prior to gluing. Figure 3 show the results from series 2 after optimization next step of the process. This results fulfilled the norms for glulam in delamination.

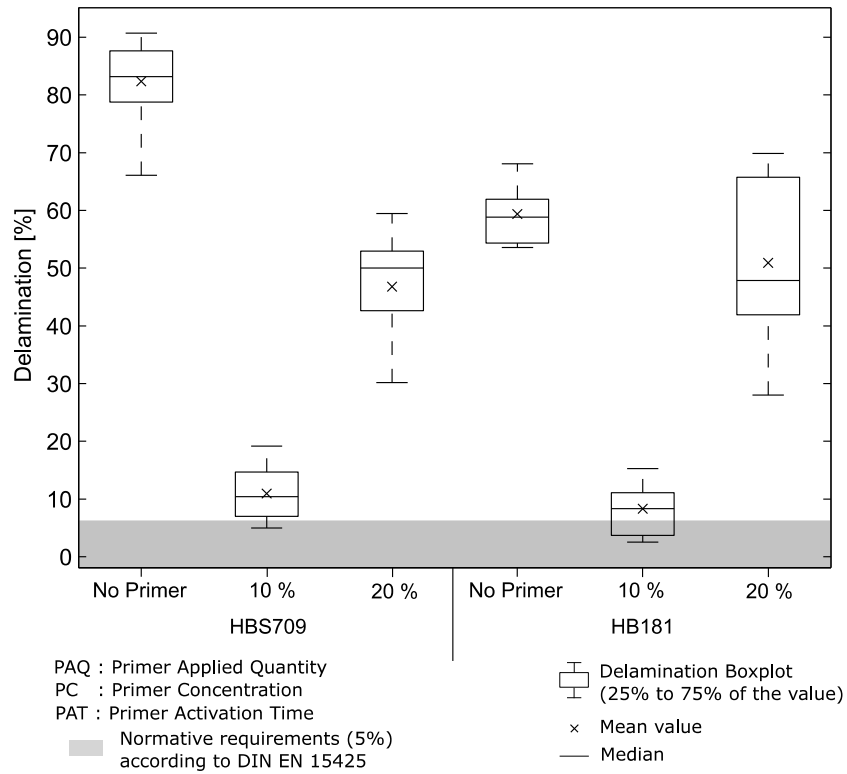


Figure 2. Delamination results with no Primer, 10 % and 20 % primer concentration (20g/m²) for the adhesive HBS709 and HB181 (test 2) series 2

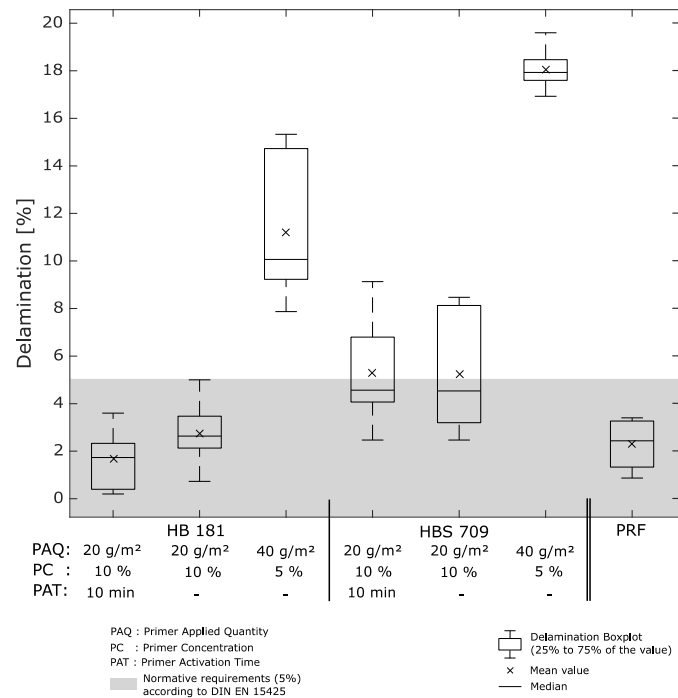


Fig 3: Delamination results with variable PAQ, PC (primer concentration) and PAT (Primer assembly time) from series 3 for the adhesives HB S709, HB 181 (Henkel) and PRF (Aerodux from Dynea), also reduced lamella thickness (25mm)

Summary and Conclusions

It is possible to reach delamination lengths below 5 % for ash wood bonded with slow-reacting special 1C-PUR in combination with primer in an industrial process. The presented investigation showed that the following parameters are essential:

- The best results were obtained with a concentration of 10 % and a primer applied quantity of 20 g/m². The influence of the absolute quantity of water and of primer should be carefully chosen
- A relatively low wood moisture content of approximately 8-10 % reduces the moisture-induced stress in the wood section, resulting in a lower delamination
- A slow-reaction adhesive system with long assembly time probably allows for further penetration into the wood structure and increases the available surface for bonding
- A reduction of the lamella thickness and is important for the reduction from internal stresses and the delamination

Acknowledgements

The authors would like to thank the Federal Office for the Swiss Environment FOEN (Project 2014.06) for the financial support of this research, as well as the provision of the adhesives substances by Henkel AG (Sempach-Station, Switzerland) and the expertise and industrial facility by "neue Holzbau AG" (Lungern, Switzerland). Also the authors like to thank for the support of "Advanced research supporting the forestry and wood-processing sector's adaptation to global change and the 4th industrial revolution", No. CZ.02.1.01/0.0/0.0/16_019/0000803 financed by OP RDE

References

- [1] V. Krackler, D. Keunecke, A. Hurst, and P. Niemz
Possible fields of hardwood application. *Wood Research*, 56(1):125-136, 2011.
- [2] U.-B. Brändli, editor
Schweizerisches Landesforstinventar. Ergebnisse der dritten Erhebung 2004-2006. Birmensdorf, Eidgenössische Forschungsanstalt für Wald, Schnee und Landschaft WSL. Bern, Bundesamt für Umwelt, BAFU, 2010. ISBN 9783905621471.
- [3] EN 302-1. Adhesives for load-bearing timber structures – Test methods. Part 1: Determination of longitudinal tensile shear strength. European Committee for Standardization (CEN), Brussels, 2013.
- [4] EN 302-2. Adhesives for load-bearing timber structures – Test methods. Part 2: Determination of resistance to delamination. European Committee for Standardization (CEN), Brussels, 2013.
- [5] M. Knorz, M. Schmidt, S. Torno, and J.-W. van de Kuilen
Structural bonding of ash (*Fraxinus excelsior* L.): resistance to delamination and performance in shearing tests. *European Journal of Wood and Wood Products*, 72(3):297_309, 2014.
- [6] O. Kläusler, P. Hass, C. Amen, S. Schlegel, and P. Niemz
Improvement of tensile shear strength and wood failure percentage of 1C PUR bonded wooden joints at wet stage by means of DMF priming. *European Journal of Wood and Wood Products*, 72(3):343_354, 2014.
- [7] G. Clerc; M. Lehmann; J. Gabriel; D. Salzgeber; F. Pichelin; T. Strahm; P. Niemz: Improvement of ash (*Fraxinus excelsior* L.) bonding quality with one-component polyurethane adhesive and hydrophilic primer for load-bearing application. *Int. J of Adhesives and Adhesion* 85(2018)303-307
- [8] S. Ammann; S. Schlegel; M. Beyer; K. Aehlig; M. Lehmann.; H. Jung; P. Niemz.
Quality assesment of glued ash wood for construction engineering
Eur. J Wood and Wood Prod. 74(2016), S. 67-74
- [9] O. Kläusler: Improvement of one -component polyurethane bonded wooden joints under wet conditions. PhD thesis ETH Zurich 2014
- [10] S. Hering: Charakterisierung und Modellierung der Materialeigenschaften von Rotbuchenholz zur Simulation von Holzverklebungen, PhD thesis,ETH Zurich 2011

Synchrotron-based analysis of densified wood impregnated with curing resin

Matthew Schwarzkopf
InnoRenew CoE & University of Primorska, Slovenia

Abstract

Consumers and policy makers are demanding the use of natural and sustainable materials for various reasons: low environmental impact, links to local cultural heritage, and benefits to human health. To this end, there has been renewed interest in the production and use of modified wood. Wood modification techniques have been used to help valorise under-utilised wood materials and increase their performance with respect to durability and mechanical characteristics and to achieve new forms and functions desired by consumers and designers. One such modification technique is a thermal-hydro-mechanical (THM) treatment. This treatment results in increased density, hardness, abrasion resistance, and improvements in some strength properties. One limitation of this modification technique is dimensional stability of the product. If this treated wood is exposed to high levels of moisture or water, it can revert partially or entirely back to its original dimensions. One proposed technique to increase dimensional stability of densified wood is to impregnate the wood micro-structure with curing resin. Cured resin improves dimensional stability of wood by chemically bonding with the wood cell wall, within the cell wall itself, and through mechanical interlocking in the cellular wood structure. To date, there is little known about the fundamental process of adhesive mobility/penetration into the micro-structure of densified wood. This behaviour is a significant component of the overall effectiveness of adhesive bonds and impregnated curing resins.

The motivation for this project is to understand the micro-scale mechanisms behind dimensional stability and mechanical performance of impregnated, densified wood. More specifically, this research is to investigate curing resin penetration into the densified wood micro-structure and mechanical performance and load transfer efficacy of impregnated, densified wood on a micro-scale. The objective of this research is to create a predictive modelling tool that will be used for technical assessment of adhesives/curing resins and densification methods.

The approach is to use the synchrotron light source located in Trieste, Italy, to obtain 3D reconstructions of densified wood samples using x-ray computed tomography (XCT) with in-situ mechanical loading, to use x-ray fluorescence microscopy (XFM) for spatial analysis of penetration, to carry out digital material separation, and to use this data as direct input for a predictive modelling tool. This tool will enable virtual experimentation of other resin/densification combinations, densification treatments, etc. Results to be presented include experimental methodology, initial results from XCT and XFM scans, and preparation of the modelling tool.

Tuesday, October 22nd

Wood Chemistry

13:45 – 15:30

Chair: Steven Keller, Miami University, USA

Lignocellulosic Materials as Biocompatible Drug Delivery System for Opioid Addiction Treatment

Dr. Gloria Oporto¹, Kelsey O'Donnell², Noelle Comolli², Luis Arroyo¹, Marina Galvez-Peralta¹,
Gustavo Cabrera³

¹ West Virginia University, Morgantown West Virginia, USA

gloria.oporto@mailwvu.edu

luis.arroyo@mail.wvu.edu

magalvezperalta@hsc.wvu.edu

²Department of Chemical Engineering, Villanova University, Villanova, Pennsylvania, USA

kodonn30@villanova.edu

noelle.comolli@villanova.edu

³ University of Concepcion, Concepción, Bío Bío Region, Chile

g.cabrera@udt.cl

Abstract

Advancements to understanding of lignocellulosic material from woody biomass from a chemical standpoint will open new opportunities of its utilization for high value and novel applications. The proposed research considers the implementation of preliminary experiments to evaluate a process to conjugate opioid antagonists on cellulosic materials and study their release performance. The overarching goal of the proposed research is to gather information regarding the effectiveness of using carboxymethyl cellulose and nanofibrillated cellulose in combination with Naltrexone, an opioid antagonist drug, to produce a natural product and lower the cost of extended release opioid treatments. This research will provide insight into a new area of utilization for lignocellulosic materials, and will add significant understanding concerning the specific characteristics of cellulosic materials in terms of their chemical functionalities to be effectively used as drug delivery systems.

Dewatering Wood Using Supercritical CO₂

Salonika Aggarwal^{1}– Shelly Johnson¹ – Marko Hakovirta² – Bhima Sastri³ – Sujit Banerjee⁴*

¹ Graduate Student, Department of Forest Biomaterials, North Carolina State University, Raleigh, NC, USA* *Corresponding author*
saggarw3@ncsu.edu

² Professor, Department of Forest Biomaterials, North Carolina State University, Raleigh, NC, USA,
mjhakovi@ncsu.edu

³ Division Director, U.S Department of Energy, Germantown, MD, USA
bhima.sastri@hq.doe.gov

⁴ Emeritus Professor, School of Chemical and Biomolecular Engineering, Georgia Tech, Atlanta, GA, USA
sb@gatech.edu

Abstract

Wood drying for the manufacture of oriented strand board (OSB) and other engineered woods is a major component of the overall product cost. Apart from the capital cost and energy costs of drying there are environmental control costs, requiring equipment such as electrostatic precipitators and thermal oxidizers. Supercritical carbon dioxide (sCO₂) dewatering could be a possible solution to reduce the cost of drying wood. Dewatering flakes with sCO₂ at 20.7-24.1 MPa and 45-60°C is highly efficient and can be applied to flakes for the manufacture of OSB. An economic analysis for the removal of water and extractives from pine flakes shows that sCO₂ treatment is potentially much more cost effective than thermal drying as water is removed by displacement rather than through evaporation, which drastically reduce the environmental costs. Moreover, the extractives removed represent a value stream instead of pollutants whose emissions need to be controlled.

Key words: Wood, OSB, Supercritical carbon dioxide (sCO₂), Extractives

Introduction

Supercritical CO₂ is the fluid state of carbon dioxide at or above its critical temperature (31.10 °C) and critical pressure (7.39 MPa). Unlike two-phase flow, sCO₂'s single-phase nature eliminates the necessity of a heat input for phase change that is required for the water to steam conversion, thereby also eliminating associated thermal fatigue and corrosion (Dodge 2014). The dissolving efficiency of sCO₂ can be enhanced with the modulation in temperature, pressure and by using cosolvents. Supercritical CO₂ can dewater wood and also remove extractives (Meder et al. 2015, Kaye et al. 2000, Schindelholz et al. 2015, Zeng et al. 2014). This preliminary research describes a method for cost effectively dewatering wood.

Materials & Methods

Softwood chips were obtained from International Paper's New Bern, North Carolina mill. The moisture of the chips was calculated using a Torbal moisture analyzer. The dry basis moisture content was 31±1%. Pine flakes were collected from the Georgia-Pacific Brookneal, VA facility. The dry basis moisture content of flakes was 80±5%. All samples were collected directly from the chipper and kept refrigerated. The supercritical extractor was bought from OCO labs and the unit was OCO labs Super C. The scanning electron microscope (SEM) used was an FEI Verios 460L unit at the NCSU Analytical Instrument Facility. Contact angles of deionized water on wood were measured using an SEO-Phoenix 150/300 contact angle analyzer. Contact angles were calculated to determine if sCO₂ treatment had any impact on the wettability of the wood surface. For each moisture content, at least 5 pieces of wood were sampled. Measurements were made at three different spots. Deionized water was used, and 50 images were captured every 0.25 seconds from each location. The contact angle decreased rapidly over a few seconds: only the initial contact angles were reported.

Green chips and flakes were cut into 12×15×2 mm and 60×15×1 mm subsamples, respectively. Small pieces from each set of the sample were cut and used to measure moisture content. Samples weighing (5-14) g were put into the extraction tube of the extractor. The temperature of the extractor vessel was kept constant at 60°C. Measurements were made 13.8 MPa and 27.6 MPa. The run time was varied from 60-90 min for the wood chips and 5-90 min for the flakes. The sCO₂/wood mass ratio was obtained by calculating the volume of dry wood using a density of 0.5. This volume was subtracted from the volume of extractor which is 120 ml. The remaining volume was occupied by sCO₂ whose density was determined from the equation of state of Span and Wagner (1996) which gave the mass of sCO₂. The quantity of extractives removed was calculated as the residual from subtracting the amount of water lost from the total weight loss. Chemical analysis of extractives was done at the Renewable Bioproducts Institute at Georgia Tech.

Results and Discussion

Results from sCO₂ extraction of pine chips and flakes are provided in Table 1. Increasing sCO₂ pressure increased water removal as expected from the work of Franich et al. 2014 on green radiate pine sapwood. Franich et al. also observed that the effect of temperature increase was insignificant. The water removal increases with increasing sCO₂/wood ratios. Insight into the mechanism of the process can be obtained by considering the solubility of water in sCO₂. The solubility of water in supercritical CO₂ is approximately 0.3% v/v (Pourmortazavi and Hajimirsadeghi 2007). At low pressure, all the water removed from flakes is free water until the fiber saturation point (FSP). Higher pressure increases extractive loss (Sparks et al. 2010, Maheshwari et al. 1992). Table 2 demonstrates that the sCO₂/wood ratio is also critical for the removal of water; increasing the sCO₂ amount increases the amount of water removed.

The water removed from wood flakes by sCO₂ over time is illustrated in Figure 1. Each measurement was made with the same mass of wood to keep the sCO₂:wood mass ratio constant for each of the two pressures used. The curve appears to plateau at about 70% water loss. The fiber saturation point of softwood is about 30% water below which the moisture is bound to the cell walls. Hence, the residual water corresponding to the plateau region in Figure 1 should be bound water. The curve flattens out because bound water is more difficult to remove than free water.

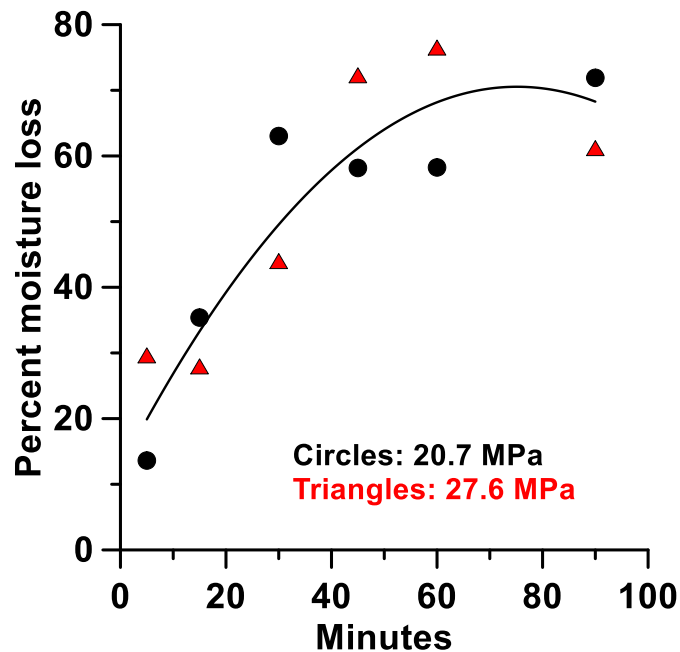


Figure 1. Moisture loss (dry basis) profiles from flakes.

Chips

*Proceedings of the 62nd International Convention of
Society of Wood Science and Technology
October 20-25, 2019 – Tenaya Lodge, Yosemite, California USA*

Pressure (MPa)	Run time (h)	Final MC % (dry basis)	MC loss % dry basis	Extractives %	Ratio Mass sCO₂/wood
13.8	1	14.96	16.8	-0.04	4.37
13.8	1	11.48	19.8	-0.36	14.41
13.8	2	11.02	18.7	-1.05	7.00
13.8	1	13.07	21.4	0.09	6.53
13.8	2	7.99	25.9	-0.74	14.75
17.2	1	14.38	18.3	1.48	7.85
17.2	1	10.69	15.8	2.42	11.82
20.7	1	12.99	19.5	1.80	8.87
20.7	1.5	9.54	21.3	0.56	10.52
24.1	1	11.23	21.6	1.12	22.13
27.6	1	11.64	21.3	1.89	13.30
27.6	1	10.99	21.4	1.23	21.81
27.6	1	14.04	17.3	3.17	9.89

OSB Flakes

27.6	1	19.05	76.5	-0.79	25.68
27.6	1	20.77	109.7	0.03	50.64

Table 1. Removal of water and extractives from softwood by sCO₂.

Pressure (MPa)	Mass(sCO₂)/ mass(wood)	moisture loss (%)
20.7	24	58
20.7	47	66
27.6	31	77
27.6	61	~100

Table 2: Effect of sCO₂/Wood mass ratio on water removal

The initial contact angles of water on flakes dried at 105°C and with sCO₂ were very similar at 83° and 81°, respectively, suggesting that their surface properties were also similar and that no differences are expected in the interaction between wood and resin. These contact angles compare well with those reported earlier by Martino et al. 2002.

SEM images (x 1,000) of flakes oven dried at 105°C and with sCO₂ are compared in Fig.2. The pore structure of sCO₂ treated wood is more open and the surface is less glazed than the thermally dried flakes. Increasing temperature is known to increase the degree of surface glazing probably by increasing the presence of extractives on the surface (Martino et al. 2002). Overall, no major differences in surface character are observed between sCO₂

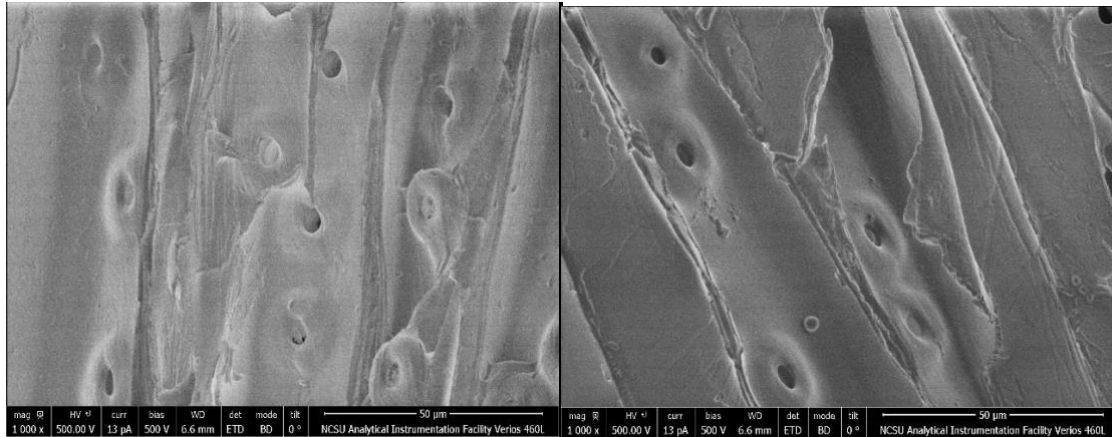


Fig.2. SEM Images of surfaces of oven-dried wood (left) and SCO₂ treated wood (right)

and thermally dried flakes, which suggests that bonding between the flakes should be largely unaffected.

Summary and Conclusions

In conclusion, sCO₂ treatment of wood removes most of the water and some of the extractives. Water is removed through displacement which is less energy intensive than evaporative removal. The CO₂ can be recycled and reused. An application to drying wood flakes for the manufacture of oriented strand board is evaluated. The extraction does not appear to affect the surface properties of the flakes, so product quality should not be compromised. The extractives can be recovered in decompression phase of the process. The extractives collected should increase the economic value of this process.

Acknowledgements

The authors thank International Paper and Georgia Pacific for providing the samples. Special thanks to Georgia Tech for the chemical analysis. Thanks to Guillermo Velarde and Barbara White for their support.

References

- 1) Dodge E (2014) [Supercritical Carbon Dioxide Power Cycles Starting to Hit the Market](#). *Breaking Energy*.
- 2) Franich R.A, Gallagher S, Kroese H (2014) Dewatering green sapwood using carbon dioxide cycled between supercritical fluid and gas phase. *The journal of Supercritical Fluids* 89: 113-118.
- 3) Kaye B, Cole-Hamilton D.J, Morphet K (2000) Supercritical Drying: A New Method for Conserving Waterlogged Archaeological Materials. *Studies in Conservation* 45(4): 233-252.
- 4) Maheshwari P, Nikolov Z. L, White T. M, Hartel R (1992) Solubility of Fatty Acids in Supercritical Carbon Dioxide. *Journal of American Oil Chemists Society* 69: 1069–1076.
- 5) Martino C.J, Shrauti S, Banerjee S, Otwell L.P, Price E.W (2002) Flake drying temperature affects mat properties during pressing. *Holzforschung* 56: 558-562.

*Proceedings of the 62nd International Convention of
Society of Wood Science and Technology
October 20-25, 2019 – Tenaya Lodge, Yosemite, California USA*

- 6) Meder R, Franich R.A, Callaghan P.T, Behr V.C (2015) A comparative study of dewatering of *Pinus radiata* sapwood using supercritical CO₂ and conventional forced air-drying via in situ magnetic resonance microimaging (MRI). *Holzforschung* 69(9): 1137–1142.
- 7) Pourmortazavi, S.M, Hajimirsadeghi, S.S (2007) Supercritical fluid extraction in plant essential and volatile oil analysis. *Journal of Chromatography A* 1163(1-2): 2-24
- 8) Schindelholz E et.al (2015) An Evaluation of Supercritical Drying and PEG/Freeze Drying of Waterlogged Archaeological Wood. National Center for Preservation Technology and Training Grant.
- 9) Span R, Wagner W (1996) A New Equation of State for Carbon Dioxide Covering the Fluid Region from the Triple-Point Temperature to 1100K at pressures up to 800MPa. *Journal of Physical and Chemical Reference Data* 25: 1509.
- 10) Sparks D. L, Estevez L. A, Hernandez R, McEwen J, French T (2010) Solubility of Small-Chain Carboxylic Acids in Supercritical Carbon Dioxide. *Journal of Chemical Engineering. Data* 55: 4922–4927.
- 11) Zeng M, Laromaine A, Roig A (2014) Bacterial cellulose films: influence of bacterial strain and drying route on film properties. *Cellulose* 21: 4455–4469.

*Proceedings of the 62nd International Convention of
Society of Wood Science and Technology
October 20-25, 2019 – Tenaya Lodge, Yosemite, California USA*

**Selective Extraction of High-Value Molecules from Forest Products
Processing Residues in the Speciality Chemicals Sector**

Dr. Andreja Kutnar
InnoRenew CoE and University of Primorska, Slovenia
Andreja.kutnar@innorenew.eu

Abstract

Not Available

Cellulose I and II Nanocrystals Derived from Sulfuric Acid Hydrolysis of Cellulose I Substrates

Jin Gu, Lichao Sun, Lida Xing, Yun Hong, Chuanshuang Hu*

College of Materials and Energy, South China Agricultural University,
Guangzhou, 510642, PR China

*Corresponding author: cshu@scau.edu.cn

Abstract: Cellulose nanocrystals (CNCs) produced from lignocellulosic biomass seem to give a range of opportunities to obtain superior materials. Cellulose polymorphism is an important factor associated with the cellulose nanomaterial properties. In this study, cellulose nanocrystals with cellulose I and II (CNC I and CNC II) allomorphs were prepared from eucalyptus cellulose I substrates by controlling the sulfuric acid hydrolysis conditions, including acid concentration (56%-66 wt%), reaction temperature (45~60 °C) and time (10-120 min). The crystalline structures of CNC I and CNC II were explored by XRD and ¹³C-NMR. CNC II only appeared at a very narrow operating window. Compared to CNC I, CNC II exhibited a smaller and more uniform nanoparticle size. The highest CNC II yield was 36.4%. The possible mechanism of cellulose allomorph conversion during the sulfuric acid hydrolysis was discussed. A connection between cellulose allomorph transition and CNC yields was established. CNCs with controllable allomorph may have potentially diverse applications.

Keywords: Cellulose nanocrystal; Cellulose allomorph; Sulfuric acid hydrolysis; Eucalyptus; X-ray diffraction

Mineralization in situ of Tropical Hardwood Species: Calcium Carbonate Formation and Wood Properties

Roger Moya

Instituto Tecnológico de Costa Rica, Costa Rica

Abstract

The process of mineralization "in situ" basically consists in the formation of salts by means of chemical reactions inside the wood to improve structural properties. This process was applied in ten tropical woods used commercially in Costa Rica, with the impregnation in a first stage of calcium chloride (CaCl_2) at 72% in ethyl alcohol, and a second stage of sodium carbonate (NaCO_3) at 99% using deionized water as a solvent, achieving an internal reaction inside the wood cells of calcium carbonate (CaCO_3). The results showed that the absorption of the first salt (CaCl_2) was 49 to 300 l/m³, with a salt retention of 2.7 to 10.1 kg/m³ with a penetration of 5 mm, however it was penetrated in an irregular manner. After drying the samples for 3 hours at 60 °C, the second impregnation (NaCO_3) was applied, which presented an absorption of 75 to 222 l/m³, with a salt retention of 4.2 to 10.2 kg/m³ and a penetration of the salt 5 mm, irregularly. According to the stoichiometry of the mineralization reaction, the reaction in situ produce irregular reaction. The observations in the Scanner Electric Microscopic (SEM), showed that the mineralization process occurs in the walls of the vessels, in the direction of the radii and in a small amount in the fibers of the wood. This unlike the coniferous species, which the mineralization process occurs in all the cellular elements of the wood. Wood density, MOE and MOR in flexion and compression test were not affected by mineralization, but the flowing properties were improvement: wood stability, water absorption, fire resistance and fungal decay. For hardwood species, the mineralization "in situ" is differenced from softwood due to mainly due to the fact that the movement of fluids inside the wood species occurs first in the direction of the vessels, followed by the radii and in a small quantity by the fibers, unlike the conifers that the liquid fluid only it is presented by the fibro-tracheids.

In-situ penetration of ionic liquids into surface-densified Scots pine

Benedikt Neyses, Wood Science and Engineering, Luleå University of Technology, Sweden, benedikt.neyeses@ltu.se

Kelly Peeters, InnoRenew CoE, Slovenia, Kelly.peeters@innorenew.eu

Lauri Rautkari, Department of Bioproducts and Biosystems, Aalto University, Finland, lauri.rautkari@aalto.fi

Michael Altgen, Department of Bioproducts and Biosystems, Aalto University, Finland, michael.altgen@aalto.fi

Surface densification of solid wood leads to an increase in hardness and wear resistance, proportional to the increase in density of the surface. This may lead to an increase in value of low-density wood species, such as Scots pine, which are abundant in boreal and temperate forests. To exploit the positive effects of surface densification commercially, a fast and cost-efficient surface densification process is required. To achieve this, several problems need to be solved. Hitherto, research into surface densification was focused on the lab-scale, and methods to reduce the moisture-induced set-recovery of the densified wood either take a long time in an open system or require a closed system. This prevents the large-scale commercialization of surface-densified wood products. A previous study has shown that a fast pre-treatment with ionic liquids can reduce the set-recovery from 90% to 10-50%, depending on the process parameters. There was also an increase in Brinell hardness in comparison to the untreated surface-densified wood. A pre-treatment with ionic liquids does not require a closed system and takes less than 10 minutes. In order to implement the combined pre-treatment and surface densification process as an industrial process, it is necessary to understand how the chemical treatment interacts with the wood material, resulting in reduced set-recovery. We studied the penetration depth of the chemical treatment and cellular level chemical changes by FT-IR spectroscopy and confocal Raman microscopy. We found that the penetration of chemical agents into the wood was limited to only a few cell layers. This low penetration cannot explain the achieved reduction in set-recovery and the increase in Brinell hardness, as the surface-densified layer has a thickness of several millimeters. Based on these findings, we hypothesize that the high temperature of the press platen during the densification process (>200°C) vaporizes the ionic liquid, which then diffuses deeper into the wood surface, where it is activated by the heat. The activated ionic liquid cleaves hydrogen bonds between cellulose chains, which allows plastic deformation of the wood cells. Further exposure to temperatures over 200°C decomposes the ionic liquid, allowing the formation of a new hydrogen bond network between the cellulose chains for a permanent reduction of the set-recovery. To test our hypothesis, we will conduct GC-MS and TGA-FT-IR analysis of the decomposition products to be found in the pre-treated wood after surface densification. The knowledge obtained from this study will enable us to implement an improved

*Proceedings of the 62nd International Convention of
Society of Wood Science and Technology
October 20-25, 2019 – Tenaya Lodge, Yosemite, California USA*

version of the treatment process, especially with regard to the development of a large-scale surface densification process.

Keywords: compressed wood, wood modification, chemical treatment, green chemistry, confocal Raman microscopy

Biomass derived high surface area carbon materials for shale gas flowback water purification

Jingxin Wang
West Virginia University, USA

Abstract

Biomass derived porous carbon materials with high surface areas can be used in various industrial cases one of which is to remove organics and metal ions from industrial waste water produced during shale gas production. In this work, three types of porous carbon materials with different specific surface areas were fabricated from hybrid willow biomass which was milled with 1 mm sieve as porous carbon precursors. Three porous carbon were labelled as Char, AC-1 and AC-2. The Char was prepared by pyrolysis of the biomass at 450 °C for 30 minutes. The AC-1 was prepared by directly carbonizing the mixture of biomass powders and KOH at 800 °C in nitrogen. The AC-2 was prepared by carbonizing the mixture of biomass char and KOH at 800 °C in nitrogen. The residence time of both carbonization are 60 minutes. The ratios of the precursor to the activation agent KOH are both 2:1. Based on original weight of the biomass, the yield of Char, AC-1 and AC-2 were 21.7%, 18.2% and 14.8%, respectively. Three porous carbon materials were characterized with N₂ adsorption and desorption to determine the porosity. The results showed that Char, AC-1 and AC-2 have specific areas of 261.9, 1071.4 and 776.6 m²/g, respectively. Then the carbon materials were applied to remove Barium from actual shale gas flowback water. The concentration of Barium was tested with inductively coupled plasma optical emission spectrometry (ICP-OES). Although the porous carbon materials are considered less effective to remove alkali metal ions when compared to organics, the results still showed that the barium concentration was decreased by 2.5%, 11.3% and 3.3%, respectively, at a relative low carbon to water ratio (0.4g:15ml) by Char, AC-1 and AC-2. The carbon materials after adsorption were also characterized with scanning electron microscopy (SEM) and energy-dispersive X-ray spectroscopy (EDS). The results showed that adsorbates were observed on porous carbon surfaces with significant Barium peaks. The future research work will be focused on how to increase the adsorption capacity of hybrid willow derived activated carbon and discover the mechanism of adsorption and desorption of metal ions.

Tuesday, October 22nd

Poster Session

15:45 -18:00

Student Posters:

**Characterization and Utilization of Epoxy/Pyrolysis Bio-Oil in Oriented Strand
Board Production**

Osei Asafu-Adjaye

Auburn, University, USA

Abstract

Epoxy resins are vastly used in construction, automotive and aerospace industries due to their excellent dry strength and thermal resistance. However, epoxies are minor wood adhesives, brittle, expensive and the linkage between epoxy and wood can become considerably weakened after exposure to moisture. Production of Oriented Strand Board (OSB) utilizing epoxy resin blended with fast pyrolysis bio-oil was studied. The aim of the study was to improve the hydrophobicity of the wood-epoxy matrix without compromising the mechanical properties. The effect of bio-oil substitution and resin content on the physical and mechanical properties of OSB was examined. The properties included internal bond (IB), modulus of rupture, modulus of elasticity, thickness swelling (TS), and water absorption (WA). Hot stacking effect on the mechanical and physical properties were also assessed. The results showed that higher bio-oil content in the epoxy resin reduced the mechanical and physical properties of the OSB. Epoxy resin with bio-oil content of 30% showed comparable bonding properties to that of polymeric diphenylmethane diisocyanate (pMDI). Bio-oil substitution of 20% improved the hydrophobicity of the OSB. Hot stacking also improved the dimensional stability and mechanical properties of the boards. It was concluded that epoxy resin could be used in the production of OSB. Addition of bio-oil could help to reduce the cost of the epoxy resin and as well improve the properties of the board.

Membrane-based thermal energy recovery system to improve the energy efficiency of kiln drying processes

Nasim Alikhani¹, Darien Dewar⁴, Ling Li¹, Jinwu Wang², Douglas Bousfield³, Mehdi Tajvidi¹

¹ School of Forest Resources, University of Maine, 5755 Nutting Hall, Orono, ME 04469

² USDA Forest Service, Forest Products Laboratory, 1 Gifford Pinchot Dr., Madison, WI 53726

³ School of Forest Resources, University of Maine, 5737 Jenness, Orono, ME 04469

⁴ College of Engineering, Valparaiso University, Valparaiso, IN 46383

Abstract:

The moisture content (MC) of woody materials is usually very high. For instance, the MC of green wood varies from 60% to 80% and in some cases up to 120%. Therefore, a kiln drying process plays an important role to reduce the MC of raw materials fast for further applications. Unlike the air-drying process, kiln drying is a very energy-demanding process, which consumes much energy to extract water from woody materials and deliver it to the atmosphere through venting. The thermal energy loss from the venting of dry kilns takes up to 20% of total energy consumed by the whole drying operation because a considerably large thermal energy is stored in the moist exhaust air. Harvesting and reusing such waste thermal energy would improve the energy efficiency of the kiln drying process. Nowadays, advanced moisture selective membranes, such as polydimethylsiloxane (PDMS), are emerging technology to remove moisture from gas streams because of the advantages of low energy requirements, the simplicity of operation, and high specificity. Therefore, this preliminary study aims to investigate the feasibility of using moisture selective membrane modules to fabricate a highly-efficient thermal energy recovery system to produce warm and dry air that can be redirected into the dry kiln. A mini-scale membrane-based dehumidification system was developed and constructed. Then the effects of air flow rate, relative humidity (RH), and vacuum pressure on the moisture separation efficiency of the system were studied through experimental and COMSOL Computational Fluid Dynamics (CFD) modeling approaches. The major results are: 1) the initial RH had little influence on the efficiency of moisture vapor removal; 2) increasing the vacuum pressure led to an increase in the efficiency of moisture vapor removal; 3) increasing the air flow rate resulted in a decrease in the efficiency of moisture vapor removal; and 4) the CFD modeling was used to predict the concentration of moisture vapor in dried air (i.e., RH of dried air) at the outlet of the membrane system.

Keywords: Kiln drying processes; Moisture selective membrane; Thermal energy recovery system; Waste thermal energy.

1. Introduction

Green woody materials usually have high moisture contents (MCs) in a wide range of 60% to 120% on a dry weight basis (Copper 2003). Therefore, a kiln drying process is a key process for the lumber industry to dry lumber/boards fast to reduce their MCs to the required final MCs for various applications. The conventional steam dry kiln is the most commonly used kiln type in North America. Steam is used as a heating medium in heating coils to heat air and as a medium to adjust the relative humidity (RH) in the kiln based on a specified drying schedule. Moisture evaporated from lumber is stored in the surrounding air as moisture vapor. Saturated humid and hot air is typically ventilated to the environment regularly. Also, relatively cold and dry air is brought in the kiln to absorb the water vapor escaping from lumber. The kiln drying process,

although greatly decreasing the time required to produce useable wood, requires high amounts of heat energy to lower the MC of wood (Simpson 1991). During the kiln drying process, energy is consumed by several elements, such as latent heat used to evaporate water, heat loss from kiln structures (walls, doors), heat loss from venting air, and sensible heat to warm lumber, air, and kiln structures, etc., most of which are irreversible. However, heat loss through ventilation can be partially recycled to serve an energy-saving purpose. There have been several energy recovery systems being applied in the conventional dry kiln, which employ the principle of air exchange to capture the sensible heat from exhaust air and stored in the incoming air. The efficiency of energy recovery of these systems varies with the environmental conditions, for example, the temperature difference of two air streams. Another drawback is that the RH of the incoming air is affected by the environmental conditions as well, for examples, moist air in rainy/snowy days.

With the rapid development of membrane technology during recent decades, it has been shown that a type of moisture selective membrane can effectively and efficiently remove moisture from the air, which has found applications in certain air conditioning units currently in use (Elustondo & Oliviera 2009). Membrane-based dehumidification systems have numerous advantages, such as, less energy consumption (because there is no phase change in this process), simplicity in maintenance and operation, high selectivity, ease of scale up and low initial cost (Liang et al. 2018 , Zhao et al. 2012), showing promising potential for the wood industry's need to reduce energy consumption.

It was reported that about 20% of heat energy loss in conventional dry kilns comes from the ventilation of humid and hot air (Garrahan 2008). A hypothesis proposed is that energy saving can be achieved when dry air is separated from the humid and hot exhaust air and the dry, hot air is rerouted back into the kiln, which reduces the energy required to heat another cold air stream coming into the kilns from the environment.

Therefore, this preliminary study aims to investigate the feasibility of using a moisture selective membrane module to develop a closed energy recovery system that can improve the energy efficiency of the wood drying process. The objectives were to 1) design and fabricate a mini-scale membrane-based dehumidification system to separate moisture vapor from moist air, and 2) study the effects of air flow rate, relative humidity, and pressure on the moisture separation efficiency of the system through experimental and COMSOL Computational Fluid Dynamics (CFD) modeling approaches.

2. Materials

2.1 Membrane Selection and Performance Factors

For an application in air dehumidification, the research group had several options for the membrane type to be used in testing. After reviewing current literature, the research group identified a hollow fiber polydimethylsiloxane (PDMS) membrane (PermSelect-MedArray Inc., <http://www.permselect.com/>) as a potential candidate due to the high water-to-gas permeability ratios (based on the coefficients of permeability) for separating water from nitrogen and from oxygen, being approximately 129 and 60, respectively (Montoya 2010 , Bergmair et al. 2015). This type of membrane takes bundles of hollow fibers made of the specific membrane material and encloses them in a tubular shell. The basic construction of this membrane is

displayed in Figure 1 (left). The membrane selected for testing had a surface area of 1 square meter, as displayed in Figure 1 (right).

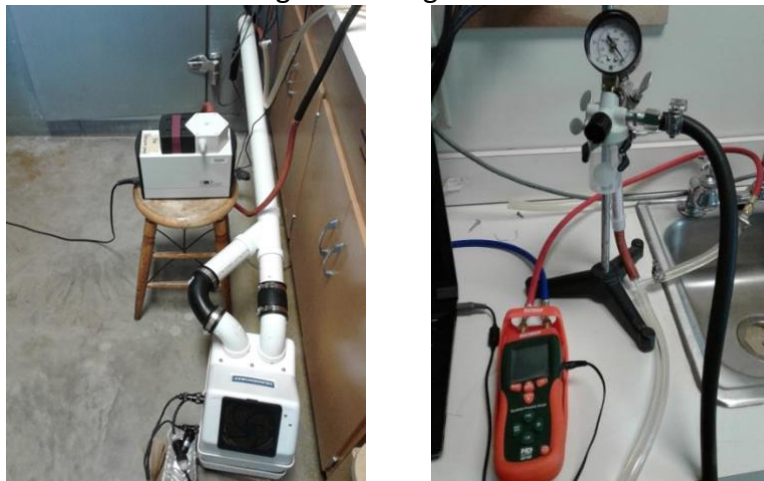


Figure 1. Exploded view of basic hollow fiber membrane (Montoya, 2010).

2.2 Design and fabrication of membrane dehumidification system

A membrane dehumidification system was designed and fabricated, as illustrated in Figure 2. An inline blower was used to blow humid air into the membrane and control the air flow rate. An in-line flow meter (Brand: Aalborg Company, Orangeburg, New York) was used to monitor the flow rate. A vacuum pressure pump (Brand: Welch) with a pressure gauge was connected to two outlets of the membrane to take away the moisture vapor that permeates across the membrane. The pressure gauge was used to alter the pressure of the vacuum pump. The dry air exhausted from another outlet was collected in a plastic bag for measuring the RH.

The entire system was placed in an environmental chamber. The RH of air entering the membrane was controlled by a humidifier (Brand: Humidifirst Ultrasonic Humidifier company, Boynton Beach, Florida). The RHs of humid air and dried air were monitored by humidistats, and the data was collected by a data logger (Brand: HOBO Remote Monitoring System, Bourne, Massachusetts). The temperature in this study was set as ambient temperature, which was also monitored and recorded by temperature sensors during the testing as a reference.



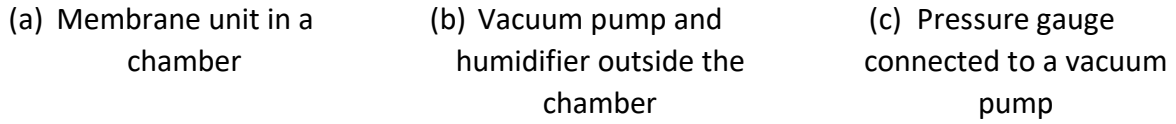


Figure 2. Membrane system and setup of experiment.

3. Methods

3.1 Experiment

The experimental design was adopted to analyze the effects of three variables and their interactions on the moisture separation efficiency of the membrane system constructed. The variables are air flow rate, relative humidity and vacuum pressure. The levels of the variables are shown in Table 1.

Experimental ranges and levels of the process factors. Table 1:

Variables	Levels		
	Low	Medium	High
Flow rate (FR) (ml/min)	600	700	1000
RH%	65	75	85
Pressure (P) (inch mercury)	20	-	26

Based on the number of variables and levels, there were a total of 18 combinations to carry out. When running each combination, the RHs of humid air and dry air with time and temperature in the chamber with time at an interval of 10 secs were recorded.

The water removal efficiency was determined according to Eq.1

$$Efficiency(\%) = \frac{(RH_{in} - RH_{out})}{RH_{in}} \times 100 \quad (1)$$

where, RH_{in} is the initial RH of humid air at the inlet; RH_{out} is the RH of dried air at the outlet (i.e., air on the permeate side of the membrane). RH_{out} was selected when a steady-state was reached, which was defined as the level-off stage of the curve of RH with time, as shown in Figure 4.

3.2 Finite element modeling

A finite element modeling was developed through COMSOL software with Computational Fluid Dynamics (CFD) module (Comsol Multiphysics Version 5.4, <https://www.comsol.com/>) to simulate the process of the moisture permeation and effects of variables on the efficiency. Experimental results were used to verify the modeling results. The mechanism of moisture selective membrane is based on the solution diffusion mechanism and the dense structure of the membrane. According to a solution-diffusion mechanism, water vapor molecules permeate preferentially through the membrane because it has a smaller kinetic diameter and also it is more condensable compared to the other gases (Liang et al. 2018). A 2-D finite element modeling based on one single hollow fiber was developed with a few assumptions outlined below:

- 1) All hollow fibers made of PDMS in the membrane module have the same dimensions;
- 2) There are no manufacturing defects in these fibers;

3) A steady-state diffusion process occurs.

A 2D-axisymmetric geometry was built to model the half-section hollow fiber membrane, as shown in Figure.3, which were divided into three domains: shell, membrane, and tube). The length and the radius of the fiber were 10000 micrometers and 80 micrometers, respectively. The radius of the fiber was measured from an SEM image of the cross-section of a fiber taken before this study. The outlet was set to atmospheric pressure, and for the wall the no-slip condition was applied. Also, in the boundary between the membrane and permeate side, Henry's Law was considered.

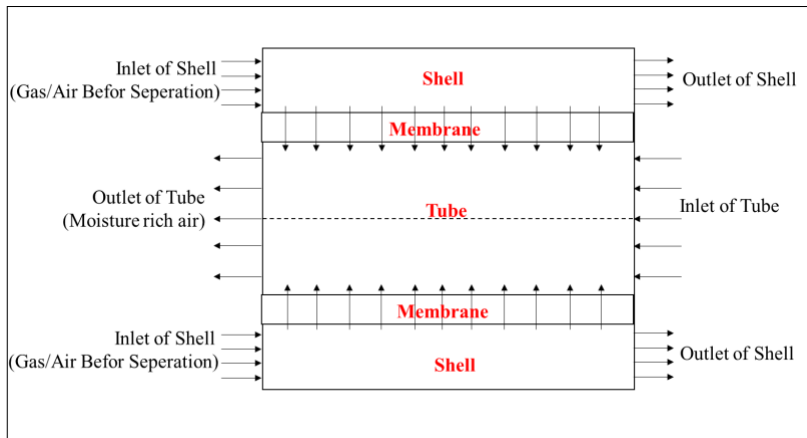


Figure 3. Schematic of a hollow fiber membrane

In the simulation, one combination was chosen and used as initial input parameters (inlet region), which are RH of 75%, the flow rate of 600 ml/min, the vacuum pressure of 26-inch mercury. The temperature was set as an ambient temperature of 25°C. In the modeling, the concentration of inlet humid air and velocity of the air instead of RH and flow rate, respectively, were input in the CFD modeling. The concentration of humid air corresponding to 75% RH is 0.96 mol/m³, which was calculated in terms of the molecular weight of the water molecule. The velocity of humid air corresponding to the flow rate of 600 ml/min is 0.0083 m/s, which was calculated in terms of the known surface area of the membrane. According to Massman (1998), the diffusion coefficient of water in the air at 298.15K (25°C) and 1 atm is $D_{H_2O-air} = 0.2630 \cdot 10^{-4} \text{ m}^2/\text{s}$. Also diffusion coefficient of water in the PDMS membrane at the same condition is $D_{H_2O-mem} = 8 \cdot 10^{-6} \text{ m}^2/\text{s}$. Vacuum pressure of 26-inch mercury is obtained by a low speed of sweeping gas on the permeate side of the membrane, in the simulation. Using COMSOL CFD modeling, the concentration of water was obtained. The inputs for the modeling are summarized in Table 2.

Table 2: Initial inputs used in CFD modeling

Parameters		Value
Inlet velocity	V	0.0083 m/s
Diffusion coefficient of water vapor in air	D_{H_2O-air}	2.2E-4 m ² /s
Diffusion coefficient of water vapor in membrane	D_{H_2O-mem}	8E-6 m ² /s
Initial concentration of water vapor in humid air	C_{H_2O-in}	0.960 mol/m ³

3. Results and discussion

3.1. Experimental results

3.1.1. General curves of reduction of RH with time

The general curves of RH reduction with time in three flow rates, three initial RHs, and two vacuum pressures are shown in Figure 4. From the collected data, we can observe a common trend among all the combinations that at the RH of dehumidified air at outlet dropped very quickly at the very beginning (less than 3 mins) after the membrane system started working and then reached a steady-state to maintain a constant RH at the whole testing period of 30 mins.

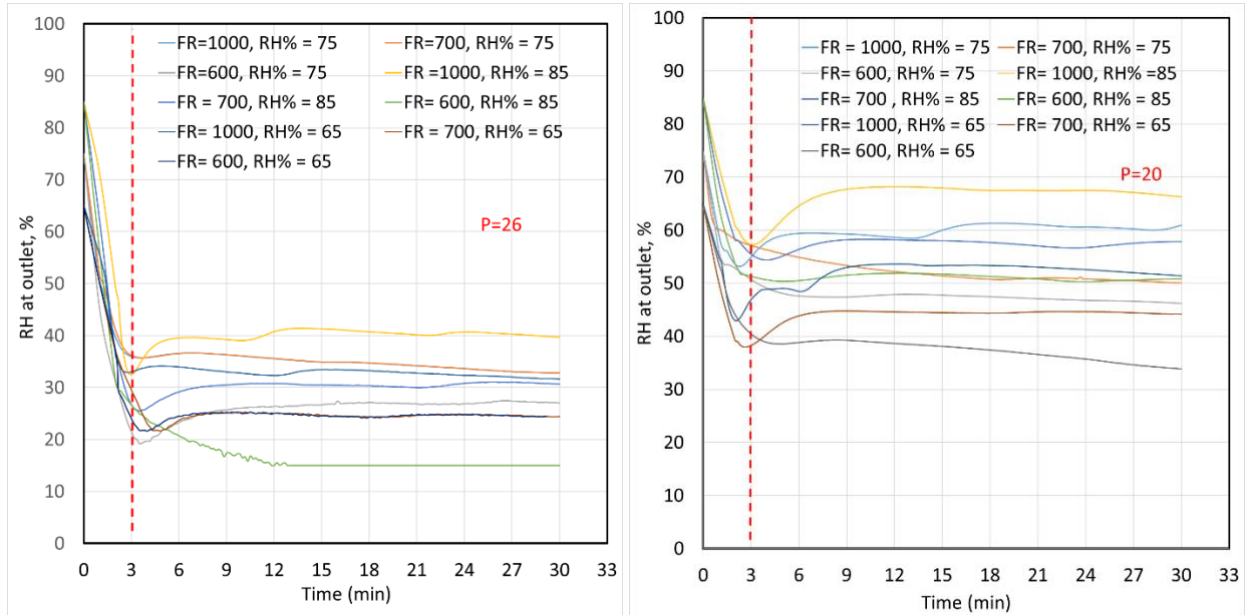


Figure 4. Effect of Flow rate and Initial Relative Humidity as a function of time, P=26-inch mercury (Left) and P=20-inch mercury (Right)

3.1.2 Effects of air flow rate, RH, and vacuum pressure on the efficiency of RH reduction

The efficiencies of moisture removal of the membrane system at all combinations calculated based on Equation (1) are plotted in Figure 5. We can observe the initial RH does not affect the efficiency of moisture removal too much when the air flow rate and vacuum pressure are at the same level, respectively. However, increasing air flow rate results in a decrease in the efficiency of moisture removal, which may due to a fast air flow rate leads to less residence time for water vapor molecules to pass through the membrane. Besides, the vacuum pressure also has a big impact on the efficiency of moisture removal: the higher the vacuum pressure, the higher the efficiency could be achieved.

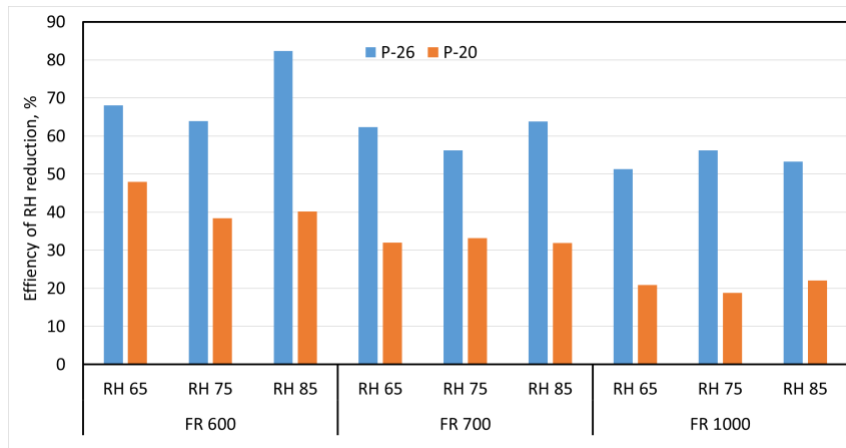


Figure 5. Efficiency of RH reduction at all combinations

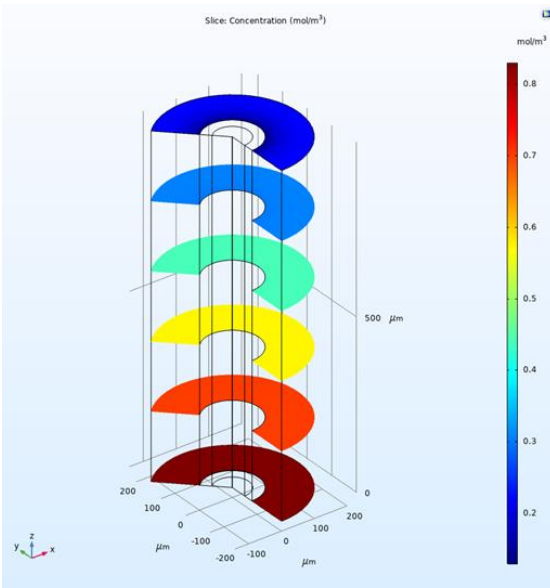
3.2. CFD simulation results

3.2.1 The concentration distribution within a fiber

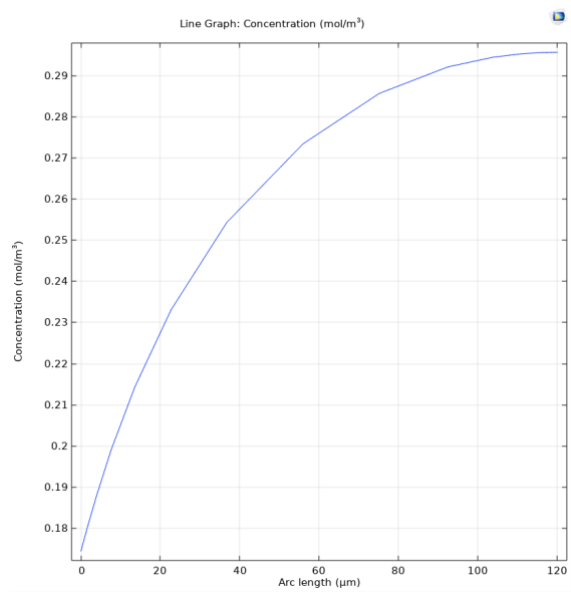
The concentration of moisture vapor at the shell domain along the length of the hollow fiber membrane in terms of slices is plotted in Figure 4 (a). The slice in dark red color shows the concentration of moisture vapor at the inlet of the membrane, which is 0.960 mol/m^3 . The slice in dark blue color shows the concentration of moisture vapor at the outlet of the membrane, which slightly increases from 0.185 mol/m^3 to 0.295 mol/m^3 with the increasing of the radius of the shell domain, as shown in Figure 4 (b). The Average water vapor concentration of dried air around the outlet is 0.258 mol/m^3 , which is corresponding to RH of 20.42%.

3.2.2 Comparison of Modeling results with experimental results

The experimental result of moisture reduction of the membrane at 75% RH, the flow rate of 600 ml/min, the vacuum pressure of 26-inch mercury was 27.06 % RH. Comparing with the average RH of 20.42 % simulated by COMSOL CFD modeling, the differential in RH between the experimental result and simulation result is 24%, which is in line with the study done by Bergmair (2012). The CFD modeling developed in this study can well predict the RH of air dehumidified by the membrane system, which will be employed to further study the efficiency of moisture removal of a scaled-up membrane unit including a bundle of hollow fiber PDMS membranes.



(a) Concentration of moisture vapor simulated along the length direction



(b) Concentration of moisture vapor at outlet along the radius direction

Figure 6. Distribution of concentration of moisture vapor of membrane

4. Summary and Conclusions

In this work, a membrane-based dehumidification system was successfully constructed. The effects of flow rate, initial RH, vacuum pressure on dehumidification of moist air were studied through experimental and CFD modeling approaches. The efficiency of water vapor removal was calculated and analyzed. The major findings are drawn below:

- 1) The initial RH had little influence on the efficiency of moisture vapor removal;
- 2) Increasing the vacuum pressure led to an increase in the efficiency of moisture vapor removal;
- 3) Increasing the air flow rate resulted in a decrease in the efficiency of moisture vapor removal; and
- 4) The COMSOL CDF modeling developed could be used to predict the concentration of moisture vapor in dried air (i.e., RH of dried air) at the outlet of the membrane system.

Acknowledgements:

This research is funded by USDA Agricultural Research Service (2018) and the 2019 National Science Foundation Research Experience for Undergraduates # 1757529.

References:

Bergmair, D., Metz, S. J., de Lange, H. C., & van Steenhoven, A. A. (2012). Modeling of a water vapor selective membrane unit to increase the energy efficiency of humidity harvesting. In *Journal of Physics: Conference Series* (Vol. 395, No. 1, p. 012161). IOP Publishing.

*Proceedings of the 62nd International Convention of
Society of Wood Science and Technology
October 20-25, 2019 – Tenaya Lodge, Yosemite, California USA*

- Cooper, G. (2003). Methods of reducing the consumption of energy on wood drying kilns (No. 211-915). Client report.
- Elustondo, D. M., Oliveira, L., & Lister, P. (2009). Temperature drop sensor for monitoring kiln drying of lumber. *Holzforschung*, 63(3), 334-339.
- Garrahan, P. (2008). Drying spruce-pine-fir lumber. By FPInnovations for Natural Resources Canada. Special Publication–SP-527E: 167pp.
- Cooper, G. (2003). Methods of reducing the consumption of energy on wood drying kilns (No. 211-915). Client report.
- Liang, C. Z., & Chung, T. S. (2018). Robust thin film composite PDMS/PAN hollow fiber membranes for water vapor removal from humid air and gases. *Separation and Purification Technology*, 202, 345-356.
- Massman, W. J. (1998). A review of the molecular diffusivities of H₂O, CO₂, CH₄, CO, O₃, SO₂, NH₃, N₂O, NO, and NO₂ in air, O₂ and N₂ near STP. *Atmospheric Environment*, 32(6), 1111-1127.
- Montoya, J. P. (2010). Membrane gas exchange using hollow fiber membranes to separate gases from liquid and gaseous streams. MedArray.
- Simpson, W. T. (Ed.). (1991). Dry kiln operator's manual. US Department of Agriculture, Forest Service, Forest Products Laboratory.
- Wai Lin, S., & Valera Lamas, S. (2011). Air dehydration by permeation through dimethylpolysiloxane/polysulfone membrane. *Journal of the Mexican Chemical Society*, 55(1), 42-50.
- Yang, B., Yuan, W., Gao, F., & Guo, B. (2015). A review of membrane-based air dehumidification. *Indoor and Built Environment*, 24(1), 11-26.
- Zhao, B., Peng, N., Liang, C., Yong, W., & Chung, T. S. (2015). Hollow fiber membrane dehumidification device for air conditioning system. *Membranes*, 5(4), 722-738.

Evaluation of NHLA Graded Yellow-Poplar Lumber Regraded for Structural Use in CLT

Panel Production

Rafael Azambuja

West Virginia University, USA

Abstract

The current cross laminated timber (CLT) standard in North America (ANSI/APA PRG 320-2018) restricts the use of hardwoods. For producers within the Appalachian Region, with a large percentage of hardwoods, this restriction limits the use of locally supplied lumber for CLTs. An additional hinderance is that most hardwood lumber is graded in respect to appearance following National Hardwood Lumber Association (NHLA) grading rules. Lumber used in structural purposes, however, requires grading system that evaluate defects in relation to mechanical properties. For example, *Liriodendron tulipifera* (yellow-poplar) can be structurally graded following North Eastern Lumber Manufacturers Association (NELMA) grading rules. Further complicating the issue, the processing steps vary between lumber produced for NHLA versus structural grading. Therefore, the objective of this study was to evaluate differences in lumber grades and quantify the influence of additional machining steps on yellow-poplar lumber prepared for CLT panels. Eight packs of dry, rough-cut, 17/16" yellow-poplar lumber with NHLA grades of "2 and below" (NHLA Grade 2A, 2B, 3A, and 3B) were obtained. The lumber used was of random width, but within a range of 6 1/4 inches to 7 3/8 inches. The lumber was graded following both NHLA and NELMA grading rules before and after processing. The processing consisted of ripping to a final width of 6-inches and surfacing both faces to achieve a final thickness of 7/8-inch. Information on which defect kept the lumber from achieving a higher grade (i.e., limiting defect) was determined. Results indicated that lumber processing

***Proceedings of the 62nd International Convention of
Society of Wood Science and Technology
October 20-25, 2019 – Tenaya Lodge, Yosemite, California USA***

considerably influence the grade, as chi-square tests showed a statistically significant difference between the lumber grade (in both systems) prior to and after processing (NHLA, $268.61 > 12.59 \times 25\%$ and NELMA, $140.97 > 7.81 \times 25\%$). In relation to NELMA grades, analyses of prior and post processing showed an increase of Select Structural and lumber that did not meet grade (i.e., below grade). The most common defects were knots (46%) followed by splits (29%), wane (7%), and shake (7%). Ripping to final width showed two main qualitative results. When the defect was in the edge areas, the defect was removed and boards achieved higher grades (e.g., Select Structural). However, when defects were located in central areas, the board overall surface area decreased and the defect area (as a percent) increased, thus decreasing the board grade. To truly quantify these results, further investigation is required with digital image comparisons for prior to and after processing. In respect to NHLA vs NELMA grading, the results showed for processed lumber graded as “2 and below”, 56% of the boards achieved a NELMA structural grade. The lumber met the following NELMA grades: 12% Select Structural; 7% No. 1; 19% No. 2; and 18% No. 3. The remaining 44% were below grade. In conclusion, a majority of yellow-poplar lumber sawn and graded for appearance possessed structural attributes required for use in the production of CLT panels. This finding suggests that there is potential value in re-grading/classifying traditionally processed hardwood lumber (in particular, yellow-poplar) for structural grades.

Design Validation of Cross-Laminated Timber Rocking Shear Walls

Esther Baas
Oregon State University, USA

Abstract

As mass timber products such as cross-laminated timber (CLT) rise in popularity and mass timber buildings are scaling taller than ever, it is crucial for designers and researchers to know how these structural elements perform throughout their lifespan. Although models have been developed to characterize phenomena of mass timber components, they have yet to be verified on large-scale, in-field applications. To complement the direction of industry, The Living Lab at Peavy Hall is a research project established at Oregon State University intended to compare long-term data and design specifications for mass timber and CLT.

George W. Peavy Hall (Peavy Hall) is a three-story building that is being constructed at Oregon State University and is built out of mass timber structural elements, including self-centering rocking CLT walls and CLT-concrete composite floor systems. As construction progresses, Peavy Hall will become equipped with sensors monitoring outdoor and indoor weather conditions, heat and moisture transfer in CLT assemblies, moisture content of timber elements, displacement of CLT floor panels, tension losses in CLT shear walls, and global dynamic behavior of the structure. The data will be collected during and construction while the structural elements are exposed to characterize drying rates and their effects on the structural integrity and serviceability throughout the lifespan of the structure.

Peavy Hall is the world's first real-world application of post-tensioned CLT rocking shear walls. Inside the building, there are 41 CLT shear wall panels that contain four unbonded steel rods that are stressed to high tensile forces to resist the horizontal loads the building is subjected to (e.g. earthquakes, wind). This system is one of performance-based design (PBD), meaning that it is not only designed to resist forces and ensure the building stays standing after an earthquake, but also designed to have minimal residual damage and movement, saving time and money post-event. The system is similar to that of a guitar string, in which the steel strings are pulled to a certain force, and when plucked, will move around but eventually return to its original position. Although these walls have been tested to be successful in seismic applications, there is still data lacking related to their long-term performance, including tension loss in the steel rods over time, creep of the wall panels, and effects of environmental exposure during construction. Sensors, including load cells monitoring the tension force in the steel rods, environmental sensors, and string potentiometers monitoring wall movements, were installed during construction and will remain throughout the lifespan of Peavy Hall to validate the shear wall design over the long-term.

The data will be made available to students, researchers, and industry professionals via implementation of a digital model, and will be used to quantitatively characterize the effects of major and minor operational and extreme events that mass timber structures are subjected to.

ACTIVITY OF ORGANIC ACIDS AND THEIR SYNERGY AGAINST THE WOOD-DECAYING FUNGUS *CONIOPHORA PUTEANA*

Aitor Barbero-López^{1}, Md Mokbul Hossain², Antti Haapala³*

¹Early Stage Researcher, School of Forest Sciences, University of Eastern Finland, Joensuu, FI-80101, Finland. *Corresponding author, *aitorb@uef.fi*

²Junior Researcher, School of Forest Sciences, University of Eastern Finland, Joensuu, FI-80101, Finland. *mdho@student.uef.fi*

³Associate Professor, School of Forest Sciences, University of Eastern Finland, Joensuu, FI-80101, Finland. *antti.haapala@uef.fi*

Abstract

Wood industry is seeking for new wood preservatives that harm the environment less than the ones used nowadays. Bio-based chemicals, usually extracted from forestry side-streams, are being studied as a possible new wood preservative. Organic acids are one of the most common constituents found in bio-based chemicals and are often considered responsible of their antimicrobial activity against fungi and insects. The aim of this study is to understand the independent and synergetic activity of acetic, formic and propionic acid against the wood-decaying fungus *Coniophora puteana*, performing *in vitro* antifungal and wood decay tests. Within all the acids and acid mixtures tested, that showed a high antifungal activity against *C. puteana*, propionic acid was the best performing one, with an estimated minimum inhibitory concentration to completely inhibit the fungus around 0.03%. The wood decay test showed that even the acids are successfully impregnated into the wood, they are easily leached out and don't protect the wood from fungal decay well enough. Thus, the high wood preserving activity of bio-based chemicals, such as pyrolysis distillates, is not coming only from the organic acids, but from their combination with other constituents.

Key words: Wood Preservatives; Pyrolysis; Organic Acids; Fungal Inhibition; Wood Degradation; Wood Decay.

1 INTRODUCTION

Wood decays naturally due to many factors, as fungi or bacteria, when used outdoors. To avoid decay, many kinds of wood preservatives have been tried and many already substituted during the years due to their toxic nature, as chromated-copper-arsenate (CCA) (Mohajerani et al. 2018). Further limitations are expected because of environmental awareness and increasingly strict chemical legislation driving the industry towards new green alternatives.

Bio-based chemicals are being broadly studied as the already cited green alternatives for wood preservation. Several extractives are known to play a role in wood decay prevention due to their antifungal and antioxidant activities, such as tannins (Anttila et al. 2013), stilbenes (Lu et al. 2016) or spent coffee's cinnamates (Barbero-López et al. 2018). These antifungals can be extracted from forestry side streams, such as bark, via different methods, such as pyrolysis, resulting in chemical mixtures rich in phenolics and organic compounds, able to inhibit wood-decaying fungi (Temiz et al. 2013; Barbero-López et al. 2019). Organic acids have been identified by previous researchers as fungal inhibitors against wood-decaying fungi, as propionic and acetic acid protect date and oil palm against decay (Bahmani et al. 2016). Acid anhydrides from formic and acetic acid are also used in commercial modified wood such as Accoya® and Kebony®, that are more durable than non-treated wood.

The aim of this study is to understand the independent and synergetic antifungal activity and wood decay retardancy of organic acids broadly found in wood pyrolysis distillates - propionic acid, acetic acid and formic acid - against the brown-rot fungus *Coniophora puteana*. The results of the study will help understanding if organic acids are the main responsible of the antifungal activity of the pyrolysis distillates, or if other constituents play also a role. The antifungal activity of the acids was tested measuring the inhibition caused by the chemicals to the fungal growth in petri dish, while the wood decay retardancy was studied exposing Scots pine sapwood impregnated with acids – and non-impregnated as control – to fungal cultures of *C. puteana* and assessing the mass loss caused by this fungus.

2 MATERIALS AND METHODS

2.1 Antifungal test

Growth media amended with acetic, propionic and formic acid (Merck KGaA, Darmstadt, Germany) and their mixtures were prepared in petri dish (Ø 90 mm). The pH of the acids and acid mixtures was neutralized adding few drops 0.1M NaOH, until pH was 4, to ensure later agar setting. The media for the antifungal test were prepared in Milli-Q water, with 4% malt powder, 2% agar and one of the organic acids or their mixtures as presented in table 1. The growth media for the control samples was prepared by mixing 4% malt powder and 2% agar in Milli-Q water, without adding acids. In each petri dish 15 mL of 1 of the media was poured. Eight replicates were prepared for each organic acid, mixture and concentration.

Table 1: concentrations of the individual organic acids and their mixtures tested in the antifungal test.

Organic acid and its mixtures	Total tested concentrations (%)
--------------------------------------	--

**Proceedings of the 62nd International Convention of
Society of Wood Science and Technology
October 20-25, 2019 – Tenaya Lodge, Yosemite, California USA**

Acetic acid	0.01	0.025	0.05	0.1
Propionic acid	0.01	0.025	0.05	0.1
Formic acid	0.01	0.025	0.05	0.1
Acetic + propionic acid (1:1, w/w)	0.02	0.05	0.1	
Propionic + Formic acid (1:1, w/w)	0.02	0.05	0.1	
Acetic + Formic acid (1:1, w/w)	0.02	0.05	0.1	
Acetic + propionic + formic acid (1:1, w/w)	0.03	0.075	0.1	

In the center of each acid-amended petri dish and in each control petri dish a spherical piece (\emptyset 5.5 mm) of an active colony of *C. puteana* (strain BAM 112), purchased to the Federal Institute for Materials Research and Testing (BAM, Berlin, Germany), was put under sterile conditions. The petri dish were then sealed with parafilm and put in a growing chamber ($22 \pm 2^\circ\text{C}$ and $65 \pm 5\%$ relative humidity), and the growth of the fungal colonies was checked daily, until the mycelia of the controls reached the edge of the petri dish (between 11 and 14 days). Fungal growth inhibition was measured by modifying the formula proposed by Chang et al. (1999):

$$\text{Inhibition (\%)} = (1 - (AT - IA)/(AC - IA)) * 100$$

Here, AT is the area of the experimental plate, AC is the area of the control plate, and IA is the surface area (mm^2) of the inoculated plug. The minimum inhibitory concentration (MIC) to inhibit the growth of the fungus completely was estimated based on this result.

2.2 Wood decay test

Scots pine (*Pinus sylvestris*) sapwood pieces of $5 \times 40 \times 10 \text{ mm}^3$ (radial x longitudinal x tangential) bought from Kerimäki sawmill, Finland, were used as wood substrate. These sapwood pieces were tagged and oven dried at 50°C until constant mass was reached, and their mass was recorded. Propionic, acetic and formic acid were prepared at 3% and 6% concentration for wood impregnation. Formic and propionic acid mixture (1:1) and acetic, formic and propionic acid mixture (1:1:1) at a total acid concentration of 3% and 6% were also prepared for wood impregnation. Wood decay test was carried out by following a modified version of EN 113 test described by Lu et al. (2016). In each acid and acid mixture, 16 sapwood pieces were submerged, and, using the PUUMA impregnation platform of the University of Eastern Finland, they were exposed to a modified Bethel impregnation process. First, wood pieces were exposed to vacuum in 0.15 bar for 20 minutes. Afterwards, the pressure was slowly increased until 10 bar, held for 60 minutes and released, and no final vacuum was applied. The wet mass of the impregnated wood specimens was then measured to ensure proper impregnation, and afterwards the wood pieces were oven dried at 50°C until constant mass was reached, and their mass was recorded to calculate the chemical retention.

Eight sapwood specimens of each treatment were then exposed to leaching following the norm EN84. After leaching, the wood specimens were oven dried at 50°C until constant mass was reached, and their mass was recorded. Then, the wood specimens – impregnated and non-treated – were sterilized in the Scandinavian Clinics Estonia OÜ (Alliku, Estonia) using gamma radiation (31.7 kGy to 32.3 kGy).

Petri dish (\varnothing 90 mm and 15 mm height) were prepared with 30 ml of 4% malt powder and 2% agar growth media, and a plug (\varnothing 5.5 mm) of the fresh *C. puteana* cultures was put in the center of the petri dish under sterile conditions. The petri dish were sealed with parafilm and kept in a growing chamber ($22 \pm 2^\circ\text{C}$ and $65 \pm 5\%$ relative humidity) until the mycelia covered the whole surface of the petri dish. Then, under sterile conditions, four plastic meshes ($\sim 50 \times 15 \text{ mm}^2$) were put in each petri dish, and four wood pieces were placed in each petri dish over the meshes. All the wood pieces in each petri dish were leached and non-leached specimens of different concentrations (3% and 6%) of the same acid or acid mixtures (see figure 1). In case of controls, two wood specimens were put in each petri dish, and two extra wood specimens – not part of the experiment – were added to the petri dish to have 4 specimens per dish. 8 replicates per treatment were used in this experiment. Then, the petri dish were sealed with parafilm and kept in a growing chamber at $22 \pm 2^\circ\text{C}$ and $65 \pm 5\%$ relative humidity. After eight weeks, the wood specimens were taken out of the petri dish, the fungal mycelia was smoothly removed with the help of a brush and the wood specimens were oven dried at 50°C until constant mass was reached. The mass of the wood specimens was measured to calculate the decay rate caused by *C. puteana* to the wood pieces.

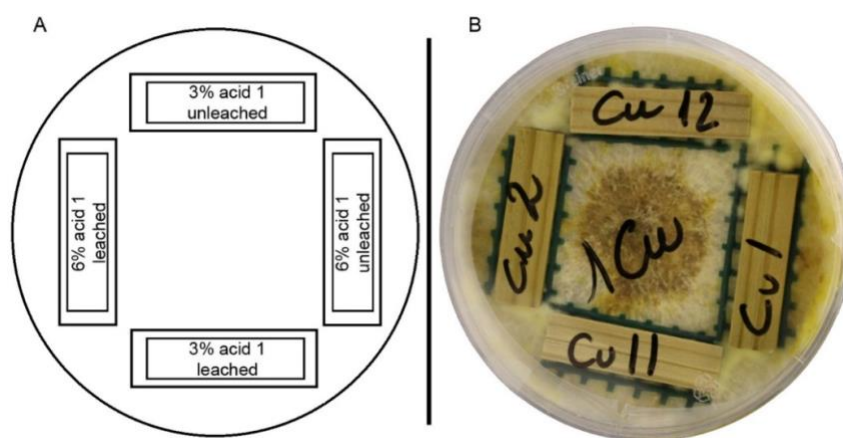


Fig 1: Schematic (A) and visual example (B) of the setup of the sapwood pieces, over the plastic meshes, in a petri dish inoculated with *C. puteana*.

3 RESULTS

3.1 Antifungal test

All the studied acids showed antifungal activity even at the lowest tested concentrations (Table 2). At 0.01%, formic acid was the most effective acid inhibiting *C. puteana* about 70%, while acetic acid and propionic acid inhibited this fungus about 40%. When the acid concentration was increased to 0.025% propionic acid was the most effective acid as it almost fully inhibited *C. puteana*. Acetic acid caused about 70% inhibition of the fungus while formic acid was able to inhibit it about 80%. At 0.05% concentration, propionic acid completely inhibited *C. puteana*, and acetic and formic acid inhibited this fungus about 90%. The decay fungus was completely inhibited by the acids at 0.1%.

The two acid mixtures were also successful inhibitors of *C. puteana* at concentration of 0.2%, the acetic acid and formic acid mixture caused *C. puteana* inhibition of 25%. Acetic acid and propionic acid mixture inhibition was 35%. The mixture of formic acid and propionic acid caused a growth increment of *C. puteana* of about 9%. The inhibition by acetic and formic acid at 0.05% did not differ from the inhibition caused at 0.02%. The formic and propionic acid mixture inhibited the fungus at 76%, while the acetic acid and propionic acid mixture caused over 90% fungal inhibition. The fungus was completely inhibited by mixtures at 0.1%. The three acid mixture inhibited *C. puteana* over 75% at 0.03% concentration, and completely at higher concentrations. Out of all the tested acids and acid mixtures, propionic acid has the lowest estimated MIC (about 0.03%). Acetic acid and the mixture of acetic acid and propionic acid have a MIC of 0.06%. Formic acid, its mixture with propionic acid and the mixture of acetic, formic and propionic acid have MIC between 0.07 and 0.08%. The highest MIC - about 0.1% - was estimated for the acetic and formic acid mixture.

Table 2. Growth inhibition (%) of *Coniophora puteana* caused by the different acids and their mixtures, and the estimated minimum inhibitory concentration (MIC) to fully inhibit *C. puteana*. Results are presented as mean \pm standard error.

Acids	0.01%	0.025%	0.05%	0.1%	MIC
Acetic acid	41.8 \pm 3.8	70.8 \pm 2.4	93.5 \pm 1.2	100 \pm 0	~ 0.06%
Formic acid	71.3 \pm 2.8	79.1 \pm 3.8	86.6 \pm 1.7	100 \pm 0	~ 0.07%
Propionic acid	38.8 \pm 4.3	98.1 \pm 0.2	100 \pm 0	100 \pm 0	~ 0.03%
	0.02%	0.05%	0.1%		
Acetic + formic acid	24.6 \pm 7.1	23.6 \pm 3.0	100 \pm 0		~ 0.1%
Acetic + propionic acid	35.4 \pm 4.8	92.4 \pm 1.2	100 \pm 0		~ 0.06%
Formic + propionic acid	-9.3 \pm 2.6	76.0 \pm 3.4	100 \pm 0		~ 0.08%
	0.03%	0.075%	0.1%		
Acetic + formic + propionic acid	77.4 \pm 3.2	100 \pm 0	100 \pm 0		~ 0.07 – 0.08%

3.2 Chemical retention in wood

All the acids and their mixtures were successfully impregnated into the wood, with retention values of 8-20 kg·m⁻³. When the dry impregnated specimens were exposed to leaching, all the treated wood presented a negative retention values between 1-6 kg·m⁻³.

3.3 Wood decay test

The acid treatment of the sapwood specimens produced in most of the cases a decrement in the mass loss caused by *C. puteana* in non-leached sapwood specimens (Table 3). Acetic acid at 3% concentration presented the best performance against wood decay caused by *C. puteana*, as it had the lowest sapwood mass loss out of all the acids and acid mixtures tested. Propionic acid at 6% presented the lowest mass loss out of all the acid and mixtures at that concentration. All the other tested acids and mixtures had a mass loss of between 15-20%, while the mass loss of the untreated controls was close to 24%.

Table 3. Dry mass loss (%) caused by *C. puteana* to acid treated leached and non-leached Scots pine sapwood specimens. Results are presented as mean \pm standard error.

Acids	Concentration (%)	Non-leached (%)	Leached (%)
Acetic acid	3	10.32 \pm 2.14	17.55 \pm 2.83
	6	13.86 \pm 3.37	20.56 \pm 3.18
Formic acid	3	17.10 \pm 3.19	25.40 \pm 4.13
	6	17.66 \pm 2.17	18.65 \pm 2.31
Propionic acid	3	13.52 \pm 3.01	21.62 \pm 2.54
	6	10.47 \pm 3.02	16.90 \pm 2.39
Formic + propionic acid	3	18.93 \pm 3.36	21.26 \pm 2.95
	6	19.69 \pm 3.54	16.42 \pm 2.06
Acetic + Formic + propionic acid	3	15.31 \pm 1.84	23.85 \pm 3.29
	6	19.68 \pm 3.43	22.53 \pm 2.87
Control		23.75 \pm 2.59	

The leached sapwood specimens has a higher mass loss than the non-leached specimens treated with the same acid and mixtures (Table 3). Only sapwood specimens treated with 3% acetic acid and 6% formic acid, propionic acid and the mixture of propionic and formic acid had less mass loss than the control specimen.

4 DISCUSSION

The results of the antifungal test proved the high inhibitory effect of the different acids against the wood-decaying fungus *C. puteana*, causing fungal inhibition even at 0.01% concentration. Propionic acid was found to be the most effective acid out of the tested independent acids, as it has a MIC value that is at least half the MIC value of the other tested acids and mixtures. These results agree with previous findings that suggested a high inhibitory effect of propionic acid against wood-decaying fungi (Barbero-López et al. 2019) and the relevance of total acid content of different chemicals, as pyrolysis distillates, in their antifungal activity (Oramahi and Yoshimura 2013).

The results of our study found that the tested acid mixtures inhibit *C. puteana* in a similar manner to independent acids, but it does not have a stronger effect. Barbero-López et al. (2019) concluded that pyrolysis distillates present a high antifungal activity due to the mixture of different organic acids and other chemicals, such as phenolics, what supports the findings of this study.

All the acids and their mixtures were successfully impregnated into the wood, but after leaching the mass of the specimens was slightly lower than their mass before impregnation, presenting a maximum estimated mass loss of about 1%. This showed that these acids and mixtures have a high leachability from wood and a possible chemical degradation of the specimens by strong acidic solutions (Kass et al. 1970).

Although some of the acids decreased the decay rate of the sapwood specimens, based on the European norms (EN 113), none of the acids provided adequate protection as the mass loss of all the sapwood specimens was over 3%. However, non-leached propionic acid and acetic acid impregnated wood showed the best performance out of all the tested acids against wood decay caused by *C. puteana*.

Both tested mixtures of acids presented very low mass loss reductions compared to control specimens, despite their higher impregnation rate compared to independent acids and although organic acids are present in chemicals with known antifungal and decay retardant properties, as pyrolysis distillates (Oasmaa and Czernik 1999; Barbero-López et al. 2019). This results show that the antifungal properties and decay retardancy caused by pyrolysis distillates it's not coming merely from the organic acids tested in this study, but from other distillates' constituents. Baimark and Niamsa (2009) concluded that the antifungal activity of these distillates was dependent in their amount of phenolics and recently, Mattos et al. (2018) highlighted that based on literature, the antimicrobial activity of these distillates are coming from their phenolics, fatty acids and acetic acid. Based on the cited literature and our findings, it could be concluded that the pyrolysis distillates' antifungal activity is based in the combined effect of their constituents and not just by the organic acids or phenolics.

The present paper focused in understanding the activity of the several organic acids against *C. puteana*. The results help understanding the pyrolysis liquids' constituents' activity against *C. puteana*, and discard the acid impregnation as such as a wood preservative, due to their low performance against the decay. Nevertheless, the study needs to be expanded to more fungi and wood species. Due to the high antifungal activity of propionic and acetic acid at very low concentration, the addition of these acids in wood preservatives formulations need to be studied further. Further studies are also necessary to understand the mechanical properties of wood are affected by these acids at low concentration and how would they affect the wood properties and durability if their pH is neutralized prior to impregnation.

5 CONCLUSIONS

Acetic, formic and propionic acid, as well as their mixtures, showed a very high antifungal activity *in vitro* against *Coniophora puteana*, but did not retard Scots pine sapwood decay caused by *C. puteana* sufficiently to meet the requirements in EN 113 standard. Propionic acid exhibited the highest inhibitory effect against *C. puteana*. Additionally, it was found that the organic acids of pyrolysis distillates are not the alone responsible of the antifungal activity of pyrolysis distillates, but their efficiency arises in combination with other constituents.

6 REFERENCES

- Anttila AK, Pirttilä AM, Häggman H, Harju A, Venäläinen M, Haapala A, Holmbom B, Julkunen-Tiitto R (2013) Condensed conifer tannins as antifungal agents in liquid culture. *Holzforschung* 67: 825–832.
- Bahmani M, Schmidt O, Fathi L, Frühwald A (2016) Environment-friendly short-term protection of palm wood against mould and rot fungi. *Wood Mater. Sci. Eng.* 11: 239–247.
- Baimark Y, Niamsa N, (2009) Study on wood vinegars for use as coagulating and antifungal agents on the production of natural rubber sheets. *Biomass Bioenergy* 33: 994-998.
- Barbero-López A, Chibily S, Tomppo L, Salami A, Ancin-Murguzur FJ, Venäläinen M, Lappalainen R, Haapala A (2019) Pyrolysis distillates from tree bark and fibre hemp against wood-decaying fungi. *Ind. Crop. Prod.* 129: 604–610.
- Barbero-López A, Ochoa-Retamero A, López-Gómez Y, Vilppo T, Venäläinen M, Lavola A, Julkunen-Tiitto R, Haapala A (2018) Activity of spent coffee ground cinnamates against wood-decaying Fungi *in vitro*. *BioResources* 13: 6555–6564.
- EN 113. “Wood preservatives – Test method for determining the protective effectiveness against wood destroying basidiomycetes - Determination of the toxic values”. European Committee for Standardization, Brussels, BE, 1996.
- Kass A, Wangaard FF, Schroeder HA (1970) Chemical Degradation of Wood: The Relationship Between Strength Retention and Pentosan Content. *Wood Fiber Sci.* 1: 31-39.
- Lu J, Venalainen M, Julkunen-Tiitto R, Harju AM (2016) Stilbene impregnation retards brown-rot decay of Scots pine sapwood. *Holzforschung* 70: 261–266.
- Mattos C, Romeiro GA, Folly E (2018) Potential biocidal applications of pyrolysis bio-oils. *J. Anal. Appl. Pyrol.* DOI: 10.1016/j.jaap.2018.12.029
- Mohajerani A, Vajna J, Ellcock R (2018) Chromated copper arsenate timber: a review of products, leachate studies and recycling. *J. Clean. Prod.* 179: 292–307.
- Oasmaa A, Czernik S (1999) Fuel oil quality of biomass pyrolysis oils - state of the art for the end users. *Energ. Fuels* 13: 914-921.
- Oramahi HA, Yoshimura T (2013) Antifungal and antitermitic activities of wood vinegar from *Vitex pubescens* Vahl. *J. Korean Wood Sci. Technol.* 59: 344–350.

***Proceedings of the 62nd International Convention of
Society of Wood Science and Technology
October 20-25, 2019 – Tenaya Lodge, Yosemite, California USA***

Temiz A, Akbas S, Panov D, Terziev N, Alma MH, Parlak S, Kose G (2013) Chemical composition and efficiency of bio-oil obtained from giant cane (*Arundo donax* L.) as a wood preservative. *BioResources* 8: 2084-2098. doi:10.15376/biores.8.2.2084-2098

**Evaluation of Shear Performance of Cross-Laminated timber Shear Wall Connections
under the Effects of Moisture**

Mr. Shrenik Bora, boras@oregonstate.edu

Dr. Arijit Sinha

Dr. Andre Barbosa

Oregon State University, USA

Abstract

Cross-laminated timber (CLT) is a promising renewable building material which enables the utilization of wood for mid-rise and even tall wood buildings owing to its high strength-to-weight ratio, fire performance, and prefabricated nature. However, moisture intrusion in CLT is a significant risk since it directly affects the durability of the structure. CLT panels have high storage capacity but relatively low vapor permeability which may result in absorption and retention of large amounts of moisture. The structural members of CLT can be exposed to moisture due to various reasons such as excessive wetting during or after construction, failure of internal plumbing, and failure of impermeable elements of facades or roofs. Performance of CLT structure is highly dependent on the performance of its connections. Most of the existing research on CLT is focused on ambient temperature and moisture control. While the influence of moisture on timber structures is well recognized, the impact of moisture intrusion on the performance of CLT connectors is less understood. Therefore, this study aims to investigate the effects of three (3) different moisture exposure conditions on shear performance of 3-ply CLT diaphragm to shear wall connectors under quasi-static loading. Four important wood species used across globe for CLT manufacturing [Douglas fir, Southern yellow pine, Norway spruce, and Spruce Pine Fir] are used for the test specimens. The test specimen is fabricated with one horizontal member of CLT having dimensions of [8" X 12"] connected to one vertical member of CLT having equal dimensions at the center with a two (2) L-brackets. The connections will be tested using Abbreviated Basic Loading History CUREE protocol to understand the effects of different moisture exposure conditions along with the variation of wood species on these connection types. This study is envisioned for the development of design guidelines of CLT connections. Consequently, the results of this study will improve our knowledge to account for effects of moisture while designing connections for mass timber buildings.

Keywords- CLT, mass timber, connections, moisture, durability, exposure, CUREE

Study on VOCs Emissions from Veneered Plywood at Closed Circumstances

Tianyu Cao^a, Jun Shen^b, *

^a College of Material Science and Engineering, Northeast Forestry University, Harbin, China
18504616802@163.com

^b College of Material Science and Engineering, Northeast Forestry University, Harbin, China
shenjun@nefu.edu.cn

In order to explore the emission characteristics of VOCs and different VOC-components from plywood in a sealed environment, three kinds of plywood with thickness of 8 mm were tested as experimental materials. Polyvinyl chloride overlaid veneered plywood (PVC-VP), melamine-impregnated paper overlaid veneered plywood (MI-VP) and unfinished plywood (UF-P) were released in a 15 L small environment cabin with the temperature of $23.5^{\circ}\text{C}\pm 0.5^{\circ}\text{C}$ and gas exchange of 0 time \cdot h⁻¹. The gas was collected after sealed 2h, 4h, 6h, 8h, 12h, 18h, 24h and 30h separately under the panel area to volume ratios were 1m²·m⁻³, 1.5m²·m⁻³, 2m²·m⁻³, 2.5m²·m⁻³. The gas chromatography-mass spectrometer was used to analysis the changes of VOCs concentration and VOC-components with the panel area to volume ratios. The results show that the VOCs concentration released from the panel increased gradually until equilibrium with the increase of the hermetical time, and the trend was non-linear. PVC-VP and MI-VP were reached equilibrium state after sealed 12h, but UF-P needed 18h. The higher the panel area to volume ratio is, the earlier VOC concentration reached equilibrium, and veneered plywood (PVC-VP and MI-VP) reached equilibrium earlier than unfinished plywood. Among them, concentration of MI-VP is the highest in equilibrium. Among the various components of VOC, categories that account for larger proportion such as aromatic hydrocarbons, esters and aldehydes changed obviously with time. The concentration of aromatic hydrocarbons increased most obviously with the increase of sealing time, also with the panel area to volume ratios. The UF-P reached equilibrium after 24h of sealing, but the veneered plywood reached fluctuation equilibrium after 12h. The concentration of esters released from PVC-VP and MI-VP changed more regularly, which increased with time and had no equilibrium period. However, only the esters released from UF-P showed a weak positive correlation with the increase of the panel area to volume ratios. The regularity of aldehydes changes with time and the panel area to volume ratios were weak, which showed an unstable upward trend. The other VOC-components had small proportion and the trends of them were not obvious.

Keywords: plywood; veneer material; closed circumstances; the panel area to volume ratio; VOC-components

INTRODUCTION

In recent years, more and more attention has been paid to the pollution caused by family decoration. And wood-based panel such as plywood and particleboard has been used more and more widely in furniture decoration. Plywood has many advantages such as not easy to deform, good transverse tensile properties, large breadth and so on. But volatile organic compounds could release from plywood when manufacturing and using, which causing indoor air pollution. VOC can do harm to human health, especially elderly and children, which can lead to cancer and even death [1-2]. Formaldehyde and benzene were mainly toxic substance which can irritate eyes and mucosa, leading headache, fatigue and nausea, and resulting in sick building syndrome (SBS) [3]. Therefore, the research of VOCs has been paid more and more attention.

There are many studies on the impact of VOCs on indoor air and health risk assessment. The level of indoor air pollution could be calculated the comprehensive index to determine according to Bernd's research [4-5]. The concentration and odor of TVOC could also be affected by changes of indoor environmental factors. The odor will be stronger when indoor temperature and relative humidity increase [6]. VOCs released from wood itself and wood surface coatings, decorative materials can also be a source of odor [7-9]. As a common decorative material, PVC is a thermoplastic polymer made from vinyl chloride monomer. The VOC released by PVC mainly includes dibutyl phthalate and dioctyl phthalate [10]. It is irritating and easy to release vinyl chloride, trichloromethane and trichloroethylene after heating, showing acid and plastic taste [11].

**Proceedings of the 62nd International Convention of
Society of Wood Science and Technology
October 20-25, 2019 – Tenaya Lodge, Yosemite, California USA**

The emission of VOCs can be affected by many factors such as environmental parameters, production process and finishing materials. The research shows that the increase of temperature can promote the release of formaldehyde and VOCs in wood-based panels more than the increase of relative humidity [12-13]. The release rate of VOCs will increase by increasing the hot-pressing temperature and time in the production process [14]. Most wood-based panels were decorated by veneers and edges, and different veneers have different sealing rates for formaldehyde and TVOC [15-17]. Not only veneer treatment, surface painting can effectively reduce TVOC release from particleboard, but surface painting and wood modification with chemical reagents often lead to increased TVOC release, which brings hidden dangers to human health [18-19].

In this experiment, the VOCs emission of three kinds of plywood were tested under the condition of air exchange rate was 0 times/h. Four panel area to volume ratios ($1\text{m}^2\cdot\text{m}^{-3}$, $1.5\text{m}^2\cdot\text{m}^{-3}$, $2\text{m}^2\cdot\text{m}^{-3}$, $2.5\text{m}^2\cdot\text{m}^{-3}$) and eight airtight storage periods (2h, 4h, 6h, 8h, 12h, 18h, 24h and 30h) were set. The total concentration and composition of VOCs were qualitatively and quantitatively analyzed by GC-MS. The characteristic curve of VOCs release from plywood under closed condition was explored, and the effects of finishing materials and panel area to volume ratios on the release of VOCs from plywood were analyzed. It is of great guiding significance to choose plywood for furniture decoration.

EXPERIMENTAL

Materials

In this experiment, three kinds of plywood were from a furniture manufacturer in Guangzhou. The length×width×thickness was 1200mm×1200mm×8mm, and the pH was 7.2-7.4. The hot-pressing temperature was 190-200°C and hot-pressing time was 210s. The initial moisture content of plywood ranges from 8.5% to 10.5%. Three kinds of plywood were cut to 150mm×50mm×8mm and 150mm×75mm×8mm. Aluminum foil was used to seal the edges of the specimens so that the VOCs do not escape from the edges, then stored at -30°C.

Equipment

The main equipment conditions are as follows:

- (1) A 15 L small environment cabin was used as the VOCs sampling chamber, which was made by Northeast Forestry University independently. 15 L small environment cabin has the advantage that simple assembly, low cost and has good correlation with 1m³ environment cabin. Nitrogen (purity was 99.99%) was used as carrier gas, the temperature was 23.5°C±0.5°C and gas exchange rate was 0 h⁻¹.
- (2) Tenax-TA tubes (200mg filler inside, L×R=89mm×3.2mm, BeifenTianpu Instrument Technology Co., Ltd. Beijing, China) were used to collect the gas released from plywood in the cabin.
- (3) A vacuum sealing machine (VS2110GB, Dongguan Yinger Electrical Appliances Co., Ltd.) was used to vacuum samples into polytetrafluoroethylene bags.
- (4) Analytical Tube Processor (TP-2040, Beijing Beifen Tianpu Instrument Technology Co., Ltd.) was used to thermal desorption of the Tenax-TA tubes and removal of residues in the tubes.
- (5) A miniature vacuum pump (ANJ6513-220V, Chengdu Xinweicheng Technology Co., Ltd.) was used as one of the sampling equipment. A Tenax-TA tubes was set between 15L small cabin and vacuum pump, and gas was collected into the tube by vacuum extraction.
- (6) Thermal Desorber (ultra&unity, Markes International Inc., Llantrisant, UK) were used as the thermal desorption equipment. The cold trap adsorption temperature is -15°C, analytical temperature is 300°C and pipeline temperature is 180°C.
- (7) GC-MS (DSQ II, Thermo Scientific, Germany) was used to characterize and quantified the VOCs. The basic parameters were as follows: the type of chromatographic column is DB-5MS, 30m×0.25mm×0.25µm, the carrier gas was helium of 99.996%, the injection port temperature was 250°C and the distribution ratio was 40. The temperature program is three steps: first kept at 40°C for 2 min, then increased to 150°C by 4°C/min and kept for 4 min, finally increased to 250°C by 10°C/min and kept for 8 min. By ionizing with EI and the energy was 70eV, the ionization temperature was 230°C, transmission line temperature was 250°C and the mass scan range was 40-450 amu with full scan.

Methods

Sampling

The samples were divided into three groups: PVC-VP, MI-VP and UF-P, and have two pieces 150mm×75mm×8mm and four pieces 150mm×50mm×8mm according to the panel area to volume ratios and exposure area of panel (1m²/m³-0.015m², 1.5m²/m³-0.225m², 2m²/m³-0.03m², 2.5m²/m³-0.0375m²).

The interior walls of 15L small cabin was cleaned by anhydrous ethanol and distilled water. Then the fan was turned on and kept for more than 30 minutes and nitrogen with 99.99% purity was injected. The main experimental parameters were: temperature 23.5°C±0.5°C controlled by air conditioner, and gas exchange rate was zero. Put samples into the cabin and then turn down the fan and nitrogen to keep the airtight condition.

Before collection, the Tenax-TA tubes should be desorbed by the analytic tube processor for 30 minutes at 325°C. A miniature vacuum pump was used to collection 3L gas in the cabin. In this way, eight experiments were conducted in each group and the airtight time was 2h, 4h, 6h, 8h, 12h, 18h, 24h and 30h, respectively.

Analytical method

Toluene-D₈ was used as the solute and dissolved in methanol to make a standard curve. 2μL of Toluene-D₈ was injected into a Tenax-TA tube and prepurge for 5 minutes. DSQII gas chromatography-mass spectrometer was used to characterize and quantified the VOCs. In the analysis of VOCs, firstly the volatile components with matching degree greater than 90% and the number of carbon atoms is 6-16 were selected, then determination the volatile components by retention time. Finally, the peak area of C₇D₈ was used to quantify VOCs concentration.

RESULTS AND DISCUSSION

Trend of VOCs of plywood with time under four panel area-volume ratios

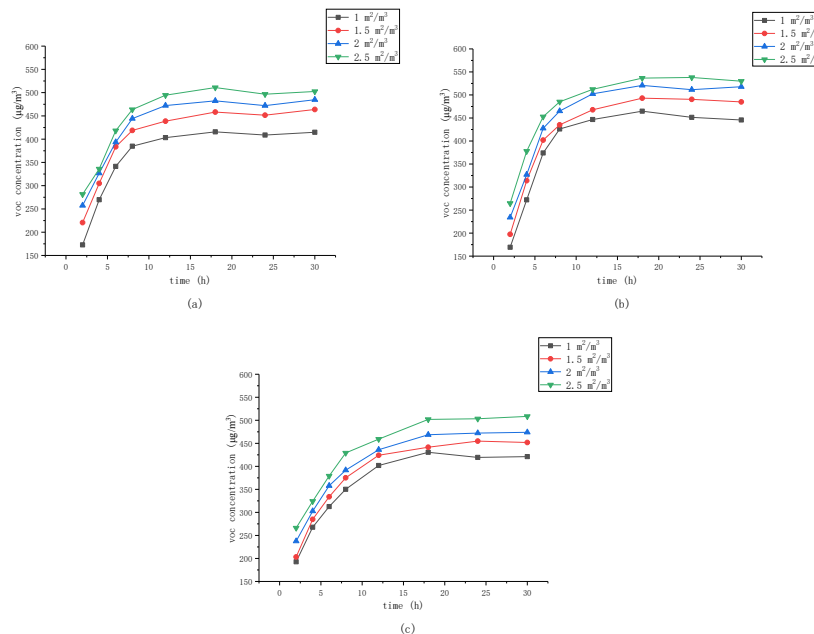


Fig. 1 Trend of VOCs with airtight time under different panel area-volume ratios: PVC-VP (a), MI-VP (b), UF-P(c)

Fig.1 shows the concentration of the VOCs released from PVC-VP, MI-VP, and UF-P after storage for 2h, 4h, 6h, 8h, 12h, 18h, 24h, and 30h respectively in airtight environment cabin. Regardless of the plywood type, VOCs concentration increased with the airtight time, and gradually reached saturation. But the speed of saturation of plywood with different veneer materials was different. The concentration of VOCs of PVC-VP after storage for 12h was 97.15% higher than after storage for 2h. MI-VP was 127.27% after storage for 12h compared with 2h. While the concentration after storage for 30h was only 3.22% (PVC-VP), 2.5% (MI-VP) higher than 12h. Therefore, the concentration of VOCs growth rapidly when storage for 2h-12h, and the growth rate slows down greatly after 12h. What's more, the concentration of VOCs released from veneered plywood (PVC-VP, MI-VP) reached saturation faster, and about only 12h needed. However, the VOCs concentration of UF-P needs 18h to reach the saturation, and increased only 0.66% from 18h to 30h.

UF-P only releases VOCs from the interior plywood, but veneer materials released VOCs along with the inner board because the veneer covered by the surface itself contains VOCs. In terms of VOCs concentration at saturation, the pollution degree of veneered plywood is PVC-VP better than MI-VP. Also, the concentration of VOCs from MI-VP is the highest among the three plywood. The higher the panel area to volume ratio is, the earlier VOC concentration reached equilibrium, and veneered plywood (PVC-VP and MI-VP) reached equilibrium earlier than unfinished plywood.

Analysis of Mainly VOC-components

VOCs are aggregates of many volatile organic compounds; they are classified into eight categories according to their composition (aromatics, alkanes, olefins, aldehydes, ketones, alcohols, esters and others). Among the various components of VOC, categories that account for larger proportion such as aromatic hydrocarbons, esters and aldehydes changed obviously with time. Figure 2 shows the trend of aromatic hydrocarbons, aldehydes and esters with the airtight time and different panel area to volume ratios at 30h.

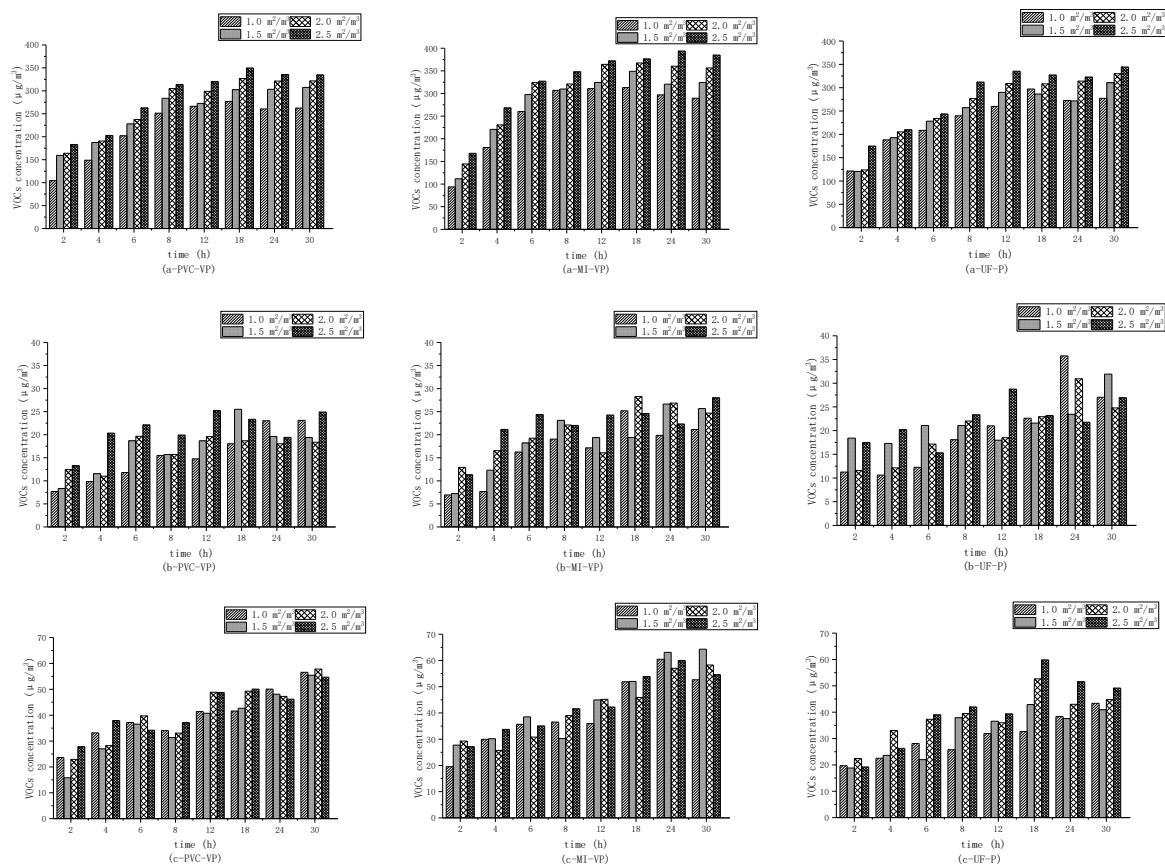


Fig. 2 trend of aromatic hydrocarbons (a), aldehydes (b) and esters (c) released from PVC-VP, MI-VP and UF-P at 30h

Aromatic hydrocarbons account for the largest proportion of VOCs, because the components with higher release rate can better represent the release characteristics of VOCs [20]. The proportion of aromatic hydrocarbons in VOC released by three kinds of plywood was 65.63% (PVC-VP), 68.34% (MI-VP) and 67.98% (UF-P), respectively. The concentration of aromatic hydrocarbons showed a good trend with the increase of airtight time, also with the panel area to volume ratios. The aromatic hydrocarbons released from MI-VP reached the saturation fastest, and its concentration was the highest. The aromatic hydrocarbons of UF-P reached equilibrium after 24h of sealing, but the aromatic hydrocarbons of veneered plywood reached fluctuation equilibrium after 12h. The concentration of aromatic hydrocarbons released from three kinds of plywood increased by more than 120% when the panel area to volume ratios from 1m²·m⁻³ to 2.5m²·m⁻³, such as PVC-VP was 127.58%, MI-VP was 132.89% and UF-P was

**Proceedings of the 62nd International Convention of
Society of Wood Science and Technology
October 20-25, 2019 – Tenaya Lodge, Yosemite, California USA**

124.19%. It shows that MI-VP is most strongly affected by the panel area to volume ratios. On the other hand, Polyvinyl chloride can prevent the release of aromatic hydrocarbons from the inside of the plywood effectively cause its concentration was lowest among the three plywood.

The regularity of aldehydes changes with time and the panel area to volume ratios were weak, which showed an unstable upward trend. The aldehydes released from PVC-VP and MI-VP increased more obviously with airtight time than those released by UF-P, and influenced by the panel area to volume ratios more obviously when the airtight time were 2h-12h. The influenced was weakened by the panel area to volume ratios after 12h. The concentration of esters released from PVC-VP and MI-VP changed more regularly, which increased with time and had no equilibrium period. However, only the esters released from UF-P showed a weak positive correlation with the increase of the panel area to volume ratios. The concentration of aldehydes from PVC-VP and MI-VP were lower than UF-P, which shows polyvinyl chloride and melamine-impregnated paper can reduce the release of aldehydes emissions. On the contrary, the concentration of esters from PVC-VP and MI-VP were higher than UF-P. This is due to the lack of decorative materials on the surface of veneer plain board, so a part of the source of esters is missing. Shen Jun, Jiang Liqun's research found that veneer treatment reduced the total amount of TVOC released from sheets, but also increased the amount of a compound released [21], which also explains the increase of esters concentration released from MI-VP and PVC-VP.

It can be seen that not all the release characteristics trend was logarithmic function growth as expected, but shows different characteristic curves because of the influence of decoration materials. Results show that the panel area to volume ratios does not have a linear relationship with VOCs concentration [22]. And the emission of VOCs from the inside of plywood could be limited when the concentration increased to maximum under the condition that the air exchange rate was zero [23], which explained the different characteristic curves above. However, the obtained characteristics curve is limited because the panel area to volume ratios chosen in this experiment was only $1\text{m}^2\cdot\text{m}^{-3}$ to $2.5\text{m}^2\cdot\text{m}^{-3}$. Therefore, it is necessary to carry out follow-up experiments which have the panel area to volume ratios greater than $2.5\text{m}^2\cdot\text{m}^{-3}$.

CONCLUSIONS

(1) VOCs concentration increased with the airtight time, and gradually reached saturation. But the speed of saturation of plywood with different veneer materials was different. PVC-VP and MI-VP reached saturation faster, and about only 12h needed, but UF-P needs 18h. The concentration of VOCs growth rapidly when storage for 2h-12h, and the growth rate slows down greatly after 12h. In terms of VOCs concentration at saturation, the pollution degree of veneered plywood is PVC-VP better than MI-VP. Also, the concentration of VOCs from MI-VP is the highest among the three plywood. The higher the panel area to volume ratio is, the earlier VOC concentration reached equilibrium, and veneered plywood (PVC-VP and MI-VP) reached equilibrium earlier than unfinished plywood.

(2) Aromatic hydrocarbons account for the largest proportion of VOCs and showed a good trend with the increase of airtight time, also with the panel area to volume ratios. The aromatic hydrocarbons released from MI-VP reached the saturation fastest, and its concentration was the highest. Polyvinyl chloride can prevent the release of aromatic hydrocarbons from the inside of the plywood effectively. The regularity of aldehydes changes with time and the panel area to volume ratios were weak, which showed an unstable upward trend. The concentration of esters released from PVC-VP and MI-VP changed more regularly, which increased with time and had no equilibrium period. However, only the esters released from UF-P showed a weak positive correlation with the increase of the panel area to volume ratios. the concentration of esters from PVC-VP and MI-VP were higher than UF-P. It can be seen that not all the release characteristics trend was logarithmic function growth as expected, but shows different characteristic curves because of the influence of decoration materials. The other VOC-components had small proportion and the trends of them were not obvious.

ACKNOWLEDGEMENTS

This study was supported by the National Key Research and Development Program of China (Grant 2016 TFD 0600706).

REFERENCES CITED

- [1] Shao, Y. L., Shen, J., Shen, X. W. & Qin, J. K. Effect of panel area–volume ratio on TVOC released from decorative particleboards. *Wood Fiber Sci.* 50, 132–142 (2018).

**Proceedings of the 62nd International Convention of
Society of Wood Science and Technology
October 20-25, 2019 – Tenaya Lodge, Yosemite, California USA**

- [2] Liu WJ, Shen J, Wang QF (2017) Design of DL-SW micro-cabin for rapid detection and analysis of VOCs from wood-based panels. *J. Forestry Eng* 4:40–45. (In Chinese)
- [3] Jiang C, Li D, Zhang P, et al. Formaldehyde and volatile organic compound (VOC) emissions from particleboard: Identification of odorous compounds and effects of heat treatment [J]. *Building and Environment*, 2017, 117:118-126.
- [4] Zhao Y, Shen J, Zhao GL. Measurement of VOC release rate of plywood and its impact on indoor environment [J]. *Journal of Safety and Environment*, 2015, 15 (01): 316-319. (In Chinese)
- [5] Liu Y, Zhu XD. Application of comprehensive index method in the evaluation of volatile organic compound pollution from wood-based panel[J]. *Journal of Environment and Health*, 2012, 28(4) : 369-370.
- [6] Wang QF, Shen J, Shen XW, Du JH (2018) Volatile Organic Compounds and Odor Emissions from Alkyd Resin Enamel-coated Particleboard. *BioResources* 13(3): 6837-6849
- [7] Liu R, Huang AM, Wang C, Lu B. Review of Odor Source and Controlling Technology for Furniture [J]. *Wood Industry*, 2018, 32 (03): 34-38. (In Chinese)
- [8] Filipy J, Rumburg B, Mount G, et al. Identification and quantification of volatile organic compounds from a dairy[J]. *Atmospheric Environment*, 2006, 40(8): 1480-1494.
- [9] Järnström H, Saarela K, Kalliokoski P, et al. Comparison of VOC and ammonia emissions from individual PVC materials, adhesives and from complete structures[J]. *Environment International*, 2008, 34(3):420-427.
- [10] Wang QF, Shen J, Jiang LQ, Dong HJ. Comprehensive evaluation on impact of melamine veneer particleboard on indoor environment [J]. *Journal of Central South Forestry University*, 2019, 39 (03): 99-106. (In Chinese)
- [11] Li ZJ, Shen J, Jiang LQ, Li XB, Dong HJ, Wang QF. Odor emission analysis of melamine faced MDF [J]. *Journal of Beijing Forestry University*, 2018, 40 (12): 117-123. (In Chinese)
- [12] Cao TY, Shen J, Liu WJ, Shao YL. Effect of Environment on the Release of VOCs from Wood-based Panel which Detected by DL-SW Micro-cabin [J]. *Journal of Northeast Forestry University*, 2018, 46 (02): 72-76. (In Chinese)
- [13] Liang W, Lv M, Yang X. The effect of humidity on formaldehyde emission parameters of a medium-density fiberboard: Experimental observations and correlations[J]. *Building and Environment*, 2016, 101:110-115.
- [14] Liu Y, Shen J, Zhu XD. Effect of hot-pressing parameters on the emission of volatile organic compounds from particleboard [J]. *Journal of Beijing Forestry University*, 2008 (05): 139-142. (In Chinese)
- [15] Shen J, Liu Y, Zhang XW, et al. Study on the volatile organic compounds emission from wood-based composites [J]. *China Forest Products Industry*, 2006, 33(1): 5—9. (In Chinese)
- [16] Shen J, Liu Y, Zhang WC, et al. Study on particleboard VOCs release [M]. Beijing: Science Press, 2013. (In Chinese)
- [17] Chen F. Study on the release characteristics and influence factors of volatile organic compounds emission from surface finishing particleboard [D]. Harbin: Northeast Forestry University, 2010. (In Chinese)
- [18] Zhang YF. Several environmentally-friendly finishing products for panel and their production technology [J]. *Forest Industry*, 2002 (04): 26-28. (In Chinese)
- [19] Deng FJ, Shen J, Li YB, Wang JX. Impacts of isocyanate concentration on TVOC emission from treated poplar wood [J]. *Forest Engineering*, 2016, 32 (04): 46-50. (In Chinese)
- [20] Li S, Shen J, Jiang SM. Characteristics of VOC Emission from Plywood in Different Environment Factors [J]. *Forestry Science*, 2013, 49 (01): 179-184.
- [21] Shen J, Jiang LQ. A review of research on VOCs release from wood-based panels [J]. *Journal of Forestry Engineering*, 2018, 3(06): 1-10.
- [22] Shao YL, Shen J, Deng FJ, Li YB, Shen XW. The influence of surface coating on TVOC emissions from the treated populus wood [J]. *Journal of Central South Forestry University*, 2018, 38 (02): 114-121.
- [23] Li CY, Shen XB, Shi Y. Study on VOC Emissions from Plywood Using a Climate Chamber [J]. *Wood Industry*, 2007 (04): 40-42.

UV-Light Protection Cellulose Nanocrystals Films Prepared through Trivalent Metal Ions

Cong Chen¹, Lu Wang¹, Jinwu Wang², Douglas Gardner¹

¹University of Maine, USA

²USDA Forest Service, Forest Products Laboratory, USA

Abstract

In order to preserve food from the effects of oxygen, moisture, and UV radiation, typical packaging is opaque or metallized. There is increasing consumer demand of transparent packaging, or a transparent viewing window to allow viewing of food stuffs during consumer purchase. Cellulose nanocrystals (CNCs), as a sustainable and biodegradable material, show huge potential for transparent food packaging, and can provide good oxygen permeation resistance, but is poor in preventing UV radiation transmission. The aim of this work is to produce high quality CNC films with UV-blocking characteristics under facile operation. CNC suspensions were modified with different concentrations of trivalent metal ions (Al^{3+} , Fe^{3+}) and homogeneous, transparent and flexible CNC films were prepared by the casting method. CNC films undergo cross-linking between metal ions and sulfate half-ester groups of CNCs and exhibit high UV absorption properties. Meanwhile, the water vapor permeability of the films was decreased slightly and the tensile strength was improved. In order to enhance the UV absorption, the addition of UV stabilizers into the CNC matrix may also be explored, and their interactions may be characterized.

Structure-related Vapor Sorption Phenomena in Wood

Raphaela Hellmayr^{1} – Rupert Wimmer²*

¹ Graduate Student, University of Natural Resources and Life Sciences, Vienna, Austria * *Corresponding author*
raphaela.hellmayr@boku.ac.at

² Professor, University of Natural Resources and Life Sciences, Vienna, Austria
rupert.wimmer@boku.ac.at

Abstract

Wood-water relations have been studied for more than a century. Doubts exist if equilibrium moisture content can be ever reached in full for wood in service, since ambient climate conditions are changing within a day. The objective of this research was to analyse vapor sorption, i.e. swelling phenomena of several wood species, by using Dynamic Vapour Sorption (DVS) in combination with a built-in video camera. DVS is a gravimetric method able to record sorption behaviour of materials by continuously monitoring the sample mass. Different softwoods and hardwoods were tested at 20 % steps of relative humidity. With the built-in video camera sample images were taken when the equilibrium moisture content was reached at each step, with the hygroexpansion coefficients determined at the acquired images. Results show that the adsorption phases were longer than the desorption phases across the species measured, with exception of beech. During adsorption the required time per step increased at higher relative humidity levels, whereas the duration in desorption was comparably stable. Different to spruce, larch responded slower to relative humidity changes. Radial swelling in earlywood of softwoods was roughly one-third of the one measured in latewood. It can be stated that a DVS apparatus with a built-in camera is suitable for determining swelling and shrinking of wood. As a next step, consecutive images will be evaluated by applying digital image correlation, delivering high spatial-resolution data for even better understanding.

Key words: Sorption, swelling, wood physics, wood anatomy, DVS, beech, oak, spruce, pine, larch

Introduction

Wood is a heterogeneous and anisotropic material with a specific multiscale anatomic structure. The orientation of the cells has a big influence on the mechanical and hygroexpansive properties. Dimensional changes occur when the moisture content drops below the fibre saturation point (FSP), with the content of bonded water in the wooden cell wall declining (Chirkova et al., 2007). According to Walker (2006) reasons for swelling differences in the radial vs. tangential direction are (1) the arrangement and density of earlywood and latewood within the annual ring, (2) microfibril angle differences of the radial vs. tangential cell walls and (3) directional influences of the radially arranged wood rays. Siau (1984) stated that swelling and shrinkage is directly proportional to density. Since the relative humidity in housings (Fischer et al., 2008) and outdoor is changing throughout the year, wood as a hygroscopic material is constantly adjusting to the ambient climate. Thybring et al. (2017) reported that the hydroxyl groups accessibility in wood is affected by drying and re-wetting procedures. A method to study swelling of wood at a cellular scale is phase-contrast X-ray tomography (Derome et al., 2011). A digital X-ray imaging system with a humid air conditioner was developed by Badel et al. (2006). With this configuration it was possible to investigate swelling phenomena at high spatial resolution, including anatomical patterns and density variations. El Hachem et al. (2017) studied the swelling of spruce during sorption cycles at the microscale. Here, the lumen as well as cell wall dimensional changes during swelling at different relative humidities were observed. Stuckenberg et al. (2018) determined the swelling velocity of different wood species relative to the anatomical cutting directions, using 50 μ m thick microtomed sections. The proportions of earlywood and latewood had a significant influence on the swelling velocity, with the latter being highest in tangential direction. Chau et al. (2015) have measured adsorption and hygroexpansion in southern pine. In this research radial and tangential swelling showed a linear relationship along with the moisture content. As reviewed by Engelund et al. (2013) wood-water relations have been studied for more than a century. It is seen doubtful that moisture equilibrium is ever fully reached in applications, since it takes a long time until wood is fully adjusted to an ambient climate. The technical development of Dynamic Vapor Sorption (DVS) apparatus enable the monitoring of adsorption and desorption processes (Wilkinson and Williams, 2016). Pfriem et al. (2007) recorded differences in sorption dynamics at high vs. low wood moisture contents. So far, no data on the sorption behaviour of wood prior to a reached moisture equilibrium.

In this research the following hypotheses are stated and tested: (a) Adsorption and desorption dynamics in wood alter with relative humidity levels, along with the prevalent moisture content. Chemisorption, physisorption and capillary condensation are mechanisms that result from different moisture uptake behavior. (b) A dynamic vapor sorption apparatus with a built-in video camera is in the position to determine high-spatial resolution swelling and shrinking movements in wood, allowing a combination of sorption dynamics with hygroexpansion. (c) Radial swelling in softwood species differs between earlywood and latewood, due to the existing density differences.

Materials & Methods

Nine wood species (Table 1) were analysed with samples having a size of 10 mm in radial

direction, 10 mm in tangential direction, and a thickness of 1 mm cut in longitudinal direction. Surfaces were sanded with a fine grit sandpaper (up to 600-grit).

Table 1: Tested wood species and samples

Scientific name	Common name	Number of samples
<i>Picea abies (L.) Karst</i>	Norway spruce	5
<i>Pinus sylvestris L.</i>	Scots pine	5
<i>Larix decidua Mill.</i>	European larch	4
<i>Fagus sylvatica L.</i>	European beech	11
<i>Quercus robur L. / petraea (Matt.) Liebl.</i>	European oak	4
<i>Fraxinus excelsior L.</i>	European ash	2
<i>Acer pseudoplatanus L.</i>	Sycamore maple	2
<i>Prunus avium L.</i>	Wild cherry	2
<i>Eucalyptus spp.</i>	Eucalyptus	3
Total		38

Dynamic Vapor Sorption (DVS, Advantage 1 by Surface measurement systems®) is a gravimetric measurement method, which is recording the sorption of the solvent in the sample by a continuous monitoring of the mass changes. The heart of the DVS is a micro-balance ($\pm 0.1 \mu\text{g}$) in a small chamber with controlled climate. The relative humidity range is between 0 % and 98 % and can be set by a mixture of two flows, one with water vapor and one with nitrogen at an accuracy of ± 1.5 %. All tests were performed at a nitrogen flow of 200 sccm. Equilibrium was defined as a relative change-rate in mass over time (dm/dt), which must be below 0.002 for 10 minutes. The built-in video camera (Dino-Lite ProX®) was mounted beneath the sample, to take sample images at each equilibrium moisture content state. The sample-surrounding climate gets changed by approaching a next climate step.

$$\alpha [\%] = \frac{d_{95} - d_0}{d_0} * 100 \quad (1)$$

The sequence was programmed with 20 % relative humidity steps starting from zero to 95 %, and back to 0 %, at a constant temperature of 25 °C. Sample mass was recorded every second and the minute averages saved. Data analysis and statistics were processed with the software SPSS (IBM, Version 24.0). ImageJ was used for image analysis and distances in radial and tangential direction were measured at 0 % and 95 % relative humidity. The resolution of the images was 1780 dpi. As shown in Equation (1), swelling was calculated by dividing the distance change by the initial distance.

Results and Discussion

Sorption dynamics

The overall sorption cycle duration is representing the speed of sorption reaching equilibrium at the ambient climate. This duration is ranging between 32 and 50 hours. The equilibrium moisture contents reached at each step, the produced isotherms as well as the hysteresis curves all showed similar levels across the species spruce, larch and pine, though spruce was adjusting

significantly faster to equilibrium moisture contents than larch (Figure 1). The saturated state at 95 % relative humidity corresponded with 16 to 18 % moisture content. For all species, adsorption required on average more time than desorption, with the exception of beech. Pfriem et al. (2007) showed that the speed of adsorption for Norway spruce was increasing with higher starting relative humidity, which is the opposite trend compared to the results obtained in this work. Compared to the other species, larch was slower in adsorption between 0 % and 60 % relative humidity, reaching a similar equilibrium moisture content. In desorption larch was slower and spruce faster than the average, a fact that was also found by Žlahtič and Humar (2017). Meyer-Veltrup et al. (2017) confirmed our finding, by reporting that the moisture uptake of European larch was significantly lower than for the other domestic wood species.

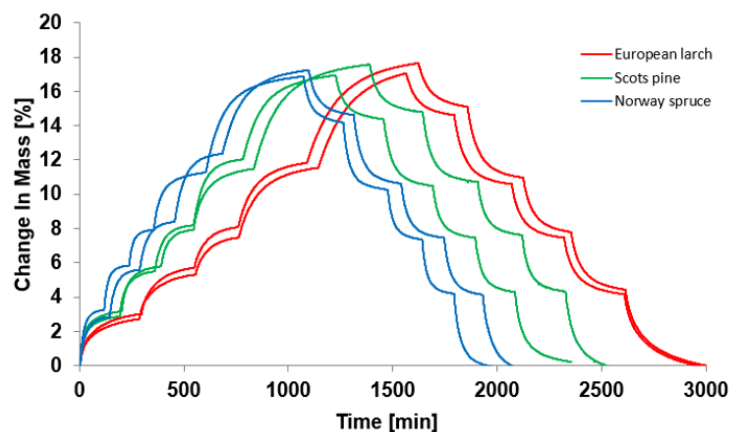


Figure 1: Change in mass over time, for spruce, larch and pine

As shown in Figure 2 (left) there is a significant difference between the time required for a complete adsorption and for a desorption cycle. The duration for desorption was longer for the lowest relative humidity step, and shorter at the highest humidity step. Moisture content changes per step followed the trend of relative humidity, (Figure 2, right) with changes per step varying between 1.5 % and 7 %. The visible outlier data in Figure 2 refer to eucalyptus, which showed high moisture uptake at low relative humidity. With eucalyptus, the first adsorption step created a 4 % change in moisture content, while in desorption it was slightly below 6 %. The continued sorption course did follow the general trend of all other species. The duration in desorption lasted longer than in adsorption, between 0 % and 60 % relative humidity, and shorter for the steps above that given range. Adsorption took longest for the step from 80 % to 95 % relative humidity, with an average of 7.5 hours. Steps between 0 % and 60 % relative humidity had no significant difference in their duration of adsorption, which equalled to an average of 2.5 hours. The same trend was observed for the change in moisture content per step, which laid between 2 % and 6 %. The achieved moisture content at half time of the step was slightly increasing and values between 80 % and 90 % were obtained. Here, Hill et al. (2010) reported similar sorption kinetics curves with Sitka spruce. The variation of the required desorption time between the steps was beyond the one for adsorption. Desorption between 20 % and 0 % relative humidity took longest with 5.5 hours on average, and the largest change in moisture with 4.5 %. The humidity step from 40 % to 20 % took the least time with only three hours. The lowest change

in moisture content was obtained for the 95 % and 80 % relative humidity step.

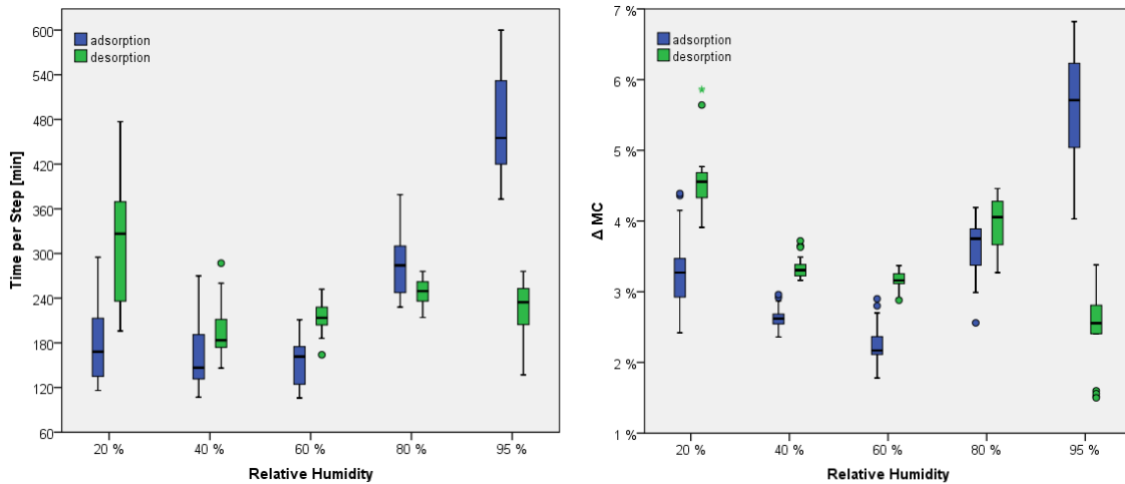


Figure 2: Sorption time per step (left) and change in moisture content (right) for adsorption and desorption

The reached moisture content at half time of the step was around 90% of the equilibrium, which showed the lowest values for the highest relative humidity step. Glass et al. (2018) described that the errors with a setting of dm/dt at 0.002, which must be held over ten minutes, are up to 1.2 % of the equilibrium moisture content and can be minimized by a stricter criterion. Since the objective of this study was to analyse the difference between relative humidity and species, including the path to get there, the accuracy of equilibrium was less critical. All samples reached more than 80 % of the equilibrium moisture content at half time of the step.

Swelling properties

The analysis of earlywood and latewood of softwoods individually in radial direction showed that there are significant difference in swelling (Figure 3). Swelling in earlywood was approximately one third of the one for latewood, which was also more or less equivalent to the total tangential swelling. Patera et al. (2018) showed that latewood is isotropic, while earlywood is orthotropic, a result that was also confirmed here. Combined swelling of earlywood and latewood showed no significant difference to total swelling in radial direction. The variance of swelling in latewood could be caused by the small distances and the limited measuring accuracy. For example, if the distance is 8 mm, one pixel is equivalent to 0.2 %, whereas if the distance is only 0.5 mm, one pixel equals to 1.5 %. It was not possible to identify the hygroexpansion of pores or single wood rays and the swelling in latewood showed a notable deviation. Latewood has a density gradient and the highest value is probably linked to the highest density. Panshin and Zeeuw (1980) stated that decreased shrinkage in radial direction is caused by wood rays and the change in density between earlywood and latewood. In tangential direction the latewood controls shrinkage and forces earlywood to shrink in the same amount. Earlywood and latewood were visually identified by the lighter and darker colour.

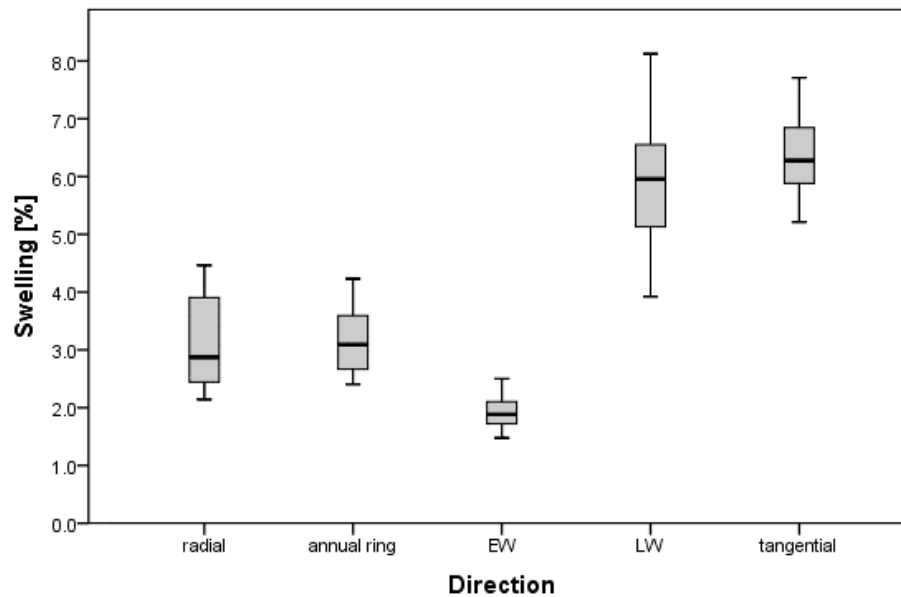


Figure 3: Radial (annual ring, earlywood (EW), latewood (LW)) and tangential swelling of softwoods

Total tangential swelling was approximately twice the swelling in radial direction for all domestic wood species. This well-known fact has been observed in various studies (e.g. Niemz and Sonderegger, 2017), and simply approved the validity of the DVS measurement method, in combination with an in-situ video camera to determine wood sorption. Chau et al. (2015) showed the moisture adsorption and hygroexpansion of southern pine and found that the swelling ratio between tangential and radial direction is increasing with moisture content. The same authors also stated that a linear correlation exists between swelling and the moisture content in wood. Tangential swelling of eucalyptus was approximately half of the one found for the domestic hardwood species. In radial direction the eucalyptus swelling was slightly lower than the one for the other species, which results in a radial to tangential ratio of 10:15. Spruce, pine and larch had a similar swelling behaviour in tangential direction, with the radial swelling being slightly higher for Scots pine than the other species. A reason for this deviation might be founded in earlywood and latewood differences, as determined by the density of the samples. Siau (1984) showed that density is directly proportional to swelling. European larch showed a high latewood proportion of approximately 40 %. The latewood proportion in Norway spruce and Scots pine was significantly less. It would be interesting to see if species differences are neglectable if the density difference is considered.

Summary and Conclusions

Sorption analyses confirmed that adsorption and desorption dynamics in wood are dependent on the prevalent relative humidities, and the moisture content levels. For the tested wood species with exception of beech the adsorption phase took longer than desorption. In adsorption the required time per relative humidity step increased as the moisture content was higher, whereas the duration in desorption was more constant. Larch reacted slower to a changed relative humidity than spruce. Dynamic vapor sorption (DVS) with a built-in video camera was

suitable for the determination of swelling and shrinkage in wood. For the combination of sorption with hygroexpansion, the spatial resolution of 1.3 megapixel of the used camera was insufficient. The difference of radial swelling in earlywood and latewood of domestic softwood species was quantified as well. DVS with a built-in camera having high-resolution has utility to analyse swelling properties of wood below the equilibrium moisture content. This would help to understand sorption in wood during real-life humidity cycles, checking also if there is a difference in swelling during adsorption and shrinkage during desorption. Further, digital image correlation could be applied to analyse the sorption images as well. Future studies are planned to better understand the swelling properties of heartwood, of coloured heartwood and of sapwood, especially of beechwood.

References

- Badel, E., Bakour, R. and Perré, P. (2006): Investigation of the relationships between anatomical pattern, density and local swelling of oak wood, *IAWA Journal*, 27(1), pp. 55–71.
- Chau, T., Ma, E. and Cao, J. (2015): Moisture Adsorption and Hygroexpansion of Paraffin Wax Emulsion-treated Southern Pine (*Pinus spp.*), *BioResources*, 10(2), pp. 2719–2731.
- Chirkova, J., Andersons, B. and Andersone, I. (2007): Study of the structure of wood-related biopolymers by sorption methods, *BioResources*, 4(3), pp. 1044–1057. doi: 10.15376/biores.4.3.1044-1057.
- Derome, D. et al. (2011): Hysteretic swelling of wood at cellular scale probed by phase-contrast X-ray tomography, *Journal of Structural Biology*. Elsevier Inc., 173, pp. 180–190. doi: 10.1016/j.jsb.2010.08.011.
- El Hachem, C., Abahri, K. and Bennacer, R. (2017): Microscopic swelling analysis of spruce wood in sorption cycle, *Energy Procedia*. Elsevier B.V., 139, pp. 322–327. doi: 10.1016/j.egypro.2017.11.215.
- Engelund, E. T. et al. (2013): A critical discussion of the physics of wood-water interactions, *Wood Science and Technology*, 47, pp. 141–161. doi: 10.1007/s00226-012-0514-7.
- Fischer, H.-M. et al. (2008): *Lehrbuch der Bauphysik*, Wiesbaden:Vieweg+Teubner Verlag.
- Glass, S. V. et al. (2018): Quantifying and reducing errors in equilibrium moisture content measurements with dynamic vapor sorption (DVS) experiments, *Wood Science and Technology*. Springer Berlin Heidelberg, 52, pp. 909–927. doi: 10.1007/s00226-018-1007-0.
- Hill, C. A. S., Norton, A. J. and Newman, G. (2010): The water vapour sorption properties of Sitka spruce determined using a dynamic vapour sorption apparatus, *Wood Science and Technology*, 44(3), pp. 497–514. doi: 10.1007/s00226-010-0305-y.
- Meyer-Veltrup, L. et al. (2017): The combined effect of wetting ability and durability on outdoor performance of wood: development and verification of a new prediction approach, *Wood Science and Technology*, 51, pp. 615–637. doi: 10.1007/s00226-017-0893-x.
- Niemz, P. and Sonderegger, W. (2017): *Holzphysik: Physik des Holzes und der Holzwerkstoffe*. München: Fachbuchverlag Leipzig im Carl Hanser Verlag.
- Panshin, A. J. and Zeeuw, C. (1980): *Textbook of wood technology: structure, identification, properties, and uses of the commercial woods of the United States and Canada*. 4th edition, New York: McGraw-Hill.

*Proceedings of the 62nd International Convention of
Society of Wood Science and Technology
October 20-25, 2019 – Tenaya Lodge, Yosemite, California USA*

- Patera, A. et al. (2018): Swelling interactions of earlywood and latewood across a growth ring: global and local deformations, *Wood Science and Technology*. Springer Berlin Heidelberg, 52(1), pp. 91–114. doi: 10.1007/s00226-017-0960-3.
- Pfriem, A., Grothe, T. and Wagenführ, A. (2007): Einfluss der thermischen Modifikation auf das instationäre Sorptionsverhalten von Fichte (*Picea abies* (L.) Karst.), *Holz als Roh- und Werkstoff*, 65, pp. 321–323. doi: 10.1007/s00107-006-0167-z.
- Siau, J. F. (1984) *Transport processes in wood*. Berlin: Springer.
- Stuckenberg, P., Wenderdel, C. and Zauer, M. (2018): Determination of the swelling velocity of different wood species and tissues depending on the cutting direction on microtome section level, *Results in Physics*. Elsevier, 9, pp. 1388–1390. doi: 10.1016/j.rinp.2018.04.059.
- Thybring, E. E., Thygesen, L. G. and Burgert, I. (2017): Hydroxyl accessibility in wood cell walls as affected by drying and re-wetting procedures, *Cellulose*. Springer Netherlands, 24, pp. 2375–2384. doi: 10.1007/s10570-017-1278-x.
- Walker, J. C. (2006): *Primary wood processing: principles and practice*, 2nd edition, Dordrecht: Springer.
- Wilkinson, J. and Williams, D. (2016): The Latest Developments in Dynamic Vapor Sorption (DVS), <https://www.azom.com/article.aspx?ArticleID=13001>, 15.03.2019.
- Žlahtič, M. and Humar, M. (2017) 'Influence of Artificial and Natural Weathering on the Hydrophobicity and Surface Properties of Wood', *BioResources*, 12(1), pp. 117–142. doi: 10.15376/biores.11.2.4964-4989.

**The Effect of Pore Size on Specific Capacitance for Activated Carbon
Supercapacitors**

Jiyao Hu, Changlei Xia, Sheldon Shi
University of North Texas, USA

Abstract

Activated carbon poses a promising supercapacitor material with its highly porous surface and low cost. Numerous publications have been made on activated carbon made supercapacitors with the conclusion that the higher the Brunauer-Emmett-Teller surface area value is, the higher the specific capacitance is. It is assumed that the high surface areas inside the porous activated carbons facilitate ion transport in the electrochemical process, and macropores (>50nm) inside the activated carbon materials can act as ion-buffering reservoirs for electrolytes. Recent studies further look into the mesopore (2-50 nm) and micropore (<2 nm) distributions inside the AC with the conclusion that the combination of highest specific surface area and porosity can result in optimum specific capacitance. However, in these studies, there are many variations in precursor material used, activation method, and have different resulting total surface area values which all could act as confounding factors in establishing concrete relationships. Self-activation is a process in which the gases released during the self-activation serve as activating agents, which eliminates possible contaminants from chemical activation processes. Previous work has used the self-activating process to produce activated carbon materials using kenaf core fibers, which is environmentally friendly and has low-cost. By varying the duration of activation, the final activated carbon materials produced have very similar surface area values of 2266 m²g⁻¹ and 2296 m²g⁻¹, while varying greatly in their mesopore volumes (0.682 cm³g⁻¹ and 1.337 cm³g⁻¹ respectively). In the current study, we seek to establish relationship with mesopore volumes and specific capacities while trying to keep all other experimental conditions as similar as possible. It is expected that the greater numbers of mesopores inside the material will increase the specific capacity of the material, and the results from this study will benefit the optimization and engineering process of future activated carbon supercapacitors.

**Sustainable Development – International Framework – Overview and Analysis
in the Context of Forests and Forest Products with Quality**

ANNIKA HYYTIÄ

University of Helsinki, Finland

Abstract

Business is more and more concerned with the sustainable development. There are opportunities in quality with sustainable development in the markets and sustainable competitive business in the markets. Business concepts and competitiveness has a link to sustainable resources and the policy framework.

Sustainable development in value added products with quality and marketing provide opportunities for competitiveness in the forest sector. There are new promising opportunities for the forest sector in the sustainable development and green policies. In the policies like Bioeconomy, sustainable development has an important significance. Policy with quality management aspects including certification and standards have a remarkable role in the value chain from forests. The value chain and innovations in the sustainable development of the forest sector provides opportunities for competitiveness and business. Markets are linked to the sustainable development framework. In Finland and in the European Union, the framework of value added products, markets and competitiveness in the sustainable development framework is highlighted. The Corporate Social Responsibility, the CSR, provides a significant framework with the sustainable development.

This is a qualitative research based on research articles and literature including academic sources, for example Proquest, Academic Search Complete (EBSCO), Agris, CAB Abstracts, SCOPUS (Elsevier), Web of Science (ISI) and Google Scholar and Internet sites.

Evaluation of Bond Integrity in Low-Value Blue-Stain Ponderosa Pine CLT

Sina Jahedi ^{1} – Lech Muszynski ² – Mariapaola Riggio ³ – Rakesh Gupta ⁴*

¹ Ph.D. Student, Wood Science and Engineering, Oregon State University, Corvallis, OR, USA *Corresponding author, sina.jahedi@oregonstate.edu

² Professor, Wood Science and Engineering, Oregon State University, Corvallis, OR, USA, lech.muszynski@oregonstate.edu

³ Assistant Professor, Wood Science and Engineering, Oregon State University, Corvallis, OR, USA, mariapaola.riggio@oregonstate.edu

⁴ Professor, Wood Science and Engineering, Oregon State University, Corvallis, OR, USA, rakesh.gupta@oregonstate.edu

Abstract

National forest restoration programs aim to reduce wildfire risks by selectively removing small-diameter trees from the forest. Each year a large number of Ponderosa pine logs are generated in these operations in Southern Oregon and Northern California. These logs have a very limited market value locally. A substantial portion of them contain blue-stain, which reduce the value even further. It is important to find a value-added market for the logs to offset the high costs of these operations. Based on the previous research, cross-laminated timber can be a promising solution to address this issue. CLT is a composite structural panel consisting of three or more odd number of orthogonally arranged layers of boards. ANSI/APA PRG 320 'Standard for Performance-Rated CLT' specifies the criteria and quality assurance requirements for fabrication of custom CLT layups of non-standard lumber. A literature review on CLT made of low-value lumber showed that the stringent bond integrity criteria are most critical of these standard requirements. Results of delamination test on blue-stain ponderosa pine CLT completed as a preliminary step to assess the potential of using it in CLT panels as a structural material are presented in this paper. The specimens were manufactured in a research laboratory under controlled environment conditions. Laboratory scale fabrication is essential for prototyping innovative CLT layups. Fabrication parameters including ambient temperature, lamination moisture content, adhesive spread rate, close assembly and press time were monitored during the tests. Of the investigated variables, the effect of the close assembly time showed to be the most important for fabrication of CLT panels in laboratory conditions. Using adequate equipment and procedures can reduce the close assembly time to a suitable duration.

Key words: cross-laminated timber; CLT; low-value lumber; Ponderosa pine; blue-stain; cyclic delamination.

Introduction

Currently, the building industry is a major consumer of nonrenewable materials, many obtained in unsustainable ways. The construction industry is responsible for a significant part of greenhouse emission and anthropocentric environmental impact (Akan et al., 2017). Wood, as a renewable material with high specific strength, is a promising material to address this issue (Green, 2013). Mass timber constructions contribute to reduce the carbon dioxide footprint of the building industry by storing carbon in buildings instead of releasing it to the environment. Cross-laminated timber (CLT) was invented in Austria and Germany in the early 1990s, (Karacabeyli et al., 2013). CLT is a structural composite panel consisted of three or more odd number of orthogonally arranged layers of boards. The layer-wise arrangement of CLT layups reduces the impact of inhomogeneity of individual boards and results in more uniform panels. In principle, layer-wise characteristic of CLT makes it possible to reach a predictable and uniform mechanical properties even when low-grade lumber is used in laminations. Since the introduction of CLT to North America in early 2000's the interest to use this product as a construction material has steadily grown, but it is not a common practice yet (Pei et al., 2016).

National forest restoration programs aim to reduce wildfire risks by thinning operations, or selectively removing small diameter trees to preserve larger and superior trees. Many of the harvested trees are either dead or diseased which can be fuel for wildfire and pest outbreaks. Currently, the market for this low-value lumber in the U.S. Northwest is very limited. It is important to find a value-added market for this material to offset the high costs of thinning operations.

Low-value lumber CLT:

ANSI/APA PRG 320, 'Standard for Performance-Rated CLT' developed in the United States since 2011 provides the specifications and requirements for the CLT components, and performance criteria, qualification, and quality assurance for the finished CLT panels. The standard allows production of custom CLT layups using alternative grades and species according to American Lumber Standards Committee (ALSC), and also arbitrary number and thickness of layers in major and minor directions, provided these custom CLT products satisfy prescribed performance qualifications. These requirements fall in two major categories: mechanical characteristics of components and panels and adhesive bond integrity (resistance to shear and delamination).

The interest in utilizing low-value lumber for making CLT panels has increased in the past few years. Previous studies have showed that utilizing low-value lumber in fabricating CLT can result in a favorable structural performance comparing to pre-defined PRG 320 CLT grades. The research on yellow-poplar CLT emphasized that CLT fabricated with low-grade lumber can provide satisfactory mechanical properties (Mohamadzadeh and Hindman, 2015). Furthermore, current research (Larkin 2017, Lawrence 2018) determined the potential of using small diameter ponderosa pine logs for hybrid CLT fabrication. The hybrid CLT consisted of low-value ponderosa

pine lumber in core layer and Douglas-fir lumber in major direction. While the studies showed that the low-value lumber CLT has sufficient strength and elastic properties compared to pre-defined CLT grades, they failed to satisfy the delamination criteria dictated by PRG 320. The study on effectiveness of adhesive systems for low-value lumber CLT panels confirmed that passing delamination test is challenging, but achievable under controlled conditions (Larkin, 2017, Lawrence 2018), although the presence of blue stain alone was shown not to interfere with the quality of the bonds formed with polyurethane adhesives (Li et al. 2018).

Materials & Methods

Given the importance of bond integrity tests, this study is focused on cyclic delamination test, which is more difficult to pass than the resistance to shear criterion. Delamination test has been selected to be the initial step towards assessing the potential of fabricating blue-stained ponderosa pine structural CLT. The aim was to evaluate the effect of various operational and environmental parameters on the delamination of blue-stain ponderosa pine CLT specimens bonded with melamine formaldehyde (MF). These parameters included ambient temperature, lamination moisture content, adhesive spread rate, close assembly and press time. The only cost efficient way to perform such prototyping work is on lab-scale fabricated CLT specimens, as opposed to specimens extracted from full-scale panels produced in commercial production lines, even as faithful reflection of full-scale fabrication at the lab-scale is not always possible.

The CLT panels used in this study were fabricated under monitored conditions in laboratory environment using two component MF adhesive system. All of the panels are made of No. 3 visually graded ponderosa pine lumber in accordance with Western Wood Products Association. Traces of blue-stain could be visually identified in some of the panels. The lumber was stored indoor before the fabrication to make sure they are stable regarding moisture content. The moisture content of the lumber during fabrication was 11 to 13% depending on the season and weather condition. The laminations were planned within 48 hours prior to the assembly. Both bonding-surfaces are planned at least 1/16 in from each side. Delamination specimens are obtained from two sizes of CLT layups, both shown in Figure 1.

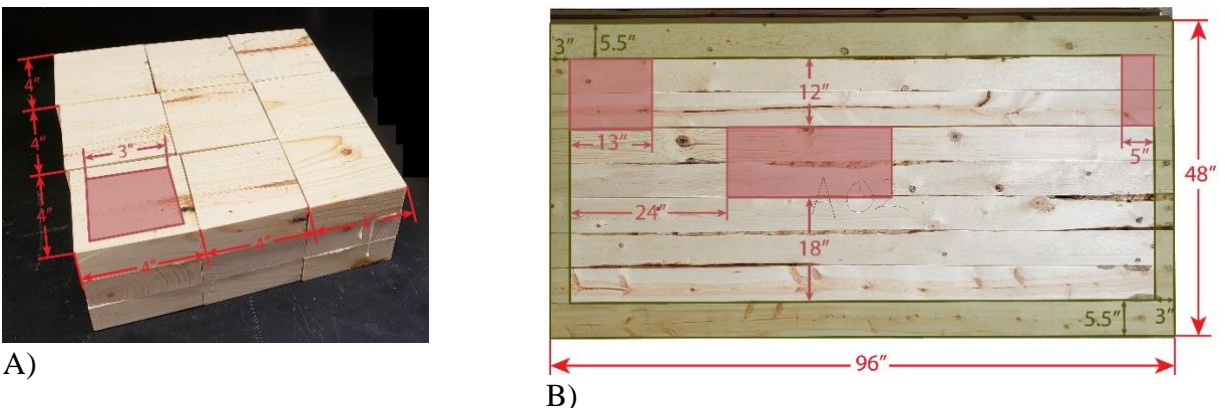


Figure 1. (A) A set of nine CLT blocks produced for delamination test. (B) A CLT panel. Red areas indicate the locations which delamination specimens are obtained from.

**Proceedings of the 62nd International Convention of
Society of Wood Science and Technology
October 20-25, 2019 – Tenaya Lodge, Yosemite, California USA**

CLT Blocks, are 4 inches by 4 inches cross-laminated lamination sections arranged in three-layer blocks as shown in Figure 1 A. This size selected to eliminate the effect of layer bridging and lamella thickness tolerances and used to determine the effect of the adhesive compatibility and fundamental fabrication conditions. To minimize the amount of glue skips, the blocks are obtained from parts of the boards with minimum defects. In ANSI/APA PRG 320 glue skips are defined as knots, checks, waness, and rough surfaces. Table 1 summarizes the fabrication parameters for CLT blocks.

The specimens were fabricated in sets of 9. The first two preliminary sets, Pre-1 and Pre-2, were fabricated strictly following the adhesive manufacturer suggestions to gain benchmark experience. Immediate failures were observed in both Pre-1 and Pre-2 due to long assembly time and low adhesive spread rates, resulting in the adhesive dryout prior to setting the layup into the press. Close assembly time is in a direct relationship with spread rate ratio. Hence, in the regular test block fabrications the spread rates were the principle variable. At the fabrication stage, the increased spread rate in sets B1, B3 and double spread rate in set B4 helped in reducing the impact of assembly time. The increased spread rates also helped in offsetting the spillage of adhesive from bonding-surfaces, which is substantial in small specimens.

Table 1. Fabrication parameters for CLT blocks. Press pressure is equal to 0.7 MPa (100 psi) on the panel for all sets. Each set is consisted of nine specimens.

Set#	Blue stain presence	MC	Temp, RH	SRR* (g/m ²)	CAT**	Press time	Oven time***
Pre-1	No	12.8 %	20.7 ⁰ C, 32 %	300	18 min	15 hr	-
Pre-2	No	12.5 %	21.2 ⁰ C, 35 %	300	14 min	17 hr	-
B1	Yes	12.0 %	22.1 ⁰ C, 22 %	300<SSR<500	15 min	23 hr	13 hr
B2	Yes	13.0 %	22.1 ⁰ C, 22 %	250<SSR <310	12 min	22 hr	13 hr
B3	No	11.6 %	21.1 ⁰ C, 30 %	300<SSR <500	14 min	15 hr	14 hr
B4	No	11.6 %	20.8 ⁰ C, 43 %	500<SSR<1000	14 min	18 hr	14 hr

*Spread rate ratio **Close assembly time ***Refers to dry-oven time in delamination test

In set B1, press time was extended beyond the duration suggested by the adhesive manufacturer in order to simulate the industrial practice, where after pressing the CLT panels are stored under a dead-load to let the adhesive complete the curing process.

CLT Panels were three 4 ft by 8 ft CLT three-layer layups fabricated in the laboratory environment. Figure 1 B shows such panel as well as the locations, from which delamination specimen obtained. As suggested by ASTM PRG, the delamination specimens were extracted from both center and corners of the CLT panel. No pre-selection is made for the boards used for

fabrication of the CLT panels. The boards were selected randomly and they highly contained knots and waness. Table 2 indicates the fabrication parameters for the CLT panels. The spread rate was increased for the fabrication of the CLT panels to extend the allowable close assembly time, which took significantly longer time than in case of the CLT blocks.

Table 2. Fabrication parameters of CLT panels. Press pressure for all sets is equal to 0.7 MPa (100 psi) on the panel.

Set#	Blue stain presence	MC	Temp, RH	SRR* (g/m ²)	CAT**	Press time	Oven time** *
P1	No	11.6 %	19.8 ⁰ C, 43%	488	43 min	18.0 hr	13.5 hr
P2	Yes	12.0 %	23.8 ⁰ C, 31%	>600	55 min	21.5 hr	13.5 hr
P3	Yes	11.6 %	20.3 ⁰ C, 50%	488	54 min	18.0 hr	13.5 hr

*Spread rate ratio **Close assembly time ***Refers to dry-oven time in delamination test.

During the fabrication it became obvious that the adhesive mixture was not adequate for the long assembly times required in producing 4 ft x 8 ft in laboratory. That was particularly apparent in fabricating P3 CLT panel which showed that the maximum allowable close assembly time is 20 minutes at the ambient conditions specified in table 2. In this research the resin and the hardener were mixed together before the application on layup. To achieve longer close assembly time, in future studies, the resin and hardener will be applied on different faces of the bonding-surface to be mixed only when the layup is pressed.

Testing procedure:

ANSI/APA PRG 320-2018 refers to AITC T110 for cyclic delamination test. Delamination percentage is defined as the sum of delaminated lengths in a specimen over the total perimeter of the bonding-surfaces. This will include sum of multiple bonding-surface perimeters if the specimen consists of a numerous bonding-surfaces. Based on the standard, the maximum allowable delamination percentage is 5%. The delamination specimens should be 3 in by 3 in in-plane and, for the purpose of certification and quality assurance, they should be obtained from a panel larger than 24 inches by 24 inches. The AITC T110 delamination procedure is summarized in figure 2.

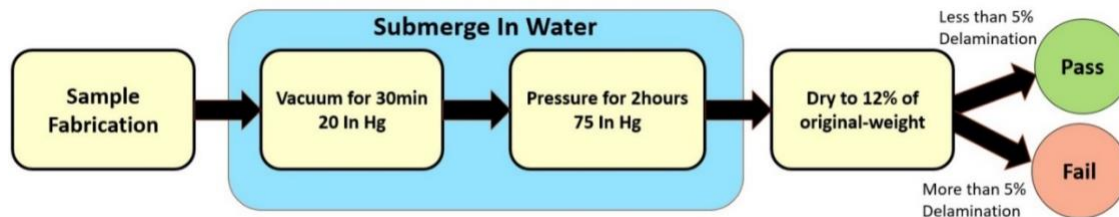


Figure 2. Delamination procedure based on AITC T110.

After taking the specimens out of the drying oven, each bonding-surface was carefully investigated. A crack is reported as delamination if the depth of the crack is more than approximately 1/16 in and no major wood fibers pulled out of either side of the crack. Only the cracks exactly located on the bonding-surfaces are considered as delamination. Chisel test found to be effective to investigate the probable reason in case of delamination (Lukowsky 2015).

Results and Discussion

The delamination in the bond lines resulting from different shrinkage rates in wood in orthogonal directions and internal stresses developed during wet-dry cycle, was assessed by visually inspecting the CLT specimens after wet-dry cycle. One visible sign of good bond is a flowing transition between the layers of the sample, as shown in figure 3. Mostly the delamination occurred at the corners of the specimens. Checks and cracks within the lamellas were observed in specimens with good quality of bonding.

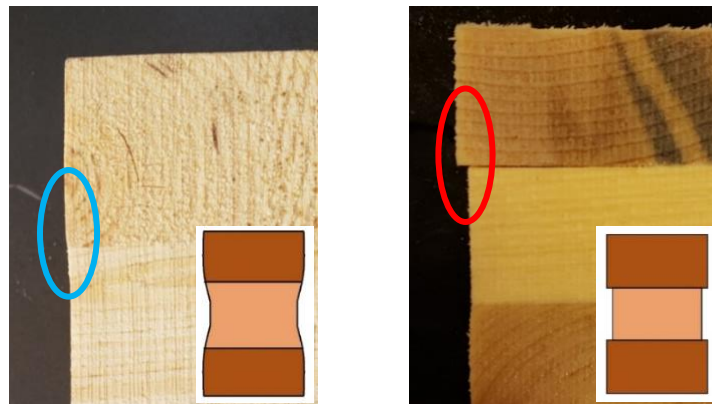


Figure 3, (Left) smooth transient between layers after wet-dry cycle. (Right) step-like transient which resulted in delamination.

It is important to note that the delaminations in some specimens coincided with the presence of defects on the bonding-surfaces, e.g. knots, checks, and rough surfaces. Also, it was common to observe a delamination formed by propagation of existing checks. No influence of blue-stain on the delamination of cross laminated ponderosa pine specimens was observed.

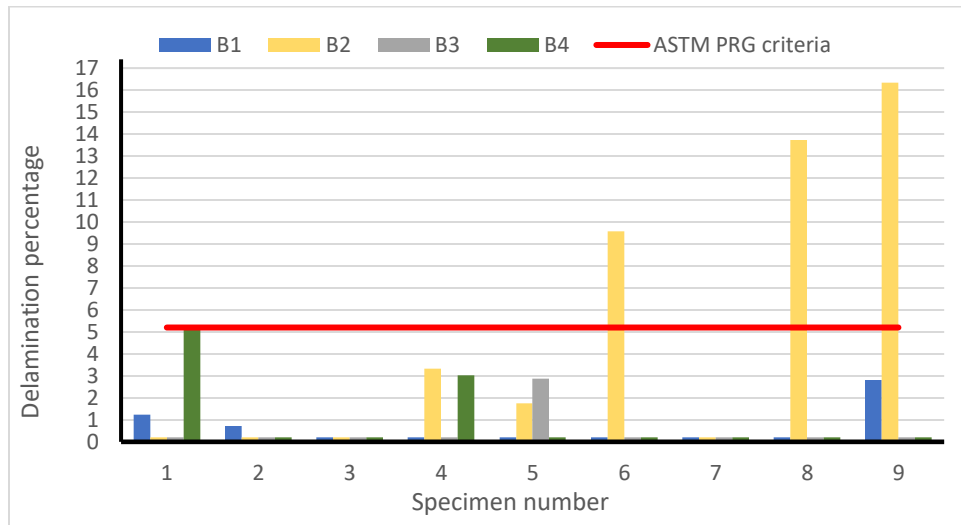


Figure 4, delamination percentage of the CLT block specimens.

Figure 4 shows the results of delamination tests on the CLT blocks. All the specimens in test sets B1, B3 and B4, and 6 out of 9 blocks in set B2, successfully met the PRG 320 criteria. Considering unavoidable spillage of adhesive, B2 set was essentially fabricated with reduced adhesive spread rate. Chisel test revealed that in blocks with the reduced spread rate delamination is caused by uneven adhesive application and areas with “starved bond line.” On the other hand, excessive adhesive spread rates in set B4 did not improve the bond integrity, since press squeezed the excess of liquid resin out of the bonding-surface. Furthermore, comparing the effect of press time of B3 and B4 with B1, it can be observed that additional press time is not necessary to reduce delamination.

The acceptable delamination tests results on blocks from sets B1, B3 and B4 prove that Ponderosa pine with blue stain presence is compatible with the MF adhesive system.

Summary and Conclusions

CLT is a promising alternative for conventional nonrenewable structural systems. As a part of ASTM/APA PRG 320 qualifications, a custom layout CLT should pass bond integrity tests to be permitted as a structural material. The results from this study indicates that MF adhesive system have a good compatibility with blue-stain ponderosa pine CLT regarding AITC T110 cyclic delamination test. Close assembly time has a significant impact on the results of the delamination test. It is important to finish the assembly within the allowable close assembly time. Assembly can take significantly longer time in producing larger CLT panels, but the time can be reduced by using adequate automations and procedures. The results showed that it is important to account for the adhesive waste caused by operator errors and spillage, especially for fabrication of smaller scale CLT specimens. Moreover, knots, waness, and rough surfaces can negatively affect the bonding, but no direct relation between blue-stain and bonding properties have found.

Acknowledgements

*Proceedings of the 62nd International Convention of
Society of Wood Science and Technology
October 20-25, 2019 – Tenaya Lodge, Yosemite, California USA*

This research is supported by USDA Forest Service (17-DG-11062765-742). The authors thank their colleagues from the department of wood science and engineering at Oregon State University who assisted greatly through this research. We would also like to gratitude CollinsWoods and AkzoNobel companies for their donations.

References

- Akan, M. Ö. A., Dhavale, D. G., and Sarkis, J. (2017). Greenhouse gas emissions in the construction industry: An analysis and evaluation of a concrete supply chain. *Journal of Cleaner Production*, 167, 1195–1207.
- ANSI/APA PRG 320 (2018). Standard for Performance-Rated Cross-Laminated Timber.
- Green, M. (2013). Why we should build wooden skyscrapers | TED Talk.
<https://www.ted.com/talks/michael_green_why_we_should_build_wooden_skyscrapers?language=en> (Jan. 2, 2019).
- Karacabeyli, E., Douglas, B., and Editors. (2013). CLT handbook: Cross-laminated timber. FPIInnovations, Pointe-Claire, Québec.
- Lawrence, C. (2018). Utilization of Low-value Lumber from Small-diameter Timber Harvested in Pacific Northwest Forest Restoration Programs in Hybrid Cross Laminated Timber (CLT) Core Layers: Technical Feasibility. Oregon State University.
- Larkin, B. (2017). Effective Bonding Parameters for Hybrid Cross-Laminated Timber (CLT). Oregon State University.
- Li X., B. Larkin, L. Muszyński, J. Morrell (2018): Effect of blue stain on bond shear resistance of polyurethane resins used for cross-laminated timber production. *Forest Products Journal*. 68(1): 67-69.
- Mohamadzadeh, M., and Hindman, D. (2015). Mechanical performance of yellow-poplar cross laminated timber. Report No. CE/VPI-ST-15-13. Virginia Polytechnic Institute and State University.
- Pei, S., Rammer, D., Popovski, M., Williamson, T., Line, P., and Lindt, J. W. van de. (2016). An Overview of CLT Research and Implementation in North America. World Conference on Timber Engineering. Vienna, Austria.
- Lukowsky, D., (2015) Failure Analysis of wood and wood-based products. P 148-154

**A Science Comic Poster: The Gender Diversity Tale in the US, Canada, Finland,
and Sweden Forest Sector**

PIPIET LARASATIE
ERIC HANSEN
OREGON STATE UNIVERSITY, USA

ABSTRACT

Comics provide a potential medium for science education and communication. In this science comic poster, the first author delivers her plan on doing her PhD in Wood Science with a dissertation about gender diversity in the forest sector in four countries: the U.S., Canada, Finland, and Sweden.

Given an aging workforce, job and career prospects for young people are extremely positive in the forest sector. Employee turnover through retirement also presents a significant opportunity for the industry to increase the diversity of its workforce.

Gender diversity is no longer just the right thing to do but also the smart thing to do. However, although there are simultaneous efforts to increase gender diversity in the forest sector, the industry is continually perceived as a male dominated and male oriented industry with a masculine culture.

This study utilizes interviews of female executives in global forest sector companies, female college student leaders, and professional women's network leaders to better understand how these female leaders perceive the impact of the situation of gender diversity in the forest sector as well as making the forest sector more attractive for young females. The results of this study will provide meaningful insights into gender aspects in the forest sector and raise awareness into the importance of diverse and inclusive workplace.

Rayleigh Mode Excitation at the Half-space Boundary in Wood using Embedded Elastic Waveguides

Yishi Lee¹ – Mohammad Mahoor² – Wayne Hall³

¹ Graduate Researcher, University of Denver, Denver, Colorado, USA
yishi.lee@du.edu

² Professor, University of Denver, Denver, Colorado, USA
Mohammad.Mahoor@du.edu

³ President, Utility Asset Management Inc., Denver, Colorado, USA
wayne.hall@utilityassetmanager.com

ABSTRACT

Due to the aging wooden utility pole infrastructure in the United States, it demands a more rigorous assessment program using an ultrasonic-based non-destructive evaluation (NDE) method. This paper focuses using novel small embedded elastic waveguides to excite and receive the so-call Rayleigh surface waves at the half-space boundary in wood in the plane geometry. The results of the proposed technique can be transferred to other NDE applications to enhance the current ultrasonic inspection capability. Using numerical and empirical approaches, the results provide strong evidence of Rayleigh surface wave propagation in wood. Through a brief discussion, the waveform of the resulted surface wave will be analyzed. This study employs (Riegert, 2006) the latest NDE device UB1000 that is jointly developed by the University of Denver and Utility Asset Management Inc. This work hopes to burgeon the future work for improving the current non-destructive evaluation technique for wooden pole structural assessments.

Key words: Elastodynamics, Ultrasonic waveguide, Rayleigh wave mode, non-destructive evaluation.

INTRODUCTION

The United States deploys approximately 100 million poles that support the power and communication infrastructures (Morrell, 2013). That demands effective and rapid inspection techniques for evaluating and monitoring their structural integrity. Non-destructive evaluation (NDE) using ultrasonic wave has been a mature technology in a wide range of industrial and academic sectors for assessing structural conditions (Riegert, 2006). The same ultrasonic excitation technique, using contact-based transducers for example, cannot be used for inspecting the wooden poles mainly due to the unpredictable surface conditions as illustrated in Figure 1. Hence, the application of contact-based transducers could lead to erroneous waveform measurements. An alternative approach is to perform a small insertion of roughly 2 mm by 2 mm by 16 mm with a waveguide to excite different wave modes in the interior of the specimen. This technique provides two immediate advantages: independence from the surface condition, and to provide structural support for mounting any NDE devices without a manual application. Despite a wide adaptation of this technique, the wave mechanics of this method has not been fully studied.

For a wooden utility pole, most of the mechanical load is concentrated at the outer shell of the cross-sectional area at the ground line region (Lovelace, 2005), approximately few inches above the ground. The mechanical property in this region plays a vital role in sustaining structural integrity. The study of Rayleigh wave propagating in this region can help infer important mechanical properties (Viktorov I. A., 1967). The methods of Rayleigh wave excitation were dated back to the 1940s by C. Minton (Minton, 1954). Since then, various techniques introduced by (Lynnworth, 1964), (Sokolinskii, 1958) and (Viktorov I. A., 1962) were developed and employed in the field of NDE (Thompson, 2012) and (Kim, 2014). The Rayleigh wave



Figure 4

propagation in a wooden utility pole has yet to be known.

Based on the academic and practical interests, this study focuses on the Rayleigh mode excitation in two-dimensional space at the flat half-space boundary using the embedded waveguide method. In order to demonstrate the excitation mechanism, a numerical approach

using the finite-element method (FEA) will be employed and the results will be analyzed. Using a jointly developed UB1000 NDT device for wooden utility pole inspections, digitized waveforms will also be presented. The numerical and empirical finding will be compared to evaluate the Rayleigh mode excitation and reception using the embedded waveguide technique.

MATERIALS & METHODS

Problem statement

Figure 2 illustrates an embedded waveguide problem. A cylindrical waveguide is inserted into a wooden medium. The origin of the inertial reference frame xz is placed at the corner of the side aperture of the waveguide the half-space boundary. Transient load generated by an ultrasonic transducer is applied at the load application interface of the waveguide. The goal is to

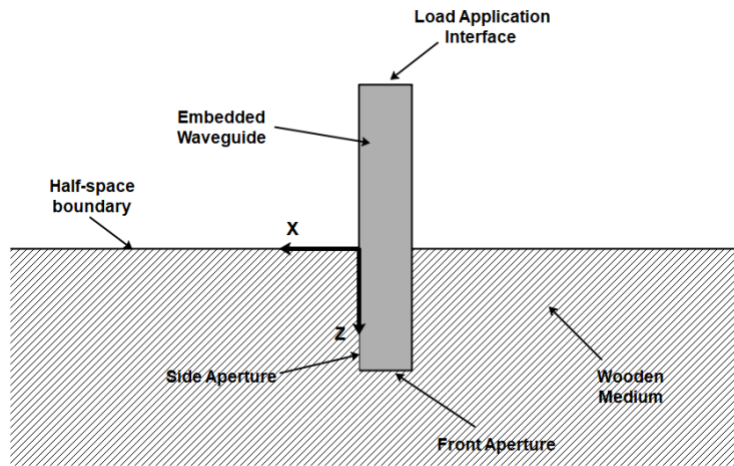


Figure 5

demonstrate the propagation of Rayleigh mode using the described method.

Assumptions and boundary conditions.

As a classical elastodynamic problem, it requires to solve the wave equations. As recalled, the displacement vector \mathbf{u} are decomposed into the longitudinal scalar ϕ and transverse vector potential fields $\boldsymbol{\psi}$ using the Helmholtz decomposition:

$$\begin{aligned}\nabla^2 \phi + k_l^2 \phi &= 0; \\ \nabla^2 \boldsymbol{\psi} + k_t^2 \boldsymbol{\psi} &= 0,\end{aligned}$$

where k_l and k_t are the wave numbers associated with the longitudinal and transverse modes. The resolution to the elliptic wave equations demands the solution to comply with the boundary conditions described as followed:

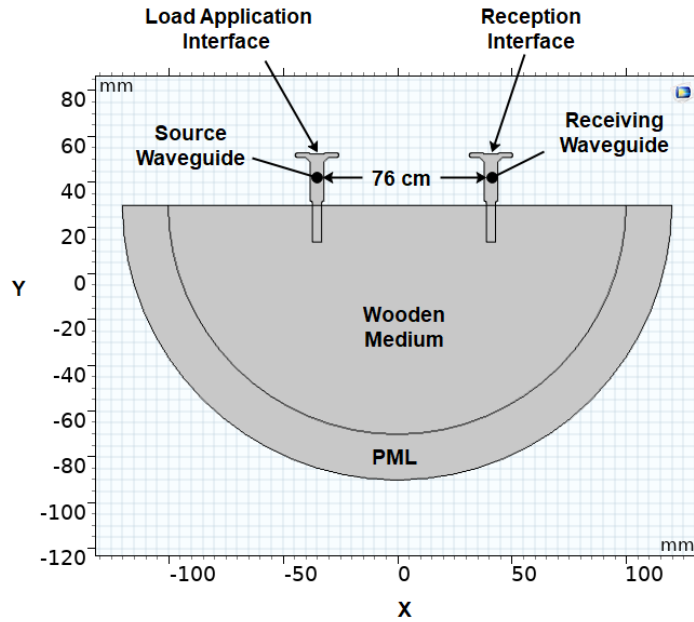


Figure 6

1. The ultrasonic transducer produces transient one-dimensional longitudinal traveling wave along the waveguide body (z-direction), expressed as

$$\phi_w = W = W_0(t)e^{i(k_0z - \omega t)} \quad x = 0, z \in [0, L], \quad (1)$$

where k_0 is the wave number of the wave travelling within the waveguide, and $W_0(t)$ denotes the displacement with time dependency in the z direction. For wave envelop, this can be a Gaussian modulated amplitude. Finally, L denotes the depth of insertion.

2. Continuity condition applies at the solid-solid boundary at $x = 0$ between the waveguide and the propagating medium. That is, $\phi_m = \phi_w$ and $\frac{\partial \phi_m}{\partial x} |_{x=0} = \frac{\partial \phi_w}{\partial x} |_{x=0}$ at $x = 0$; $\forall t$. The subscript m denotes the wooden medium and w denotes the waveguide medium.
3. Only the longitudinal wave mode is permissible. Mode conversion only occurs when the incident wavefront is parallel to the load application interface.
4. Neglect energy absorption in the body of the waveguide.
5. Traction-free boundary condition at the half-space boundary ($z = 0$). That is, $\sigma_{zz} = 0$ and $\sigma_{xz} = 0$. We exploit the fact that the atmospheric pressure is at least many orders of magnitude smaller than the internal stress of the propagating medium.
6. Isotropic medium is assumed.

Numerical Method

To discretize the computational domain illustrated in Figure 2, finite-element simulation model using COMSOL Multiphysics is employed to study the excitation mechanism. Figure 3 shows a sinusoidal transient load with Gaussian modulated amplitude is imposed at the load application interface. The perfectly matched layer (PML) is placed around the computational domain to eliminate interference from the reflection without constructing a large computational domain. Transient load is imposed on the load application interface of the source waveguide and the received stress is measured at the reception interface of the receiving waveguide. Both waveguides are made of aluminum and placed about 76 cm or 2 ½ feet apart. The propagating medium mimics the Douglas-firs species with the averaged mechanical properties obtained from (Ross, 2010).

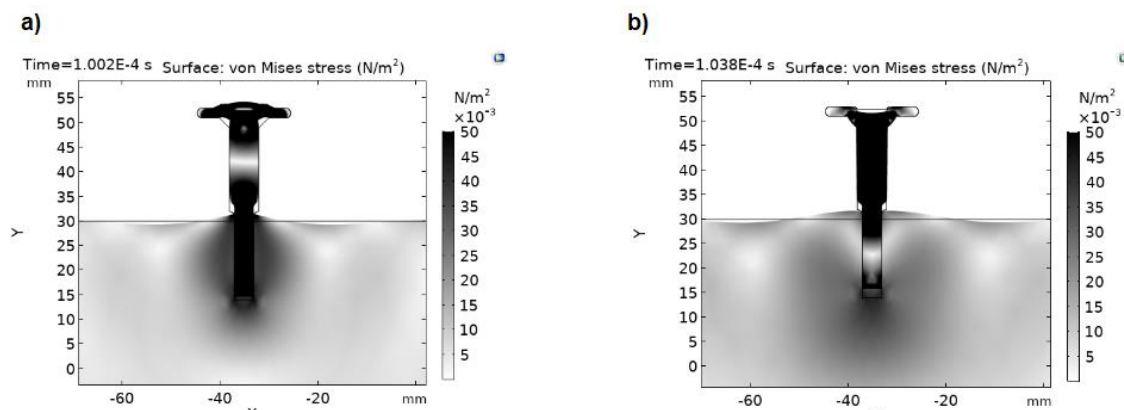


Figure 7

The result of the time domain Von Mises Stress is illustrated in Figure 4a and Figure 4b. At $t = 102 \mu\text{s}$, the source waveguide emitting longitudinal wave which excites ripples on either side of the waveguide at the half-space boundary ($x=0$) due to the imposed traction free boundary condition. By comparing the embedded side and the front apertures, energy emission appears to be stronger on the side aperture due to a large contact area. At $t = 104 \mu\text{s}$, as the sinusoidal

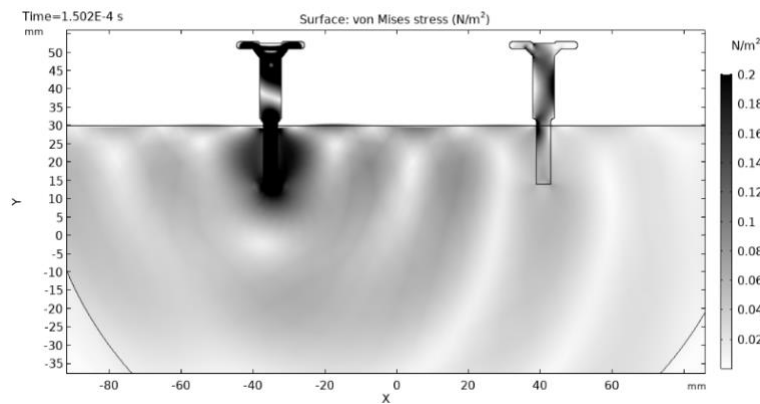


Figure 8

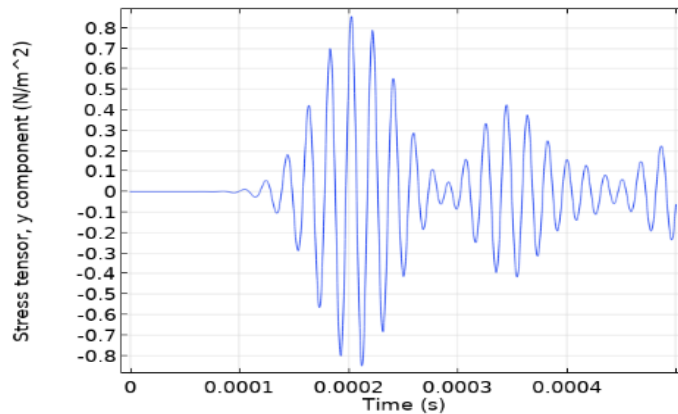


Figure 9

waveform propagating along the waveguide, the continuity condition demands the transmitted waveform to mirror the phase speed of longitudinal wave propagating along the waveguide. Simultaneously, the wave also propagates symmetrically outward in the x directions. The propagation in both x and z directions creates ‘bubbles’ about the source vividly shown in the figure. This is a classical response of a Rayleigh wave propagation along the half-space boundary. In Figure 5, traveling Rayleigh wave first reaches the side aperture of the receiving waveguide that is closest to the source creating asymmetrical wave mode propagating upward along the waveguide. At the reception interface, the time domain stress in the y-direction is depicted in Figure 6. The first wave envelop occurs between 100 to 280 μs , the time of the occurrence corresponds to the wavefront reaching the side aperture of the receiving waveguide as depicted in Figure 5. The shape of the amplitude suggests that it is Gaussian modulated similar to the imposed BC. Due to dissimilar material between the wooden medium and the aluminum waveguide, some of the energy are reflected between the two waveguides generating subsequent wave envelops as seen in Figure 6.

Empirical Method

An inserted waveguide (Figure 7c) was designed to resonate in the longitudinal direction in order to produce the highest displacement amplitude at the pre-determined frequency of the transducer. In order to transmit and receive the ultrasonic signal, a device jointly developed by the University of Denver and the Utility Asset Management Inc. called UB1000 (Figure 7b) was used. Each probe equips with a high-power ultrasonic transducer. An onboard printed circuited assembly (PCA) was designed to excite the resonance mode of the ultrasonic transducer by transmitting a sequence of modulated energy at the resonant frequency. Through a set of passive filters and amplifiers, the conditioned signals are transmitted to a high throughput analog-to-digital converter (ADC). A developed Android-based commanding app (Figure 7c) is to receive conditioned ultrasonic signal and command the units using the Bluetooth protocol.

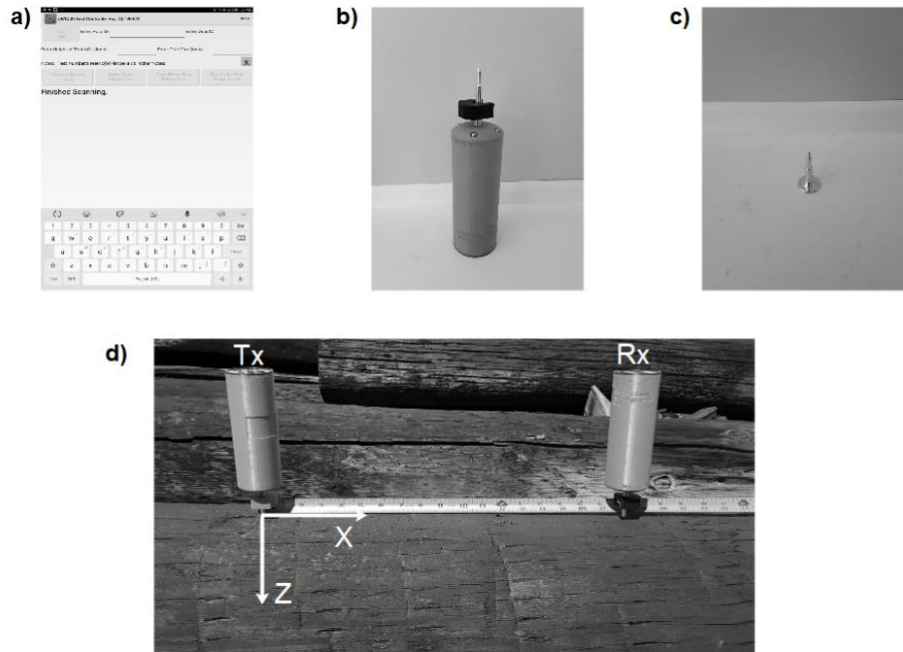


Figure 10

In this study, a brand-new pre-treated Douglas-firs utility pole laid in a horizontal position was used for this experiment (see Figure 7d). The portion facing upward is used to mimic the half-space boundary illustrated in Figure 2. A source waveguide is inserted at a fixed location denoted as Tx. Receiving waveguide denoted as Rx is placed at a distance about 76 cm away from the transmitting location. Figure 8 depicts the conditioned waveform.

RESULTS AND DISCUSSION

In this section, we will compare the waveforms generated by the numerical and empirical results. Figure 8 is the conditioned Analog-to-digital (ADC) data obtained by the Rx UB1000 device. The first wave envelope shows an apparent symmetry that correlates with a Gaussian modulated amplitude. Qualitatively speaking, the empirical waveform agrees with the numerical prediction suggesting a Gaussian amplitude modulated waveform. The arrival time of flight (TOF) is approximately $280 \mu\text{s}$. In order to verify the identity, as we recall, the Rayleigh wave is a transverse wave. Its phase speed can be estimated by calculating the corresponding transverse wave propagating in the same direction. Transverse wave speed is defined as $c_T = \sqrt{\mu/\rho}$, where μ is the shear modulus, and ρ is the density of the material. Based on the wood species, the values can be obtained from (Ross, 2010). The calculating wave speed is about 500 us which is significantly higher than the measured TOF.

SUMMARY AND CONCLUSIONS

This study compares the numerical results generated using the finite-element method to simulate the excitation of Rayleigh mode with the empirical results using UB1000 system. A qualitative agreement of the Gaussian modulated amplitude is established, between the two

approaches, suggesting the possibility of the embedded waveguide excitation of the Rayleigh mode. The empirical result suggests the measured TOF be significantly faster than the theoretical estimation of the transverse wave speed. The result shows that the excited Rayleigh wave mode using this technique might be different from the classical one. An analytical deviation might be beneficial to obtain more valuable insight into the propagational characteristics of using the embedded waveguide excitation method.

ACKNOWLEDGMENTS

This work was sponsored by the National Science Foundation (NSF) RoSe-Hub Center for and the Utility Asset Management Inc. (UAM). The authors are grateful to Mr. Wayne Hall for the funding, supplying industrial equipment and industrial cooperation.

REFERENCES

- Achenbach, J. D. (1967). Dynamic interaction of a layer and a half-space. *Journal of the Engineering Mechanics Division*, 93(5), 27*42.
- Kim, G. I. (2014). Air-coupled detection of nonlinear Rayleigh surface waves in concrete— Application to microcracking detection. *Ndt & E International*, 64-70.
- Lovelace, W. R. (2005). *The wood pole 2005: Design considerations, service benefits, and economic reward*. Hi-Line Engineering, LLCm Tech. Rep.
- Lynnworth, L. (1964). Shear wave robes and applications. *IEEE trans., Sonics and ultrasonics*.
- Minton, C. (1954). Inspection of metals with ultrasonic surface waves. *Nondestructive Testing*, 12(4), 13-16.
- Morrell, J. J. (2013). *Estimated service life of wood poles*. *Technical Bulletin, North American Wood Pole Council*,. Retrieved April 5, 2013, from http://www.woodpoles.org/documents/TechBulletin_EstimatedServiceLifeofWoodPole_12-08.pdf
- Rayleigh, L. (1885). On wave propagated along the plane surfaces of an elastic solid. *London Math Society*, 17, pp. 4-11. London.
- Riegert, G. e. (2006). Modern methods of NDT for inspection of aerospace structures. *ECNDT*.
- Ross, R. J. (2010). *Wood handbook: wood as an engineering material*. USDA Forest Service, , Forest Products Laboratory, . General Technical Report FPL-GTR-190.
- Sokolinskii, A. G. (1958). Technique for the Excitation and Reception of Surface Waves. . *Author Certificate*.
- Thompson, D. &. (2012). *Review of progress in quantitative nondestructive evaluation*. Springer Science & Business Media.
- Viktorov, I. A. (1962). Investigation of methods for exciting Rayleigh waves. *Soviet Physics-Acoustics*.
- Viktorov, I. A. (1967). *Rayleigh and Lamb Waves*. Moscow: Springer Science + Business Media, LLC.

Industry 4.0 Readiness in the US Forestry Industry

Ms. Brooklyn Legg, Oregon State University, USA
Ms. Bettina Dorgner, Oregon State University, USA
Dr. Scott Leavengood, Oregon State University, USA
Dr. Eric Hansen, Oregon State University, USA

Abstract

Advances in technology have promoted evolution across all sectors of manufacturing. The forestry industry has also implemented many new manufacturing technologies and techniques. Given these changes, this work sought to identify the overall readiness of the industry with respect to implementing the principles and technologies associated with Industry 4.0 (the fourth industrial revolution). Preliminary results from a pilot study show that industry professionals feel well prepared for Digital Connectivity, Digital Customer Interaction and New Business Models, but the majority are not familiar with Virtualization, Robotics, Big Data, Predictive Analytics, Cloud Computing and Autonomous Systems. A survey of US-based primary wood products manufacturers will be conducted in summer 2019. Survey questions cover a variety of industry advancements including new technologies. We hope to develop insights that can help improve the sector by understanding the current technological growth and eliminating roadblocks that hinder the growth of future technologies.

Reducing the set-recovery of surface-densified Scots Pine by furfuryl alcohol modification

Han Lei

Dick Sandberg

Luleå University of Technology, Sweden

Abstract

It is well known that there is a positive relationship between wood density and its mechanical properties. That means the densification process is a reasonable method to increase the value of low-density species like Scots Pine and Norway Spruce. In the past, most of the densification processes are aim to densify the whole thickness of the wood. However, the bulk densification not only consumes a quite long time and the huge amount of energy during the process but also lose most of the volume after the process which results in the lower total bending capacity and much higher price per unit. In some case, only one surface of the product is exposed during use periods such as the wooden flooring and worktop. Therefore, the surface densified wood is relative fast, low energy consuming, retained overall thickness and enough to provide favorable hardness and strength during the application period. How to avoid the moisture-induced set-recovery of the densified wood is still the main obstacle in wood densification. Although there are several methods like post heat treatment can almost eliminate the set-recovery, they are either time consuming or difficult to translate into a continuous process which makes the advantage of densification for cheap low-density species lost. On the point of fixing the deformation by increasing the dimensional stability of wood, furfurylation performs the best in improving the anti-swelling efficiency compared with other methods. Besides, furfuryl alcohol is a renewable and natural material which can be obtained from biomass waste. Furfurylation can also protect the wood from biodegradation at a high level without unharmed emission or leaching during the application period. Considering about wettability, curing conditions and viscosity, furfuryl alcohol owns similar properties like phenolic resin. Based on the above properties, it has been proved by the present study that the polymerization of furfuryl alcohol is able to be used to impregnate wood for fixing bulk densified deformation.

The objective of this thesis is to verify whether the furfuryl alcohol can also be used in reducing the set-recovery of surface densified Scots Pine. The study will focus on the interactive effect of the process parameters on the end properties such as immediately spring back, surface hardness, set-recovery under several dry-wet cyclic climate changes, etc. In order to achieve this objective and find the optimal processing parameter, the two-level full factorial design was used combined with following ANOVA and multivariate analysis. Microstructure and density profile measurement after the surface densification and dry-wet cyclic climate test were carried out at the same time as a supplementary tool to learn the mechanism of this two-step modification process further.

Keywords: surface densification; set-recovery; hardness; furfuryl alcohol; microstructure

Composition Analysis and Health Risk Assessment of Benzene Series for Nitrocellulose Paint Lacquered MDF

Huifang Lia, Jun Shen ^{b,*}

^a College of Material Science and Engineering, Northeast Forestry University, Harbin, China, 150040 lihuifang@nefu.edu.cn

^b College of Material Science and Engineering, Northeast Forestry University, Harbin, China, 150040 shenjun@nefu.edu.cn

Abstract: [objective] To evaluate the effect of board thickness and diluents of lacquered panel on human health. [method] The 18mm and 8mm MDF were used as the research object. The nitrocellulose paint was diluted by mixed solvent (alcohols, esters, benzene mixture), Anhydrous Ethanol and Ethyl Acetate, respectively. The 15L small climate chamber was used to simulate indoor environment, and GC – MS was used to analyze the concentration of benzene series released from nitro-lacquered panels. Health risk assessment was evaluated by EPA/US health risk assessment model, it showed the influence of different diluents on the release of benzene series to human body. [results] Under the simulated indoor condition of using MDF alone, 18 kinds of benzene series were detected from mixed diluent painted MDF (NC-M) with thickness of 18mm and 8mm. Thickness of board had no significant effect on the release of benzene. There were significant carcinogenic and non-carcinogenic risks to humans; MDF painted with Anhydrous Ethanol diluent (NC-A) released 14 kinds of benzene series with a total mass concentration of 174.82 $\mu\text{g}\cdot\text{m}^{-3}$, it had no significant non-carcinogenic risk to human body; MDF painted with Ethyl Acetate diluent (NC-E) released 16 kinds of benzene series with a total mass concentration of 218.76 $\mu\text{g}\cdot\text{m}^{-3}$, it had no significant non-carcinogenic risk to human body; [conclusion] Under the indoor conditions of using lacquered MDF alone, thickness has no significant effect on the release of benzene series. Of the three kinds of diluents, benzene series varieties and mass concentration releasing from NC-A and NC-E were both far lower than from NC-M, health risk of NC-A was the lowest. Choosing suitable organic solvent as the diluent of nitro-lacquer can greatly reduce the release of benzene series from the source.

Keywords: nitrocellulose paint; MDF; diluent; benzene series; health risk

Introduction

With the improvement of people's living standards and environmental protection consciousness, varieties of lacquered panel furniture are widely used for interior decoration [1]. Nitro-lacquered furniture is especially common in home storage, while is also getting more and more air irritating attention [2]. Studies have shown that indoor air pollution can cause diseases of the respiratory, nervous and circulatory systems [3]. Volatile organic compounds (VOCs) released from nitro-lacquered furniture, especially benzene series, can irritate people's skin, eyes and respiratory tract, and pose a serious threat to people's health [4]. Therefore, the nitro-lacquered MDF was tested to study the effect of different diluents on the release of benzene series and scientifically evaluated for air quality and human health risks. It is of great significance for ensuring indoor air quality and human health.

Health risk assessment is used to evaluate the degree of harm of toxic substances to human health [5]. It includes carcinogenic risk and non-carcinogenic risk [6]. Non-carcinogenic risk assessment is expressed by Hazard Index (HI), it's the ratio of long-term intake to reference dose. Carcinogenic risk is expressed in terms of risk value (Risk), it's expressed by the product of the reference intake and average exposure concentration of lifetime. The formula is as follows.

$$HQ = EC / (Rfc \times 1000) \quad (1)$$

$$HI = \sum HQ_i \quad (2)$$

$$\text{Risk} = EC \times IUR \quad (3)$$

Note: HQ is Hazard Quotient, EC is Exposure Concentration, Rfc is the concentration of inhaled carcinogenic risk ($\text{mg}\cdot\text{m}^{-3}$), HI is the sum of hazard quotients of pollutants, IUR is the reference concentration that causes a cancer risk ($\text{m}^3\cdot\mu\text{g}^{-1}$) [7].

To evaluate the effect of different thickness and diluents of lacquered panels on human health, in this study, 8mm and 18mm nitro-lacquered MDF panels were examined as the research object, the nitrocellulose paint was diluted by mixed solvent (alcohols, esters, benzene mixture), Anhydrous Ethanol and Ethyl Acetate, respectively. The panels were placed in a 15L small climate chamber, which was used to simulate indoor environment. Benzene series released from three kinds of nitro-lacquered panels was examined by GC – MS.

The health risk assessment model was used to evaluate the risk of benzene series to human health. Based on assessment result, to protect human health, the study proposed to control benzene series pollution from the choice of paint diluent.

Materials and Methods

Experimental materials

Undecorated MDF panels, produced in Guangdong, were chosen as our experimental material. The panels had the dimensions (length × width × thickness) of 150mm×75mm×18mm and had a formaldehyde emission of level of E1. The adhesive used in MDF production was urea-formaldehyde resin adhesive.

Ash was used as veneer material for MDF with a thickness of 0.6mm, the hot-pressing temperature was 200°C, the hot-pressing time was 10min, and the thermal pressure was 4MPa[8].

The nitrocellulose paint was diluted by three types of diluents, the first type was Anhydrous Ethanol (NC-A), the second was Ethyl Acetate (NC-E), and the last was mixed solvents that mixed with alcohol, ester and benzene (NC-M). Painting proportion was the main agent: diluent=2:1. Painted panels were placed in a naturally ventilated room with 23°C for 28 days[9]. Tin foil is used to seal the side of the plate when collecting gas to prevent the benzene series from being released [10].

Experimental equipment

The following equipment was used in the experiments. (1) A small climate chamber with the volume of 15 liter. It had been verified had a good correlation [11] with 1m³ chamber [12]. The chamber simulated the indoor environment, with the temperature of 23°C, air humidity of 50%, air exchange rate of 1 [13]. (2) Tenax-TA sampling tubes were obtained from Beifen Tianpu Instrument Technology Limited Company [14]. (3) A DSQ II series GC-MS (Thermo Fisher, America) was used [15]. Thermal desorption apparatus made by MARKES UK performed with a DB-5 quartz capillary column, the carrier gas was Helium [16].

Experimental design


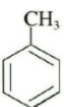
Collection of benzene series- In this study, painted MDF were placed in a naturally ventilated room with 23°C for 28 days. The panels were placed horizontally in the center of the climate chamber, the benzene series released from the specimen surface was absorbed using Tenax-TA tubes. The collected gas was analyzed by thermal desorption apparatus for 5 minutes. The GC-MS and built-in software were used to analyze the concentration of benzene series according to GB/T29899-2013 [17]. The EPA/US health risk assessment model were used to evaluate the risk of harm of benzene series to human health.

Results and Discussion

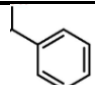
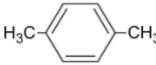
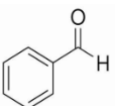
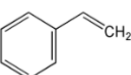
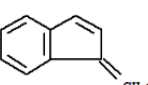
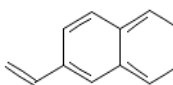
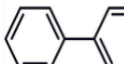
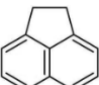
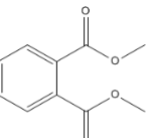
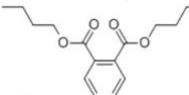
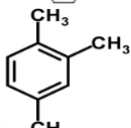
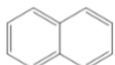
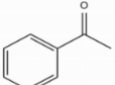
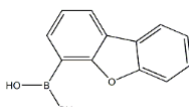
Benzenes eries components released from MDF with different thicknesses

Table 1 summarizes the release of benzene series from MDF lacquered with different thickness. 18 kinds of benzene series were detected in 8mm and 18mm MDF, 13 kinds of benzene series were detected in undecorated MDF.

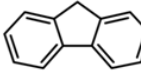
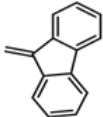
Table 1 Release of benzene series components from three kinds of MDF

substance	chemical formula	structural formula	functional group	Toxicity	Concentration / ($\mu\text{g}\cdot\text{m}^{-3}$)		
					18mm MDF	8mm MDF	18mm undecorated MDF
benzene	C ₆ H ₆		/	high	45.61	45.42	44.4
toluene	C ₇ H ₈		methyl	high	27.65	14.75	60.24

**Proceedings of the 62nd International Convention of
Society of Wood Science and Technology
October 20-25, 2019 – Tenaya Lodge, Yosemite, California USA**

ethylbenzene	C ₈ H ₁₀		ethyl	high	62.62	63.35	59.37
p-xylene	C ₈ H ₁₀		methyl	high	61.1	72.11	43.17
Benzaldehyde	C ₇ H ₆ O		Aldehyde group	high	3.09	3.82	/
styrene	C ₈ H ₈		carbon-carbon double bond	high	9.54	7.54	/
1-methylene-1H-indene	C ₁₀ H ₈		carbon-carbon double bond	low	2.57	2.45	/
2-vinylnaphthalene	C ₁₂ H ₁₀		carbon-carbon double bond	low	5.22	3.61	4.98
biphenyl	C ₁₂ H ₁₀		/	low	1.96	1.51	10.47
acenaphthene	C ₁₂ H ₁₀		/	low	3.14	3.79	12.38
dimethyl phthalate	C ₁₀ H ₁₀ O ₄		/	low	3.45	3.58	3.15
dibutyl phthalate	C ₁₆ H ₂₂ O ₄		Ester group	low	28.57	27.65	21.49
1,2,4-trimethylbenzene	C ₉ H ₁₂		methyl	high	1.59	1.21	5.31
naphthalene	C ₁₀ H ₈		/	low	4.09	4.2	21.2
Acetophenone	C ₈ H ₈ O		/	low	1.49	2.42	/
Dibenzofuran	C ₁₂ H ₈ O		carboxyl	low	6.91	6.14	1.95

**Proceedings of the 62nd International Convention of
Society of Wood Science and Technology
October 20-25, 2019 – Tenaya Lodge, Yosemite, California USA**

Fluorene	C ₁₃ H ₁₀		/	low	10.12	11.59	16.64
9H-Fluorene-9-methylene-	C ₁₄ H ₁₀		carbon-carbon double bond	low	5.72	5.92	/

The benzene series released from the nitro-lacquered MDF is mainly from the paint. Table 1 shows the total mass concentration of benzene series released from undecorated MDF was 316.24 $\mu\text{g}\cdot\text{m}^{-3}$, concentrations of Benzene, Toluene, Ethyl Benzene and P-xylene were 44.4 $\mu\text{g}\cdot\text{m}^{-3}$, 60.24 $\mu\text{g}\cdot\text{m}^{-3}$, 59.37 $\mu\text{g}\cdot\text{m}^{-3}$ and 43.17 $\mu\text{g}\cdot\text{m}^{-3}$ respectively. The mass concentration of Toluene was the highest, followed by Benzene and Ethyl Benzene. It can be seen that BTEX contributed the most to the benzene series of the undecorated MDF, it mainly derived from the tree itself and the adhesive applied when the wood fiber was produced.

The total concentration of 18 benzene series released from 18mm MDF was 284.44 $\mu\text{g}\cdot\text{m}^{-3}$, concentration of BTEX was 196.98 $\mu\text{g}\cdot\text{m}^{-3}$, Benzene, Toluene, Ethyl Benzene and P-xylene were 45.61 $\mu\text{g}\cdot\text{m}^{-3}$, 27.65 $\mu\text{g}\cdot\text{m}^{-3}$, 62.62 $\mu\text{g}\cdot\text{m}^{-3}$, 61.1 $\mu\text{g}\cdot\text{m}^{-3}$, respectively. The five highest components of total benzene series from high to low was Ethyl Benzene, P-xylene, Benzene, Dibutyl Phthalate and Toluene. The mass concentration of the other 13 benzene series was lower than 10.12 $\mu\text{g}\cdot\text{m}^{-3}$, and the concentration of Biphenyl was the lowest.

The total concentration of 18 benzene series released from 8mm MDF was 281.06 $\mu\text{g}\cdot\text{m}^{-3}$, concentration of BTEX was 195.65 $\mu\text{g}\cdot\text{m}^{-3}$, the mass concentrations of Benzene, Toluene, Ethyl Benzene and P-xylene were 45.42 $\mu\text{g}\cdot\text{m}^{-3}$, 14.75 $\mu\text{g}\cdot\text{m}^{-3}$, 63.35 $\mu\text{g}\cdot\text{m}^{-3}$, 72.11 $\mu\text{g}\cdot\text{m}^{-3}$, respectively. The concentration of P-xylene was the highest, then Ethyl Benzene and Benzene, and then Dibutyl Phthalate. The mass concentration of the other 14 kinds of benzene series were lower than 14.75 $\mu\text{g}\cdot\text{m}^{-3}$.

It was found that benzene series types released from 18mm and 8mm nitrocellulose lacquered MDF were same, the total mass concentration was not much different, and the concentration of BTEX was almost equal. It shows that under this experimental condition, thickness had no significant effect on the release of benzene series. The benzene series types of undecorated MDF were the least, but the total mass concentration was the highest. First, because the plate was veneered with ash before painting, it had a significant sealing effect on benzene series release from the plate itself. Secondly, the existence of paint film closed the contact between wood and air, and hindered the benzene series released from wood itself and adhesive, lacquer material becomes the main source of the benzene series released from lacquered MDF. This experiment also corrected the general view that "unpainted board is more environmentally friendly". Reasonable painting can not only protect wood, but also hinder the release of volatile organic compounds, and protect the home environment.

Composition ratio of benzene series released from nitro-lacquered MDF with different diluents

Benzene series release mainly from main agent and diluents of the paint. Figures 1 to 3 visually show the composition and proportion of benzene series released from nitro-lacquered MDF using three diluents. The main ingredients include three major parts of BTEX (Benzene, Toluene, Ethyl benzene, P-xylene) which is the most harmful to humans, Styrene and other benzene-containing compounds.

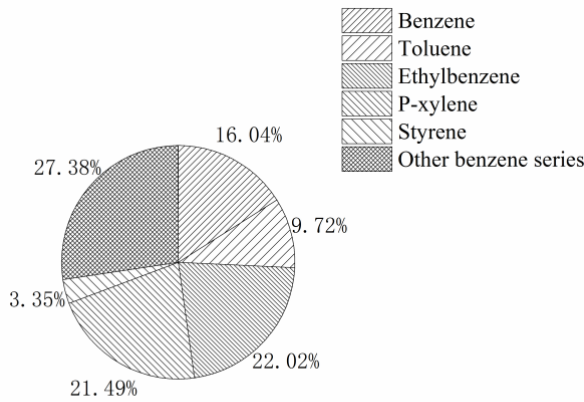


Figure 1 benzene series released from NC-M

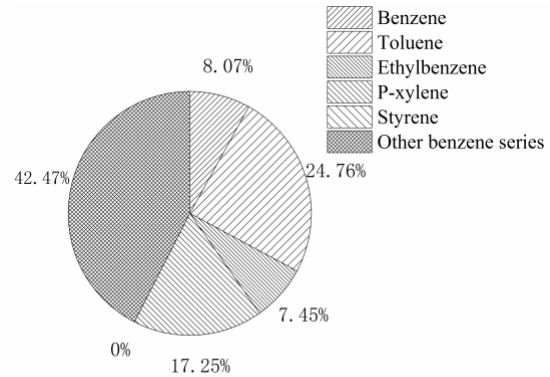


Figure 2 benzene series released from NC-A

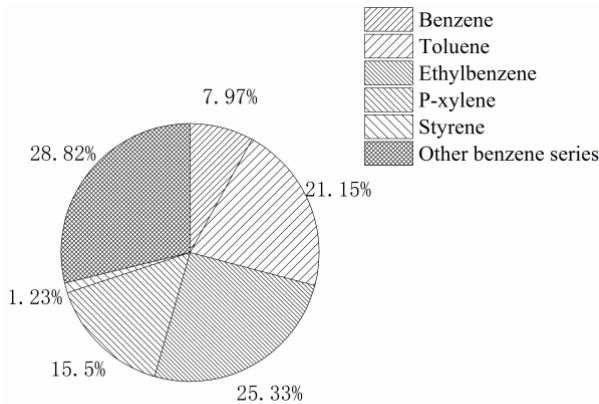


Figure 3 benzene series released from NC-E

Among the benzene series released from the nitro-lacquered MDF with three diluents, there were 12 common components, and BTEX accounted for the largest proportion.

BTEX accounted for 69.26% of the total mass concentration of benzene series released from NC-M lacquered MDF, Ethyl Benzene and P-xylene accounted for more than 1/5, which was 22.02% and 21.49%, respectively, and Styrene accounted for 3.35%, which may cause a potential health risks;

From NC-A lacquered MDF, BTEX accounted for 57.6% of the total mass concentration, Toluene and P-xylene accounted for 24.76% and 17.25% respectively, without releasing Styrene;

From NC-E lacquered MDF, BTEX accounted for 69.94% of the total mass concentration, Toluene and Ethyl Benzene accounted for 21.15%, 25.33% and Styrene for 1.23% respectively. Other compounds such as Naphthalene, Fluorene, Biphenyls, etc., had a lower release amount and a faster volatilization rate, causing less harm to health.

At present, the national standard limits the amount of benzenes added to the paint to not more than 0.5%, so that Benzene released from the lacquered panels get controlled. However, there is no specific limit of other single components of BTEX, and the potential hazards of various benzene series to human body still exist. Therefore, it is necessary to improve the monitoring of BTEX releasing level of lacquered panels, especially Toluene, Ethyl Benzene and P-xylene, in home life.

Health risk assessment

A health risk assessment is to further clarify the toxicity of the benzene series released from three lacquered MDF.

At present, only the Rfc and IUR values of Benzene, Toluene, Ethyl Benzene, P-xylene and Styrene can be found in the database of EPA/US Integrated Risk Information System (IRIS) [18]. Therefore, this study only evaluated the health risks of these five benzene series. Referring to the health risk assessment model, the daily

**Proceedings of the 62nd International Convention of
Society of Wood Science and Technology
October 20-25, 2019 – Tenaya Lodge, Yosemite, California USA**

average exposure concentration (EC), non-carcinogenic risk hazard quotient (HQ), hazard index (HI) and lifetime carcinogenic risk (Risk) of the five benzene series mentioned above in three kinds of lacquered MDF were calculated according to formulas (1) ~ (3), respectively. The results are shown in Table 2~4.

Table 2 Health Risk Assessment of Benzenes Released from NC-M

Benzenes	EC/($\mu\text{g}\cdot\text{m}^{-3}$)	Rfc/ ($\text{mg}\cdot\text{m}^{-3}$)	IUR/ ($\text{m}^3\cdot\mu\text{g}^{-1}$)	HQ	Risk
Benzene	45.61	0.03	7.80E-06	1.52	3.56E-04
Toluene	27.65	5	—	5.53E-03	—
Ethyl	62.62	1	—	6.26E-02	—
Benzene					
P-xylene	61.1	0.10	—	0.06	—
Styrene	9.54	1	—	9.54E-03	—
$\text{HI}_{\text{NC-M}}=\sum\text{IHQ}_{\text{NC-M}}=1.66$					

Table 3 Health Risk Assessment of Benzenes Released from NC-A

Benzenes	EC/($\mu\text{g}\cdot\text{m}^{-3}$)	Rfc/ ($\text{mg}\cdot\text{m}^{-3}$)	IUR/ ($\text{m}^3\cdot\mu\text{g}^{-1}$)	HQ	Risk
Benzenes	14.1	0.03	7.80E-06	0.47	1.1E-04
Toluene	43.28	5	—	8.66E-03	—
Ethyl	13.02	1	—	1.3E-02	—
Benzene					
P-xylene	30.16	0.10	—	0.3	—
Styrene	—	1	—	—	—
$\text{HI}_{\text{NC-A}}=\sum\text{IHQ}_{\text{NC-A}}=0.79$					

Table 4 Health Risk Assessment of Benzenes Released from NC-E

Benzenes	EC/($\mu\text{g}\cdot\text{m}^{-3}$)	Rfc/ ($\text{mg}\cdot\text{m}^{-3}$)	IUR/ ($\text{m}^3\cdot\mu\text{g}^{-1}$)	HQ	Risk
Benzene	17.44	0.03	7.80E-06	0.58	1.36E-04
Toluene	46.26	5	—	9.25E-03	—
Ethyl	55.41	1	—	5.54E-02	—
Benzene					
P-xylene	33.9	0.10	—	0.34	—
Styrene	2.69	1	—	2.69E-03	—
$\text{HI}_{\text{NC-E}}=\sum\text{IHQ}_{\text{NC-E}}=0.99$					

Note: “—” means no relevant data.

Assessment of non-carcinogenic risk

Table 2 shows in the benzene series released from NC-M, the HQ of Benzene was two to three orders of magnitude higher than the other four benzene series, Benzene was the most harmful benzene series. The EC ranged from 9.54 to 62.62 $\mu\text{g}\cdot\text{m}^{-3}$, HQ ranged from 5.53E-03 to 1.52, and HI was 1.66. According to the EPA/US standard, adverse reactions will occur when people are exposed to environmental conditions with HI of Benzene greater than 1 for a long time. In this study, the HI of benzene series was greater than 1, which indicated that the benzene series released from NC-M lacquered MDF had obvious non-carcinogenic risk to human body.

Table 3 shows the HI of benzene series released from NC-A lacquered MDF was the lowest, much lower than NC-M. The HQ of Benzene and P-xylene was one to two orders of magnitude higher than that of the other three benzene series. EC ranged from 3.64 to 17.67 $\mu\text{g}\cdot\text{m}^{-3}$, HQ ranged from 8.66E-03 to 0.47, HI was 0.79,

**Proceedings of the 62nd International Convention of
Society of Wood Science and Technology
October 20-25, 2019 – Tenaya Lodge, Yosemite, California USA**

and there was no obvious non-carcinogenic risk to human body.

Table 4 shows the HI of benzene series released from NC-E lacquered MDF was lower than NC-M, the HQ of Benzene and P-xylene was one to two orders of magnitude higher than that of the other three benzene series. The EC range of the five benzene series was 2.69~46.26 $\mu\text{g}\cdot\text{m}^{-3}$, the HQ range was 8.66E-03~0.47, and the HI was 0.99. The HI was lower than the NC-M, higher than the NC-A, close to 1, may have potential non-carcinogenic risks to the human body.

It should be pointed out that no obvious non-carcinogenic risk is not equal to no harm. The HI of benzene series released from NC-M lacquered MDF had exceeded 1. It is advisable to monitor the concentration of benzene series released from the nitrocellulose lacquered MDF for a long time, and be alert to the potential effects of benzenes in the environment on the human body.

Assessment of carcinogenic risk

According to the relevant definition of EPA/US, for the cancer risk, the acceptable carcinogenic risk value is in the range of 10^{-6} ~ 10^{-4} , when the risk value is less than 10^{-6} , it is considered to be acceptable, whereas the risk value is greater than 10^{-4} , it indicates that the benzene released from the lacquered board has a higher risk of cancer, and certain measures must be taken. Table 2~4 shows the risk value of benzene series released from NC-M lacquered MDF was 3.56E-04, which is 3.56 times the upper limit of carcinogenic risk. The carcinogenic risk values of benzenes released from NC-A and NC-E were significantly lower than those of NC-M, which were 1.1E-04 and 1.36E-04, respectively. The carcinogenic risk of these two kinds of paints has reached the upper limit, it indicates that benzene released from the two kinds of painted panels still has a certain carcinogenic risk to human body under this painting condition.

It can be seen that the type of diluents will directly affect the carcinogenic risk of gases. Using appropriate organic solvents as diluents can greatly reduce the toxicity of the released gases. Close attention should be paid to the release of benzene, and take measures such as window ventilation to promote the discharge of benzene.

The study shows that it feasible to use appropriate organic solvents as nitro-lacquer diluent, which not only guarantees the stable performance of the film, but also reduces the pollution of benzene series from the source. It has certain reference value for industrial improvement of nitro-lacquer.

Conclusion

- (1) Under the indoor conditions of using lacquered MDF alone, thickness has no significant effect on the release of benzene series.
- (2) The health risk of benzene series released from NC-A and NC-E lacquered MDF were both lower than NC-M, NC-A had the lowest health risk.
- (3) Choosing suitable organic solvent as the diluent of nitro-lacquer can greatly reduce the release of benzene series from the source.

Reference

- [1] Wang Zhenjie, Gao Li. Application and Demand of Wood-based Panel Products in Modern Interior Decoration [J]. *China Wood-based Panel*, 2018, 25 (04): 22-25.
- [2] Lu boqi. Effect of decoration materials on indoor air quality [J]. *Farmer's Staff*, 2018 (15): 210.
- [3] Peng Qi, Rao Jun, Yang Zhiwen, Zhou Chunliang. A review of the correlation between indoor inhalable particulate matter pollution and asthma and lung cancer [J]. *Practical preventive medicine*, 2018, 25 (08): 1022-1025.
- [4] Shen Jun, Jiang Liqun. Progress in VOCs release from wood-based panels [J]. *Journal of Forestry Engineering*, 2018,3(06): 1-10.
- [5] Committee on the Institutional Means for Assessment of Risks to Public Health, National Research Council (US). Risk Assessment in the Federal Government: Managing the Process [R] . *Washington, DC: National Academy Press*, 1983.
- [6] Feng Huanyin, Fu Xiaoqin, Zhang Qian, et al. Residual status and health risk assessment of persistent toxic pollutants in agricultural soils in suburbs of Ningbo [J]. *Modern Scientific Instruments*, 2012 (4): 128-133.
- [7] Li Lei, Li Hong, Wang Xuezhong. Pollution characteristics and health risk assessment of volatile organic compounds (VOCs) in the ambient air of downtown Guangzhou [J]. *Environmental Science*, 2013, 34 (12): 4558-4564.

**Proceedings of the 62nd International Convention of
Society of Wood Science and Technology
October 20-25, 2019 – Tenaya Lodge, Yosemite, California USA**

- [8] Tang Qiheng, Tan Hongwei, Wei Qifeng, Cui He Shuai, Guo Wenjing, Zhou Guanwu. Preparation and properties of low formaldehyde emission high density fiberboard [J]. *Journal of Forestry Engineering*, 2019, 4 (02): 26-30.
- [9] Xu Wei, Han Jiatong, Feng Yuefei, Wu Zhizhi, Luo Jianfeng. Effects of film thickness on sound absorption properties of spruce wood [J]. *Journal of Forestry Engineering*, 2016, 1(04): 156-160.
- [10] Shao Yali, Shen Jun, Deng Fujie et al. Study on the effect of surface finishing on the release of TVOC from strengthened poplar wood [J]. *Journal of Central South University of Forestry Science and Technology*, 2018, 38 (2): 114-121.
- [11] Du Chao, Shen Jun. Comparison of VOCs rapid detection method and climatic box method for wood-based panels [J]. *Forestry Science*, 2015, 51 (3): 109-115.
- [12] Afshari A, Lundgren B, Ekberg L E. 2003. Comparison of three small chamber test methods for the measurement of VOC emission rates from paint. *Indoor Air*, 13: 156–165
- [13] Du Chao, Shen Jun. Comparison of VOCs rapid detection method and climatic box method for wood-based panels [J]. *Forestry Science*, 2015, 51 (3): 109-115.
- [14] Du Chao, Shen Jun. Rapid Detection of Volatile Organic Compounds Release from MDF [J]. *Journal of Northeast Forestry University*, 2014, 42 (10): 115-117, 131.
- [15] Cao Tianyu, Shen Jun, Liu Wanjun, et al. Effects of environmental conditions on VOCs release from wood-based panels detected by DL-SW microchip [J]. *Journal of Northeast Forestry University*, 2018, 46 (2): 72-76
- [16] Zhao Yang, Shen Jun, Cui Xiaolei. VOC Release and Rapid Detection of 3-storey Solid Wood Composite Flooring [J]. *Forestry Science*, 2015, 51(2): 99-104.
- [17] Wu Qingsi, Wang Xuan, Xia Jinwei, Shen Lijin, Zhang Yaoli. Wood structural characteristics and GC-MS analysis of *Dalbergia alba* and *Dalbergia alba* [J]. *Journal of Forestry Engineering*, 2017, 2 (06): 26-30.
- [18] US EPA. Risk Assessment Guidance for Superfund Volume I: Human Health Evaluation Manual (Part F, Supplemental Guidance for Inhalation risk Assessment) [R] . Washington D C: Office of Superfund Remediation and Technology Innovation Environmental Protection Agency, 2009.

**Using crack-growth experiments to study the moisture and thermal durability
of MDF,OSB and PB**

Ms. Sweta Mahapatra, Dr. Arijit Sinha, Dr. John Nairn
Oregon State University, USA

Abstract

Fracture resistance curves or R curves for Medium Density Fiber Board (MDF), Oriented Strand Board (OSB) and Particle Board (PB) were measured in replicates of 3 and the average values of fracture resistance curves were found for each. We studied the development of crack growth in each of the specimens using a digital image correlation technique and generated the load-displacement curve from Universal testing machine (UTM). Further we exposed the specimens to an elevated temperature from 400C to 200 0C, tested them and generated the R Curves for each. In the second phase we exposed our specimen to different moisture conditions by submerging the samples in water using a vacuumed desiccator and tested them to generate R curves. After conducting above experiments we compared the fracture toughness of specimens and inferred the change in toughness when exposed to different moisture and temperature changes. We would like to suggest that fracture toughness should be considered when characterizing durability of wood based composites.

Moment-rotation behaviour of beam-column connections fastened using compressed wood connectors

Sameer Mehra¹, Iman Mohseni¹, Conan O’Ceallaigh¹, Zhongwei Guan², Adeayo Sotayo²,
Annette M. Harte¹

¹ Timber Engineering Research Group, College of Engineering and Informatics & Ryan Institute, NUI Galway, Ireland

² School of Engineering, University of Liverpool, Liverpool, United Kingdom

ABSTRACT: Over the last few decades, there has been a renewed interest in the use of timber in building construction in response to concerns related to the challenges of global warming and climate change. This transition towards sustainable and bio-based construction has led to developments in mass timber products and associated novel connection typologies. Considering the demand, the use of traditional carpentry type connections has been largely replaced by fast, efficient and cost-effective modern connections using mechanical fasteners and adhesives. However, metallic fasteners have high embodied energy while adhesives have negative implications for end of life disposal. Therefore, it is favourable to replace these products with sustainable wood-based connectors. The traditional carpentry connections rely on load-transfer in compression via contact between the connected elements or through the use of timber dowels and plates. Numerous examples of such techniques can be seen in historic buildings many of which have been standing for centuries and have endured severe loading situations. These connections are completely adhesive free and non-metallic and can be easily disassembled and reconfigured for replacement or repair. However, connections using hardwood dowels have been reported to loosen over time and necessitate regular tightening so alternative approaches that overcome this drawback are desirable.

Recent studies on modified wood have found that densified or compressed wood (CW) can be used to provide reinforcement in the joint area and could be a potential alternative to adhesives and energy intensive metallic connectors in timber connections. Densified or CW connectors have higher load-carrying capacity and greater ductility than the equivalent hardwood dowels due to their high density. Furthermore, the moisture dependent swelling and springback of CW connectors ensures a tight fit in the connection over time. Also, these connectors have been found to have better compatibility with timber in the connections compared to steel fasteners, which have far greater stiffness than timber. In this study, seven configuration of beam-column moment resisting connection were developed using CW dowels with or without compressed wood plates. The study has considered specimens with CW dowels of 10 mm diameter and CW plates of 20 mm thickness. The load carrying capacity, typical failure modes, moment resistance and rotational stiffness of each connection system were evaluated based on experimental results. Results have shown that connection with CW plates provide a greater load carrying capacity and moment resistance than comparable connections without plates. However, it was found that connections without CW plates allow for more energy dissipation and ductility in the connection.

KEYWORDS: Connections, compressed wood dowels, compressed wood plates, moment-rotation

Evaluation of a Renewable Wood Composite Sandwich Panel for Building Construction

Mr. Mostafa Mohammadabadi
Dr. Vikram Yadama
Washington State University, USA

Abstract

Finding a solution for small diameter timber from hazardous fuel treatments contributes to forest health as well as rural economic development. The issue is with lower wood quality of the wood derived from these trees as well as lower rate of conversion into higher value products such as lumber and veneer. However, wood strand technology, such as OSB, can offer a solution. However, can we produce a wood strand composite panel of greater performance than OSB with improved functionality and with less materials (wood and resin)? To this aim, wood strand composite sandwich panel with biaxial corrugated core(s) was developed to serve as a material for construction of building envelopes, such walls, floors, or roofs.

Thin wood strands with an average thickness of 0.36 mm were produced from ponderosa pine (pp) logs ranging in diameter from 191 to 311 mm, using a CAE strander operating at a rotational speed of 500 rpm. Wood strands were dried to a target moisture content of 3-5% and sprayed with aerosolized liquid phenol formaldehyde (PF) resin in a drum blender to a target resin content of 8%.

Subsequently, resinated wood strands were oriented unidirectionally to fabricate a wood strand mat and hot-pressed into a corrugated core using a matched-die mold. Single or multiple cores can then be bonded with flat wood strand panels on the faces to fabricate a sandwich panel. When used in walls, these panels can be subjected to gravity loads from the roof and other floors, and transverse wind loads. Therefore, this presentation will focus on performance evaluation of wood strand sandwich panels in compression and bending conducted following the standard testing guidelines in ASTM E72-15. Additionally, to improve the energy performance, the cavities in the sandwich panel resulting from the corrugated geometry of the core were filled with two-part closed-cell foam. Prefabricated wall panel filled with insulation foam and instrumented with moisture, temperature, and relative humidity sensors was evaluated for its hygrothermal performance at Washington State University's Natural Exposure Testing (NET) facility. Hygrothermal performance of this wall will be compared with the performance of a structurally insulated panel installed and evaluated at the NET facility as well.

Dynamic Assessment of Dimensional Change of Wood-Based Composite Materials in Moist Environments

Mr. Luis Molina
Dr. Fred Kamke
Oregon State University, USA

Abstract

Engineered wood composites can be manufactured using various materials, such as wood fibers, particles, and veneer. Some of these materials are used for laminating stock and other applications where the dimensional stability of the material is essential. The dimensional stability of MDF and veneer products is primarily the result of changing moisture content, which is driven by fluctuating humidity conditions or exposure to liquid water.

The goal of this research is to measure the dynamic effect of the experimental accelerated weathering techniques on the dimensional change of engineered wood composites. This ongoing project is evaluating three experimental methods of inducing dimensional change in engineered wood products: (1) water spray, (2) water soaking, and (3) changes in relative humidity conditions. Digital image correlation (DIC), an optical method of measuring dimensional changes, is being incorporated, along with conventional measuring technics.

The materials under investigation include commercially-produced engineered panels that are designed for exceptional water resistance. Using an environmental chamber, with water spray and partial submersion in water applied in the same chamber, all specimens will be tested under the same ambient conditions. The DIC camera is mounted in the chamber, and protected by an enclosure, to monitor the dimensional changes of the specimens on a continuous basis. Results will include plots of thickness swell and linear expansion as a function of exposure time.

Keywords: dimensional stability, wood-based composites, moisture exposure, thickness swell, linear expansion.

INVESTIGATING THE THERMAL AND MECHANICAL PROPERTIES OF FLY ASH/METAKAOLIN-BASED GEOPOLYMER REINFORCED WITH ALIEN INVASIVE WOOD SPECIES

MR. HAMED OLAFIKU OLAYIWOLA
DR. STEPHEN AMIANDAMHEN
DR. LUVUYO TYHODA

Stellenbosch University, South Africa

Abstract

Alien invasive wood species pose serious threat to the sustainable biodiversity of natural ecosystems. They add to the fuel load of above-ground biomass and lead to excessive loss of groundwater storage through evapotranspiration. The impacts have manifested in the incessant fire outbreaks and acute water shortage being experienced in South Africa in recent times. The prevailing approach of total clearing to contain the spread of these invasive plants is generating enormous biomass wastes. This study seeks to find alternative uses for these residues in geopolymer composite manufacturing, which can be applied in low cost building construction as an alternative beneficial control measure and a novel pathway of converting biomass and industrial wastes to value added products. *Acacia mearnsii* and *A. longifolia* were incorporated into geopolymer binder developed from a binary precursor system of fly ash and metakaolin. The production process was established using Central Composite Design (CCD) coded to utilize as much biomass as technically possible. Influence of factors related to the precursor materials and chemical activators such as binder to activator ratio, activator moduli ($\text{SiO}_2/\text{Na}_2\text{O}$), dosage ($\% \text{Na}_2\text{O}/\text{binder}$) and curing pattern on the thermal and mechanical properties of the final products were investigated. Preliminary results have indicated that the final products have comparable properties to conventional inorganic-bonded composite products.

Evaluating Stem and Wood Quality of Planted Longleaf Pines Using Bio-Imaging Techniques

Sameen Raut^{1} – Joe Dahlen²*

¹ MS Student, University of Georgia, Warnell School of Forestry and Natural Resources, Athens, GA, USA
sameen.raut@uga.edu

² Associate Professor, University of Georgia, Warnell School of Forestry and Natural Resources, Athens, GA, USA
jdahlen@uga.edu

Abstract

The conversion of forest land to agriculture resulted in the loss of 97 percent of longleaf pine forests in the southern U.S. Reforestation efforts in the 1950's established other southern pines across the southeast, namely loblolly and slash pine. However, recent efforts have led to the reestablishment of approximately 4 million acres of longleaf pine throughout the south on both converted agricultural fields and cutover forestlands. The application of modern silvicultural practices, combined with the lack of genetic improvement, has proven detrimental to longleaf pine stem wood and quality, with some sites having over 50% stem defect rate. Defects including sweep, forking, and ramicorn branching will result in the formation of compression wood which is undesirable for manufacturing. This study will investigate the applicability of bio-imaging techniques to quantify the amount of compression wood from longleaf pine. We are in the process of collecting cross sectional disks, extracted at multiple height levels, from approximately 400 trees. Green disk surfaces will be machined using a CNC router and subsequently photographed. An RGB image will be collected for making inferences about wood and bark volume and disk shape. A second image taken using circular polarized light will fluorescence the compression wood and allow for accurate quantification of the compression wood quantity. Following imaging, wood and bark volume, specific gravity and moisture content will be

determined manually with comparisons made between the two volume measurements. Analysis of Variance using linear mixed models with stand and tree sampled as random factors will be conducted to determine differences in wood and bark properties between the converted agricultural fields and cutover forestland sites.

Results from this study will help inform forest landowners and state foresters about the quality of longleaf pine stem and wood so that they can better assess product quality and ultimately the economic returns on their investment. With growing interests of landowners towards planting longleaf pine in their cutover forestlands and old agricultural fields due to lucrative incentives, and the broader community of longleaf supporters making somewhat a leap of faith in attaching the same values of physical wood properties (specific gravity, moisture content, etc.) that natural, slow growing longleaf is known for to the more quickly grown plantation longleaf, our research, in my point of view, is of great importance.

Key words: Longleaf pine, compression wood, specific gravity, moisture content, bio-imaging

Development of a Leach Resistant Fire Retardant System for Wood

Mr. Alexander Scharf
Luleå University of Technology, Sweden

Abstract

Wood is a traditional and promising raw material which can meet the increasing demands on building products regarding sustainability and environmental impact. Recent developments in wood modification and engineered wood products have proven that wood is a serious competitor for steel and concrete constructions, not only in regard to sustainability.

The fire performance of materials used for construction is one of the main selection criteria. By introducing chemicals into wood, the usually high instability of untreated wood to fire, can be strongly limited. The reduction in fire resistance of fire-retardant-treated wood by exposure to outdoor conditions is often an issue when developing new retardants. Commonly used fire-retardants are inorganic salts of the elements phosphorus, nitrogen and boron. These compounds alter the thermal degradation of wood as single compounds, but also by synergistic effects. However, the solubility of inorganic salts makes them susceptible to leaching. This may lead to a loss in fire-performance but also to a higher introduction of leached out chemicals into the environment.

The durability of fire-retardant-treated wood in outdoor use is dependent on the leaching resistance. Östman and Tsantaridis (2017) showed that commercially fire-retardant-treated wood may lose its improved fire performance over time under service conditions. High amount of chemicals or protective paint systems allow the wood to keep its fire performance. Furuno et al. (1993) introduced water glass solution (sodium silicate) and boron compounds into wood with subsequent precipitation of silicate by soaking specimens in aluminum sulphate. The treated samples showed improved fire resistance and increased hygroscopicity. The precipitation of an insoluble inorganic substance like aluminum silicate may provide the wood with leaching resistance. It could lower the amount of needed chemicals and reduce the environmental impact of fire-retardant-treated wood.

In this project Scots pine (*Pinus Sylvestris*) samples with dimensions of 150x10x10 mm³ (L x W x T) were treated in a two-step process. Initial pressure impregnation with an aqueous solution containing guanylurea phosphate, borax and sodium silicate was followed by drying and then by soaking in aluminum sulphate for precipitation of insoluble compounds. The dried samples were exposed to leaching in water (EN 84) and limited oxygen index (LOI) was determined. The formed insoluble compounds may provide the material with leaching resistance to secure fire resistance under service conditions. The analyses were supported by thermogravimetric analysis, SEM and FTIR spectroscopy.

The applied 2-step treatment of the samples led to a reduction in leaching compared to the single treatment reference. Samples lost 80-90% of the initially introduced material but still showed improved fire resistance despite the leaching losses. Without the second treatment all compounds were leached out and had a fire resistance similar to untreated wood. Different ratios of the chemicals were tested, and the results were evaluated by multivariate data analysis. Higher concentrations of chemicals did not lead to a significant improvement in leaching resistance or fire retardancy.

Key words: wood modification, wood-mineral composite, water glass, leaching resistance, fire resistance

Mycelium-Assisted Bonding: Influence of the Aerial Hyphae on the Bonding Properties of White-Rot Modified Wood

Ms. Wenjing Sun
Dr. Mehdi Tajvidi
University of Maine, USA

Abstract

Biological pretreatment of wood before the production of bio-composites may increase the properties of the products by facilitating more adhesion. At the initial stage of colonization, white-rot fungi produce enzymes to breakdown lignin and hemicellulose. The generated phenoxy radicals can form covalent bonding by radical-radical coupling. At the same time, the aerial hyphae of the fungi grow on the surface and form fibrous films that cover the substrate. The formed mycelium changes the surface morphology and may contribute to the bonding by its constituents (protein and carbohydrates) under certain processing condition. The aim of this work is to investigate the influence of aerial hyphae on the bonding properties of white-rot modified wood veneers. The effect of the life condition and density of aerial fungi on the change of roughness, surface energy and bonding property of wood veneer were characterized and compared.

INFLUENCE OF PARTICLEBOARD THICKNESS AND VENEERS ON ODOR EMISSIONS

Qifan Wang¹, Jun Shen^{2*}
Northeast Forestry University, China

ABSTRACT

It is well known that the release of volatile organic compounds (VOCs) and odors from wood-based panels is harmful to human health. To reduce the problem of volatile organic compounds (VOCs) and odor emissions from veneered particleboard, this study focused on identifying odorant compounds and exploring the thickness and veneers on VOCs and odor emissions. Veneered particleboard coated with polyvinyl chloride (PVC) and melamine was studied via gas chromatography-mass spectroscopy/olfactometry. In total, 17 (55%) different odor types were identified from PVC-veneered particleboard among the 31 detected compounds. The predominant odor impressions of PVC veneered particleboard were *pungent*, *spicy* and *sweet*, and the main odorant compounds identified were aromatics, ketones, and esters. Over time, the odorant esters and ketones released from the PVC-covered particleboard decreased, whereas the release of alcohols and aldehydes odors increased, the release of aromatic compounds changed little. Among the 29 compounds detected from the melamine-veneered particleboard, 13 (45%) had odorant characteristics, the predominant odor impressions were *fresh*, *bitterness of plants* and *sour*, and the main odorant compounds identified were aromatics and esters. The release of odorant aromatic was relatively weak, but the release of ketones, esters, and aldehydes increased over time. In the early stage, the TVOC and total odor intensity was greatest, and over time, those values gradually decreased until a state of equilibrium was reached. There was no direct correlation between odor intensity and the mass concentration of different odorant compounds, but, for a odorant compound, its concentration affected the odor intensity somewhat. It is proved that veneer can help prevent the release of odors from particleboard, but it cannot completely prevent the emission for the voids in the structure of the veneer. Increasing thickness will increase the emission of VOCs and odor. Compared to veneered particleboard, the thickness influence odor emission from unvarnished particleboard more greatly.

Keywords: emission characteristics, melamine veneer, particleboard, PVC veneer, thickness, volatile organic compounds

INTRODUCTION

Volatile organic compounds (VOCs) from interior decorating have been identified as a silent killer by the medical community (Klepeis et al. 2001; Shen et al. 2001), and the problem of odor from furniture is receiving increasing attention (Nibbe 2017). People make subjective judgments about an environment based on its odors, and odors can affect a person's mood. Therefore, combining instrumental analysis with the subjective, human sense of smell provides more complete odor analysis and increases our ability to control VOCs.

In this study, a gas chromatography-mass spectroscopy-olfactometry (GC-MS-O) analysis combined the excellent separation techniques of gas chromatography, the abundant structural information produced by a mass spectrometer (Hsu and Shi 2013), and the human sense of smell, which can exceed that of many chemical detectors (Xia and Song 2006). This method has been widely used to select and evaluate active odor substances from complex mixtures (Zhang et al. 2009). At present, GC-MS-O has been used to analyze tobacco (Cotte et al. 2010), food (Frank et al. 2004; Gómez-Míguez et al. 2007; Machiels et al. 2003), and flavorings and spice (Choi 2005; Dharmawan et al. 2009) and has been used in environmental monitoring (Bulliner et al. 2006; Rabaud et al. 2002). However, GC-MS-O has not been widely used in the wood industry. GC-MS-O, based on GC-MS first proposed by Fuller et al. (1964) and Acree et al. (1976), analyzes the outflow components of GC-MS directly. In 1976, Acree et al. improved the original GC-MS technology by adding humidified air and by having evaluators smell the GC outflow after film chromatography processing. In

¹ Northeast Forestry University, 26 Hexing Road, Harbin 150040, China. Email: wangqifan66@163.com

² Northeast Forestry University, 26 Hexing Road, Harbin 150040, China. Email: shenjunnr@126.com. Corresponding author.

the mid-1980s, Acree et al. (1984) and Ullrich and Grosch (1987) used dilution-analysis to analyze the intensity of various odors at the same time, which made GC-MS technology widely applicable in many situations. Currently, there are four major GC-MS-O detection methods (Maarse and van der Heij 1994), including dilution analysis, time-intensity analysis, detection-frequency methods, and posterior-intensity evaluation. Time-intensity analysis was used in this study.

Polyvinyl chloride (PVC) and melamine veneers are widely used in furniture and interior decor composed of particleboard. In this study, those two types of veneered particleboards were analyzed. A Micro-Chamber/Thermal Extractor M-CTE250 (Markes International, Cardiff, UK) and GC-MS-O were used to analyze VOCs and odor emissions within a standard environment (temperature 23°C, relative humidity 40%). The characteristic odor of the compounds and their possible sources were identified, and variations caused by the thickness of the particleboard were investigated.

MATERIALS AND METHODS

Experimental Materials

In this experiment, PVC and melamine veneers were applied to particleboard ((Suofeiya, Guangdong, China). The density and moisture content of the particleboard were 0.60 g cm⁻³ and 8%, respectively. The samples were cut into round pieces (60 mm diameter) for the microchamber/thermal extractor apparatus, and the exposed surface area was 5.65 × 10⁻³ m². The samples were all taken from the center of the same plate to ensure the stability of the experimental material. For each experimental condition, four particleboard samples were used. After the edges of the specimens were sealed with aluminum foil to prevent the release of compounds, the samples were stored in polytetrafluoroethylene bags and refrigerated until needed.

Experimental Equipment

Sampling devices

The Micro-Chamber/Thermal Extractor μ -CTE 250 consists of four cylindrical micropools (each with a microcell diameter of 64 mm wide × 36 mm deep). The sampling temperature can be adjusted up to 250°C and can test four samples at the same time. The Tenax TA tube (Markes International Inc.) used had a stainless steel pipe body and contained 200 mg of 2,6-dibenzofurans porous polymer, which efficiently adsorbs or desorbs the VOC gases.

Detection and analysis device

Three detection and analysis devices were used. The Unity thermal analysis desorption unit (Markes International Inc.) used nitrogen as the carrier gas and was set with the following related parameters: thermal desorption temperature, 280°C; cold-trap adsorption temperature, -15°C; thermal analysis time, 10 min; and injection time, 1 min.

The second device used was a DSQ II series GC-MS (Thermo Fisher Scientific, Schwerte, Germany). Chromatography was performed with a DB-5 quartz capillary column (3,000 mm [length] × 0.26 mm [inner diameter] × 0.25 μ m [particle sizes]). Helium was used as the carrier gas with a constant velocity of 1.0 mL min⁻¹ by splitless injection. The chromatographic column was initially kept at 40°C for 2 min; then, the temperature was increased to 50°C (in 2°C min⁻¹ increments) and was held at that temperature for 4 min. Finally, the temperature was increased to 250°C (in 10°C min⁻¹ increments) and held at that temperature for 8 min. The injection port temperature was 250°C. The following GC-MS parameters were used: ionization mode, electron ionization; ion energy, 70 eV; transmission line temperature, 270°C; ion source temperature, 230°C; and mass scan range, 50 to 650 atomic mass units.

The third detection device used was a Sniffer 9000 Olfactory Detector (Brechtbühler, Echallens, Switzerland). Combined with GC-MS, quantitative and qualitative analyses can be made, and the compound's odor intensity can be reflected directly and recorded. The effluent of the GC capillary is divided into two parts, one part enters the mass spectrometer, and the other part is used for human sensory evaluation (ratio 1:1). The transmission line temperature was 150°C, and nitrogen was used as the carrier gas through a purge valve. Humidified air was added to prevent dehydration of the nasal mucosa.

Experimental Method

Sampling method

The experiment used the Tenax TA sampling tubes to adsorb a 2 liter amount of VOCs from the alkyd resin enamel coating on the particleboards under constant experimental conditions. Four samples were collected under each condition, with a sampling cycle of 8 hours; 2 L of the content was sampled and analyzed. After sampling, the Tenax TA sampling tubes were wrapped in polytetrafluoroethylene plastic bags until needed. The experimental scheme is shown in Table 1.

Analytic method

GC-MS and its built-in software were used to analyze the VOCs. The MS detection peaks were identified in the 2008 spectral library of the National Institute of Standards and Technology (NIST, Gaithersburg, MD) (matching degrees up to 800 or above). An internal-standard method was used in this experiment, with deuterium substituted for toluene at a concentration of 200 ng μL^{-1} , which added 2 μL . The internal-standard quantitative-analysis method used the following equation:

$$M_i = A_i \times \left(\frac{M_s}{A_s} \right) \quad (1)$$

where M_i is the mass of the internal standard added to the calibration standard; A_i and A_s are the peak areas of the products tested and the internal standard, respectively; and M_s is the amount of internal standard.

The time-intensity method was chosen for analysis of the compounds. As the sample was injected and the chromatogram yielded peaks, the human sensory-evaluation assessors perceived and described the column outflow from the odor port simultaneously. The timing of the odor, the odor type, and the intensity of the odor were recorded. After specific training, four assessors (with ages between 20 and 30 y, no history of smoking, and no olfactory organ disease) formed an odor-analysis evaluation group. The experimental environment was set to reference standard EN 13725-2003 (NSAI 2003). The room was well ventilated, and there were no peculiar smells within the room. The temperature was kept $23^\circ\text{C} \pm 2^\circ\text{C}$ throughout the entire experiment. Activities, such as eating, which might have an effect on indoor odors, were forbidden for 5 h before the experiment. Experimental results were recorded when the same odor characteristics were described by at least two assessors at the same time. The intensity value was based on the average value of the four assessors. The experiment's discrimination of odor intensity was based on the human sense of smell according to Japanese standards (Table 2; Ministry of Japan 1971).

After detection by GC-MS, the compounds were identified through the NIST (2008 standard spectrum) and Wiley (Hoboken, NJ) MS libraries. The primary odor compounds were identified by GC-MS-O. The refractive index value was calculated by the retention time of *n*-alkane under the same conditions (van Den Dool and Kratz 1963).

RESULTS AND DISCUSSION

Odor Constituents From Two Types of Veneered Particleboard

The odor constituents arising from of 8-mm-thick, PVC-veneered particleboard, melamine-veneered particleboard, and unfinished particleboard were identified within a standard environment (temperature, 23°C ; relative humidity, 40%). Figure 1 shows the intensities of the odor-time spectrum for the two types of veneered particleboard. The greatest odor intensities from the PVC- and melamine-veneered particleboard were less than that arising from the unvarnished particleboard, that is, both veneer coatings lessened the odor intensity of the particleboard alone. The odor intensities from the two veneered particleboard were not high, with an average intensity of about 1. Odors from the PVC veneer reached their maximum intensity at about 4 min and 30 min, whereas those from the melamine veneer reached their maximum in about 27 min and had a maximum intensity of 2.

Table 3 shows the primary odor constituents emitted from the two types of veneered particleboard and the particleboard alone. Aromatics comprised most of the VOCs in both the veneered boards and the particleboard itself. For comparison and analysis, Table 4 shows the composition of the odorant compounds from the particleboard. Table 5 shows the acute-toxicity classification by the World Health Organization of the various odorants released from each veneer and from the particleboard, whereas the actual constituents of the odor are shown in Tables 6 and 7.

Among the 31 compounds detected from PVC-veneered particleboard, 17 (55%) produced the odorant characteristics. According to the UL 2821-2013 standard (Greenguard Environmental Institute 2006), those of

the greatest concern were benzene, *p*-xylene, butyl acetate, and 2-butanol, which are listed as VOCs from office furniture if measured in greater than 10% of all products. Aromatics, ketones, and esters primarily produced the odors, which also contained alcohol and aldehyde odorants. The odor from aromatics produces a plant aroma and was in the low-toxicity range (only *p*-xylene was categorized as slightly toxic). Aromatics were emitted from the particleboard itself, from the raw materials used in PVC film coating, from the polyester resin stabilizer, from adhesives used in hot pressing, and from high-temperature lubricants used in making PVC. Ketones produced an aroma of soil and spice and were in the low to slight toxicity range. Ketones were mainly produced from the adhesive mundificant, the preparation of the adhesives, and the use of solvents. Most esters produce a fruity odor and had only slight toxicity. Esters were primarily produced by the making of PVC, from adhesive solvents, and from the particleboard itself. Only one constituent was categorized as alcohol, and it had a sour and bitter aroma and was classified as low toxicity. The alcohol was produced by the adhesive detergent, the PVC plasticizer, and the cosolvent. Aldehydes, which produce an aroma described as green grass, belong to low-toxicity classification and were derived from releases from the particleboard itself.

Among the 29 compounds detected from the melamine-veneered particleboard, 13 (45%) had odorant characteristics. The compounds of greatest concern from this veneer board were benzene, *p*-xylene, butyl acetate, and 2-butano, according to the UL 2821-2013 standard. Those compounds were listed as VOCs from office furniture if measured in greater than 10% of all products. Most of the odors from this type of veneered particleboard were aromatics and esters and, in small amounts, ketones and aldehydes. These aromatics produced the same plant aromas and were listed as being of low toxicity (only *p*-xylene was listed as slightly toxic, whereas naphthalene is moderately toxic). Aromatics were mainly produced by the particleboard itself, from the raw materials of synthetic ester, and from the adhesives and lubricants used in hot pressing. There was only a single compound in the ketone category—acetone—which has a slight toxicity classification, produces spicy odors, and is produced primarily from the adhesives, mundificants, and ester solvents. Esters produce fruity odors with only slight toxicity and are primarily produced by the adhesive solvents, resin solvents, organic solvents, and the particleboard itself. Aldehydes smell like green grass and have a low-toxicity classification. They were derived from the particleboard itself; however, the mass concentration from the aldehydes was greater than that released from the particleboard itself, so it may also be derived from the synthesis of resin in melamine-impregnated paper.

We found no direct correlation between odor intensity and the number of different odorant compounds in either veneered particleboard. A greater concentration of a single odorant compound, however, affected the odor intensity to a certain extent. The extent to which a constitution added to the overall atmosphere is related to the threshold of that species (Sun 2003). When a compound's mass concentration was relatively low, the sensory evaluators might not even perceive it as they would at a higher threshold. For example, the ethyl acetate (which smells fresh and sweet) and the acetic acid 1-methylpropyl ester (which smells like fresh and sweet fruit) from the melamine-veneered particleboards, which obviously have odor characteristics, were not detected at low mass concentrations.

Effect of Particleboard Thickness on VOCs and Odor Release

Figure 2 shows the TVOC and total odor intensity released by the different thicknesses of particleboard with PVC and melamine veneer coatings were basically the same. In the early stage, the TVOC and total odor intensity reached their maximum values; then, they decreased over time until a stable phase was achieved. The VOC concentrations decreased sharply on d 1 to d 7; after which, the rate of the decline slowed. That trend was due to the larger concentration difference between the VOCs and the external environment during the early release. According to the theory of mass transfer, the VOCs inside the particleboard plate continue to off-gas until the concentration difference disappears (Liu et al. 2017). The TVOC and total odor intensity for the two types of veneer studied were all less than particleboard itself with the same thickness. In the initial stages, PVC and melamine veneers effectively prevent the release of VOCs and odor from the particleboard, but over time, those distinctions gradually diminish, until no difference is seen between the veneers and the particleboard alone.

The TVOC and total odor intensity increases as the thickness of the particleboard increased. Compared with the TVOC, the increasing trend from the total odor intensity was not large. In the early stages, the TVOC and total odor intensity from 18-mm-thick PVC-veneered particleboard was greater than it was from the 8-mm-thick PVC-veneered particleboard at about $106.53 \mu\text{g m}^{-3}$ and $0.75 \mu\text{g m}^{-3}$, respectively. The TVOC and total odor intensity of 18-mm-thick melamine-veneered particleboard was stronger than it was for 8-mm-thick

melamine-veneered particleboard at about $113.73 \mu\text{g m}^{-3}$ and $0.5 \mu\text{g m}^{-3}$, respectively. When the emissions reached a plateau, the TVOC and total odor intensity of 18-mm-thick PVC-veneered particleboard were still more than they were in the 8-mm-thick boards at about $31 \mu\text{g m}^{-3}$ and $0.5 \mu\text{g m}^{-3}$, respectively. The TVOC of 18-mm-thick melamine-veneered particleboard was greater than it was for the 8-mm-thick board at about $12.72 \mu\text{g m}^{-3}$, whereas the total odor intensity remained the same. Substrate thickness produced those results, with the 18-mm-thick particleboard emitting more VOCs than 8-mm-thick board did (Sun 2011). The veneer prevented the release of only some of the particleboard gases, but because of the void structure within the veneer, it could not completely deter their release. The amount off-gassing from particleboard at various thicknesses was greater than it was for veneered particleboard. In their initial state, the concentration difference between two different thicknesses of particleboard was $549.69 \mu\text{g m}^{-3}$, whereas the concentration difference from two different thicknesses for the PVC-veneered particleboard was $106.53 \mu\text{g m}^{-3}$ and was $113.73 \mu\text{g m}^{-3}$ from the melamine surface. Similarly, at equilibrium, the concentration differences between the two different thicknesses of particleboard was $92.91 \mu\text{g m}^{-3}$, whereas the difference in the thickness of PVC veneer was $31.00 \mu\text{g m}^{-3}$ and was $12.72 \mu\text{g m}^{-3}$ for the melamine surface.

VOCs and Odors Released From Two Types Of Veneered Particleboards

Figure 3 shows the percentage of TVOC and total odor intensity in the initial and stable phases of PVC- and melamine-veneered particleboard. The gases released from the particleboard with a PVC veneer included aromatics, alkanes, ketones, esters, alcohols, aldehydes, and alkenes; among which, aromatics, ketones, esters, alcohols, and aldehydes had odorant characteristics. The gases released from melamine-veneered particleboard included aromatics, alkanes, ketones, esters, aldehydes, and alkenes; among which, aromatics, ketones, esters, and aldehydes had odorant characteristics.

For the PVC-veneered particleboards, over time, the odorant compounds emitted were esters and ketones, which decreased, whereas the release of alcohols and aldehydes strengthened over time. Aromatics showed little change in odor intensity over time. In a state of equilibrium, the proportion of VOC components, from most to least, were esters (34.26%), aromatics (16.98%), alkanes (14.16%), ketones (13.26%), alcohols (11.48%), and aldehydes (9.86%) from the PVC veneer. The proportion of gases with odor components, from most to least were esters (50.26%), aromatics (15.29%), ketones (13.11%), alcohols (11.48%), and aldehydes (9.86%).

For melamine-veneered particleboards, emissions of aromatics decreased over time, whereas the release of ketones, esters, and aldehydes increased somewhat. In a state of equilibrium, the proportion of VOC components, from most to least, were aromatics (59.58%), esters (26.58%), aldehydes (7.26%), and ketones (6.58%). The proportions of gases with odor components, most to least, were aromatics (44.25%), esters (20.01%), aldehydes (14.89%), alkanes (12.58%), and ketones (8.27%).

CONCLUSIONS

PVC- and melamine-veneered particleboards were analyzed by GC-MS-O in this experiment. The results showed that the primary odor emissions released from PVC particleboards were aromatics, ketones, and esters, whereas the melamine particleboard off-gassed aromatics and esters. Both the TVOC and the odor intensity increased with thicker particleboards, even when coated with either veneer. The release characteristics of TVOC and total odor intensity from PVC and melamine particleboards remained consistent with the different thicknesses. In the early stage, the TVOC and total odor intensity was greatest, and over time, those values gradually decreased until a state of equilibrium was reached. Both veneers slowed the release of gas from the particleboard, but because of the void structure of veneers, they could not completely prevent the release. Thickness had a greater effect on the particleboard itself than it did on the veneered particleboard. There was no direct correlation between odor intensity and the number of different odorant compounds, but, for any particular odorant compound, its concentration affected the odor intensity somewhat. Over time (28 d), the off-gassing of esters and ketones from the PVC particleboard weakened, whereas the release of alcohols and aldehydes increased. The release of aromatic compounds changed little with time. For the melamine particleboard, the aromatic compounds weakened over time, whereas the release of ketones, esters, and aldehydes increased.

LIST OF FIGURES

Figure 1. Odor–time intensity spectrum from particleboard and two types veneered particleboard. (a) Particleboard. (b) Particleboard with polyvinyl chloride (PVC) veneer. (c) Particleboard with melamine veneer.

Figure 2 The trends in total volatile organic compound (TVOC) and odors released from different thicknesses of particleboard coated with polyvinyl chloride (PVC) and with melamine. (a) TVOC of PVC-veneered particleboard. (b) Total odor intensity from PVC-veneered particleboard. (c) TVOC from melamine-veneered particleboard. (d) Total odor intensity from the melamine-veneered particleboard

Figure 3. The percentage of various constituents of the gases released from polyvinyl chloride (PVC) and melamine particleboard and the mass concentration of the odorant substances during the initial and stable phases (a) Volatile organic compounds (VOC) from PVC-coated particleboard. (b) Odorant components from PVC-veneered particleboard. (c) VOC compounds from melamine particleboard. (d) Odorant components from the melamine particleboard.

REFERENCES

- Acree TE, Barnard J, Cunningham DG (1984) A procedure for the sensory analysis of gas chromatographic effluents. *Food Chem* 14(4):273-286.
- Acree TE, Butts RM, Nelson PR, Lee, CY (1976) Sniffer to determine the odor of gas chromatographic effluents. *Anal Chem* 48(12):1821-1822.
- Bulliner EA, Koziel JA, Cai LS, Wright, D (2006) Characterization of livestock odors using steel plates, solid-phase microextraction, and multidimensional gas chromatography-mass spectrometry-olfactometry. *J Air Waste Manag Assoc.* 56(10):1391-1403.
- Choi HS (2005) Characteristic odor components of kumquat (*Fortunella japonica* Swingle) peel oil. *J Agric Food Chem* 53(5):1642-1647.
- Cotte VME, Prasad SK, Wan PHW, Linforth, RST, Taylor, AJ (2010) Cigarette smoke: GC-Olfactometry analyses using two computer programs. Pages 498-502 in I Blank, M Wüst, C. Yeretzián, eds. *Expression of Multidisciplinary Flavour Science—Proc 12th Weurman Symposium, July 2008, Interlaken, Switzerland.* Zürcher Hochschule für Angewandte, Wissenschaften, Winterthur.
- Dharmawan J, Kasapis S, Sriramula P, Lear MJ, Curran P. (2009) Evaluation of aroma-active compounds in Pontianak orange peel oil (*Citrus nobilis* Lour. Var. *micropa* Hassk) by gas chromatography-olfactometry, aroma reconstitution, and omission test. *J Agric Food Chem* 57(1):239-244.
- Frank CO, Owen CM, Patterson J. (2004) Solid phase microextraction (SPME) combined with gas-chromatography and olfactometry-mass spectrometry for characterization of cheese aroma compounds. *LWT Food Sci Technol* 37(2):139-154.
- Fuller GH, Stellencamp R, Tisserand GA. (1964) The gas chromatograph with human sensor: perfumer model. *Ann N Y Acad Sci.* 116:711-724.
- Gómez-Miguez MJ, Cacho JF, Ferreira V, Vicario IM, Heredia FJ (2007) Volatile components of Zalema white wines. *Food Chem* 100(4):1464-1473.
- Greenguard Environmental Institute (2006) Standard Method for Measuring and Evaluating Chemical Emissions From Building Materials, Finishes and Furnishings Using Dynamic Environmental Chambers. GG Publications UL 2821-2013, Marietta, GA.
- Hsu CS, Shi Q. (2013) Prospects for petroleum mass spectrometry and chromatography. *Sci. China Chem.* 56(7):833-839.
- Klepeis NE, Nelson WC, Ott WR, Robinson JP, Tsang AM, Switzer P, Behar JV, Hern SC, Engelmann WH (2001) The National Human Activity Pattern Survey (NHAPS): A resource for assessing exposure to environmental pollutants. *J Expo Anal Environ Epidemiol* 11(3): 231-252.
- Liu WJ, Shen J, Wang QF (2017) Design of DL-SW micro-cabin for rapid detection and analysis of VOCs from wood-based panels. *J For Eng* 2(4):40-45. In Chinese.

- Maarse H, van der Heij DG, eds. (1994) Pages 211–220 *in* Trends in flavour research, Proc 7th Weurman Flavour Res Symp, 15-18 June 1993, Noordwijkerhout, Netherlands. Elsevier, Amsterdam.
- Machiels D, van Ruth SM, Posthumus MA, Istasse L (2003) Gas chromatography-olfactometry analysis of the volatile compounds of two commercial Irish beef meats. *Talanta* 60(4):755-764.
- Ministry of the Environment. (1971) Law No. 91: Offensive Odor Control Law. Government of Japan, Tokyo, Japan.
- NSAI. National Standards Authority of Ireland. (2003) Air Quality—Determination of Odour Mass Concentration by Dynamic Olfactometry. SN EN 13725-2003. NSAI, Dublin, Ireland.
- Nibbe N (2017) How to select train and maintain a human sensory panel. *In* Olfasense: Proc Odour Workshop on Product and Material Testing. 26-27 January 2017, Kiel, Germany.
- Rabaud N, Ebeler SE, Ashbaugh LL, Flocchini RG (2002) The application of thermal desorption GC/MS with simultaneous olfactory evaluation for the characterization and quantification of odor compounds from a dairy. *J Agric Food Chem.* 50(18):5139-5145.
- Shen XY, Luo XL, Zhu LZ (2001) Progress in research on volatile organic compounds in ambient air. *J Zhejiang Univ (Sci Ed)* 28(5):547-556. In Chinese with abstract in English.
- Sun BG (2003) Edible flavoring surgery. Chemical Industry Publishing House, Beijing, China. In Chinese.
- Sun SJ. (2011) Study on evaluation of the influencing factors for VOC emissions from wood-based panels. MS thesis. Northeast Forestry University, Harbin, China.
- Ullrich F, Grosch W (1987) Identification of the most intense volatile flavor compounds formed during autoxidation of linoleic acid. *Z Lebensm Unters Forsch.* 1987; 184(4):277-282.
- van Den Dool, H., Kratz, PD (1963) A generalization of the retention index system including linear temperature programmed gas-liquid partition chromatography. *J. Chromatogr.* 11:463–470.
- Xia LJ, Song HL (2006) Aroma detecting technique—application of the GC-olfactometry. *Food Ferment Ind.* 32(1):83-87. In Chinese.
- Zhang Q, Wang XC, Liu Y (2009) Applications of gas chromatography-olfactometry (GC-O) in food flavor analysis. *Food Sci* 30(3):284-287.

TABLE 1 Testparameters

Testparameters	Condition
Exposure area /m ²	5.65×10 ⁻³
Cabin volume /m ³	1.35×10 ⁻⁴
Loading rate /(m ² /m ³)	41.85
The ratio of air exchange rate and loading factor /(m ³ ·m ⁻² ·h ⁻¹)	0.5±0.05
Temperature /°C	23±1
Relative humidity /%	40±5

TABLE 2 Odor intensity Criteria (Japan)

Odor intensity	0	1	2	3	4	5
Representation	Odorless	Barely perceptible (Detection threshold)	Slightly perceptible (Identification threshold)	Obvious perceptible	Strong smell	Extremely strong smell

TABLE 3 Main components emitted from two types veneer particleboards and particleboards

Classification	VOCs components of particleboard	VOCs components of PVC veneer particleboard	VOCs components of melamine veneer particleboard
Aromatic compounds	Benzene, Toluene, Ethylbenzene, 1,3-dimethyl-Benzene, Styrene, 1-ethyl-2-methyl-Benzene, propyl-Benzene, 1-ethyl-3-methyl-Benzene, 1-ethyl-4-methyl-Benzene, 1,2,4-trimethyl-Benzene, 1-methyl-2-(1-methylethyl)-Benzene, 1-methylene-1H-Indene, 1,2-Benzisothiazole, hexyl-Benzene, 1-methyl-Naphthalene, Acenaphthene, Fluorene, Phenanthrene, Dibutyl phthalate	Benzene, Toluene, Ethylbenzene, 1,3-dimethyl-Benzene, p-Xylene, 1-ethyl-3-methyl-Benzene, 1-ethyl-4-methyl-Benzene, 1,3,5-trimethyl-Benzene, 1,2,3-trimethyl-Benzene, 1-methylene-1H-Indene, 1-methyl-Naphthalene, Dibenzofuran	Benzene, Toluene, Ethylbenzene, p-Xylene, 1,3-dimethyl-Benzene, 1-ethyl-3-methyl-Benzene, 1-ethyl-4-methyl-Benzene, 1,2,3-trimethyl-Benzene, 1,2,4-trimethyl-Benzene, 1-methyl-3-(1-methylethyl)-Benzene, Naphthalene, 2-methyl-Naphthalene, 1-methyl-Naphthalene, Acenaphthene, Dibenzofuran, Fluorene
Alkanes	hexamethyl-Cyclotrisiloxan, octamethyl-Cyclotetrasiloxane, Undecane, dodecamethyl-Cyclohexasiloxane	dimethoxy-Methane, 3-methylene-Heptane, 2,2,4,6,6-pentamethyl-Heptane, Decane	dimethoxy-Methane, Hexane, Decane, 5-ethyl-2,2,3-trimethyl-Heptane
Ketones	(1S)-1,7,7-trimethyl-Bicyclo[2.2.1]heptan-2-one	Acetone, 2-Butanone, Methyl Isobutyl Ketone, 2-methyl-Cyclopentanone, (1S)-1,7,7-trimethyl-Bicyclo[2.2.1]heptan-2-one	Acetone, Cyclohexanone, (1S)-1,7,7-trimethyl-Bicyclo[2.2.1]heptan-2-one
Esters	Acetic acid, butyl ester	2-methyl-2-Propenoic acid, methyl ester, Acetic acid, 1-methylpropyl ester, Acetic acid, 2-methylpropyl ester, Acetic acid, butyl ester, 2-Pentanol, acetate, 2-methyl-2-Propenoic acid, butyl ester, Ethyl Acetate	Ethyl Acetate, Acetic acid, 1-methylpropyl ester, Acetic acid, 2-methylpropyl ester, Acetic acid, butyl ester, 2-Pentanol, acetate
Alcohols	2-ethyl-1-Hexanol	2-Butanol, 2-methyl-1-Propanol	-
Aldehydes	Hexanal, Nonanal	Hexanal	Hexanal
Alkenes	(ñ)-2,6,6-trimethyl-Bicyclo[3.1.1]hept-2-ene, D-Limonene	2-Butene, 3,6,6-trimethyl-Bicyclo[3.1.1]hept-2-ene	Copaene

TABLE 4 Composition of odorant compounds of particleboard

Compounds	Retention time(RT)	Retention index(RI)	Mass concentration/ $\mu\text{g}\cdot\text{m}^{-3}$	Odor character	Odor intensity
Aromatic compounds					
Benzene	6.42	642	4.56	Burnt	1
Ethylbenzene	15.00	849	187.25	Aromatic	1
1,3-dimethyl-Benzene	15.46	858	152.56	Aromatic, sweet	2
Styrene	16.37	875	101.16	Charcoal, cream	3
1-ethyl-2-methyl-Benzene	18.25	912	2.42	Mixed smell	0
1,2,4-trimethyl-Benzene	21.38	981	4.15	Aromatic	0
1-methylene-1H-Indene	28.13	1165	75.60	Bitter, oil	2
1-methyl-Naphthalene Aldehyde	31.67	1340	9.44	Wheat	1
Hexanal	11.20	775	6.25	Sweet	2
Nonanal	25.43	1085	3.31	Oil, flower, fresh	1
Esters					
Acetic acid, butyl ester	12.39	800	20.47	Fresh and sweet fruit	1
Alkenes					
D-Limonene	23.09	1023	3.36	Lemon	0

TABLE 5 Acute toxicity classification of compounds by World Health Organization

Toxicity classification	Rats orally LD50 (mg/kg)	Rats inhalation and dead 1/3-2/3 in 4 hours	Rabbit transdermal LD50 (mg/kg)
Severe toxicity	≤ 1	≤ 10	≤ 5
Highly toxicity	1-50	10-100	5-43
Moderate toxicity	51-500	101-1000	44-350
Low toxicity	501-5000	1001-10000	351-2180
Slight toxicity	5001-15000	10001-100000	2181-22590
Non-toxic	>15000	>100000	>22600

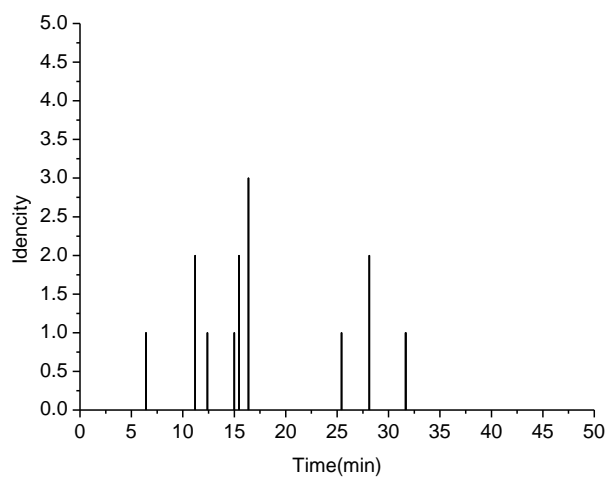
TABLE 6 Composition of odorant compounds from PVC venveer particleboards

Compounds Retention Time	Retenti on index(RI)	Mass concentr ation/ $\mu\text{g}\cdot$ m^{-3}	Toxicity classificati on	Odor character	Odor intensit y	Possible sources
Aromatic compounds						
Benzene	5.05	3.73	Low toxicity	Burnt	0.5	Particleboard emission
1,3-dimethyl-Benzene	13.55	43.00	Low toxicity	Fresh Pungent, aromatic	1	Particleboard emission
p-Xylene	13.63	13.62	Slight toxicity		0	PVC film coating agent and adhesive
1,3,5-trimethyl-Benzene	19.88	4.63	Low toxicity	Mixed smell	1.75	Stabilizer of polyester resin
1-methylene-1H-Indene	27.32	9.53	Low toxicity	Bitter, oil	0	Particleboard emission
1-methyl-Naphthalene	30.90	4.55	Low toxicity	Wheat	1	Particleboard emission
Dibenzofuran	38.36	2.41	Low toxicity	Almond, licorice	0	High temperature lubricant in the preparation of PVC
Ketones						
Acetone	3.34	6.39	Slight toxicity	Special spicy Pungent,	0	Adhesive mundificant
2-Butanone	4.11	7.27	Low toxicity	spicy, sweet	2	Adhesive mundificant
Methyl Isobutyl Ketone	6.97	64.00	Low toxicity	Pleasant fragrance	1.25	Adhesive
2-methyl-Cyclopentanone	14.96	92.44	Low toxicity	Soil	1	Solvent
Esters						
Acetic acid, 1-methylpropyl ester	7.60	330.67	Slight toxicity	Fresh and sweet fruit	0.75	Preparation of PVC
Acetic acid, 2-methylpropyl ester	8.30	1.20	Slight toxicity	Fresh and sweet fruit	0	Preparation of PVC
Acetic acid, butyl ester	10.27	18.38	Slight toxicity	Fresh and sweet fruit	0	Particleboard emission, organic solvent
Ethyl Acetate	4.31	5.84	Slight toxicity	Fresh and sweet	0	Adhesive solvent
Alcohols						
2-Butanol	4.19	1.38	Low toxicity	Sour, bitter	0	Adhesive mundificant, PVC plasticizer and cosolvent
Aldehydes						
Hexanal	9.50	5.10	Low toxicity	Grass	0	Particleboard emission

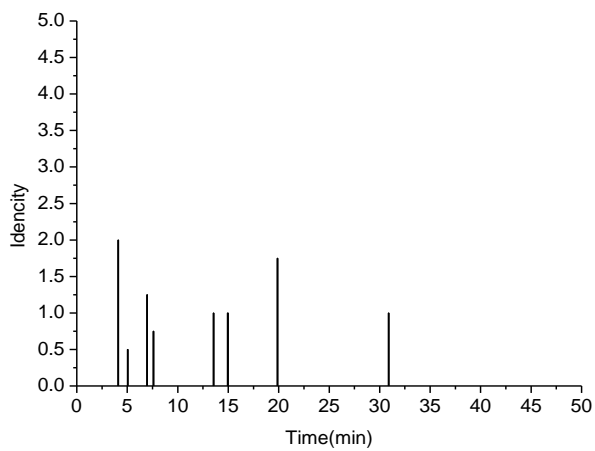
TABLE 7 Composition of odorant compounds from melamine venveer particleboards

Compounds Retention Time	Retenti on index(RI)	Mass concentr ation/ $\mu\text{g}\cdot$ m^{-3}	Toxicity classificati on	Odor character	Odor intensit y	Possible sources
Aromatic compounds						
Benzene	5.06	8.91	Low toxicity	Burnt	0.75	Particleboard emission, additive
Ethylbenzene	13.05	104.30	Low toxicity	Aromatic Pungent, aromatic	0	Particleboard emission
p-Xylene	13.57	133.95	Slight toxicity		1	Adhesive
1,3-dimethyl- Benzene	14.84	80.79	Low toxicity	Fresh	0.75	Particleboard emission
Naphthalene	27.33	69.56	Moderate toxicity	Fresh, bitterness of plants,sour	1.75	Raw material of resin
1-methyl- Naphthalene	31.39	15.16	Low toxicity	Wheat	1	Particleboard emission
Dibenzofuran	38.35	11.42	Low toxicity	Almond, licorice	1	Lubricant
Ketones						
Acetone	3.36	16.28	Slight toxicity	Special spicy	0	Adhesive mundificant, Resin solvent
Esters						
Ethyl Acetate	4.33	10.65	Slight toxicity	Fresh and sweet	0	Adhesive solvent
Acetic acid, 1- methylpropyl ester	7.65	27.72	Slight toxicity	Fresh and sweet fruit	0	Resin solvent
Acetic acid, 2- methylpropyl ester	8.33	5.03	Slight toxicity	Fresh and sweet fruit	0	Resin solvent
Acetic acid, butyl ester	10.32	77.10	Slight toxicity	Fresh and sweet fruit	0.5	Particleboard emission, organic solvent
Aldehydes						
Hexanal	9.53	16.58	Low toxicity	Grass	1	Particleboard emission, Synthesis of resin

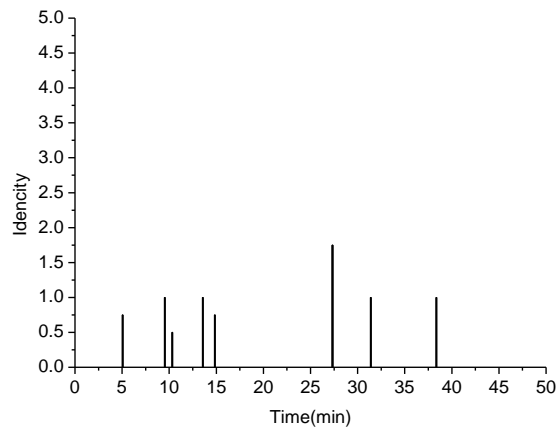
FIGURE 1



(a)

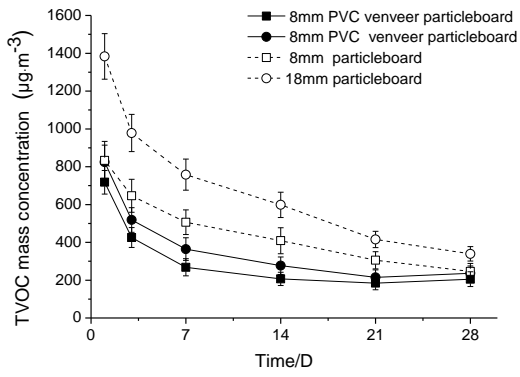


(b)

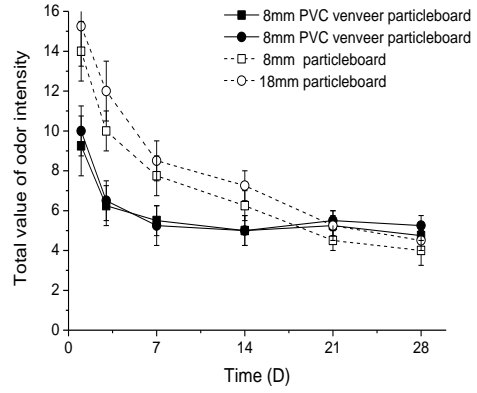


(c)

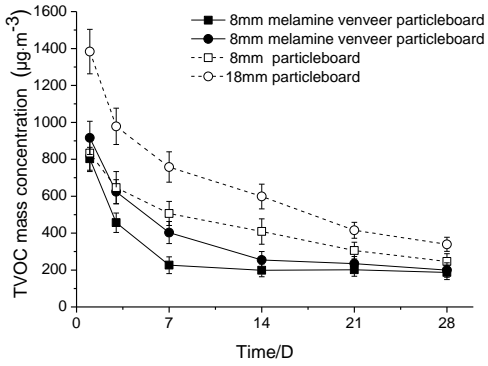
FIGURE 2



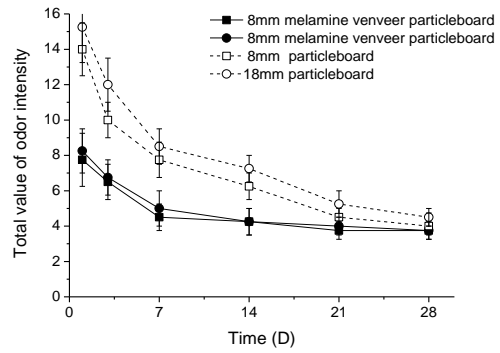
(a)



(b)

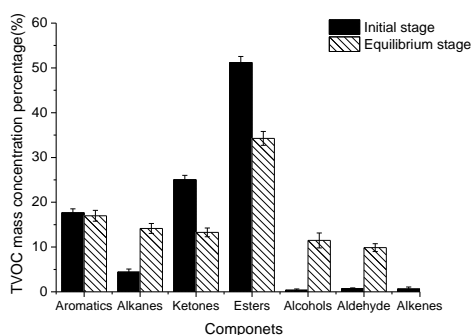


(c)

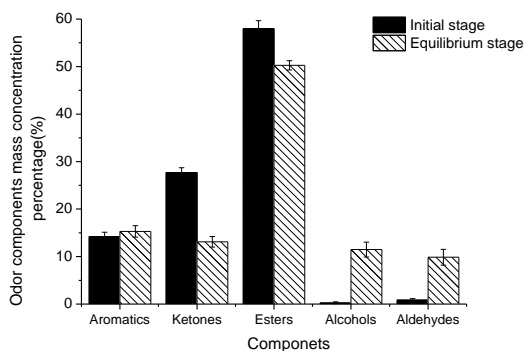


(d)

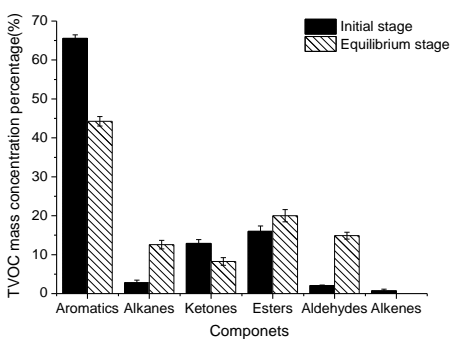
FIGURE 3



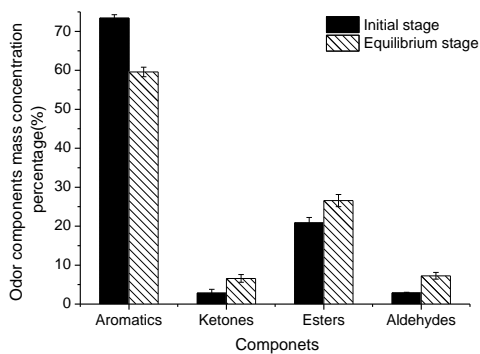
(a) VOCs component of PVC particleboards



(b) Odorant Components of PVC particleboards



(c) VOCs component of melamine particleboards



(d) Odorant Components of melamine particleboards

Converting Industrial Waste Cork to Biochar as Cu (II) Absorbents via Effective Pyrolysis

Qihang Wang, Zongyuan Lai, Demiao Chu, Jun Mu*

Key Laboratory of Wood Material Science and Utilization (Beijing Forestry University), Ministry of Education, Beijing, 100083, P.R. China;

*Corresponding author: mujun@bjfu.edu.cn

Abstract:

Cork is a renewable biomass material with many excellent properties, which makes it widely applicable to a diverse array of applications all over the world. Cork powders being generated throughout the fabrication stages of various cork products is the main waste of the cork industry. It is with an annual production estimated to reach around 50,000 t only by the granulation process. This aspect of cork manufacturing is considered highly problematic, as the cork powders has almost no commercial value, and thus, has been mainly combusted for energy generation, due to its high calorific value. The purpose of this study was to use cork waste to prepare cork-based biochar (CBC) that can be used to removal heavy metal ions from wastewater, which could be a more eco-friendly, cost-effective, and sustainable cork waste recycling method.

The cork powders were heated under different pyrolysis temperatures (450, 550, 650, and 750°C) and pyrolysis time (0.5, 1.0, 1.5, and 2.0 hr) at 10 °C/min in a tubular electric furnace under nitrogen gas to obtain CBC. The physicochemical properties of CBC were characterized by elemental analysis, FT-IR, XRD, N₂ adsorption and SEM. The adsorption capacity of CBC on heavy metal ions was further evaluated by Cu ion adsorption testing.

The results showed that the CBC produced under conditions of higher pyrolysis temperature and time, has a more stable carbon structure, larger specific surface area, and enhanced Cu ion adsorption capacity. The maximum specific surface area of CBC prepared at 750°C for 0.5 h was 392.5m²/g, which surpasses most other biochars reported in previous studies, which are beneficial to the application of wastewater management. The SEM image demonstrated that the biochar retains the special hollow polyhedral cell structure of raw material cork. Furthermore, a large number of pores formed on the cell wall after high temperature pyrolysis, causing independent cells to communicate with each other. Finally, CBC exhibits superior Cu ion adsorption capacity (18.5mg/g) with a shorter equilibrium time, which gives it a competitive advantage to similar adsorbents.

In summary, pyrolysis of cork waste to obtain biochar is a solution to recycling these large residues, and facilitates adsorbent development with no exploitation of natural resources. In addition, it also reduces the carbon footprint by taking advantage of industrial by-products that have no significant value. Therefore, regardless of ecological or economic perspective, this method can be regarded as a feasible alternative to recycling waste in the cork industry.

Key words:

Industrial Waste Cork, Biochar, Cu (II) Absorbents, Pyrolysis

A novel method for fabricating an electrospun polyvinyl alcohol/cellulose nanocrystals composite nanofibrous filter with low air resistance for high-efficiency filtration of particulate matter

Qijun Zhang[†], Qian Li ^{*,‡†}, Timothy M. Young[†], David P. Harper[†], Siqun Wang ^{*,†}

[†]Center for Renewable Carbon, University of Tennessee, 2506 Jacob Drive, Knoxville, TN 37996, USA

[‡]School of Engineering, Zhejiang A&F University, 666 Wusu Street, Hangzhou 311300, China

*To whom correspondence should be addressed

Qian Li, Email: liqian_polymer@126.com

Siqun Wang, E-mail: swang@utk.edu

Abstract

Particulate matter (PM) air pollution poses a risk to public health, especially in rapidly industrializing countries. One major way to protect individuals from PM exposure is to use fiber-based filters for indoor air purification. In this study, a new low pressure drop poly(vinyl alcohol) (PVA)/cellulose nanocrystals (CNCs) composite nanofibrous filter was fabricated using electrospinning. This electrospun PVA/CNCs filter was demonstrated as an air filter for the first time. The CNCs not only contributed to the PVA/CNCs system as mechanical reinforcement agents, but also increased the surface charge density of the electrospinning solution, thereby reducing fiber diameter. The thinner fibers reduced pressure drop significantly and increased the efficiency of the PM removal. Our results indicate that high PM_{2.5} removal efficiency was achieved (99.1%) under extremely polluted conditions (PM_{2.5} mass concentration > 500 $\mu\text{g m}^{-3}$) with low pressure drop (91 Pa) at an airflow velocity of 0.2 m s^{-1} . Considering that PVA and CNCs are both nontoxic and biodegradable, this high-efficiency composite filter with low air resistance is environmentally friendly and shows promise in indoor air purification applications.

Keywords: Air filtration; Cellulose nanocrystals; Electrospinning; PM_{2.5}; PM₁₀

Regular Posters:

Environmental Impacts of Redwood Lumber: A Cradle-to-Gate Assessment

Kamalakanta Sahoo^{1} – Richard D. Bergman²*

¹ Post-doctoral Research Fellow, USDA Forest Service, Forest Products Laboratory, Madison, Wisconsin, USA, * *Corresponding author*

kamalakanta.sahoo@usda.gov

² Supervisory Research Wood Scientist, USDA Forest Service, Forest Products Laboratory, Madison, Wisconsin, USA

richard.d.bergman@usda.gov

Abstract

Global demand for construction materials has grown greatly in the last century, contributing to unsustainable growth and detrimental impacts on the ecosystem. To aid in sustainable growth and reduce our environmental footprint, renewable construction materials, such as lumber, have been incorporated into green building activities. To quantify the environmental footprints of construction products, a method called life-cycle assessment is used. This study determined the environmental attributes associated with manufacturing redwood lumber in northern California using the unit process approach (1 m³ or 380 oven-dry kg of lumber as the declared unit). The cradle-to-gate cumulative fossil energy demand of redwood lumber was found to be 1,120 MJ/m³ of redwood lumber produced. Greenhouse gas emissions were estimated at about 69.8 kgCO₂e/m³ of lumber produced excluding carbon storage in the lumber. Upstream operations (including silviculture, harvesting, and transport) and mainstream (mill) operations (including sawing, drying, and planing) contributed 52% and 48% of total greenhouse gas emissions, respectively. Carbon stored in redwood lumber is about twelve times more than its cradle-to-gate carbon footprint, a substantial environmental benefit. Many redwood lumber products such as decking are used green, and a large portion of green lumber is only air-dried, which has a much lower carbon footprint than kiln-dried lumber. In addition, even if the lumber requires kiln-drying, the heat comes from burning on-site mill residues, considered a carbon-neutral energy source. For wood production life-cycle stages, force- (kiln-) drying lumber tends to use a lot of thermal energy (albeit mostly from mill residues) compared with the whole life cycle. However, the carbon footprint for the redwood lumber drying unit process is low, only 14%, because the product tends to be used green. Furthermore, using mill residues to produce on-site combined heat and power (co-generation) was shown to be the most efficient way to reduce the environmental footprints of lumber production. Overall, the results showed that redwood lumber used in the construction sector can act as a carbon sink and can mitigate impacts to our ecosystem.

Key words: Lifecycle assessment, redwood, lumber, forest products, co-generation, carbon, green building materials, EPD, carbon footprint

Introduction

Globally, the use of raw materials, especially for construction, has increased exponentially since the nineteenth century (Matos 2017). Buildings and construction account for more than 35% of global final energy use and nearly 40% of energy-related CO₂ emissions (Abergel et al. 2017). The demand for construction materials is predicted to grow because of global population growth and increased standard of living (Bringezu et al. 2017). However, climate change and resource depletion pose a serious threat to human civilization. Resources from forests provide renewable construction materials, pulp and paper, energy, bioproducts, and more. Forests sequestering carbon and wood products storing carbon have the greatest potential to mitigate climate change (Canadell and Raupach 2008, Malmheimer et al. 2011). Combining wood carbon storage and avoiding greenhouse gas (GHG) emissions by using forest-based instead of fossil fuel-based construction materials, especially in building construction, is one of the most efficient options to mitigate climate change (Bergman et al. 2014a, Oliver et al. 2014, Sathre and O'Connor 2010). Because of environmental awareness and regulations, documenting the environmental performance of building products using life-cycle assessment (LCA) is becoming widespread and is the new normal. Quantifying environmental performance for structural wood products is one way to generate green building certifications (Bergman et al. 2014b), scientific documentation [e.g., environmental product declarations (EPDs)], and provide information to stakeholders including consumers, regulating agencies, and policymakers. EPDs, based on the underlying LCA data, not only provide verified data on the environmental performance of products and services but can also identify the environmental hot spots for continuous improvements in a consumer-friendly format (ISO 2006a, ISO 2007).

Redwood lumber is used to build decking, fencing, etc. in the western United States, and its demand has increased since the great recession because of the growing housing market. Bergman et al. (2014b) estimated the environmental impact of redwood decking (38 by 138 mm) compared with other alternative materials. However, with changes in the manufacturing process, sawmill size, and sawlog procurement distances, other input resources especially electricity and drying requirements to produce redwood lumber of various dimensions have gone through substantial changes. Therefore, the objective of this study was to measure the environmental performance of redwood lumber (*Sequoia sempervirens*) and compare the results with previous results. This will serve two important purposes: (i) the study results will be used to develop a redwood lumber EPD, and (ii) the changes (positive and negative) in the environmental performance of redwood lumber will be tracked. This study lists material flows, energy consumption, and emissions for the redwood lumber manufacturing process on a per-unit basis. Primary data were collected by surveying redwood sawmills primarily with a questionnaire. Peer-reviewed literature provided secondary data. Material balances constructed with a spreadsheet algorithm used data from primary and secondary sources. From material and energy inputs and reported emissions, SimaPro 8 software (PRé Consultants,

Amersfoort, the Netherlands) modeled the estimates for raw material consumption, environmental outputs, and associated impacts (Pré-Consultants 2017).

Materials & Methods

Scope

This study followed the ISO 14040 and 14044 international standards to perform LCA of redwood lumber (ISO 2006b, ISO 2006c) and estimated the cradle-to-gate life-cycle impacts of redwood lumber produced in northern California, USA. The scope of this study covered the unit operations starting from forest management (silvicultural) and harvesting of redwood to the production of redwood lumber, i.e., redwood log transportation, sawing, drying, and planing. The focus of this study was the sawmill operations. However, the data related to redwood forest management and harvesting were taken from a previous study (Han et al. 2015). Major redwood lumber producing sawmills in northern California were surveyed and visited in 2018 to collect detailed information on redwood log logistics and lumber manufacturing. The surveyed mills provided detailed annual production data on their facilities including log volumes and transport distance, on-site fuel and materials consumption, electrical usage, and lumber production for 2017. This study included all dimensions and categories (redwood lumbers are classified into rough-green, rough-dry, and planed-dry) of redwood lumber produced from three sawmills. The studied sawmills produced redwood lumber along with another softwood species, i.e., Douglas-fir (*Pseudotsuga menziesii*). Redwood and Douglas-fir were tracked separately to remove any effect from processing Douglas-fir. Given that lumber production generates mill residues, an allocation approach was necessary to assign the environmental impacts associated with the final product of redwood lumber and its associated coproducts. For this analysis, all environmental impacts were assigned to the redwood lumber and none to its coproducts because redwood lumber and its coproducts have a large price differential (>10:1). This is consistent with previous redwood decking LCA studies (Bergman et al. 2013, Bergman et al. 2014b).

Declared Unit

It is important to provide a reference to which inputs (materials and energy) and outputs (products/coproducts and emissions) can be related. LCAs use a functional or declared unit as the reference depending on the scope. A declared unit of 1 m³ of redwood lumber was used in this analysis because the whole life cycle (i.e., cradle-to-grave) was not covered. The life-cycle inventory (LCI) flows and life-cycle impact assessment (LCIA) results were reported on this per-declared-unit basis.

System Boundary and Unit Processes

This study considered the cradle-to-gate system boundary of redwood lumber, which included resource extraction (cradle) and product manufacturing. The boundary ended at the mill gate with products ready to ship. Figure 1 shows the system boundary of the cradle-to-gate LCA study of redwood lumber. Demarcating the boundary helps to track the material and energy flows crossing the boundary precisely. To track flows tied to redwood lumber production, two system boundaries were considered: (i) the gate-to-gate boundary (the dotted line in Fig. 1)

shows the on-site system boundary of the mill and the four unit processes involved (log yard, sawing, drying, and planing); and (ii) the cradle-to-gate boundary shown by the solid line included gate-to-gate and upstream operations (this boundary considered both on- and off-site emissions for all material and energy consumed and began with forest management and ended with products at the sawmill gate ready for dispatch to consumers).

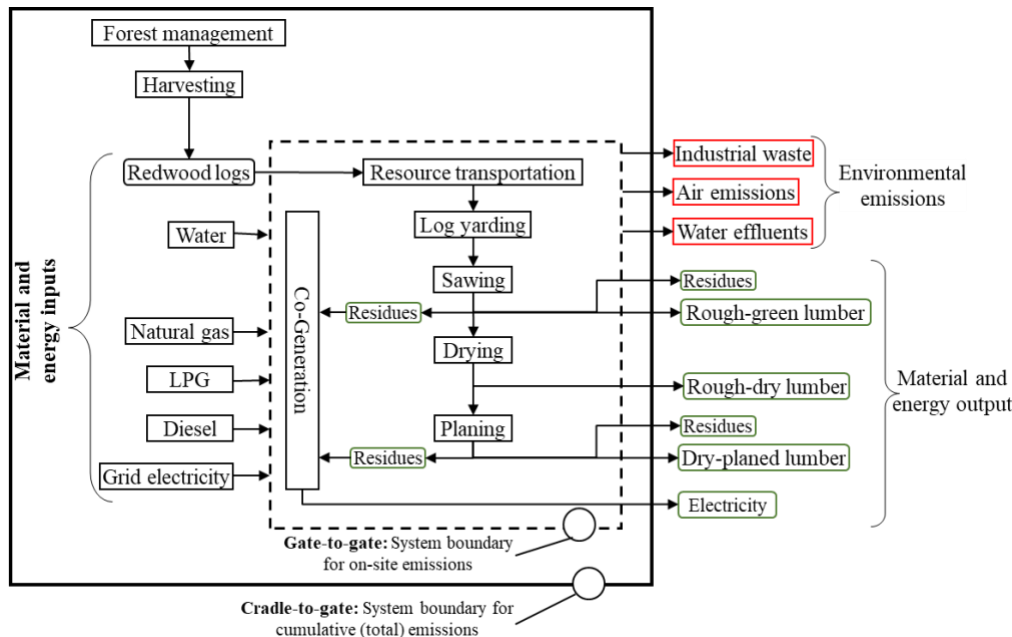


Figure12. System boundaries for redwood lumber manufacturing.

The resources used for the cradle-to-gate production of fossil energy and electricity were included within the cumulative system boundary. Off-site emissions included grid electricity production, transportation of logs to the mill, and fuels produced off-site but consumed on-site. Ancillary material data such as motor oil, paint, and hydraulic fluid were collected and were part of the analysis. The main unit processes in the manufacturing of redwood lumber were resource transport, log yard, sawing, drying, and planing with cogeneration of electricity and heat considered as auxiliary processes. As mentioned previously, all emissions (i.e., environmental outputs) and energy consumed were assigned to the redwood lumber and none to the coproducts (i.e., mill residues). Green wood residues included bark, chips, sawdust, and hog fuel. Some mills ground all wood residues into hog fuel. Redwood logs were transported in logging trucks from forest landings to the log yard. The procurement of redwood logs is seasonal, i.e., during the summer months. Logs in the log yard were wetted as needed to maintain log quality and prevent checking or splitting depending on the season and the mill. Log stackers or front-end loaders transported logs from the yard to the sawmill (the debarking unit). Sawing the debarked logs produces rough-green redwood lumber of different dimensions based on product demand. The sawing process (less the bark) produces rough-green lumber (58.9%), wood chips (16.0%), sawdust (5.3%), hog fuel (12.2%), and shavings (7.6%). Rough-green lumber can be sold directly to customers or dried to be sold as rough-dry lumber. The drying of lumber can be performed by either air-drying or kiln-drying based on the climate and

time to fulfill customer demand. Overall, drying rough-green lumber occurs mostly by air-drying with minimal kiln-drying to reach the desired moisture content (MC). A certain volume of the rough-green and rough-dry lumber is planed and sold as surfaced-green lumber or surfaced-dry lumber (or planed-dry lumber), respectively. Both drying and surfacing can be full or partial based on customer demand.

Inventory Approach

Primary (mill) data were collected from three major redwood lumber manufacturing sawmills (for the year 2017) through a survey questionnaire to generate the gate-to-gate LCI for the LCA study. The data related to upstream forest operations for redwood logs came from Han et al. (2015). Secondary data, such as diesel, gasoline, natural gas, propane, grid electricity, chemicals, and transport, were taken from DATASMART LCI database (LTS 2017) in SimaPro and peer-reviewed literature.

Mass balances of the material flow (ins and outs) for each unit operation were performed to verify data consistencies and quality. Two levels of mass balances (individual facilities level and industry level) were performed, and the data were found to be consistent for the surveyed mills. A difference of less than 10% is considered good for wood product production. The primary data obtained from the surveys were analyzed using the weighted-average approach.

Life-Cycle Impact Assessment

SimaPro 8.5 software was used to generate the LCI flows, and the LCIA was performed using the TRACI 2.1 method (Bare 2011). Six impact categories were examined, including global warming (GW [kg CO₂ eq]), acidification (kg SO₂ eq), eutrophication (kg N eq), ozone depletion (kg chlorofluorocarbons-11 eq), photochemical smog (kg O₃ eq), and fossil fuel depletion (MJ). The six impact categories evaluated in this study were in line with the requirement of the structural and architectural wood products product category rule (PCR) currently under external review (UL-Environment 2019).

Results and Discussion

SimaPro 8.5 modeled weight-averaged 2017 survey data to estimate raw material use, emission profile, and environmental impacts on a 1.0 m³ redwood lumber basis.

Mass Balance

Table 1 summarizes the mass balance of the redwood lumber production. Using a weight-averaged approach, 1.8 m³ [656 oven-dried (OD) kg] of incoming redwood logs produced 1.0 m³ (380 OD kg) of planed-dry redwood lumber. The sawing process yielded 386 kg of rough-green lumber with no loss of wood substance occurring during the drying process. Planing the rough lumber into a surfaced product decreased the 386 OD kg of rough-dry lumber to 380 OD kg of redwood lumber, for a 2% reduction in mass. This low value indicates a partial planing practice common among redwood lumber products. Some wood waste was converted on-site to thermal energy in a boiler; boilers burned all 6 OD kg of dry shavings produced per declared unit on-site for thermal process energy. Overall, an average redwood log was decreased to

51.2% (380/741) of its original dry mass (with bark) during its conversion to planed-dry redwood lumber. The conversion rate of lumber from redwood logs was higher compared with hardwood species [43.7-46.5% (Bergman and Bowe 2008, 2012)] and similar compared with other softwood species in the pacific northwest [53% (Milota et al. 2005)] as estimated in previous studies, which can be attributed to differences in the size of the logs and end product use. Overall, 355 OD kg of residues were generated and 78.3% (284 OD kg) of wood residues were used in the cogeneration unit to produce renewable electricity and thermal energy. The rest was sold for multiple uses such as land cover, soil amendments, etc.

Table 2: Mass balance for 1 m³ planed-dry redwood lumber

Material (OD kg)	Sawing process		Dryer process		Planer process		Co-generation process
	In	Out	In	Out	In	Out	In
Green logs (wood only)	656	-	-	-	-	-	-
Green logs (bark only)	85	-	-	-	-	-	-
Green chips	-	105	-	-	-	-	82
Green sawdust	-	34	-	-	-	-	27
Green bark	-	85	-	-	-	-	67
Green shaving	-	50	-	-	-	-	39
Green hog fuel	-	80	-	-	-	-	63
Rough green lumber	-	386	386	-	-	-	-
Rough dry lumber	-	-	-	386	386	-	-
Planed dry lumber	-	-	-	-	-	380	-
Dry shavings	-	-	-	-	-	6	6
Sum	741	741	386	386	386	386	284

Material Inputs and Outputs

Table 2 provides the inputs of the material for the gate-to-gate product manufacturing stage. The main material inputs were natural inputs, i.e., redwood logs and water. Most water usages were for the drying, power generation, and log yard unit operations at the sawmills.

Table 2: Gate-to-gate material flow analysis of 1 m³ of redwood lumber

Description	Unit	Value	Description	Unit	Value
<i>Products</i>			<i>Chemicals</i>		
Lumber	m ³	1	Oxygen scavenger (sulfite)	L	6.98E-03
Green chips (sold)	OD kg	22.918	Corrosion scale inhibitor	L	1.72E-02
Green sawdust (sold)	OD kg	7.501	pH adjuster	L	1.35E-01
Green bark (sold)	OD kg	18.561	Transport		
Green shaving (sold)	OD kg	10.874	Resource transport	tkm	125.625
Green hog fuel (sold)	OD kg	17.454	Chemicals transport	tkm	84.62
Renewable electricity	kWh	103.629	<i>Ancillary material</i>		
<i>Resources inputs</i>			Hydraulic fluid	kg	0.115
Water, well, in-ground	L	12.771	Motor oil	kg	0.101
Water, municipal	L	51.861	Grease	kg	0.001
Round redwood log	kg	741.385	Plastic strapping	kg	0.051
<i>Fuels and energy</i>			Paint	kg	0.001
Diesel	L	1.420	Replacement sticker	kg	1.072
Gasoline	L	0.067			
Natural gas	Nm ³	1.923			
Electricity	kWh	34.593			

Redwood lumber in service stores carbon. The carbon content for wood products is assumed to be 50% by mass of OD wood (Bergman et al. 2014a). Therefore, the carbon stored in 1 m³ (380 OD kg) of redwood lumber is equivalent to 697 kg CO₂.

Cumulative Energy Consumption

Table 3 shows the cumulative unallocated energy consumption for 1 m³ of redwood lumber. Cumulative energy consumption for cradle-to-gate manufacturing redwood lumber was 1,573 MJ/m³ with wood fuel comprising about 44.5%. Crude oil (38.1%), natural gas (10.0%), and coal (3.5%) were the next three highest fossil energy resources consumed. Compared with a previous study (Bergman et al. 2014b), this study estimated a drastic reduction in energy from coal and natural gas but a multifold increase in energy from crude oil. Crude oil is the feedstock used to produce diesel, which is consumed in forest machines and logging trucks. Contrarily, the use of wood fuel increased ~3 times. However, wood fuel was used to generate electricity on-site. In this analysis, we did not take the credit of the extra electricity that was generated on-site but sold off-site. In retrospect, the wood products industry generates energy in-house by burning wood fuel generated on-site (Puettmann et al. 2010a). Overall, energy consumption increased compared with the previous redwood decking study (Bergman et al. 2014b). Still, redwood lumber production requires substantially lower energy compared with most other lumber products. The cumulative allocated energy consumption for 1 m³ of planed-dry hardwood and softwood lumbars in the United States varied between 2,500 and 6,000 MJ/m³ (Milota et al. 2005, Bergman and Bowe 2008, 2010, 2012, Puettmann et al. 2010b, Milota and Puettmann 2017,). The low cumulative energy consumption for redwood lumber occurs because of the minimal use of kiln-drying, which is the most energy-intensive part of producing dry lumber products (Bergman 2010).

Table 3: Cumulative energy (higher heating values (HHV)) consumed during the production of redwood lumber, cumulative, unallocated, and cradle-to-gate LCI values^a

Fuel ^{b,c}	(kg/m ³)	(MJ/m ³)	(%)
Wood fuel/wood waste	33.5	700.0	44.5
Coal ^d	2.1	55.2	3.5
Natural gas ^d	2.9	157.0	10.0
Crude oil ^d	13.2	599.0	38.1
Hydro	0	13.0	0.8
Uranium ^d	0.00011	40.6	2.6
Energy, unspecified	0	8.7	0.5
Total	—	1,573	100

^a Includes fuel used for electricity production and for log transportation (unallocated).

^b Values are unallocated, cumulative, and based on HHV.

^c Energy values were found using their HHV in MJ/kg: 20.9 for wood oven-dry, 26.2 for coal, 54.4 for natural gas, 45.5 for crude oil, and 381,000 for uranium.

^d Materials as they exist in nature and have neither emissions nor energy consumption associated with them.

Environmental Emission Profile

Table 4 lists the unallocated environmental outputs for manufacturing one m³ of redwood lumber for the cumulative and on-site system boundaries. The cumulative values included all

emissions and were higher than the on-site emissions, as expected. For the cumulative system boundary, biogenic CO₂ and fossil CO₂ were 56.8 and 54.2 kg/m³, respectively. For the cumulative case, fossil CO₂ was about three times the fossil CO₂ emitted for the on-site case, whereas biogenic CO₂ emissions were the same. For on-site, the only sources of fossil CO₂ came from rolling stock such as front-end loaders moving logs, forklifts moving lumber around the mill, and natural gas used for kiln-drying.

Table 4: Environmental outputs for manufacturing 1 m³ of redwood lumber

Substance	Cumulative (kg/m ³)	On-site (kg/m ³)
<i>Water effluents</i>		
BOD5 (biological oxygen demand)	7.66E-02	6.86E+01
Chloride	2.06E+00	2.06E+00
COD (chemical oxygen demand)	5.29E-02	3.62E-02
DOC (dissolved organic carbon)	4.81E-02	4.56E-02
Oils, unspecified	3.00E-03	2.08E-03
Suspended solids, unspecified	7.91E-01	6.86E-01
<i>Industrial waste^a</i>		
Waste in inert landfill	2.67E-01	2.67E-01
Waste to recycling	2.22E-01	2.22E-01
Solid waste ^b	1.11E-01	9.20E-02
<i>Air emissions</i>		
Acetaldehyde	1.56E-04	6.16E-05
Acrolein	5.41E-05	4.26E-05
Benzene	3.17E-04	2.02E-04
CO	1.04E+00	7.69E-01
CO ₂ (biomass (biogenic))	6.03E+01	6.03E+01
CO ₂ (fossil)	5.20E+01	1.69E+01
CH ₄	6.57E-02	6.16E-02
Formaldehyde	6.24E-04	4.77E-04
Mercury	2.50E-07	2.21E-07
NO _x	6.39E-01	1.52E-01
Nonmethane VOC	2.77E-01	2.56E-01
Particulate (PM10)	4.01E+00	4.01E+00
Particulate (unspecified)	4.06E-03	7.68E-04
Phenol	2.07E-05	2.07E-05
SO _x	3.35E-02	1.58E-02
VOC	4.82E-02	3.28E-02

^a Includes solid materials not incorporated into the product or coproducts but that left the system boundary.

^b Solid waste was boiler ash from burning wood. Wood ash is typically used as a soil amendment or landfilled.

Life-Cycle Impact Assessment

Figure 2 shows the six midpoint environmental impact categories for redwood lumber without considering the credits from co-generating renewable electricity from burning mill residues. Forestry operation has a substantial contribution toward all categories of environmental impacts except ozone depletion. Forestry operation, sawing, and planing unit operations are the three major contributors to ozone depletion. Because of the use of diesel in harvesting equipment and logging trucks, most global warming and fossil fuel depletion impacts were from forestry operation and transportation of logs from landing to the mills. This study's environmental profiles of redwood lumber production (gate-to-gate) such as GW, ozone

depletion, and smog were reduced by two to three times compared with the previous study (Bergman et al. 2014b) mainly because of energy and power mix improvements such as more energy coming from co-generation and notable reduction in electricity usage in sawmill operations.

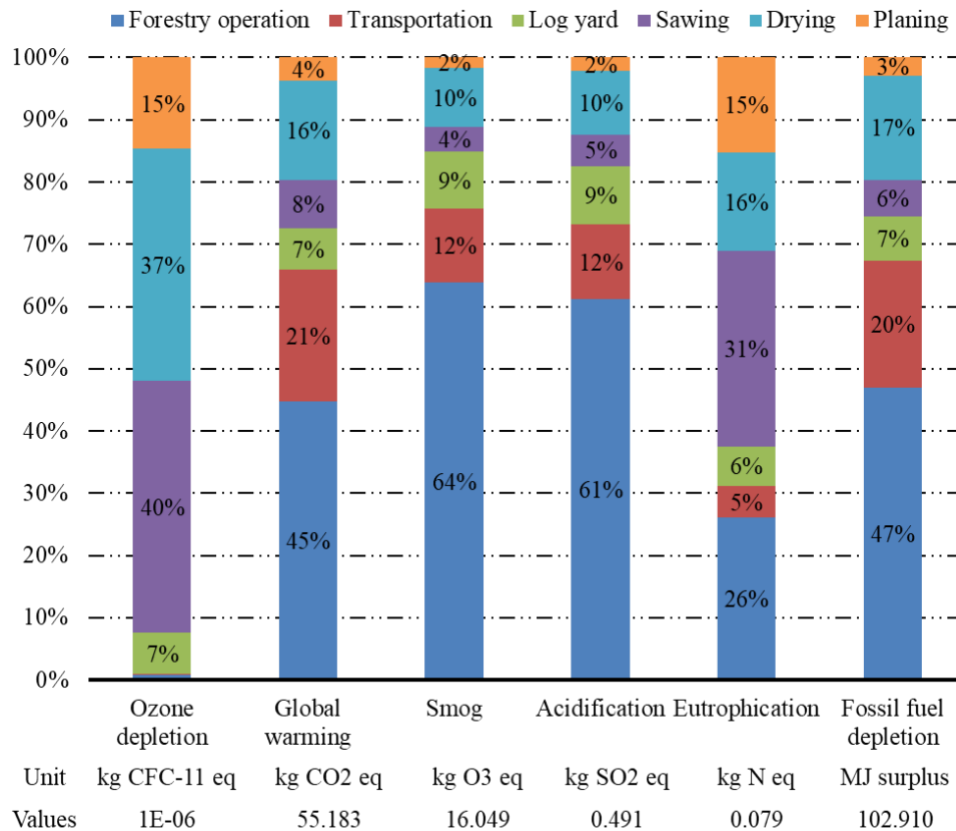


Figure 2. Contribution of environmental impacts for the cradle-to-gate life-cycle stages of redwood lumber production.

Summary and Conclusions

Construction materials made from wood have numerous environmental attributes. Redwood lumber, because of how it is processed, showed in this analysis an even greater benefit than other wood products. On resource efficiency, redwood lumber makes up about 51.2% of the incoming redwood logs while the rest is mill residues, primarily from sawing, that are used for other purposes and are not wasted. On GHG mitigation potential, our analysis showed redwood lumber stored about 12 times the total GHG emissions released during cradle-to-gate product manufacturing. CO₂ uptake from the atmosphere into the raw materials (i.e., trees) used to make wood products and the storage of the resultant carbon in long-lived building products are a substantial environmental attribute because this carbon is kept from the atmosphere. Other wood building products have this environmental advantage of storing carbon while in service to offset the effects from production while also avoiding the production of fossil fuel-intensive products (Puettmann and Wilson 2005, Puettmann 2010b; Bergman et al. 2016).

The unit process approach shows how product production facilities can improve their environmental profiles because of the many inherent details required compared with a system process approach. For most wood products, the drying process tends to have the greatest environmental impacts on the cradle-to-gate manufacturing process compared with other unit processes. However, compared with almost all other lumber species, redwood lumber drying process consumes less energy because it tends to be produced and sold green or air-dried. Contrary to most other wood products, forestry operation for redwood lumber production was found to be the most dominant life-cycle stage, contributing to most of the environmental impact categories. In retrospective, the impacts from the forest operation stage were still consistent with other wood products (Han et al. 2015, Oneil and Puettmann 2017), but because redwood lumber has minimal kiln-drying, the forest operation stage contributed a higher percentage of the overall impacts, as was reported.

This study showed substantial reductions in environmental profiles compared with the previous study in 2013 (Bergman et al. 2014b) because of the usage of heat and electricity from co-generation and reduction in electricity usage in the sawmill.

Acknowledgments

We gratefully acknowledge those companies and their employees that participated in the surveys to obtain production data and those who provided financial assistance to the USDA Forest Service, Forest Products Laboratory, for this research project (19-CO-1111137-010). The authors acknowledge the following peer reviewers: Charlie Jourdain, Manager, Business Development, Mendocino Forest Products and Humboldt Redwood; Sevda Alanya-Rosenbaum, Postdoctoral research fellow, USDA Forest Service, Forest Products Laboratory; Steven Hubbard, Lead Consultant, Hubbard Forest Solutions, LLC.

References

- Abergel T, Dean B, Dulac J (2017) Towards a zero-emission, efficient, and resilient buildings and construction sector: Global Status Report 2017. Paris, France: UN Environment, International Energy Agency.
- Bare J (2011) TRACI 2.0: the tool for the reduction and assessment of chemical and other environmental impacts 2.0. *Clean Technologies Environmental Policy* 13: 687-696.
- Bergman RD, Bowe SA (2008) Environmental impact of producing hardwood lumber using life-cycle inventory. *Wood and Fiber Sci* 40: 448-458.
- Bergman RD (2010) Drying and control of moisture content and dimensional changes. In: *Wood handbook—wood as an engineering material*. General Technical Report FPL–GTR–113. Madison, WI: U.S. Department of Agriculture, Forest Service, Forest Products Laboratory. pp. 13-1–13-20.

Bergman RD, Bowe SA (2010) Environmental impact of manufacturing softwood lumber determined by life-cycle inventory. *Wood Fiber Sci* 42(CORRIM SpecialIssue):67-68.

Bergman RD, Bowe SA (2012) Life-cycle inventory of manufacturing hardwood lumber in southeastern US. *Wood and Fiber Sci* 44: 71-84.

Bergman R, Han H-S, Oneil E, Eastin I (2013) Life-cycle assessment of redwood decking in the United States with a comparison to three other decking materials. Seattle, WA: Consortium for Research on Renewable Industrial Materials.
https://www.fpl.fs.fed.us/documnts/pdf2013/fpl_2013_bergman001.pdf

Bergman R, Puettmann M, Taylor A, Skog KE (2014a) The carbon impacts of wood products. *Forest Products Journal* 64: 220-231.

Bergman RD, Oneil E, Eastin IL, Han HS (2014b) Life cycle impacts of manufacturing redwood decking in Northern California. *Wood and Fiber Sci* 46: 322-339.

Bergman RD, Kaestner D, Taylor AM (2016) Life cycle impacts of North American wood panel manufacturing. *Wood and Fiber Sci* 48: 40-53.

Bringezu S et al. (2017) Assessing global resource use: A systems approach to resource efficiency and pollution reduction. A report of the International Resource Panel. Nairobi, Kenya: United Nations Environment Programme.

Canadell JG, Raupach MR (2008) Managing forests for climate change mitigation. *Science* 320: 1456-1457.

Han HS, Oneil E, Bergman RD, Eastin IL, Johnson LR (2015) Cradle-to-gate life cycle impacts of redwood forest resource harvesting in northern California. *Journal of Cleaner Production* 99: 217-229.

ISO (2006a) Environmental labels and declarations-type iii environmental declarations-principles and procedures. International Organization for Standardization.

ISO (2006b) Environmental management: Life cycle assessment; principles and framework. International Organization for Standardization.

ISO (2006c) Environmental management: Life cycle assessments: Requirements and guidelines. International Standardization Organization.

ISO (2007) Sustainability in building construction: Environmental declaration of building products. ISO 21930. International Organization for Standardization.

LTS (2017) DATASMART LCI package (US-EI SimaPro® Library).
<https://ltsexperts.com/services/software/datasmart-life-cycle-inventory/>.

Malmsheimer RW et al. (2011) Managing forests because carbon matters: integrating energy, products, and land management policy. *Journal of Forestry* 109: S7-S50.

Matos GR (2017) Use of raw materials in the United States from 1900 through 2014. U.S. Geological Survey Fact Sheet 2017-3062. 6 p., <https://doi.org/10.3133/fs20173062>. Reston, VA: National Minerals Information Center.

Milota M, Puettmann ME (2017) Life-cycle assessment for the cradle-to-gate production of softwood lumber in the pacific northwest and southeast regions. *Forest Products Journal* 67(Special Issue): 331-342.

Milota MR, West CD, Hartley ID (2005) Gate-to-gate life-cycle inventory of softwood lumber production. *Wood and Fiber Sci* 37(Special Issue): 47-57.

Oliver CD, Nassar NT, Lippke BR, McCarter JB (2014) Carbon, fossil fuel, and biodiversity mitigation with wood and forests. *Journal of Sustainable Forestry* 33: 248-275.

Oneil E, Puettmann ME (2017) A life-cycle assessment of forest resources of the Pacific Northwest, USA. *Forest Products Journal* 67: 316-330.

Pré-Consultants (2017) SimaPro8 life-cycle assessment software package, version 8.5.2. Plotter 12. 3821 BB Amersfoort, the Netherlands.

Puettmann ME, Wilson JB (2005) Life-cycle analysis of wood products: Cradle-to-gate LCI of residential wood building materials. *Wood and Fiber Sci* 37(Special Issue):18–29.

Puettmann ME, Bergman R, Hubbard S, Johnson L, Lippke B, Oneil E, Wagner FG (2010a) Cradle-to-gate life-cycle inventory of US wood products production: CORRIM Phase I and Phase II products. *Wood and Fiber Sci* 42(Special Issue): 15-28.

Puettmann ME, Wagner FG, Johnson L (2010b) Life cycle inventory of softwood lumber from the inland northwest US. *Wood and Fiber Sci* 42(Special Issue): 52-66.

Sathre R, O'Connor J (2010) Meta-analysis of greenhouse gas displacement factors of wood product substitution. *Environmental Science & Policy* 13: 104-114.

UL-Environment (2019) Guidance for building-related products and services: Part b: Structural and architectural wood products epd requirements. Washington, DC: UL Environment.

Data Science at the University of Primorska: Combining Fundamentals with Data and Challenges from Buildings, Wood and Processing Science

Dr. Mike Burnard
InnoRenew CoE & University of Primorska
Prof. Klavdija Kutnar
University of Primorska

Abstract

The University of Primorska has developed a new master's degree program within the Faculty of Mathematics, Natural Sciences, and Information Technology (FAMNIT). This innovative program teaches data science fundamentals using data and challenges from wood science, wood value chains (processing, logistics), and building science. Data science is an interdisciplinary field blending computer science, mathematics, and domain knowledge. Key computer science skills like data management, algorithm development, parallel and distributed computing, and visualization are taught alongside topics in mathematics including statistics, probability theory, algebra, and graph theory to provide students with the skills necessary to collect, store, process, and analyze data to provide value insights to scientific work and industry. The novelty of FAMNIT's data science program is the inclusion of specialized domain knowledge from the fields of wood science, processing, tracking, and logistics in wood value chains, and data collected from sensors in buildings.

As new devices are developed, wood scientists have found novel uses of them to provide new insights and wood assessment techniques. For example, as prices drop on tools like near infrared (NIR) spectrometers they can be deployed in wood production lines to provide useful quality management information (amongst other uses). The chemometric data produced by a single NIR device is significant, but as more and more devices are deployed there is a need to develop solutions that provide rapid and insightful information to users (production staff, managers, etc.). Scalable solutions require interdisciplinary skills data scientists can provide, but to generate truly useful information domain knowledge from wood science and processing is required. Another example is creating advanced tag and trace systems in chain-of-custody applications that may combine multiple technologies like radio frequency identification, blockchain, and integration with existing enterprise resource planning software and life cycle assessment impact databases.

Sensors deployed in buildings allow researchers and manufacturers to gain insight into product and system performance in buildings. For example, monitoring temperature, relative humidity, vibrations, strain, etc. in cross-laminated timber plates can help researchers and manufacturers to optimize product and process design, engineers to improve seismic, acoustic, and wind-load design, and facilities managers to predict maintenance intervals and improve building energy performance. Sensors in buildings are also used to monitor indoor environments and users, which introduces both ethical and privacy issues that data scientists from FAMNIT's new program are prepared to confront.

The data science master's at FAMNIT is a 2-year program requiring a thesis and industry internships to ensure students are prepared to advance in both as academics and professionals. The program leverages FAMNIT's excellent research and teaching staff from existing computer science, mathematics, and sustainable building programs along with expertise from its partners in industry and external research organizations.

Quantifying Dimensional Changes in Wood Pellets as a Function of Relative Humidity

Daniel Burnett, Surface Measurement Systems, Ltd.; Fahimeh Yazdan Panah, Shahabaddine Sokhansanj, and Hamid Rezaei; Biomass and Bioenergy Research Group, Chemical and Biological Engineering Department, The University of British Columbia

Wood pellet as an international renewable energy source is usually exposed to humid air, and the changes in relative humidity and temperature during storage and shipment. Such a variation in environmental conditions is responsible for dimensional variation as well as mechanical stress. More than 90 percent of wood pellets produced in Canada are exported overseas and thus exposed to different environment conditions e.g. high humidity and rain during shipping and handling. Moreover, when pellets are produced on the plant, they will spend some time on the plant in the storages and exposed to different environmental conditions before being shipped. In addition, even a small amount of moisture sorption could lead to self-heating of the pellets and eventual spontaneous combustion. Thus, it's essential to study the pellet dimension and porosity change and its effect on pellet durability and strength when exposed to different environment conditions such as humid weather and rain exposure. In addition, moisture content changes can lead to aesthetic variations and rates of photochemical degradation. To assess the behavior of wood pellet in an environment where humidity is present and may change over time, too, reliable micro-scale data are required to predict the ultimate performance of these materials.

In this research, Dynamic Vapor Sorption (DVS) studies have been performed on wood pellets. The pellets had been produced commercially from compacting wood milling residues like sawdust and bark in a pellet press. The source of wood was from BC forest species spruce, fir, and pine. One sample was made out of pine sawdust ('white wood') and the other sample was wood pellets made out of pine wood and some bark along with some other species ('dark wood'). The samples were exposed to a linear ramp in relative humidity from 0 to 95% (15% RH/hour), then held at 95% RH for 6 hours. During this time, images of the pellets were collected *in-situ*. Digital image analysis technique was used to measure dimensional changes (via pellet cross-section) with respect to humidity. For both samples, there was negligible swelling below 30% RH. For the dark wood sample, swelling occurred at a lower RH compared to the white wood sample (30% RH versus 50% RH). In addition, the dark wood sample exhibited larger relative dimensional changes compared to the white wood sample.

The combination of moisture sorption studies with *in-situ* video monitoring allowed the simultaneous determination of moisture content and swelling behavior in real-time. This information is critical to the stability and ultimate performance of wood pellets under various processing and storage conditions.

Keywords: moisture, sorption, wood pellets, swelling

A potential thermal energy storage material used for green buildings

Xi Guo, Jinzhen Cao*

Key Laboratory of Wood Material Science and Utilization (Beijing Forestry University)

Two types of porous materials, expanded graphite (EG) and diatomite, were used as stabilizers for paraffin by using vacuum impregnation method to prepare form-stable phase change materials (FSPCMs), and they were compound with wood flour (WF) and high-density polyethylene (HDPE) to prepare a thermal energy storage wood-polymer composite (TES-WPC). Mercury intrusion test indicates that the pores of EG are filled by paraffin and the porosity of EG decreased from 81% to 27% after full impregnation of paraffin. Compared with EG stabilized paraffin FSPCM, diatomite stabilized paraffin FSPCM showed better thermal stability. It can be contributed to the smaller pore diameter as well as the special isolated microporous structure of diatomite. XRD test indicates that the FSPCMs had perfect stability without showing any chemical reaction between paraffin and the stabilizers. Both prepared TES-WPCs show constant temperature range during phase change process, which fits the comfortable temperature zone of human. Thermal performance indicates that both TES-WPCs had great TES capacity which can effectively alleviate or even prevent the temperature vibration in indoor environment. The TES capacity can be enhanced with the increasing paraffin ratios in FSPCM and the mass fraction of FSPCM in TES-WPC. But it should be noted that high EG addition would improve the thermal conductivity and therefore promote the heat transfer of TES-WPC obviously. The enthalpy of TES-WPC decreases only about 6% after 500 heating-cooling recycles, suggesting a great thermal durability. The addition of paraffin endows the composites satisfying moisture resistance while also slightly decreases the mechanical strength due to the damaged interface between WF and HDPE. In this study, liquid leakage of PCM was fundamentally solved by using porous EG or diatomite as the primary stabilizer and then WF/HDPE as the secondary encapsulation material. The TES-WPC fabricated either by EG or diatomite shows satisfying mechanical properties, thermal stability and durability. Therefore, we suggest it as a potential TES material used in green buildings for energy conservation.

Improvement of Weathering Performance of Painted Wood Applying Laser Micro Incisions

DR. SATOSHI FUKUTA, fukuta@aichi-inst.jp

Aichi Center for Industry and Science Technology, Japan

Abstract

A short pulse laser with ultraviolet wavelength was applied to the incising process. Spread amount of paint (penetrating-type wood preservative semi-transparent coating) significantly increased by applying the “Laser Micro Incisions (LMI)” to wood surface, and the remarkable improvement of weathering performance of painted wood was predicted by accelerated weathering test; changes in color and water repellency of LMI-treated samples were suppressed. And we investigated the influences of processing form of LMI and distribution of paint on deterioration of painted wood by nondestructive observation using X-ray microscope and considered the factors.

Performance Test of Chairs - Joints Design by Use of Lower Tolerance Limits

Dr. Eva Haviarova,

ehaviar@purdue.edu

Mr. Mesut Uysal

Purdue University, USA

Abstract

Joints are the weakest part of furniture structure and therefore unreliable joints result in unreliable products. If the reliability of joints is increased, an increase in reliable products could be obtained. Design values for furniture structures and their joints are not well addressed in available literature sources. If design values of joints are known, then the joints can be designed with safety measures.

In this study, the statistical lower tolerance limits method, which ensure product reliability and safety, was used to determine design values of rectangular mortise and tenon joints. A chair structure was designed to resist a load capacity of 2000 N and its internal forces were obtained. By using design values and calculated internal forces, joint sizes were determined to resist a 2000 N load level. After calculating the load level, chairs specimens were produced and then subjected to a vertical static load test on front legs. These test results were expected to be higher than a 2000 N load level. Moreover, a front-to-back cyclic load test was applied on chairs and results were compared with American Library Association (ALA) specifications. Research findings are indicating that chair strength could be increased for intended service if design values are used for design of chair joints. This study is also proposing a systematic procedure on how to use design values for construction of a chair and its joints.

In conclusion, this study provides design values for rectangular mortise and tenon joints while considering the safety and reliability of furniture joints. Also, research findings are providing methods on how to determine design values for joints in furniture industry and how to select a specific joint for best-suited applications.

Keywords: Design values, furniture joint, performance testing of chair, lower tolerance limits

Mechanical Properties of 3D Printed Sustainable Bio-based Sandwich Structures

Dr. Eva Haviarova,

ehaviar@purdue.edu

Purdue University, USA

Prof. Nadir Ayrilmis

Istanbul University - Cerrahpasa, Turkey

Dr. Manja Kitek Kuzman

University of Ljubljana, Slovenia

Abstract

Commercial use of 3D printers has rapidly increased in the last 10 years due to the fact that it enables the creation of rapid prototypes in complex shapes based on virtual computer models. A type of 3D printer known as fused deposition modeling has gained popularity due to its relatively low cost. The purpose of this study is to increase knowledge in the mechanical properties of parts created with wood-plastic composite materials by using 3D printing. This study focused on the mechanical properties of 3D printed sandwich structures produced from various natural fibers and bio polymers by additive manufacturing technique. With this aim, a comprehensive literature review was conducted on the 3D printed sandwich structures. 3Dprinting can be exceptionally useful for civil engineers and designers to produce scaled-down prototypes of complex shapes with different sandwich structures. In addition, the furniture industry is also currently focusing on the lightweight materials, not only for light-weight product development but also for material savings. Internal and external geometrical structures of the lightweight materials significantly affects properties of the final product. Specifically, different honeycomb core structures affect the tensile, bending, shear and viscoelastic behaviors of the sandwich structures. This review of the study would be beneficial to designers and civil engineers working with wood-plastic composited in order to analyse small size prototypes before real production.

Key words: mechanical properties; 3D printing; wood-plastic; sandwich structures

Applying Zero-Slot Learning to Wood Identification

Eva Haviarova¹, Fanyou Wu², Rado Gazo³, Bedrich Benes⁴

^{1,2,3}Purdue University, Department of Forestry and Natural Resources,

⁴Purdue University, Department of Computer Graphics Technology

West Lafayette, IN, USA;

ehaviar@purdue.edu

wu1297@purdue.edu

gazo@purdue.edu

bbenes@purdue.edu

ABSTRACT

Recently, deep-learning techniques have demonstrated their usefulness in automated wood identification based on analysis of macroscopic cross-section images of wood samples. These techniques, however, require that large number of images of all species exist in training set. This makes them lose their practical application, since macroscopic images of some wood species are hard to obtain (e.g. rare and endangered species).

Zero-slot learning is a process that addresses unavailability of a complete training image set. By using attribute vectors instead of species label, zero-slot learning attempts to recognize occasions that were potentially missed during the deep-learning training process. In this case study, we use Convolutional Neural Network-ResNet as a discriminant network and minimal distance as the final decision rule. By separating 30 tropical wood species into two sets without overlapping species, we demonstrate the power of zero-slot learning.

Key words: Wood ID; zero-slot, deep-learning, automated wood identification

**Fire Resistance of Unprotected Cross-Laminated Timber Assemblies of Walls and Floors
Made in U.S.**

Mr. Seung Hyun Hong, hongseu@oregonstate.edu
Prof. Lech Muszynski
Dr. Rakesh Gupta
Oregon State University, USA
Dr. Brent Pickett
Western Fire Center, Inc, Kelso, Washington, USA

Abstract

Fire is one of the major concerns of wood construction because wood-based materials are more flammable than other commonly used structural materials. The flammability of wood has led to tall wood building code restrictions in the U.S. despite data on the fire resistance of cross-laminated timber (CLT) from research conducted in Europe, Japan, and Canada. The major reason for CLT building code restrictions in the U.S. is the lack of full-scale tests conducted on structural CLT manufactured in the U.S. Therefore, the objective of this project was to provide the necessary evidence for removing this legal use barrier by analyzing data of full-scale unprotected CLT fire tests conducted using CLT made in the U.S. The assemblies represented two species groups, spruce-pine-fir (SPF) and Douglas fir-Larch (DF-L), and two adhesive systems, polyurethane (PUR) and melamine urea formaldehyde (MUF). All assemblies were tested under working load conditions. All wall assemblies and floor assemblies met the ASTM E119 standard qualifying criteria for 2-hours Time-Temperature Area except for the SPF/PUR wall assembly which passed 101 minutes. A statistically significant difference was observed between the adhesive types where the MUF adhesive system held a char layer more effectively than PUR. While the major driving force of char rate was furnace temperature, adhesive type appeared to influence char rate more than wood species. The unprotected half-lap joints provided an adequate barrier against the transmission of hot gases and flames through the assemblies before the char depth reached half of the total assembly thickness.

KEYWORDS: Fire resistance; cross-laminated timber; CLT; floors; walls; half-lap joints; polyurethane; PUR; melamine urea formaldehyde; MUF; spruce-pine-fir; SPF; Douglas fir-larch; DF-L

Preparation of Biomorphic Porous SiC Ceramics from Bamboo by Combining Sol-Gel Impregnation and Carbothermal Reduction

Ke-Chang Hung^{1}–Tung-Lin Wu²–Jin-Wei Xu³–Jyh-Horng Wu^{4*}*

¹ Postdoctoral research fellow, Department of Forestry,
National Chung Hsing University, Taichung 402, Taiwan.
d9833004@mail.nchu.edu.tw

² College Student, College of Technology and Master of Science in Computer
Science, University of North America, Virginia 22033, USA
tonywuwu22@gmail.com

³ Graduate Student, Department of Forestry,
National Chung Hsing University, Taichung 402, Taiwan.
ecsgunro@gmail.com

⁴ Professor, Department of Forestry, National Chung Hsing University, Taichung
402, Taiwan. * *Corresponding author*
eric@nchu.edu.tw

Abstract

This study investigated the feasibility of using bamboo to prepare biomorphic porous silicon carbide (bio-SiC) ceramics through a combination of sol–gel impregnation and carbothermal reduction. The effects of sintering temperature, sintering duration, and sol–gel impregnation cycles on the crystalline phases and microstructure of bio-SiC were investigated. X-ray diffraction patterns revealed that when bamboo charcoal–SiO₂ composites (BcSiCs) were sintered at 1700°C for more than 2 h, the resulting bio-SiC ceramics exhibited significant β-SiC diffraction peaks. In addition, when the composites were sintered at 1700°C for 2 h, scanning electron microscopy micrographs of the resulting bio-SiC ceramic prepared using a single impregnation cycle showed the presence of SiC crystalline particles and nanowires in the cell wall and cell lumen of the carbon template, respectively. However, bio-SiC prepared using three and five repeated cycles of sol–gel impregnation exhibited a foam-like microstructure compared with that prepared using a single impregnation cycle. Moreover, high-resolution transmission electron microscopy and selected area electron diffraction revealed that the atomic plane of the nanowire of bio-SiC prepared from BcSiCs had a planar distance of 0.25 nm and was perpendicular to the (111) growth direction. Similar results were observed for the bio-SiC ceramics prepared from bamboo–SiO₂ composites (BSiCs). Accordingly, bio-SiC ceramics can be directly and successfully prepared from BSiCs, simplifying the manufacturing process of SiC ceramics.

Key words: Bamboo; Carbothermal reduction; Ceramic; Silicon carbide; Sol–gel process.

Introduction

Over the past few decades, silicon carbide (SiC) ceramics have been extensively used in the structures of modern aviation vehicles, such as rocket nozzles, aeronautic jet engines, and aircraft brake materials, because such ceramics exhibit remarkable physical properties, including wear, corrosion, and thermal resistance (Qian et al. 2004a; Mao et al. 2016). In particular, SiC ceramics hold considerable promise for use as solar energy absorbers; solar-energy-absorbing devices require ceramics with open porosity, excellent solar energy absorption performance, and high thermal conductivity. In general, SiC ceramics that exhibit larger grain sizes and are supplemented with α -SiC can produce relatively high thermal conductivity levels (Locs et al. 2011).

Reaction processing of SiC is a technique for producing advanced SiC-based structural ceramics; this technique involves a chemical reaction between carbon (C) and silicon (Si) during sintering (Mao et al. 2016). In recent years, the use of wood as a carbon template for preparing SiC ceramics with a wood-like microstructure (wood-like SiC ceramics) has emerged as a relatively new research area (Locs et al. 2009). Therefore, several techniques have been developed for fabricating porous wood-like SiC ceramics, including reactive infiltration with Si-containing melts (Esposito et al. 2004), reactive silicon vapor infiltration (Qian et al. 2003), and SiO₂ sol-gel impregnation combine with carbothermal reduction (Herzog et al. 2004; Sieber 2005). SiO₂ sol-gel impregnation combined with carbothermal reduction has several advantages; for example, it is a low-cost approach, involves easy synthesis procedures, involves relatively low temperatures of synthesis, provides high-purity resultant products, and can retain the structure and morphology of starting carbonaceous materials (Qian and Jin 2006).

Bamboo, a perennial woody plant belonging to the Gramineae family, is widely distributed across Asia and exhibits higher growth rates than do other woody plants. In Taiwan, bamboo is extensively used as a raw material for handicraft, furniture, and construction applications (Wu et al. 2013). Bamboo materials are similar to wood, and they have a porous structure that renders them useful for realizing different penetration and treatment procedures (Liu et al. 2015). Studies have focused on the crystalline-phase composition of wood-like SiC ceramics. The use of bamboo as an industrial raw material can improve economic efficiency. Accordingly, this study explored the feasibility of using bamboo to produce porous biomorphic SiC (bio-SiC) ceramics by combining sol-gel impregnation and carbothermal reduction. In addition, the study investigated the effects of sintering temperature, sintering duration, and repeated cycles of sol-gel impregnation on the crystalline phase and microstructure of the bio-SiC ceramics.

Materials & Methods

Experimental materials and procedure: This study obtained 4-year-old moso bamboo (*Phyllostachys pubescens* Mazel) from a local bamboo-processing factory. The obtained bamboo was air dried and then cut into rectangular specimens measuring approximately 50 mm (L) × 25 mm (T) × 5 mm (R). Each of the bamboo specimens was converted to a porous biocarbon template (bamboo charcoal) through carbonization in a nitrogen atmosphere at a temperature of 850°C, heating rate of 5 °C/min, and holding time of 1 h. A SiO₂ precursor sol was formulated by mixing methyltrimethoxysilane (MTMOS) (Acros Chemical) and methanol at a molar ratio of 0.13:1. In the sol-gel process, the bamboo and bamboo charcoal specimens were impregnated with the prepared sol under reduced pressure for 2 days. The impregnated specimens were then

placed in an oven controlled to 105°C for 24 h to age the gels. Repeated impregnation cycles (one, three, and five cycles) were applied, producing various bamboo charcoal–SiO₂ composites (BcSiCs) and bamboo–SiO₂ composites (BSiCs). The derived BcSiCs and BSiCs were subjected to carbothermal reduction reactions in nitrogen atmosphere (flow rate: 2.5 L/min) in a heater furnace (Nabertherm, LHT 04/17 SW) at 1500–1700°C for 0.5–3 h to form porous bio-SiC ceramics.

Characterization: The crystalline phases of bamboo charcoal and porous SiC ceramics were characterized through a powder X-ray diffraction (XRD) instrument (MAC Science, MXP18) operated in the 2 θ range of 2°–85° using CuK α ($\lambda = 1.5406 \text{ \AA}$) radiation at 40 kV and 30 mA. The morphology and detailed structural features of the specimens were determined using a scanning electron microscopy (SEM) instrument (JEOL, JSM-7401F) and high-resolution transmission electron microscopy (HRTEM) instrument (JEOL, JEM-2100F), respectively. Field-emission measurements for the nanowires of the synthesized SiC were performed in a vacuum chamber at a pressure of approximately 5.0×10^{-7} Torr. A thermal analyzer (PerkinElmer, Pyris 1) was used to elucidate the synthesis and oxidation mechanisms of the samples. Thermogravimetric analysis (TGA) was conducted in an air atmosphere from 50°C to 950°C at a heating rate of 10 °C/min.

Results and Discussion

Effect of sintering temperature on the properties of porous bio-SiC ceramics

To understand the effect of sintering temperature on the properties of the porous bio-SiC ceramics fabricated in this study, the following test conditions were applied: impregnation of bamboo charcoal with a SiO₂ precursor sol (BcSiC) in a single cycle and then sintering at different temperatures for 2 h. Figure 1A illustrates the XRD patterns of bamboo charcoal and the BcSiCs sintered at 1500°C, 1600°C, and 1700°C for 2 h. When the samples were sintered at temperatures below 1700°C, two broad carbon diffraction peaks could be clearly observed at 2 θ values of approximately 24° and 43°, which were attributed to the (002) and (101)/(100) planes of carbon, respectively; these results indicate that the samples had some unreacted carbon (Qian and Jin 2006; Gordic et al. 2014). However, both specific carbon peaks almost completely disappeared after the samples were sintered at 1700°C. Furthermore, when the samples were sintered at 1600°C and 1700°C, peaks associated with the α -SiC (2 $\theta = 33.6^\circ$ and 38.1°) and β -SiC phases (2 $\theta = 35.3^\circ$, 60.0° , and 71.8°) were observed, and the intensity of the peaks increased with the sintering temperature. Similar observations were reported by Qian and Jin (2006), who suggested that preparing β -SiC through carbothermal reduction usually results in a minor amount of α -SiC.

Figure 1B presents the TGA curve of bamboo charcoal, indicating a considerable decrease in weight residue at sintering temperatures higher than 300°C in an air atmosphere. A weight residue of only 2.7% was observed when the sintering temperature was up to 620°C; this is because the carbon substrate was completely thermally degraded at approximately 600°C (Ding et al. 2014). By contrast, for the BcSiCs sintered at 1500°C, 1600°C, and 1700°C, the thermal degradation onset temperatures were nearly 520°C, 600°C, and 610°C, respectively. When the sintering temperature reached 950°C, the weight residues of the three sintered BcSiCs were 4.7%, 5.3%, and 17.0%. Figure 1B also presents the derivative thermogravimetry (DTG) curves of the samples; as shown in the figure, the maximum thermal degradation temperature of bamboo charcoal was 590°C, whereas the maximum thermal degradation temperatures of the BcSiCs sintered at 1500°C, 1600°C, and 1700°C were 695°C, 700°C, and 710°C, respectively, signifying

that the thermal stability of the BcSiCs could be improved by increasing the sintering temperature. The primary reason for this phenomenon is that SiC was generated through the carbothermal reduction of bamboo charcoal and SiO₂ during high-temperature sintering. A higher sintering temperature typically results in a more complete reaction and thus a more thermally stable SiC ceramic. Figure 2 depicts the SEM micrographs of the BcSiCs sintered at 1500–1700°C for 2 h. According to these micrographs, all specimens retained the inherently porous microstructure of bamboo, and the resulting bio-SiC ceramics replicated the original texture of the carbon template (Figure 2C–2H). After the sintering process, SiC grains were prominently formed on the cell wall and roughened the cell wall surface. However, among the specimens, only the BcSiC specimen sintered at 1700°C formed a large amount of SiC nanowires on the cell wall (carbon template) surface (Figure 2H), and the obtained SiC nanostructures comprised a nanowire core with extensional platelets. A similar phenomenon has been observed by Ding et al. (2014). Accordingly, 1700°C was considered the optimum sintering temperature for the preparation of bio-SiC ceramics in this study.

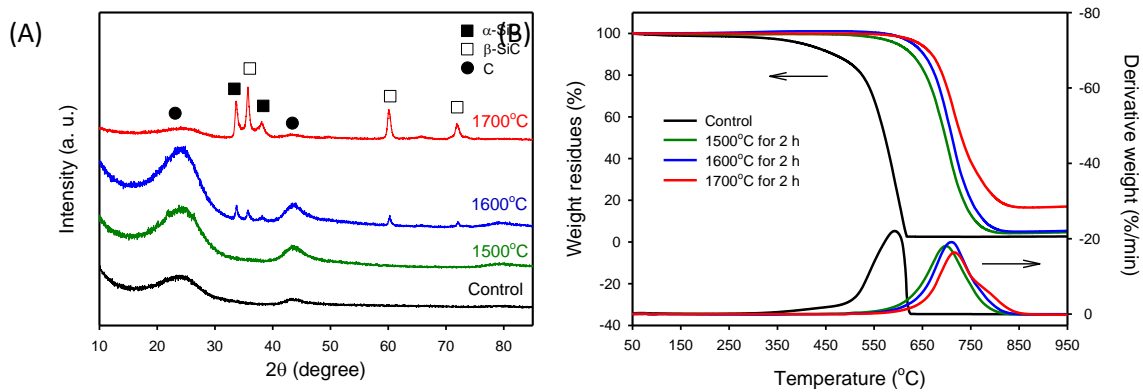


Figure 1 XRD patterns (A) and TGA/DTG curves (B) of BcSiCs sintered at different temperatures for 2 h.

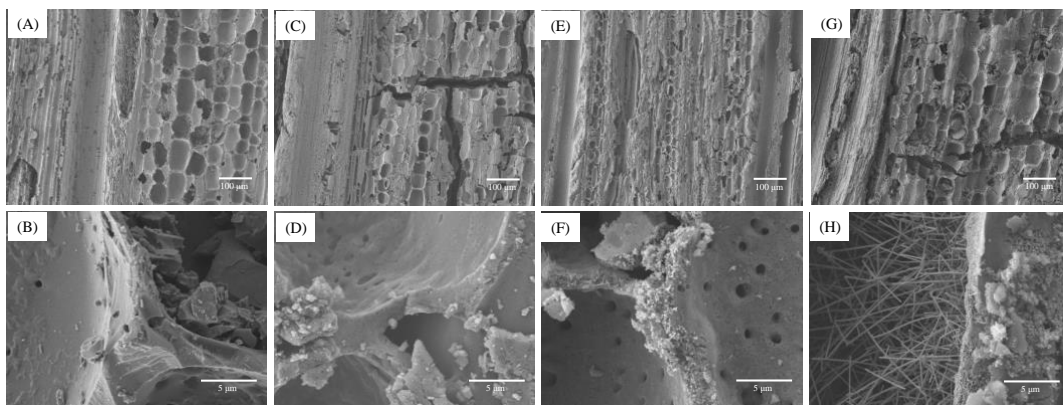


Figure 2 SEM micrographs of bamboo charcoal (A, B) and BcSiCs sintered at 1500°C (C, D), 1600°C (E, F), and 1700°C (G, H) for 2 h.

Effect of sintering duration on the properties of porous bio-SiC ceramics

To understand the effect of sintering duration on the properties of porous bio-SiC ceramics, this study applied the following test conditions: impregnation of bamboo charcoal with the SiO₂-precursor sol (in one cycle) and then the execution of sintering at 1700°C for different durations.

Figure 3 shows the XRD patterns of the BcSiCs sintered at 1700°C for 0.5–3 h. For the specimen prepared at 1700°C for 0.5 h, five distinct diffraction peaks of α - and β -SiC were observed along with two major peaks of carbon. However, as the sintering duration increased, the intensity of the SiC-associated peaks increases, whereas that of the carbon-associated peak decreased. This result is similar to that reported by Locs et al. (2011), who demonstrated that prolonged sintering positively influenced SiC formation. After 2 h of sintering, the peak of carbon nearly disappeared, whereas the peaks of the SiC crystal phase were clearly observed. A similar result has also been reported by Qian and Jin (2006) and Locs et al. (2011); when a sufficient reaction time was allocated, a favorable reaction between carbon and SiO₂ was achieved. Accordingly, a well-crystallized bio-SiC ceramic could be produced through sintering at 1700°C for more than 2 h.

Figure 4 depicts the SEM micrographs of the BcSiCs sintered at 1700°C for different durations. Observing the microstructure of the specimen sintered for 0.5 h (Figure 4A) revealed that the cell wall surface was similar to the smooth surface of bamboo charcoal, but a small amount of SiC nanowires was formed in the cell lumen. However, when the sintering duration was extended to 1–2 h, the cell wall surface became rough and the cell lumen comprised a higher amount of SiC nanowires (Figure 4B and 4C). After 3 h of sintering, this study observed the formation of a large amount of SiC crystal particles and nanowires on the surface of the specimen (Figure 4D). Additionally, the SiC nanowires in this specimen were significantly shorter and wider than those in the other specimens.

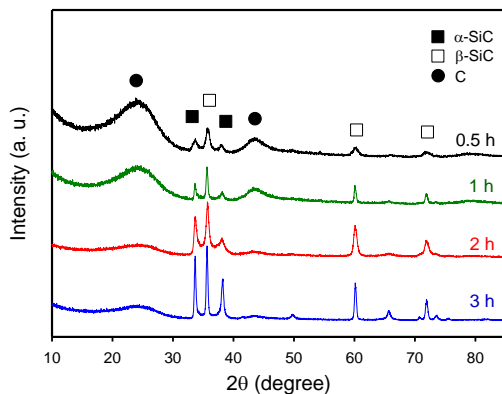


Figure 3 XRD patterns of BcSiCs sintered at 1700°C for different durations.

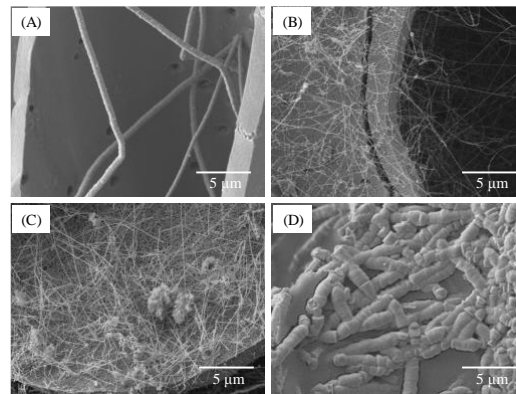


Figure 4 SEM micrographs of BcSiCs sintered at 1700°C for 0.5 h (A), 1 h (B), 2 h (C), and 3 h (D).

Effect of sol–gel impregnation cycle on the properties of porous bio-SiC ceramics

To further investigate the effect of sol–gel impregnation cycle on the properties of the derived porous bio-SiC ceramics, bamboo charcoal specimens impregnated with the SiO₂ precursor sol in one, three, and five repeated cycles were analyzed. Figure 5 illustrates the XRD patterns of the bio-SiC ceramics that were prepared from the BcSiCs prepared using different sol–gel impregnation cycles. The XRD patterns did not show obvious differences among all bio-SiC ceramics; peaks associated with β -SiC were observed at 2 θ values of 35.3°, 60.0°, and 71.8°, along with three peaks associated with amorphous carbon. However, the intensity of the peaks associated with carbon decreased as the number of sol–gel impregnation cycles increased, and this finding is consistent with that reported by Qian et al. (2004b). This phenomenon can be attributed to the fact that the amount of SiO₂ in the BcSiCs increased with the number of

impregnation cycles, which resulted in more efficient conversion of charcoal to SiC ceramics during the carbothermal reduction reaction.

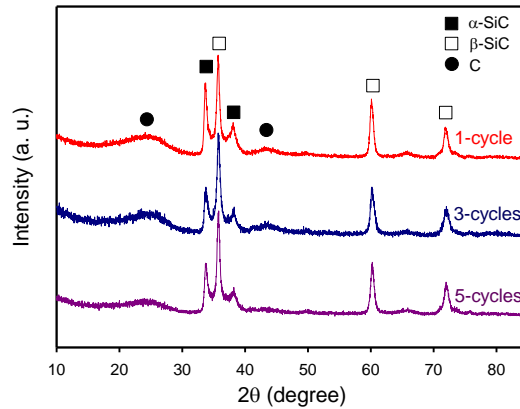


Figure 5 XRD patterns of sintered BcSiCs prepared using different repeated cycles of sol-gel impregnation process.

Figure 6 presents the microstructure of the bio-SiC ceramics prepared using three and five repeated cycles of sol-gel impregnation. The surface morphology of the cell walls of the bio-SiC ceramic prepared using three impregnation cycles (Figure 6A) was similar to that of the rough surface of the bio-SiC ceramic prepared using a single impregnation cycle (Figure 4C), except that SiC nanowires were not observed within the cell lumen. A foam-like cell wall was observed for the bio-SiC ceramic prepared using three impregnation cycles (Figure 6B). As reported by Qian and Jin (2006), a possible reason for this observation is that CO was produced in addition to SiC during the reaction of carbon with SiO₂. Moreover, the microstructure of the bio-SiC ceramic prepared using five impregnation cycles (Figure 6C and 6D) was similar to that of the bio-SiC ceramic prepared using three impregnation cycles; however, some SiC nanowires were formed on the surface of the cell wall of the bio-SiC ceramic. These results reveal that the microstructures of the bio-SiC ceramics did not differ significantly when the number of repeated sol-gel impregnation cycles exceeded three. Figure 7 depicts the HRTEM images and selected area electron diffraction (SAED) patterns of SiC nanowires of the bio-SiC ceramics prepared using five impregnation cycles. The nanowires had a diameter of nearly 100 nm and a single crystal structure (Figure 7A). The (111) plane, representing the atomic plane perpendicular to the growth direction, of β-SiC (Figure 7B) had a planar distance of 0.25 nm (Figure 7C), indicating that the preferred growth direction of the nanowires was perpendicular to the (111) plane. A similar result was reported by Ding et al. (2014).

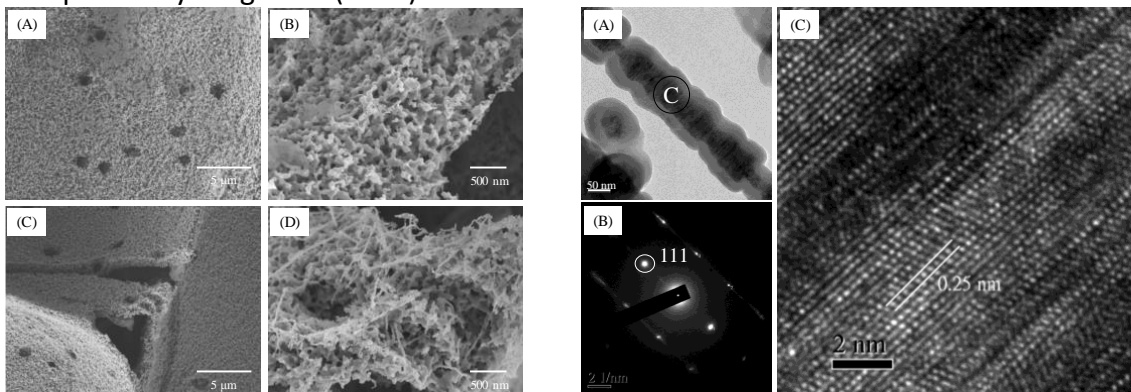


Figure 6 SEM micrographs of sintered BcSiCs prepared using three (A, B) and five repeated cycles (C, D) of sol-gel impregnation.

Figure 7 TEM image of a single β -SiC nanowire of sintered BcSiC prepared using five repeated cycles of sol-gel impregnation process (A); SAED pattern (B) and HRTEM image (C) obtained for the β -SiC nanowire.

To further investigate the feasibility of directly producing bio-SiC ceramics from bamboo, BSiCs were prepared from air-dried bamboo by using MTMOS and a sol-gel process and then sintered at 1700°C for 2 h in a nitrogen atmosphere. Figure 8 illustrates the XRD patterns of bio-SiC ceramics prepared from the BSiCs by using different sol-gel impregnation cycles. Similar to the XRD patterns of the sintered BcSiCs, β -SiC-associated peaks were observed at 2θ values of 35.3°, 60.0°, and 71.8°, in addition to peaks associated with carbon; the intensity of the peaks associated with carbon decreased as the number of repeated impregnation cycles increased. Figure 9 shows the HRTEM images and SAED patterns of a single SiC nanowire of a bio-SiC ceramic prepared from BSiCs using five impregnation cycles. The results in these images are similar to those obtained for the bio-SiC ceramic prepared from BcSiCs using five impregnation cycles. Accordingly, bio-SiC ceramics can be directly prepared from BSiCs, thus simplifying the manufacturing process of SiC ceramics. To the best of our knowledge, this is the first study to prepare biomorphic porous SiC ceramics directly from bamboo by combining sol-gel impregnation and carbothermal reduction.

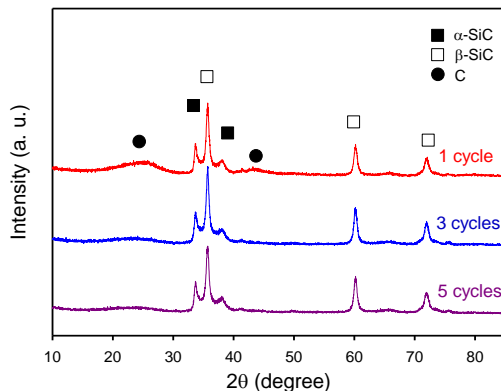


Figure 8 XRD patterns of sintered BSiCs prepared using different repeated cycles of sol-gel impregnation.

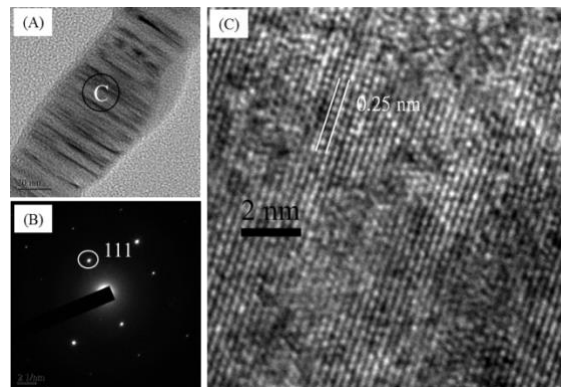


Figure 9 TEM image of a single β -SiC nanowire of sintered BSiC prepared using five repeated cycles of sol-gel impregnation (A); SAED pattern (B) and HRTEM image (C) observed for the β -SiC nanowire.

Summary and Conclusions

In this study, bio-SiC ceramics were prepared by combining sol-gel impregnation and carbothermal reduction, with MTMOS and bamboo serving as the precursors. The results reveal that a higher sintering temperature resulted in a more complete reaction and thus more thermally stable SiC. The resulting SiC ceramics comprised β -SiC and a trace amount of α -SiC. In addition, the microstructures of the cell walls of bio-SiC ceramics prepared using three and five impregnation cycles were determined to be foam-like (porous SiC) structures, in contrast to the microstructure of a bio-SiC ceramic prepared using a single impregnation cycle. Moreover, bio-SiC ceramics could also be successfully prepared from BSiC in this study, and their XRD patterns and HRTEM images were similar to those obtained for bio-SiC ceramics prepared from BcSiCs. According to a review of the literature, this is the first study to synthesize bio-SiC ceramics directly from bamboo using sol-gel and carbothermal reduction.

*Proceedings of the 62nd International
Convention of Society of Wood Science and
Technology*

Acknowledgements

This work was financially supported by a research grant from the Ministry of Science and Technology, Taiwan (NSC 102-2628-B-005-006-MY3).

References

- Ding J, Zhu H, Li G, Deng C, Li J (2014) Growth of SiC nanowires on wooden template surface using molten salt media. *Appl Surf Sci* 320:620–626.
- Esposito L, Sciti D, Pinacastelli A, Bellosi A (2004) Microstructure and properties of porous β -SiC template from soft woods. *J Eur Ceram Soc* 24:533–540.
- Gordic M, Bucevac D, Ruzic J, Gavrilovic S, Hercigonja R, Stankovic M, Mtovic B (2014) Biomimetic synthesis and properties of cellular SiC. *Ceram Int* 40:3699–3705.
- Herzog A, Klingner R, Vogt U, Graule T (2004) Wood-derived porous SiC ceramics by sol infiltration and carbothermal reduction. *J Am Ceram Soc* 87:784–793.
- Liu H, Jiang Z, Fei B, Hse C, Sun Z (2015) Tensile behavior and fracture mechanism of moso bamboo (*Phyllostachys pubescens*). *Holzforschung* 69:47–52.
- Locs J, Berzina-Cimdina L, Zhurinsh A, Loca D (2009) Optimized vacuum/pressure sol impregnation processing of wood for the synthesis of porous, biomorphic SiC ceramics. *J Eur Ceram Soc* 29:1513–1519.
- Locs L, Berzina-Cimdina L, Zhurinsh A, Loca D (2011) Effect of processing on the microstructure and crystalline phase composition of wood derived porous SiC ceramics. *J Eur Ceram Soc* 31:183–188.
- Mao WG, Chen J, Si MS, Zhang RF, Ma QS, Fang DN, Chen X (2016) High temperature digital image correlation evaluation of in-situ failure mechanism: An experimental framework with application to C/SiC composites. *Mat Sci Eng A-Struct* 665:26–34.
- Qian JM, Jin ZH (2006) Preparation and characterization of porous, biomorphic SiC ceramic with hybrid pore structure. *J Eur Ceram Soc* 26:1311–1316.
- Qian JM, Wang JP, Jin ZH (2003) Preparation and properties of porous microcellular SiC ceramics by reactive infiltration of Si vapor into carbonized basswood. *Mater Chem Phys* 82:648–653.
- Qian JM, Wang JP, Jin ZH (2004a) Preparation of biomorphic SiC ceramic by carbothermal reduction of oak wood charcoal. *Mat Sci Eng A-Struct* 371:229–235.
- Qian JM, Wang JP, Qiao GJ, Jin ZH (2004b) Preparation of porous SiC ceramic with a woodlike microstructure by sol-gel and carbothermal reduction processing. *J Eur Ceram Soc* 24:3251–3259.
- Sieber H (2005) Biomimetic synthesis of ceramics and ceramic composites. *Mat Sci Eng A-Struct* 412:43–47.
- Wu TL, Chien YC, Chen TY, Wu JH (2013) The influence of hot-press temperature and cooling rate on thermal and physicomechanical properties of bamboo particle-poly(lactic acid) composites. *Holzforschung* 67:325–331.

Fire-retardant & Sound absorption performance of WM Board

Seok-un Jo^{1, a *}, Hee-jun Park^{1, b}, Chun-won Kang¹

¹Department of Housing Environmental Design

College of Human Ecology, Chonbuk National University, Korea

^ajo18041@naver.com, ^bphjun@jbnu.ac.kr

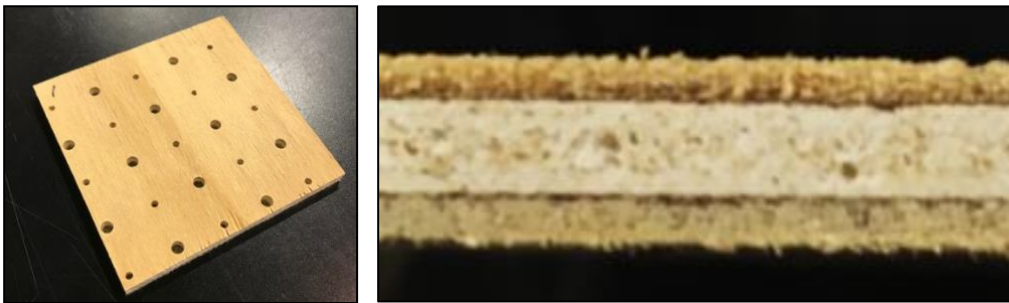
Keyword : Wood composite, Fire-retardant, Sound absorption, EN 13823, THR

Recently, as people spend more time indoors, the demand for eco-friendly indoor space that is pleasant and good for the body is also increasing. Wood is the most representative eco-friendly material that is easily accessible and used in building such eco-friendly indoor spaces.

However, despite wood's renewability, humidifying conditioning, strong specific strength, high heat insulation property and beautiful pattern, it is vulnerable to fire and thus cannot be applied to spaces that require fire-retardant performance.

This research develops wood veneer and magnesium board laminated composite (WM Board), which allows wood to be more widely used, complements its vulnerability to fire, and improves its sound absorption performance that helps create a good acoustical environment. Moreover, the research aims to confirm the newly developed material's fire-retardant performance and sound absorption performance.

Fig.1 Face & cutting surface of WM board-1.



The WM board-1 was produced by laminating and attaching Wood veneer (*Pinus radiate*) (T: 1.6mm) on the face and back of the board and a magnesium board (T: 3.0mm) in its core. And, to improve sound absorption, punchings were made and felt were attached.¹²³

The WM Board-1 was treated by fire-retardant chemicals and we tested its fire-retardant performance with the KS F ISO 5660-1, KS F 2271 methods. We also tested its sound absorption performance with the KS F 2805.

Conditions of satisfactory fire-retardant performance are: the THR (total heat released) needs to be less than or equal to 8MJ/m² for 10 minutes under 50kW/m², the HRR (heat release rate) cannot surpass 200kW/m² for more than 10 seconds, and the sample should not be penetrated, cracked, or form a hole. Also, time to incapability of moving of test mouse needs to be more than or equal 9 minutes by generated gas.

*Proceedings of the 62nd International
Convention of Society of Wood Science and
Technology*

Items	Unit	Results			Criteria	Testing Methods	Density	Moisture
		No.1	No.2	No.3				
Total heat released	MJ/m ²	6.2	5.5	5.4	≤ 8 MJ/m ²	KS F ISO 5660-1: 2015	Ave. 0.82	Ave. 12.8%
Duration of consecutive HRR over 200 kw/m ²	s	0	0	0	≤ 10 seconds			
Crack, hole or melting through the specimen	-	No	No	No	Yes/No			
Average time to stopped behavior of the white lab mice	min:s	14:42	14:17	-	≥9 minutes	KS F 2271: 2016		

Graph.1 Results of fire-retardant performance.

As a result, the WM Board treated with fire-retardant chemical satisfied the above conditions of fire-retardant performance. As for the sound absorption performance, we measured 0.51 in NRC (Noise Reduction Coefficient). Compared to plaster board's NRC 0.06, the result is approximately 8.8 times higher.

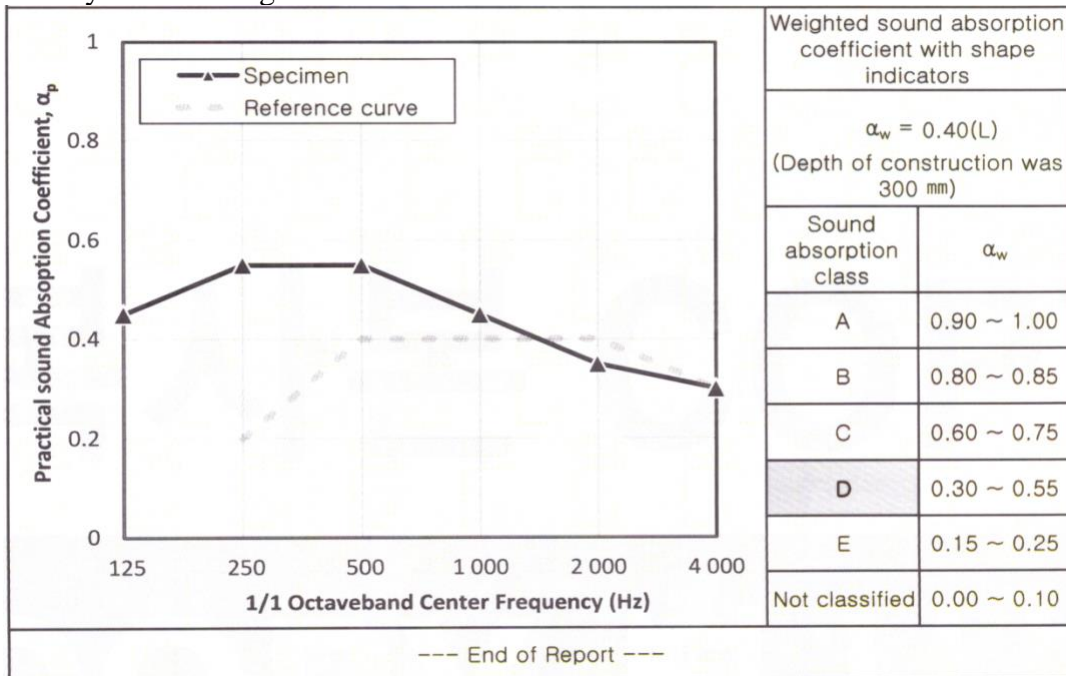


Fig.2 Results of the sound absorption performance (by Korea Standard KS F 2805)



Fig.3 The test specimen installed (Test of sound absorption class)

Additionally, for the foreign market entry of WM Board as a fire-retardant interior material, we produced a WM board-2 with different proportions of wood(T:0.8 mm) and magnesium board(T:6.0mm) and conducted the EN 13823 (Single burning items) test. As a result, we confirmed an A2 rating from an A1 to F range of the finishing material fire-retardant classification in Europe. Also, we will test by ASTM E 84 (surface burning characteristics of building materials) of the United States, and are currently in the process of investigating the WM Board's fire-retardant performance according to fire safety criteria of various countries.

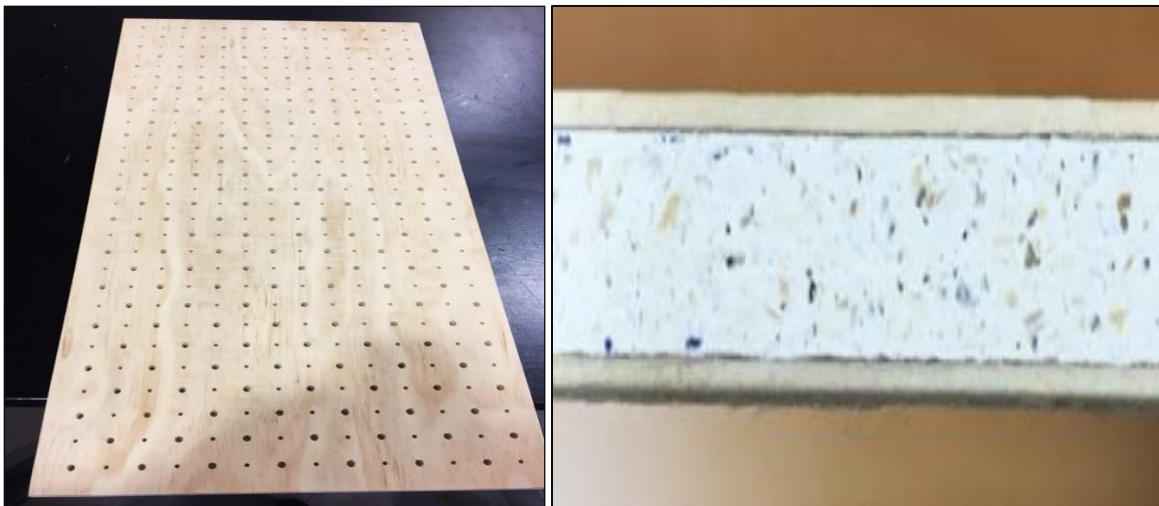


Fig.4 Face & cutting surface of WM board-2.

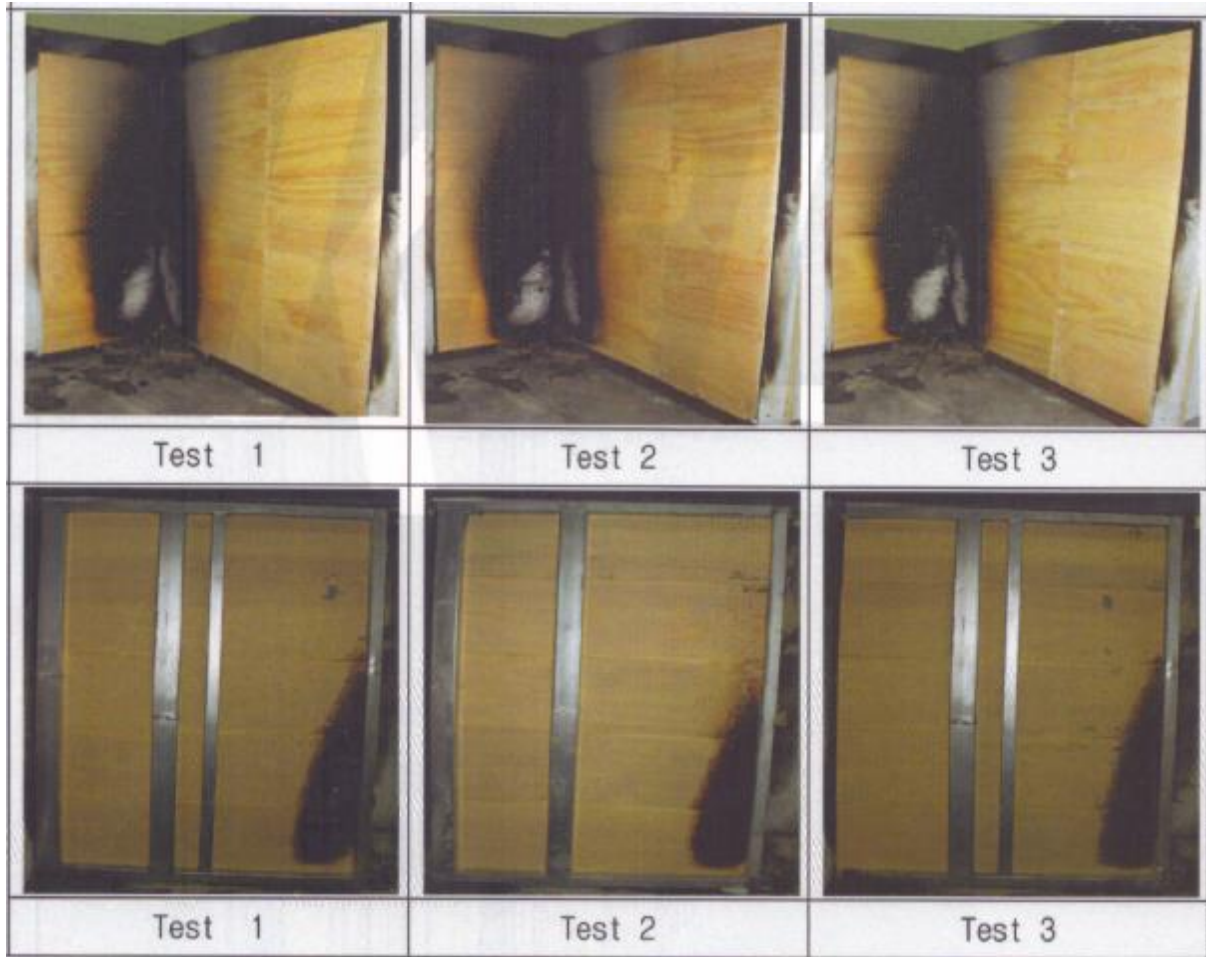


Fig. 5 Photo of the specimen (After the SBI test)

Items	Meaning	Results			Level A2
		Test 1	Test 2	Test 3	Criteria
FIGRA (w/s)	Fire growth rate	3.7	11.6	6.6	Below 120
THR _{600S} (MJ)	Total heat release	0.9	1.3	0.3	Below 7.5
SMOGRA (m ² /s ²)	Smoke growth rate	12.7	12.4	10.2	Below 30
LFS	Lateral flame spread reach the edge	None	None	None	None
Flaming droplets/particles (FDP) (flaming ≤ 10s)	Flaming droplets/particles	None	None	None	None
Flaming droplets/particles (FDP) (flaming > 10s)	Flaming droplets/particles	None	None	None	None

Graph.2 Results of fire-retardant performance (by SBI test)

In conclusion, with its outstanding fire-retardant performance and sound-absorption test results, the WM Board is expected to pave way for a new product and new industry that can replace the pre-existing minerals, metallic, and Resins interior materials.

*Proceedings of the 62nd International
Convention of Society of Wood Science and
Technology*

Acknowledgments

This study was carried out with the support of 'R&D Program for Forest Science Technology (Project No. "FTIS2018116B10-1920-AB01)' provided by Korea Forest Service(Korea Forestry Promotion Institute).

References

1. Korean standards association. Burning performance test - Heat release rate, smoke generation rate, mass reduction rate, KS F ISO 5660-1:2015
2. Korean standards association . Testing method for gas toxicity of finish materials of buildings, KS F 2271:2016
3. Korean standards association. Reverberation method Sound absorption performance measurement method, KS F 2805
4. BSI Reaction to fire tests for building products. Building products excluding floorings exposed to the thermal attack by a single burning item, EN 13823

**Thermal Stability of Glued Wood Joint Reinforced with Nanocrystalline
Cellulose in Shear Loading**

Mr. Gourav Kamboj

Prof. Milan Gaff

Mr. Vladimír Záborský

Mr. Gianluca Ditommaso

Mr. Roberto Corleto

Mr. Adam Sikora

Mrs. Fatemeh Rezaei

Dr. Miroslav Sedlecký

Mr. Štěpán Hýsek

Czech University of Life Sciences Prague, Czech Republic

Abstract

Nanocrystalline is used to improve the performance of the adhesive under thermal conditions with lap wood joint. NCC were added to poly urethane adhesive (2%, 4% and 6%) and blends were used as binder of wood. The thermal stability of glued lap joints is an important criterion to determine the stability of adhesive in field of engineered wood. Joining of wood materials has traditionally been achieved by mechanical fastening or adhesive bonding. During their product life, glued wood joints can be exposed to high temperature. The investigation covers the influence of the different temperature (30 to 180) on the shear strength of glued lap wood joints. Poly urethane adhesives with added of Nano crystalline cellulose were used in this work with increasing of temperature.

Wood modification using in situ polyesterification treatment with cost-effective and eco-friendly biomass material

Shanming Li¹, Enguang Xu¹, Xuefeng Xing², Lanying Lin¹, Yongdong Zhou¹ and Feng Fu^{1,2}
¹ Research Institute of Wood Industry, Chinese Academy of Forestry, Xiangshan Road, Haidian District, Beijing 100091, China

² College of Materials Science and Engineering, Nanjing Forestry University, Nanjing 210037, China

Email: lishanming@caf.ac.cn

Abstract: Due to its commercial applications, wood modification with cost-effective and eco-friendly biomass materials is attracting enhanced attention from researchers and industry. The aim of this work is to determine the potential for in-situ polyesterification of maltodextrin and citric acid in wood modification. Various techniques are applied to characterize the dimensional stability and polyester reaction. Permeability of modified reagents is improved by high power density microwave pretreatment. A small amount of isocyanate and silane coupling agent are used to enhance the water-resistance of polyesters. Results indicate that the optimization of microwave and bio-polyester treatment parameters can lead to significant improvement in wood properties. The modification with polyesterification enhanced dimensional stability. The anti-swelling efficiency (ASE) value of around 60%. The flexural strength and modulus of the treated specimens decreased, during degradation by acidic modification solution, compared to the control specimen. Such modified wood could be potentially utilized as wood flooring and wallboard for home furnishing applications.

Keywords: Wood modification, Polymerization, Polyester, Wood dimensional stability, Cost-effective

1. Introduction

Wood is a unique and renewable resource material that has been used for thousands of years delivering relatively high strength values with relatively low density, and beautiful appearance. However, wood is available in many species that vary in density, color, strength, and durability. Many kinds of woods have a low quality which restricted the applications. Recently, significant research has focused on modifying the low-quality wood to improve properties for value-added applications. Four main types of treatments can be implemented: (1) thermo-hydro and thermo-hydro-mechanical treatments; (2) chemical treatments; (3) biological processes; and (4) physical treatment with the use of electromagnetic irradiation or plasma (Sandberg, D. et al. 2017). The modification strategies based on chemical treatments are significant to improve properties such as dimensional stability, biodegradability, and fire resistance (Elizabeth Dunningham and Rosie, 2015). However, most of the chemicals involved in the reaction are toxicity, which may present serious environmental and health issues. To overcome these limitations and improve the renewability, several bio-based resins such as starch, polylactic acid, and polyfurfuryl alcohol have been developed instead of petrochemicals (Rowell Roger M, 2006 and Hill Callum A.S 2006).

Wood modification with furfuryl alcohol significantly enhances the durability and dimensional stability of wood, but the comparatively high cost is assumed to be the main obstacles in its commercialization (Kong Lizhuo et al. 2018). Wood modification in future research will more focus on cost-effective and eco-friendly. The polyesterification of sorbitol and citric acid in wood has been proven with increased dimensional stability, increased durability against decay fungi and less susceptibility to blue-stain fungi (Larnøy, E. et al. 2018).

Recently, our group started to look at the high power density microwave and eco-friendly adhesive treat wood, with a common goal: making direct use of the biological scaffold to develop new advanced functional materials, using new cost-effective and eco-friendly modification technologies. Microwave pretreatment creates pores and cracks in the cell walls which improve the impregnation performance of wood (Torgovnikov G. et al. 2009).

Maltodextrin which is a starch-based polysaccharide and citric acid which is a weak organic acid from the natural origin are both non-toxic, low price, renewable character, and good processability. The esterification reaction based on the maltodextrin and citric acid is particularly suitable for ecofriendly impregnation modification wood as it can be formed a three-dimensional polymeric structure. The modification process is water-soluble and used thermal curing. Once the polymerization reaction is completed the water is only obtained as the by-product which makes the wood modification technology attractive to the industry due to its green credentials (Berube, Marc-Andre et al. 2017).

The aim of this work is to in-situ synthesize a thermosetting polymer with the polymerization of maltodextrin and citric acid for eco-friendly wood modification applications. Two types of treatments were compared: one is directly impregnated modification solutions; the other one is high power density microwave pretreatment, then impregnated modification solutions. Wood with treatments may improve the quality of wood and can offer wood products with new functional opportunity for utilization.

2. Methods

Powdered maltodextrin (dextrose equivalent, DE 15 to 17) was purchased from Xiwang Group Company Limited (Shandong, China). The citric acid reagent was supplied by Suzhou Wang'an Fine Chemical Co., Ltd. Toluene-p-sulphonic was purchased from Sinopharm Chemical Reagent Co., Ltd. (Shanghai, China). Isocyanate was supplied by Guangzhou Guanzhi New Material Technology Co., Ltd. All chemicals were used as without additional purification. Deionized (DI) water was used as the solvent for preparation of the impregnation solutions.

The water-based impregnation solutions consisted of maltodextrin, citric acid, toluene-p-sulphonic, and Toluene-p-sulphonic was used as a catalyst and isocyanate as a curing agent. Typically, citric acid (21 wt%) was dissolved in DI water under mechanical stirring and then maltodextrin (12.5 wt%) was added to the solution under the same stirring.

All wood specimens were *Pinus sylvestris* produced from Russia. All specimens were divided into two groups. The specimens which need microwave pretreatment were puffed with 100kW (frequency 915MHz) and the conveyor speed is 1.2m/min using an industrial MW equipment (Figure 1a). For the microwave pretreatment, specimens with dimensions of 2000×220×120mm were used. The wood moisture contents were in the range of 40-50%. Then, all specimens were cut to impregnation specimens with dimensions of 300×80×30mm and oven-dried at 103°C for 10h. All specimens, except for the untreated controls, were impregnated with the solution performing an initial vacuum (-0.1MPa) treatment for 30min, followed by a pressure treatment (1.2MPa) for 24h. A part of specimens was then cured for 20h at a temperature 100°C. The other parts of specimens which have been microwave pretreatment were hot-pressed for 0.5h.

An X-ray diffractometer (XRD) was used to analyze the crystal structure with D8 advance (Bruker). The chemical structure was estimated by a Fourier Transform Infrared

Spectrometer (FTIR). The FTIR spectra were recorded from 400 cm⁻¹ to 4000 cm⁻¹ with a resolution of 4 cm⁻¹.

The surface morphology was observed by a field emission scanning electron microscope (XL30 S-FEG). The specimens were analyzed in a vacuum chamber that was less than 5×10⁻⁵ Pa and were scanned at a voltage of 10 kV.

The thermogravimetric analysis (TGA) was conducted with a STA 449F3 analyzer (Netzsch, Germany) at a 10 °C/min constant heating rate. The TGA tests were conducted in a flowing nitrogen atmosphere and heated to 650 °C.

The thermal properties were characterized by a Differential Scanning Calorimeter (DSC 214, Netzsch, Germany) from room temperature to 200 °C at 5 °C/min under nitrogen with a flow rate of 40 mL/min.

The flexural properties of specimens were measured using a universal mechanical testing machine (Instron 5982) according to “Chinese National Standard Testing Methods for Wood Physical and Mechanical Properties (GB/T 1928-2009)”. A three-point bending with a span of 240 mm and a speed of 5 mm/min was used for the test.

The weight percentage gain (WPG), bulking efficiency (BE) and volumetric swelling (S) of the specimens were calculated according to Eq.1 and Eq.2 (Wang Wang et al. 2014),

$$\text{WPG (\%)} = (W_2 - W_1) / W_1 \times 100 \quad (1)$$

$$\text{BE (\%)} = (V_2 - V_1) / V_1 \times 100 \quad (2)$$

$$\text{S (\%)} = (V_3 - V_2) / V_2 \times 100 \quad (3)$$

Where W_1 and W_2 are the oven-dried weight of the wood specimen before and after treatment, respectively (g), V_1 and V_2 are the volume of the wood specimen before and after treatment, respectively (mm³). V_3 is the volume of specimens after 24h of immersion at room temperature (mm³) for the control and treated wood specimens.

Anti-swelling efficiency (ASE) for the control and treated wood specimens were calculated as follows,

$$\text{ASE (\%)} = (S_u - S_t) / S_t \times 100 \quad (4)$$

Where S_u and S_t are the volumetric swelling of the control and treated wood specimens, respectively.

The water uptake (WU) after 24h, 48h, 72h, 96h, and 120h of immersion in deionized water at room temperature was calculated as follows,

$$\text{WU (\%)} = (W_3 - W_2) / W_2 \times 100 \quad (5)$$

Where W_3 is the weight of the sample after immersion in deionized water (g).

3. Results and discussion

Schematic diagram of the modification procedures of wood is illustrated in Figure 1a. As shown in the figure, one group is directly impregnated modification solutions; the other one is high power density microwave pretreatment to puff and increase permeability, then impregnated modification solutions.

Wood, maltodextrin and citric acid can react with heat to form a three-dimensional polymeric structure. The citric acid will react with free hydroxyl groups from wood chains and maltodextrin initiating the cross-linked polymer (M. Castro-Cabado, et al. 2016). The reaction mechanism for esterification of wood cell wall maltodextrin and citric acid is illustrated in Figure 1b.

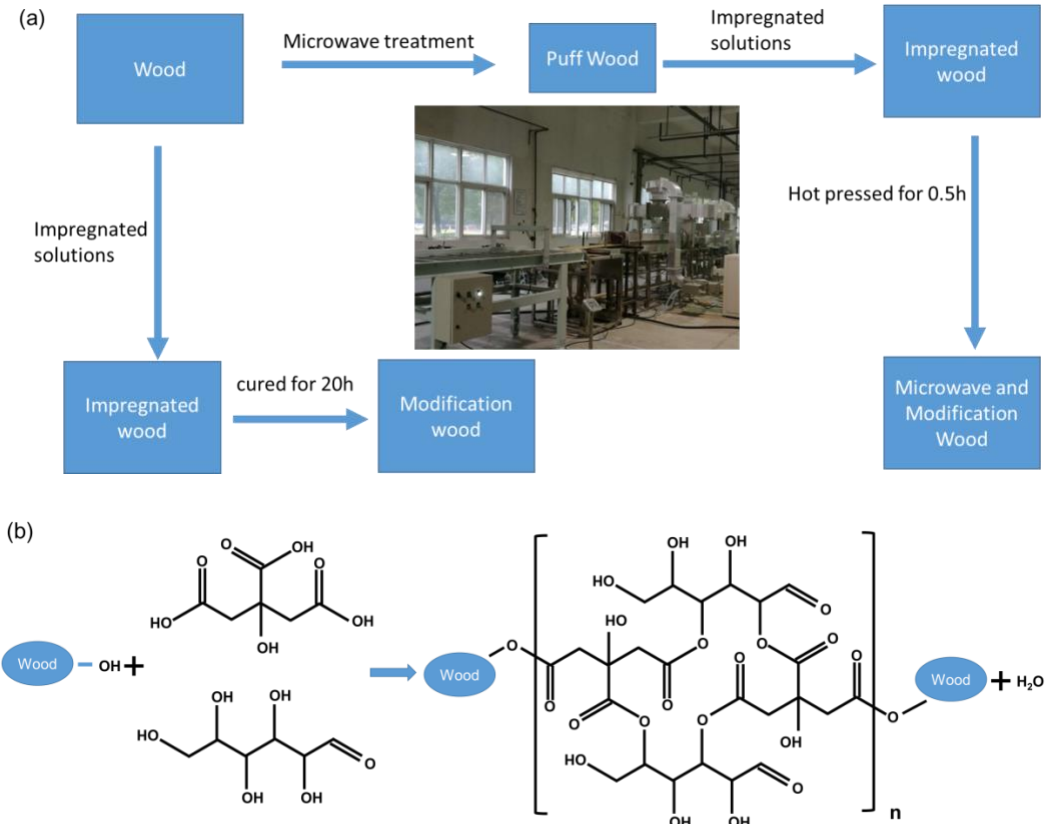


Figure 1. (a) Schematic illustration of experimental procedures and objectives of experiment design; (b) Esterification of the wood cell wall and citric acid, maltodextrin and citric acid formed.

Figure 2a shows the XRD results that the major peaks at approximately 17° and 22.5° corresponding to the cellulose (101) and (002) crystal planes, respectively. The peak position did not change and not addition peaks described in the profile indicating that the crystallinity is not influenced by the treatments.

To investigate the possible the OH stretching band evolve as esterification reaction is progressing between maltodextrin, wood and citric acid. The FTIR spectra for the specimens is shown in Figure 2b. Compared with the control wood, new bands in the range of 1712 to 1720 cm⁻¹ can be identified to C=O stretching band, which assigned to the ester bond between the hydroxyl groups of maltodextrin and the carboxyl group of citric acid in the modification and MW/modification specimens.

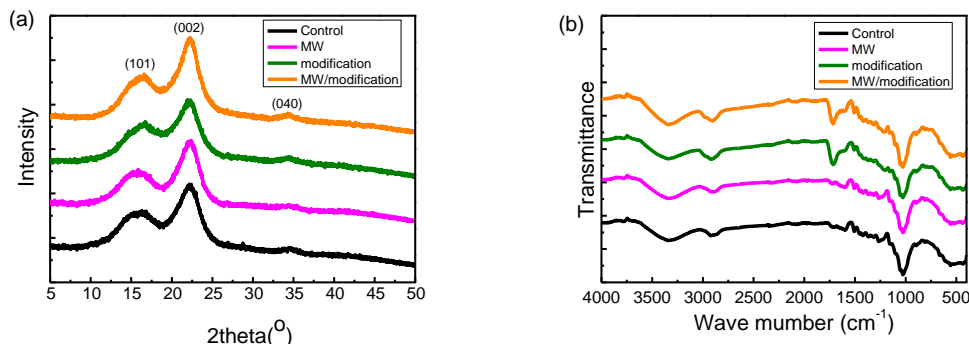


Figure 2. (a) XRD and (b) FTIR spectra of the wood specimens: control; microwave treatment; modification; microwave treatment and modification

In microwave pretreatment, the wood material is heated and cracked with pressure difference steam which reduces the strength and improves the impregnation performance of wood. Bio-polyester treatment specimens were increased weight percentage gain and density. However, due to the impregnation modification solution is acidic, the strength of specimens is reduced by degradation.

Table 1 Preparation, mechanical properties, and characterization of the specimens

Labels	Specimen preparation	Weight percentage gain, WPG (%)	Density (g/cm ³)	Flexural strength (MPa)
Control	No treatment	--	0.468	64.00
MW	Microwave treatment	-8.33±5.22	0.447	43.10
modification	bio-polyester treatment	29.85±4.41	0.604	43.84
MW/modification	microwave and bio-polyester treatment	20.68±2.5	0.802	20.20

The water uptakes of the specimens as a function of time at room temperature are shown in Figure 3a. The value of the control specimens increased from 35.2% (3h of immersion) to 114.9% (13 days of immersion). Due to increased permeability by high-intensity microwave treatment, the water uptakes of the MW specimens were higher than that of control. For group modification and MW/modification, the values decreased slightly and 52%, respectively. Two mechanisms might be proposed for explanation: (1) Microwave pretreatment increases the permeability for modification solutions; (2) Hot pressing improves acid and alcohol polyesterification quality.

The average anti-swelling efficiency (ASE) was calculated for each group of specimens shown in Figure 3c. Results show the increase for modification and MW/modification specimens. The best ASE value was achieved in MW/modification specimens with an average value of 60%; this is higher than the modification specimens which is 25%. The polymerization of citric acid with both hydroxyl groups of wood macromolecules and maltodextrin explain the high values of ASE. The increased dimensional stability can be attributed to the increased permeability of the MW. Materials impregnated to a greater extent resulting in a more cross-linked polymer after curing, which suggest better dimensional stability of the wood.

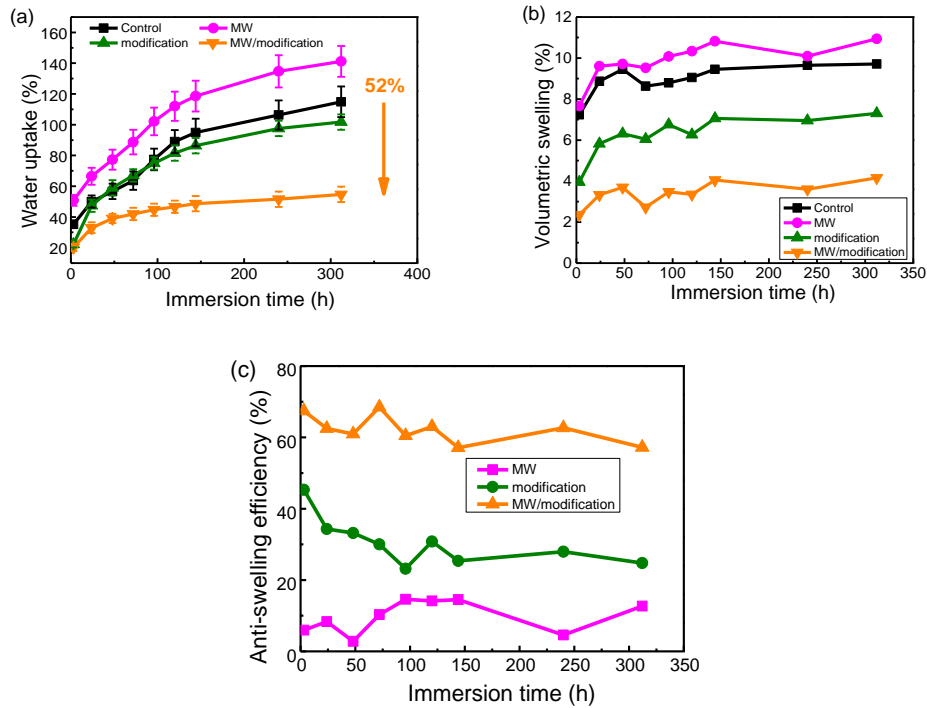


Figure 3. Effects of the different treatments on (a) water uptake (WU), (b) volumetric swelling (S), and (c) Anti-swelling efficiency (ASE).

As shown in Figure 4a and 4b, the TG and DTG curves show a three-stage decomposition process. The first mass loss occurs between 8-200°C which corresponds to the volatilization of water and other volatile derivatives in wood. The second mass loss shows an average loss of 55-60% of the total weight in the range from 220-380°C, which corresponds to the thermal degradation of the remaining polymer chains, fatty acid methyl esters impurities, and carbonization. The final mass corresponds to ashes and coke attributed to the thermal cracking process between 400 and 650°C. Thermograms show that the thermal stability increases while modification caused by the length of crosslinks between the polymer chains.

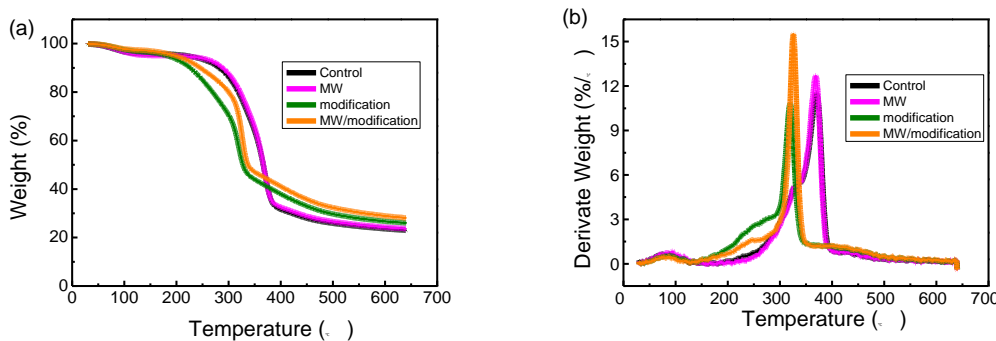


Figure 4. The (a) TG; (b) DTG curves of the wood specimens: control; microwave treatment; modification; microwave treatment and modification

The SEM images show the morphologies of the wood surfaces taken in cross-sections in Figure 5. It can be observed from that wood cell walls are damaged from the MW and curing step of the polymerization. The wood cell lumens of the control and MW specimens are empty

*Proceedings of the 62nd International
Convention of Society of Wood Science and
Technology*

(Figure 5a, 5a', 5b, 5b'). The images show a full or partial filling of cell lumens by the modification, microwave treatment/modification (Figure 5c, 5c', 5d, 5d'). Fillers are formed by the citric acid react with free hydroxyl groups from wood chains and maltodextrin initiating the cross-linked polymer.

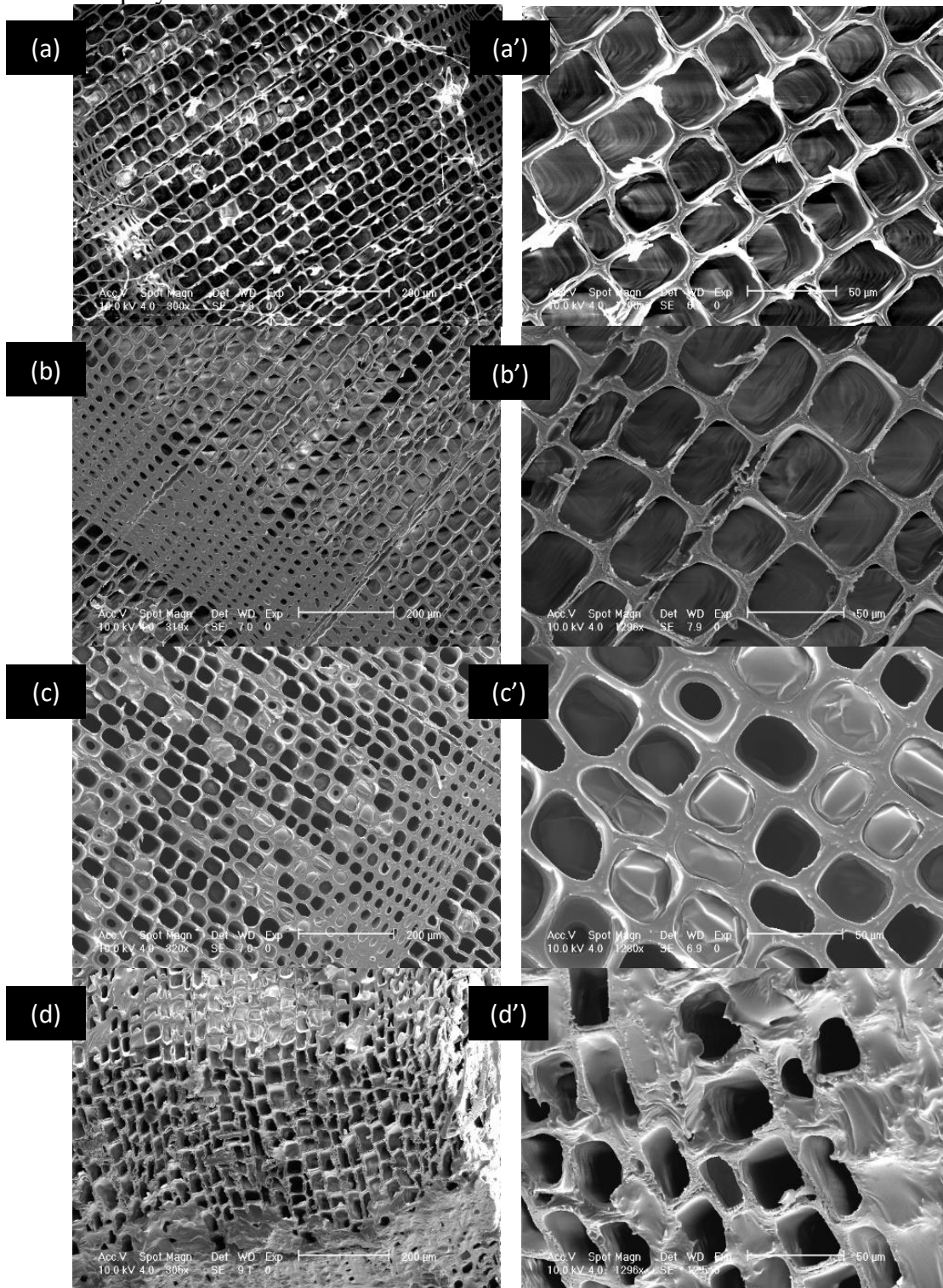


Figure 5. SEM images of cross-sectional (a, a') control; (b, b') microwave treatment; (c, c') modification; (d, d') microwave treatment and modification. The scale bar is (a,b,c,d) 200 μ m; (a',b',c',d') 50 μ m.

4. Conclusion

Chemical modification of wood requires chemical agents with cost-effective and eco-friendly. Therefore, the biomass materials are preferred for wood modification. Two different strategies have been applied to achieve this aim. In one approach, bio-polyester impregnation; In another approach, the two-step method proposed, high power density microwave pretreatment to puff and increase permeability, then bio-polyester impregnation. Compared with untreated wood, microwave treated wood, bio-polyester modified wood, and microwave and bio-polyester modified wood, shows higher weight percentage gain, density, thermal stability, and ASE value.

With an ASE value of around 60% after water leaching, microwave and bio-polyester treatment appear to be most promising for modification of the wood. Overall, results show that the optimization of microwave and bio-polyester treatment parameters can lead to significant improvement in wood properties. More work is needed to adjust the acidity of the modification solutions to improve mechanical properties and evaluate the durability against fungal decay and weathering.

Acknowledgments

This work was financially supported by the National Natural Science Foundation of China (NSFC Grant No. 31700641).

References

- Berube, Marc-Andre, Diane Schorr, Richard J. Ball, Veronic Landry and Pierre Blanchet. "Determination of in Situ Esterification Parameters of Citric Acid-Glycerol Based Polymers for Wood Impregnation." *Journal of Polymers and the Environment* 26, 3 (2017): 970-979.
- Castro-Cabado M., Francisco J. Parra-Ruiz, A.L. Casado. "Thermal Crosslinking of Maltodextrin and Citric Acid. Methodology to Control the Polycondensation Reaction under Processing Conditions." *Polymers & Polymer Composites* 24, 8 (2016): 643-54.
- Elizabeth Dunningham and Rosie. "Review of New and Emerging International Wood Modification Technologies." *Forest & Wood Products Australia Limited*, (2015).
- Hill, Callum A.S. "Wood modification: Chemical, Thermal and Other Processes." *Wiley Series in Renewable Resources*. Chichester: Wiley (2006).
- Kong, Lizhuo, Hao Guan, and Xiaoqing Wang. "In Situ Polymerization of Furfuryl Alcohol with Ammonium Dihydrogen Phosphate in Poplar Wood for Improved Dimensional Stability and Flame Retardancy." *ACS Sustainable Chemistry & Engineering* 6, 3 (2018): 3349-57.
- Sandberg, D., A. Kutnar and G. Mantanis. "Wood Modification Technologies - a Review." *iForest - Biogeosciences and Forestry* 10, 6 (2017): 895-908.
- Larnøy, E., A. Karaca, L. R. Gobakken, and C. A. S. Hill. "Polyesterification of Wood Using Sorbitol and Citric Acid under Aqueous Conditions." *International Wood Products Journal* 9, 2 (2018): 66-73.
- Rowell, Roger M. "Chemical Modification of Wood: A Short Review." *Wood Material Science and Engineering* 1, 1 (2006): 29-33.
- Torgovnikov G., Vinden P. . "High Intensity Microwave Wood Modification for Increasing Permeability." *Forest Products Journal* 59, 4 (2009): 84-92.
- Wang, Wang, Yuan Zhu, Jinzhen Cao, and Ru Liu. "In-Situ Synthesis of Organo-Montmorillonite in Southern Yellow Pine Wood: Preparation, Characterization and Properties." *Holzforschung* 68, 1 (2014): 29-36.

Effects of Physical Extraction on the Acoustic Vibration Performance of *Picea jezoensis*

Yuanyuan Miao, Rui Li, Xiaodong Qian, Yuxue Yin, Xianglong Jin, Bin Li, Zhenbo Liu*³
(School of Materials Science and Engineering, Northeast Forestry University, Harbin, China
150040)

In order to investigate the effects of physical extraction on the acoustic vibration performance of wood, deionized water (DW), dichloromethane (DE), benzyl alcohol (BA), and absolute ethanol (ET) were used to extract spruce. The results showed that the specific dynamic elastic modulus values E/ρ of spruce increased by 6.92%, 12.97%, 14.52% and 11.57%, respectively, and it can be seen that the effect of extraction was ranked as dichloromethane > benzyl alcohol > absolute ethanol > deionized water with respect to the specific dynamic elastic modulus E/ρ ; the acoustic radiation quality constants R increased by 11.20%, 18.11%, 17.42% and 14.89%, respectively, and in terms of the acoustic radiation quality constant R , the changes were ranked as dichloromethane > benzyl alcohol > ethanol > deionized water; both the logarithmic attenuation coefficient σ and the acoustic impedance ω decreased, and the logarithmic attenuation coefficient σ decreased most significantly by benzyl alcohol extraction (-52.0%); after dichloromethane extraction, the acoustic impedance decreased the most (-4.35%); from the sound quality of the material, the E/G value decreased by deionized water and dichloromethane extraction, while the E/G value increased after the extraction of benzyl alcohol and ethanol. The maximum value added (only 1.02%) was ethanol extraction. It can also be seen that the effect of the extraction treatment on the E/G value was not obvious. From the perspective of energy utilization, after four kinds of solvent-extracted spruce, the transmission parameter v/σ and the acoustic conversion efficiency $v/(\sigma \rho)$ were improved. The transmission parameter v/σ and the acoustic conversion efficiency $v/(\sigma \rho)$ were maximally increased by benzyl alcohol extraction: 124% and 145%, respectively. It can be seen that the benzyl alcohol extraction process was beneficial to improving the utilization efficiency of vibrational energy and prolonging the vibration time.

After the extraction treatment, the infrared characteristic curve of spruce did not change significantly, but the intensity of the absorption peak by hydroxyl and hemicellulose was slightly weakened; in the SEM electron micrograph, the duct walls and pits were more clear and clean after extraction, and the porous properties of the wood were retained; XRD tests showed that the crystallinity of spruce increased by 4.45%, 4.59%, 8.24% and 6.31%, respectively, and that the relative crystallinity of the wood treated with benzyl alcohol increased the most (11.70%). In summary, the extraction effect of the organic solvent was better than that of the polar solvent (deionized water), so the extract of the organic matter was not conducive to the acoustic properties of the wood. Hence, the effect of different extraction solvents on the acoustic performance of wood was different from the rate of change. In the future, a number of extraction methods can be considered to comprehensively improve the acoustic vibration

³The authors gratefully acknowledge the financial support from the National Natural Science Foundation of China (Grant No. 31670559), the Fundamental Research Funds for the Central Universities (2572016EBJ1), and State key research and development program funding (2017YFD0600204).

* Corresponding author: : Zhenbo Liu (liu.zhenbo@foxmail.com)

The stress-strain behavior of joint components in the surrounding of oak dowels

Jaromir Milch^{1} – Pavlina Suchomelova² – Hana Hasnikova³ – Martin Hataj⁴ –
Martin Brabec⁵ – Jiri Kunecky⁶*

¹ Researcher, Dr., Mendel University in Brno, Brno, Czech Republic *

Corresponding author

jaromir.milch@mendelu.cz

² Ph.D. student, Ing, Mendel University in Brno, Brno, Czech Republic

Pavlina.suchomelova@mendelu.cz

³ Researcher, Dr., Institute of Theoretical and Applied Mechanics of the Czech
Academy of Sciences, Prague, Czech Republic

hasnikova@itam.cas.cz

⁴ Researcher, Dr., University Centre for Energy Efficient Buildings of Technical
University in Prague, Prague, Czech Republic

martin.hataj@cvut.cz

⁵ Researcher, Dr., Mendel University in Brno, Brno, Czech Republic

martin.brabec@mendelu.cz

⁶ Researcher, Dr., Institute of Theoretical and Applied Mechanics of the Czech
Academy of Sciences, Prague, Czech Republic

kunecky@itam.cas.cz

Abstract

The timber structures cannot do without traditional all-wooden joints, especially, when historically valuable constructions are being reconstructed. The connections are usually the masterpieces that testify to the high carpentry skills and knowledges of the overall mechanical behavior. The mutual position of joint components is most commonly fixed by means of wooden dowels. However, the know-how for designing of these traditional joints remained only in the carpentry masters' mind and they were forwarded by long-term experiences to following generations. Therefore, the authors deal with the mechanical behavior of oak dowels within a comprehensive project granted by Technology agency of Czech Republic. This study addresses issue of missing available information about deformations experienced by joint components in the surrounding of oak dowels. The timber joint components made from Norway spruce (*Picea Abies* L. Karst.) were connected using cylindrical wooden dowels with diameter of 20, 24 and 30 mm made from English oak (*Quercus robur* L.). The mechanical force acting in double-shear mode

*Proceedings of the 62nd International
Convention of Society of Wood Science and
Technology*

was applied as a tensile loading parallel, resp. as a compressive loading parallel, perpendicular and at 45° to timber grain direction within the joint components. The experiments were done on full-scale specimens meeting the requirements listed in European standard EN 383. A statistically appropriate number of specimens (almost 300) were tested. The results characterize the timber embedment strength and joints load-bearing capacity, which are necessary for designing of structures according to the limit states theory.

Key words: wood; dowel; capacity; grain orientation; construction

Acknowledgements

This research was created at the Research Center Josef Ressel, Brno-Útěchov, Mendel University in Brno and was funded by TAČR - Zéta project “Oak fastener in timber structures: materials for normative anchorage” reg. No, TJ01000412.

*Proceedings of the 62nd International
Convention of Society of Wood Science and
Technology*

**Intensified Pulping Process to Produce High Value Materials from
Underutilized Appalachian Hardwood Biomass**

Dr. Gloria Oporto
Dr. Rory Jara-Moreno
Dr. Joseph McNeel
West Virginia University, USA

Abstract

An examination of prospective applications for nanocellulose from woody biomass suggests that U.S. markets exist that could use approximately 6.4 million metric tons annually. To date, nanocellulose is been produced mainly at small scale from bleached kraft pulps using mechanical processing. One significant disadvantage of any mechanical treatment is the high energy consumption associated with the fiber delamination, which decreases the final product's profit margin. A current limitation to introducing nanocellulose in the market is high production costs. Our goal is to demonstrate the feasibility of using an intensified and cost-effective process to produce nanocellulose for novel applications. Based on our preliminary research, we propose to produce nanocellulose from underutilized sawdust that considers lignin dissolution using acetic acid as a pulping solvent followed by mechanical fibrillation using a tubular high efficiency small reactor. Our hypothesis is that high quality low cost nanocellulose can be produced using an efficient intensified pulping process that utilizes low cost raw material from underutilized forestry sources highly available in the Appalachian hardwood forest.

**Comparison of Small- and Intermediate-Scale Fire Performance Tests of Southern Pine
Cross-Laminated Timber**

Mr. Bryan Dick

Dr. Perry Peralta

Dr. Phil Mitchell

Dr. Ilona Peszlen, Ilona_peszlen@ncsu.edu

Department of Forest Biomaterials, North Carolina State, USA

Abstract

Already well established in low and mid-rise construction in Europe, cross-laminated timber (CLT) is gaining acceptance in the U.S. and several manufacturers are now producing CLT in the U.S. and Canada. A critical question for the adoption of CLT is an understanding of the fire performance of all new design configurations. This study was performed to evaluate the effectiveness of a small-scale fire testing protocol from the ASTM PS-1 standard compared to intermediate-scale fire testing. The small-scale fire test, originally intended for plywood, demonstrated an ability to assess the fire performance of adhesive/species combinations with much less effort and readily available construction and testing equipment than what was required for intermediate panels.

Three cold-set adhesives [polyurethane (PUR), melamine formaldehyde (MF) and phenol resorcinol formaldehyde (PRF)] that are commonly used in CLT or other engineered wood products were tested. All CLT test panels were constructed of three layers of southern pine lumber, combined to mimic a 19mm plywood test panel. For both small-scale and intermediate-scale fire performance tests, MF and PRF adhesives were found to perform well, with little or no delamination of the outer lamina. In both scales tested, PUR-based CLT panels demonstrated easily observed delamination and charring of the exposed middle lamina in qualitative assessment. Measured delamination was also significantly higher in PUR-glued panels than in those glued with PRF and MF.

While not an adopted standard by building codes, the use of the ASTM PS-1 small-scale fire test is useful for easier construction and replication in new CLT product development prior to formal horizontal fire testing.

Keywords: Cross-laminated timber, fire test, southern pine, adhesive, polyurethane, melamine formaldehyde, phenol resorcinol formaldehyde

Hierarchy of Efficient Carbon Displacement & Storage in Products

Prof Bruce Lippke
University of Washington, College of Environment, USA
Dr. Maureen Puettmann
Dr. Elaine Oneil
CORRIM

Abstract

Research on the environmental impacts of fossil fuels and alternative renewable fuels and products has escalated since the early 1990's focused on opportunities to reduce CO₂ in the atmosphere. Life Cycle Inventories (LCIs) & environmental Assessments (LCAs) provide measures of carbon displaced and carbon stored. In this paper we analyze recent updates to LCI/LCA data for wood products and non-wood substitutes published over the last 20 years by CORRIM, a nonprofit research consortium. While CORRIM's primary mission has been to provide quality environmental data, when using wood to substitute for non-wood products, every product use and production process alters carbon resulting in interactions that inadvertently impact best practices. We consider the interactions of changes to different products, their uses, and raw material supply arrangements that may inadvertently influence carbon policy and investment decisions.

This paper uses recently updated LCI data revealing substantial differences in energy use across products and regions largely resulting from near universal adoption of energy intensive Environmental Control Devices to reduce particulate matter & other pollutants. We develop a hierarchy of efficiency options for displacing fossil carbon and storing carbon in wood products per unit of carbon in the wood used, ranging from 0.2 (20%) to 0.4 (40%) for ethanol substituting for gasoline fuels to highly leveraged uses of wood products at 6.0 (600%) revealing many opportunities to reduce Global Warming Potential (GWP) and contribute to more effective carbon policies, innovative research and productive investments. The complexity of many different processes and products reveals many interactions that if not understood contribute to unintended consequences counterproductive to carbon mitigation objectives.

**Optimization of Milling Process of Iroko Wood (*Chlorophora excelsa*) Depending on
Temperature of Thermal Modification**

Dr. Miroslav Sedlecký, sedlecky@fld.czu.cz

Prof Milan Gaff

Mrs. Fatemeh Rezaei

Mr. Gourav Kamboj

Mr. Gianluca Ditommaso

Mr. Roberto Corleto

Mrs. Monika Sarvasová Kvietková

Mr. Adam Sikora

Mr. Štěpán Hýsek

Czech University of Life Sciences, Prague, Czech Republic

Abstract

Wood species from tropical regions are a very attractive commodity in the world. Most of them have good mechanical and physical properties and are mainly sought after by end users for their hardness, color and beautiful look. The paper deals with the evaluation of the different temperatures of thermal modification (160, 180 and 210 °C) of Iroko wood (*Chlorophora excelsa*) on selected chemical components of wood in interaction with machining parameters (cutting speed: 20, 30, 40 and 60 m*s⁻¹; feed rate: 4, 8, and 11 m*min⁻¹ and rake angle: 15, 20 and 25°) and their effect on the quality of the milled surface. Quality is assessed by the roughness and waviness of the profile and these properties are represented by Ra/Wa: arithmetical mean deviation of the roughness/waviness profile. Another indicator of the effects of thermal modification temperature and milling variables was energy consumption. The results show that the density is decreases if the temperature of the thermal modification is increasing. Temperature change the various chemical components of the wood differently, and this is reflected in the final quality and energy consumption of the milled surface. Thanks to the research results we can optimize the milling process of Iroko wood.

This paper was supported by Project No. QK1920391 financed by Ministry of Agriculture of the Czech Republic called Diverzifikace vlivu biohospodářství na strategické dokumenty lesnicko-dřevařského sektoru jako podklad pro státní správu a návrh strategických cílů do roku 2030.

Behavior of Layered Beech Wood Reinforced with Glass and Carbon Fibers under Bending Loading

Adam Sikora*, Milan Gaff, Tomáš Svoboda, Štěpán Hýsek

¹Institute of Chemistry and Technology of Macromolecular Materials,
Department of Wood Processing,
Czech University of Life Sciences in Prague, Czech Republic
Corresponding author sikoraa@fd.czu.cz

Key words: layered wood, glass fiber, carbon fiber, bending loading

From a scientific and practical point of view, knowledge about the plasticity properties of wood-based laminates reinforced with non-wood components is an important part of a better understanding of the behavior of these materials during stresses. This paper deals with the analysis of the influence of the wood component (*Fagus sylvatica* L.), its thickness (5 and 9 mm), degree of densification (without densification, 10%, 20%, 30%, 40% and 50% densification of individual wood layers); and type of the non-wood components (stitched glass and carbon fibers) located on the convex side with respect to the direction of stress. On these layered materials were monitored the plastic characteristics of the force-deflection diagram at the three-point bend. The observed characteristics were the modulus of rupture "MOR" and the "CHM, EE, EMV, EP" plasticity moduli. The adhesive used to connect the individual components was a PVAc dispersion glue. A part of the work is a microscopic analysis declaring deformation of beech wood cells at the individual degrees of densification. The results provide important insights from the plastic area required for the production of wood-based composite materials reinforced with non-wood components with specific properties for a specific purpose.

Acknowledgement: The authors are grateful for the support of project Advanced Research Supporting the Forestry and Wood-processing Sector's Adaptation to Global Change and the 4th Industrial Revolution, No.CZ.02.1.01/0.0/0.0/16_019/0000803, financed by OPRDE. The authors also are grateful for the support of the Internal Grant Agency (IGA) of the Faculty of Forestry and Wood Sciences, project No B_19_03.

Impact of Gas Concentrations on the Self-Activation of Wood Biomass throughout its Processing

Lee M. Smith , Sheldon Q. Shi*

Department of Mechanical and Energy Engineering, University of North Texas, Denton Texas,
USA

*Corresponding Author: Sheldon.Shi@unt.edu

Self-Activation is a form of physical/thermal activation that uses high temperature (1000C) and oxygen free environment to cause the gasification of a biomass source and utilizes the syn gases produced to serve as the activation agent to treat and activate the resulting carbonized biomass to improve its surface properties. Because the self-activation process is a closed process it is currently difficult to monitor and understand the interactions between the syn gases present and the state of the material activation. The focus of this study is to subject southern yellow pine a common form of structural lumber to self-activation and to record the changes in gases at different intervals of the activation schedule and compare them to the surface properties of the resulting carbon. With this data it is hoped it can be used to help develop a model for the self-activation of this wood species.

Key Words: activated carbon, self-activation, gasification, syn-gases

**Survey of the Needed Changes in forestry Related Curricula – for Improving the
Competitiveness of Estonian Forest Sector**

Dr. Meelis Teder, meelis.teder@emu.ee

Chair of Forest Management Planning and Wood Processing Technologies
Estonian University of Life Sciences, Estonia

Abstract

Estonian forest area is 2.3 million ha, forests cover nearly 52% of the land territory and the use of this resource is important for the national economy. In 2017, the forest related sectors employed 33.8 thousand persons, which is 5.1% of the total number of employed persons. The foreign trade balance is positive; in 2017, the share of the export of forest related sectors in the total export was 21.4%, while the corresponding import share was 6.9%. However, due to recent forestry debates and changes in public opinion, the number of forestry students has been decreasing and reforms are needed.

The opinion survey was targeted at three forest sector related curricula - Forest Management (FM), Forest Industry (FI) and Natural Resources Management (NRM). Mixed methods were used. The qualitative part consisted of two internet based surveys: (1) MSc level graduates of 2013–2017 and (2) different kind of employers, with the focus of aforementioned graduates' first supervisors/mentors.

From 145 graduates 65 started to answer to the survey questions. Of these, 54 full surveys (37.2% of all graduates) were submitted: FM 16 (50.0%), FI 17 (31.5%) and NRM 16 (32.7%). From the 65 respondents 46% have worked on their profession after graduation; 22% partly worked according to their profession and additionally had other jobs or studied another speciality; 14% continued their professional studies on PhD level; 9% had applied for a professional job, but were not selected; 2% declared that already during the university studies it was obvious they are not willing to work according to the profession, and 8% declared other options.

There were 164 responses from employers' representatives, the majority of them had forestry (68.9%) or forest industry (12.2%) educational background, 28.0% were the leaders/ managers of their organizations, 24.4% top specialists, 27.4% technicians or middle level managers and 10.4% were officials.

The employers' general satisfaction with young specialists' education was 3.55 (max 5), the averages by field of activity were: officials – 3.75, forest management – 3.53, forest industry – 3.20. The main strengths and weaknesses of young specialists in forest industry: strengths – specific theoretical knowledge, knowledge of biology, willingness to learn independently. Weaknesses – knowledge of further processing of wood products (e.g. gluelam timber), lack of knowledge of practices in woodworking industries, volume estimation, price levels of wood products, lack of practical skills, lack of trust to the knowledge obtained in university – what is relevant and up-to-date and what is outdated? The lack of leadership skills and involvement of people.

For evaluation of different subjects in curriculum gap analysis was mostly used (gaps between satisfaction with university activities and importance in forest sector or in specific position, using five level Likert scale). Generally the gaps were smaller for silviculture related subjects, followed by forest management, and higher for forest industry related subjects.

*Proceedings of the 62nd International
Convention of Society of Wood Science and
Technology*

Additionally all the respondents were asked about the recommendations for changes in curriculum, especially what kind of new subjects are needed by labor market.

KEYWORDS: forest sector; education; employment; opinion survey; curricula developme

Comparison of acoustic non-destructive methods and semi-destructive methods for logs and timber assessment

**JAN TIPPNER^{1*} – MICHAL KLOIBER² – JAROSLAV HRIVNÁK² – JAN ZLÁMAL¹ –
VÁCLAV SEBERA¹**

¹ Research Scientist, Mendel University in Brno, Faculty of Forestry and Wood
Technology, Brno, Czech Republic* *Corresponding author*
jan.tippner@mendelu.cz, vaclav.sebera@mendelu.cz, jan.zalamal@mendelu.cz

² Research Scientist, Czech Academy of Sciences, Institute of Theoretical and
Applied Mechanics, Prague/Telč, Czech Republic

KLOIBER@ITAM.CAS.CZ, KUNECKY@ITAM.CAS.CZ

Abstract

The selection of high quality material is one of the first step in building of timber constructions. Hence, there is a call for techniques that would provide reliable methods for assessment of logs and timber. The goal of this study is to test spruce logs and subsequently evaluate timber by several methods, and to describe relationships between the evaluated material parameters. The trees from stand in Czech Republic with optimal ecological conditions for Norway spruce were felled during 3 seasons, consequently milled to logs and tested by several methods. Logs were processed into 68 beams made by 1. traditional carpentry way or 2. machine milling. The influence of traditional way of water treatment of timber was tested too. All the beams were tested by frequency-resonant method in the course of almost 2 years. Wood densities, sound velocities, dynamic moduli of elasticity, micro- drilling and indentation resistances were measured. The visual assessment was carried out as well. The relationships between properties were statistically tested to determine significance of manufacturing parameters, reliability of used non-destructive and semi-destructive methods to predict wood quality and also to describe the significance of harvest period or timber treatment to quality and properties of timber.

Key words: Spruce, Logging, Hewing, Beam, Assessment

Introduction

The high demand for spruce timber in central Europe in the centuries has led to the expansion of Norway spruce monocultures outside its natural ecological area (Slodičák and Novák 2007). It results in a wide-range and gradual variation of behaviour and properties of the spruce trees due to the change in original habitat conditions. Norway spruce is the dominant wood species used for building; the material with balanced physical and mechanical properties e.g. elasticity modulus vs. wood density and it is frequently used for restoration of historic timber structures too. The wood quality plays an important role in structure mechanics and durability thus the individual selection of material is the first important step of traditional carpentry technique of restoration of valuable constructions.

The selection of trees in the forest should be emphasized to reach a balance between properties for better processing and material behaviour. An appropriately selected timber at the entry (e.g. in the forest) is basic step of using of high-quality material for structural purposes. Therefore, simple and reliable methods for *in-situ* assessment of standing trees, logs and timber are searched.

Next to the natural variability of properties, the way of processing of wood can influence the timber quality. In the spruce regions of central Europe, the traditional ways of processing of spruce wood for achieve the desired qualities were developed in the past. Many of traditional proverbs says when to cut the trees in the year seasons, even in moon phase or the zodiac sign and how to consequently process it. Toreli (2009) presents proverbs from the Alpine region, which narrates logging at certain moon phases or on a specific day. Bues and Triebel (2004) mentioned similar old-known rules related to year season: traditionally, winter is mentioned as the ideal time for felling the trees, which is respected in many current technological regulations or standards. Zürcher (2010) adds that after the full moon in the winter it is preferable to cut down trees. Taking these principles into account in current practices is rather rare. Also, the strong wood-water relations open questions about the possible effect of timber rafting or any traditional wood treatment by water.

During reconstructions of valuable timber structures, there are strong requirements for sensitive approach with respect to cultural value of structures, traditional techniques and use of material with corresponding quality and properties. This opens questions of reconstruction designers, preservationist, truss builders or, finally, carpenters. How and where to choose high-quality spruce wood? What is the effective and easy way to choose wood *in-situ*? How the traditional logging and carpentry practices can affect the properties of processed wood This article attempts to provide an answer using practical experiment based on devices.

Materials & Methods

For the experiment a forest stands in Bohemian-Moravian Highlands with optimal ecological conditions for Norway spruce (*Picea abies* L. Karst) were selected. First group of 28 standing trees were selected for visual evaluation and device-supported methods. The

Proceedings of the 62nd International Convention of Society of Wood Science and Technology

assessed trees had a straight trunk with no signs of rot or any internal defects, they looked vital and healthy in general. The individual selection of trees was followed by the requirements for production of quality building elements. The average tree trunk diameter (*Diameter at breast height, DBH*) was 0.43 m and the average height of tree was the 31 m. Drilling resistance (parameter *RM Tree*) through the tree trunk was obtained using *Resistograph® 4453-S* (max. drilling depth 440 mm and resolution 0.010 mm, Rinn et al. 1996), velocity of stress wave propagation in radial direction - *VelocityR Tree* was obtained by *Fakopp 2D Microsecond Timer* (as presented in Tippner et al. 2015), and trunk diameter (*BHD Tree*) was measured using caliper; the tree dominance status in canopy (5 grades) and tree crown canopy closure (5 grades) were visually assessed on all the standing trees.

Drilling resistance was again measured on the lying trees; velocity of stress wave propagation was measured in the longitudinal direction and indentation resistances measurement (Kloiber et al. 2011, 2014). The small wood samples (discs and small beams) were prepared from the base of every trunk. Moisture content (*MC*) and density (*Rho*) of wood was evaluated on the discs and beams.

The tree trunks were bucked into the logs (2.5 m), which were processed into beams (dimensions of 0.2 x 0.24 x 2.5 m) in the spring 2017 in four different ways: a) hand hewing, b) standard saw cutting, c) hand hewing of water dipped logs, and d) hand hewing and subsequent dipping in water. Logs and beams were dipped in a river for four months. Immediately after production of beams, the selected physical and mechanical properties of wood were measured. Subsequently, the beams were stored (open-air covered piles), measurements were taken a year later in autumn 2018. The second group of 24 trees was harvested in three different seasons: 1) in the winter, 2) in the spring and 3) in the summer of 2017. Felling dates were predominantly set for the 1st and 2nd quarters of the moon phase.

The tree logging was divided up to eight time periods. In every felling period were harvested three trees. In the winter, we harvested 12 trees, in the spring and summer we harvested 6 trees in total. Subsequently, two beams from every logged tree were processed by hand hewing. Every beam was assessed by frequency-resonance acoustic method in longitudinal and bending mode (based on Baar et al. 2012). The long. velocity (*VEL-L Beam*), long. (*EDYN-L*) and bend. (*EDYN-B*) dynamic moduli of elasticity were then calculated. The evidence of cracks and other defects was monitored during testing.

Results and Discussion

All parameters measured on 4 types of beams (different methods of production) were scattered at the first measurement, but for almost all these parameters the scatter diminished after repeated measurements. The most changed parameter was the beam volume (Fig. 1 left). The sawn (group no. 2 and repeated measurement group no. 10) and hewed beams (group 1 & 9) showed a larger volume reduction after repeated measuring than the other (dipped) groups, although the dimensions and volumes measured immediately after production were very balanced and in agreement with designed shape. Beams made by hewing and sawing have statistically different values after 1 year of production. The mean volumes decreased by 9.7% for the hewed and 8.4% for the sawed beams respectively. This fact could be explained by the relationship between wood hygroexpansion levels at different

MC, when the wood do not change dimensions with decreasing of MC from green state to the fibre saturation point (approx. 30% of MC), after which the wood shrinks quite significantly. The weight of beams decreased constantly with decreasing of MC.

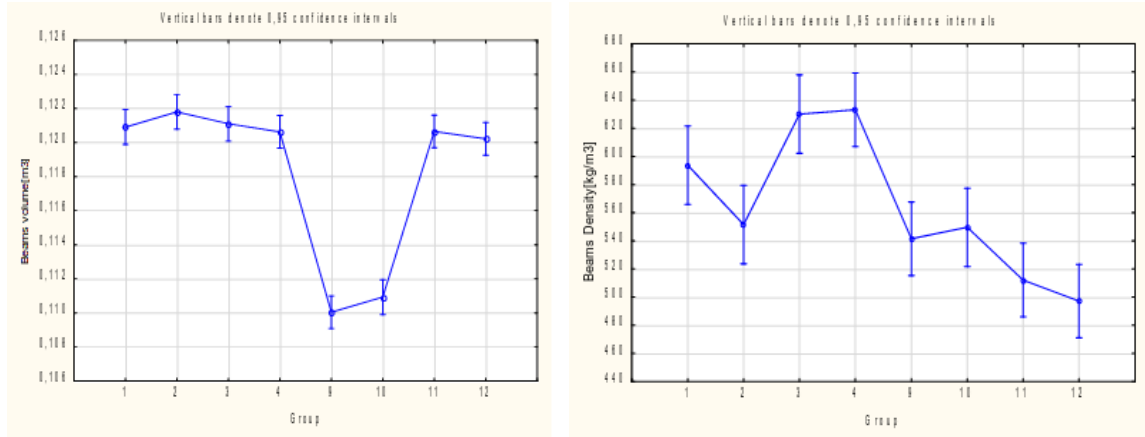


Figure 1: Left: beam volume [m³] changes between measurements (1-hewed, 2 sawed, 3 dipped-hewed, 4 hewed-sawed beams at 1st term; 9-12 the same order of groups for 2nd term); right: the average wood densities [kg/m³] for beam groups.

Density was significantly highest for beams which were dipped in water during the first measurement. There were no statistically significant differences ($\alpha = 0.05$) in densities measured in the second measurement, but the hewed and sawn beams (not dipped) had a slightly higher mean density than the other ones. This could be interpreted as a result of leaching of substances from wood into water. The second measurement showed the values of dynamic modulus of elasticity in the longitudinal direction and the bending dynamic modulus of elasticity had the similar differences between the groups as the densities. The occurrence of larger cracks in hewed and sawed beams was confirmed compared to beams dipped in water. Fig. 1 (right) illustrates the wood density changes. Density statistically differs between both terms of measurement in case of group 3 and 4, whereas variances of values of groups 1 and 2 overlaps with the one of repeated measurements (9 and 10). It corresponds to above mentioned developments of beam volumes and weight. The changes are contradicted by the smaller volumes of groups 9 and 10 when the weight is similar across all groups.

The analysis of variance (ANOVA, $\alpha = 0.05$) of the dynamic elastic moduli in the longitudinal direction based on the frequency-resonance method (*EDYN-L*) shows (Fig. 2) that the mean values for the sawn and hewed beams were about 1.8 GPa lower than the one of repeated measurement. The mean of *EDYN-L* for beams hewed from dipped logs and dipped beams were about 1.25 GPa lower from their repeated measurements. However, Tuckey's test showed that the statistically significant differences are only between group 4 and groups 9–11.

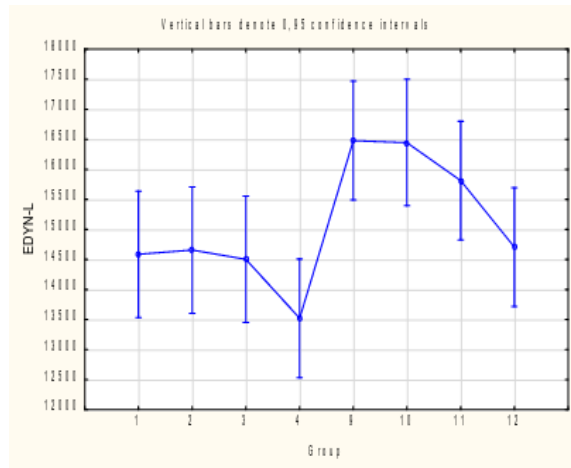


Figure 2: The dynamic elastic moduli in longitudinal direction [Mpa].

Prediction based on relationships between methods

Data from trees, logs, small cut samples and all beams were correlated. A strong relationship was found between resistance drilling values (*RM Tree*), wood sample density with 12% MC (*Rho-2 Cut*), beam density (*Rho Beam*), and beam elastic moduli (*EDYN-L*, *EDYN-B*).

Furthermore, the micro-drilling and indentation resistances from the logs correlated with each other. A strong relationship has been also demonstrated between the densities measured in different samples (*Rho... Cut*) and beams (*Rho Beam*) as well as between these densities and the dynamic elastic moduli. Tree dominance status does not correlate with any monitored material properties, it is related to the tree height and diameter only.

Table 1: The correlation coefficients of selected monitored variables.

Variable	Correlations - Marked correlations are significant at p < 0.05										
	BHD Tree	RM Tree	VEL-R Tree	Rho-green Cut	Rho-12 Cut	W-green Cut	Rho-K Cut	Rho Beam	VEL-L Beam	EDYN-L Beam	EDYN-B Beam
BHD Tree	----										
RM Tree	-0.311	----									
VEL-R Tree	0.842	-0.339	----								
Rho-green Cut	-0.516	0.534	-0.539	----							
Rho-12 Cut	-0.429	0.735	-0.442	0.834	----						
MC-green Cut	-0.363	0.073	-0.294	0.654	0.176	----					
Rho-K Cut	-0.429	0.647	-0.499	0.859	0.969	0.175	----				
Rho Beam	-0.503	0.748	-0.532	0.731	0.916	0.113	0.869	----			
VEL-L Beam	-0.493	0.470	-0.467	0.572	0.463	0.558	0.371	0.428	----		
EDYN-L	-0.586	0.737	-0.603	0.771	0.849	0.338	0.772	0.882	0.801	----	
EDYN-B	-0.503	0.759	-0.526	0.791	0.892	0.314	0.815	0.911	0.738	0.985	----

Based on strong correlations, data from resistance drilling (*RM Tree*) and the wood density at 12% of MC (*Rho-12 Cut*) were used for a theoretical derivation of the global beam material parameters - elastic moduli in longitudinal direction (*EDYN-L*), and bending elastic

**Proceedings of the 62nd International
Convention of Society of Wood Science and
Technology**

modulus (*EDYN-B*) for beam groups produced by four different technologies. Furthermore, the linear regression models were determined for monitored values. These simple models could be used in practice for individual selection of trees based on drilling resistance.

For example, the *EDYN-L* of beams can be estimated by:

$$EDYN-L = -14561.6 + 190.9 \cdot RM \text{ Tree}, \quad \text{Equation (1)}$$

and wood density at 12% MC can be estimated by:

$$Rho-12 \text{ Cut} = -19.2608 + 3.2296 \cdot RM \text{ Tree}. \quad \text{Equation (2)}$$

The influence of harvest period

The effect of logging season to wood density is described by Fig. 3. The groups of beams from spring and summer logging were alike, but beams from winter harvest period differ.

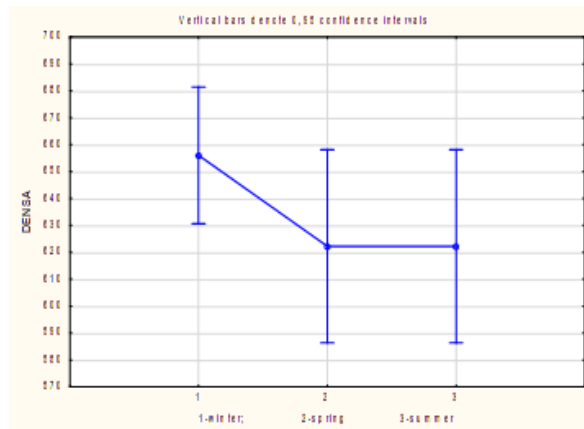


Figure 3: The effect of the logging season to the wood density variance [kg/m³].

Fig. 3 shows the higher average density for the winter timber beams. However, the Tuckey's test did not show a statistical difference. The longitudinal stress-wave velocity (*VEL-L Beam*) was lower for the winter-logged timber. The beams from spring and summer harvest have similar values with each other. The elastic modulus in the longitudinal direction applies the same trend and differences as for beam density. The flexural elastic moduli (*EDYN-B*) were statistically different too (see Fig. 4). The beams processed from winter harvest show statistically lower values when compared with the beams from spring and summer harvest. Statistical differences were confirmed by Tuckey's test of multiple comparisons.

The monitored properties for each beam were evaluated according to the harvesting (cutting) terms of the trees. The term of harvest corresponded to the phases before the full moon or after the full moon. The variance analyses of the individual monitored parameters exposed the differences in the mean values of variables. However, the statistical tests did not confirm significant differences.

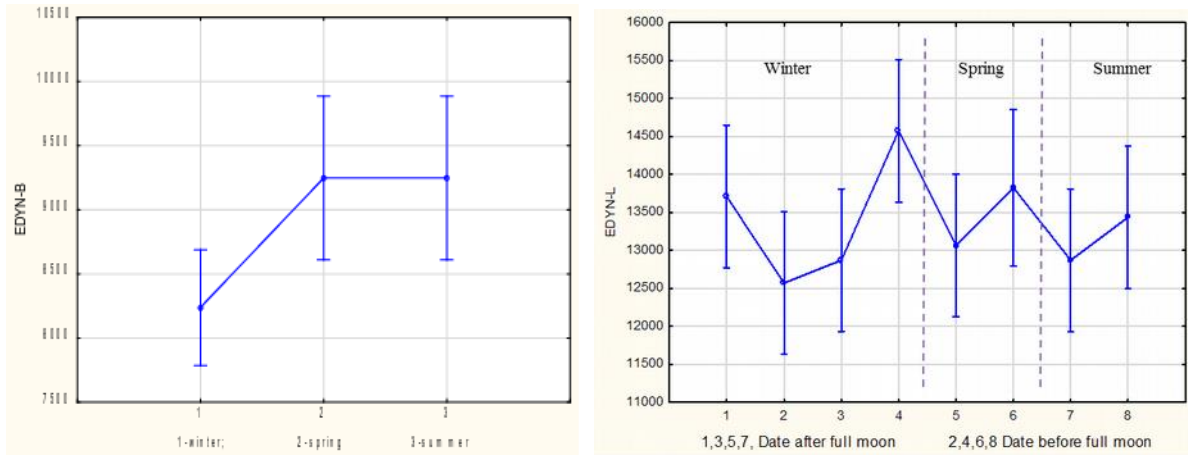


Figure 4: Left: the effect of the harvest season to flexural elastic modulus variance [Mpa]; right: the longitudinal dynamic moduli [MPa] at different moon phases (1-8).

The moon phase influence on the monitored variables might have been confirmed when the monitored values changed significantly and regularly according to the phases. The example of changes of *EDYN-L* (variance analyses) is visible in Fig 4. The mean values regularly changed at the end of winter, spring and summer, the mean values for the timber harvested before the full moon are higher but the scatters overlaps. Also, the Tuckey's multiple comparison test shows that these differences are not statistically significant.

Summary and Conclusions

We have tested several practice-friendly techniques for a prediction of spruce timber properties based on data measured at logs or even at standing trees. Four different technologies of processing and storage of beams and several harvest periods of trees give us opportunity to try to find out changes in timber properties too. Statistical analysis of data obtained from 68 true-scale spruce beams show no significant differences between the sawn and hewed beams. The difference was found between the group of water treated beams and untreated beams. The density of dipped beams and beams made from dipped logs decreased more significantly in one year when compared with hewed and sawn beams without dipping. After more than one-year-long dry storage of beams, the differences were still present due to the different MC levels in each group and probably due to the amount of leached extracts from the wood. The mean values of densities of the hewed and sawn beams were higher than the mean values of the beams that were dipped, but based on variance analysis, these differences are insignificant.

The most significant correlations were found between: 1) drilling resistance of tree trunks and density of final beams, 2) density of a small samples cut from tree base and global dynamic elastic moduli of beams. According to the correlation, the linear regression models were created for estimation of the density of wood

*Proceedings of the 62nd International
Convention of Society of Wood Science and
Technology*

of monitored properties. The values of beams from trees harvested in winter differed slightly and statistically insignificantly (the significant difference was demonstrated only in 1 case - the flexural elastic moduli). The effect of moon phases on properties of wood beams was not confirmed. However, certain differences were observed between the individual moon phases in terms of the dynamic longitudinal elastic moduli, but these differences were not statistically significant.

Acknowledgements

This research is supported from project “Historical Timber Structures: Typology, Diagnostics and Traditional Wood Working” NAKIII, reg. No. DG16P02M026, provided by the Ministry of Culture of the Czech Republic.

References

- Baar J, Tippner J, Gryc V (2012) The influence of wood density on longitudinal wave velocity determined by the ultrasound method in comparison to the resonance longitudinal method, *European Journal of Wood and Wood Products* 70(5), 767-769.
- Bues CT, Triebel J (2004) Sorgloser Umgang mit Mondholz schadet dem Image des Holzes allgemein Mondholz – alles erlaubt? *Wald und Holz* 2004(3):31-35.
- Kloiber M, Tippner J, Hrivnák J (2014) Mechanical properties of wood examined by semi- destructive devices. In: *Materials and Structures*, Vol.47(1):199-212.
- Kloiber M, Tippner J, Drdácký M (2011) Semi-destructive tool for "In-situ" measurement of mechanical resistance of wood. In: SHATIS´ International Conference on Structural Health Assessment of Timber Structures. June 2011. Lisbon. Portugal.
- Rinn F, Schweingruber F, Schär E (1996) Resistograph® and x-ray density charts of wood comparative evaluation of drill resistance profiles and x-ray density charts of different wood species. *Holzforschung – International Journal of the Biology, Chemistry, Physics and technology of Wood*, Vol.50(4):303-311.
- Slodičák M, Novák J (2007) Growth structure and static stability of Norway spruce stands with different thinning regimes, *Lesnická práce* 2007, 128, *Folia Forestalia Bohemica* 3.
- Tippner J, Hrivnák J, Kloiber M (2015) Experimental Evaluation of Mechanical Properties of Softwood using Acoustic Methods. *BioResources* 11(1):503-518.
- Torelli N (2009) Lunarni les. mit ali resničnost. *Zbornik gozd. in les*, 76: 71-101.
- Zürcher E (2010) Looking for differences in wood properties as a function of the felling date: lunar phase-correlated variations in the drying behavior of Norway Spruce (*Picea abies* Karst.) and Sweet Chestnut (*Castanea sativa* Mill.), *Trees* 10.

Preparation and UV-aging resistant properties of Eu(III) complex-modified poplar wood-based materials

Di Wang¹

1. Material Science and Engineering College, Northeast Forestry University, Harbin 150040, China

Abstract

Wood surface always attacks by solar irradiation even used indoors, Eu³⁺ complex is chosen to protect the surface by absorbing the ultraviolet energy and releasing with fluorescence at the same time. The influence on surface and fluorescence characteristics of the poplar veneer and fluorescent wood with ultraviolet radiation was investigated in this paper. Based on the previously studies, two kinds of materials exposure for 480h in the same condition. The properties of samples were quantified after fixed time of exposure, could be checked by FTIR, SEM combined with CIE L*a*b* system for color change. Fluorescence recorded by luminescence spectra and TG analysis for thermal performance. The results showed, Chemical structure of modified wood surface didn't had substantial change with SEM supported the found. Modified wood had less color change values than nature wood after 480h ultraviolet irradiation, it implied modified wood has better stability on surface color changing. The fluorescence change during the aging decreased relatively slow with exposed time.

Keywords: wood-based materials; Eu(III) complex-modified; UV-aging resistant properties; CIE system

Impact of Torrefaction on the Chemical Component of Nigerian Grown *Pinus caribaea* Morelet

Faruwa F.A₁*¹, Anyacho M₂, Iyiola E.A₃, Wekesa A₄

¹* Research scientist, Department of Forestry and Wildlife Technology, Federal
University of Technology Owerri, Imo State, Nigeria
Email: francis.faruwa@futo.edu.ng or faruwa@gmail.com

² Research scientist, Department of Forestry and Wildlife Technology
Federal University of Technology Owerri, Imo State
ebenezeriyiola@gmail.com

³ Research scientist, Department of Forestry and Wood Technology
Federal University of Technology Akure, Ondo State, Nigeria
ea iyiola@futa.edu.ng

⁴ Research scientist, Department of Agroforestry and Rural
Development, University of Kabianga, P.O. Box 2030 -20200 Kericho
Kenya
annehabwe@gmail.com

Abstract

Wood is a three-dimensional biopolymer composite; comprising of cellulose, hemicelluloses and lignin with minor amounts of extractives and inorganic. The combination of cellulose and the hemicelluloses are called hollocellulose. The amount of each of these carbohydrate polymers can be altered or changed by age, sex, type of species, location of growth and through a heat treatment called torrefaction. Hence, this study determined the impact of torrefaction on the chemistry of selected pine grown in Nigeria. Torrefied samples of *Pinus caribaea* were subjected to different temperatures regime at 225, 250, 275 and 300 °C in this study. Extractives analysis and ash content were determined using gravimetric and proximate analysis respectively for the torrefied wood. The chemical characterization determination was carried out across the different temperatures and parts for the samples using the wet chemistry method. The result from this study revealed that, as the torrefied temperature increases from 225 to 300, the volatiles within the torrefied wood samples reduced from 8.00 to 4.47 %. The analysis of variance revealed that significant difference was recorded within different temperatures regime, and no significant difference was recorded within the different parts. The ash content varied between 1.44 and 2.7%, the hemicelluloses were found to range between 21 to 33%, the lignin content from 33- 53% for torrefied sample and this was found to increase with temperature. The cellulose content reduced with increasing temperature from 24% to 13 %. This study evidently showed that the composition of polymers of *Pinus caribaea* was affected by the different temperatures and slightly by different tree parts. The work shows that most of the polymers were evidently degraded between 225 and 250 °C and more evidently at the temperature approaches 300 °C.

Key Words: *Pinus caribaea Morelet*, Torrefaction, Biofuel, Energy, Wet chemistry

INTRODUCTION

The energy crisis and obvious overuse of fossil fuels globally which has caused major concerns for environmentalist has led to a worldwide interest in sustainable biofuels. This core interest in the search for an alternative has led to a search for plant biomass, which is seen as an ideal source of sustainable energy and biobased products because it is renewable and available in high amounts and relatively low cost (Del, 2012).

Most plant biomass is lignocellulosic and mainly consists of three biopolymers: cellulose, hemicelluloses, and lignin with minor amount of extractives, and inorganic which together form a complex and rigid structure (Xu *et al.*, 2013 and Roger *et al.*, 2013). This chemical composition varies with tree species, part (root, stem, or branch), type of wood (i. e., normal and reaction wood), geographic location, climate, and soil conditions. The amount of each of these carbohydrate polymers can be altered or changed by the age, sex, type of species and through a heat treatment (torrefaction). Torrefaction of biomass e.g.; wood, is a mild form of pyrolysis at temperatures between 200°C to 300°C (392 to 608°F). It is a heat treatment on wood to improve the properties of the treated material. Torrefaction changes the biomass properties to provide a better fuel quality for combustion and gasification applications. It leads to a dry product with no biological activity like rotting. Biomass can be an important energy source; however, nature provides a large diversity of biomass with varying characteristics. To create highly efficient biomass to energy chains, torrefaction of biomass is a promising step to overcome logistics economics in large-scale sustainable energy solutions. Since torrefaction affects the organic nature of biomass, it is essential to have an evaluation of the level of chemical alteration in the basic wood polymer subjected to this process. Therefore, the objective of this study was to determine hollocellulose, lignin, ash and extractive content of a torrefied *Pinus caribaea Morelet* species grown in Nigeria using the wet chemistry method.

MATERIAL AND METHODS

Torrefaction and Sample Preparation

The Wood of *Pinus caribaea Morelet* torrefied at Federal University of Technology Akure (FUTA), Nigeria was used in this study. The dimension of the pine wood chips of 10 x 10 x 60 mm was used in this study. The temperature range of 225°C, 250°C, 275°C and 300°C was used as torrefaction regimes. The moisture content of each sample was determined using an electrically powered oven.

Extractives and Ash Content Analysis

Wood extractive (WE) were quantified by the procedure as reported by Rabemanolontsoa (2011) and (TAPPI, 1988). This procedure was based on gravimetric analysis method to quantify extractives. By acetone extraction, lipophilic wood components, such as fatty acids, resins, fatty alcohol, sterols and glycerides were extracted. In addition, low molecular phenolic compounds

like lagans were also extracted. (Chacha *et al.*, 2011). The extractives were expressed as percent weight by weight of dry biomass, WE were calculated as:

$$WE = \frac{W_0 - W_1}{W_0} \dots\dots\dots \text{Equation (1)}$$

WE =Wood Extractive
W₀=Weight of Wood before Extraction
W₁=Weight of wood after extraction

The proximate analysis was carried out on all the torrefied samples to determine the percentage of volatile matter content (PVM), percentage of ash content (PAC), percentage of fixed carbon (PFC) following Kurada (2000) procedures.

Hemicellulose

1 g of dried biomass (W₂, g) was weighed after the extractive analysis and carefully transferred into a 250 mL Erlenmeyer flask. 150 mL (Mililitre) of 0.5 M NaOH was measured out accurately into the Erlenmeyer flask. The mixture was allowed to boil in a water bath for 3.5 hrs using distilled water. After the 3.5 h boiling of the mixture, it was left to cool at room temperature. The slurry was filtered through the vacuum filtration and set until the pH of the solution approached the residues were dried to a constant weight of 103 ± 2 °C. The dried residues were cooled in a desiccator and then weighed (W₃, g)

$$WH = \frac{W_2 - W_3}{W_2} \dots\dots\dots \text{Equation (2)}$$

WH =Wood Hemicelluloses
W₂=Weight of Wood before Extraction (but after extractive removal)
W₃=Weight of wood after extraction

Lignin Content Determination

The acetone extracted wood samples of 200mg were weighed into small test tubes. Then tetra-oxo-sulphate VI acid (H₂SO₄) (2mL, 72%) was added to each sample and incubated for 60 minutes at 30^oC with regular stirring using a glass rod, this is commonly known as the primary hydrolysis step. Thereafter, the primary hydrolyzates were transferred into a 200mL Erlenmeyer flask with the aid of distilled water of 56mL, thereby resulting to the final sulphuric acid concentration of 4% and the flask was then covered with a small beaker. It was covered and placed in a pressure cooker and heated until it started hissing. It was left for 30 minutes of heating after hissing; this step is called secondary hydrolysis. The pressure cooker was allowed to cool down slowly and then the samples were then removed. The secondary hydrolyzates were filtered in pre-weighed sintered glass crucible with the aid of 40ml of distilled water. The remaining sample (known as klason lignin) in the crucible after filtration were oven dried overnight at

104°C and cooled in a desiccator for 10 minutes and the weight of the crucible containing lignin was taken. The klason lignin content (%KL) is calculated in relation to the extractive-free wood basis and the oven-dried original wood basis as expressed in equation 3

$$\% \text{KL}_{\text{ext-free}} = \frac{A}{W} \times 100 \dots \dots \dots \text{Equation (3)}$$

A = Extract free wood

W = Drendy weight

Determination of cellulose content

The cellulose content, WC, was calculated by difference, assuming that extractives, hemicellulose, lignin, ash, and cellulose are the only components of the entire biomass in equation 4

$$\text{WC} = 100 - (\text{WA} + \text{WE} + \text{WH} + \text{WL}) \dots \dots \dots \text{Equation (4)}$$

WC= Weight of Cellulose

WA= Weight of Ash

WE= Weight of Extractive WH= Weight of Hemicellulose

WL= Weight of Lignin

RESULT AND DISCUSSION

The result of Moisture content, Wood Extractive, Hemicellulose, Ash, Lignin and Cellulose on a torrefied Nigerian grown *Pinus caribaea Morelet* was represented using statistical models such as tables as relevant to the objective of the study. The results of ANOVA's for moisture content, extractives, lignin, hemicelluloses and celluloses were presented in Table 3 and their respective mean values in Table 4.

Moisture content (mc)

The result of ANOVA's in Table 3 revealed that, for moisture content, a significant difference was recorded within the different temperatures of the sample at P-value ≤ 0.05 , and within the different parts, no significant difference was recorded as P value > 0.05 . The result of the mean value for Pine in Table 4 showed that the moisture content reduces with an increase in temperature of which the raw has the highest value of 11.48% and the temperature 300 has the lowest value of 2.92%. This is lower than the reported results of Maciejewska *et al.*,(2006) where the moisture content of torrefied samples falls between 5-10% but similar to the study conducted by Carl Wilen *et al.*,(2013) where the value is between 2-12%.

*Proceedings of the 62nd International
Convention of Society of Wood Science and
Technology*

Table 3: ANOVAs' for Moisture content, Ash content, Extractive content, Lignin, Cellulose, Hemicelluloses and Lignin of Pinus caribaea Morelet

	Source	Sum of Squares	Df	Mean Square	F	P value
MC	Tor temp	127.10	4	31.77	4.13	0.04*
	Tree parts	3.84	2	1.92	0.25	0.78 _{ns}
	Error	61.51	8	7.69		
	Total	192.46	14			
Extractive	Tor temp	28.89	4	7.22	4.59	0.03*
	Tree parts	10.05	2	5.02	3.19	0.09 _{ns}
	Error	12.56	8	1.57		
	Total	51.50	14			
Hemicelluloses	Tor temp	60.40	4	15.10	3.39	.07 _{ns}
	Tree parts	3.73	2	1.87	0.42	.67 _{ns}
	Error	35.60	8	4.45		
	Total	99.73	14			
Lignin	Tor temp	1009.10	4	252.27	41.00	0.00*
	Tree parts	42.17	2	21.08	3.43	0.08 _{ns}
	Error	49.22	8	6.15		
	Total	1100.49	14			
Celluloses	Tor temp	482.13	4	120.53	5.80	0.01*
	Tree parts	62.17	2	31.09	1.49	0.28 _{ns}
	Error	166.18	8	20.77		
	Total	710.48	14			
Ash Content	Temp	3.811	3	1.270	0.962	0.42 _{ns}
	Part	1.350	2	.675	0.511	0.61 _{ns}
	Error	39.604	30	1.320		
	Total	44.765	35			

Table 4: Mean value for Moisture content, extractives, Hemicelluloses, lignin and Celluloses of *Pinus caribaea* Morelet

Samples	MC (%)	Extractives	Ash	Hemicelluloses	Lignin(klasson)	Celluloses
Raw	11.48 ^a	8.00 ^a	1.44	28.56 _a	32.48 _c	29.52 ^a
225	6.85 ^{ab}	7.53 ^{ab}	1.50 ^c	33.00 _a	33.70 _c	24.27 ^{ab}
250	4.38 ^b	5.20 ^{bc}	2.33 ^{ab}	30.67 _a	42.60 _b	22.20 ^{abc}
275	5.91 ^b	4.47 ^c	2.55 ^{ab}	25.00 _a	46.05 _a	18.48 ^{bc}
300	2.92 ^b	7.20 ^{ab}	2.70 ^a	21.00 _b	53.49 _a	13.98 ^c

Values are means. Means with the superscript are not significantly different from each other.

Extractive

The results of ANOVAs' of Extractive content were presented in Table 3 and their respective mean values for the weight of Extractive in Table 4. The result of ANOVAs' in Table 1 revealed that significant difference was recorded within different temperatures as P value ≤ 0.05 , and within the different parts, no significant difference was recorded as P value was > 0.05 . The result of mean value for *Pinus* in Table 4 showed that the value for extractive content ranges from the lowest 4.47% to the highest at 8.00%. This is higher than the reported result of Shebani *et al.*, (2008); where the extractive content varies between 2-5% but later stated that it can exceed 15% in some species. The result of this work is similar to the study conducted by Sixta (2006) where the Extractive content ranges between 2- 8%.

Ash content

As shown in Table 3, the Ash value for *Pinus caribaea* revealed from the ANOVA that there were no significant differences recorded for the different temperatures and different parts of the tree at P-value ≤ 0.05 . Though there were no significant differences recorded, the result of mean separation revealed that the value increased with increase in temperature i.e. 1.44 to 2.70% for raw and 300 respectively as shown in Table 4. It is evident from this study that as the torrefied temperature increases, the volatiles reduces while the fixed carbon is increased. The result of this work also shows a similar trend with the work of Ho *et al.*, (2014) where they reported that in Ash analysis for Larch wood, increasing the reaction temperature.

Hemicellulose

The result of ANOVAs' in Table 3 revealed that no significant difference was recorded within the different temperatures of the sample as P value > 0.05, and within the different parts, no significant difference was recorded as P value > 0.05. This means that irrespective of the different temperatures of the samples, the mean value was not statistically different from one another.

Lignin content (LC)

The results of ANOVAs' for Lignin content were presented in Table 3 and their respective mean values in Table 4. The result of ANOVAs' in Table 3 revealed that significant difference was recorded within the different temperatures of the sample as P value \leq 0.05, and within the different parts, no significant difference was recorded as P value > 0.05. The result of the mean value for Lignin content of *Pinus caribaea* in Table 4 showed that the raw untorrefied sample had the lowest value of 32.48% for lignin and temperature 300 has the highest value of 53.49%. This means that lignin content was slightly affected by temperature used in this study and this is corroborated with the work of Wenjia *et al.*, (2013) that reported that the thermal decomposition of lignin occurs at 280 to 500 °C yielding phenol via cleavage of ether and carbon-carbon linkages. As the temperature increases, the lignin content increases as well. This result is higher than the result reported by Yongfeng Li. (2011) where the lignin content ranges from 25 and 35% but similar to the study conducted by Dardick *et al.*, (2010) where the Lignin content ranges from 32-54%. The result of this work also showed a similar trend with the study conducted by Reyes *et al.*, (2015) where the lignin percentage were 32-56.8%.

Cellulose content (CC)

The results of ANOVAs' for Cellulose content were presented in Table 3 and their respective mean values for the Cellulose content in Table 4. The ANOVAs for cellulose content of *Pinus* revealed that, significant difference were recorded for the different temperatures as P \leq 0.05 and for different parts of the tree, no significant difference were recorded for tree parts as P value > 0.05. The result of the mean value for cellulose content revealed that the cellulose content reduced with increasing temperature, that is, the raw untorrefied sample had the highest value of 29.52% and temperature 300 had the lowest value of 13.98% for cellulose. This result is lower than the reported result of Sixta (2006) that cellulose content of wood ranges from 40-44% but similar and within the range of the study conducted by Bhuiyan and Hirai (2005) that the cellulose content ranges from 13-49%. This shows that within the torrefaction temperature used in this work, celluloses degradation was initiated massively.

CONCLUSION

This study evidently showed that the composition of carbohydrate polymers of *Pinus caribaea* Morelet were affected by the different temperatures and slightly by different tree parts.

Extractive content, Ash and weight of Hemicellulose were significantly affected. The cellulose content reduced with increasing temperature while the lignin content increased with increasing temperature. The work shows that most of the sugars were evidently degraded between 225 and 250°C and more evidently at the temperature approaches 300°C. The decrease in pine wood component can be attributed not to volatiles production but also the char formation during torrefaction.

Finally, additional work is required to relate the end use properties such as energy value, hydrophilic, grind ability and bio degradability to the chemical changes experienced in the torrefaction regimes and also to make a comparison on effect of temperature between soft wood and hard species to allow for improved fuel flexibility.

ACKNOWLEDGEMENT

I acknowledge the moral and academic support of my colleagues throughout the course of this research in person of Mr Iyiola, Mrs Wekesa, Mr Anyacho and other people that contributed to the success of this study. I also appreciate the staff at the wood workshop of the Federal University of Technology, Akure for their contribution to the success of this study.

REFERENCE

- Bhuiyan, M. T.; Hirai, N.; Sobue, N. (2000) Changes of crystallinity in wood cellulose by heat treatment under dried and moist conditions. *Journal of Wood Science* 46(6):431-436.
- Chacha, N., Toven, K, Mtui, G., Katima, J., Mrema, G. (2011) Steam pretreatment of Pine (*Pinus patula*) wood residue for the production of reducing sugar. *Cellulose Chemistry Techno.* 45(7-8) pp 459-501.
- Delgado, C.; Prinsen, P.; Encoret, S.; Nieto, L.; Jimenez-Barbero, J.; Ralph, J.; Martínez, T.; Gutiérrez, A. (2012) Structural characterization of the lignin in the cortex and pith of elephant grass (*Pennisetum purpureum*) stems. *J. Agric. Food. Chem.*, 60, 3619–3634.
- Ho Seong Yoo, Hang Seok Choi, Hoon Chae Park, Jae Gyu Hwang (2014) Torrefaction of woody biomass. A report on Knowledge-based environmental service (Waste to Energy recycling, Ecodesign) Human resource development Project” A National Research Foundation of Korea Grant funded by the Korean Government (NRF)” supported by Korea Ministry of Environment (MOE)
- Kurada K. Mokuzai bunseki (2000) In: Yoshida H, editor. Mokushitsu kagaku jikken manual, Tokyo: Buneido shuppan; p. 87-98.
- Maciejewska, A., H, Veringa, J., Sander and S.D. Pefves (2006) Co-firing of biomass with coal: constarin role of biomass pre-treatment: Institute of Energy, European communities.
- Rabemanolontsoa, Harifara; Ayada, Sumiko; Saka, Shi (2011) Quantitative method applicable for various biomass species to determine their chemical composition *Biomass and Bioenergy* (2011), 35(11): 4630-46/hdl.handle.net/2433/1518
- Reyes-Rivera J, Canché-Escamilla G, Soto-Hernández M, Terrazas T (2015) Wood Chemical Composition in Species of Cactaceae: The Relationship between Lignification and Stem Morphology. *PLoS ONE* 10(4): e0123919. doi:10.1371/journal.pone.0123919
- Roger M. Rowell, (2013) *The Chemistry of Solid Wood* Advances in Chemistry Series 20, Chapter 2, pp. 57-126, Washington, DC: ACS.05-180.

**Proceedings of the 62nd International Convention of
Society of Wood Science and Technology
October 20-25, 2019 – Tenaya Lodge, Yosemite, California USA**

- <https://www.ecn.nl/docs/library/report/2005/rx05180.pdf> [Cited 3.4.2015].
- Shebani, A.N., van Reenen, A.J. and Meincken, M. (2008) The effect of wood extractives on the thermal stability of different wood species. *Thermochimica Acta* 471:43–50.
- Sixta H. (2006) Introduction to industrial pulping. Handbook of Pulp.
- Tappi Standard T204 om-88: Solvent extractives of wood and pulp. Tappi test methods; 1988
- Wenjia Jin Kaushlendra Singh and John Zondlo (2013) Pyrolysis Kinetics of Physica Components of Wood and Wood-Polymers Using Isoconversion Method *Agriculture* 2013, 3ISSN 2077-0472
- Xu, F.; Yu, J.M.; Tesso, T.; Dowell, F.; Wang, D.H. (2013) Qualitative and quantitative analysis of lignocellulosic biomass using infrared techniques: A mini-review. *Appl. Energy*, 104, 801–809.
- Yongfeng Li. (2011) Wood Polymer composite, Key Laboratory of Bio-based Material Science and Technology of Ministry of Education, Northeast Forestry University, Harbin 150040, P. R. China

Novel enzyme-modified lignin adhesive to substitute PVAc carpenter's glue?

Raphaela Hellmayr^{1} – Sabrina Bischof¹ – Georg M. Guebitz¹ –
Gibson Stephen Nyanhongo¹ – Rupert Wimmer¹*

¹ University of Natural Resources and Life Sciences, Vienna, Austria

** Corresponding author: raphaela.hellmayr@boku.ac.at*

Abstract

The application of industrial lignin adhesive modified with laccase as a biocatalyst to be used for solid wood was developed and compared with PVAc, known as carpenter's glue.

Lignin solutions at a viscosity of approximately 0.4 Pas on freshly sanded or planed surfaces of beech wood were used. Samples were cured under pressure for two days, at room temperatures. Tensile shear strength measurements showed a performance that was at the same level as the PVAc-glued samples (11 MPa). As there was no significant difference in the mechanical properties, the PVAc had 100 % wood failure while the lignin adhesive glued samples failed mainly in the bondline. The demonstrated data showed potential in using an enzyme-polymerized lignin adhesive as a well performing wood-glue.

Key words: Laccase, industrial lignin, bio-based adhesive, wood bonding, tensile shear strength, failure mode

Introduction

Lignin, a product of photosynthesis by plants representing 30 % of all non-fossil based organic carbon source worldwide is emerging as a potential raw material that can replace many fossil-based products (Vanholme et al. 2013). Although lignin has the potential to replace fossil-based products, its industrial exploitation has been limited to only 2% of the 40 and 50 million tons lignin per annum produced worldwide by the pulp and paper industry (Fang & Smith 2016). Advances in biotechnology have witnessed enzyme-based technologies, using especially laccases, emerging as highly promising green catalysts for synthesizing and modifying lignin-based materials. Hüttermann et al. (2001) have shown that in situ polymerization of lignin is leading to adhesives that can be used to produce particle boards. The adhesive cure was based on the oxidative polymerization of lignin using phenoloxidases (laccase) as radical donors. Laccases as oxidoreductase enzymes are widely distributed in nature, able to react with a variety of aromatic substrates including lignin, generating reactive species with concomitant reduction of molecular oxygen to water. The most attractive feature of laccases is therefore the ability to generate reactive species able to cross-link among themselves or with other (functional) molecules. The supply of oxygen during the enzyme-catalysed reaction gives rise to the production of high-molecular weight polymerized lignin, which forms solid products. Polyvinylacetate (PVAc) is known as "white glue", or "carpenter's glue", which is a widely used, non-toxic and very easy to apply adhesive. PVAc dispersions give a thermoplastic glueline and the curing is a physical process where the dispersion particles melt together when the water evaporates. In this research, we intended to create a laccase-polymerized lignin adhesive to be used for solid wood gluing. Due to the similarity in cure-type and applications, we have chosen PVAc as the adhesive to be compared with our new lignin-based adhesive. We therefore hypothesize that it is possible to provide a fully lignin-based adhesive that is comparable to PVAc glue.

Materials & Methods

Pre-purified industrial lignin was obtained from the paper industry as a brown liquid, which was dried at 80 °C and ground to powder. For the polymerization process the powder that was at the end also the main component of the adhesive, was dissolved in water to a solution. Industrial lignin was neutralized to pH 7 which allowed the enzyme treatment with i.e. laccase from *Myceliophthora thermophila*. The enzyme concentration was not the limiting factor, and the solution was constantly supplied with oxygen, which constituted a mediator-free polymerization process. Polymerization was stopped at a proper viscosity, the polymerized lignin was applied on freshly sanded-cleaned, as well as on planed beech wood surfaces, always on both sides of the planks. The bondline was cured in a hydraulic press for two days at room temperature, at an applied pressure of 0.8 MPa. Only during the first 5 hours the pressing temperature was set at 50 °C. Samples were stored in the climatized chamber, at 20 °C and 65 % relative humidity. After two weeks of storage boards were cut into 10 samples each, following EN 302-1. Tensile shear tests were carried out on a Zwick Universal testing machine, at a testing speed of 1 kN/min.

Results and Discussion

Laccase polymerization of lignin resulted in increased molecular weight and viscosity. In Figure 1 it can be seen that the PVAc reference tensile shear strength was 11.0 ± 1.07 MPa. The tensile shear strength of the lignin adhesive was 10.6 ± 1.42 MPa. The lignin-based adhesive showed no significant difference in tensile shear strength to PVAc (ANOVA post-hoc mean test, $p > 0.05$). Remarkable was the mode of failure mode, i.e. there was wood failure for PVAc, while the lignin-glued samples failed mainly within the bondline. The differences between ground and planed surface were insignificant ($p > 0.05$). There was a tendency that the ground surface had slightly higher tensile shear strength.

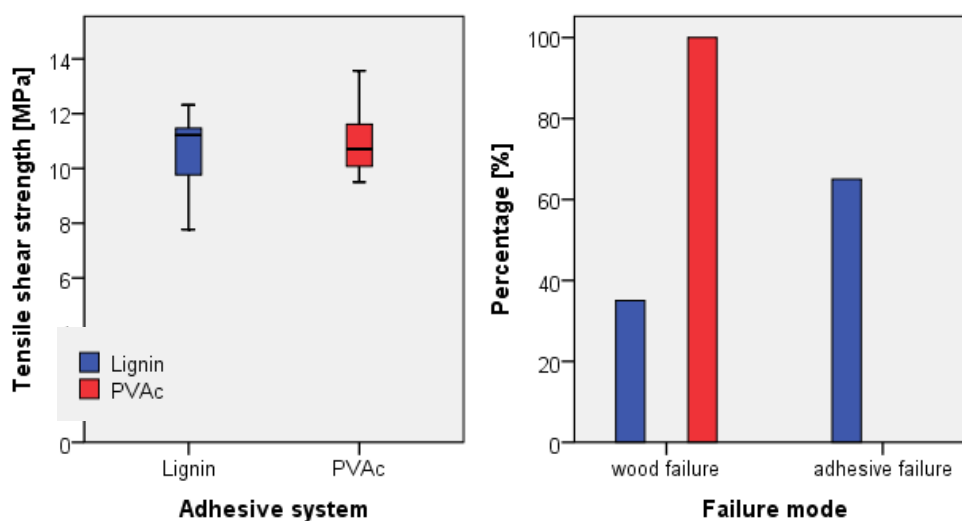


Figure 1: Strength and wood failure of lignin adhesive and PVAc (n=20 in each group)

While the PVAc samples showed wood failure only, the lignin samples predominately demonstrated adhesive failure. Surprisingly, there were selected samples that reached higher strengths than PVAc samples, but with clear bondline failure. Microscopic images showed that PVAc formed a 50 μ m thick bondline and the pores close to the bondline were filled with PVAc, seemingly due to a capillary effect. In contrast, the lignin-based adhesive did not form such a visible bondline but penetrated well into cell walls. No pore lumens were found filled with lignin adhesive. The bonding mechanisms need to be better understood, which is subject of continued research.

Summary and Conclusions

We developed an enzyme-polymerized lignin adhesive, which has shown a maximum tensile shear strength of $10,6 \pm 1,42$ MPa. The tensile shear strength compared with the PVAc reference, i.e. no significant difference was found. PVAc penetrated well into the pore lumens, while the lignin adhesive was found in the cell walls only. We have also seen a significant difference in wood failure vs. bondline failure. PVAc showed 100 % wood failure, while only one third of lignin adhesive glued samples had partly wood failure. There is a huge potential for enzyme-modified

*Proceedings of the 62nd International Convention of
Society of Wood Science and Technology
October 20-25, 2019 – Tenaya Lodge, Yosemite, California USA*

lignin adhesives in future applications, as they are capable of reaching comparable properties with conventional adhesive systems, as used in the wood industry.

References

Fang Z, Smith R.L. (2016) Production of Biofuels and Chemicals from Lignin. Springer Singapore. doi: 10.1007/978-981-10-1965-4

Hüttermann, A., Mai, C. & Kharazipour, A. (2001) Modification of lignin for the production of new compounded materials. *Appl Microbiol Biotechnol* 55: 387. doi: 10.1007/s002530000590

Vanholme B, Desmet T, Ronsse F, Rabaey K, Van Breusegem F, De Mey M, Soetaert W and Boerjan W (2013) Towards a carbon-negative sustainable bio-based economy. *Front. Plant Sci.* 4:174. doi: 10.3389/fpls.2013.00174

Thursday, October 24th

Composites and Adhesives 2

8:30 -10:30

Chair: Ilona Peszlen, North Carolina State University, USA

**CHARACTERIZATION OF PLASTIC BONDED COMPOSITES REINFORCED WITH *Delonix regia*
PODS**

AJAYI B., ADENIRAN A. T., FALADE O. E., ALADE B. O.

*Department of Forestry and Wood Technology, Federal University of Technology Akure, Akure,
Ondo State, Nigeria. E-mail: bajayi.futa.edu.ng*

Abstract

The influence of production variables on the properties of *Delonix regia* particles based plastic bonded composites were characterized based on strength and dimensional movement. The boards were produced at three levels of mixing ratio (MR) of 1:1, 2:1, and 3:1; and two levels of board densities (BD) of 1000 kg/m³ and 1200 kg/m³. The study evaluated the dimensional movement and strength properties of the boards which result into ranges in mean values obtained. As mixing ratio and board density increases, Modulus of Elasticity (MOE) and Modulus of Rupture (MOR) also increases while Thickness Swelling (TS) and Water Absorption (WA) decreases. From the values obtained from this study, the production variables had significant effect on the boards at different levels of combination. The result also proved that *Delonix regia* pods and car battery case are suitable raw materials in the production of Plastic Bonded Composites. This research therefore provide basic information on the use of particles derived from *Delonix regia* pods and plastic wastes as binder for the manufacturing of Plastic Bonded Composites.

Keywords: Composites, Dimensional Stability, Flexural, Pods, Tropical tree species

Introduction

Wood Plastic Composite (WPC) is a panel product manufactured from mixture of lignocellulosic materials such as wood flours, wood fiber, wood particles, agricultural wastes, paper wastes, common weeds and virgin or recycled plastics under controlled heat and pressure (Ajayi and Aina, 2010). Lignocellulosic waste materials are used in the production of wood plastic composites in accordance with the sustainable principle of cascading exploitation and resource efficiency (Teuber *et al.*, 2016). The plastic components that can be used in the manufacturing process include thermosets or thermoplastics. However, recycled thermoplastics also provide great opportunities for wood plastic composites production (Kazemi-Najafi 2013; Sommerhuber *et al.*, 2015).

Wood and wood products are considered environmentally friendly and sustainable due to their renewability and biodegradability (Sadiku *et al.*, 2016). However, scarcity of economically preferred wood species, over-exploitation of both natural and artificial forests as a result of high

demand for wood and wood products, lack of effective utilization of wood resources due to huge wastes incurred in wood processing and encroachment into the free and reserved forests by unlicensed timber exploiters have resulted in deforestation and degradation of the forests (Ajayi, 2011). This phenomenon has caused shortages in the availability of wood and wood products in the wood industry. There is therefore urgent need for concerted effort to find alternative to sawn timber in order to meet the demand for wood products in perpetuity.

Several research works have been done into the improvement and performance of WPCs (Ajayi and Olufemi 2011; Adhikari *et al.*, 2012; Adefisan 2013; Falemara *et al.*, 2015; Falemara and Ajayi 2018; Mármol and Savastano 2017) and others are still ongoing but little or no research has been carried out on the inclusion of the pods of *Delonix regia* in the production of WPC and any other panel products. *Delonix regia* grows in the tropical and sub-tropical region as ornamental tree, the seeds of this tree are used for many important things among which is the production of oil, but it had been noticed that once the seeds has been extracted from the pods, the pods are disposed as they are of no economic value.

Disposal of non-degradable plastic wastes is a huge challenge confronting the world due to the large volumes used and discarded daily. Disposing plastic waste in landfills is a common practice but has not been an effective way in getting rid of such unwanted materials. There is therefore the need for effective and sustainable method in managing the hazard posed by the accumulation of plastic wastes in the environment. Recycling of these wastes can proffer a solution to manage the situation and this study offers an alternative mode of recycling plastic waste in the manufacturing of value added Plastic Bonded Composites (PBCs). Value addition to plastic wastes is of paramount importance for serene and conducive environment. Composite formation is one of the ways by which plastic waste can be recycled. Research into the development and manufacturing of this boards using simple technologies is increasing due to the following factors: 1) recognition of the suitability of a wide range of raw materials for board production in order to reduce pressure on existing forest resources; 2) desire to increase wood resources utilization; 3) acceptability of the new product in the markets as alternative to sawn timber so as to meet wood product needs on sustainable basis; and 4) the desire to protect forest biodiversity (Ajayi, 2006). The collection, processing and utilization of this waste materials could have the following benefit: increase farmer's income and alleviate poverty, introduce new product in the market place that is capable of bringing about industrial development, increase raw material supplies for construction, create job opportunities, and reduce pressure on forest resources (Ajayi, 2006). This study is designed to evaluate the influence of mixing ratio and density on the dimensional stability and the flexural strength of plastic bonded composites produced from *Delonix regia* pods particles and recycled plastic wastes.

Materials and Methods

The post-consumer plastic waste used for this research were obtained from dumpsites and milled into granulated particles. The particles were screened to obtain uniform size materials. The raw material base, *Delonix regia* pods were collected from the mother trees, split into two to remove the seeds and the fluffy part of the pods. Thereafter, the pods were converted into chips by a

chipping machine and dried in an open air. Hammermill was used to reduce the dried chips into fine particles. The fine particles were then sieved in order to obtain uniform size particles. The required quantities of *Delonix regia* pods particles and granulated plastic wastes were measured at different mixing ratios (1:1, 1:2 and 1:3) of wood/plastic and board densities (1000 kg/m³ and 1200 kg/m³). The two components were premixed before they were fed into a co-rotated twin-screw extruder/compounder. The temperatures of the extruder were controlled at 170°C, 180°C, 185°C and 190°C for zones 1, 2, 3 and 4 respectively while the temperature of the extruder die was held at 200°C. The gradual increment in temperature at each zone was to ensure rapid flow of the plastic and to ensure that the *Delonix regia* pods particles do not char. The screw speed was varied between 150 revolution per minutes and the pressure from 33 to 47 bars. The extruded strand passed through a water bath and was subsequently pelletized. The pelletized compounded materials (mixtures of *Delonix regia* pods and recycled plastic) were measured and placed in a mold of 300 mm x 180 mm x 6 mm. The inside of the mould was greased with engine oil for easy de-molding. The hot platen press was heated to 200°C before placing the pellet-filled mold on it for ten minutes and then transferred to a cold press for complete setting. This procedure was repeated for the remaining boards. The boards were de-molded after hot pressing and allow to cool for about five (5) minutes. After which the boards were trimmed and cut into test specimen.

Thickness Swelling (TS) and Water Absorption (WA) properties were assessed using test specimen of 50 mm x 50 mm x 6 mm subjected into cold water immersion for 24 and 48 hours respectively, while Modulus of Rupture (MOR) and Modulus of Elasticity (MOE) of the boards were assessed using test specimen of 194 mm x 50 mm x 6 mm. MOE and MOR was determined with the aid of Universal testing machine.

The data obtained were analyzed using Statistical Package for Social Science (SPSS). Analysis of Variance (ANOVA) was conducted to investigate the influence of mixing ratios (1:1, 1:2 and 1:3) and board density of 1000 kg/m³ and 1200 kg/m³ on the physical and mechanical properties of the composites. In line with assumptions of Analysis of Variance (ANOVA) the data set obtained from the water absorption and thickness swelling as expressed in percentages were transformed using square root transformation prior to analysis.

Results and Discussion

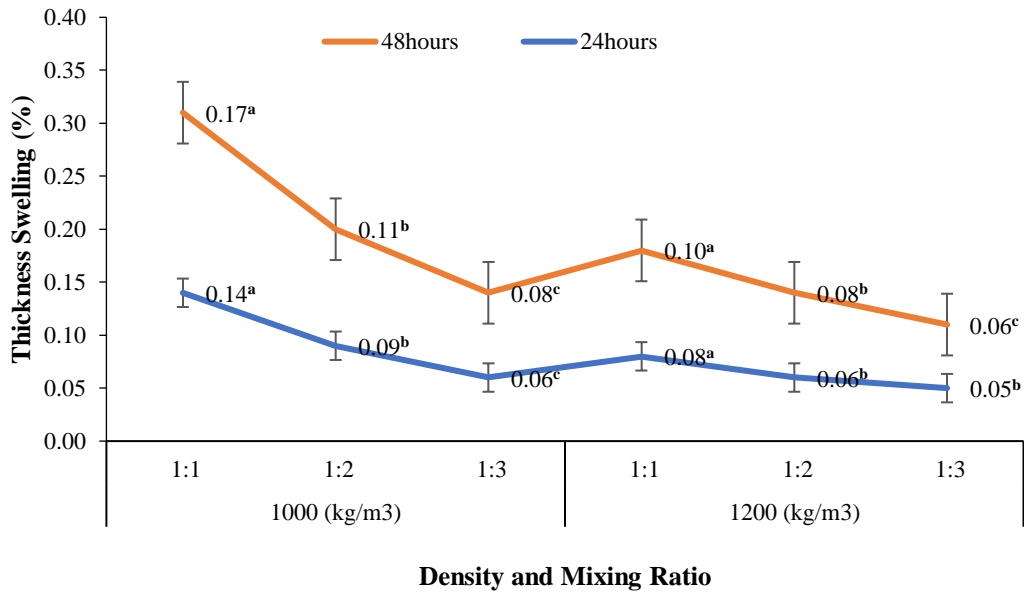
Effects of Density and Mixing Ratio on the Dimensional Stability of the Composite Board

The composite boards were subjected to water immersion for a period of 24 hours and 48 hours respectively. The mean thickness swelling of the composite boards soaked in water for 24 hours and 48 hours ranged from 0.05% to 0.14% and 0.06% to 0.17% respectively (Figure 1). The mean value for water absorption after 24 hours and 48 hours immersion ranged from 1.22% to 2.03% and 1.24% to 2.08% respectively (Figure 2). These values are comparatively lower than the submission of Hung *et al.* (2017) who obtained values ranging between 3.6% and 6.8% for thickness swelling and 7.3% to 15.4% for water absorption, indicating that the board produced from these materials shows higher resistant to water intake. As mixing ratio (1:1, 1:2 and 1:3) and board density (1100 kg/m³ and 1200 kg/m³) increases, water absorbed decreases. Boards produced at higher board density (1200 kg/m³) and mixing ratio (1:3) had the lowest intake of water, while boards produced at lower board density (1000 kg/m³) and mixing ratio (1:1) had

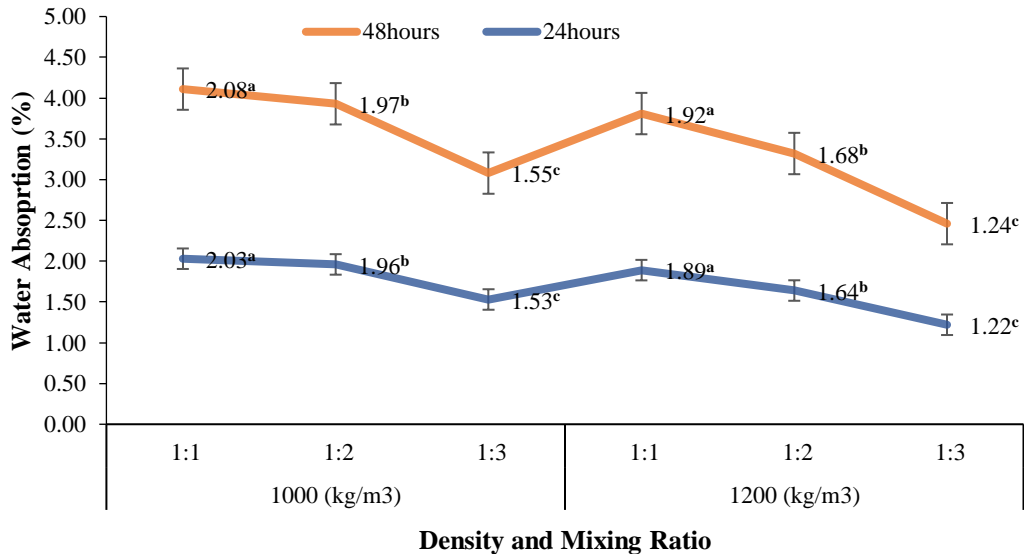
higher intake of water. Thickness swelling and water absorption of boards is significantly influenced by mixing ratio and density at 5% level of significance ($p \leq 0.05$). The follow-up test shows significant ($p \leq 0.05$) differences in the TS and WA for mixing ratio 1:1 and 1:2; 1:2 and 1:3; and 1:1 and 1:3.

These observed values were lower than those obtained in previous studies (Aina *et al.*, 2008; Ajigbon and Fuwape, 2005; Stark *et al.*, 2003). The result also revealed slight increase in dimensions and weight of the composite board after continual immersion in water beyond 24 hours up till 48 hours. The result further revealed that as the ratio of plastic to fiber increased from 1:1 to 1:3, the thickness swelling and water absorption property of the composite boards significantly ($p \leq 0.05$) decreased, after 24 hours and 48 hours immersion in water. This implies that higher plastic content reduces the intake of water into the composite. The board produced from the highest mixing ratio (1:3) and board density (1200 kg/m^3) is highly dimensionally stable and resistant to moisture intake (Figure 1). This is because the particles of *Delonix regia* pods were adequately encased by the molten recycled plastic.

However, the increase in rate of water intake in the composite board with lowest ratio of plastic to fiber (1:1) can be attributed to the affinity of *Delonix regia* pods to moisture and its hygroscopic nature. The WA and TS reduces as BD increases, the BD reflects the quantity of materials in the board produced and this aided effective compaction of the board because there is more fibre to fibre bond (Olufemi *et al.*, 2012). This observation could be attributed to the resistance to hydrostatic force against the bonds, high compression ratio and compatibility, strong bonds formation with little or no void spaces to accommodate water (Ajayi, 2003). At a lower mixing ratio (1:1) and board density (1000 kg/m^3), high rate of water absorption was observed as a result of the decrease in the level of plastic. This observed inference is in line with the previous findings of Aina *et al.* (2016) and Carus *et al.* (2015) who both asserted the fact that increase in plastic content in the board matrix caused improvement in the physical properties (TS and WA) of the boards as well as reduced moisture intake. The moisture absorption in the composites is mainly due to the presence of both visible and invisible void spaces present in the board (Ajayi, 2008). The presence of hydroxyl and other polar groups in various constituents of the *Delonix regia* pods particles resulted in water absorption between the hydrophilic *Delonix regia* pods particles and the hydrophobic plastics.



Means on the same line graph having similar superscripts are not significantly different ($p \geq 0.05$)
Figure 1: Effect of Density and Mixing Ratio on Thickness Swelling (%) of the Composite Board after 24hrs and 48hours immersion in water

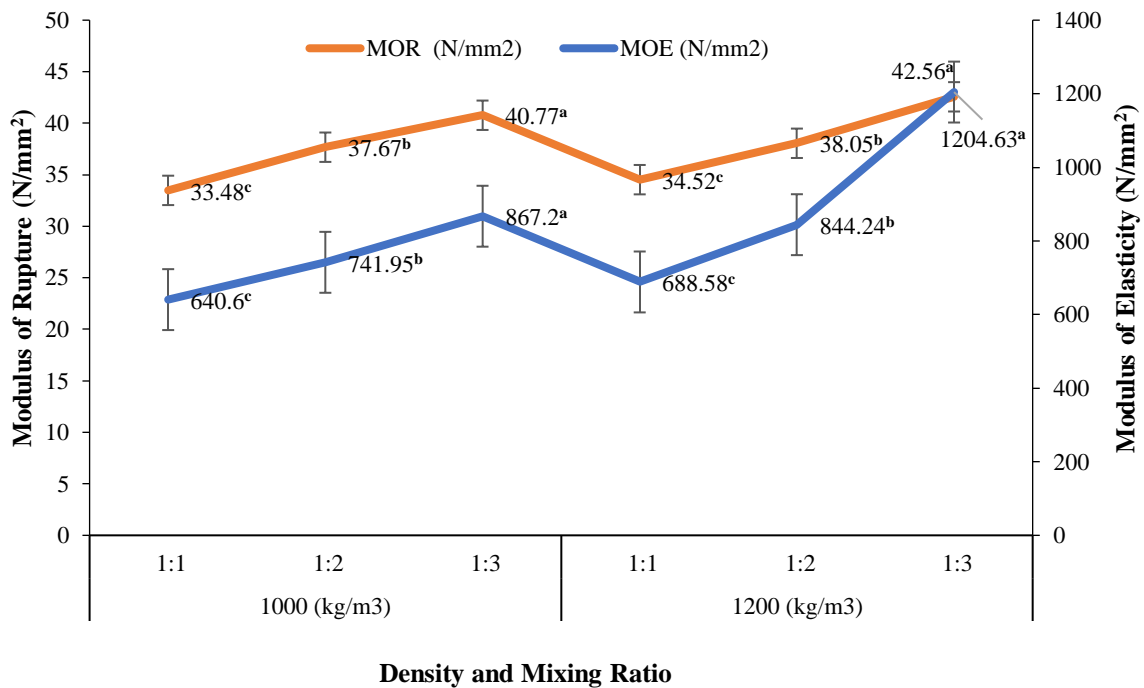


Means on the same line graph having similar superscripts are not significantly different ($p \geq 0.05$)
Figure 2: Effect of Density and Mixing Ratio on Water Absorption (%) of the Composite Board after 24hrs and 48hours immersion in water

Effects of Density and Mixing Ratio on the Strength Properties of the Composite Board

The mean values for the Modulus of Elasticity (MOE) and Modulus of Rupture (MOR) as presented in Figure 3, ranged from 640.6 N/mm² to 1204.6 N/mm² and 33.48 N/mm² to 42.56 N/mm² respectively. The MOE and MOR of the plastic boards produced increased with increase in the board density (BD) and mixing ratio (MR) as illustrated in Figure 3.

The mean values of the MOE and MOR in this study are within the values (MOE: 206 N/mm² to 2195 N/mm²; MOR: 10.0 N/mm² to 54.9 N/mm²) obtained by Hillig *et al.* (2017) when they assessed the strength properties of composite boards produced from coconut shell. As similarly reported by Hillig *et al.* (2017), the strength and stiffness properties were higher for composites produced at the highest density (1200 kg/m³) and mixing ratio (1:3). This therefore suggests that the higher the BD and MR, the higher the resistance to bending strength and stress elongation stiffness of the board and as asserted by Adhikary (2008) that as the density increases the mechanical properties (MOE and MOR) of the WPC increased. Boards produced at the highest density (1200 kg/m³) and mixing ratio (1:3) had the strongest and stiffest properties. This therefore suggests that board density and mixing ratio dictates the inherent strength characteristics of composite boards. Board density and mixing ratio has significant influence on MOE and MOR at 5% level of significance ($p \leq 0.05$). The follow-up test shows significant ($p \leq 0.05$) differences in the MOE and MOR for mixing ratio 1:1 and 1:2; 1:2 and 1:3; and 1:1 and 1:3.



Means on the same line graph having similar superscripts are not significantly different ($p \geq 0.05$)
Figure 3: Effects of Density and Mixing Ratio on Strength Properties (MOR and MOE) of the Composite Board

Conclusion

This study shows that the pods of *Delonix regia* can be used to produce value added Plastic Bonded Composites using recycled plastic as binder. TS and WA decreases and MOE and MOR increases proportionately as board density and mixing ratio increases. The board produced at mixing ratio of 1:3 and board density of 1200 kg/m³ is the most stable and showed highest resistance to bending. The mixing ratio and board density had significant effect on the TS, WA,

**Proceedings of the 62nd International Convention of
Society of Wood Science and Technology
October 20-25, 2019 – Tenaya Lodge, Yosemite, California USA**

MOE and MOR of PBC. This study demonstrate that *Delonix regia* pods as suitable and potential raw material for PBCs that can be used for both indoor and outdoor applications. Also, production of PBC from *Delonix regia* pods and recycled plastic will help to mitigate environmental pollution, siltation of waterways, incursion of plastic in the ocean, destruction to land and marine animals arising from plastic wastes prevalent worldwide. This study therefore serves as a baseline for the inclusion of pods of *Delonix regia* and other pods in the production of value added panel products.

References

Adefisan, O.O. (2013). Pre-treatment effects on the strength and sorption properties of cement composites made from mixed particles of *Eremospatha macrocarpa*. In: the proceeding of the 38th Annual Conference of the Forestry Association of Nigeria held in Sokoto State. 11th – 16th February, 2013. pp438 – 444

Adhikari, R., Bhandari, N.L., Le, H.H., Henning, S., Radusch, H.J., Michler, G.H., Garda, M.R., and Saiter, J.M. (2012). Thermal, mechanical and morphological behavior of poly (propylene)/ wood flour composites. *Macromol. Symp.* 315, 24-29. DOI: 10.1002/masy.201250503

Adhikary, B.K. (2008). *Development of wood flour-recycled polymer composite panels as Building material*. PhD Thesis in Chemical and Processing Engineering, University of Canterbury: pp. 226 – 229.

Aina, K.S, Osuntuyi E.O. and Aruwajoye A.S. (2013). Comparative Studies of Physico-mechanical properties of Wood Plastic Composites produced from three indigenous wood species. *International Journal of Science and Research.* 2(8): pp178.

Aina, K.S., Badejo, S.O., Baiyewu, R.A., Ademola, I.T., Taleat, O.S., Agbigbi, J.O and Alao, O.J. (2008). Assessment of Dimensional Stability of Plastic bonded particleboard produced from *Gmelina arborea*. *African Journal of Agric Research and Development*, Vol 1 (1): 98 – 103.

Ajayi, B and Aina, K.S (2010). Effect of production variables on the Strength Properties of Plastic-bonded Particle Board from Bamboo. *Journal of Tropical Forest Resources*, 24(1): 99-105.

Ajayi, B. (2003). *Assessment of the dimensional stability of cement bonded particle board from Post-harvest banana stem residues and saw dust*. World Forestry Congress at Quebec City, Canada. Vol. A: Pp. 157.

Ajayi, B. (2008). The dimensional stability and Strength properties of inorganic bonded particleboards made from *Eupatorium odorata* particles. *62nd Forest Product Society Conference. St Louis, Missouri, USA, Book of Biographies and Abstracts.* Pp. 27.

Ajayi, B. (2011) Durability characteristics of Cement Bonded Particleboards manufactured from an agricultural residue. *Journal of Forestry*, 22(1):111-115

**Proceedings of the 62nd International Convention of
Society of Wood Science and Technology
October 20-25, 2019 – Tenaya Lodge, Yosemite, California USA**

Ajayi, B. and Olufemi, B. (2011). Properties of cement-bonded flake-boards from *Gmelina arborea* and *Leucaena leucocephala*. *Int. J. Biol. Chem. Sci.*, 5(2), 586-594

Ajigbon, A.A. (2005). *Strength and Dimensional Properties of Plastic bonded Boards produced from Terminalia superba sawdust*. Thesis project in the Department of Forestry and Wood Technology, Federal University of Technology, Akure. pp98

American Society for Testing and Materials (2005). American Society for Testing and Materials. Annual book of ASTM standards. 100 Barr Harbor Dr., West Conshohocken, PA 19428, ASTM D570-98, reapproved in 2005, pp. 35-37.

Carus, M., Eder, A., Dammer, L., Korte, H., Scholz, L., Essel, R., Breitmayer, E., and Barth, M. (2015). WPC/NFC Market Study 2014-10 (Update 2015-06): Wood-Plastic Composites (WPC) and Natural Fibre Composites (NFC): European and Global Markets 2012 and Future Trends in Automotive and Construction. Market study by nova Institut GmbH, Hürth, DE, available under www.biobased.eu/markets

Falemara, B.C. and Ajayi, B. (2018). Effects of Additives levels on Dimensional Stability and Strength of Cement Composite before and after Aging Procedure. Conference Proceedings IIBCC 2018. Editor: Holmer Savastano Jr. International Inorganic-Bonded Fiber Composites Conference (IIBCC). Cape Town International Conference Centre (CTICC), Cape Town, South Africa, 23–26 October 2018. 213-224

Falemara, B.C., Ajayi, B. and Owoyemi, J.M. (2015). Strength and Sorption Properties of Bamboo (*Bambusa vulgaris*) Wood-Plastic Composites. *Pro Ligno*; Sep. 2015, Vol. 11(3):21

Hillig, E., Ignacio Bobadilla, Ademir José Zattera, Érick Agonso Agnes de Lima and Raquel Marchesan (2017). Influence of Coconut Shell Addition on Physico-Mechanical Properties of Wood Plastic Composites. *Revista Árvore*; 41(4):e410412. <http://dx.doi.org/10.1590/1806-90882017000400012>

Hung Ke-Chang, Heng Yeh, Teng-Chun Yang, Tung-Lin Wu, Jin-Wei Xu and Jyh-Horng Wu (2017). Characterization of Wood-Plastic Composites Made with Different Lignocellulosic Materials that Vary in Their Morphology, Chemical Composition and Thermal Stability. *Polymers*, 9, 726. doi:10.3390/polym9120726

Kazemi-Najafi, S., Hamidinia, E., and Tajvidi, M. (2006). Mechanical properties of composites from sawdust and recycled plastics. *J. Appl. Polym. Sci.* 100(5): 3641-3645. DOI: 10.1002/app.23159

Mármol, G. and Savastano, H. Jr (2017). Study of the degradation of non-conventional MgO-SiO₂ cement reinforced with lignocellulosic fibers. *Cement and Concrete Composites* 80, 258-267

**Proceedings of the 62nd International Convention of
Society of Wood Science and Technology
October 20-25, 2019 – Tenaya Lodge, Yosemite, California USA**

N. A. Sadiku, A. O. Oluyeye and **B. Ajayi** (2016): Fibre dimension and chemical characterization of naturally grown *Bambusa vulgaris* for pulp and paper production. *J. Bamboo and Rattan*, 15, Nos. 1-4, pp. 33-43

Olufemi, A.S., Abiodun, O.O., Omaojor O. and Paul, F.A. (2016). Evaluation of Cement Bonded Particle boards made from Banana stalk (*Musa sapientum*). *Global Journal of Advance Engineering Technologies and Sciences*. 2(675): 2349-2368

Sommerhuber, P. F., Welling, J., and Krause, A. (2015). Substitution potentials of recycled HDPE and wood particles from post-consumer packaging waste in wood-plastic composites. *Waste Manag.* 46: 76-85. DOI: 10.1016/j.wasman.2015.09.011

Stark, M.N. (2008). Improving the Colour Stability of Wood Plastic Composites through Fibre Pretreatment. *Journal of Wood and Fibre Science*, 40(2): 271-278.

Sudar, A., Lopez, M. J., Keledy, G., Vargas –Garcia, M.C., Enstrella, S.F., Moreno, J. and Burgstaller, C. (2013). Bio-deterioration and Eco-toxicity of PP/ Wood Composites: Effect of Wood content and Coupling. *Journal of Chemosphere*, 93(2): 408-414.

Teuber, L., Osburg, V.S., Toporowski, W., Militz, H., and Krause, A. (2016). Wood polymer composites and their contribution to cascading utilization. *J. Clean. Prod.* 110: 9-15. DOI: 10.1016/j.jclepro.2015.04.009

Mycelium-Assisted Bonding, Influence of the Aerial Hyphae on the Bonding Properties of White-Rot Modified Wood

Ms. Wenjing Sun, wenjing.sun@maine.edu
Dr. Mehdi Tajvidi
University of Maine, USA

Abstract

Biological pretreatment of wood before the production of bio-composites may increase the properties of the products by facilitating more adhesion. At the initial stage of colonization, white-rot fungi produce enzymes to breakdown lignin and hemicellulose. The generated phenoxy radicals can form covalent bonding by radical-radical coupling. At the same time, the aerial hyphae of the fungi grow on the surface and form fibrous films that cover the substrate. The formed mycelium changes the surface morphology and may contribute to the bonding by its constituents (protein and carbohydrates) under certain processing condition. The aim of this work is to investigate the influence of aerial hyphae on the bonding properties of white-rot modified wood veneers. The effect of the life condition and density of aerial fungi on the change of roughness, surface energy and bonding property of wood veneer were characterized and compared.

Characterization and Properties of PLA-Based Biomass Composites for FDM Technology

Dr. Rui Guo, guorui0527@163.com
Prof. Min Xu
Northeast Forestry University, China

Abstract

In recent years, conductive polymeric composites have attracted wide attention due to their good electrical and thermal conductivity as well as the wide application, especially those filled with conductive fillers such as graphite. Carbonaceous materials such as graphite and carbon nanotubes are considered to be potential fillers due to their high conductivity and light weight, which can be incorporated into polymer matrix to improve their electrical and thermal conductivity. Among carbonaceous fillers, nanographite is an ideal nanofiller for reinforcing polymer matrix due to its low manufacturing cost and unique two-dimensional structure. In order to adapt to its broad application, the composites can be realized in 3D printing with complex structures and special shapes and geometries that can be customized.

With the emphasis on environmental issues in recent years, degradable materials have become a research hotspot. Polylactic acid (PLA), with good biocompatibility and biodegradability, can be completely degraded to carbon dioxide and water under natural conditions without environmental pollution. The mechanical processability of PLA is good and its performance can be comparable to many petroleum-based plastics, but does not rely on petroleum-based resources. However, its application may be limited by the brittleness and the high cost of PLA. Wood flour, which is cost-effective, renewable, and biodegradable, can be a kind of good filler adding into PLA to reduce the cost. To improve the toughness of the PLA composites, polymer blending and polymer grafting may be an efficient way.

Studies have shown that the addition of TPU significantly improved the performance of PLA-based wood-plastic composites, and with the addition of TPU, the compatibility between PLA and WF improved. GMA grafted PLA polymer was prepared by melt blending in a Haake torque rheometer with wood flour as a carrier. The wood flour is loose and porous, and can absorb more liquid of GMA, which can increase the grafting rate of PLA-g-GMA. The PLA-g-GMA can slightly improve the mechanical properties of the composite, but the flexural strength decreases slightly. In summary, the mechanical properties and compatibility of the PLA/WF/TPU composites can be better.

To improve the electrical and thermal conductivity of the polylactic acid /wood flour /thermoplastic polyurethane composites by Fused Deposition Modeling, nano-graphite was incorporated into the ternary blends. The results showed that, when the addition amount of nano-graphite reached 25wt%, the volume resistivity of the composites decreased to $10^8 \Omega \cdot m$, which was a significant reduction, indicating that the conductive network was already formed. The thermal conductivity, mechanical

***Proceedings of the 62nd International Convention of
Society of Wood Science and Technology
October 20-25, 2019 – Tenaya Lodge, Yosemite, California USA***

properties and thermal stability were also good. The adding of rGO combined with graphite into the composites, compared to the tannic acid-functionalized graphite or the multi-walled carbon nanotubes, can be an effective method to improve the performance of the biocomposites, because the resistivity reduced by one order magnitude and the thermal conductivity increased by 25.71%. Models printed by FDM illustrated that the composite filaments have a certain flexibility and can be printed onto paper or flexible baseplates.

Keywords: Polylactic Acid; Biocomposites; Toughening Agents; Nano-Graphite; Electrical Conductivity; Fused Deposition Modeling; Tannic Acid-Functionalized Graphite

Evaluation of a Renewable Wood Composite Sandwich Panel For Building Construction

Mr. Mostafa Mohammadabadi, m.mohammadbadi@wsu.edu

Dr. Vikram Yadama
Washington State University, USA

Abstract

Finding a solution for small diameter timber from hazardous fuel treatments contributes to forest health as well as rural economic development. The issue is with lower wood quality of the wood derived from these trees as well as lower rate of conversion into higher value products such as lumber and veneer. However, wood strand technology, such as OSB, can offer a solution. However, can we produce a wood strand composite panel of greater performance than OSB with improved functionality and with less materials (wood and resin)? To this aim, wood strand composite sandwich panel with biaxial corrugated core(s) was developed to serve as a material for construction of building envelopes, such walls, floors, or roofs.

Thin wood strands with an average thickness of 0.36 mm were produced from ponderosa pine (pp) logs ranging in diameter from 191 to 311 mm, using a CAE strander operating at a rotational speed of 500 rpm. Wood strands were dried to a target moisture content of 3-5% and sprayed with aerosolized liquid phenol formaldehyde (PF) resin in a drum blender to a target resin content of 8%.

Subsequently, resinated wood strands were oriented unidirectionally to fabricate a wood strand mat and hot-pressed into a corrugated core using a matched-die mold. Single or multiple cores can then be bonded with flat wood strand panels on the faces to fabricate a sandwich panel. When used in walls, these panels can be subjected to gravity loads from the roof and other floors, and transverse wind loads. Therefore, this presentation will focus on performance evaluation of wood strand sandwich panels in compression and bending conducted following the standard testing guidelines in ASTM E72-15. Additionally, to improve the energy performance, the cavities in the sandwich panel resulting from the corrugated geometry of the core were filled with two-part closed-cell foam. Prefabricated wall panel filled with insulation foam and instrumented with moisture, temperature, and relative humidity sensors was evaluated for its hygrothermal performance at Washington State University's Natural Exposure Testing (NET) facility. Hygrothermal performance of this wall will be compared with the performance of a structurally insulated panel installed and evaluated at the NET facility as well.

The Use of Soy Flour to Replace pMDI in Wood Composites

Prof. Brian Via¹, bkv0003@auburn.edu

Mr. Osei Asafu-Adjaye¹

Dr. Sujit Banerjee²

¹Forest Products Development Center, Auburn University, USA

²Georgia Tech, USA

Abstract

The use of methylene diphenyl diisocyanate (pMDI) adhesive is common in oriented strand board (OSB) and becoming more feasible for particleboard if tack is not an issue. pMDI has been replacing phenol formaldehyde in OSB due to the perception of formaldehyde removal. While in particleboard, pMDI has been proposed to replace urea formaldehyde for the same reason. In both cases, pMDI can be more expensive than other adhesives. Ways to lower the cost of pMDI without affecting composite physical and mechanical properties is desirable by industry. Soy flour is 3 times cheaper than pMDI and could be a possible candidate for substitution. However, ways to disperse can be difficult as the addition of soy to pMDI increases viscosity. Additionally, soy flour is hydrophilic and can retain water resulting in board distortion or failure in the field. This presentation will demonstrate how to disperse pMDI-soy mixtures without viscosity and moisture degradation issues.

UV-Light Protection Cellulose Nanocrystals Films Prepared through Trivalent Ions

Ms. Cong Chen¹

Dr. Lu Wang¹

Dr. Jinwu Wang²

Prof. Douglas Gardner¹

¹University of Maine, USA

²USDA Forest Service, Forest Products Laboratory, USA

Abstract

In order to preserve food from the effects of oxygen, moisture, and UV radiation, typical packaging is opaque or metallized. There is increasing consumer demand of transparent packaging, or a transparent viewing window to allow viewing of food stuffs during consumer purchase. Cellulose nanocrystals (CNCs), as a sustainable and biodegradable material, show huge potential for transparent food packaging, and can provide good oxygen permeation resistance, but is poor in preventing UV radiation transmission. The aim of this work is to produce high quality CNC films with UV-blocking characteristics under facile operation. CNC suspensions were modified with different concentrations of trivalent metal ions (Al^{3+} , Fe^{3+}) and homogeneous, transparent and flexible CNC films were prepared by the casting method. CNC films undergo cross-linking between metal ions and sulfate half-ester groups of CNCs and exhibit high UV absorption properties. Meanwhile, the water vapor permeability of the films was decreased slightly and the tensile strength was improved. In order to enhance the UV absorption, the addition of UV stabilizers into the CNC matrix may also be explored, and their interactions may be characterized.

Study of Refiner Plates as a Possibility to Improve the Production of Wood Fiber Insulation Materials

Simon Barth
Prof Andreas Michanickl
Rosenheim Technical University of Applied Sciences, Germany

Abstract

In central Europe, modern wood fiber insulation materials (WFI) have had a notable increase in production capacity over the past 15 years. Currently, they are of great interest for R&D and industry. This is due to their good performance in sound and thermal insulation of buildings and the use of the sustainable raw material wood. However, compared to synthetic and mineral insulation materials, WFI are still a niche product with a market share of only 3 % to 5 % in Germany. Currently, the main obstacle preventing further market penetration of WFI are high production costs.

The processing technology for modern WFI offers a large potential for optimization. The state of the art is based on the dry process that is used in MDF production. In particular, the central processing step of fiber generation uses refiner plates for MDF production. However, the requirements for MDF and WFI are quite different. Therefore, it is questionable whether the fibers currently used in the production of WFI are optimal. To date, studies of the influence of refiner plates on fiber morphology, usable raw materials, electrical and thermal energy consumption, and other cost factors such as binders, have been sadly neglected. Thus, the development of refiner plates for the production of WFI is a promising possibility to improve product properties, processing technology and reduce production costs.

The aim of this study is to determine the optimal fiber morphology in technical and economic terms. Improvements are intended in energy related aspects, as well as, in mechanical and physical product properties e.g. low heat conductivity. This also includes an enlargement of the raw material base. So far, the raw material selection in the production WFI has been limited to expensive softwood assortments. Therefore, one aspect of this study deals with currently unused, but favorable, and abundantly available hardwood assortments. The study takes place within an experimental setup that includes a laboratory refiner plant to determine the efficiency of new plate designs. Industrial scale trials are currently underway in several plants.

The results to date confirm a direct and positive influence of the refiner plate design on the fiber morphology and the thermal and specific electrical energy consumption. The development of special refiner plates makes it possible to produce wood fibers that are more suitable for the requirements of wood fiber insulation materials and helps to decrease production costs. Furthermore, it seems possible not only to use softwoods, but also hardwoods for the production of WFI.

Environmentally-friendly bio-adhesives from renewable resources – WooBAdh project

Milan Sernek¹, Jasa Sarazin¹, Siham Amirou², Antonio Pizzi², Marie-Pierre Laborie³, Detlef Schmiedl⁴, Thelmo A. Lú Chau⁵, María Teresa Moreiras

¹ University of Ljubljana, Biotechnical Faculty, 101 Jamnikarjeva, 1000 Ljubljana Slovenia, milan.sernek@bf.uni-lj.si

² Universite de Lorraine LERMAB-ENSTIB, 34 Cours Léopold, 54000 Nancy France, antonio.pizzi@univ-lorraine.fr

³ Albert Ludwig University of Freiburg Institute of Earth and Environmental Sciences - Chair of Forest Biomaterials, 6 Werthmanstrasse, 79085 Freiburg im Br Germany, marie-pierre.laborie@fobawi.uni-freiburg.de

⁴ Fraunhofer ICT Environmental Engineering, 7 Joseph-von-Fraunhofer-Str., 76327 Pfinztal Germany, detlef.schmiedl@ict.fraunhofer.de

⁵ Universidade de Santiago de Compostela, Dept. Chemical Engineering, Rúa Lope Gómez de Marzoa s/n, 15782 Santiago de Compostela Spain, maite.moreira@usc.es

Wood adhesives are of tremendous industrial importance as more than two-thirds of wood products in the world are totally, or at least partially, bonded together using a variety of adhesives. Synthetic adhesives on formaldehyde basis greatly dominate the field of binders for wood-based panels. The WooBAdh project aims to study the feasibility of replacing formaldehyde in wood adhesives by natural components derived from wood or other vegetable matter. The proposed solution is focused on different modifications of polyphenols, namely lignin and tannins, for producing bioadhesives. Shear strength of the specimens bonded with adhesive mixtures made of pine tannin, different types of lignin and hexamine was studied. Three types of kraft lignin and three types of organosolv lignin were tested. The mixing ratio between dry weight tannin and lignin was always 1:1; 6 % of hexamine was used as a hardener. Bioadhesives from kraft lignins shown significantly higher shear strength than those from organosolv lignins. Two adhesive formulations from kraft lignins reached required shear strength according to EN standards for use in interior conditions.

October 24th

Business, Marketing and Regulations

11:00 – 12:15

Chair: Henry Quesada, Virginia Tech, USA

KEEPING THE HOME FIRES FROM BURNING: THE LATEST ON FIRE-RETARDANT-TREATED WOOD AND THE MODEL CODES

Mike Eckhoff, Ph.D.^{1}*

¹ Marketing Representative, Hoover Treated Wood Products, Inc., Thomson, GA,
USA* *Corresponding author*
meckhoff@frtw.com

ABSTRACT

At the end of 2018, wildfires continued to burn with increased intensity and efficiencies. As a result, more and better solutions to help reduce their impacts are needed. Traditional approaches, such as defensible space and removing combustible materials from around structures, can help. However, solutions that help improve structures' ignition resistance while also reducing forest fuel loads in the wildland-urban interface (WUI) are also needed. Pressure-impregnated, fire-retardant-treated wood (FRTW) is one such solution.

Modern, pressure-impregnated FRTW technology modifies wood with mineral salts that reduce the wood's combustibility. When exposed to high heat, the treatment releases water vapor and non-flammable gases that reinforce a protective char layer that forms around the wood thereby insulating it. The result is that while the wood is not fireproof, it is unable to support combustion and is self-extinguishing. By substituting untreated wood with FRTW, structures will not add to fuel loads, and people will have more time to evacuate and/or to try to save those structures. FRTW can also help mitigate climate change; whereas steel and concrete emit large sums of carbon, FRTW sequesters it.

This paper defines FRTW, compares it to non-pressure-impregnated wood products, and then qualitatively reviews several incentives and code-permitted applications for using FRTW in the WUI. The paper concludes that FRTW is such a solution, but barriers exist to its more widespread use.

Key words: building, fire-retardant-treated wood, pressure-impregnated, wildland-urban interface, wildfire

INTRODUCTION

At a little after 6:30AM on November 8, 2018, what would be known as the Camp Fire erupted from faulty Pacific Gas & Electric equipment in Butte County, CA (Serna 2019). The Camp Fire would be the most expensive natural disaster on the planet for 2018 in terms of insurance losses (\$16.5 billion) and the deadliest in California's history (Munich Re 2019, Serna 2019).

Accounts, like the Camp Fire's, confirm that wildfires are continuing to burn with greater intensity and efficiency. According to data from the National Interagency Fire Center's (NIFC), since 2000, the average number of acres burned by wildfires in the U.S. each year is increasing, while the average number of wildfires each year is decreasing (NIFC 2019). In other words, a smaller number of fires are burning a larger number of acres each successive year.

Incentives exist to reduce wildfire severity while also minimizing risks to public and life safety in the wildland-urban interface (WUI). One option for homeowners, land managers, or building tenants is to create defensible space, which is "the area around a home or other structure that has been modified to reduce fire hazard. In this area, natural and manmade fuels are treated, cleared or reduced to slow the spread of wildfire" (Colorado State Forest Service [CSFS] 2019). Another option is to remove potential fuel sources from on and next to the home. For instance, cleaning out gutters and areas where leaves and needles could be trapped on a roof, raking debris away from the exterior walls of a home, and even moving firewood piles away from the home could help reduce potential home ignition sources relatively inexpensively (Insurance Institute for Business and Home Safety [IBHS] 2019).

However, a third tack is worth exploring: what can be done to harden the physical structures in the WUI i.e., how can we improve the materials we use to build in the WUI?

WHAT IS PRESSURE-IMPREGNATED FIRE-RETARDANT-TREATED WOOD?

Hardening structures in the WUI against the wildfire threat means relying more on ignition-resistant building materials. Owners and managers could increase a structure's resistance to fire while also providing an option for lowering hazardous forest fuel loads by using ignition-resistant wood products for their structures. One such product is pressure-impregnated fire-retardant-treated wood (FRTW). FRTW products are defined in the 2018 International Building Code (IBC) as "wood products that, when impregnated with chemicals by a pressure process or other means during manufacture, exhibit reduced surface-burning characteristics and resist the propagation of fire" (International Code Council [ICC] 2018).

Most FRTW will be chemically impregnated using a pressure process, although other, non-pressurized methods are possible. Pressure impregnation, however, is the only effective means for treating wood with fire-retardants (Bueche 2010). First patented in 1893, this pressure-impregnation process consists of a simple six-step process, as shown in Figure 1.

First, untreated wood is loaded into an empty, horizontal treating cylinder (A); then, the cylinder door is sealed and a vacuum is applied to remove air from the cylinder and the wood (B); next, the treatment is pumped into the cylinder (C); the pressure in the cylinder is then increased, forcing the treating solution deep into the wood (D); after pressurizing, the treating solution is then pumped out, and a second vacuum removes any excess treatment (E); finally, the treated wood is moved to a kiln to be dried using carefully controlled moisture conditions (F). Once kiln-dried after the treatment to moisture content levels prescribed by the IBC, the FRTW is ready to be labeled and is then subsequently ready for use.

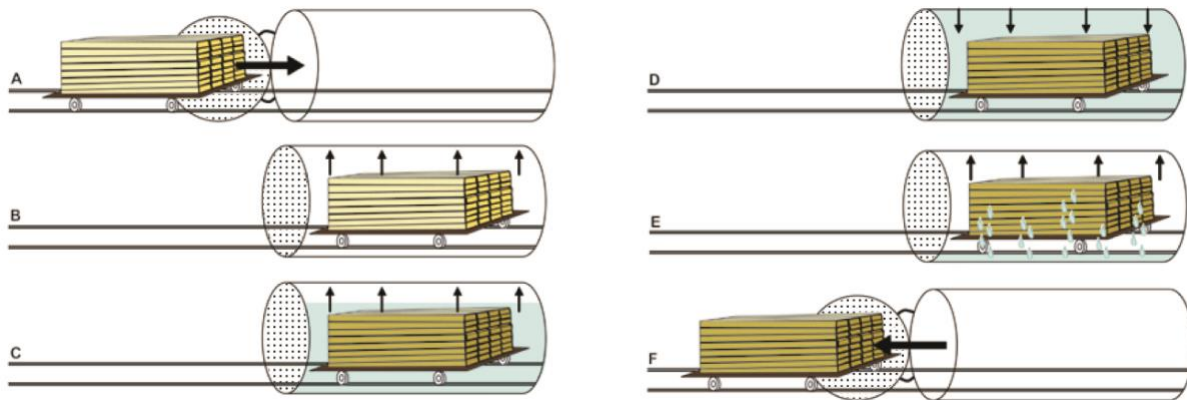


Figure 1. The FRTW Manufacturing Process (Adapted from USDA Forest Service, Forest Products Laboratory 2010)

This pressure-impregnation process helps differentiate FRTW from other materials, like intumescent-painted wood panels or cementitious-coated oriented strandboard. These products are covered in a vulnerable surface layer and typically do not cover all six sides of a wood panel. This distinction was recognized in the 2018 IBC, Section 2303.2.2: “The use of paints, coating, stains or other surface applications are not an approved method of protection as required in this section” (ICC 2018). In other words, those painted or coated products are not code-compliant substitutes for FRTW because they are not pressure-impregnated.

HOW DOES FRTW WORK?

Once through the chemical impregnation process, fire-retardant treatment of wood improves fire performance by greatly reducing the amount of flammable gases released, thus reducing the rate at which flames spread over the surface. Treatments reduce the amount of heat available or released by the volatiles during the initial stages of fire and result in the wood self-extinguishing once the primary source of external fuel is exhausted.

To ensure that the treatment is effective, FRTW is required to pass the UL 723 “Standard for Test for Surface Burning Characteristics of Building Materials” (UL, Inc. 2018). This test is designed to gauge the firespread over the surface of a material and the smoke developed due to the burning. The test apparatus, originally developed by Steiner, consists of a 25-foot-long

***Proceedings of the 62nd International Convention of
Society of Wood Science and Technology
October 20-25, 2019 – Tenaya Lodge, Yosemite, California USA***

rectangular tunnel with two gas burners at one end that direct a 4.5-foot flame under controlled conditions of draft and temperature onto the surface of a 24-foot-long by 20-inch-wide specimen (Steiner 1936). Flame spreads along the surface of the material as the test progresses. The distance of flame travel and rate at which the flame front advances during a 10-minute exposure determine the calculated flame spread index (FSI).

However, UL realized that this 10-minute period only demonstrated delayed ignition and gave little indication of non-combustibility. At the request of several insurance rating bureaus, UL wrote a performance standard for pressure impregnated FRTW that requires the test period to be extended an additional 20 minutes to a total of 30 minutes. Malcomson and Bono wrote that during the 20-minute extension, “the test samples are observed to determine that the flame spread does not exceed the equivalent of 25 (5 ft. beyond the standard igniting flame) and that there is no evidence of significant progressive combustion” (Malcomson and Bono 1967).

Over the years, changes to the standard affected the calculation procedures used to determine FSI values from raw data. In order to allow listed FRTW from older tests to remain compliant, an additional criterion was added to the codes to address what was already required by the UL Listings. This additional code criterion requires that “the flame front shall not progress more than 10-½ feet beyond the centerline of the burners at any time during the test.” (ICC 2018)

HOW CAN FRTW BE USED?

FEDERAL GOVERNMENT

Department of Defense Qualified Producer List

The Department of Defense maintains a Qualified Products List (QPL). Defined a QPL “is a listing of products or family of products that have met the qualification requirements set forth in the applicable specification, including appropriate product identification, tests or qualification reference, and the name and plant address of the manufacturer and authorized distributor” (Defense Logistics Agency 2019). Federal entities, such as the U.S. Department of Defense and U.S. Department of Energy, use QPL listings to determine approved sources of supply for items they wish to procure, which includes FRTW since FRTW is on the QPL.

Executive Order 13728

Promulgated in May 2016, this Executive Order applies to all agencies responsible for planned/existing federal buildings (or leasing space in buildings or financing the construction of buildings) of 5,000 or more square feet in the WUI and at moderate or greater risk to wildfire, should apply the wildfire-resistant design provisions outlined in the most current edition of the International Wildland-Urban Interface Code (IWUIC) or an equivalent nationally recognized code (Obama 2016). FRTW applications are permitted in the IWUIC (see IWUIC below).

**Proceedings of the 62nd International Convention of
Society of Wood Science and Technology
October 20-25, 2019 – Tenaya Lodge, Yosemite, California USA**

MODEL CODES

These code references identify applications where an architect may decide to use FRTW or where a building or fire inspector may encounter FRTW in the field. These applications can be significant for providing an outlet for merchantable material removed from the WUI. For instance, UL Design Number V314 is a two-hour rated exterior wall assembly permitted by the code in Type IIIA construction. It consists of two sheets of 5/8” Type X Gypsum Board on an interior face, with 2x4 FRTW studs and either mineral wool or fiberglass insulation, with FRTW plywood on the exterior face, and finished with any exterior cladding as permitted by the authority having jurisdiction. Material harvested from the WUI, thus, could then be fire-retardant treated and used in multi-family wood structures in the WUI or even in increasingly densified urban corridors in proximity to the WUI.

International Building Code

Because of its working properties stemming from the chemical impregnation, FRTW has been accepted by the IBC and legacy building codes for a myriad of applications, including as a substitute for untreated wood in any rated assembly without altering its fire resistance, as stated in references such as UL’s Fire Resistance Directory (Bueche 2013). See Table 1 for a list.

Table 1: FRTW Applications and Corresponding Code Citations in the 2018 IBC

Code Application	Citation
Architectural trim, exterior wall coverings	1405.1.1#3
Attics, elimination of sprinklers in residential occupancy	903.3.1.2.3
Awnings & canopies	3105.2
Balconies and similar projections	603.1#1.4
Bay and oriel windows	705.2.4
Children playground structures in malls	424.2#1
Combustible projections	705.2.3
Exterior bearing & nonbearing walls: Type III const.	602.3
Exterior bearing & nonbearing walls: Type IV const.	602.4.1
Exterior nonbearing walls in Types I & II construction	603.1#1.2
Enclosed combustible spaces in sprinklered buildings of all types of construction: Sprinklers not required	NFPA 13: 1999 ed. 8-13.1.1#9; 2002 ed. 8.14.1.2.11; 2007, 2010, 2013, 2016 ed. 8.15.1.2.11
Fire barrier: See partitions Types I & II construction	603.1#1.1
Fuel dispensing station (marine and motor vehicle)	406.7.2
Interior finish with flame spread index < 25 (Class A)	803.1.2
Kiosks in covered and open mall buildings	402.6.2#1.1
Liquid storage rooms (shelving, racks, and wainscotting)	415.11.5.2#3
Mechanical equipment screens	1510.6.2#2
Parapet not required when using FRTW sheathing:	
Exterior walls	705.11#5.1
Fire and party walls in Types III, IV, and V	706.6#4.3
Townhouses: Exterior and common wall use within 4ft of such walls	International Residential Code: R302.2.4
Partitions (2 hr or less) in Types I & II construction	603.1#1.1
Partitions (fixed) establishing corridors in buildings with one tenant serving no more than 30 people	603.1#11
Pedestrian walkways	3104.3#2

**Proceedings of the 62nd International Convention of
Society of Wood Science and Technology
October 20-25, 2019 – Tenaya Lodge, Yosemite, California USA**

Platforms in Types I, II, and IV construction	410.3
Plenums in all types of construction	International Mechanical Code: 602.2.1
Roof construction in Types I & II construction	603.1#1.3
Roof construction in Types I, II, III, & VA construction when > 20 ft. above the floor	Table 601, Footnote b
Rooftop structures (penthouses)	1510.2.4
Shakes and shingles: Wood	1505.6
Wood veneer	1404.5.1
Walls and ceiling furred & dropped more than 1-3/4"	803.15.2.1

International Wildland-Urban Interface Code (IWUIC)

FRTW is also accepted for use in the WUI per the IWUIC for all three ignition-resistance construction classes. For instance, FRTW could be used for decking, siding, roof coverings, and eaves and soffits (Fig. 2).

National Fire Protection Association (NFPA)

FRTW is also permitted in several NFPA Codes and Standards, including 101, 220, 221, and 5000. FRTW is also defined in NFPA 703. Many FRTW applications identified in the 2018 IBC also pertain to the NFPA Codes and Standards (Table 2).

Table 2: Some FRTW Applications in NFPA 5000 and NFPA 101

Code Application	NFPA 5000	NFPA 101
	Citation	
Architectural trim, exterior wall coverings	37.2.1	See a building code
Attics, elimination of sprinklers in residential occupancy	26.2.3.5.6.2(4)	28.3.5.3.1(3)
Awnings & canopies	32.4.2.1(3)	See a building code
Balconies and similar projections	37.2.2.2	See a building code
Bay and oriel windows	37.2.2.1	See a building code
Combustible projections	37.2	See a building code
Exterior bearing & nonbearing walls: Type III const.	7.2.4.2.1	NFPA 220: 4.4.2.1
Exterior bearing & nonbearing walls: Type IV const.	7.2.5.6.7(3)	NFPA 220: 4.5.6.7
Exterior nonbearing walls in Types I & II construction	7.2.3.2.12.1	NFPA 220: 4.3.2.12.1
Enclosed combustible spaces in sprinklered buildings of all types of construction: Sprinklers not required	NFPA 13: 1999 ed. 8-13.1.1#9; 2002 ed. 8.14.1.2.11; 2007, 2010, 2013, 2016 ed. 8.15.1.2.11	
Fire barrier: See partitions Types I & II construction	7.2.3.2.11.2	NFPA 220: 4.3.2.11.2
Fuel dispensing station (marine and motor vehicle)	32.4.5.2	See a building code
Interior finish with flame spread index < 25 (Class A)	32.7.5.2(5)	12.4.9.3.3
Kiosks in covered and open mall buildings	27.4.4.13.1(1)	36.4.4.11(1)(a)
Parapet not required when using FRTW sheathing:		
Exterior walls	37.1.3.1(6)(b)	See a building code
Fire and party walls in Types III, IV, and V	8.3.3.7.4.2	NFPA 221: 6.6.4.2
Townhouses: Exterior and common wall use within 4ft of such walls	22.5.4	See a building code
Partitions (2 hr or less) in Types I & II construction	7.2.3.2.11.2	NFPA 220: 4.3.2.11.2
Partitions (fixed) establishing corridors in buildings with one tenant serving no more than 30 people	7.2.3.2.11.2	See a building code
Pedestrian walkways	7.2.3.2.9.2	See a building code
Platforms in Types I, II, and IV construction	7.2.3.2.7	NFPA 220: 4.3.2.7
Plenums in all types of construction	7.2.3.2.14.2	NFPA 220: 4.3.2.15

**Proceedings of the 62nd International Convention of
Society of Wood Science and Technology
October 20-25, 2019 – Tenaya Lodge, Yosemite, California USA**

Ramps		7.2.5.4.1(3)
Roof construction in Types I & II construction	7.2.3.2.9.2	NFPA 220: 4.3.2.9.2
Roof construction in Types I, II, III, & VA construction when ≥ 20 ft. above the floor	7.2.3.2.8 (Types I & II)	NFPA 220: 4.3.2.9.1 (Types I & II)
Shakes and shingles: Wood	38.3.2	12.4.6.11.3
Wood veneer		13.4.6.11.3

Summary and Conclusions

FRTW has many incentives and accepted applications in the model codes. FRTW could even be manufactured sustainably to meet Forest Stewardship Council (FSC) standards, which, in turn, could be used to engender points used for Leadership in Energy and Environmental Design (LEED) designations. By sourcing sustainably, FRTW can contribute in perpetuity to lowering hazardous fuels loads in local forests, create local jobs and strengthen local economies, and provide fire-resistant building materials useful in construction, for building, rebuilding, and/or retrofitting in the WUI or even in urban corridors in multi-family structures.

Architectural Feature	Class 1 (Extreme Severity)	Class 2 (High Severity)	Class 3 (Moderate Severity)
Roof covering	Class A Roof Assembly	Class B or noncombustible	Class C or noncombustible
Eaves and soffits	Ignition-resistant material, or 1-hour fire-resistance-rated construction, or 2-inch dimensional lumber, or 1-inch exterior fire-retardant-treated lumber, or ¾-inch exterior fire-retardant-treated plywood	Combustible eaves, facias and soffits shall be enclosed with solid materials with a minimum thickness of ¾ of an inch. No exposed rafter tails are permitted unless constructed of heavy timber.	No special requirement
Gutters and downspouts	Constructed of noncombustible materials and provided with approved means to prevent the accumulation of leaves and debris in the gutter.	Constructed of noncombustible materials and provided with approved means to prevent the accumulation of leaves and debris in the gutter.	No special requirement
Exterior walls	1-hour fire resistance from the exterior side, or Approved noncombustible materials, or Heavy timber or log wall construction, or Exterior of fire-retardant treated wood , or Exterior of ignition-resistant material	1-hour fire resistance from the exterior side, or Approved noncombustible materials, or Heavy timber or log wall construction, or Exterior of fire-retardant-treated wood , or Exterior of ignition-resistant material	No special requirement
Unenclosed underfloor protection	1-hour fire-resistance-rated construction, or Heavy timber construction, or Exterior fire-retardant-treated wood	1-hour fire resistance-rated construction, or Heavy timber construction, or Exterior fire-retardant-treated wood	1-hour fire resistance-rated construction, or Heavy timber construction
Appendages and projections, such as decks	1-hour fire resistance from the exterior side, or Heavy timber construction, or Approved noncombustible materials, or Exterior fire-retardant-treated wood, or Ignition-resistant building materials	1-hour fire resistance from the exterior side, or Heavy timber construction, or Approved noncombustible materials, or Exterior fire-retardant-treated wood, or Ignition-resistant building materials	No special requirement
Exterior glazing	Tempered glass, or Multilayered glazed panels, or Glass block, or Fire protection rating of not less than 20 minutes	Tempered glass, or Multilayered glazed panels, or Glass block, or Fire protection rating of not less than 20 minutes	No special requirement
Exterior doors	Approved noncombustible construction, or Solid core wood not less than 1¾-inch thick, or Fire protection rating of not less than 20 minutes	Approved noncombustible construction, or Solid core wood not less than 1¾-inch thick, or Fire protection rating of not less than 20 minutes	No special requirement
Vent location	Not allowed in soffits, eave overhangs, between rafters at eaves or in other overhang areas.	Not allowed in soffits, eave overhangs, between rafters at eaves or in other overhang areas.	No special requirement

Figure 2. FRTW Applications in the IWUIC (Adapted from CSFS 2010)

*Proceedings of the 62nd International Convention of
Society of Wood Science and Technology
October 20-25, 2019 – Tenaya Lodge, Yosemite, California USA*

The main problem with using FRTW tends to be two-fold: lack of awareness by architects, code officials, and other stakeholders and the additional incurred expense over untreated wood. Efforts could be made through educational institutions, including architecture, construction, and forestry/wood products programs, to include more FRTW in their curricula. Code officials could opt for trainings involving FRTW. Stakeholder groups, particularly in the WUI, could arrange for FRTW educational seminars. Greater familiarity with FRTW could lead to increased demand and usage and help discourage code officials from accepting painted or coated wood products when they are not appropriate for some WUI applications.

While manufacturing FRTW does incur additional expense over untreated wood through the additional handling, treating, and transportation required, it will outperform untreated wood, coated/painted wood, and even steel and concrete under real fire conditions, thus earning it the same premium from the Insurance Service Office as if a building were using steel or concrete. Furthermore, the cost of FRTW results in potentially giving occupants more time to evacuate a burning structure while giving first responders more time to try to save it, potentially lowering the costs for repair and for insurance when using FRTW for the code applications shown above.

References

Bueche D (2010) Wood use in type I and II (noncombustible) construction. Challenges, Opportunities and Solutions in Structural Engineering and Construction, pp. 581-585. Boca Raton, FL, CRC Press.

Bueche D (2013) NFPA code provisions and fire-retardant-treated wood in New Developments in Structural Engineering and Construction, pp. 245-250. Singapore: Research Publishing Services.

Colorado State Forest Service [CSFS] (2010) FireWise construction: Site design & building materials. Available: <https://static.colostate.edu/client-files/csfs/pdfs/firewise-construction2012.pdf>. [Accessed 15 Aug 2019].

Colorado State Forest Service [CSFS] (2019) Protect your home, property & forest from wildfire. Available: <https://csfs.colostate.edu/wildfire-mitigation/protect-your-home-property-forest-from-wildfire/> [Accessed 15 Aug 2019].

Defense Logistics Agency (2019) DLA troop support industrial hardware. U.S. Department of Defense, 2019. Available: <https://www.dla.mil/TroopSupport/IndustrialHardware/Engineering-and-Technical-services/Qualified-Products-List/> [Accessed 15 Aug 2019].

*Proceedings of the 62nd International Convention of
Society of Wood Science and Technology
October 20-25, 2019 – Tenaya Lodge, Yosemite, California USA*

Insurance Institute for Business and Home Safety [IBHS] (2019) Reduce wildfire damage to homes. Available: <https://disastersafety.org/wildfire/reduce-wildfire-damage-homes/> [Accessed 15 Aug 2019].

International Code Council [ICC] (2018). International Building Code. Country Club Hills, IL: ICC Publications.

Malcomson RW and Bono JA (1967) Underwriters' Laboratories, Inc. issues new labels for FRTW. Wood Preserving News.

Munich Re (2019) Extreme storms, wildfires and droughts cause heavy nat cat losses in 2018. Munich Re, 8 Jan 2019. Available: <https://www.munichre.com/en/media-relations/publications/press-releases/2019/2019-01-08-press-release/index.html> [Accessed 15 Aug 2019].

Obama B (2018) Executive Order 13728: Wildland-urban interface federal risk mitigation. Homeland Security Digital Library, 20 May 2016. Available: <https://www.hsdl.org/?abstract&did=790206> [Accessed 15 Aug 2019].

Serna, J (2019) PG&E power lines caused California's deadliest fire, investigators conclude. L.A. Times. 15 May 2019.

Steiner A (1936). Investigation of Effectiveness of Fireproofed Red Oak and Maple Lumber. MS Thesis. Chicago, IL: Armour Institute of Technology.

UL, Inc. (2018) UL 723: Standard for Test for Surface Burning Characteristics of Building Materials. 11th Ed. Northbrook, IL: UL Publications.

USDA Forest Service, Forest Products Laboratory (2010) Wood handbook: Wood as an engineering material. Gen. Tech. Rep. FPL-GTR-190. Madison, WI: U.S. Department of Agriculture, Forest Service, Forest Products Laboratory. 509 p. Graphic adapted from page 15-19.

Marketing of Urban and Reclaimed Wood Products

Dr. Omar Espinoza¹, espinoza@umn.edu

Ms. Anna Pitti¹

Dr. Robert Smith²

¹University of Minnesota, USA

²Virginia Tech, USA

Abstract

In the United States, trees felled in urban areas and wood generated through construction and demolition are primarily disposed of as low-value resources, such as biomass for energy, landscaping mulch, composting, or landfill. An emerging industry makes use of these underutilized resources to produce high-value added products, with associated benefits for the environment, the local economy, and consumers. Research was carried out to increase the understanding of the marketing practices of urban and reclaimed wood industries. This paper presents the results from a nationwide survey of these companies. The results indicate that a majority of companies in this industry are small firms, operating for less than 10 years, which produce mostly to order and sell their products at comparatively higher prices than comparable products made from traditional sources. Promotional messages included quality, aesthetics, and customization, conveyed through company webpages, word of mouth, and social media. Distribution channels used include direct sales, online sales, and retail sales. Partnerships are critical for effective raw material procurement. Respondents indicated optimistic growth expectations, despite barriers associated with urban and reclaimed wood materials and production.

**Drivers Impacting Supplying Decisions of Construction Companies: A Case Study in the
Southeastern Region of the US**

Dr. Henry Quesada, quesada@vt.edu

Dr. Robert Smith

Ms. Alison Bird

Mr. Joe Pomponi

Virginia Tech, USA

Abstract

Spending in the construction industry in the US reached over \$1.2 trillion in 2017 where single family residential construction reached \$267 billion in 2016 and commercial construction \$85 billion for the same year. Consumption of solid lumber, engineered lumber, and composite panels continues to be a critical construction raw material for the residential and commercial construction business in the United States. Thirteen years ago it was reported that the construction industry consumed 71.3 billion board feet of lumber, 39.8 billion ft² of structural panels, and 27 billion ft² of non-structural panels. Softwood species accounted for 85% of the lumber market. Despite the economic impact of wood products in the construction industry little is known about purchasing and supply chain decision practices of construction companies. This project aims to identify the main drivers behind supply chain and purchasing decision of construction companies in the Southeastern region of the United States. The research uses a combination of case study, survey, and data analytics research methods to answer this question. In this paper, data and analysis conducted through the case study research is presented. It was determined that for large construction companies the most important factor when purchasing raw materials was cost while for smaller construction companies honesty fairness, and quality were were the most important factors.

Acknowledgement: Research funded through a competitive grant from the South Carolina Forestry Commission.

Productivity of Firms in the Swedish Industry for Wooden Single-Family Houses

Schauerte, Tobias^{1} – Vestin, Alexander²*

¹ Ass.-Prof. PhD, Linnæus University,
Inst. of Mechanical Engineering, Växjö, Sweden

** Corresponding author*

Tobias.Schauerte@lnu.se

² Ph.D. candidate, Jönköping University, Inst. of Industrial Product Development,
Production and Design, Jönköping, Sweden

Alexander.Vestin@ju.se

Abstract

In Sweden, wooden single-family houses have been prefabricated for a long time, instead of being built on-site. However, it was mentioned that in several firms, many working tasks just were brought from outside into a manufacturing hall, yet the tasks were not adjusted to utilize potential benefits that prefabrication offers. Production development was not prioritized and thus, the firms' productivity and efficiency were on a second-rate level, with profitability numbers following accordingly. In the past years, however, and especially related to the rapid development within the areas of digitalization and automation, several firms have been investing into different types of development. As the production of wooden single-family houses is very unstable in the past decade, yet, production costs per m² more than doubled since 2002 and the industry is characterized of a very high degree of competition, productivity is a key performance indicator (KPI) in this industry.

The aim of this study is to investigate in the productivity of Swedish firms producing wooden single-family houses in the past ten years. This is done by using the activity ratio Total Asset Turnover ratio, measuring a firm's operational efficiency from 2008 to 2017, i.e. the latest data available. For 47 firms, data from annual reports were collected and analyzed.

Data shows a productivity loss by 4.7%, aggregated for all firms in the industry. Further, the productivity for individual firms developed very different, varying from +141.7% to -68.4% and it can be concluded that a change in fixed assets affects productivity.

Key words: Wooden Single-Family Houses, Productivity, Activity Ratios, Efficiency

Introduction

The demand on the Swedish market for wooden single-family houses (WSFH) was unstable in the past years. Before the economic crisis, in 2007, 12 100 WSFH were built. By 2012, numbers decreased to 4 800 units but recovered again until 2017, when circa 12 500 WSFH were produced (TMF 2014, 2018). Concurrently, the firms had to adopt to these changes and many of them chose to lay off employees when the market went down (Schauerte and Lindblad 2015). Yet, when conditions improved and orders were taken, workers had to be hired again. This fluctuation of personnel is reflected in the firms' profitability (Lindblad et al. 2016, Schauerte et al. 2017). As the industry of interest is characterized by high competition (Schauerte et al. 2017), the individual firm's profitability plays a decisive role for its competitiveness (Besanko et al. 2017).

Profitability is related to operation efficiency, productivity and used for strategic purposes, when trying to outperform competitors (Singh and Kaur 2016). For some, productivity is the key to survival (Syverson 2011). Compared to other industries, the industry at hand is lagging behind concerning utilizing the possibilities that digitalization offers. That shortcoming might as well be one explanation for the disproportionate development of production costs per m², which increased from 25 100 SEK in 2008 to 34 062 SEK net in 2017. This equals 35.7 % and should be compared with the consumer price index that only increased by 7.2 % in the same period (SCB 2019a, 2019b). Firms in this industry e.g. still apply a relatively high degree of manual work to transfer data between different IT-systems. Some firms use Building Information Modelling, yet, operators in production often still use their technical procedure documentation in paper form. Even for production activities, suggestions have been made to improve efficiency in operations to increase productivity. These are e.g. related to stock utilization, material handling, bottleneck reduction, facilities planning and an increased level of automation (a.o. Svensson and Allhorn 2014, Schauerte et al. 2015, Andersson and Björk 2016, Andersson and Jönsson 2016, Popovic and Winroth 2016, Johansson et al. 2018). This indicates that the firms are not utilizing their assets in an efficient manner.

One and the same product can be produced by different means and varying usage of production factors (Lundmark 2018). A lower production level in terms of output does thus not necessarily imply a low level of productivity. The output needs to be regarded in relation to the input. This can be done by means of different ratios that are used as key performance indicators. In general, there are different (kinds of) ratios for different fields of interest, e.g. for liquidity, market trend, debt management etc. (Park 2016). Capturing a firm's operational efficiency and productivity, *activity ratios* can be used. These ratios describe how efficiently a firm is using its assets (Coulter 2010).

Related to the industry at hand and regarding the period 2008 to 2017, the aim of this study is to investigate the productivity of Swedish firms producing WSFHs, i.e. how efficient these firms

are using their assets to generate sales. For this aim, the activity ratio Total Asset Turnover is being used.

Materials & Methods

Total Asset Turnover (TAT) is an activity ratio that measures a firm's ability to use its total assets in generating sales (David and David, 2015), and is calculated according to Equation (1) (Park 2016).

$$TAT = \frac{\text{Turnover}}{\text{Total assets}} \quad (1)$$

It shows, how many times a firm's assets are turned-over during a year. In general, firms with a higher TAT have processes that are more efficient and are more productive. However, there are cases, where firms cannot directly be compared in that manner. Firms with a low amount of facilities, machinery or other fixed assets, tend to have a higher TAT, as current assets dominate their total assets. These used to be raw material and the like, and are turned-over relatively often. Conversely, firms with a high book value in fixed assets tend to show lower values in TAT, as these assets can represent a relatively large proportion of the total assets (Öberg 2012). By conducting rationalization activities in workflow, the TAT value can be increased (Gabler 1994). Here, upgraded machinery and IT-systems and processes may be of concern for the industry at hand.

Therefore, additional data was consulted for the analysis and values for the firms' fixed assets and aggregated turnover for the entire industry were used.

All data were gathered from a statistical online database, where annual reports from all registered firms in Sweden are available. To select the relevant firms, various threshold criteria were applied. To start with, the segment *trähus, tillverkning* (wooden houses, manufacturing) was chosen. Further, firms with *more than 10 employees* in at least one of the years between 2008 to 2017 were included. Third, relevant data for Equation (1) had to be available for that entire timeframe. Finally, it was checked that the firms *prefabricated* wooden single-family houses and not only produced wooden houses on-site. This was done in different ways, e.g. homepages, mail contact etc. This final list resulted in 47 firms.

The industry at hand is highly competitive, as described above. Even though the used annual reports are free available, their content and its analysis may be sensitive and could be used to gain competitive advantage over rivals. As many of the analyzed firms are taking part in projects together with the authors' universities, the names of the involved firms are not revealed in this study but kept anonymous.

Table 1 shows the TAT for the 47 chosen Swedish firms that prefabricate WSFHs for the period 2008 to 2017, where

***Proceedings of the 62nd International Convention of
Society of Wood Science and Technology
October 20-25, 2019 – Tenaya Lodge, Yosemite, California USA***

- Firm # is the respective firms number in this study,
- TAT₀₈ to TAT₁₇ is the Total Asset Turnover ratio from 2008 to 2017,
- $\bar{\text{TAT}}_{t=10}$ is the average Total Asset Turnover ratio for the studied 10-year period,
- $\bar{\text{TAT}}_t$ is the average Total Asset Turnover ratio for the respective year t,
- ΔTAT_{08-17} in % is the relative change in Total Asset Turnover ratio from 2008 to 2017.

Results and Discussion

**Proceedings of the 62nd International Convention of
Society of Wood Science and Technology
October 20-25, 2019 – Tenaya Lodge, Yosemite, California USA**

firm #	TAT ₀₈	TAT ₀₉	TAT ₁₀	TAT ₁₁	TAT ₁₂	TAT ₁₃	TAT ₁₄	TAT ₁₅	TAT ₁₆	TAT ₁₇	ØTAT _{t=10}	ΔTAT ₀₈₋₁₇ in %
1	1,7	1,3	1,8	2,0	1,8	1,7	2,1	2,2	2,1	2,3	1,9	31,6
2	2,8	2,0	2,1	3,3	2,8	2,4	2,7	2,6	2,4	2,3	2,5	-16,9
3	3,2	2,2	2,6	1,0	2,4	2,4	3,0	3,1	2,8	3,1	2,6	-3,0
4	3,7	2,7	3,5	4,0	3,7	3,9	5,1	3,7	3,9	2,3	3,6	-38,6
5	0,6	0,6	0,4	0,4	0,4	0,4	0,5	0,7	1,0	0,7	0,6	18,3
6	2,4	1,8	2,1	2,2	2,3	2,1	1,5	2,4	2,7	2,6	2,2	7,9
7	2,0	3,0	2,6	2,6	2,1	2,1	2,7	2,5	3,2	2,3	2,5	17,7
8	1,5	1,2	1,4	1,5	1,4	1,4	1,4	1,6	1,9	2,0	1,5	33,5
9	3,1	2,3	2,4	2,2	1,9	1,7	2,4	2,7	2,5	2,1	2,3	-32,9
10	4,6	3,0	4,8	4,4	4,6	3,4	3,5	3,9	5,2	7,0	4,5	53,8
11	2,1	2,5	2,0	2,0	2,4	1,9	2,1	1,8	1,6	5,0	2,3	132,7
12	2,1	1,6	1,4	1,9	1,9	1,8	1,8	1,7	2,4	2,1	1,9	1,0
13	1,1	1,0	1,2	1,0	1,0	0,9	0,9	0,8	1,0	1,0	1,0	-10,4
14	4,6	4,8	4,1	3,8	3,8	2,2	3,9	3,9	3,4	3,1	3,8	-33,8
15	1,7	1,5	1,5	2,2	2,7	3,7	3,0	2,7	4,0	4,2	2,7	141,7
16	1,3	1,1	1,0	1,0	1,0	0,8	0,6	0,8	1,1	0,8	0,9	-35,3
17	4,2	2,3	2,0	3,0	3,9	4,9	3,4	2,3	2,2	2,3	3,0	-45,5
18	0,4	0,9	0,7	0,5	0,3	0,4	0,5	0,5	0,7	0,7	0,6	65,7
19	2,2	2,5	1,2	2,1	1,5	1,7	1,7	2,6	2,9	3,3	2,2	49,2
20	2,5	2,3	1,4	2,0	1,7	1,4	1,5	1,8	2,0	2,6	1,9	4,9
21	3,0	3,7	3,6	3,8	3,3	4,6	3,0	3,7	3,4	3,7	3,6	23,9
22	2,2	2,5	2,1	2,1	2,5	2,3	1,3	1,7	2,2	1,8	2,1	-19,8
23	3,3	2,8	4,3	3,3	3,0	3,0	3,0	2,6	2,8	2,5	3,1	-22,6
24	3,7	3,9	3,3	3,2	2,8	1,9	2,7	2,4	1,5	1,8	2,7	-51,5
25	2,5	3,6	1,9	2,2	3,0	1,6	1,5	2,5	4,4	2,3	2,5	-7,2
26	1,9	1,6	1,2	1,1	1,3	1,7	1,9	2,8	2,8	2,4	1,9	25,0
27	5,1	3,7	3,5	3,9	3,6	4,8	4,8	4,4	3,9	4,4	4,2	-13,8
28	3,1	2,7	2,9	3,1	2,6	2,8	2,7	2,9	3,2	4,3	3,0	39,0
29	0,0	2,0	1,6	3,0	3,2	3,9	1,7	5,3	1,7	3,6	2,6	85,8
30	4,4	2,4	2,5	2,8	2,5	2,6	2,5	3,0	3,5	3,2	3,0	-27,8
31	2,9	3,0	1,6	2,4	1,6	2,1	2,8	2,4	2,1	1,8	2,3	-39,9
32	4,0	3,5	2,7	2,1	2,0	1,8	2,7	2,4	3,1	2,3	2,7	-42,0
33	2,6	2,6	2,7	2,9	2,9	2,9	3,3	2,4	2,2	2,5	2,7	-1,0
34	1,8	1,9	1,4	1,6	1,9	1,8	2,0	2,0	2,4	2,5	1,9	34,0
35	2,5	1,8	1,6	1,2	1,1	1,1	2,9	3,0	2,2	2,9	2,0	15,7
36	3,6	2,5	2,6	2,4	2,2	1,9	1,9	2,4	2,0	2,3	2,4	-35,5
37	2,8	1,2	1,0	0,7	1,0	0,7	0,8	1,6	2,0	1,7	1,3	-40,5
38	1,5	1,7	1,5	1,7	1,8	1,6	1,4	2,4	1,1	0,9	1,5	-39,1
39	3,8	1,7	1,5	1,8	1,5	2,7	2,2	2,3	2,4	3,0	2,3	-21,8
40	1,1	0,8	0,7	0,7	0,6	0,7	0,5	0,8	0,8	0,8	0,7	-28,9
41	5,2	4,9	3,9	5,9	3,6	2,2	1,8	1,3	1,0	1,6	3,1	-68,4
42	5,3	4,1	3,4	2,5	2,6	4,6	2,8	3,0	3,0	3,0	3,4	-43,6
43	2,6	2,2	2,0	3,4	4,3	4,2	3,3	2,4	2,3	2,8	2,9	6,9
44	0,6	0,5	0,5	0,4	0,4	0,4	0,4	0,6	0,6	0,4	0,5	-25,8
45	1,8	2,2	2,6	2,5	2,7	1,9	2,3	2,5	2,3	2,6	2,3	46,7
46	3,3	1,7	2,3	2,8	2,1	2,2	2,9	2,6	3,5	3,5	2,7	6,6
47	0,3	0,3	0,3	0,2	0,2	0,3	0,3	0,5	0,5	0,5	0,3	69,4
ØTAT _t	2,6	2,3	2,1	2,3	2,2	2,2	2,2	2,3	2,4	2,5	2,3	-4,7

Table 1: Total Asset Turnover (TAT) from 2008 to 2018 for 47 firms prefabricating WSFH in Sweden.

**Proceedings of the 62nd International Convention of
Society of Wood Science and Technology
October 20-25, 2019 – Tenaya Lodge, Yosemite, California USA**

Table 1 shows that the average TAT_t for the industry from 2008 to 2017 declined by 4.7%. The average TAT for that period is 2.3, varying from 2.1 at the lowest to 2.6 at a top value. Overall, it seems that the average values for the entire period are on a relatively constant level, regarded from year to year. Yet, the two mentioned upper and lower values appear within a relatively short period of three years. Looking at additional market data for these years, it appears that the total market volume decreased by ca 23% from 2008 to 2010. After a consolidation phase, the market volume increased again by ca 52% until 2017, compared to 2008. This is mirrored by the firms TATs, which, however, for the entire industry increased slower than they decreased before. This can be interpreted as if the firms adopted to the market development with a certain time gap, resulting in decreasing productivity numbers. In a similar manner, adopting to positive market changes might occur gradually, possibly with a quite distinct risk minimization, which leads to a relatively long time for productivity indicators to recover.

The above could be a point when looking at the aggregated industry numbers only. Nevertheless, different firms developed in different ways. Looking at the five firms with the highest TAT_{08} , i.e. #42, 41, 27, 14 and 10, only #27 and 10 remain in the top five in 2017. Regarding the column to the right in Table 1, differences in productivity from 2008 to 2017 are shown in %. It can be seen that differences vary from +141.7% to -68.4%. The four firms with the highest productivity in 2008 all lost ground until 2017 with numbers ranging from -68.4% to -13.8%. However, what actions are hiding behind these numbers? As mentioned above, the level of TAT can depend on the amount of book value for fixed assets and rationalization activities in workflow and other processes can affect as well. Table 2 shows the five firms with the highest TAT_{08} and the change in their TAT, fixed assets (FA) and turnover (TO) from 2008 to 2017.

firm #	ΔTAT_{08-17}	ΔFA_{08-17}	ΔTO_{08-17}
42	-43.6%	+26%	-4%
41	-68.4%	+377%	+504%
27	-13.8%	+160%	+193%
14	-33.8%	-80%	+58%
10	+53.8%	-25%	+11%

Table 2: Top five firms in Total Asset Turnover (TAT) from 2008 to 2018.

Firm #42 increased its fixed assets by 26%, yet, lost 4% in turnover, whilst the entire industry grew by 52%, see above. This, alongside with a 43.6% decline in productivity. An analysis solely based on this data would suggest that even though fixed assets increased, processes in e.g. marketing and sales were not focused on or at least not succeeded in.

Firm #41 invested a large amount in fixed assets (+377%) and gained a lot on market share (+504%); yet, productivity declined with the largest number in the entire industry, i.e. -68.4%. Even firm #27 invested in fixed assets and increased its turnover with remarkable numbers, but here as well a decline in productivity of -33.8% can be seen. Trying to analyze these two firms, it could be possible that both follow a corporate growth strategy. They invested a lot of money

into (a) market development, like e.g. marketing and sales, new customer segments, possibly product development etc., and (b) fixed assets, like e.g. larger facilities and upgraded machinery and IT-systems, yet, these are probably not fully applied and production processes are still to be rationalized and further developed, maybe towards the changed product.

Firm #14 in turn acted differently. Its growth between 2008 to 2017 lies almost parity with the industry's growth (58% vs. 52%), however, the firm's fixed assets did not develop accordingly but decreased by 80%. Depreciation and amortization might be a key factor here, but it seems very likely that the growth in sales could not be handled within the given technical and production preconditions and happened at the expense of productivity (-33.8%). Thus, further investments in the needed kind of fixed assets might be the current concern.

Firm #10 grew below industry average (11% vs. 52%), but is the fourth largest firm in the industry, based on turnover. It seems to handle the growth within the given boundaries of its facilities and processes. Even though fixed assets decrease with 25%, this might be in line with depreciations and amortizations. This firm actually has the highest TAT value for 2017, as well as the highest average value for TAT for the investigated period.

Summary and Conclusions

The aim of this study was to study the productivity from 2007 to 2010 of Swedish firms producing WSFHs. Data from the relevant firms' annual reports were gathered and the Total Asset Turnover ratio used, alongside with additional data on fixed assets and turnover in the industry. Results show that the average accumulated productivity from 2008 to 2017 decreased by 4.7%. Further, when firms adjusted their operations to the market situation, profitability decreased faster in the downturn phase than it increased when the market turned up again. The results show as well that the five firms with the highest productivity in 2008, show great differences in how and why the productivity value developed until 2017. The differences could, at least partly, be based on the handling of their fixed assets and other rationalization activities in workflow. Possibly, adopting upgraded machinery and IT-systems may play a role when fixed assets increased but productivity numbers lag behind, as they may not be fully in use yet.

The data in Table 1 and especially Table 2 supports the reasoning that a change in fixed assets affects productivity. Yet, firms can be different in structure, processes etc. and it might be downright disputable to compare all firms within a given industry, without consulting additional data that can explain the determining background factors. At least they have somehow to be considered in the analysis. In the current case, data on fixed assets was tried be used for that account. Nevertheless, it seems that the probability of residual information loss still exists to some extent.

References

Andersson A, Jönsson F (2016) Effektivisering av produktion på producerande företag [Increasing production efficiency in manufacturing companies]. Bachelor Thesis in Industrial Organisation and Economics, Department of Mechanical Engineering, Linnaeus University, Växjö, Sweden. In Swedish.

Andersson M, Björk S (2016) Effektivisering av industriell tillverkning [Increasing efficiency in industrialized production]. Bachelor Thesis in Industrial Organisation and Economics, Department of Mechanical Engineering, Linnaeus University, Växjö, Sweden. In Swedish.

Besanko D, Dranove D, Shanley M, Schaefer S (2017) Economics of Strategy. Hoboken, NJ: John Wiley & Sons, Inc.

Coulter M (2010) Strategic Management in Action. Upper Saddle River, New Jersey: Pearson education ltd.

David Fred R, David Forest R (2015) Strategic Management – Concepts and Cases. Essex: Pearson education ltd.

Gabler Wirtschaftslexikon (1994) [business and economics lexicon] Keyword: Kapitalumschlag. 13th edition, Wiesbaden: Gabler. In German.

Johansson J, Schauerte T, Lindblad F (2018) Balancing the production flow in prefabrication of wooden houses. Proceedings of the 72nd Forest Products Society International Convention.

Lindblad F, Schauerte T, Flinkman M (2016) Evaluating profitability of firms in the Swedish industry for wooden single-family houses. Proceedings of the 70th Forest products Society International Convention.

Lundmark R (2018) Produktion och marknad [Production and market]. Lund: Studentlitteratur. In Swedish.

Öberg C (2012) Bättre ekonomi [Better economy]. Lund: Studentlitteratur. In Swedish.

Park CS (2016) Contemporary engineering economics. Essex: Pearson education ltd.

Popovic, D. and Winroth, M. (2016). Industrial timber house building – levels of automation. Proceedings of the 33rd International Symposium on Automation and Robotics in Construction.

*Proceedings of the 62nd International Convention of
Society of Wood Science and Technology
October 20-25, 2019 – Tenaya Lodge, Yosemite, California USA*

SCB, Statistics Sweden (2019a) Total production price.

http://www.statistikdatabasen.scb.se/pxweb/en/ssd/START_BO_BO0201_BO0201C/PrisPerAreorSM02/table/tableViewLayout1/

SCB, Statistics Sweden (2019b) Inflation in Sweden.

<https://www.scb.se/en/finding-statistics/statistics-by-subject-area/prices-and-consumption/consumer-price-index/consumer-price-index-cpi/pong/tables-and-graphs/consumer-price-index-cpi/inflation-in-sweden/>

Schauerte T, Lindblad F (2015) Corporate economic distress in the wood construction industry: current state and trend after the economic crisis. *PRO LIGNO*, 11:4, pp. 389-396.

Schauerte T, Lindblad F, Flinkman M (2017) Critical success factors determining economic health of firms producing wooden single-family houses. *Arkitektur N*, ISSN 1504-7628 and conference papers for the 6th Forum Wood Building Nordic in Trondheim, pp. 73-84.

Schauerte T, Svensson V, Allhorn S (2015) Improving Production Efficiency to Increase the Capacity and Profitability of a Swedish Wooden Single-Family House Producer. *Proceedings of the 58th International Convention of Society of Wood Science and Technology*.

Singh RI, Kaur S (2016) Efficiency and Profitability of Public and Private Sector Banks in India: Data Envelope Analysis Approach. *The IUP Journal of Bank Management*, XV (1), pp. 50-68.

Svensson V, Allhorn S (2014) Kapacitetsökning på ett producerande företag [Increasing capacity in manufacturing industries]. Bachelor Thesis in Industrial Organisation and Economics, Department of Mechanical Engineering, Linnaeus University, Växjö, Sweden. In Swedish.

Syverson C (2011) What determines productivity? *Journal of Economic Literature*, 49:2, pp. 326-365.

TMF "Trähusbarometern" (wooden house barometer) (February 2014) Web:

<http://www.tmf.se/statistik/statistiska-publikationer/trahusbarometern/> .

TMF "TMF i siffror" (TMF in numbers) (2018) Web:

<https://www.tmf.se/siteassets/statistik/statistiska-publikationer/tmf-i-siffror/tmf-i-siffror-2-2018.pdf>

***Proceedings of the 62nd International Convention of
Society of Wood Science and Technology
October 20-25, 2019 – Tenaya Lodge, Yosemite, California USA***

Building the Future with Social Media

Mrs. Candra Burns, candra@talkingforests.com
Talking Forests, Germany

Abstract

Social media is a new frontier for most, but even those with experience can use some tips. This presentation will walk participants through the journey from not having any social media, to strategies to build your online presence, leverage social media to achieve goals in your life, explain advantages it gives you to have a voice in the forest industry, and help you navigate social media effectively. This hands-on workshop will cover Facebook, Twitter, LinkedIn, and Instagram.

Facebook is all-inclusive; every age group is using this platform. You can use Facebook to reach everyone, create groups for local use which would feed into the larger Facebook page communities at a regional level. Twitter is the place for quick news and you can use a few hashtags and tag people here to get their attention. LinkedIn is the best place to network with professionals in your industry and build your virtual resume that goes with you anywhere you go. Instagram is visually beautiful and the place where you can show off what you do in the woods. The best way to create content and build your organic following is to feature other people and create contests that give away swag.

October 24th

Wood Physics and Mechanics

14:00 – 17:00

Chair: Tetsuya Inagaki, Nagoya University, Japan

Sorption Hysteresis in Wood and Its Coupling to Swelling Investigated by Atomistic Modeling

Prof. Jan Carmeliet¹, cajan@ethz.ch

Mr. Mingyang Chen¹

Dr. Benoit Coasne²

Dr. Dominique Derome³

¹ETHZ, Switzerland

² Laboratoire Interdisciplinaire de Physique CNRS and University Grenoble Alpes, France

³Université de Sherbrooke, Canada

Abstract

Wood displays hysteresis in moisture sorption. In order to investigate its origin, we used atomistic simulations to study the hysteresis behavior of a similar soft nano-porous material, i.e. amorphous cellulose. A detailed analysis reveals that water molecules first adsorb at free sorption sites, i.e. hydroxyl sites, leading to a swelling of the material. The swelling is followed by a distancing of the polymer chains favoring the creation of new sorption sites, as demonstrated by an increase of cellulose-water and water-water hydrogen bonds. Upon desorption however, these newly exposed sorption sites remain favorably occupied by water molecules and the material remains longer in a swollen state at higher moisture content. The atomistic numerical investigation thus allows to identify the molecular mechanism responsible for hysteresis in sorption-induced swelling. The moisture content and swelling exhibit hysteresis upon ad- and desorption but not swelling versus moisture content, as seen also experimentally. In addition, the atomistic approach allows to see that different hydrogen bond networks are established: cellulose swells to form water-cellulose bonds upon adsorption but these bonds do not break upon desorption at the same chemical potential.

Considering the evidence that swelling plays a determining role in sorption hysteresis, we propose a hysteresis model based on elastic dependent domain theory, where the filling of a site depends not only on the relative humidity but also on the strain state of the sorption site. This model is able to adequately describe sorption hysteresis and sorption induced swelling for wood exposed to different moisture loading protocols.

Sorption, Swelling and Mechanical Behavior of Wood: A Multiscale Study

Dr. Dominique Derome¹, dominique.y.derome@gmail.com

Mr. Chi Zhang²

Mr. Mingyang Chen²

Dr. Benoit Coasne³

Prof. Jan Carmeliet²

¹Université de Sherbrooke, Canada

²ETHZ, Switzerland

³ Laboratoire Interdisciplinaire de Physique CNFS and University Grenoble Alpes, France

Abstract

Wood is a hierarchical material, where the configuration at different scales (lumber, growth ring, cellular and cell wall material) plays different roles in its behavior: adsorption/desorption, swelling/shrinkage and mechanical softening. Different modeling approaches are required at different scales and upscaling between models is required. Our approach allows us to study holistically this material hygromechanical behavior.

As the origin of swelling lies at the nanoporous material scale, where water molecules are adsorbed into the hydrophilic matrix in the cell walls and the induced fluid-solid interaction forces result in swelling of these cell walls, we study in-depth the coupled effects of water sorption on the hygric and mechanical properties of different polymeric components with atomistic modeling. Our aim is to understand all the ramifications of this intricate nanocomposite, and then we have the specific aim of upscaling the results to cellular and macroscopic scales. In order to study the behavior of S2 layer, we analyze the different configurations of cellulose microfibril aggregates and S2 matrix using Molecular Dynamics (MD). Atomistic simulations are used to mimic water adsorption and relate this hygromechanical behavior as observed from the breaking and reforming of hydrogen bonds in complex polymeric composites.

In a multiscale framework, we upscale the hygromechanical observations using a poromechanical constitutive model. Upscaling to cellular scale is informed through accurate geometrical description of the cellular structure using X-ray CT at different relative humidity, at different scales, namely sub-cellular, cellular and growth ring scales. The ensemble of results documents the co-occurrence of sorption and swelling. This methodology provides new insights in understanding wood behavior and its material properties. Such insights cannot be directly determined solely from experiments. This multiscale methodology is used to explore new pathways for material development and durability of wooden components.

EFFECT OF PYROLYSIS-OIL BASED MICROEMULSIONS ON MECHANICAL PROPERTIES OF SCOTS PINE

Antti Haapala^{1}, Vitaly Bulavtsev², Aitor Barbero-López³, Juhani Marttila⁴*

¹Associate Professor, School of Forest Sciences, University of Eastern Finland, Joensuu, FI-80101, Finland. *Corresponding author, *antti.haapala@uef.fi*

²Senior Researcher, School of Forest Sciences, University of Eastern Finland, Joensuu, FI-80101, Finland.
bulavtsevvv@yandex.ru

³Early Stage Researcher, School of Forest Sciences, University of Eastern Finland, Joensuu, FI-80101, Finland.
aitorb@uef.fi

³Early Stage Researcher, School of Forest Sciences, University of Eastern Finland, Joensuu, FI-80101, Finland.
juhani.marttila@uef.fi

ABSTRACT

A potential new method for enhancing the mechanical properties and durability of wood is to introduce chemicals in a form of microemulsions. Microemulsion is a micellar system of water, oil and an amphiphile that can make lipids disperse in water as miniscule droplets that can readily penetrate wood structure and achieve good penetration performance. Once dried inside the wood they coalesce and form stable structures that should provide beneficial changes for wood properties. In this study we demonstrate novel approach to impregnate the sapwood of Scots pine (*Pinus sylvestris*) with pyrolysis-oil based microemulsions and present the performance of these systems regarding retention, leaching, fungal decay and mechanical strength of wood.

Key words: Impregnation, Leaching, Polymerization, Modulus of Elasticity, Modulus of Rupture

1 INTRODUCTION

To avoid decay, many kinds of wood preservatives have been tried and many well-performing compounds have been utilized but some of them have also become substituted during the

years due to their toxic and/or carcinogenic nature, as chromated-copper-arsenate (CCA) (Mohajerani et al. 2018). Further limitations are expected because of increasing environmental awareness and the ongoing trend of chemicals legislation.

Bio-based chemicals have been considered as green alternatives for wood preservation and several extractives are known to play a role in wood decay prevention due to their antifungal and antioxidant activities, such as bark, heartwood and cone tannins (Anttila et al. 2013), stilbenes (Lu et al. 2016) or cinnamates (Barbero-López et al. 2018). Extraction of antifungals can be achieved using different methods but many means to extract and purify a specific compound are too expensive for industrial scale wood preservation. Among the chemical processes that can convert large volumes of solid biomass to liquids are different types of pyrolysis that result in chemical mixtures rich in phenolics and organic compounds that are able to inhibit wood-decaying fungi (Temiz et al. 2013; Barbero-López et al. 2019). The aqueous and oily phases of pyrolytic liquids have components that prevent decay in different ways. Organic acids have been identified as fungal inhibitors against wood-decaying fungi (Bahmani et al. 2016). The oily substances have lipids that can form miniscule emulsion droplets, but also wide array of phenolics shown to prevent decay (Miettinen et al. 2015; Venäläinen et al. 2004).

2 AIM AND METHODOLOGY

The aim of this study is to investigate the potential and performance of pyrolytic liquids in wood decay and mechanical properties utilizing them for the first time in the form of microemulsions. Microemulsion is a micellar system of water, oil and an amphiphile that can make lipids disperse in water whereas they would naturally form a separate continuous phase (Fig. 1.)

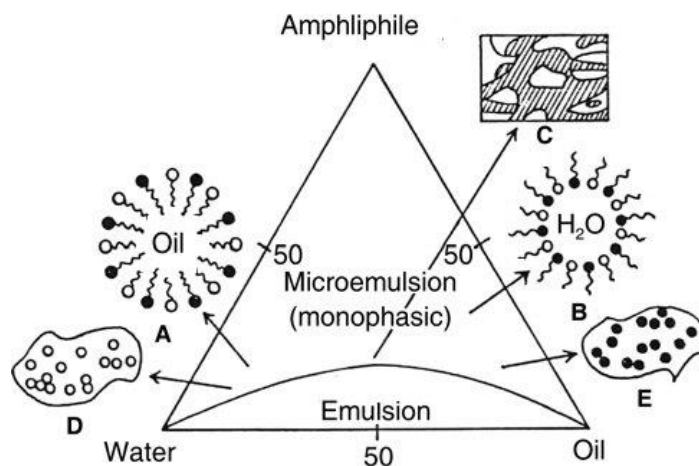


Fig 1. Phase diagram showing probable internal structures: (A) oil in water microemulsion; (B) water in oil microemulsion; (C) continuous (macro)emulsion; (D) isolated and aggregated oil in water dispersion; and (E) isolated and aggregated water in oil dispersion (modified from Paul and Moulik 1997).

Microemulsions are generally considered as monodispersed spherical droplets (10–200 nm in diameter) of water in oil or oil in water depending on the nature of surfactants and the composition of the microemulsion (shape can vary). The outcome is a single-phase, optically isotropic and thermodynamically stable liquid solution referred to as emulsion, but with immensely small droplet size for lipid particles stabilized by surfactant(s).

We pose a hypothesis that the lipids in pyrolytic liquids can interact with surfactants to form emulsions of miniscule drop size that would benefit the chemical penetration and yield in pressure impregnation processing of wood. They should coalesce and form stable structures that should provide beneficial changes for wood properties. In microemulsion, lipids and fatty acids act as a natural biocide and water repellent, while organic acids and phenolics provide additional decay resistance.

Scots pine (*Pinus sylvestris*) sapwood pieces of 5×40×10 mm³ (tangential × longitudinal × radial) bought from Kerimäki sawmill, Finland, were used as wood substrate following 32 kGy gamma irradiation before decay trial. Microemulsions were made from pyrolytic liquid from pine using water, sodium dodecyl sulphate, and aliphatic alcohol (ethanol and 1-pentanol), and quantified using cryo-EM imaging at Vienna BioCenter, Austria. The performance of these microemulsion systems are referenced with linseed oil emulsions and copper-based wood preservative, and evaluated comparing:

- retention and oil leaching from wood according to EN 84 (*Wood preservatives – Accelerated ageing of treated wood prior to biological testing – Leaching procedure*)
- microemulsion treated wood decay according to EN 113 (*Wood preservatives – Test method for determining the protective effectiveness against wood destroying basidiomycetes - Determination of the toxic values*) using *Coniophora puteana*
- development of mechanical strength of wood; ultimate strength (ISO 13061-3 *Physical and mechanical properties of wood – Test methods for small clear wood specimens – Part 3: Determination of ultimate strength in static bending*) and modulus of elasticity (ISO 13061-4 *Part 4: Determination of modulus of elasticity in static bending*).

3 REFERENCES

Anttila AK, Pirttilä AM, Häggman H, Harju A, Venäläinen M, Haapala A, Holmbom B, Julkunen-Tiitto R (2013) Condensed conifer tannins as antifungal agents in liquid culture. *Holzforschung* 67: 825–832.

Bahmani M, Schmidt O, Fathi L, Frühwald A (2016) Environment-friendly short-term protection of palm wood against mould and rot fungi. *Wood Mater. Sci. Eng.* 11: 239–247.

**Proceedings of the 62nd International Convention of
Society of Wood Science and Technology
October 20-25, 2019 – Tenaya Lodge, Yosemite, California USA**

Barbero-López A, Chibily S, Tomppo L, Salami A, Ancin-Murguzur FJ, Venäläinen M, Lappalainen R, Haapala A (2019) Pyrolysis distillates from tree bark and fibre hemp against wood-decaying fungi. *Ind. Crop. Prod.* 129: 604–610.

Barbero-López A, Ochoa-Retamero A, López-Gómez Y, Vilppo T, Venäläinen M, Lavola A, Julkunen-Tiitto R, Haapala A (2018) Activity of spent coffee ground cinnamates against wood-decaying Fungi *in vitro*. *BioResources* 13: 6555–6564.

EN 84:1997 “Wood preservatives – Accelerated ageing of treated wood prior to biological testing – Leaching procedure”. European Committee for Standardization, Brussels, BE, 1997.

EN 113:1996 “Wood preservatives – Test method for determining the protective effectiveness against wood destroying basidiomycetes - Determination of the toxic values”. European Committee for Standardization, Brussels, BE, 1996.

ISO 13061-3:2014 “Physical and mechanical properties of wood - Test methods for small clear wood specimens - Part 3: Determination of ultimate strength in static bending”. International Organization for Standardization, Geneva, Switzerland.

ISO 13061-4:2014 “Physical and mechanical properties of wood - Test methods for small clear wood specimens - Part 4: Determination of modulus of elasticity in static bending”. International Organization for Standardization, Geneva, Switzerland.

Lu J, Venäläinen M, Julkunen-Tiitto R, Harju AM (2016) Stilbene impregnation retards brown-rot decay of Scots pine sapwood. *Holzforschung* 70: 261–266.

Miettinen I, Mäkinen M, Vilppo T, Jänis J (2015) Compositional Characterization of Phase-Separated Pine Wood Slow Pyrolysis Oil by Negative-Ion Electrospray Ionization Fourier Transform Ion Cyclotron Resonance Mass Spectrometry. *Energy Fuels* 29(3): 1758–1765.

Mohajerani A, Vajna J, Ellcock R (2018) Chromated copper arsenate timber: a review of products, leachate studies and recycling. *J. Clean. Prod.* 179: 292–307.

Paul BK, Moulik SP (1997) Microemulsions: an overview. *Journal of Dispersion Science and Technology* 18(4): 301–367.

Temiz A, Akbas S, Panov D, Terziev N, Alma MH, Parlak S, Kose G (2013) Chemical composition and efficiency of bio-oil obtained from giant cane (*Arundo donax* L.) as a wood preservative. *BioResources* 8: 2084–2098.

*Proceedings of the 62nd International Convention of
Society of Wood Science and Technology
October 20-25, 2019 – Tenaya Lodge, Yosemite, California USA*

Venäläinen M, Harju AM, Saranpää P, Kainulainen P, Tiitta M, Velling P (2004) The concentration of phenolics in brown-rot decay resistant and susceptible Scots pine heartwood. *Wood Sci. Tech.* 38(2): 109–118.

Thermal modification influences on permeability and sorption properties of wooden shingles

Authors: Dominik Hess *

Department of Wood Science and Technology, Faculty of Forestry and Wood Technology, Mendel University in Brno, Zemědělská 3, 613 00 Brno, Czech Republic; office phone: +420545134550; e-mail: hessdominikcloud.com

Abstract

The present study aims to analyze the influence of thermal modification (TM) on permeability and sorption properties of wood shingle manufactured in two different ways. Wood-water interaction has always been one of the main issues when using wood in the construction industry. Quality of wooden shingles is influenced by the manufacturing process — hand-split and sawn. The specimens for experiment were made of fir wood (*Abies alba*). Each shingle's specimen was cut and sorted into four groups (control, thermally modified at 160, 180, and 200°C). Thermal modification (TM) at three different temperatures was applied in a laboratory chamber using atmospheric pressure and super-heated steam. The degree of modification was determined by mass loss. The first part of the measurements was focused on water absorption in transverse direction for two drying-soaking cycles. Specimens were oven-dried and then immersed in water, soaked and weighted at certain intervals (2, 4, 6, 8, 10, 20, 40, and 72 h). Those specimens were then oven-dried again and soaking cycle was repeated. The second part of the research was to determine the equilibrium moisture content (EMC) of all groups. Specimens were placed in conditioning room (99% RH and 20°C) for 7 weeks and their equilibrium moisture was detected. The mass loss of hand-split and sawn shingles was not as significant as expected. An average mass loss after TM of 200°C and 2 hours was between 1.2 - 1.8%. The mass loss depends on the density, but also on the nature of wood species and other factors of the thermal modification process (i.e. time, temperature, type of wood are the most significant). Specimens with sawn surface showed less water absorption than hand-split one. The higher the level of thermal modification, the bigger the difference in water absorption, and thus the moisture content of a hand-split and sawn wood shingle surface. This was valid for up to 10h intervals of immersion. The reference specimen showed 1-2% difference in hand-split and sawn specimens, whereas for TM at 200°C the difference was 4-5%. During the second soaking cycle, the thermal modification had a negative effect on water absorption. Wood moisture and water absorption increased in all sample groups. While the average moisture content of the hand-split control samples increased from 20% to 21% after 10 hours, the TM samples increased the moisture content from 18% to 26%. The increase in moisture after the second soaking cycle could be due to the release of degraded substances formed by the thermal modification, which created new sites for binding more water molecules. The equilibrium moisture content was continuously measured for 7 weeks. During the first 3 weeks, surprisingly, EMC was lower in sawn samples in comparison with hand-split once. After 4 weeks, samples with hand-split surface showed lower EMC as expected. The hand-split and sawn wood shingle surface absorbs water and moisture differently. However, there was no significant difference between those two methods of manufacturing shingles. This result can be affected by the fact that the surface characterization of our specimens wasn't equalized.

Key words: wooden shingle; thermal modification; hand-split; sawn; water absorption; soaking; equilibrium moisture content

Rayleigh Mode Excitation at the Half-space Boundary in Wood using Embedded Elastic Waveguides

Yishi Lee¹ – Mohammad Mahoor² – Wayne Hall³

¹ Graduate Researcher, University of Denver, Denver, Colorado, USA
yishi.lee@du.edu

² Professor, University of Denver, Denver, Colorado, USA
Mohammad.Mahoor@du.edu

³ President, Utility Asset Management Inc., Denver, Colorado, USA
wayne.hall@utilityassetmanager.com

ABSTRACT

Due to the aging wooden utility pole infrastructure in the United States, it demands a more rigorous assessment program using an ultrasonic-based non-destructive evaluation (NDE) method. This paper focuses using novel small embedded elastic waveguides to excite and receive the so-call Rayleigh surface waves at the half-space boundary in wood in the plane geometry. The results of the proposed technique can be transferred to other NDE applications to enhance the current ultrasonic inspection capability. Using numerical and empirical approaches, the results provide strong evidence of Rayleigh surface wave propagation in wood. Through a brief discussion, the waveform of the resulted surface wave will be analyzed. This study employs (Riegert, 2006) the latest NDE device UB1000 that is jointly developed by the University of Denver and Utility Asset Management Inc. This work hopes to burgeon the future work for improving the current non-destructive evaluation technique for wooden pole structural assessments.

Key words: Elastodynamics, Ultrasonic waveguide, Rayleigh wave mode, non-destructive evaluation.

INTRODUCTION

The United States deploys approximately 100 million poles that support the power and communication infrastructures (Morrell, 2013). That demands effective and rapid inspection techniques for evaluating and monitoring their structural integrity. Non-destructive evaluation (NDE) using ultrasonic wave has been a mature technology in a wide range of industrial and academic sectors for assessing structural conditions (Riegert, 2006). The same ultrasonic excitation technique, using contact-based transducers for example, cannot be used for inspecting the wooden poles mainly due to the unpredictable surface conditions as illustrated in Figure 1. Hence, the application of contact-based transducers could lead to erroneous waveform measurements. An alternative approach is to perform a small insertion of roughly 2 mm by 2 mm by 16 mm with a waveguide to excite different wave modes in the interior of the specimen. This technique provides two immediate advantages: independence from the surface condition, and to provide structural support for mounting any NDE devices without a manual application. Despite a wide adaptation of this technique, the wave mechanics of this method has not been fully studied.

For a wooden utility pole, most of the mechanical load is concentrated at the outer shell of the cross-sectional area at the ground line region (Lovelace, 2005), approximately few inches above the ground. The mechanical property in this region plays a vital role in sustaining structural integrity. The study of Rayleigh wave propagating in this region can help infer important mechanical properties (Viktorov I. A., 1967). The methods of Rayleigh wave excitation were dated back to the 1940s by C. Minton (Minton, 1954). Since then, various techniques introduced by (Lynnworth, 1964), (Sokolinskii, 1958) and (Viktorov I. A., 1962) were developed and employed in the field of NDE (Thompson, 2012) and (Kim, 2014). The Rayleigh wave



Figure 1

propagation in a wooden utility pole has yet to be known.

Based on the academic and practical interests, this study focuses on the Rayleigh mode excitation in two-dimensional space at the flat half-space boundary using the embedded waveguide method. In order to demonstrate the excitation mechanism, a numerical approach

using the finite-element method (FEA) will be employed and the results will be analyzed. Using a jointly developed UB1000 NDT device for wooden utility pole inspections, digitized waveforms will also be presented. The numerical and empirical finding will be compared to evaluate the Rayleigh mode excitation and reception using the embedded waveguide technique.

MATERIALS & METHODS

Problem statement

Figure 2 illustrates an embedded waveguide problem. A cylindrical waveguide is inserted into a wooden medium. The origin of the inertial reference frame xz is placed at the corner of the side aperture of the waveguide the half-space boundary. Transient load generated by an ultrasonic transducer is applied at the load application interface of the waveguide. The goal is to

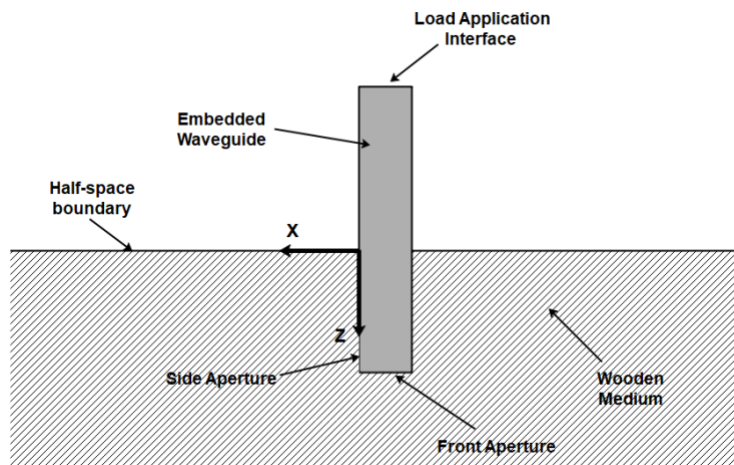


Figure 2

demonstrate the propagation of Rayleigh mode using the described method.

Assumptions and boundary conditions.

As a classical elastodynamic problem, it requires to solve the wave equations. As recalled, the displacement vector \mathbf{u} are decomposed into the longitudinal scalar ϕ and transverse vector potential fields Ψ using the Helmholtz decomposition:

$$\begin{aligned}\nabla^2 \phi + k_l^2 \phi &= 0; \\ \nabla^2 \Psi + k_t^2 \Psi &= 0,\end{aligned}$$

where k_l and k_t are the wave numbers associated with the longitudinal and transverse modes. The resolution to the elliptic wave equations demands the solution to comply with the boundary conditions described as followed:

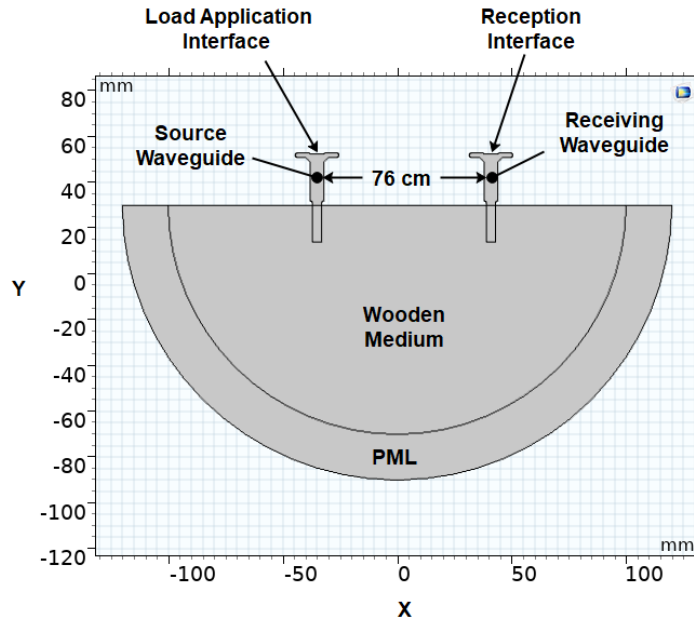


Figure 3

1. The ultrasonic transducer produces transient one-dimensional longitudinal traveling wave along the waveguide body (z-direction), expressed as

$$\phi_w = W = W_0(t)e^{i(k_0z - \omega t)} \quad x = 0, z \in [0, L], \quad (1)$$

where k_0 is the wave number of the wave travelling within the waveguide, and $W_0(t)$ denotes the displacement with time dependency in the z direction. For wave envelop, this can be a Gaussian modulated amplitude. Finally, L denotes the depth of insertion.

2. Continuity condition applies at the solid-solid boundary at $x = 0$ between the waveguide and the propagating medium. That is, $\phi_m = \phi_w$ and $\frac{\partial \phi_m}{\partial x} \Big|_{x=0} = \frac{\partial \phi_w}{\partial x} \Big|_{x=0}$ at $x = 0$; $\forall t$. The subscript m denotes the wooden medium and w denotes the waveguide medium.
3. Only the longitudinal wave mode is permissible. Mode conversion only occurs when the incident wavefront is parallel to the load application interface.
4. Neglect energy absorption in the body of the waveguide.
5. Traction-free boundary condition at the half-space boundary ($z = 0$). That is, $\sigma_{zz} = 0$ and $\sigma_{xz} = 0$. We exploit the fact that the atmospheric pressure is at least many orders of magnitude smaller than the internal stress of the propagating medium.
6. Isotropic medium is assumed.

Numerical Method

To discretize the computational domain illustrated in Figure 2, finite-element simulation model using COMSOL Multiphysics is employed to study the excitation mechanism. Figure 3 shows a sinusoidal transient load with Gaussian modulated amplitude is imposed at the load application interface. The perfectly matched layer (PML) is placed around the computational domain to eliminate interference from the reflection without constructing a large computational domain. Transient load is imposed on the load application interface of the source waveguide and the received stress is measured at the reception interface of the receiving waveguide. Both waveguides are made of aluminum and placed about 76 cm or 2 ½ feet apart. The propagating medium mimics the Douglas-firs species with the averaged mechanical properties obtained from (Ross, 2010).

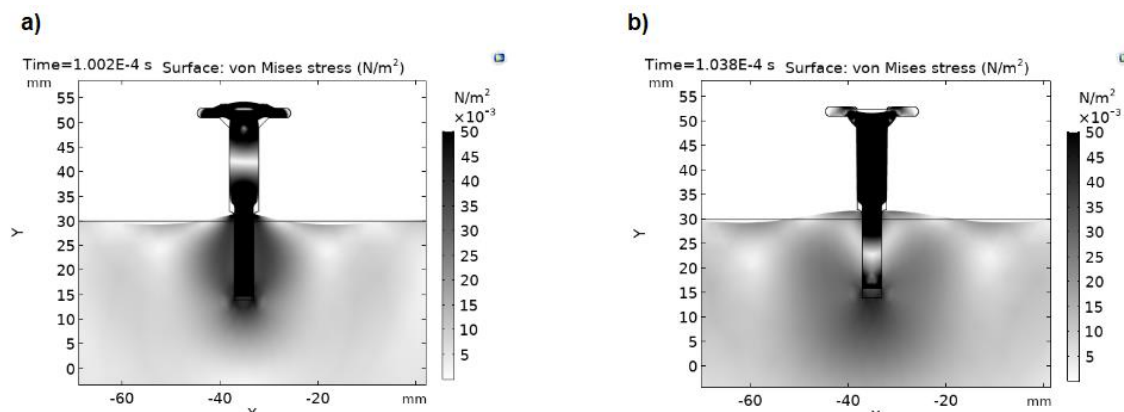


Figure 4

The result of the time domain Von Mises Stress is illustrated in Figure 4a and Figure 4b. At $t = 102 \mu\text{s}$, the source waveguide emitting longitudinal wave which excites ripples on either side of the waveguide at the half-space boundary ($x=0$) due to the imposed traction free boundary condition. By comparing the embedded side and the front apertures, energy emission appears to be stronger on the side aperture due to a large contact area. At $t = 104 \mu\text{s}$, as the sinusoidal

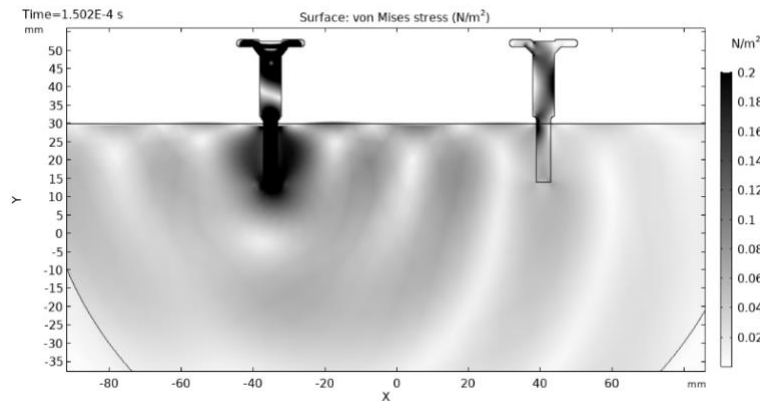


Figure 5

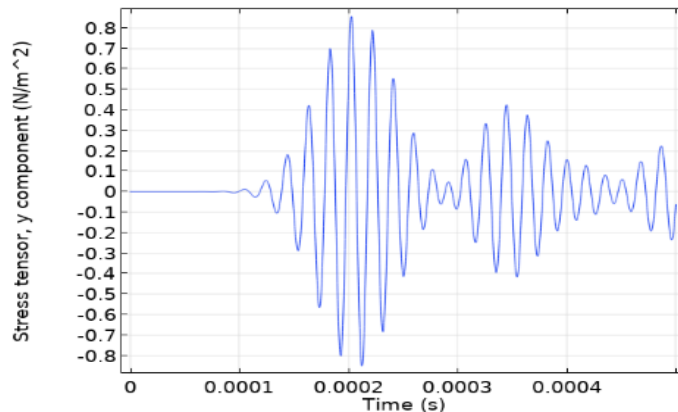


Figure 6

waveform propagating along the waveguide, the continuity condition demands the transmitted waveform to mirror the phase speed of longitudinal wave propagating along the waveguide. Simultaneously, the wave also propagates symmetrically outward in the x directions. The propagation in both x and z directions creates ‘bubbles’ about the source vividly shown in the figure. This is a classical response of a Rayleigh wave propagation along the half-space boundary. In Figure 5, traveling Rayleigh wave first reaches the side aperture of the receiving waveguide that is closest to the source creating asymmetrical wave mode propagating upward along the waveguide. At the reception interface, the time domain stress in the y-direction is depicted in Figure 6. The first wave envelop occurs between 100 to 280 μs , the time of the occurrence corresponds to the wavefront reaching the side aperture of the receiving waveguide as depicted in Figure 5. The shape of the amplitude suggests that it is Gaussian modulated similar to the imposed BC. Due to dissimilar material between the wooden medium and the aluminum waveguide, some of the energy are reflected between the two waveguides generating subsequent wave envelops as seen in Figure 6.

Empirical Method

An inserted waveguide (Figure 7c) was designed to resonate in the longitudinal direction in order to produce the highest displacement amplitude at the pre-determined frequency of the transducer. In order to transmit and receive the ultrasonic signal, a device jointly developed by the University of Denver and the Utility Asset Management Inc. called UB1000 (Figure 7b) was used. Each probe equips with a high-power ultrasonic transducer. An onboard printed circuited assembly (PCA) was designed to excite the resonance mode of the ultrasonic transducer by transmitting a sequence of modulated energy at the resonant frequency. Through a set of passive filters and amplifiers, the conditioned signals are transmitted to a high throughput analog-to-digital converter (ADC). A developed Android-based commanding app (Figure 7c) is to receive conditioned ultrasonic signal and command the units using the Bluetooth protocol.

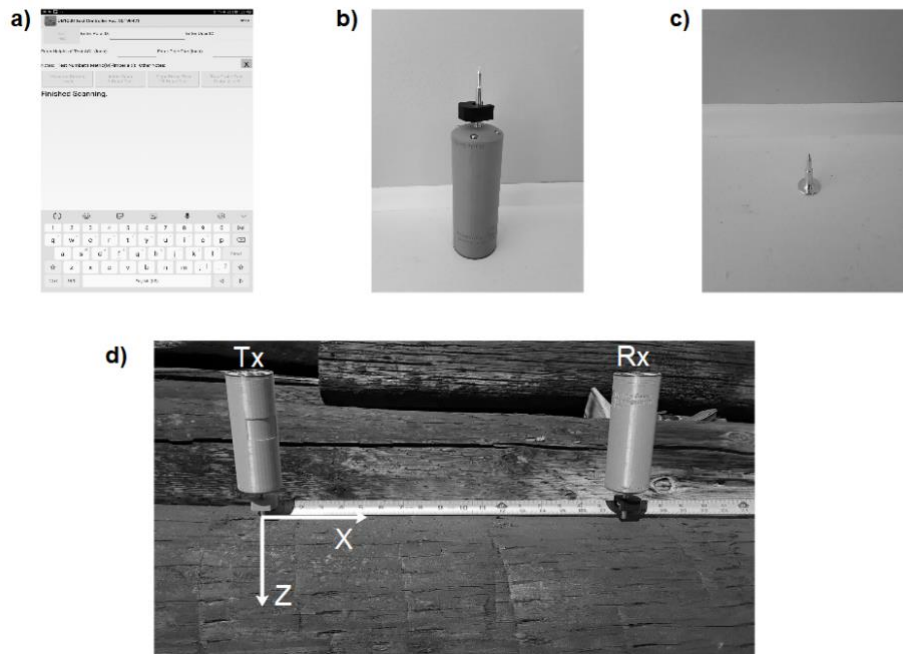


Figure 7

In this study, a brand-new pre-treated Douglas-firs utility pole laid in a horizontal position was used for this experiment (see Figure 7d). The portion facing upward is used to mimic the half-space boundary illustrated in Figure 2. A source waveguide is inserted at a fixed location denoted as Tx. Receiving waveguide denoted as Rx is placed at a distance about 76 cm away from the transmitting location. Figure 8 depicts the conditioned waveform.

RESULTS AND DISCUSSION

In this section, we will compare the waveforms generated by the numerical and empirical results. Figure 8 is the conditioned Analog-to-digital (ADC) data obtained by the Rx UB1000 device. The first wave envelope shows an apparent symmetry that correlates with a Gaussian modulated amplitude. Qualitatively speaking, the empirical waveform agrees with the numerical prediction suggesting a Gaussian amplitude modulated waveform. The arrival time of flight (TOF) is approximately $280 \mu\text{s}$. In order to verify the identity, as we recall, the Rayleigh wave is a transverse wave. Its phase speed can be estimated by calculating the corresponding transverse wave propagating in the same direction. Transverse wave speed is defined as $c_T = \sqrt{\mu/\rho}$, where μ is the shear modulus, and ρ is the density of the material. Based on the wood species, the values can be obtained from (Ross, 2010). The calculating wave speed is about 500 us which is significantly higher than the measured TOF.

SUMMARY AND CONCLUSIONS

This study compares the numerical results generated using the finite-element method to simulate the excitation of Rayleigh mode with the empirical results using UB1000 system. A qualitative agreement of the Gaussian modulated amplitude is established, between the two

approaches, suggesting the possibility of the embedded waveguide excitation of the Rayleigh mode. The empirical result suggests the measured TOF be significantly faster than the theoretical estimation of the transverse wave speed. The result shows that the excited Rayleigh wave mode using this technique might be different from the classical one. An analytical deviation might be beneficial to obtain more valuable insight into the propagational characteristics of using the embedded waveguide excitation method.

ACKNOWLEDGMENTS

This work was sponsored by the National Science Foundation (NSF) RoSe-Hub Center for and the Utility Asset Management Inc. (UAM). The authors are grateful to Mr. Wayne Hall for the funding, supplying industrial equipment and industrial cooperation.

REFERENCES

- Achenbach, J. D. (1967). Dynamic interaction of a layer and a half-space. *Journal of the Engineering Mechanics Division*, 93(5), 27*42.
- Kim, G. I. (2014). Air-coupled detection of nonlinear Rayleigh surface waves in concrete— Application to microcracking detection. *Ndt & E International*, 64-70.
- Lovelace, W. R. (2005). *The wood pole 2005: Design considerations, service benefits, and economic reward*. Hi-Line Engineering, LLCm Tech. Rep.
- Lynnworth, L. (1964). Shear wave robes and applications. *IEEE trans., Sonics and ultrasonics*.
- Minton, C. (1954). Inspection of metals with ultrasonic surface waves. *Nondestructive Testing*, 12(4), 13-16.
- Morrell, J. J. (2013). *Estimated service life of wood poles. Technical Bulletin, North American Wood Pole Council*. Retrieved April 5, 2013, from http://www.woodpoles.org/documents/TechBulletin_EstimatedServiceLifeofWoodPole_12-08.pdf
- Rayleigh, L. (1885). On wave propagated along the plane surfaces of an elastic solid. *London Math Society*, 17, pp. 4-11. London.
- Riegert, G. e. (2006). Modern methods of NDT for inspection of aerospace structures. *ECNDT*.
- Ross, R. J. (2010). *Wood handbook: wood as an engineering material*. USDA Forest Service, , Forest Products Laboratory, . General Technical Report FPL-GTR-190.
- Sokolinskii, A. G. (1958). Technique for the Excitation and Reception of Surface Waves. . *Author Certificate*.
- Thompson, D. &. (2012). *Review of progress in quantitative nondestructive evaluation*. Springer Science & Business Media.
- Viktorov, I. A. (1962). Investigation of methods for exciting Rayleigh waves. *Soviet Physics-Acoustics*.
- Viktorov, I. A. (1967). *Rayleigh and Lamb Waves*. Moscow: Springer Science + Business Media, LLC.

The Mechanics of Engineered Wood Flooring

Joseph R. Loferski, Ph.D.

Department of Sustainable Biomaterials

Virginia Tech

Blacksburg, Virginia USA

Email: jloferski@vt.edu

This paper addresses the performance and mechanics of engineered wood flooring used in residences.

The wood flooring industry is a multi-billion dollar per year activity. In 2015 the engineered and solid flooring market in the USA was \$2.2 billion in sales and 74 million square meters (800 million square feet) representing 10 % of the total flooring market. Laminate flooring sales approached \$1.2 billion in sales with more than 19 million square meters (200 million square feet).

Traditionally, wood flooring was made from solid wood strips with widths between 57 mm to 127 mm wide (2-¼ inch to 5 inch). The edges had tongues and grooves milled into them and the strips were fastened to the subfloor with nails or staples. Then, the flooring was sanded and finished after installation. Today many advances in technology have led to developments in engineered wood flooring and laminate flooring.

Engineered flooring is made as a glued, laminated composite with a high quality veneer as a wear layer (top surface) that is glued to the core. The core maybe plywood or solid wood strips oriented with the grain direction at 90 degrees to the top layer. The bottom layer may be a “balancing layer” which is a veneer of the same (or similar) species as the top layer to help keep the floorboard flat when subjected to moisture content (MC) changes. In some cases the flooring may lack a balancing layer. Laminate flooring is made from high-density fiberboard with wood grain pattern overlays and scratch resistant wear layers. Traditional tongue and grooves have been replaced by patented glue-less edge connections to fasten the boards together. Floating floors have been developed to replace nailed down flooring.

With advances in manufacturing technology engineered flooring is often made in widths of 200 mm, 250 mm, and even up to 300 mm (8 inches, 10 inches to 12 inches). These wide boards can be problematic when subjected to MC cycling as found in typical residences in which the relative humidity can fluctuate between 25% to 60+% annually. Because of the cross laminated construction of engineered wood flooring the various layers are subjected to differential shrinking and swelling and internal stresses that can cause a variety of problems including delamination of the wear layer from the core or even delamination of the core itself. Other potential problems include checks and splits in the wear layer, excessive cup or crown, warp, and gaps between boards.

This paper presents an approach to understanding the performance of engineered flooring. The concept of balanced construction using the theory of orthotropic mechanics for layered systems

***Proceedings of the 62nd International Convention of
Society of Wood Science and Technology
October 20-25, 2019 – Tenaya Lodge, Yosemite, California USA***

is developed for predicting dimensional stability caused by MC changes. Tests for measuring the performance of engineered flooring are presented including dimensional stability, cup/crown, warp and flatness, and delamination potential.

Key words: Engineered wood flooring, laminate flooring, orthotropic mechanics, delamination, dimensional stability, warp, moisture content cycling

References

1. Bodig J.B. and Jayne B.A.1982*Mechanics of Wood and Wood Composites.* Van Nostrand Reinhold Co., NY. New York. pp712.
2. Suchsland O. 2004.*The Swelling and Shrinking of Wood: A Practical Primer.* The Forest Products Society. Madison WI. pp 189

“Water in wood – the gel-theory revised”

Martin Nopens* (corresponding author)
Universität Hamburg
Faculty of Mathematics, Informatics and Natural Sciences
Department Biology
Institute of Wood Science, Wood Physics
Leuschnerstr. 91 c, 21031 Hamburg, Germany
Email: martin.nopens@uni-hamburg.de

Prof. Dr. Michael Fröba
Universität Hamburg
Faculty of Mathematics, Informatics and Natural Sciences
Department Chemistry
Institute of Inorganic and Applied Chemistry
Martin-Luther-King-Platz 6, 20146 Hamburg, Germany
Email: froeba@chemie.uni-hamburg.de

Prof. Dr. Bodo Saake
Universität Hamburg
Faculty of Mathematics, Informatics and Natural Sciences
Department Biology
Institute of Wood Science, Wood Chemistry
Leuschnerstr. 91 b, 21031 Hamburg, Germany
Email: bodo.saake@uni-hamburg.de

Dr. Dr. h.c. Uwe Schmitt
Thünen Institute
Institute of Wood Research
Leuschnerstraße 91, 21031 Hamburg, Germany
Email: uwe.schmitt@thuenen.de

Prof. Dr. Andreas Krause
Universität Hamburg
Faculty of Mathematics, Informatics and Natural Sciences
Department Biology
Institute of Wood Science, Wood Physics
Leuschnerstr. 91 c, 21031 Hamburg, Germany

Email: andreas.krause@uni-hamburg.de

Wood-water-relation, cell wall, surface area, porosity, sorption enthalpy, swelling gel, absorption
The interaction between water and wood influences the structure and different material properties. Although it was studied over decades, the existing wood-water-theories lack by describing the phenomena completely. A revised view in this field could be to assume that wood components act like a swelling gel. This approach is supported by a critical view on the existing literature and a new composition of different research topics as well as own research data of porosity, surface area, sorption enthalpy and others.

The entrance of water into the dry wood cell wall leads to a linear swelling within the hygroscopic region. Length and mass change occur simultaneously while sorption takes place. A change of the cell wall dimensions is in contrast to an adsorption theory where molecules are being adsorbed from a gas phase onto a stable surface. The water forms the spaces, which were not filled with another gas before. Therefore the mechanism could be explained by gaseous water molecules condensing on the outer surface of cell wall and then transported in the liquid state into the cell wall matrix, which leads to a swelling. This mechanism is the characteristic of a gel. Therefore not adsorption of gaseous water onto the inner surface of the cell wall is the underlying physical process. This process can be understood as absorption coming from diffusion within a liquid or an osmotic transport process

The cell wall is shown to be free of mesopores and macropores below fiber saturation. Therefore the gel-approach would explain why no pores can be measured within the bulk cell wall material. When wood is dissolved by water the resulting mixture contains no spaces which are large enough to form water clusters that can freeze.

This would support that the polarity and the amount of sorption sites is not the only basis for water sorption in wood. When wood is seen as a gel, the concentration of wood components is one dominant part, even if the water molecules are bonded directly to an OH-group within the wood. The approach is in line with the state of the art knowledge of the wooden cell wall structure. Parts of the cell wall, such as hemicelluloses, are getting dissolved and therefore participate in the water sorption phenomena, were other parts are constant like the fibril structure.

Applying this changed perspective could lead to a better and more comprehensive consideration of the wood-water-interaction. Including this perspective in future, ongoing research in wood modification as well as the understanding of the wooden structure and wood decay can be improved.

Cell Morphology and Mechanical Properties of Transgenic Poplar with Reduced Cellulose Content

Dr. Ilona Peszlen, Ilona_peszlen@ncsu.edu

Dr. Zhouyang Xiang

Dr. Perry Peralta

North Carolina State University, USA

Abstract

Recent advances in cell wall biosynthesis of plants make it possible to investigate the role of cell wall chemical components and compositions on anatomical structure and mechanical properties. In this study, genetically modified *Populus trichocarpa* wood with reduced cellulose content was investigated. Five xylem-specific cellulose synthase genes were knocked down in three ways. Five lines were produced by silencing gene PtrCesA4, three lines were obtained by silencing gene pair PtrCesA7/17, and one line was obtained by silencing gene pair PtrCesA8/18. A total of thirty-four young trees (two to six plants per line and three wild type plants) growing in the greenhouse were harvested at eight months.

Cell morphology was studied by using quantitative wood anatomy methods; modulus of elasticity (MOE) and modulus of rupture (MOR) in three-point bending were measured using a modified micromechanical test method. The wood of transgenics with reduced cellulose content had significantly larger fibers with thinner cell wall and exhibited severe reduction in MOE and MOR compared to the wild types. The reduced mechanical strength may be due to thinner fiber cell walls. Collapsed vessels were observed in some transgenics indicating that water transport in xylem may be affected but otherwise no specific pattern of vessel variation was found.

Keywords: *Populus trichocarpa*, genetic modification, transgenic tree, cellulose, quantitative wood anatomy, modulus of elasticity, modulus of rupture, mechanical properties.

Triboelectrical charging of wood: a neglected wood property with potential applications

*Roman Myna¹– Stephan Frybort²– Raphaela Hellmayr¹–
Falk Lieber³– Rupert Wimmer¹*

¹ University of Natural Resources and Life Sciences, Vienna, Institute of Wood Technology and Renewable Materials, Austria

²Kompetenzzentrum Holz GmbH , Linz, Austria

³ University of Natural Resources and Life Sciences, Vienna, Institute of Chemistry of Renewable Resources, Austria

** Corresponding author: rupert.wimmer@boku.ac.at*

Abstract

Triboelectrification is a charging process that results from the contact and separation between two dissimilar materials. When two charging partners are colliding, equal and opposite charges may result, with obtained polarities depending on the effective charging work of the two materials. The amount of charge developed depends on several factors, including kinetic energy, area of contact, and the chemical-structural layout of the involved materials. Materials can be listed in order of polarity of charge separation, when getting in touch and released with another object. A material towards the bottom of that series acquires a more negative charge, when touched to a material near the top of the series. In a triboelectric series wood is located around the middle, which means that wood could be charged negatively as well as positively, depending on the collision partners above and below in the series. The triboelectrical charging of wood particles was investigated by means of a self-built charging, field strength and coagulation apparatus. It was shown that most wood particles carry initial charges, and this charge could be altered through collisions with selected materials mounted in a laminar air stream pipe. Wood particles obtained were then either positively or negatively charged. The triboelectric charge turned out to be quite stable, and the field strength depended on wood species, particle sizes, or on included adhesives as it is with particleboards or fiberboards. The triboelectric effects can be utilized in various ways, such as facilitating particle agglomerations with differently charged wood particles, which can get removed more effectively in an existing filtering system.

Key words: dust removal, wood particle, triboelectricity, electrical charge, wood structure, chemistry, exhaust system

Introduction

The European wood-based industries cover a range of downstream activities, including the woodworking industries, furniture industry, and pulp and paper manufacturing. Together, some 430 000 enterprises are active in wood-based industries across the EU-28 (2017 data). The wood industry is representing one in five (20.0 %) manufacturing enterprises across the EU, which also highlights that many belong to small or medium-sized enterprises. In Austria, with more than 27,000 employees the wood industrial sector ranks among the largest and most important employers in the country. Here, the wood-based industry is traditionally known to be an export-oriented sector, showing a constantly positive trade balance (Schwarzbauer 2002).

During wood processing activities such as sawing, cutting, routing, turning and sanding, particulate matter such as chips, particles, fibers or wood flour are created, and these particles are posing risks to the workers' health. The breathing in dust is the most common type of exposure to wood dust. A person's upper respiratory system can filter out larger particles, but smaller particles can go deep into the lungs causing damage and scarring to the lung tissue. Each time this happens a small amount of irreversible damage occurs. This damage reduces the lungs' ability to take in oxygen and over time makes it increasingly difficult to breathe. Also, swallowing wood dust can affect the intestines, bloodstream and vital organs, which can make people ill. Getting dust in the eyes causes irritation and damage, and skin contact with wood dust may cause ulceration of the skin, irritation and dermatitis.

In Austria, the limit-value regulatory (called GKV 2011, annex V), lists wood species with their particles being carcinogenic. While dust derived from oak and beech is clearly cancer-causing, the dust of all the wood species are suspected carcinogens. Therefore, a fast and efficient extraction of wood dust is of foremost importance, due to the following facts:

1. During machining multiple particles may be generated, which could create higher tool-wear (Heisel & Dressler 2002), reducing also the surface quality (Scheurich 2000).
2. Insufficient extraction of particles leads to higher cleaning effort (Heisel und Dressler 2002), und
3. Multiple milling processes may also raise the proportion of fine particles. Higher process speed and better surface quality may have an additional effect on more fine particles.

An improved particle extraction and dust collection in wood processing have been traditionally achieved through oversized exhaust systems (Heisel et al. 2000). However, improving dust extraction purely through a higher exhaust power has limitation due to high energy consumption and a reduced economic viability. These so-far adopted strategies have been leading to high investments, creating also additional noise. According to Seeger & Tönsing (1999) dust exhaust systems in Germany are consuming 24% of the entire electric energy, which ranks amongst the highest, next to machining (29%), and heating (13%). The energy saving potential of exhaust and compressed air systems are reported to lay between 25% und 30% (Seeger & Tönsing 1999).

A central problem is that respirable dust having a median aerodynamic diameter of 2,5 μm is especially harmful (Figure 1). Then, particles with a median aerodynamic diameter of <5 μm behave like aerosols, which means they are airborne ("dust cloud"). In addition to the particle

size, health risks are also linked to the particle shape, the particle surface structure, including surface chemistry (Klouda et al. 2012).

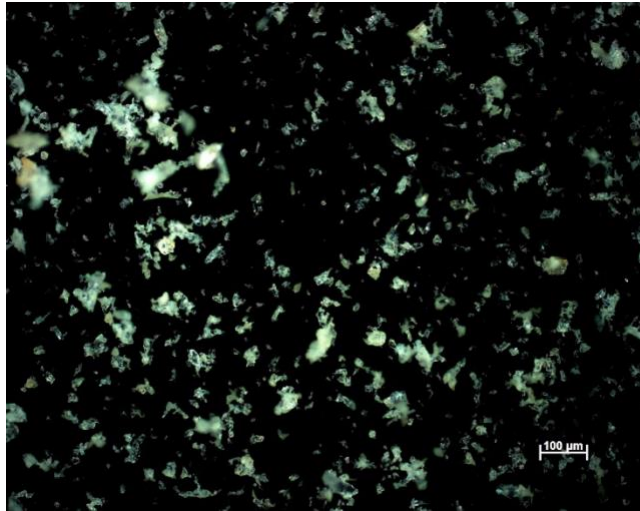


Figure 1: Wood fine dust particles, $<10\ \mu\text{m}$ (PM10), and $<2,5\ \mu\text{m}$ (PM25), health risks increase with smaller particles

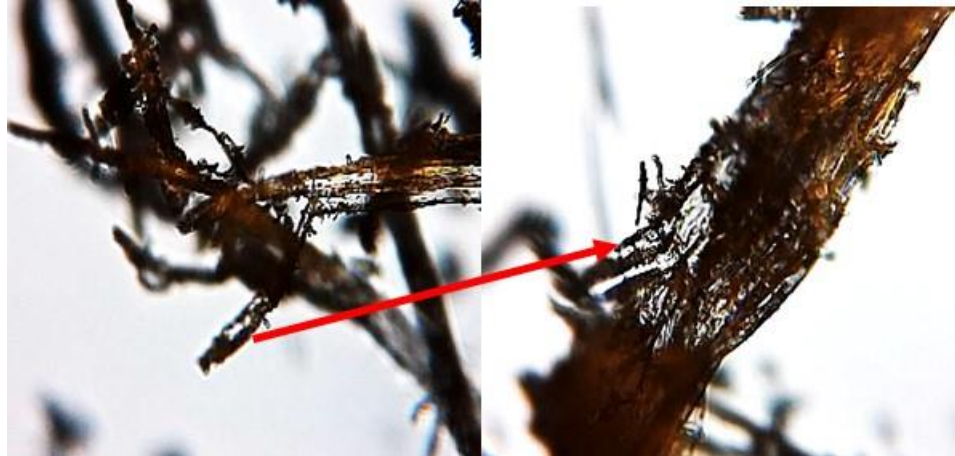


Figure 2: Spruce dust particle, consisting of single and agglomerated fibers and wood tissue fractions (magnification: left 30 x, right 120x).

Wood dust consists of tissue fractions, with single and agglomerated fibers that may be branched or show tiny hooks (Figure 2). By their pin-like structure wood fibers are prone to get caught in the alveoli of the lung parenchyma, subsequently leading to irritations and inflammations (IARC Working Group on the Evaluation of Carcinogenic Risks to Humans 1995).

Triboelectric charging of wood particles

Triboelectric charging refers to the transfer of charge via contact. The triboelectric effect is therefore a contact electrification, with materials becoming electrically charged after they are separated from a different material that they have contacted. For example, rubbing glass with a plastic comb through the hair can build up triboelectricity. Polarity and strength of the charges produced differ according to the materials, surface roughness, temperature, strain, and other physical and chemical properties. Substances can be arranged into triboelectric series, which is a list that ranks materials according to their tendency to gain or lose electrons. It shows materials in order of decreasing tendency to charge positively (=lose electrons) and increasing tendency to charge negatively (=gain electrons). In the middle of the list are materials that do not show strong tendency to behave either way, and right next to cotton wood is also positioned there (Figure 3).

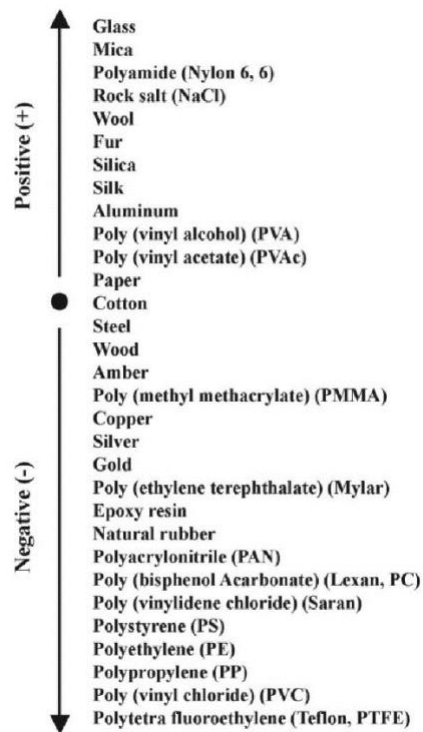


Figure 3: Triboelectric series is ranking materials according to their tendency to gain or lose electrons. Wood is positioned in the middle, being either negative, nor positive, but can be charged in any direction by colliding with materials listed below and above.

In this work, we investigated if triboelectric charging takes place on wood particles that are generated in machining processes, such as sawing or sanding. The motivation for this research evolved from the search for new methods reducing wood dust development during processing. This has led to the issue of triboelectric charging of wood particles, and we are hypothesizing that the triboelectric effect is a prevalent characteristic of any wood particle that evolved from a cutting process. The obtained charges may have the potential to be used in the reduction of wood dust-related health risks.

Materials and Methods

A fully sensor-equipped measuring equipment was designed and built, able to measure the triboelectric charge of wood particles (Figure 4). Dust particles are fed into the ventilated system from the left, and drawn to the right, with particle size distribution and the triboelectric charge measured along the air stream. At the same time, the streaming velocity, pressure differences, and the humidity are constantly monitored and recorded.

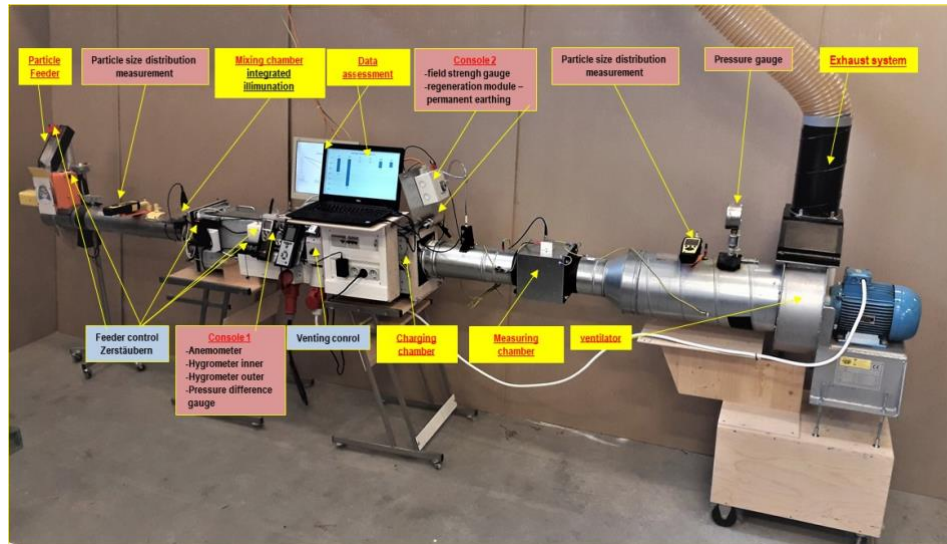


Figure 4: Measuring stand to detect triboelectric charging of wood particles

Figure 5 shows the measuring equipment adapted to circular saw cutting. Chrome-vanadium steel circular saw blades were used for the cutting. Particles generated from that process were sucked into the system, to measure the triboelectric charge occurring as a consequence of the cutting process.

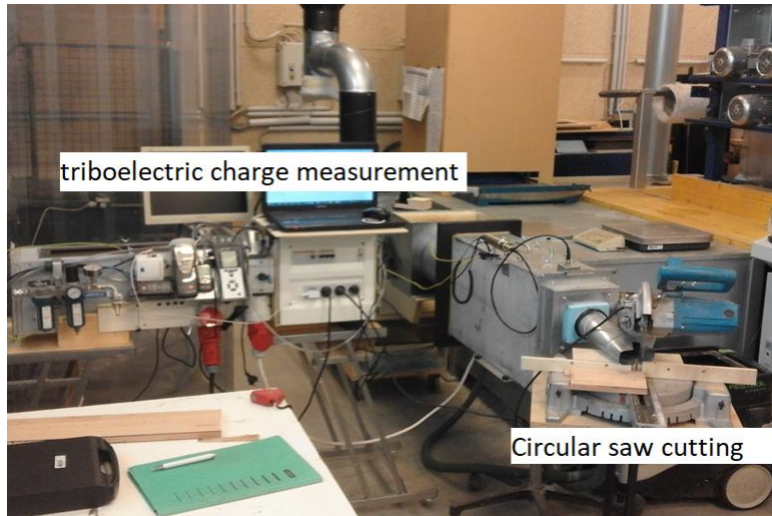
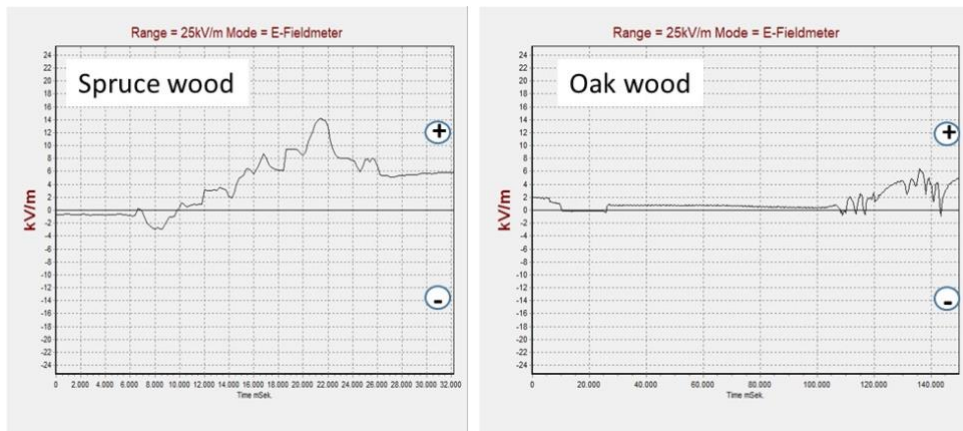


Figure 5: Adapted measuring equipment for the detection of triboelectric charging of wood particles during circular saw cutting

Results and Discussion

The measured data are preliminary and need ongoing confirmation and extension, assessing also effects such as different moisture contents, particle sizes, extractive contents, chemical composition. However, data obtained from circular saw processes have shown clear trends as followed: (1) Wood particles from cutting solid wood during circular saw cutting always get positively charged (Figure 6); (2) Wood particles from wood-based panel cuttings, i.e. particleboards and fiberboards, receive negative charging (Figure 7).



**Proceedings of the 62nd International Convention of
Society of Wood Science and Technology
October 20-25, 2019 – Tenaya Lodge, Yosemite, California USA**

Figure 6: Triboelectric charging (KV/m) with time (seconds) of wood particles when circular cutting spruce (left) and oak (right). Wood particles are positively charged throughout.

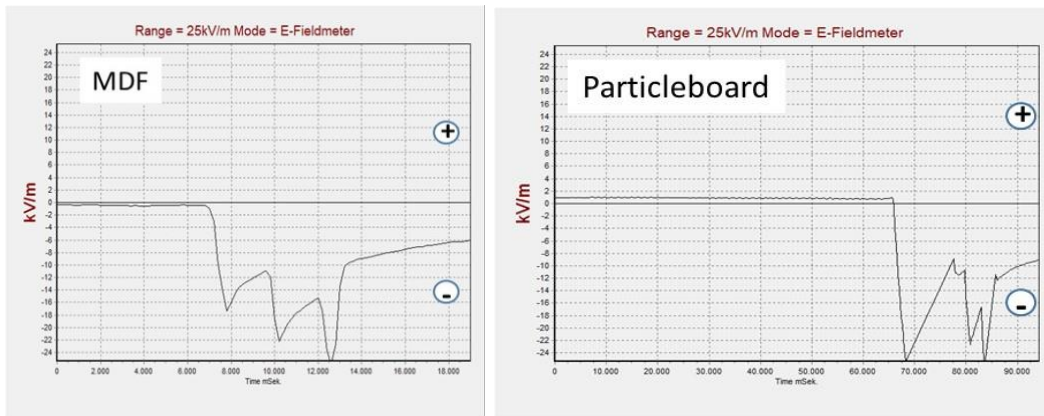


Figure 7:

Triboelectric charging (KV/m) with time (seconds) of wood particles when circular cutting MDF (left) and a particleboard (right). Wood particles are negatively charged throughout.

Additional data confirmed that the moisture content affects the triboelectric charging: dry wood particles received higher charges, which declined as the moisture content of the wood particles increased. Higher charges were also shown with circular saws that were more serrated. The negative charge obtained with particles cut from wood-based panels are most likely due to the intrinsic thermosetting resin in the panel. More specific data are subject of ongoing research. The lower charge at higher moisture contents are due to the fact that the higher electric conductivity is removing charges immediately after particle collision. Triboelectric charges may also alter when the steel circular saw blades are carbide tipped or carry any other tip-coating type. Charging turned out to be persistent and could be re-measured on particles after weeks.

Experiments were also done with sanding, testing different sandpaper types. The chemical composition of the sandpaper determined if wood particles got positively or negatively charged. While rubin-sandpaper had led to positively charged wood particles, the zircon and brilliant sandpaper delivered a positive charge. Depending on the sanded wood material, an either positive or negative charge could be achieved.

Summary and Conclusions

We have found that wood particles during cutting processes consistently received triboelectric charges. During circular saw cutting of solid wood the particles get positively charged, while cutting of wood-based panels - glued with standard urea-formaldehyde resin – were negatively charged. The positive charge of solid wood particles complies with cellulose and hemicellulose positioned in the triboelectric series. It is shown that triboelectric charging during cutting processes will lead to repulsive forces of wood particles (particles have the same charge), which provokes a greater dust dispersion and, since dust sedimentation processes are reduced. Through defined opposite-poled charging of wood particles it is possible to agglomerate particles, which is leading to reduced fractions of fine dust, and to a reduced “dust cloud” formation.

*Proceedings of the 62nd International Convention of
Society of Wood Science and Technology
October 20-25, 2019 – Tenaya Lodge, Yosemite, California USA*

Through designed triboelectric charging processes, a novel dust removal technology can be established. The authors have patented this new approach.

References

Heisel U., Dressler M. (2002) Auslegung von Absaughauben bezüglich der Späneerfassung durch Simulationsrechnung. Stuttgart, Lehrstuhl und Institut für Werkzeugmaschinen, Universität Stuttgart.

Heisel U., Tröger J., Müller S., Dressler M. (2000) Analyse des Partikelstrahlverhaltens ist Basis für effiziente Späneerfassung. Maschinenmarkt - Das Industrie Magazin 8: 60-63.

Klouda K., Brádka S., Otáhal P. (2012) Experiences with Anthropogenic Aerosol Spread in the Environment, in Atmospheric Aerosols-Regional Characteristics-Chemistry and Physics. Chapter 17, 415pp.

Scheurich H. (2000) Ermittlung des Späneauswurfs aus dem Werkzeug und Dokumentation des Spanflugverhaltens im Spanraum. Institut für Werkzeugmaschinen, Universität Stuttgart: 128.

Seeger K., Tönsing E. (1999). Stromeinsparpotentiale in der Holzverarbeitenden Industrie. Energie effizient nutzen - Schwerpunkt Strom. P. Radgen and E. Jochem, Wirtschaftsministerium Baden-Württemberg.

Schwarzbauer P. (2002) The wood resources in Europe - Availability, Trade flows, value added. Lignovisionen 2: 11-20.

Friday, October 25th

8:30 – 11:30

Timber Engineering and Mass Timber

Chair: Dave Devallance, InnoRenewCoe, Slovenia

Evaluation of NHLA Graded Yellow-Poplar Lumber Regraded for Structural Use in CLT Panel Production

Mr. Rafael Azambuja¹, rdazambuja@mix.wvu.edu

Dr. David DeVallance²

Dr. Joseph McNeel¹

Dr. Curt Hassler¹

¹ West Virginia University, USA

²InnoRenewCoE, Slovenia

Abstract

The current cross laminated timber (CLT) standard in North America (ANSI/APA PRG 320-2018) restricts the use of hardwoods. For producers within the Appalachian Region, with a large percentage of hardwoods, this restriction limits the use of locally supplied lumber for CLTs. An additional hinderance is that most hardwood lumber is graded in respect to appearance following National Hardwood Lumber Association (NHLA) grading rules. Lumber used in structural purposes, however, requires grading system that evaluate defects in relation to mechanical properties. For example, *Liriodendron tulipifera* (yellow-poplar) can be structurally graded following North Eastern Lumber Manufacturers Association (NELMA) grading rules. Further complicating the issue, the processing steps vary between lumber produced for NHLA versus structural grading. Therefore, the objective of this study was to evaluate differences in lumber grades and quantify the influence of additional machining steps on yellow-poplar lumber prepared for CLT panels. Eight packs of dry, rough-cut, 17/16" yellow-poplar lumber with NHLA grades of "2 and below" (NHLA Grade 2A, 2B, 3A, and 3B) were obtained. The lumber used was of random width, but within a range of 6 1/4 inches to 7 3/8 inches. The lumber was graded following both NHLA and NELMA grading rules before and after processing. The processing consisted of ripping to a final width of 6-inches and surfacing both faces to achieve a final thickness of 7/8-inch. Information on which defect kept the lumber from achieving a higher grade (i.e., limiting defect) was determined. Results indicated that lumber processing considerably influence the grade, as chi-square tests showed a statistically significant difference between the lumber grade (in both systems) prior to and after processing (NHLA, $268.61 > 12.59 \times 25\%$ and NELMA, $140.97 > 7.81 \times 25\%$). In relation to NELMA grades, analyses of prior and post processing showed an increase of Select Structural and lumber that did not meet grade (i.e., below grade). The most common defects were knots (46%) followed by splits (29%), wane (7%), and shake (7%). Ripping to final width showed two main qualitative results. When the defect was in the edge areas, the defect was removed and boards achieved higher grades (e.g., Select Structural). However, when defects were located in central areas, the board overall surface area decreased and the defect area (as a percent) increased, thus decreasing the board grade. To truly quantify these results, further investigation is required with digital image comparisons for prior

***Proceedings of the 62nd International Convention of
Society of Wood Science and Technology
October 20-25, 2019 – Tenaya Lodge, Yosemite, California USA***

to and after processing. In respect to NHLA vs NELMA grading, the results showed for processed lumber graded as “2 and below”, 56% of the boards achieved a NELMA structural grade. The lumber met the following NELMA grades: 12% Select Structural; 7% No. 1; 19% No. 2; and 18% No. 3. The remaining 44% were below grade. In conclusion, a majority of yellow-poplar lumber sawn and graded for appearance possessed structural attributes required for use in the production of CLT panels. This finding suggests that there is potential value in re-grading/classifying traditionally processed hardwood lumber (in particular, yellow-poplar) for structural grades.

**Evaluation of Shear Performance of Cross Laminated Timber Shear Wall Connections
under the Effects of Moisture Intrusion**

Mr. Shrenik Bora, boras@oregonstate.edu

Dr. Arijit Sinha

Dr. Andre Barbosa

Oregon State University, USA

Abstract

Cross-laminated timber (CLT) is a promising renewable building material which enables the utilization of wood for mid-rise and even tall wood buildings owing to its high strength-to-weight ratio, fire performance, and prefabricated nature. However, moisture intrusion in CLT is a significant risk since it directly affects the durability of the structure. CLT panels have high storage capacity but relatively low vapor permeability which may result in absorption and retention of large amounts of moisture. The structural members of CLT can be exposed to moisture due to various reasons such as excessive wetting during or after construction, failure of internal plumbing, and failure of impermeable elements of facades or roofs. Performance of CLT structure is highly dependent on the performance of its connections. Most of the existing research on CLT is focused on ambient temperature and moisture control. While the influence of moisture on timber structures is well recognized, the impact of moisture intrusion on the performance of CLT connectors is less understood. Therefore, this study aims to investigate the effects of three (3) different moisture exposure conditions on shear performance of 3-ply CLT diaphragm to shear wall connectors under quasi-static loading. Four important wood species used across globe for CLT manufacturing [Douglas fir, Southern yellow pine, Norway spruce, and Spruce Pine Fir] are used for the test specimens. The test specimen is fabricated with one horizontal member of CLT having dimensions of [8" X 12"] connected to one vertical member of CLT having equal dimensions at the center with a two (2) L-brackets. The connections will be tested using Abbreviated Basic Loading History CUREE protocol to understand the effects of different moisture exposure conditions along with the variation of wood species on these connection types. This study is envisioned for the development of design guidelines of CLT connections. Consequently, the results of this study will improve our knowledge to account for effects of moisture while designing connections for mass timber buildings.

Keywords- CLT, mass timber, connections, moisture, durability, exposure, CUREE

Evaluation of Bond Integrity in Low-Value Blue-Stain Ponderosa Pine CLT

Sina Jahedi ^{1} – Lech Muszynski ² – Mariapaola Riggio ³ – Rakesh Gupta ⁴*

¹ Ph.D. Student, Wood Science and Engineering, Oregon State University, Corvallis, OR, USA *Corresponding author, sina.jahedi@oregonstate.edu

² Professor, Wood Science and Engineering, Oregon State University, Corvallis, OR, USA, lech.muszynski@oregonstate.edu

³ Assistant Professor, Wood Science and Engineering, Oregon State University, Corvallis, OR, USA, mariapaola.riggio@oregonstate.edu

⁴ Professor, Wood Science and Engineering, Oregon State University, Corvallis, OR, USA, rakesh.gupta@oregonstate.edu

Abstract

National forest restoration programs aim to reduce wildfire risks by selectively removing small-diameter trees from the forest. Each year a large number of Ponderosa pine logs are generated in these operations in Southern Oregon and Northern California. These logs have a very limited market value locally. A substantial portion of them contain blue-stain, which reduce the value even further. It is important to find a value-added market for the logs to offset the high costs of these operations. Based on the previous research, cross-laminated timber can be a promising solution to address this issue. CLT is a composite structural panel consisting of three or more odd number of orthogonally arranged layers of boards. ANSI/APA PRG 320 'Standard for Performance-Rated CLT' specifies the criteria and quality assurance requirements for fabrication of custom CLT layups of non-standard lumber. A literature review on CLT made of low-value lumber showed that the stringent bond integrity criteria are most critical of these standard requirements. Results of delamination test on blue-stain ponderosa pine CLT completed as a preliminary step to assess the potential of using it in CLT panels as a structural material are presented in this paper. The specimens were manufactured in a research laboratory under controlled environment conditions. Laboratory scale fabrication is essential for prototyping innovative CLT layups. Fabrication parameters including ambient temperature, lamination moisture content, adhesive spread rate, close assembly and press time were monitored during the tests. Of the investigated variables, the effect of the close assembly time showed to be the most important for fabrication of CLT panels in laboratory conditions. Using adequate equipment and procedures can reduce the close assembly time to a suitable duration.

Key words: cross-laminated timber; CLT; low-value lumber; Ponderosa pine; blue-stain; cyclic delamination.

Introduction

Currently, the building industry is a major consumer of nonrenewable materials, many obtained in unsustainable ways. The construction industry is responsible for a significant part of greenhouse emission and anthropocentric environmental impact (Akan et al., 2017). Wood, as a renewable material with high specific strength, is a promising material to address this issue (Green, 2013). Mass timber constructions contribute to reduce the carbon dioxide footprint of the building industry by storing carbon in buildings instead of releasing it to the environment. Cross-laminated timber (CLT) was invented in Austria and Germany in the early 1990s, (Karacabeyli et al., 2013). CLT is a structural composite panel consisted of three or more odd number of orthogonally arranged layers of boards. The layer-wise arrangement of CLT layups reduces the impact of inhomogeneity of individual boards and results in more uniform panels. In principle, layer-wise characteristic of CLT makes it possible to reach a predictable and uniform mechanical properties even when low-grade lumber is used in laminations. Since the introduction of CLT to North America in early 2000's the interest to use this product as a construction material has steadily grown, but it is not a common practice yet (Pei et al., 2016).

National forest restoration programs aim to reduce wildfire risks by thinning operations, or selectively removing small diameter trees to preserve larger and superior trees. Many of the harvested trees are either dead or diseased which can be fuel for wildfire and pest outbreaks. Currently, the market for this low-value lumber in the U.S. Northwest is very limited. It is important to find a value-added market for this material to offset the high costs of thinning operations.

Low-value lumber CLT:

ANSI/APA PRG 320, 'Standard for Performance-Rated CLT' developed in the United States since 2011 provides the specifications and requirements for the CLT components, and performance criteria, qualification, and quality assurance for the finished CLT panels. The standard allows production of custom CLT layups using alternative grades and species according to American Lumber Standards Committee (ALSC), and also arbitrary number and thickness of layers in major and minor directions, provided these custom CLT products satisfy prescribed performance qualifications. These requirements fall in two major categories: mechanical characteristics of components and panels and adhesive bond integrity (resistance to shear and delamination).

The interest in utilizing low-value lumber for making CLT panels has increased in the past few years. Previous studies have showed that utilizing low-value lumber in fabricating CLT can result in a favorable structural performance comparing to pre-defined PRG 320 CLT grades. The research on yellow-poplar CLT emphasized that CLT fabricated with low-grade lumber can provide satisfactory mechanical properties (Mohamadzadeh and Hindman, 2015). Furthermore, current research (Larkin 2017, Lawrence 2018) determined the potential of using small diameter ponderosa pine logs for hybrid CLT fabrication. The hybrid CLT consisted of low-value ponderosa

pine lumber in core layer and Douglas-fir lumber in major direction. While the studies showed that the low-value lumber CLT has sufficient strength and elastic properties compared to pre-defined CLT grades, they failed to satisfy the delamination criteria dictated by PRG 320. The study on effectiveness of adhesive systems for low-value lumber CLT panels confirmed that passing delamination test is challenging, but achievable under controlled conditions (Larkin, 2017, Lawrence 2018), although the presence of blue stain alone was shown not to interfere with the quality of the bonds formed with polyurethane adhesives (Li et al. 2018).

Materials & Methods

Given the importance of bond integrity tests, this study is focused on cyclic delamination test, which is more difficult to pass than the resistance to shear criterion. Delamination test has been selected to be the initial step towards assessing the potential of fabricating blue-stained ponderosa pine structural CLT. The aim was to evaluate the effect of various operational and environmental parameters on the delamination of blue-stain ponderosa pine CLT specimens bonded with melamine formaldehyde (MF). These parameters included ambient temperature, lamination moisture content, adhesive spread rate, close assembly and press time. The only cost efficient way to perform such prototyping work is on lab-scale fabricated CLT specimens, as opposed to specimens extracted from full-scale panels produced in commercial production lines, even as faithful reflection of full-scale fabrication at the lab-scale is not always possible.

The CLT panels used in this study were fabricated under monitored conditions in laboratory environment using two component MF adhesive system. All of the panels are made of No. 3 visually graded ponderosa pine lumber in accordance with Western Wood Products Association. Traces of blue-stain could be visually identified in some of the panels. The lumber was stored indoor before the fabrication to make sure they are stable regarding moisture content. The moisture content of the lumber during fabrication was 11 to 13% depending on the season and weather condition. The laminations were planned within 48 hours prior to the assembly. Both bonding-surfaces are planned at least 1/16 in from each side. Delamination specimens are obtained from two sizes of CLT layups, both shown in Figure 1.

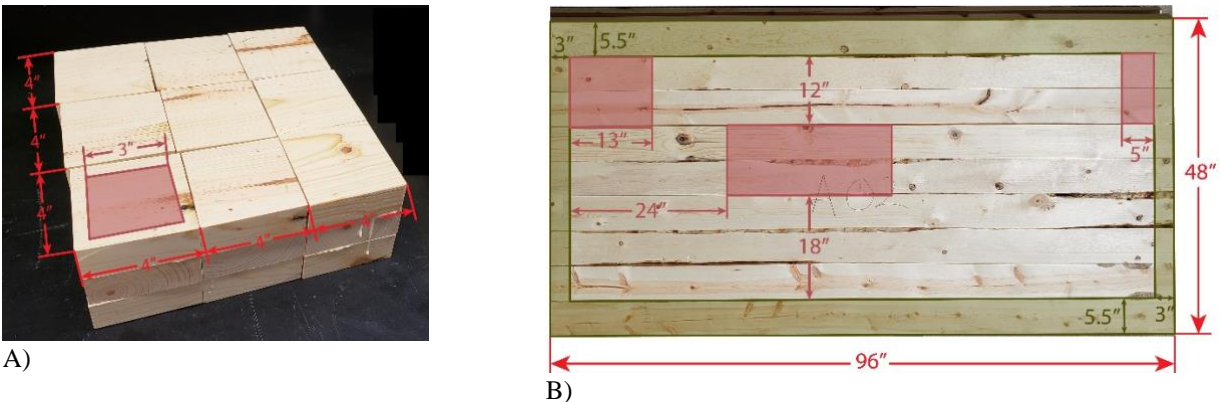


Figure 1. (A) A set of nine CLT blocks produced for delamination test. (B) A CLT panel. Red areas indicate the locations which delamination specimens are obtained from.

CLT Blocks, are 4 inches by 4 inches cross-laminated lamination sections arranged in three-layer blocks as shown in Figure 1 A. This size selected to eliminate the effect of layer bridging and lamella thickness tolerances and used to determine the effect of the adhesive compatibility and fundamental fabrication conditions. To minimize the amount of glue skips, the blocks are obtained from parts of the boards with minimum defects. In ANSI/APA PRG 320 glue skips are defined as knots, checks, waness, and rough surfaces. Table 1 summarizes the fabrication parameters for CLT blocks.

The specimens were fabricated in sets of 9. The first two preliminary sets, Pre-1 and Pre-2, were fabricated strictly following the adhesive manufacturer suggestions to gain benchmark experience. Immediate failures were observed in both Pre-1 and Pre-2 due to long assembly time and low adhesive spread rates, resulting in the adhesive dryout prior to setting the layup into the press. Close assembly time is in a direct relationship with spread rate ratio. Hence, in the regular test block fabrications the spread rates were the principle variable. At the fabrication stage, the increased spread rate in sets B1, B3 and double spread rate in set B4 helped in reducing the impact of assembly time. The increased spread rates also helped in offsetting the spillage of adhesive from bonding-surfaces, which is substantial in small specimens.

Table 1. Fabrication parameters for CLT blocks. Press pressure is equal to 0.7 MPa (100 psi) on the panel for all sets. Each set is consisted of nine specimens.

Set#	Blue stain presence	MC	Temp, RH	SRR* (g/m ²)	CAT**	Press time	Oven time***
Pre-1	No	12.8 %	20.7 ⁰ C, 32 %	300	18 min	15 hr	-
Pre-2	No	12.5 %	21.2 ⁰ C, 35 %	300	14 min	17 hr	-
B1	Yes	12.0 %	22.1 ⁰ C, 22 %	300<SSR<500	15 min	23 hr	13 hr
B2	Yes	13.0 %	22.1 ⁰ C, 22 %	250<SSR <310	12 min	22 hr	13 hr
B3	No	11.6 %	21.1 ⁰ C, 30 %	300<SSR <500	14 min	15 hr	14 hr
B4	No	11.6 %	20.8 ⁰ C, 43 %	500<SSR<1000	14 min	18 hr	14 hr

*Spread rate ratio **Close assembly time ***Refers to dry-oven time in delamination test

In set B1, press time was extended beyond the duration suggested by the adhesive manufacturer in order to simulate the industrial practice, where after pressing the CLT panels are stored under a dead-load to let the adhesive complete the curing process.

CLT Panels were three 4 ft by 8 ft CLT three-layer layups fabricated in the laboratory environment. Figure 1 B shows such panel as well as the locations, from which delamination specimen obtained. As suggested by ASTM PRG, the delamination specimens were extracted from both center and corners of the CLT panel. No pre-selection is made for the boards used for fabrication of the CLT panels. The boards were selected randomly and they highly contained knots and waness. Table 2 indicates the fabrication parameters for the CLT panels. The spread rate was increased for the fabrication of the CLT panels to extend the allowable close assembly time, which took significantly longer time than in case of the CLT blocks.

Table 2. Fabrication parameters of CLT panels. Press pressure for all sets is equal to 0.7 MPa (100 psi) on the panel.

Set#	Blue stain presence	MC	Temp, RH	SRR* (g/m ²)	CAT**	Press time	Oven time***
P1	No	11.6 %	19.8 ⁰ C, 43%	488	43 min	18.0 hr	13.5 hr
P2	Yes	12.0 %	23.8 ⁰ C, 31%	>600	55 min	21.5 hr	13.5 hr
P3	Yes	11.6 %	20.3 ⁰ C, 50%	488	54 min	18.0 hr	13.5 hr

*Spread rate ratio **Close assembly time ***Refers to dry-oven time in delamination test.

During the fabrication it became obvious that the adhesive mixture was not adequate for the long assembly times required in producing 4 ft x 8 ft in laboratory. That was particularly apparent in fabricating P3 CLT panel which showed that the maximum allowable close assembly time is 20 minutes at the ambient conditions specified in table 2. In this research the resin and the hardener were mixed together before the application on layup. To achieve longer close assembly time, in future studies, the resin and hardener will be applied on different faces of the bonding-surface to be mixed only when the layup is pressed.

Testing procedure:

ANSI/APA PRG 320-2018 refers to AITC T110 for cyclic delamination test. Delamination percentage is defined as the sum of delaminated lengths in a specimen over the total perimeter of the bonding-surfaces. This will include sum of multiple bonding-surface perimeters if the specimen consists of a numerous bonding-surfaces. Based on the standard, the maximum allowable delamination percentage is 5%. The delamination specimens should be 3 in by 3 in in-plane and, for the purpose of certification and quality assurance, they should be obtained from a panel larger than 24 inches by 24 inches. The AITC T110 delamination procedure is summarized in figure 2.

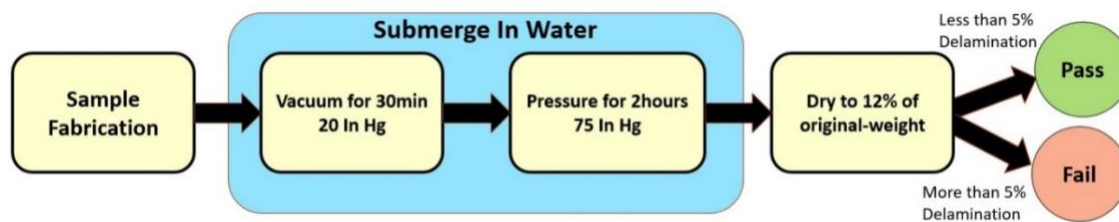


Figure 2. Delamination procedure based on AITC T110.

After taking the specimens out of the drying oven, each bonding-surface was carefully investigated. A crack is reported as delamination if the depth of the crack is more than approximately 1/16 in and no major wood fibers pulled out of either side of the crack. Only the cracks exactly located on the bonding-surfaces are considered as delamination. Chisel test found to be effective to investigate the probable reason in case of delamination (Lukowsky 2015).

Results and Discussion

The delamination in the bond lines resulting from different shrinkage rates in wood in orthogonal directions and internal stresses developed during wet-dry cycle, was assessed by visually inspecting the CLT specimens after wet-dry cycle. One visible sign of good bond is a flowing

transition between the layers of the sample, as shown in figure 3. Mostly the delamination occurred at the corners of the specimens. Checks and cracks within the lamellas were observed in specimens with good quality of bonding.

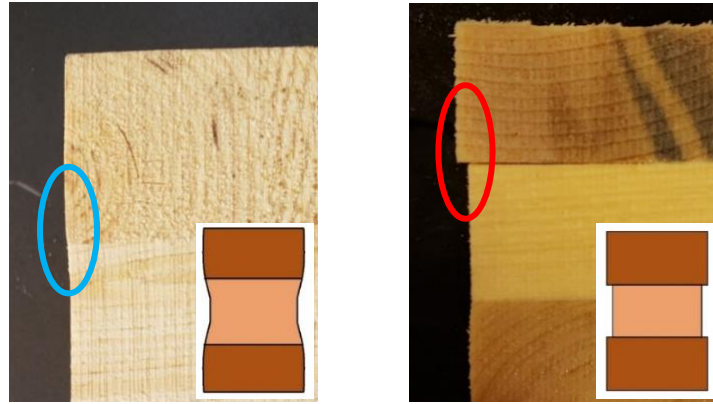


Figure 3, (Left) smooth transient between layers after wet-dry cycle. (Right) step-like transient which resulted in delamination.

It is important to note that the delaminations in some specimens coincided with the presence of defects on the bonding-surfaces, e.g. knots, checks, and rough surfaces. Also, it was common to observe a delamination formed by propagation of existing checks. No influence of blue-stain on the delamination of cross laminated ponderosa pine specimens was observed.

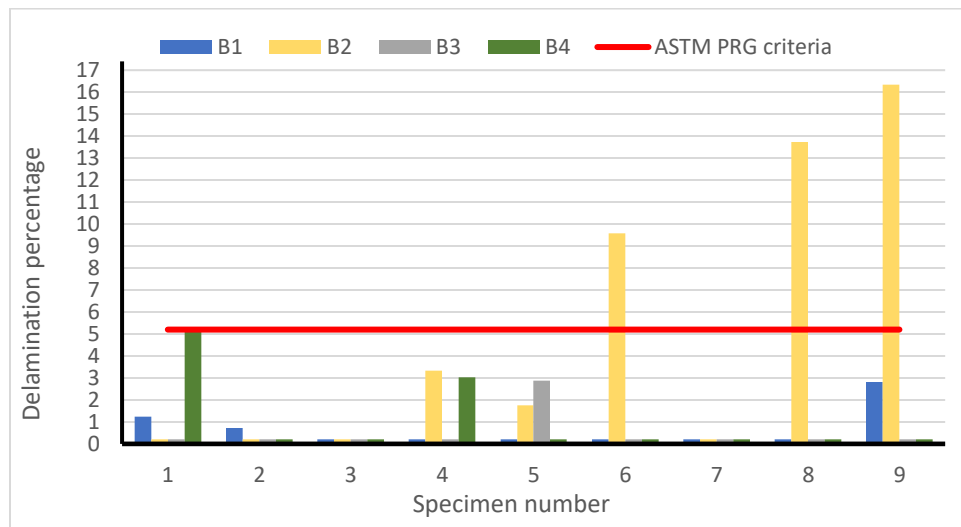


Figure 4, delamination percentage of the CLT block specimens.

Figure 4 shows the results of delamination tests on the CLT blocks. All the specimens in test sets B1, B3 and B4, and 6 out of 9 blocks in set B2, successfully met the PRG 320 criteria. Considering unavoidable spillage of adhesive, B2 set was essentially fabricated with reduced adhesive spread rate. Chisel test revealed that in blocks with the reduced spread rate delamination is caused by uneven adhesive application and areas with “starved bond line.” On the other hand, excessive adhesive spread rates in set B4 did not improve the bond integrity, since press squeezed

***Proceedings of the 62nd International Convention of
Society of Wood Science and Technology
October 20-25, 2019 – Tenaya Lodge, Yosemite, California USA***

the excess of liquid resin out of the bonding-surface. Furthermore, comparing the effect of press time of B3 and B4 with B1, it can be observed that additional press time is not necessary to reduce delamination.

The acceptable delamination tests results on blocks from sets B1, B3 and B4 prove that Ponderosa pine with blue stain presence is compatible with the MF adhesive system.

Summary and Conclusions

CLT is a promising alternative for conventional nonrenewable structural systems. As a part of ASTM/APA PRG 320 qualifications, a custom layup CLT should pass bond integrity tests to be permitted as a structural material. The results from this study indicates that MF adhesive system have a good compatibility with blue-stain ponderosa pine CLT regarding AITC T110 cyclic delamination test. Close assembly time has a significant impact on the results of the delamination test. It is important to finish the assembly within the allowable close assembly time. Assembly can take significantly longer time in producing larger CLT panels, but the time can be reduced by using adequate automations and procedures. The results showed that it is important to account for the adhesive waste caused by operator errors and spillage, especially for fabrication of smaller scale CLT specimens. Moreover, knots, waness, and rough surfaces can negatively affect the bonding, but no direct relation between blue-stain and bonding properties have found.

Acknowledgements

This research is supported by USDA Forest Service (17-DG-11062765-742). The authors thank their colleagues from the department of wood science and engineering at Oregon State University who assisted greatly through this research. We would also like to gratitude CollinsWoods and AkzoNobel companies for their donations.

References

- Akan, M. Ö. A., Dhavale, D. G., and Sarkis, J. (2017). Greenhouse gas emissions in the construction industry: An analysis and evaluation of a concrete supply chain. *Journal of Cleaner Production*, 167, 1195–1207.
- ANSI/APA PRG 320 (2018). Standard for Performance-Rated Cross-Laminated Timber.
- Green, M. (2013). Why we should build wooden skyscrapers | TED Talk. <https://www.ted.com/talks/michael_green_why_we_should_build_wooden_skyscrapers?language=en> (Jan. 2, 2019).
- Karacabeyli, E., Douglas, B., and Editors. (2013). CLT handbook: Cross-laminated timber. FPIInnovations, Pointe-Claire, Québec.

***Proceedings of the 62nd International Convention of
Society of Wood Science and Technology
October 20-25, 2019 – Tenaya Lodge, Yosemite, California USA***

Lawrence, C. (2018). Utilization of Low-value Lumber from Small-diameter Timber Harvested in Pacific Northwest Forest Restoration Programs in Hybrid Cross Laminated Timber (CLT) Core Layers: Technical Feasibility. Oregon State University.

Larkin, B. (2017). Effective Bonding Parameters for Hybrid Cross-Laminated Timber (CLT). Oregon State University.

Li X., B. Larkin, L. Muszyński, J. Morrell (2018): Effect of blue stain on bond shear resistance of polyurethane resins used for cross-laminated timber production. Forest Products Journal. 68(1): 67-69.

Mohamadzadeh, M., and Hindman, D. (2015). Mechanical performance of yellow-poplar cross laminated timber. Report No. CE/VPI-ST-15-13. Virginia Polytechnic Institute and State University.

Pei, S., Rammer, D., Popovski, M., Williamson, T., Line, P., and Lindt, J. W. van de. (2016). An Overview of CLT Research and Implementation in North America. World Conference on Timber Engineering. Vienna, Austria.

Lukowsky, D., (2015) Failure Analysis of wood and wood-based products. P 148-154

Flexural Properties of Dowel-Type Fastener-Laminated Timber

Dr. Olayemi Ogunrinde¹, oogunrin@unb.ca

Dr. Meng Gong¹

Dr. Ying-Hei Chui²

Dr. Ling Li³

¹University of New Brunswick, Canada

²University of Alberta, Canada

³University of Maine, USA

Abstract

Mass timber products (MTP) describes a family of engineered wood products of large section size that offers the construction industry a viable and attractive solution. Nail laminated timber (NLT) and dowel laminated timber (DLT) are two members of this family. This study was aimed at assessing the flexural stiffness and strength capacity of full-scale 7-layer NLT and DLT beam specimens, which were manufactured with different fastener spacings (250 mm and 450 mm), fastener types (nails and hardwood dowels) and fastening pattern (parallel and inclined nailing and butt joint). Third-point bending tests were conducted to assess the flexural bending properties of the beam specimens, which included apparent modulus of elasticity (MOE_{app}) and apparent modulus of rupture (MOR_{app}). Failure modes were also recorded. Findings revealed that group NS2, which was made with 89-mm-long nails and 250-mm nailing spacing, had MOE_{app} and MOR_{app} of 11,700 MPa and 34 MPa, which were 4% and 9%, respectively, higher than NM4 made with 102-mm-long nails and 450-mm nailing spacing recommended in the Canadian Standard CSA O86. On average, NLT beam specimens had MOE_{app} of 11,500 MPa and MOR_{app} of 32 MPa, which were 2% and 28% higher than DLT ones and 5% and 21% lower than those of GLT, respectively. The failure modes observed for all NLT and DLT were similar, which were mainly caused by knots and holes. The failure of GLT beams was mainly dominated by fracture in the bottom layer(s) subjected to the tensile stresses. It could be concluded that 89-mm-long nails used in group NS2 could be used in the manufacturing of NLT beams. Likewise, DLT could also be used as an alternative for NLT.

**Mass Timber Building Construction Cost and Life Cycle Cost Analysis with Comparison to
Concrete and Steel Buildings**

Dr. Hongmei Gu¹, hongmeigu@fs.fed.us

Dr. Shaobo Liang²

¹USDA Forest Service, Forest Products Laboratory, USA

²North Carolina State University, USA

Abstract

Sustainability in the building sector has become increasingly vital. The United States Department of Agriculture Forest Service Forest Products Laboratory (USDA FS FPL) has long been providing critical research to support wood industry with sustainability in social, economic and environmental aspects. Recent movement of mass timber buildings with the innovated wood material called cross-laminated-timber (CLT) opens a new market for timber use in US building sector. Mass timber buildings offer many advantages including long term carbon sequestrations, renewable raw material, lighter carbon footprint during construction process, low concrete mass for foundations and footings, and many social benefits for building occupants. While the social and environmental benefits from Mass Timber buildings have been recognized publicly, the cost effectiveness of mass timber buildings is receiving more attentions from many stake holders. The construction cost differential between mass timber and alternative concrete and steel building structures is under intense debate. This presentation provides a case study on the CLT mass timber building construction cost analysis and potential savings with life cycle cost analysis when comparing to a functional equivalent concrete-steel alternative. The results could help to understand the cost differentials on building constructions and other cost components effect in the whole building life cycles including operations, maintenance, residual values, and end-of-life management. This study will also help stakeholders to identify economic potentials and competitiveness of the mass timber use in the US building sectors.

Potential Use of Hardwood Lumber in Cross Laminated Timber: A Manufacturer Perspective

Henry Quesada
Virginia Tech University
Blacksburg, Virginia, USA
quesada@vt.edu

Abstract

The goal of this study is to understand current cross-laminated timber (CLT) manufacturing practices and explore the opportunity and challenges to use hardwood lumber in CLT manufacturing. The method used to collect data is face-to-face interview as well as industry tours. Two US-based CLT manufacturers have considered using hardwood lumber in CLT fabrication. With the experience of these two CLT manufacturers, it is clear that there is opportunity for using hardwood lumber in CLT production, but the current hardwood lumber supply needs to be adjusted to meet CLT raw material specifications including volume, grading practices, and current dimensions. CLT manufacturers are interested in collaborating with hardwood lumber producers to use hardwood lumber as raw material for CLT manufacturer that can benefit not only the hardwood industry but also the end-consumers.

Moment-rotation behaviour of beam-column connections fastened using compressed wood connectors

Sameer Mehra¹, Iman Mohseni¹, Conan O’Ceallaigh¹, Zhongwei Guan², Adeayo Sotayo², Annette M. Harte¹

¹ Timber Engineering Research Group, College of Engineering and Informatics & Ryan Institute, NUI Galway, Ireland

² School of Engineering, University of Liverpool, Liverpool, United Kingdom

ABSTRACT: Over the last few decades, there has been a renewed interest in the use of timber in building construction in response to concerns related to the challenges of global warming and climate change. This transition towards sustainable and bio-based construction has led to developments in mass timber products and associated novel connection typologies. Considering the demand, the use of traditional carpentry type connections has been largely replaced by fast, efficient and cost-effective modern connections using mechanical fasteners and adhesives. However, metallic fasteners have high embodied energy while adhesives have negative implications for end of life disposal. Therefore, it is favourable to replace these products with sustainable wood-based connectors. The traditional carpentry connections rely on load-transfer in compression via contact between the connected elements or through the use of timber dowels and plates. Numerous examples of such techniques can be seen in historic buildings many of which have been standing for centuries and have endured severe loading situations. These connections are completely adhesive free and non-metallic and can be easily disassembled and reconfigured for replacement or repair. However, connections using hardwood dowels have been reported to loosen over time and necessitate regular tightening so alternative approaches that overcome this drawback are desirable.

Recent studies on modified wood have found that densified or compressed wood (CW) can be used to provide reinforcement in the joint area and could be a potential alternative to adhesives and energy intensive metallic connectors in timber connections. Densified or CW connectors have higher load-carrying capacity and greater ductility than the equivalent hardwood dowels due to their high density. Furthermore, the moisture dependent swelling and springback of CW connectors ensures a tight fit in the connection over time. Also, these connectors have been found to have better compatibility with timber in the connections compared to steel fasteners, which have far greater stiffness than timber. In this study, seven configuration of beam-column moment resisting connection were developed using CW dowels with or without compressed wood plates. The study has considered specimens with CW dowels of 10 mm diameter and CW plates of 20 mm thickness. The load carrying capacity, typical failure modes, moment resistance and rotational stiffness of each connection system were evaluated based on experimental results. Results have shown that connection with CW plates provide a greater load carrying capacity and moment resistance than comparable connections without plates. However, it was found that connections without CW plates allow for more energy dissipation and ductility in the connection.

KEYWORDS: Connections, compressed wood dowels, compressed wood plates, moment-rotation

Experimental Investigation of a Mass Plywood Panel Self-Centering Rocking Wall System

Ian Morrell, Rajendra Soti Ph.D., Arijit Sinha Ph.D., Byrne Miyamoto, Dillon Fitzgerald Ph.D.

There has been recent interest into both structural systems that reduce damage from natural disasters and are made of large mass timber elements. These two concepts can work hand in hand, especially using mass timber shear walls to resist lateral loads. This is due to the resistance of mass-timber panelized shear walls being controlled by the boundary conditions, allowing for damage to be isolated outside of the mass-timber element. One more recent mass timber material, mass plywood panels (MPP), was investigated for use as a rocking wall system with a self-centering element and supplemental energy dissipation. This allowed for testing of the self-centering element, the crushing of the MPP wall, and supplemental energy dissipators. The self-centering was achieved through two 91cm center hold-down rods, one per side of wall, with Belleville washers. After installation the Belleville spring washers were tightened until flat to apply post-tensioning forces. The design philosophy was to allow the hold-down rod to yield during testing, but to limit the plastic deformation to be less than the initial compression of the Belleville washers, causing post-yield cycles to have enough stiffness to reduce residual deformations.

A total of six quasi static cyclic tests were conducted on full scale 76 mm thick MPP walls measuring 1220 by 2440 mm. Two tests were conducted with only the central self-centering rods, to characterize the constitutive response of the MPP wall. Two tests were conducted with the self-centering rods and Kinematically Expanding Hysteretic Dampers (KEHDs) at the corners of the wall for supplemental energy dissipation. The KEHDs are a rod hold-down system with a fixed connection to the base and the connection to the wall with a pre-stressing chuck. This chuck resists tension while the rod is being elongated but allows the rod to slide through the chuck during compression. This results in a system that does not have a pinching response seen in conventional hold-down connections, as the chuck removes any plastic deformation from each cycle, always pulling on the same length of rod. These hold-downs eventually fracture during testing and are designed to be small in diameter to avoid shock loading from fracture. The last two tests included a slip-friction system on the corners of the wall to dissipate energy during an event. All testing was conducted using the abbreviated CUREE protocol.

The results of testing showed positive results. The walls, with the exception of the slip friction connection, would crush at the toes at approximately two percent story-drift. This crushing tended to cause larger capacity degradation when a scarf joint was located near the bottom of the panel. However, even after this crushing occurred, the system would still self-center. The KEHD test did result in fracture of the rods during testing but no adverse effects occurred in the system due to this fracture and a flag-shaped hysteretic response did occur while the rods were still resisting load. The tests with slip-friction dissipators also showed promise for energy dissipation and resistance. Further results and conclusions will be discussed during the presentation.

*Proceedings of the 62nd International Convention of
Society of Wood Science and Technology
October 20-25, 2019 – Tenaya Lodge, Yosemite, California USA*

Hardwoods for CLTs: Opportunities, Issues and Barriers

David DeVallance
InnoRenew CoE
devallance@innorenew.eu

Abstract

Not Available



List of 2019 Participating Sponsors

Gold

- Norbord, North America



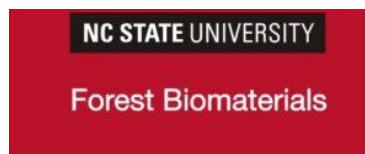
Silver

- Surface Measurement Systems, USA



Copper

- West Virginia University, USA
- University of Maine, USA
- North Carolina State University, USA
- Virginia Tech, USA
- Oregon State University, USA
- Mississippi State University, USA



Bronze

- InnoRenew CoE, Slovenia
- Université Laval, Centre de Recherche sur les Matériaux Renouvelables, Canada
- TallWood Design Institute, Oregon State University, USA



ISBN 978-0-9817876-9-5

9 0 0 0 0 >

9 780981 787695

